EMERGING INFECTIOUS DISEASES®

CDC
Centers for Disease Control and Prevention

Vectorborne Infections

January 2023

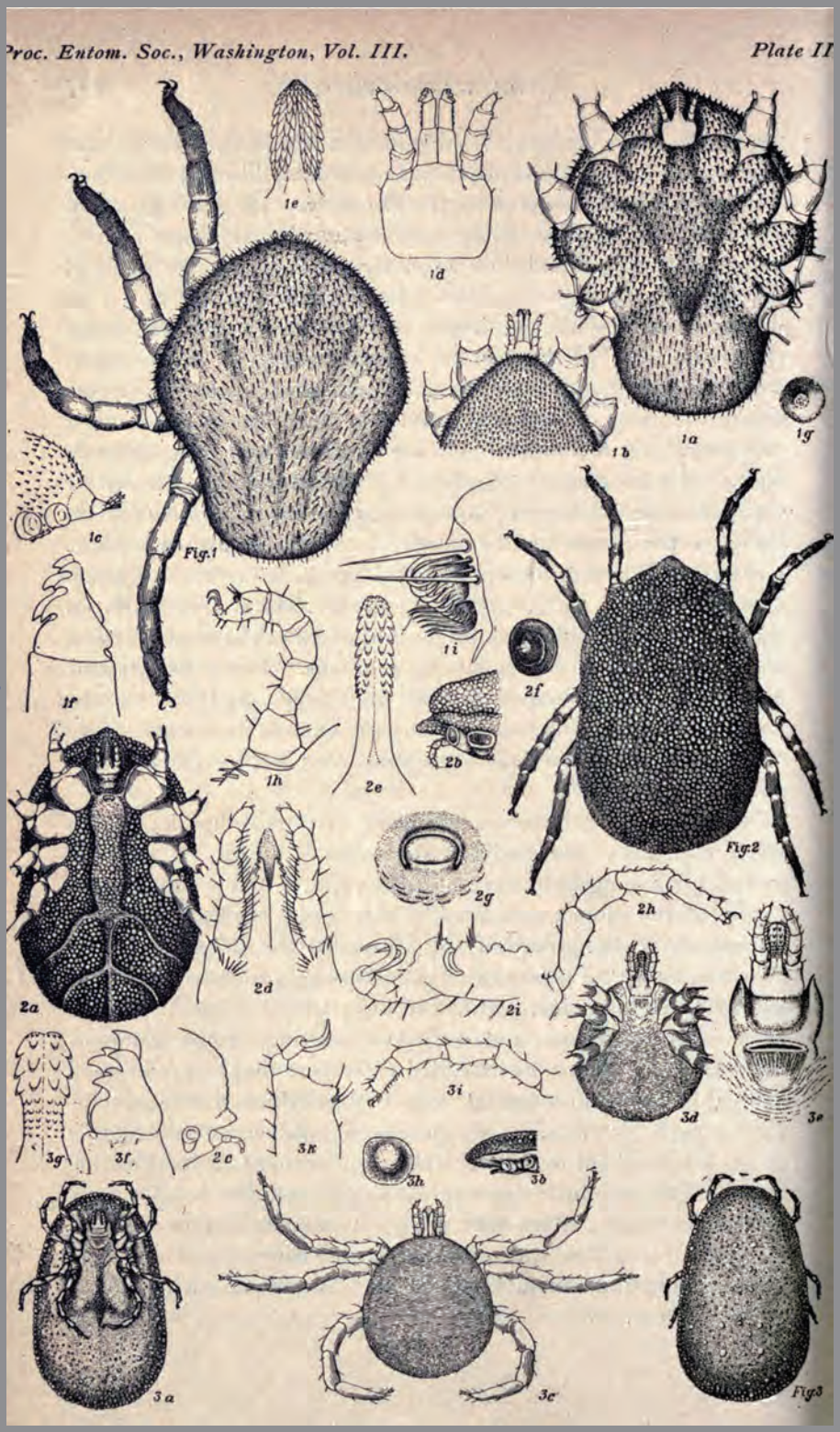

George Marx (1838–1895), *Illustration of ticks (Ixodida)*, 1892. Plate II from Proceedings of the Entomological Society of Washington. Ink on paper. Public domain image from Biodiversity Heritage Library. Holding institution: Smithsonian Libraries, Washington, DC, USA.

EMERGING INFECTIOUS DISEASES®

EDITOR-IN-CHIEF
D. Peter Drotman

ASSOCIATE EDITORS

Charles Ben Beard, Fort Collins, Colorado, USA
Ermias Belay, Atlanta, Georgia, USA
Sharon Bloom, Atlanta, Georgia, USA
Richard Bradbury, Melbourne, Victoria, Australia
Corrie Brown, Athens, Georgia, USA
Benjamin J. Cowling, Hong Kong, China
Michel Drancourt, Marseille, France
Paul V. Effler, Perth, Western Australia, Australia
Anthony Fiore, Atlanta, Georgia, USA
David O. Freedman, Birmingham, Alabama, USA
Peter Gerner-Smidt, Atlanta, Georgia, USA
Stephen Hadler, Atlanta, Georgia, USA
Nina Marano, Atlanta, Georgia, USA
Martin I. Meltzer, Atlanta, Georgia, USA
David Morens, Bethesda, Maryland, USA
J. Glenn Morris, Jr., Gainesville, Florida, USA
Patrice Nordmann, Fribourg, Switzerland
Johann D.D. Pitout, Calgary, Alberta, Canada
Ann Powers, Fort Collins, Colorado, USA
Didier Raoult, Marseille, France
Pierre E. Rollin, Atlanta, Georgia, USA
Frederic E. Shaw, Atlanta, Georgia, USA
David H. Walker, Galveston, Texas, USA
J. Scott Weese, Guelph, Ontario, Canada

Deputy Editor-in-Chief
Matthew J. Kuehnert, Westfield, New Jersey, USA

Managing Editor
Byron Breedlove, Atlanta, Georgia, USA

Technical Writer-Editors Shannon O'Connor, Team Lead; Dana Dolan, Thomas Gryczan, Amy Guinn, Tony Pearson-Clarke, Jill Russell, Jude Rutledge, Cheryl Salerno, P. Lynne Stockton, Susan Zunino

Production, Graphics, and Information Technology Staff
Reginald Tucker, Team Lead; William Hale, Barbara Segal, Hu Yang

Journal Administrators J. McLean Boggess, Susan Richardson

Editorial Assistants Letitia Carelock, Alexandria Myrick

Communications/Social Media Sarah Logan Gregory, Team Lead; Heidi Floyd

Associate Editor Emeritus
Charles H. Calisher, Fort Collins, Colorado, USA

Founding Editor
Joseph E. McDade, Rome, Georgia, USA

EDITORIAL BOARD

Barry J. Beaty, Fort Collins, Colorado, USA
David M. Bell, Atlanta, Georgia, USA
Martin J. Blaser, New York, New York, USA
Andrea Boggild, Toronto, Ontario, Canada
Christopher Braden, Atlanta, Georgia, USA
Arturo Casadevall, New York, New York, USA
Kenneth G. Castro, Atlanta, Georgia, USA
Gerardo Chowell, Atlanta, Georgia, USA
Christian Drosten, Berlin, Germany
Clare A. Dykewicz, Atlanta, Georgia, USA
Isaac Chun-Hai Fung, Statesboro, Georgia, USA
Kathleen Gensheimer, College Park, Maryland, USA
Rachel Gorwitz, Atlanta, Georgia, USA
Duane J. Gubler, Singapore
Scott Halstead, Westwood, Massachusetts, USA
David L. Heymann, London, UK
Keith Klugman, Seattle, Washington, USA
S.K. Lam, Kuala Lumpur, Malaysia
Shawn Lockhart, Atlanta, Georgia, USA
John S. Mackenzie, Perth, Western Australia, Australia
Jennifer H. McQuiston, Atlanta, Georgia, USA
Nkuchia M. M'ikanatha, Harrisburg, Pennsylvania, USA
Frederick A. Murphy, Bethesda, Maryland, USA
Barbara E. Murray, Houston, Texas, USA
Stephen M. Ostroff, Silver Spring, Maryland, USA
W. Clyde Partin, Jr., Atlanta, Georgia, USA
Mario Raviglione, Milan, Italy, and Geneva, Switzerland
David Relman, Palo Alto, California, USA
Connie Schmaljohn, Frederick, Maryland, USA
Tom Schwan, Hamilton, Montana, USA
Wun-Ju Shieh, Taipei, Taiwan
Rosemary Soave, New York, New York, USA
Robert Swanepoel, Pretoria, South Africa
David E. Swayne, Athens, Georgia, USA
Kathrine R. Tan, Atlanta, Georgia, USA
Phillip Tarr, St. Louis, Missouri, USA
Neil M. Vora, New York, New York, USA
Duc Vugia, Richmond, California, USA
J. Todd Weber, Atlanta, Georgia, USA
Mary Edythe Wilson, Iowa City, Iowa, USA

Emerging Infectious Diseases is published monthly by the Centers for Disease Control and Prevention, 1600 Clifton Rd NE, Mailstop H16-2, Atlanta, GA 30329-4027, USA. Telephone 404-639-1960; email, eideditor@cdc.gov

The conclusions, findings, and opinions expressed by authors contributing to this journal do not necessarily reflect the official position of the U.S. Department of Health and Human Services, the Public Health Service, the Centers for Disease Control and Prevention, or the authors' affiliated institutions. Use of trade names is for identification only and does not imply endorsement by any of the groups named above.

All material published in *Emerging Infectious Diseases* is in the public domain and may be used and reprinted without special permission; proper citation, however, is required.

Use of trade names is for identification only and does not imply endorsement by the Public Health Service or by the U.S. Department of Health and Human Services.

EMERGING INFECTIOUS DISEASES is a registered service mark of the U.S. Department of Health & Human Services (HHS).

EMERGING INFECTIOUS DISEASES®

Vectorborne Infections **January 2023**

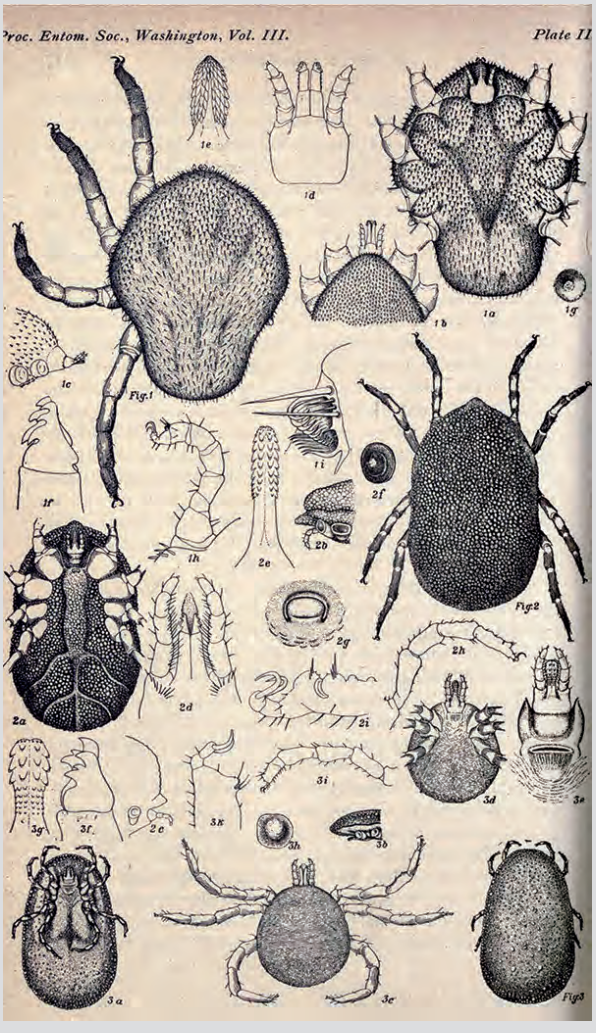

On the Cover

George Marx (1838–1895), *Illustration of ticks* (*Ixodida*), 1892. Plate II from Proceedings of the Entomological Society of Washington. Ink on paper. Public domain image from Biodiversity Heritage Library. Holding institution: Smithsonian Libraries, Washington, DC, USA.

About the Cover p. 229

Synopses

Research

EMERGING INFECTIOUS DISEASES®

January 2023

Dispatches

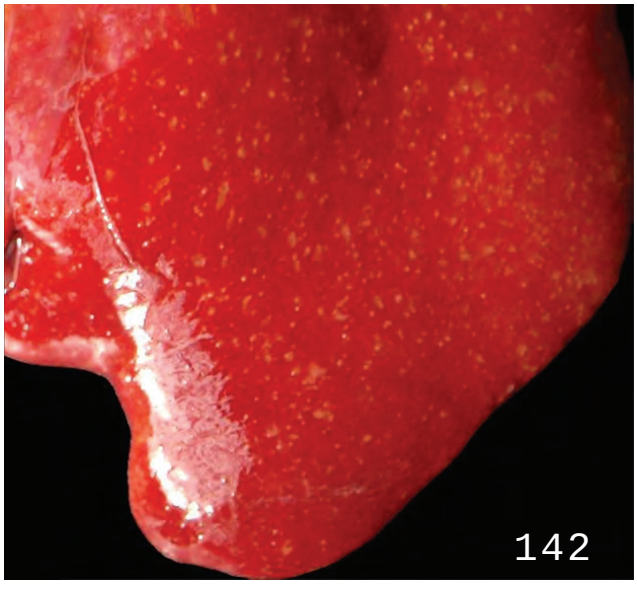

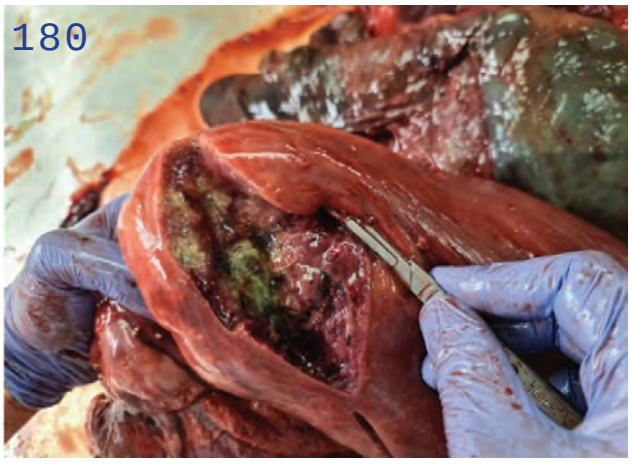

Research Letters

EMERGING INFECTIOUS DISEASES®

January 2023

About the Cover

Online Report

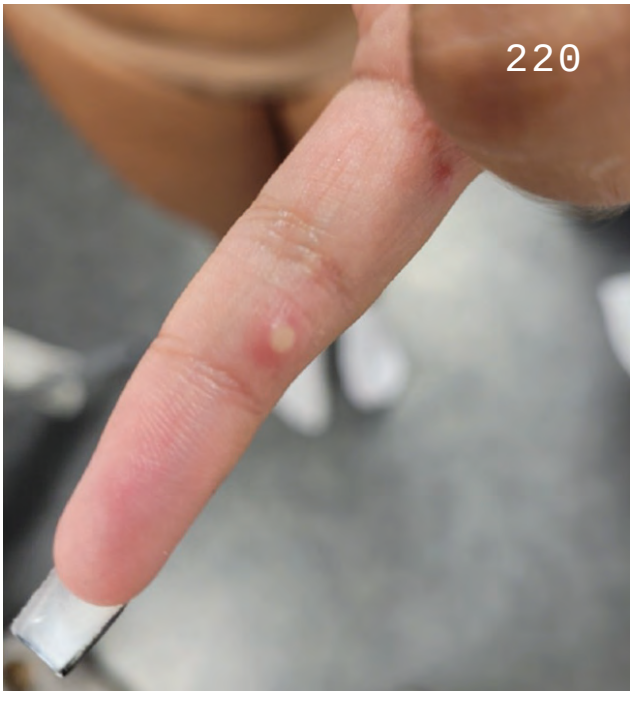

Emerging Infectious Diseases

Spotlight Topics

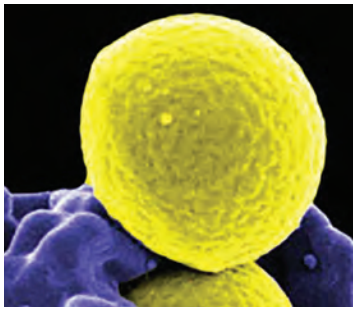


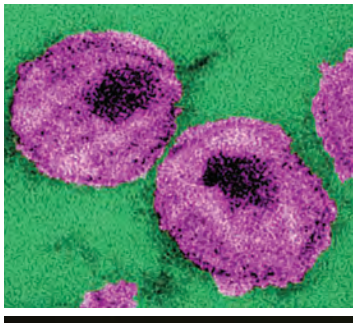

Antimicrobial resistance
Ebola • Etymologia
Food safety • HIV-AIDS
Influenza • Lyme disease
Malaria • MERS • Pneumonia
Rabies • Ticks • Tuberculosis
Coronavirus • Zika • mpox

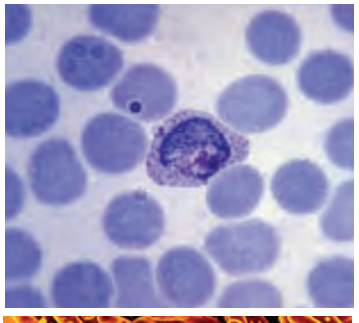
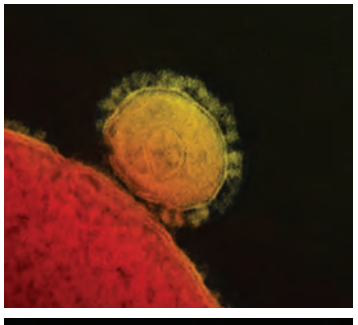
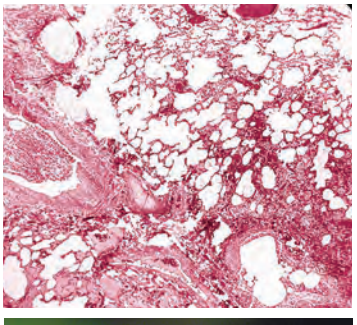
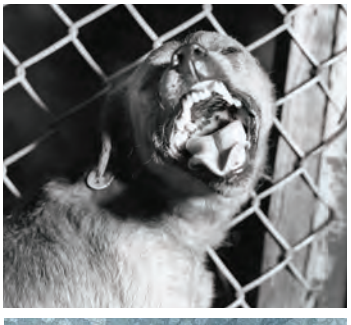




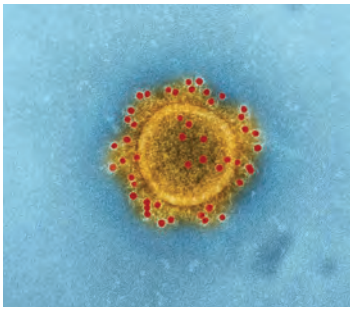

EID's spotlight topics highlight the latest articles and information on emerging infectious disease topics in our global community

https://wwwnc.cdc.gov/eid/page/spotlight-topics

Comprehensive Review of Emergence and Virology of Tickborne Bourbon Virus in the United States

Molly K. Roe,[1] Elise R. Huffman,[1] Yara S. Batista, George G. Papadeas, Sydney R. Kastelitz, Anna M. Restivo, Christopher C. Stobart

In support of improving patient care, this activity has been planned and implemented by Medscape, LLC and Emerging Infectious Diseases. Medscape, LLC is jointly accredited with commendation by the Accreditation Council for Continuing Medical Education (ACCME), the Accreditation Council for Pharmacy Education (ACPE), and the American Nurses Credentialing Center (ANCC), to provide continuing education for the healthcare team.

Medscape, LLC designates this Journal-based CME activity for a maximum of 1.00 ***AMA PRA Category 1 Credit(s)™***. Physicians should claim only the credit commensurate with the extent of their participation in the activity.

Successful completion of this CME activity, which includes participation in the evaluation component, enables the participant to earn up to 1.0 MOC points in the American Board of Internal Medicine's (ABIM) Maintenance of Certification (MOC) program. Participants will earn MOC points equivalent to the amount of CME credits claimed for the activity. It is the CME activity provider's responsibility to submit participant completion information to ACCME for the purpose of granting ABIM MOC credit.

All other clinicians completing this activity will be issued a certificate of participation. To participate in this journal CME activity: (1) review the learning objectives and author disclosures; (2) study the education content; (3) take the post-test with a 75% minimum passing score and complete the evaluation at http://www.medscape.org/journal/eid; and (4) view/print certificate. For CME questions, see page 232.

Release date: December 21, 2022; Expiration date: December 21, 2023

Learning Objectives

Upon completion of this activity, participants will be able to:

- Assess the virology of the Bourbon virus
- Distinguish the geographic distribution of the Bourbon virus infection in the US
- Evaluate the transmission of the Bourbon virus
- Assess the clinical picture of the Bourbon virus infection

CME Editor

Susan Zunino, PhD, Technical Writer/Editor, Emerging Infectious Diseases.

CME Author

Charles P. Vega, MD, Health Sciences Clinical Professor of Family Medicine, University of California, Irvine School of Medicine, Irvine, California. *Disclosure: Charles P. Vega, MD, has the following relevant financial relationships: consultant or advisor for GlaxoSmithKline; Johnson & Johnson Pharmaceutical Research & Development, L.L.C.*

Authors

Molly K. Roe, BS; Elise R. Huffman, BS; Yara S. Batista, BS; George G. Papadeas, BS; Sydney R. Kastelitz, BS; Anna M. Restivo, BS; and ***Christopher C. Stobart, PhD.***

Author affiliation: Butler University, Indianapolis, Indiana, USA

[1]These first authors contributed equally to this article.

DOI: https://doi.org/10.3201/eid2901.212295

The emergence of SARS-CoV-2 and the worldwide COVID-19 pandemic triggered considerable attention to the emergence and evolution of novel human pathogens. Bourbon virus (BRBV) was first discovered in 2014 in Bourbon County, Kansas, USA. Since its initial discovery, several cases of BRBV infection in humans have been identified in Kansas, Oklahoma, and Missouri. BRBV is classified within the *Thogotovirus* genus; these negative-strand RNA viruses appear to be transmitted by ticks, and much of their biology remains unknown. In this review, we describe the emergence, virology, geographic range and ecology, and human disease caused by BRBV and discuss potential treatments for active BRBV infections. This virus and other emerging viral pathogens remain key public health concerns and require continued surveillance and study to mitigate human exposure and disease.

The first case of Bourbon virus (BRBV) was identified in June 2014 in Bourbon County, Kansas, USA, after severe febrile illness developed in a previously healthy middle-aged (>50 years of age) man (*1*). Several days after he removed an engorged tick from his shoulder, nonspecific symptoms of disease appeared. After 3 days of worsening fever, myalgia, arthralgia, and diarrhea, the patient visited his primary care physician and was prescribed doxycycline. The next day, the patient was admitted to the hospital because of dehydration, syncope, and a possible tickborne illness. Doxycycline treatment was continued; however, the patient did not respond, and symptoms continued to progress toward multiorgan failure. Laboratory results revealed progressive leukopenia and thrombocytopenia (which are now considered identifiers of potential BRBV infection). Patient blood samples tested negative for all known regional tickborne diseases. Therefore, a whole blood sample was sent to the US Centers for Disease Control and Prevention (CDC) to test for Heartland virus (HRTV), a similar emerging tickborne virus in the region. The index patient died 11 days after symptom onset.

Initial efforts at CDC to identify the causative agent of disease in this first case revealed heterologous (non-HRTV) viral plaques in plaque reduction neutralization tests performed by using serum from the deceased patient and including a control HRTV strain. Subsequent electron microscopy revealed pleiomorphic viral particles consistent with the family Orthomyxoviridae (*1*). Phylogenetic analyses revealed a close relationship between the patient's novel virus and Thogoto and Dhori viruses, placing it within the genus *Thogotovirus*. Subsequent genetic analyses supported this initial genus classification (*2*,*3*). Recently, another novel thogotovirus (Oz virus) was discovered in ticks in Japan; this virus was capable of replicating in mammalian cell lines and is the closest known relative of BRBV (*3*). BRBV was the first human pathogen in the genus *Thogotovirus* identified in the Western Hemisphere; Aransas Bay virus, another pathogenic member of this genus, was reported in ticks found in seabird nests in the United States (*2*). Since its initial identification, ≥5 human cases of BRBV-associated disease have been reported in the Midwest region of the United States (*1*,*4*–*8*). Because little is known about BRBV biology and no specific treatments or vaccines are available, further studies of BRBV are needed.

Bourbon Virus Genetics and Replication

Genetics and Classification

BRBV consists of a segmented, ≈10–11-kb, single-stranded negative-sense RNA genome (Figure 1) (*2*,*3*). Phylogenetic analysis indicates that BRBV has the greatest similarity to Oz, Dhori, and Batken viruses within the genus *Thogotovirus* and family Orthomyxoviridae (*1*–*3*). The 6 negative-strand RNA segments of the BRBV genome encode the putative glycoprotein (GP), nucleoprotein (NP), matrix protein (M), and the 3 polymerase subunits PA, PB1, and PB2 (*2*). Gene expression and genetic organization are consistent with other orthomyxoviruses.

The genus *Thogotovirus* contains several other emerging viruses: Araguari, Aransas Bay, Dhori (including the subtype Batken), Jos, Oz, Thogoto, and Upolu viruses (*3*). Most of these species have yet to be accepted by the International Committee on Taxonomy of Viruses. Thogoto, Dhori, and Bourbon viruses are known to cause infectious disease in humans.

Despite BRBV sharing several properties with Thogoto and Dhori viruses, such as dependence on hard ticks for transmission and similar virion structures, BRBV disease pathology remains distinct from those viruses and more closely resembles that of HRTV and severe fever with thrombocytopenia syndrome virus. However, genomic analysis of virus open reading frames (ORFs) revealed that BRBV has genetic identity with Dhori and Oz viruses ranging from ≈59% in the most divergent GP gene to ≈82% in the most conserved PB1 gene (*2*,*3*). Consequently, BRBV is classified in the *Thogotovirus* genus and recognized as a relative of both Oz and Dhori viruses.

BRBV Virion Structure and Replication

BRBV forms a pleomorphic (filamentous or round), ≈100–130-nm enveloped virion that is consistent with virions of other orthomyxoviruses (Figure 2) (*1*,*3*).

Electron microscopy of BRBV virions shows multiple genomic segments that are likely coated internally with NPs and numerous GP molecules studding the virion surface (*1*,*5*). Although replication of BRBV has not yet been directly investigated, BRBV genetic analysis, recent crystallization of the BRBV postfusion GP, and studies of replication of related thogotoviruses provide several clues regarding the replication cycle of this virus.

All thogotoviruses use a single attachment GP to mediate virus attachment to and fusion with the host cell (*5*,*9*). The postfusion conformation of BRBV GP was recently crystallized; several structural similarities and distinct differences to previously crystallized Dhori and Thogoto virus GPs were observed (*2*,*5*). The BRBV GP is a type III fusion protein related to baculovirus Gp64 and consists of 5 distinct domains that assemble into homotrimers on the virus surface (*5*,*10*). The cell receptor for BRBV remains unknown; however, ecologic surveillance and in vitro cell culture studies collectively suggest that BRBV exhibits wide vertebrate and invertebrate species tropism (*2*,*11*,*12*). Electron microscopy and postfusion GP crystal structure suggest that BRBV attaches to host cells through a glycan-like cellular receptor and initiates entry by endocytosis (*1*,*5*).

After an endosome has formed, acidification of the endocytic compartment triggers a conformational change in the GP that causes fusion of the viral envelope with the endosomal membrane and release of the genome into the cytoplasm (*5*,*13*). All 6 genomic RNA segments are encapsidated by viral NPs, forming viral ribonucleoprotein complexes (*14*). Intracellular trafficking of viral ribonucleoprotein complexes into the nucleus, the site of replication for thogotoviruses, is driven by viral NPs, which contain a nuclear translocation signal and are known to accumulate in the nucleus during active infection (*14*,*15*). Virus replication is induced by heterotrimeric polymerase complexes formed from PB1, PB2, and PA protein subunits and is believed to be consistent with mechanisms described for other orthomyxoviruses (*16*). Similar to influenza virus and other orthomyxoviruses, thogotoviruses depend on host RNA polymerase II activity and a unique cap-snatching mechanism, whereby the viral polymerase complex cleaves the 5′-methylated cap of cellular mRNA and uses this capped leader sequence to prime viral mRNA transcription (*16*–*18*). Little is known about the nuclear export pathways of newly formed viral ribonucleoprotein complexes, but both M and NP have been implicated in aiding this process (*15*,*19*). Thogotovirus assembly and release appears to occur at the plasma membrane, activated by pH-dependent oligomerization of M particles in the cytoplasm (*1*,*19*).

Vectors, Hosts, and Geographic Range of BRBV

Detection and Distribution of BRBV in Invertebrates

To date, all known human cases of BRBV infection have been found in 3 US states, Kansas, Oklahoma, and Missouri (Figure 3). In each case, recent tick bites were associated with the onset of disease (*1*,*8*). Since the initial identification of BRBV in a tick-infected person, several studies have used PCR-based surveillance testing to show that BRBV can be detected in all life stages (larvae, nymph, and adult) of lone star ticks (*Amblyomma americanum*) (*4*,*20*). Lone star ticks (also known as northeastern water ticks or turkey ticks) are a species of hard tick with a wide range throughout the eastern and central United States (Figures 3, 4); they are commonly found in both wooded and grassy areas and known to harbor several human pathogens, including HRTV and Tacaribe virus and the bacteria *Ehrlichia* spp., *Francisella tularensis*, *Coxiella burnetti*, and *Rickettsia amblyommii* (*21*). Although other common species of ticks have been tested at surveillance sites, such as *Amblyomma maculatum*, *Dermacentor*

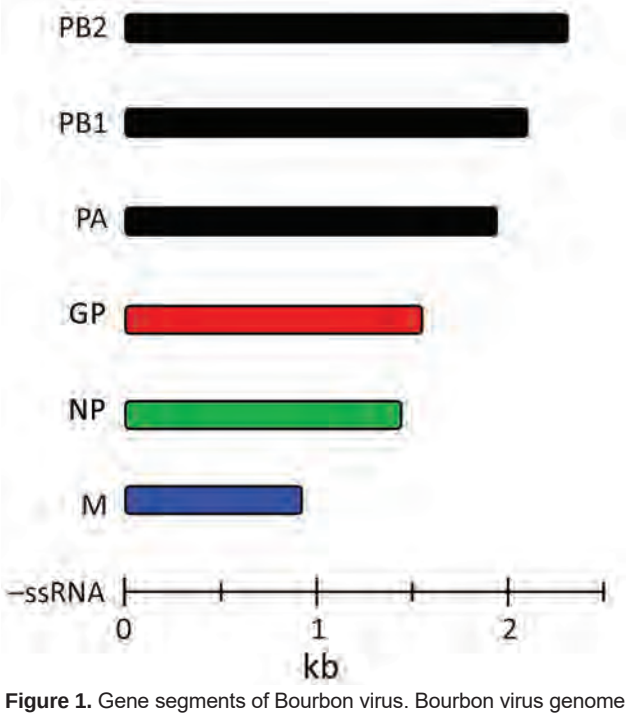

Figure 1. Gene segments of Bourbon virus. Bourbon virus genome comprises segmented, ≈10–11-kb, single-stranded negative-sense RNA. Specific proteins are encoded by 6 gene segments. GP, glycoprotein; M, matrix protein; NP, nucleoprotein; PA, polymerase acidic protein, PB1, polymerase basic protein 1; PB2, polymerase basic protein 2; –ssRNA, negative single-strand RNA.

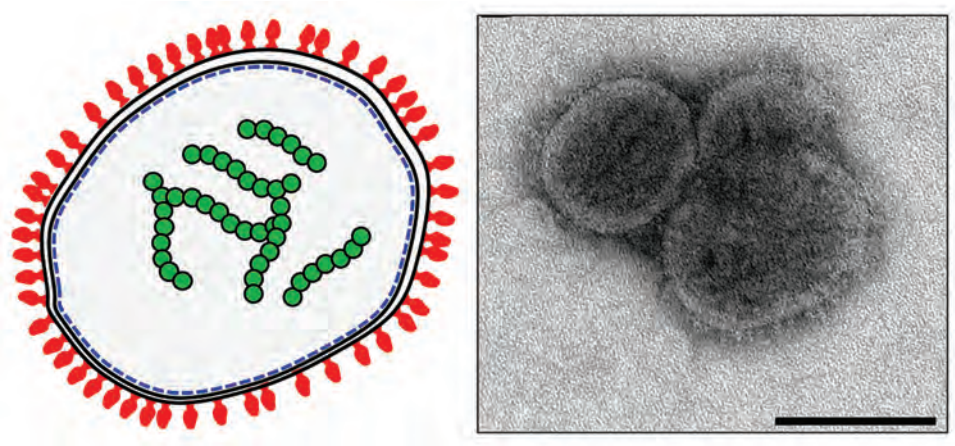

Figure 2. Diagram (left) and electron micrographic image (right) of Bourbon virus showing putative structural organization of the virion. Red structures represent glycoproteins attached to the outside of the virion; green structures represent the 6 RNA gene segments coated with nucleoproteins. Scale bar is 100 nm. Electron micrographic image credit: Public Health Image Library (https://phil.cdc.gov).

variabilis, *Haemaphysalis leporispalustris*, *Ixodes scapularis*, and *Ixodes dentatus*, to date, BRBV has only been found in *A. americanum* ticks (*4*,*20*). Recently, *A. americanum* ticks were shown to be capable of sustaining and transmitting BRBV through cofeeding on animal hosts (*22*). Although the *A. americanum* tick remains the only vector to harbor BRBV thus far, in vitro studies using cell culture have shown wide species tropism of BRBV. Multi-logarithmic BRBV replication was shown in the vertebrate cell lines Vero, Vero E6, LLC-MK2, BHK21Cl-15, HeLa, and HUH-7 and tick cell lines RAE/CTVM1, HAE/CTVM9, and AVL/CTVM17, indicating further surveillance will be necessary to detect additional invertebrate hosts (*2*).

Detection of BRBV in Nonhuman Vertebrates

Similar to many other tickborne viruses, BRBV is believed to be transmitted to and amplified in nonhuman vertebrate hosts. Serologic testing was performed on a wide array of common mammal and avian fauna found near the sites of confirmed human cases in Missouri and at a distant site in North Carolina (still within the range of *A. americanum* ticks); numerous mammals were seropositive for BRBV, including domestic dogs, eastern cottontail rabbits, horses, raccoons, and white-tailed deer (*11*,*12*). The 2 most common seropositive animals identified were raccoons and white-tailed deer. No evidence of prior infections was observed in any

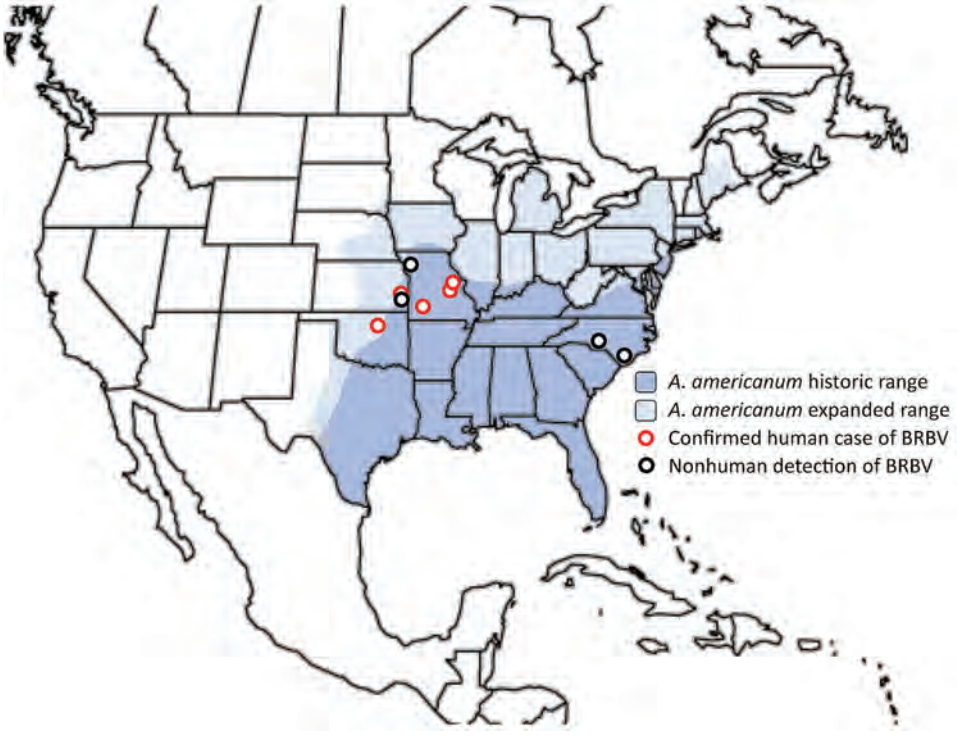

Figure 3. Geographic range of BRBV and its vector, the *Amblyomma americanum* tick . Confirmed human cases of BRBV infection and virus detection in nonhuman animals are superimposed over historic and expanded geographic ranges of the lone star tick (*A. americanum*). Confirmed human cases of BRBV infection were identified by the US Centers for Disease Control and Prevention, and detection of virus in nonhuman animals occurred primarily through sampling of ticks and subsequent testing by using PCR and serologic testing of mammals. BRBV, Bourbon virus.

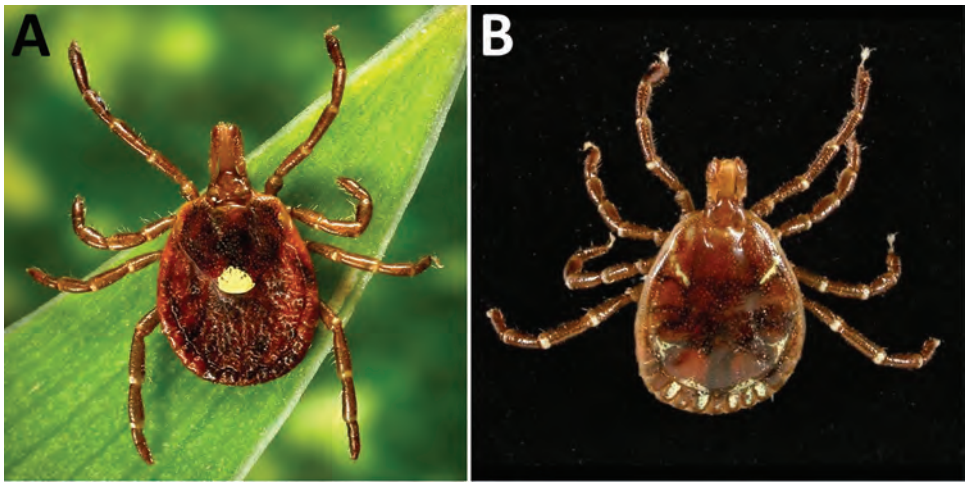

Figure 4. Female (A) and male (B) lone star ticks (*Amblyomma americanum*). Image credit: Public Health Image Library (https://phil.cdc.gov).

tested bird species, suggesting that common nonhuman mammals likely serve as potential BRBV amplifier hosts (*12*).

Bourbon Virus Disease in Humans and Potential Treatments

Five confirmed cases of BRBV infection have been reported in humans (*5*,*7*), and all 5 cases are believed to have been caused by tick bites. Although *A. americanum* ticks remain the only confirmed competent vector for BRBV, no tick species identification was made in those human cases (*22*). Limited data are available on BRBV disease in humans; however, initial symptoms of infection appear ≈2–7 days postexposure (tick bite) and include weakness, nausea, myalgia, arthralgia, fatigue, and diarrhea (*1*,*7*,*8*). Concurrently or shortly after the onset of initial symptoms, a fever and papular rash developed in all described cases. Laboratory testing of blood samples from infected persons showed consistent evidence of thrombocytopenia, leukopenia, lymphopenia, and elevated levels of aspartate transferase and alanine transferase (*1*,*8*). Late-stage BRBV disease is associated with shock, cardiac dysregulation, and pleural effusions (*1*,*7*,*8*). In confirmed fatal cases, time from initial symptoms to death was ≈11–24 days. In postmortem analysis of the index case, acute bone marrow suppression was noted (*1*).

The pathogenesis of BRBV in humans remains largely unknown. However, studies using footpad or intraperitoneal BRBV inoculations in type I interferon receptor deficient *Ifnar1*$^{-/-}$ mice showed the virus caused active viremia and lethal systemic infection; the highest viral loads were detected in the liver and spleen, and lower viral loads were detected in the blood, kidneys, and heart (*8*,*23*). Pathogenesis observed in those mice was consistent with progressive infection from the initial entry site to multiple organs, including the liver (supported by altered aspartate transferase and alanine transferase levels), lungs (pleural effusions), and heart (cardiac dysregulation). Efforts to establish infection or lethal disease in wild-type mice were largely unsuccessful (*8*,*23*). BRBV is highly sensitive to type I and II interferons, suggesting that advanced human disease and death might be caused, in part, by existing weaknesses in antiviral innate host immunity (*23*).

Because of the low incidence rate of BBRV infection and similarities to other tickborne diseases, additional cases of BRBV disease have likely been either misidentified or unreported. All cases to date have been confirmed at CDC by using PCR (*4*,*24*). No established treatment for BRBV disease has been reported other than supportive care. Studies in *Ifnar1*$^{-/-}$ mice indicate that early introduction of several known antiviral treatments might be effective, including interferon-α or the viral replication inhibitors ribavirin, favipiravir, or myricetin (*8*,*23*,*25*). Recently, a reporter system for BRBV was developed, which will enable more efficient screening of putative inhibitors of this virus (*25*).

Future Outlook

During the past 3 years, the emergence and pandemic spread of SARS-CoV-2 has highlighted the potential for evolution and proliferation of new pathogens. Thus far, BRBV has remained limited to a small number of confirmed human cases. However, many unanswered questions persist that are related to both virology and ecology of BRBV. Most of what is currently known about BRBV originates from 2 published confirmed cases of disease or ecologic surveillance

studies in a small number of states in the US Midwest or North Carolina. Therefore, a substantial need remains to determine mechanisms of viral replication, detect other potential vector hosts, and conduct additional surveillance in unexplored regions within the geographic range of *A. americanum* ticks.

The *A. americanum* tick is the only known vector responsible for BRBV spread to humans. The expanding range of *A. americanum* ticks, partly driven by climate change, might lead to more exposure events (*26*). Monitoring trends in tickborne and mosquitoborne diseases has become more prominent in recent literature (*27*). Proactive safety and awareness of tickborne diseases has been encouraged, especially because ticks such as *A. americanum* continue to be dominant health threats in much of the forested regions of the United States (*21*). Because of the lack of knowledge and established treatments or vaccines for BRBV, CDC recommends using insect repellent, wearing long sleeves and pants, and conducting a thorough tick check after spending time in known tick-infested regions (*28*).

Recent evidence suggests increasing potential for BRBV genetic evolution through recombination with related thogotoviruses. The recent discovery in Japan of Oz virus, which exhibits high sequence identity to BRBV, in *Amblyomma* sp. ticks, which share the same genus as the lone star tick, illustrates the necessity for further examination of thogotoviruses and their geographic distribution (*3*). To survive in its human host, BRBV must first overcome the interferon-induced myxovirus resistance protein A (MxA) to avoid the host's innate antiviral defense system. Thogotoviruses are normally susceptible to inactivation by MxA, but a recent study of Jos virus showed that mutations in the viral NP can lead to resistance (*14*). Although this position is conserved among viruses in the *Thogotovirus* genus, only 1 amino acid change in the viral NP was required to fully escape MxA without replicative fitness loss. As described previously, BRBV is particularly sensitive to interferon signaling, which suggests a possible therapeutic agent for active BRBV infections (*23*). However, those studies indicate that thogotoviruses, including BRBV, might find novel mechanisms to evade host interferon-stimulated gene expression.

A substantial need exists for further research on other possible tick vectors of BRBV and the role of amplifier hosts. Seropositivity of several common animals and the ability of BRBV to replicate in multiple animal and tick cells in vitro collectively highlight the need for more BRBV surveillance to mitigate human exposure and disease. Increases in population dynamics, climate change, and vectors mean that vectorborne pathogens such as BRBV remain a major public health concern. More surveillance of both viruses and vectors will elucidate the potential for increased transmission to and pathogenicity in humans.

Addendum

As of 2022, Bourbon virus has now been detected in the Asian longhorned tick (*Haemaphysalis longicornis*) through a surveillance study performed in Virginia, USA (*29*). This recent finding provides evidence of possible transmission of Bourbon virus in 2 separate species of ticks, *A. americanum* and *H. longicornis*. In addition, that study expands the known region of Bourbon virus to include Virginia.

This work was supported by an Indiana Academy of Sciences Senior Research Grant (C.C.S.), a Holcomb Awards Committee Grant of Butler University (C.C.S.), and the Butler University Department of Biological Sciences (C.C.S.).

About the Author

During the writing of this manuscript, Ms. Roe was an undergraduate research assistant in the Department of Biological Sciences at Butler University.She is now a doctoral graduate student at Yale University, New Haven, Connecticut, USA.

References

1. Kosoy OI, Lambert AJ, Hawkinson DJ, Pastula DM, Goldsmith CS, Hunt DC, et al. Novel thogotovirus associated with febrile illness and death, United States, 2014. Emerg Infect Dis. 2015;21:760–4. https://doi.org/10.3201/eid2105.150150
2. Lambert AJ, Velez JO, Brault AC, Calvert AE, Bell-Sakyi L, Bosco-Lauth AM, et al. Molecular, serological and in vitro culture-based characterization of Bourbon virus, a newly described human pathogen of the genus *Thogotovirus*. J Clin Virol. 2015;73:127–32. https://doi.org/10.1016/j.jcv.2015.10.021
3. Ejiri H, Lim C-K, Isawa H, Fujita R, Murota K, Sato T, et al. Characterization of a novel thogotovirus isolated from *Amblyomma testudinarium* ticks in Ehime, Japan: a significant phylogenetic relationship to Bourbon virus. Virus Res. 2018;249:57–65. https://doi.org/10.1016/j.virusres.2018.03.004
4. Savage HM, Burkhalter KL, Godsey MS Jr, Panella NA, Ashley DC, Nicholson WL, et al. Bourbon virus in field-collected ticks, Missouri, USA. Emerg Infect Dis. 2017;23:2017–22. https://doi.org/10.3201/eid2312.170532
5. Bai C, Qi J, Wu Y, Wang X, Gao GF, Peng R, et al. Postfusion structure of human-infecting Bourbon virus envelope glycoprotein. J Struct Biol. 2019;208:99–106. https://doi.org/10.1016/j.jsb.2019.08.005
6. Schweon SJ. Bourbon virus: a novel pathogen. Nursing. 2016;46:65. https://doi.org/10.1097/01.NURSE.0000481418.81092.98

7. Miller M. Bourbon virus linked to death of Park official—CDC testing tick samples. March 8, 2018 [cited 2021 Oct 31]. The Missourian. https://www.emissourian.com/local_news/county/bourbon-virus-linked-to-death-of-park-official—cdc-testing-tick-samples/article_057f0f0a-bddd-5f7a-aa0d-735187e4c379.html
8. Bricker TL, Shafiuddin M, Gounder AP, Janowski AB, Zhao G, Williams GD, et al. Therapeutic efficacy of favipiravir against Bourbon virus in mice. PLoS Pathog. 2019;15:e1007790. https://doi.org/10.1371/journal.ppat.1007790
9. Portela A, Jones LD, Nuttall P. Identification of viral structural polypeptides of Thogoto virus (a tick-borne orthomyxo-like virus) and functions associated with the glycoprotein. J Gen Virol. 1992;73:2823–30. https://doi.org/10.1099/0022-1317-73-11-2823
10. Peng R, Zhang S, Cui Y, Shi Y, Gao GF, Qi J. Structures of human-infecting *Thogotovirus* fusogens support a common ancestor with insect baculovirus. Proc Natl Acad Sci USA. 2017;114:E8905–12. https://doi.org/10.1073/pnas.1706125114
11. Komar N, Hamby N, Palamar MB, Staples JE, Williams C. Indirect evidence of *Bourbon virus* (*Thogotovirus, Orthomyxoviridae*) infection in North Carolina. N C Med J. 2020;81:214–5. https://doi.org/10.18043/ncm.81.3.214
12. Jackson KC, Gidlewski T, Root JJ, Bosco-Lauth AM, Lash RR, Harmon JR, et al. Bourbon virus in wild and domestic animals, Missouri, USA, 2012–2013. Emerg Infect Dis. 2019;25:1752–3. https://doi.org/10.3201/eid2509.181902
13. Relich RF, Grabowski JM. Tick-borne viruses of North America. Clin Microbiol Newsl. 2020;42:79–86. https://doi.org/10.1016/j.clinmicnews.2020.05.001
14. Fuchs J, Oschwald A, Graf L, Kochs G. Tick-transmitted thogotovirus gains high virulence by a single MxA escape mutation in the viral nucleoprotein. PLoS Pathog. 2020; 16:e1009038. https://doi.org/10.1371/journal.ppat.1009038
15. Cros JF, Palese P. Trafficking of viral genomic RNA into and out of the nucleus: influenza, Thogoto and Borna disease viruses. Virus Res. 2003;95:3–12. https://doi.org/10.1016/S0168-1702(03)00159-X
16. Guilligay D, Kadlec J, Crépin T, Lunardi T, Bouvier D, Kochs G, et al. Comparative structural and functional analysis of orthomyxovirus polymerase cap-snatching domains. PLoS One. 2014;9:e84973. https://doi.org/10.1371/journal.pone.0084973
17. Leahy MB, Dessens JT, Nuttall PA. In vitro polymerase activity of Thogoto virus: evidence for a unique cap-snatching mechanism in a tick-borne orthomyxovirus. J Virol. 1997;71:8347–51. https://doi.org/10.1128/jvi.71.11.8347-8351.1997
18. Siebler J, Haller O, Kochs G. Thogoto and Dhori virus replication is blocked by inhibitors of cellular polymerase II activity but does not cause shutoff of host cell protein synthesis. Arch Virol. 1996;141:1587–94. https://doi.org/10.1007/BF01718257
19. Yang M, Feng F, Liu Y, Wang H, Yang Z, Hou W, et al. pH-dependent conformational changes of a Thogoto virus matrix protein reveal mechanisms of viral assembly and uncoating. J Gen Virol. 2016;97:2149–56. https://doi.org/10.1099/jgv.0.000551
20. Savage HM, Godsey MS Jr, Panella NA, Burkhalter KL, Manford J, Trevino-Garrison IC, et al. Surveillance for tick-borne viruses near the location of a fatal human case of Bourbon virus (family Orthomyxoviridae: genus *Thogotovirus*) in eastern Kansas, 2015. J Med Entomol. 2018;55:701–5. https://doi.org/10.1093/jme/tjx251
21. Kennedy AC, Marshall E; BCE1. Lone star ticks (*Amblyomma americanum*): an emerging threat in Delaware. Dela J Public Health. 2021;7:66–71. https://doi.org/10.32481/djph.2021.01.013
22. Godsey MS Jr, Rose D, Burkhalter KL, Breuner N, Bosco-Lauth AM, Kosoy OI, et al. Experimental infection of *Amblyomma americanum* (Acari: Ixodidae) with Bourbon virus (Orthomyxoviridae: *Thogotovirus*). J Med Entomol. 2021;58:873–9. https://doi.org/10.1093/jme/tjaa191
23. Fuchs J, Straub T, Seidl M, Kochs G. Essential role of interferon response in containing human pathogenic Bourbon virus. Emerg Infect Dis. 2019;25:1304–13. https://doi.org/10.3201/eid2507.181062
24. Warang A, Zhang M, Zhang S, Shen Z. A panel of real-time PCR assays for the detection of Bourbon virus, Heartland virus, West Nile virus, and *Trypanosoma cruzi* in major disease-transmitting vectors. J Vet Diagn Invest. 2021;33:1115–22. https://doi.org/10.1177/10406387211039549
25. Hao S, Ning K, Wang X, Wang J, Cheng F, Ganaie SS, et al. Establishment of a replicon reporter of the emerging tick-borne Bourbon virus and use it for evaluation of antivirals. Front Microbiol. 2020;11:572631. https://doi.org/10.3389/fmicb.2020.572631
26. Ma D, Lun X, Li C, Zhou R, Zhao Z, Wang J, et al. Predicting the potential global distribution of *Amblyomma americanum* (Acari: Ixodidae) under near current and future climatic conditions, using the maximum entropy model. Biology (Basel). 2021;10:1057. https://doi.org/10.3390/biology10101057
27. Rosenberg R, Lindsey NP, Fischer M, Gregory CJ, Hinckley AF, Mead PS, et al. Vital signs: trends in reported vectorborne disease cases—United States and Territories, 2004–2016. MMWR Morb Mortal Wkly Rep. 2018;67:496–501. https://doi.org/10.15585/mmwr.mm6717e1
28. Centers for Disease Control and Prevention. Bourbon virus [cited 2021 Nov 8]. https://www.cdc.gov/bourbon-virus/index.html
29. Cumbie AN, Trimble RN, Eastwood G. Pathogen spillover to an invasive tick species: first detection of Bourbon virus in *Haemaphysalis longicornis* in the United States. Pathogens. 2022;11:454

Address for correspondence: Christopher C. Stobart, Butler University, 4600 Sunset Ave, Indianapolis, IN 46208, USA; email: cstobart@butler.edu

Multicenter Case–Control Study of COVID-19–Associated Mucormycosis Outbreak, India

In support of improving patient care, this activity has been planned and implemented by Medscape, LLC and Emerging Infectious Diseases. Medscape, LLC is jointly accredited with commendation by the Accreditation Council for Continuing Medical Education (ACCME), the Accreditation Council for Pharmacy Education (ACPE), and the American Nurses Credentialing Center (ANCC), to provide continuing education for the healthcare team.

Medscape, LLC designates this Journal-based CME activity for a maximum of 1.00 ***AMA PRA Category 1 Credit(s)™***. Physicians should claim only the credit commensurate with the extent of their participation in the activity.

Successful completion of this CME activity, which includes participation in the evaluation component, enables the participant to earn up to 1.0 MOC points in the American Board of Internal Medicine's (ABIM) Maintenance of Certification (MOC) program. Participants will earn MOC points equivalent to the amount of CME credits claimed for the activity. It is the CME activity provider's responsibility to submit participant completion information to ACCME for the purpose of granting ABIM MOC credit.

All other clinicians completing this activity will be issued a certificate of participation. To participate in this journal CME activity: (1) review the learning objectives and author disclosures; (2) study the education content; (3) take the post-test with a 75% minimum passing score and complete the evaluation at http://www.medscape.org/journal/eid; and (4) view/print certificate. For CME questions, see page 233.

Release date: December 19, 2022; Expiration date: December 19, 2023

Learning Objectives

Upon completion of this activity, participants will be able to:

- Assess risk factors for COVID-19–associated mucormycosis (CAM), including potential associations of COVID-19 treatment practices with the occurrence of CAM, based on a nationwide case-control study across 25 hospitals in India from January to June 2021
- Determine the clinical outcomes of CAM and factors associated with mortality in CAM at 12 weeks, based on a nationwide case-control study across 25 hospitals in India from January to June 2021
- Evaluate the clinical implications of risk factors for and clinical outcomes of CAM, including potential associations of COVID-19 treatment practices with the occurrence of CAM, and factors associated with mortality in CAM at 12 weeks, based on a nationwide case-control study across 25 hospitals in India from January to June 2021

CME Editor

Jill Russell, BA, Technical Writer/Editor, Emerging Infectious Diseases. *Disclosure: Jill Russell, BA, has disclosed no relevant financial relationships.*

CME Author

Laurie Barclay, MD, freelance writer and reviewer, Medscape, LLC. *Disclosure: Laurie Barclay, MD, has the following relevant financial relationships: formerly owned stocks in AbbVie Inc.*

Authors

Valliappan Muthu, DM; Ritesh Agarwal, DM; Shivaprakash Mandya Rudramurthy, MD; Deepak Thangaraju, MD; Manoj Radhakishan Shevkani, MD; Atul K. Patel, MD; Prakash Srinivas Shastri, MD; Ashwini Tayade, MD, DNB, FNB; Sudhir Bhandari, MD; Vishwanath Gella, DM; Jayanthi Savio, MD; Surabhi Madan, MD; Vinay Kumar Hallur, MD; Venkata Nagarjuna Maturu, DM; Arjun Srinivasan, DM; Nandini Sethuraman, MD; Raminder Pal Singh Sibia, MD; Sanjay Pujari, MD; Ravindra Mehta, MD; Tanu Singhal, MD; Puneet Saxena, DM; Varsha Gupta, MD; Vasant Nagvekar, MD; Parikshit Prayag, MD; Dharmesh Patel, MD; Immaculata Xess, MD; Pratik Savaj, DNB; Naresh Panda, MS; Gayathri Devi Rajagopal, MD; Riya Sandeep Parwani, B Pharm; Kamlesh Patel, MD; Anuradha Deshmukh, MD; Aruna Vyas, MD; Srinivas Kishore Sistla, MS; Priyadarshini A. Padaki, MD; Dharshni Ramar, MD; Saurav Sarkar, MS; Bharani Rachagulla, MD; Pattabhiraman Vallandaramam, MD; Krishna Prabha Premachandran, MD; Sunil Pawar, MD; Piyush Gugale, DNB; Pradeep Hosamani, MS; Sunil Narayan Dutt, MS; Satish Nair, MS; Hariprasad Kalpakkam, DM; Sanjiv Badhwar, MS; Kiran Kumar Kompella, MD; Nidhi Singla, MD; Milind Navlakhe, MS; Amrita Prayag, MS; Gagandeep Singh, MD; Poorvesh Dhakecha, MD; and ***Arunaloke Chakrabarti, MD.***

Valliappan Muthu, Ritesh Agarwal,[1] Shivaprakash Mandya Rudramurthy, Deepak Thangaraju, Manoj Radhakishan Shevkani, Atul K. Patel, Prakash Srinivas Shastri, Ashwini Tayade, Sudhir Bhandari, Vishwanath Gella, Jayanthi Savio, Surabhi Madan, Vinay Kumar Hallur, Venkata Nagarjuna Maturu, Arjun Srinivasan, Nandini Sethuraman, Raminder Pal Singh Sibia, Sanjay Pujari, Ravindra Mehta, Tanu Singhal, Puneet Saxena, Varsha Gupta, Vasant Nagvekar, Parikshit Prayag, Dharmesh Patel, Immaculata Xess, Pratik Savaj, Naresh Panda, Gayathri Devi Rajagopal, Riya Sandeep Parwani, Kamlesh Patel, Anuradha Deshmukh, Aruna Vyas, Srinivas Kishore Sistla, Priyadarshini A Padaki, Dharshni Ramar, Saurav Sarkar, Bharani Rachagulla, Pattabhiraman Vallandaramam, Krishna Prabha Premachandran, Sunil Pawar, Piyush Gugale, Pradeep Hosamani, Sunil Narayan Dutt, Satish Nair, Hariprasad Kalpakkam, Sanjiv Badhwar, Kiran Kumar Kompella, Nidhi Singla, Milind Navlakhe, Amrita Prayag, Gagandeep Singh, Poorvesh Dhakecha, Arunaloke Chakrabarti[1]

We performed a case–control study across 25 hospitals in India for the period of January–June 2021 to evaluate the reasons for an COVID-19–associated mucormycosis (CAM) outbreak. We investigated whether COVID-19 treatment practices (glucocorticoids, zinc, tocilizumab, and others) were associated with CAM. We included 1,733 cases of CAM and 3,911 age-matched COVID-19 controls. We found cumulative glucocorticoid dose (odds ratio [OR] 1.006, 95% CI 1.004–1.007) and zinc supplementation (OR 2.76, 95% CI 2.24–3.40), along with elevated C-reactive protein (OR 1.004, 95% CI 1.002–1.006), host factors (renal transplantation [OR 7.58, 95% CI 3.31–17.40], diabetes mellitus [OR 6.72, 95% CI 5.45–8.28], diabetic ketoacidosis during COVID-19 [OR 4.41, 95% CI 2.03–9.60]), and rural residence (OR 2.88, 95% CI 2.12–3.79), significantly associated with CAM. Mortality rate at 12 weeks was 32.2% (473/1,471). We emphasize the judicious use of COVID-19 therapies and optimal glycemic control to prevent CAM.

Mucormycosis is an invasive fungal infection associated with high death rates. Poorly controlled diabetes mellitus, organ transplantation, hematological malignancies, and immunosuppression are the known predisposing factors for mucormycosis (*1*). During the second wave of the COVID-19 pandemic (April–June 2021), a large number of cases of COVID-19–associated mucormycosis (CAM) were reported globally, primarily in India (*2*–*5*). The explanation for this outbreak of CAM in India remains unclear. Diabetes mellitus and glucocorticoids (used for treating COVID-19) have been identified as risk factors for CAM (*2*,*6*). Other factors proposed in the pathogenesis of CAM include altered iron metabolism, the severity of COVID-19, and immune dysfunction resulting from COVID-19 (e.g., lymphopenia and others) (*7*,*8*).

A high burden of Mucorales (in the hospital and outdoor environments) has been reported in India

Author affiliations: Postgraduate Institute of Medical Education and Research, Chandigarh, India (V. Muthu, R. Agarwal, S.M. Rudramurthy, N. Panda, A. Chakrabarti); Kovai Medical Center and Hospital, Coimbatore, India (D. Thangaraju, G.D. Rajagopal); Avron Hospitals, Ahmedabad, India (M.R. Shevkani, R.S. Parwani); Sterling Hospital, Ahmedabad (A.K. Patel, K. Patel); Sir Gangaram Hospital, New Delhi, India (P.S. Shastri); Kingsway Hospital, Nagpur, India (A. Tayade, A. Deshmukh); Sawai Man Singh Medical College, Jaipur, India (S. Bhandari, A. Vyas); Asian Institute of Gastroenterology, Hyderabad, India (V. Gella, S.K. Sistla); St. John's Medical College and Hospital, Bengaluru, India (J. Savio, P.A. Padaki); Care Institute of Medical Sciences, Ahmedabad (S. Madan, D. Ramar); All India Institute of Medical Science Bhubaneswar, Odisha, India (V.K. Hallur, S. Sarkar); Yashoda Hospitals, Hyderabad (V.N. Maturu, B. Rachagulla); Royal Care Hospital, Coimbatore (A. Srinivasan, P. Vallandaramam); Apollo Hospitals, Chennai, India (N. Sethuraman, K.P. Premachandran); Government Medical College, Patiala, India (R.P.S. Sibia, S. Pawar); Poona Hospital and Research Centre, Pune, India (S. Pujari, P. Gugale); Apollo Hospitals, Bengaluru (R. Mehta, H. Kalpakkam, P. Hosamani, S.N. Dutt, S. Nair); Kokilaben Dhirubhai Ambani Hospital and Medical Research Institute, Mumbai, India (T. Singhal, S. Badhwar); Army Hospital (Research and Referral), New Delhi (P. Saxena, K.K. Kompella); Government Medical College, Chandigarh (V. Gupta, N. Singla); Global Hospital, Mumbai (V. Nagvekar, M. Navlakhe); Deenanath Mangeshkar Hospital, Pune (P. Prayag, A. Prayag); City Clinic and Bhailal Amin General Hospital, Vadodara, India (D. Patel); All India Institute of Medical Sciences, New Delhi (I. Xess, G. Singh); Institute of Infectious Disease and Critical Care Hospital, Surat, India (P. Savaj, P. Dhakecha)

DOI: https://doi.org/10.3201/eid2901.220926

[1]These senior authors contributed equally to this article..

during and even before the CAM epidemic (*9*,*10*). We also found no difference in the Mucorales species causing mucormycosis before and during the COVID-19 pandemic (*2*,*11*). The epidemiologic triad of agent, environmental, and host factors is helpful to explain the occurrence of a new illness or the recrudescence of an old disease (*6*,*8*,*9*). Because the data indicate no change in the environment or the agent (Mucorales), we hypothesized that COVID-19, its treatment, and specific host factors contributed to the CAM outbreak.

We evaluated the risk factors and clinical outcomes of CAM in a nationwide study. The main objective of our study was to assess whether treatment practices in COVID-19 were associated with the occurrence of CAM. We also evaluate the factors associated with death from CAM at 12 weeks.

Methods

Study Design and Setting

We performed a multicenter (25 centers across India) case–control study during January 1–June 30, 2021 (Appendix Figure, https://wwwnc.cdc.gov/EID/article/29/1/22-0926-App1.pdf). We included CAM patients (cases) and at least 2 COVID-19 patients without mucormycosis (controls) for each case. Only those centers willing to provide data on ≥15 cases of mucormycosis during the outbreak were included (Appendix Table 1).

The Institute Ethics Committees approved the study protocol at the individual study sites. A consent waiver was granted because we used anonymized patient data for analysis. The study is reported according to the Strengthening the Reporting of Observational Studies in Epidemiology (STROBE) guidelines (Appendix) (*12*).

Cases and Controls

We confirmed COVID-19 diagnosis by SARS-CoV-2 RNA positivity in respiratory specimens by reverse transcription PCR or a positive rapid antigen test. We included only confirmed (proven and probable) cases of mucormycosis diagnosed and managed at the individual centers (*13*). Participating centers were tertiary care referral hospitals or research institutes equipped with the facilities required to evaluate and manage mucormycosis. We evaluated patient samples at the study sites by conventional microscopy (KOH-calcofluor method), culture, histopathology, or molecular diagnostic techniques, as appropriate. We identified positive cultures on the basis of macroscopic and microscopic characteristics of the growth or by sequencing of the internal transcribed spacer region of rDNA. We subjected tissue samples for histopathological examination and used hematoxylin and eosin, periodic acid Schiff, or Gomori's methenamine silver stain. We diagnosed invasive mucormycosis on the basis of existing guidelines and as previously described (*11*,*13*). In brief, we categorized participants' illness as proven mucormycosis if Mucorales were isolated or broad ribbon-like aseptate hyphae were demonstrated from sterile sites or deep tissue biopsy. We defined probable mucormycosis in the presence of host risk factors, consistent imaging (e.g., reversed halo sign, thick-walled cavity, and others on computed tomography), and the demonstration of Mucorales by either microscopy or culture from a nonsterile site (sputum, nasal smear, or bronchoalveolar lavage fluid) (*13*,*14*). We defined disseminated mucormycosis as >1 noncontiguous site being involved. We excluded cases without microbiological or pathological confirmation of mucormycosis. We considered isolation of Mucorales from respiratory secretions without compatible host factors, clinical features, or radiology as colonization, and these cases were not included. We further classified CAM as concurrent (occurrence of mucormycosis within 7 days before or after diagnosing COVID-19) or nonconcurrent (after 7 days but within 3 months of COVID-19 diagnosis).

We enrolled ≥2 age-matched (±5 years) persons with confirmed COVID-19 as controls for each CAM case. The controls were selected randomly by the individual centers. We also reviewed patient records or contacted control-patients by telephone 3 months after COVID-19 diagnosis to ensure CAM had not developed.

Patients were managed per the local institutional protocol and the treating physician's discretion. Mucormycosis was treated according to the standard recommendations, subject to the availability of drugs and other factors (*1*,*15*). We recorded the first antifungal medication (amphotericin B, posaconazole, isavuconazole, or a combination) used for managing mucormycosis and whether lack of availability of the intended drug led to the use of an alternate agent. We defined the use of ≥2 antifungal agents effective against Mucorales within the first 14 days of CAM as primary combination antifungal therapy. We also noted whether ≥1 doses were missed because of drug unavailability.

Exposures and Confounding Variables

The primary exposure variable was the type of treatment offered for COVID-19. The therapies consisted of glucocorticoids, remdesivir, tocilizumab, baricitinib zinc supplements, antibacterial agents, and antifungal

therapy (before onset of mucormycosis). We defined inappropriate glucocorticoid therapy as use of systemic glucocorticoids for COVID-19 without related hypoxemia. We recorded information on the dose and duration of glucocorticoids used for COVID-19 and calculated the cumulative dose of glucocorticoids by multiplying the number of days of therapy and the dose used (dexamethasone equivalent).

We accounted for potential confounding variables pertaining to CAM by retrieving demographic and clinical information about COVID-19 illness from patient records. That information was sex; place of residence (rural or urban); investigations performed during admission (the first available values) for acute COVID-19 illness, including glycated hemoglobin (HbA1C), plasma glucose, complete blood count, serum ferritin, C-reactive protein, and neutrophil-to-lymphocyte ratio; host factors, including diabetes mellitus (labeled as recent-onset if diagnosed during the current admission and there was no previous history of diabetes), diabetic ketoacidosis during admission for COVID-19, hematological malignancy, stem cell or organ transplantation, and immunosuppressive therapy (for indications unrelated to COVID-19); chronic comorbidities (chronic liver, kidney, lung, and other diseases); hypoxemia during acute COVID-19 (<94% oxygen saturation while breathing ambient air or requiring supplemental oxygen); and the need for mechanical ventilation.

We also evaluated factors associated with 12-week mortality in CAM patients. We collected the following data: time to diagnosis of mucormycosis after confirmed COVID-19, diagnosis of mucormycosis (microscopy, culture, histopathology), anatomic site of involvement (rhino-orbital mucormycosis, pulmonary, or others), treatment details (antifungal therapy, surgery, and others), and outcome at 6 and 12 weeks.

Study Size

We assumed the primary exposure of interest (treatment practices, primarily glucocorticoids) would be present in 60% of controls and 70% of cases. The estimated sample size was 374 cases and 747 controls for a case: control enrollment ratio of 1:2, at a power of 90% for detecting 1.25 odds (in cases than controls). We planned a convenient sample size by enrolling ≥15 consecutive CAM cases from each participating center.

Statistical Analysis

We analyzed data by using the commercial statistical package SPSS Statistics 22.0 (IBM, https://www.ibm.com). As appropriate, descriptive data are presented as frequencies, means and SDs, or medians and interquartile ranges. We compared categorical variables by using the χ^2 test or Fisher exact test and analyzed the differences between continuous data by using the Student *t*-test or Mann-Whitney U test, as appropriate. We considered a p value <0.05 significant.

We imputed the missing data for performing the subsequent logistic regression analysis. The pattern of missing data (missing at random or not) was ascertained. We then performed multiple imputations (50 iterations) by using the Markov Chain Monte Carlo method (Appendix Table 2). We performed multivariate logistic regression analyses to identify the factors associated with the development of CAM (vs. COVID-19 controls) and ascertain factors associated with 12-week mortality in persons with CAM. The variables included in the logistic regression model were decided on the basis of the univariate analysis and biologic plausibility. The strength of association was reported as an adjusted odds ratio (aOR) with 95% CI. To elucidate the confounding resulting from the difference in severity among the controls and cases, we repeated the multivariate analysis in the following subgroups: nonhypoxemic versus hypoxemic COVID-19 control-patients and COVID-19 control-patients with and without comorbidities. We also report the sensitivity analysis on the available data (complete case analysis) for the logistic regression.

Results

We included 1,733 CAM case-patients and 3,911 control-patients in the study (Table 1). Of the study participants, 684 did not require hospitalization for the management of acute COVID-19.

Exposure

Glucocorticoids were used for COVID-19 in 71.6% (3,890/5,431) patients (cumulative dose range 0.76–679.53 mg dexamethasone equivalent), and their use was more frequent in CAM case-patients. The median dose and duration of glucocorticoid use was also higher in case-patients than control-patients (Table 1). The proportion of persons receiving glucocorticoids in the absence of hypoxemia (inappropriate use) was even higher in CAM patients (34.2% vs. 22.3%; p = 0.0001) than control-patients. In addition, the percentage of persons receiving more than the recommended dose (>60 mg of dexamethasone or equivalent) of glucocorticoids was higher among CAM case-patients than COVID-19 control-patients (Figure), both for hypoxemic (269/439 [61.3%] vs. 683/1389 [49.2%]; p = 0.0001) and nonhypoxemic (124/329 [37.7%] vs. 143/633 [22.6%]; p = 0.0001) persons. Zinc

supplementation during COVID-19 illness was higher among case-patients than controls (47.9% vs. 41.3%; p = 0.0001). Remdesivir (49.2% vs. 20.6%; p = 0.0001) and antibacterial therapy (64.2% vs. 61.1%; p = 0.03) were more commonly used in controls. No difference was noted in the proportion of participants receiving tocilizumab, baricitinib, or antifungal therapy before the development of CAM.

Table 1. Baseline features of CAM case-patients and COVID-19 control-patients at admission for COVID-19, India, January–June 2021*

Category	Controls, n = 3,911	CAM, n = 1,733	p value
Age, y, mean (SD)	52.7 (13.5)	52.6 (12.5)	0.66
Male sex	2,738/3,911 (70.0)	1,285/1,733 (74.1)	0.002
Rural residence, n = 3,924	309/2,615 (11.8)	360/1,309 (27.5)	0.0001
Risk factors for mucormycosis			0.0001
None	2,076/3,911 (53.1)	316/1,733 (18.2)	
1 risk factor	1,743/3,911 (44.5)	1,374/1,733 (79.3)	
>1 risk factors	92/3,911 (2.4)	43/1,733 (2.5)	
Details of potential risk factors for mucormycosis†			
Diabetes mellitus	1,763/3,911 (45.1)	1,402/1,733 (80.9)	0.0001
Hyperglycemia at admission, n = 5,236	998/3,625 (27.5)	758/1,611 (47.1)	0.0001
Plasma glucose at admission, mg/dL, mean (SD), n = 3,487	195 (94)	235 (106)	0.0001
Glycated hemoglobin, mean (SD), n = 1,856	7.7 (2.5)	10.1 (2.9)	0.0001
Duration of diabetes, y, mean (SD), n = 861	9.6 (9.5)	8.4 (6.8)	0.04
Recent onset of diabetes mellitus	319/1,763 (18.1)	246/1,402 (17.5)	0.66
DKA at the time of admission for COVID-19	48/1,763 (2.7)	73/1,402 (5.2)	0.0003
Renal transplant	36/3,911 (0.9)	31/1,733 (1.8)	0.005
Bone marrow transplant	0/3,911 (0)	1/1,733 (0.1)	0.31
Hematological malignancy	36/3,911 (0.9)	6/1,733 (0.3)	0.02
Immunosuppressive therapy	76/3,911 (1.9)	22/1,733 (1.3)	0.07
HIV	7/3,911 (0.2)	6/1,733 (0.3)	0.23
Others‡	2/3,911 (0.0)	2/1,733 (0.1)	0.23
Comorbidities			
Any comorbidity	828/3,911 (21.5)	265/1,733 (15.3)	0.0001
Coronary artery disease	285/3,911 (7.3)	126/1,733 (7.3)	0.98
Chronic kidney disease	284/3,911 (7.3)	98/1,733 (5.7)	0.03
Chronic heart failure	59/3,911 (1.5)	17/1,733 (1.0)	0.11
Chronic liver disease	71/3,911 (1.8)	13/1,733 (0.8)	0.002
Chronic respiratory disease	104/3,911 (2.7)	17/1,733 (1.0)	0.0001
Others§	151/3,911 (3.9)	35/1,733 (2.0)	0.0001
Laboratory parameters during COVID-19 illness			
Hemoglobin, g/dL, mean (SD), n = 4,506	12.2 (2.4)	12.1 (2.2)	0.11
Total leukocyte count, cells/μL, mean (SD), n = 4,501	9,853 (6,844)	11,396 (6,110)	0.0001
Median absolute lymphocyte count, cells/μL (IQR), n = 4,129	1,135 (720–1,706)	1,275 (803–1,833)	0.0001
Median absolute neutrophil count, cells/μL (IQR), n = 4,071	6,177 (3,658–10,244)	7,858 (4,943–11,867)	0.0001
Median NLR (IQR), n = 4,061	5.5 (2.7–11.4)	5.7 (3.2–11.7)	0.04
Platelet count, $\times 10^3$/μL, mean (SD), n = 4,454	222 (107)	240 (105)	0.0001
Median C-reactive protein mg/dL (IQR), n = 3,972	26.7 (8.4–79.3)	48.8 (20–102.5)	0.0001
Median serum ferritin, μg/L (IQR) n = 3,168	454 (189–977)	580 (238–1,052)	0.02
Details of COVID-19 illness			
Hypoxemia, n = 5,476	2,100/3,851 (54.5)	751/1,625 (46.2)	0.0001
ICU admission, n = 5,425	1,551/3,809 (40.7)	331/1,616 (20.5)	0.0001
Mechanical ventilation, n = 5,376	1,126/3,765 (29.9)	153/1,611 (9.5)	0.0001
Management during COVID-19			
Glucocorticoid therapy, n = 5,431	2,690/3,827 (70.3)	1,200/1,604 (74.8)	0.001
Glucocorticoid use in the absence of hypoxemia, n = 5,021	789/3,532 (22.3)	509/1,489 (34.2)	0.0001
Median cumulative dose of glucocorticoids in milligram equivalent of dexamethasone (IQR), n = 2,809	52.8 (30–84)	62.6 (30.2–120)	0.0001
Median no. days on glucocorticoid treatment (IQR), n = 2,887	8 (5–12)	10 (6.3–14)	0.0001
Zinc supplementation, n = 5,179	1,502/3,633 (41.3)	741/1,546 (47.9)	0.0001
Remdesivir, n = 5,167	1,785/3,631 (49.2)	317/1,536 (20.6)	0.0001
Tocilizumab, n = 5,167	72/3,631 (2.0)	37/1,536 (2.4)	0.41
Baricitinib, n = 5,167	38/3,631 (1.0)	13/1,536 (0.8)	0.50
Antibacterial therapy, n = 5,396	2,467/3,841 (64.2)	952/1,555 (61.2)	0.04
Antifungal therapy before CAM, n = 5,039	174/3,513 (5.0)	68/1,526 (4.5)	0.45

*Values are no. observed/total no. (%) unless otherwise indicated. CAM, COVID-19–associated mucormycosis; DKA, diabetic ketoacidosis; DM, diabetes mellitus; ICU, intensive care unit; IQR, interquartile range; NLR, neutrophil-to-lymphocyte ratio.
†A single person might have had >1 risk factor; hence the numbers do not sum to 5,644.
‡Others include neutropenia (n = 3) and primary immunodeficiency (n = 1).
§Others include neurologic, endocrinologic, and rheumatologic illnesses.

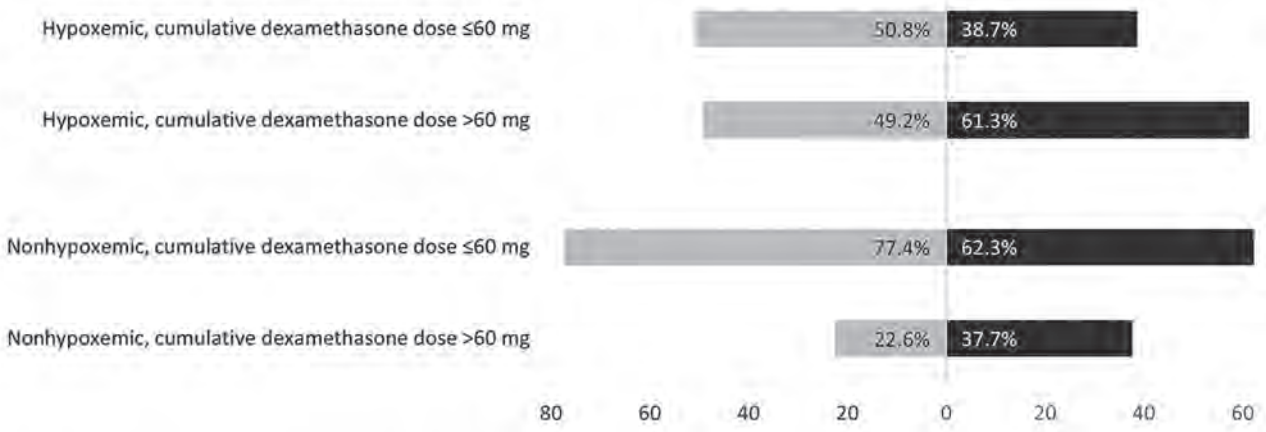

Figure. Percentages of hypoxemic and nonhypoxemic participants receiving cumulative glucocorticoid doses above and below the current recommendations (cumulative dexamethasone dose equivalent to 60 mg) as determined in multicenter case-control study of COVID-19–associated mucormycosis outbreak, India, January–June 2021. Case-patients are shown in black and control-patients are shown in gray. More case-patients than control-patients had received higher-than-recommended doses of glucocorticoids.

Confounders

Chronic comorbidities (chronic liver, kidney, lung, and other diseases) were present in 37% of study participants and were seen more often in controls than in CAM patients. Significantly higher plasma glucose, neutrophil-to-lymphocyte ratio, platelet count, C-reactive protein, and serum ferritin were seen in CAM patients during their hospitalizations for COVID-19. We identified ≥1 host factors for mucormycosis in 46.9% of controls versus 81.8% of case-patients (p = 0.0001). The proportion of diabetes mellitus was significantly higher in case-patients (80.9% vs. 45.1%; p = 0.0001) than in controls. Recent-onset diabetes mellitus was similar in both the study groups, whereas diabetic ketoacidosis was significantly more common among CAM than in the controls (5.2% vs. 2.7%; p = 0.0003). We found hypoxemia during acute COVID-19 (54.5% vs. 46.2%), admission to an intensive care unit (40.7% vs. 20.5%), and mechanical ventilation (29.9% vs. 9.5%) significantly higher among control-patients.

Association of COVID-19 Treatment Practices with CAM

We found the cumulative dose of glucocorticoid used (OR 1.006, 95% CI 1.004–1.007) and zinc supplementation (OR 2.76, 95% CI 2.24–3.40) independently associated with CAM, in addition to elevated C-reactive protein, host factors (renal transplantation, diabetes mellitus, diabetic ketoacidosis during COVID-19), and rural residence (Table 2). Hypoxemia during COVID-19 and comorbidities were associated with lower odds of CAM. The results were similar on a complete case analysis (Appendix Table 3). Because the proportion of persons with hypoxemia and comorbidities was higher in COVID-19 controls than in CAM patients, we also performed a subgroup analysis (hypoxemic vs. nonhypoxemic controls and any

Table 2. Multivariate logistic regression analysis showing factors associated with CAM, India, January–June 2021*

Parameter	Adjusted OR (95% CI)	p value
Female sex	0.92 (0.74–1.14)	0.46
Rural residence	2.88 (2.12–3.79)	0.0001
Risk factor		
No risk factor	Referent	
Diabetes mellitus	6.72 (5.45–8.28)	0.0001
Renal transplantation	7.58 (3.31–17.40)	0.0001
Others†	1.20 (0.67–2.18)	0.54
Presence of any comorbidity	0.50 (0.39–0.63)	0.0001
Hypoxia during COVID-19	0.26 (0.21–0.32)	0.0001
Diabetic ketoacidosis during COVID-19	4.41 (2.03–9.60)	0.0001
Cumulative glucocorticoid dose for COVID-19‡	1.006 (1.004–1.007)	0.0001
Zinc supplementation during COVID-19	2.76 (2.24–3.40)	0.0001
C-reactive protein at admission	1.004 (1.002–1.006)	0.0001
Serum ferritin, μg/L	1.00 (1.00–1.00)	0.21
Neutrophil-to-lymphocyte ratio	1.0 (0.99–1.01)	0.92

*CAM, COVID-19–associated mucormycosis.
†Includes malignancies, hematological malignancies, immunosuppressive therapy, HIV, and others.
‡In milligram equivalent of dexamethasone.

comorbidity vs. no comorbidity; Appendix Tables 4, 5). We found the primary exposure of interest (COVID-19 treatment factors) significantly associated with CAM in both the subgroups (Appendix Tables 4, 5).

We also assessed the association of inappropriate glucocorticoid therapy (i.e., glucocorticoids administered in the absence of hypoxemia) with CAM. In an alternative logistic regression model, we replaced glucocorticoid doses with inappropriate glucocorticoid therapy (Appendix Table 6) and found inappropriate therapy also significantly associated with CAM.

Additional Analyses of Clinical Features, Diagnosis, Treatment, and Outcome of CAM

CAM occurred nonconcurrently (>7 days after COVID-19 diagnosis) in 1,405 (81.7%) of 1,720 persons; the remaining 315 (18.3%) cases were concurrent with the COVID-19 illness (within 7 days of diagnosis). The duration between COVID-19 and the diagnosis of CAM was shorter for those hospitalized for COVID-19 (mean 20, 95% CI 19–21 days) versus those isolated at home (mean 25, 95% CI 24–27 days). The median duration between symptoms of CAM and confirmation of the diagnosis was 6 (interquartile range 3–10) days (n = 1,024 persons). Rhino-orbital mucormycosis accounted for 92.4% of the cases, followed by pulmonary (7%) and other sites (0.6%). The proportion of pulmonary mucormycosis was higher in persons who had undergone organ transplants (17.2%) and persons with hematological malignancies (33.3%) than in those with diabetes mellitus (6.4%). Of the 1,602 patients with rhino-orbital mucormycosis, we noted intracranial extension in 261 (16.3%) cases. Nearly two thirds (1,143/1,733; 66.0%) of the CAM patients had evidence of mucormycosis from >1 sample (smear, culture, or histopathology) (Table 3). The most common etiologic agent causing mucormycosis was *Rhizopus* spp. (mainly *R. arrhizus*). The other reported organisms included *Mucor* and *Rhizomucor* spp.,

Table 3. Diagnosis, treatment practices, and survival in patients with CAM, India, January–June 2021*

Parameter	No. observed/total no. (%)
Site of mucormycosis†	
Rhino-orbito-cerebral	
Sinus	1,526/1,733 (88.1)
Orbit	789/1,733 (45.5)
Palate	373/1,733 (21.5)
Jaw	315/1,733 (18.2)
Brain	261/1,733 (15.1)
Blackening of skin over face	102/1,733 (5.9)
Cavernous sinus	44/1,733 (2.5)
Skull base	65/1,733 (3.8)
Pulmonary†	122/1,733 (7.0)
Cutaneous or soft tissue	5/1,733 (0.3)
Gastrointestinal	2/1,733 (0.1)
Renal†	2/1,733 (0.1)
Diagnosis of mucormycosis	
Microscopy alone	352/1,733 (20.3)
Culture growth of Mucorales alone	61/1,733 (3.5)
Histopathology alone	177/1,733 (10.2)
≥1 evidence (smear, culture, or histopathology) of mucormycosis	1,143/1,733 (66.0)
Treatment practices	
Intended therapy could not be administered	321/1,526 (21.0)
Missed doses due to drug non-availability	248/1,457 (17.0)
Primary therapy	
Any formulation of amphotericin B‡	1,634/1,733 (94.3)
Primary combination therapy§	
Any combination	699/1,733 (41.6)
Amphotericin B and posaconazole	541/699 (77.4)
Amphotericin B and isavuconazole	121/699 (17.3)
Amphotericin B and isavuconazole or posaconazole	37/699 (5.3)
Surgery	
Combined medical and surgical treatment	1,449/1,773 (83.6)
Survival	
Death by 6 weeks	442/1,546 (28.6)
Death by 12 weeks	473/1,471 (32.2)

*CAM, COVID-19–associated mucormycosis
†Total number does not sum to 1,733 since patients might have had involvement at >1 site. There were 18 cases of disseminated mucormycosis (17 had pulmonary in addition to rhino-orbital, while 1 person had rhino-orbito-cerebral and renal mucormycosis).
‡Of the 1,634 persons receiving amphotericin B, liposomal amphotericin B alone was used in 1,210 (74.1%) patients, amphotericin B deoxycholate in 143 (8.7%) patients, amphotericin B lipid emulsion in 21 (1.3%) patients, >1 formulation in 236 (14.4%) patients, and the information was not clear in 24 (1.5%) patients.
§Primary therapy with a combination of amphotericin and isavuconazole or posaconazole within the first 14 days was used in 699/1,733 (41.6%) patients.

Table 4. Factors associated with death at 12 weeks in persons with CAM, India, January–June 2021*

Parameter	Adjusted odds ratio (95% CI)	p value
Age	1.02 (1.01–1.04)	0.0001
Sex	1.00 (0.74–1.34)	0.99
Risk factor		
No risk factor	Referent	
Diabetes mellitus	1.27 (0.93–1.74)	0.13
Renal transplantation	2.66 (1.04–6.81)	0.04
Others†	1.51 (0.55–4.18)	0.42
Presence of any comorbidity	1.38 (0.97–1.97)	0.08
Hypoxemia during COVID-19 illness	1.31 (0.93–1.83)	0.12
Site of mucormycosis		
Rhino-orbital mucormycosis	Referent	
Rhino-orbital mucormycosis with brain involvement	2.30 (1.66–3.19)	0.0001
Other sites‡	1.44 (0.90–2.32)	0.13
Primary combination medical therapy	0.53 (0.37–0.77)	0.001
Combined medical and surgical treatment	0.20 (0.14–0.27)	0.0001

*CAM, COVID-19–associated mucormycosis.
†Includes hematological malignancies, immunosuppressive therapy, and HIV infection.
‡Includes pulmonary, gastrointestinal, disseminated, and renal mucormycosis.

and rarely *Cunninghamella*, *Syncephalastrum*, *Apophysomyces*, *Lichtheimia* spp., and others.

The treatment of CAM varied widely and was influenced by antifungal drug availability. The intended antifungal agent could not be administered in 21.0% (321/1,526) of cases, and ≥1 dose was missed because the antifungal drugs were unavailable in 17% (248/1,547) of CAM cases. Amphotericin B was the most prescribed antifungal agent. A combination of antifungal agents was used for primary therapy in 41.6% of patients. Surgery was performed in most case-patients (1,449/1,733; 83.6%). The mortality rate at 6 weeks (data available for 89.2% of cases) was 28.6% and at 12 weeks (data available for 84.9% cases) was 32.2%.

We found surgical resection and primary antifungal combination therapy independently associated with better odds of survival at 12 weeks (Table 4). We also found increasing age and intracranial extension associated with worse odds of survival after adjusting for sex, comorbidities, and COVID-19–related hypoxemia. The results were similar on a complete case analysis (Appendix Table 7).

Discussion

In this large case-control study, we found that glucocorticoid use and zinc supplementation in the treatment of COVID-19 were significantly associated with CAM. In addition, several host factors for mucormycosis (i.e., renal transplantation, diabetes mellitus, and diabetic ketoacidosis), elevated C-reactive protein, and rural residence were also associated with CAM. The unprecedented rise in the number of CAM cases during the second wave of the COVID-19 pandemic indicates that COVID-19 or its treatment had a role in causing CAM (*2*,*16*).

We provide strong evidence to incriminate glucocorticoid therapy in CAM even after adjusting for host factors. Our results strengthen the current recommendation of avoiding glucocorticoid use in COVID-19 patients not experiencing hypoxemia (*17*,*18*). More critically, we found that the cumulative glucocorticoid dose is also a contributory factor for CAM. Thus, even in hypoxemic COVID-19 patients, glucocorticoids should be used judiciously (dexamethasone at a dose of 6 mg 1×/d for up to 10 days or until hospital discharge, whichever is earlier) (*19*). We also found zinc supplementation an independent factor associated with CAM. A small study suggested a protective role of zinc in CAM (*6*), but 2 other studies found an association between zinc and CAM (*20*,*21*). The biologic plausibility (*22*) and in vitro evidence of abundant growth of Mucorales strains (isolated from CAM patients) demonstrated on zinc-supplemented media supports the possible role of zinc in causing CAM (*20*). Although we found a few factors related to the severity and treatment of COVID-19 in the development of CAM, we did not evaluate the role of COVID-19–related immune dysfunction in this study. Nonetheless, we provide weak indirect evidence implicating the severity of COVID-19 illness (elevated C-reactive protein) in the development of CAM. Finally, rural residence was significantly associated with CAM and might be attributed to higher levels of fungal spores in the rural environment (*23*–*26*).

The time to develop CAM was significantly shorter in hospitalized persons than in persons isolated at home. This finding could suggest hospital-acquired mucormycosis; however, the hospitalization could simply mean that severe COVID-19 led to mucormycosis early in the course of illness or, more likely, that CAM was diagnosed earlier simply because these persons were hospitalized. Based on a few media reports, 1 review hypothesized that the burning of cow dung led to the mucormycosis outbreak in India (*27*).

However, a recent experimental aeromycological study found no evidence for this theory (*25*).

Several case-control studies (n = 13) have assessed the risk factors associated with CAM (Appendix Table 8) (*6*,*7*,*20*,*21*,*28*–*36*). In 8 studies (sample sizes ranging from 46 to 870), risk factors for CAM were assessed using multivariate analysis (*6*,*7*,*29*–*33*,*35*). Diabetes mellitus and glucocorticoid therapy were shown to be the major contributors for CAM in the case–control studies and large case series (*2*,*3*,*6*,*21*,*35*,*37*). Further, in addition to zinc and elevated inflammatory markers (C-reactive protein), which were also associated with CAM in this study, the use of cloth masks, nasal washing during COVID-19, and elevated serum glucose-regulated protein 78 were other possible associations described in smaller case–control studies (*29*,*30*,*33*). In our study, mean glycated hemoglobin values were significantly higher in the CAM cases. In another study, optimal glycemic control and adherence to low-dose glucocorticoid protocol eliminated the occurrence of mucormycosis in a COVID-19 intensive care unit even during the surge in CAM cases (*38*). Unfortunately, because of the overwhelming case burden, many COVID-19 patients were taking various prescription or over-the-counter medications (including glucocorticoids and zinc) unmonitored, which probably contributed to the outbreak.

We found lower rates of mortality in mucormycosis patients than in previous reports (*11*,*39*,*40*). The lower mortality rate in our study might be attributed to several factors. First, more severe forms of the disease, including pulmonary and disseminated mucormycosis, could have been underrepresented (*41*,*42*). For instance, pulmonary mucormycosis accounted for only 7% of the cases in this study (vs. 13% in a pre-COVID-19 large multicenter study from India) (*11*). Second, the increased awareness about mucormycosis because of the outbreak led to timely diagnosis (median time to diagnosis 6 days) and surgical intervention in a higher percentage of cases (84%) than in the pre–COVID-19 era (62%) (*11*). Also, the predisposing factors in CAM cases, such as glucocorticoid therapy and hyperglycemia, were mostly reversible. The use of primary combination antifungal therapy might have contributed to improved outcomes. A previous multicenter observational study on CAM also indicated that combining amphotericin B with posaconazole might be associated with better outcomes than monotherapy (*2*). However, attributing the benefit of combination treatment to survival without a randomized clinical trial is difficult. Our results also confirm the existing knowledge that surgical treatment is associated with better outcomes in mucormycosis (*1*,*11*).

The first limitation of our study is that data were collected during the peak of the pandemic with limited resources, and some information was missing as a result. Although our study supports the definite association of glucocorticoids with CAM, the same might not be accurate for zinc. Zinc might be synergistic to glucocorticoids or other factors in the development of CAM. However, it was an independent risk factor across different subgroups and in different multivariate models. Although we could obtain information on zinc supplementation during the treatment of COVID-19, the wide variation in prescription practice, over-the-counter availability of drugs, and use of different formulations and dosages precluded establishing a dose-response relationship between zinc and CAM. Thus, prospective studies and animal experiments are warranted to establish the association of zinc with CAM. Even though we enrolled a large number of control-patients, the control-patients were sicker than case-patients. This difference in severity of COVID-19 symptoms influenced a few of our results. For instance, the presence of any comorbidity and the need for mechanical ventilation were associated with a lower risk for CAM. One could argue that our association of the primary exposure variable with CAM is invalid because the control-patients critically ill with COVID-19 might not have survived long enough for CAM to develop. Imperfect matching for COVID-19 severity is thus a major limitation. To adjust for the severity of COVID-19, we performed a subgroup analysis in which we compared the CAM patients with either hypoxemic or nonhypoxemic COVID-19 control-patients. We found the COVID-19 treatment factors (primary exposure) remained significantly associated with CAM in both groups (Appendix Table 4). We restricted our data collection to information that could be accessed reliably despite the pandemic. Thus, we cannot exclude residual confounders. Not all the participating centers could provide the desired number of control subjects, and there was variation in mortality reported from different centers (Appendix Table 1). A referral bias to the participating study centers and underrecognition of certain forms of mucormycosis (pulmonary and others) could have influenced our observations. We could not assess the burden of CAM among COVID-19 case-patients. Also, we included cases diagnosed by conventional microbiological techniques, and we might have missed several presumed cases of mucormycosis. However, the objective of our study was to evaluate the risk factors in a case-control model, and hence we included confirmed cases only. Finally, the results might not be generalizable because the information is from just

1 country. The key strength of our study is the large sample size and representation from across the country, which lends credibility to our observations.

In conclusion, we found several treatment practices associated with CAM in addition to rural residence and host factors. Our results suggest the judicious use of COVID-19 therapies and optimal glycemic control to prevent CAM.

Other members of the MuCovi-2 network: Goverdhan Dutt Puri, Inderpaul Singh Sehgal, Ashish Bhalla, Ram Gopalakrishnan, Ritu Kumari, Prayag Mathukia, Ketan Patel, Mohnish Grover, Pradipta Parida, Aaron Charles Lobo, Ruchita Chhabra, Sahana Devakumar, Rajeshwari V, Mohammed Ismail, Ledo Thankachan, Adla Sandhya Rani, Garela Parimala Devi, Alok Thakar, Anjan Trikha, and Naveet Wig

Funding was provided by the World Health Organization.

A.K.P. received honoraria and lecture fees from Gilead Sciences, Pfizer (India), Intas Pharmaceuticals, Mylan (India), Bharat Serum Vaccine Ltd, and Cipla India Ltd. T.S. received lecture fees from Mylan (India), Cipla India Ltd, MSD, Intas Pharmaceuticals, Pfizer (India), Glenmark Pharmaceuticals.

A.C. and R.A. conceptualized the study. V.M., S.M.R., D.T., M.R.S., A.K.P., P.S.S., A.T., S.B., V.G., J.S., S.M., V.K.H., V.N.M., A.S., N.S., R.P.S.S., S.P., R.M., T.S., P.S., V.G., V.N., P.P., D.P., I.X., P.S., N.P., G.D.R., R.S.P., K.P., A.D., A.V., S.K.S., P.A.P., D.R., S.S., B.R., P.V., K.P.P., S.P., P.G., P.H., S.N.D., S.N., H.K., S.B., K.K.K., N.S., M.N., A.P., G.S., and P.D. curated data. V.M., R.A., and A.C. conducted the formal analysis. A.C. acquired funding. R.A., A.C., S.M.R., and V.M. implemented the study methodology. A.C., R.A., and S.M.R. oversaw the project administration and provided the required resources. A.C., R.A., S.M.R., A.K.P., and P.S. validated the data. V.M. and R.A. wrote the original draft. S.M.R., D.T., M.R.S., A.K.P., P.S.S., A.T., S.B., V.G., J.S., S.M., V.K.H., V.N.M., A.S., N.S., R.P.S.S., S.P., R.M., T.S., P.S., V.G., V.N., P.P., D.P., I.X., P.S., N.P., G.D.R., R.S.P., K.P., A.D., A.V., S.K.S., P.A.P., D.R., S.S., B.R., P.V., K.P.P., S.P., P.G., P.H., S.N.D., S.N., H.K., S.B., K.K.K., N.S., M.N., A.P., G.S., P.D., and A.C. reviewed and edited the article. The first and corresponding authors had full access to the data and vouch for the data integrity.

About the Author

Dr. Muthu is a pulmonologist at the Postgraduate Institute of Medical Education and Research, Chandigarh, India. His research interests include mucormycosis and allergic bronchopulmonary aspergillosis.

References

1. Cornely OA, Alastruey-Izquierdo A, Arenz D, Chen SCA, Dannaoui E, Hochhegger B, et al.; Mucormycosis ECMM MSG Global Guideline Writing Group. Global guideline for the diagnosis and management of mucormycosis: an initiative of the European Confederation of Medical Mycology in cooperation with the Mycoses Study Group Education and Research Consortium. Lancet Infect Dis. 2019;19:e405–21. https://doi.org/10.1016/S1473-3099(19)30312-3
2. Patel A, Agarwal R, Rudramurthy SM, Shevkani M, Xess I, Sharma R, et al.; MucoCovi Network3. Multicenter epidemiologic study of coronavirus disease-associated mucormycosis, India. Emerg Infect Dis. 2021;27:2349–59. https://doi.org/10.3201/eid2709.210934
3. Sen M, Honavar SG, Bansal R, Sengupta S, Rao R, Kim U, et al.; members of the Collaborative OPAI-IJO Study on Mucormycosis in COVID-19 (COSMIC) Study Group. Epidemiology, clinical profile, management, and outcome of COVID-19–associated rhino-orbital-cerebral mucormycosis in 2826 patients in India—collaborative OPAI-IJO study on mucormycosis in COVID-19 (COSMIC), report 1. Indian J Ophthalmol. 2021;69:1670–92. https://doi.org/10.4103/ijo.IJO_1565_21
4. Hoenigl M, Seidel D, Carvalho A, Rudramurthy SM, Arastehfar A, Gangneux JP, et al.; ECMM and ISHAM collaborators. The emergence of COVID-19 associated mucormycosis: a review of cases from 18 countries. Lancet Microbe. 2022;3:e543–52. https://doi.org/10.1016/S2666-5247(21)00237-8
5. Garg D, Muthu V, Sehgal IS, Ramachandran R, Kaur H, Bhalla A, et al. Coronavirus disease (COVID-19) associated mucormycosis (CAM): case report and systematic review of literature. Mycopathologia. 2021;186:289–98. https://doi.org/10.1007/s11046-021-00528-2
6. Arora U, Priyadarshi M, Katiyar V, Soneja M, Garg P, Gupta I, et al. Risk factors for coronavirus disease–associated mucormycosis. J Infect. 2022;84:383–90. https://doi.org/10.1016/j.jinf.2021.12.039
7. Kumar H M, Sharma P, Rudramurthy SM, Sehgal IS, Prasad KT, Pannu AK, et al. Serum iron indices in COVID-19-associated mucormycosis: a case-control study. Mycoses. 2022;65:120–7. https://doi.org/10.1111/myc.13391
8. Muthu V, Rudramurthy SM, Chakrabarti A, Agarwal R. Epidemiology and pathophysiology of COVID-19–associated mucormycosis: India versus the rest of the world. Mycopathologia. 2021;186:739–54. https://doi.org/10.1007/s11046-021-00584-8
9. Biswal M, Gupta P, Kanaujia R, Kaur K, Kaur H, Vyas A, et al. Evaluation of hospital environment for presence of Mucorales during COVID-19–associated mucormycosis outbreak in India—a multi-centre study. J Hosp Infect. 2022;122:173–9. https://doi.org/10.1016/j.jhin.2022.01.016
10. Prakash H, Singh S, Rudramurthy SM, Singh P, Mehta N, Shaw D, et al. An aero mycological analysis of Mucormycetes in indoor and outdoor environments of northern India. Med Mycol. 2020;58:118–23. https://doi.org/10.1093/mmy/myz031
11. Patel A, Kaur H, Xess I, Michael JS, Savio J, Rudramurthy S, et al. A multicentre observational study on the epidemiology, risk factors, management and outcomes of mucormycosis in India. Clin Microbiol Infect. 2020;26:944.e9–e15.
12. von Elm E, Altman DG, Egger M, Pocock SJ, Gøtzsche PC, Vandenbroucke JP; STROBE Initiative. Strengthening the Reporting of Observational Studies in Epidemiology (STROBE) statement: guidelines for reporting observational

studies. BMJ. 2007;335:806–8. https://doi.org/10.1136/bmj.39335.541782.AD
13. Donnelly JP, Chen SC, Kauffman CA, Steinbach WJ, Baddley JW, Verweij PE, et al.; Revision and Update of the Consensus Definitions of Invasive Fungal Disease From the European Organization for Research and Treatment of Cancer and the Mycoses Study Group Education and Research Consortium. Revision and update of the consensus definitions of invasive fungal disease from the European Organization for Research and Treatment of Cancer and the Mycoses Study Group Education and Research Consortium. Clin Infect Dis. 2020;71:1367–76. https://doi.org/10.1093/cid/ciz1008
14. Muthu V, Agarwal R, Patel A, Kathirvel S, Abraham OC, Aggarwal AN, et al. Definition, diagnosis, and management of COVID-19–associated pulmonary mucormycosis: Delphi consensus statement from the Fungal Infection Study Forum and Academy of Pulmonary Sciences, India. Lancet Infect Dis. 2022;22:e240–e253.
15. Rudramurthy SM, Hoenigl M, Meis JF, Cornely OA, Muthu V, Gangneux JP, et al.; ECMM and ISHAM. ECMM/ISHAM recommendations for clinical management of COVID-19–associated mucormycosis in low- and middle-income countries. Mycoses. 2021;64:1028–37. https://doi.org/10.1111/myc.13335
16. Seidel D, Simon M, Sprute R, Lubnow M, Evert K, Speer C, et al. Results from a national survey on COVID-19–associated mucormycosis in Germany: 13 patients from six tertiary hospitals. Mycoses. 2022;65:103–9. https://doi.org/10.1111/myc.13379
17. Muthu V, Sehgal IS, Dhooria S, Prasad KT, Aggarwal AN, Agarwal R. Corticosteroids for non-severe COVID-19: primum non nocere. Indian J Crit Care Med. 2022;26:403–4. https://doi.org/10.5005/jp-journals-10071-24138
18. Agarwal A, Rochwerg B, Lamontagne F, Siemieniuk RA, Agoritsas T, Askie L, et al. A living WHO guideline on drugs for COVID-19. BMJ. 2020;370:m3379. https://doi.org/10.1136/bmj.m3379
19. Horby P, Lim WS, Emberson JR, Mafham M, Bell JL, Linsell L, et al.; RECOVERY Collaborative Group. Dexamethasone in hospitalized patients with COVID-19. N Engl J Med. 2021;384:693–704. https://doi.org/10.1056/NEJMoa2021436
20. Muthu V, Kumar M, Paul RA, Zohmangaihi D, Choudhary H, Rudramurthy SM, et al. Is there an association between zinc and COVID-19–associated mucormycosis? Results of an experimental and clinical study. Mycoses. 2021;64:1291–7. https://doi.org/10.1111/myc.13365
21. Kumar S, Acharya S, Jain S, Shukla S, Talwar D, Shah D, et al. Role of zinc and clinicopathological factors for COVID-19–associated mucormycosis (CAM) in a rural hospital of central India: a case-control study. Cureus. 2022;14:e22528. https://doi.org/10.7759/cureus.22528
22. Foster JW, Waksman SA. The specific effect of zinc and other heavy metals on the growth and nutrition of Rhizopus. J Bacteriol. 1939;37:599–617. https://doi.org/10.1128/jb.37.6.599-617.1939
23. Adhikari A, Sen MM, Gupta-Bhattacharya S, Chanda S. Airborne viable, non-viable, and allergenic fungi in a rural agricultural area of India: a 2-year study at five outdoor sampling stations. Sci Total Environ. 2004;326:123–41. https://doi.org/10.1016/j.scitotenv.2003.12.007
24. Abrego N, Crosier B, Somervuo P, Ivanova N, Abrahamyan A, Abdi A, et al. Fungal communities decline with urbanization-more in air than in soil. ISME J. 2020;14:2806–15. https://doi.org/10.1038/s41396-020-0732-1
25. Kathirvel S, Muthu V, Rudramurthy SM, Kaur H, Chakrabarti A, Agarwal R. Could cattle dung burning have contributed to the epidemic of COVID-19–associated mucormycosis in India? Results of an experimental aero-mycological study. Mycoses. 2022;65:1024–9. https://doi.org/10.1111/myc.13487
26. Ghosh AK, Singh R, Reddy S, Singh S, Rudramurthy SM, Kaur H, et al. Evaluation of environmental Mucorales contamination in and around the residence of COVID-19–associated mucormycosis patients. Front Cell Infect Microbiol. 2022;12:953750. https://doi.org/10.3389/fcimb.2022.953750
27. Skaria J, John TM, Varkey S, Kontoyiannis DP. Are unique regional factors the missing link in India's COVID-19–associated mucormycosis crisis? MBio. 2022;13:e0047322. https://doi.org/10.1128/mbio.00473-22
28. Bansal SB, Rana A, Babras M, Yadav D, Jha P, Jain M, et al. Risk factors and outcomes of COVID associated mucormycosis in kidney transplant recipients. Transpl Infect Dis. 2022;24:e13777. https://doi.org/10.1111/tid.13777
29. Karat S, Lobo AC, Satish D, Devaraj R, Manjooran RR, Nithyanandam S. Uncontrolled diabetes mellitus exacerbated by COVID-19–induced inflammation is the risk factor for COVID-19–associated rhino-orbito-cerebral mucormycosis: a matched pair case-control study. Indian J Ophthalmol. 2022;70:3096–101. https://doi.org/10.4103/ijo.IJO_448_22
30. Muthu V, Dhaliwal M, Sharma A, Nair D, Kumar HM, Rudramurthy SM, et al. Serum glucose-regulated protein 78 (GRP78) levels in COVID-19-associated mucormycosis: results of a case-control study. Mycopathologia. 2022;187:355–62. https://doi.org/10.1007/s11046-022-00645-6
31. Pandit AK, Tangri P, Misra S, Srivastava MVP, Bhatnagar S, Thakar A, et al. Mucormycosis in COVID-19 patients: a case-control study. Microorganisms. 2022;10:1209. https://doi.org/10.3390/microorganisms10061209
32. Patel AK, Bakshi H, Shah K, Patel S, Patel T, Patel K, et al. Risk factors for COVID-19 associated mucormycosis in India: a case control study. Med Mycol. 2022;60:myac044. https://doi.org/10.1093/mmy/myac044
33. Ponnaiah M, Ganesan S, Bhatnagar T, Thulasingam M, Majella MG, Karuppiah M, et al. Hyperglycemia and steroid use increase the risk of rhino-orbito-cerebral mucormycosis regardless of COVID-19 hospitalization: case-control study, India. PLoS One. 2022;17:e0272042. https://doi.org/10.1371/journal.pone.0272042
34. Popli H, Gupta A, Singh V, Agarwal V, Akilan R, Kumar A. Are low serum vitamin D levels a risk factor for advent of COVID-19 associated rhinocerebral mucormycosis: a preliminary case control study. Indian J Otolaryngol Head Neck Surg. 2022 Jan 11 [Epub ahead of print]. https://doi.org/10.1007/s12070-022-03080-7
35. Vasanthapuram VH, Gupta R, Adulkar N, Nair AG, Bradoo RA, Hegde R, et al. A fungal epidemic amidst a viral pandemic: risk factors for development of COVID-19 associated rhino-orbital-cerebral mucormycosis in India. Orbit. 2022 Feb 22 [Epub ahead of print]. https://doi.org/10.1080/01676830.2021.2020851
36. Yesupatham ST, Mohiyuddin SMA, Arokiyaswamy S, Brindha HS, Anirudh PB. Estimation of Ferritin and D-Dimer levels in COVID-19 patients with mucormycosis: a cross-sectional study. J Clin Diagn Res. 2022;16:BC12–5. https://doi.org/10.7860/JCDR/2022/52844.15908
37. Hoenigl M, Seidel D, Sprute R, Cunha C, Oliverio M, Goldman GH, et al. COVID-19-associated fungal infections. Nat Microbiol. 2022;7:1127–40. https://doi.org/10.1038/s41564-022-01172-2
38. Mulakavalupil B, Vaity C, Joshi S, Misra A, Pandit RA. Absence of case of mucormycosis (March 2020–May 2021)

under strict protocol driven management care in a COVID-19 specific tertiary care intensive care unit. Diabetes Metab Syndr. 2021;15:102169. https://doi.org/10.1016/j.dsx.2021.06.006

39. Jeong W, Keighley C, Wolfe R, Lee WL, Slavin MA, Chen SC, et al. Contemporary management and clinical outcomes of mucormycosis: a systematic review and meta-analysis of case reports. Int J Antimicrob Agents. 2019;53:589–97. https://doi.org/10.1016/j.ijantimicag.2019.01.002
40. Muthu V, Agarwal R, Dhooria S, Sehgal IS, Prasad KT, Aggarwal AN, et al. Has the mortality from pulmonary mucormycosis changed over time? A systematic review and meta-analysis. Clin Microbiol Infect. 2021;27:538–49. https://doi.org/10.1016/j.cmi.2020.12.035
41. Muthu V, Agarwal R, Chakrabarti A. COVID-19–associated pulmonary mucormycosis: an underdiagnosed entity with high mortality. Mycopathologia. 2022;187:405–6. https://doi.org/10.1007/s11046-022-00638-5
42. Pruthi H, Muthu V, Bhujade H, Sharma A, Baloji A, Ratnakara RG, et al. Pulmonary artery pseudoaneurysm in COVID-19–associated pulmonary mucormycosis: case series and systematic review of the literature. Mycopathologia. 2022;187:31–7. https://doi.org/10.1007/s11046-021-00610-9

Address for correspondence: Ritesh Agarwal, Department of Pulmonary Medicine, Postgraduate Institute of Medical Education and Research, Sector-12, Chandigarh 160012, India; email: agarwal.ritesh@outlook.in

The Public Health Image Library

The Public Health Image Library (PHIL), Centers for Disease Control and Prevention, contains thousands of public health–related images, including high-resolution (print quality) photographs, illustrations, and videos.

PHIL collections illustrate current events and articles, supply visual content for health promotion brochures, document the effects of disease, and enhance instructional media.

PHIL images, accessible to PC and Macintosh users, are in the public domain and available without charge.

Visit PHIL at: http://phil.cdc.gov/phil

Role of Seaports and Imported Rats in Seoul Hantavirus Circulation, Africa

Guillaume Castel, Claudia Filippone, Caroline Tatard, Jacques Vigan, Gauthier Dobigny

Seoul orthohantavirus (SEOV) is not considered a major public health threat on the continent of Africa. However, Africa is exposed to rodentborne SEOV introduction events through maritime traffic after exponential growth of trade with the rest of the world. Serologic studies have already detected hantavirus antibodies in human populations, and recent investigations have confirmed circulation of hantavirus, including SEOV, in rat populations. Thus, SEOV is a possible emerging zoonotic risk in Africa. Moreover, the range of SEOV could rapidly expand, and transmission to humans could increase because of host switching from the usual brown rat (*Rattus norvegicus*) species, which is currently invading Africa, to the more widely installed black rat (*R. rattus*) species. Because of rapid economic development, environmental and climatic changes, and increased international trade, strengthened surveillance is urgently needed to prevent SEOV dissemination among humans in Africa.

Rodents are widespread, opportunistic, and competent host reservoirs involved in the maintenance, circulation, and transmission of a wide panel of zoonotic pathogens (*1*). Rodent-related zoonoses cause up to 400 million human infections worldwide each year (*1*,*2*). Among zoonotic pathogens, hantaviruses (order Bunyavirales, family Hantaviridae, genus *Orthohantavirus*) are among agents considered most likely to emerge and have a global public health impact (*3*).

Hantaviruses are enveloped, negative, single-stranded RNA viruses with a tripartite genome comprised of large, medium, and small segments. Transmitted to humans via inhalation of aerosolized virus in contaminated rodent urine and feces, hantaviruses can cause hemorrhagic fever with renal syndrome (HFRS) or hantavirus pulmonary syndrome (*4*). Hantaviruses are generally carried by a rodent species host, and geographic distribution of the host can determine the area in which the associated disease occurs among humans. From this perspective, Seoul orthohantavirus (SEOV), identified in South Korea in 1982, deserves special attention because its cosmopolitan host, the Norwegian rat (*Rattus norvegicus*), also known as the brown rat, has been dispersed worldwide, resulting in a global distribution of the virus today (*5*). Detection of SEOV is often considered anecdotal and speculated to be driven by sporadic introduction of infected brown rats via transportation but also by pet or laboratory rats (*6*,*7*). Diagnosing SEOV in humans remains a challenge due to milder and atypical HFRS pathology (*8*). However, mild symptoms can progress to acute renal disease associated with HFRS, in which patients experience low blood pressure, acute shock, and acute kidney failure, and the case-fatality rate is ≈1% (*9*).

History of Hantaviruses in Africa

Fifteen years ago, no indigenous hantavirus was known in Africa (*10*). Since then, few studies have investigated hantaviruses, including SEOV, in Africa and consequences for human health. The dearth of studies gives the appearance that SEOV is not a major public health threat on the continent because of the lack of local specific testing for SEOV among human serum samples (*11*). Nonetheless, suspicions of SEOV-like agents in humans and wild rats in 17 different countries in Africa are strong (*5*). Until recently, immunofluorescence assays positive for Hantaan virus (HTNV), a closely related orthohantavirus in rats, was the only indication that SEOV probably was in Africa. Unfortunately, these serologic analyses were mainly based on cross-reactivity with better documented hantaviruses from Eurasia within the *Murinae*-associated hantavirus virus genera

Author affiliations: CBGP, INRAE, CIRAD, IRD, Institut Agro, University of Montpellier, Montpellier, France (G. Castel, C. Tatard, G. Dobigny); European Research Infrastructure on Highly Pathogenic Agents, Bruxelles, Belgium (C. Filippone); National University Hospital Center, Cotonou, Benin (J. Vigan); Institut Pasteur de Madagascar, Antananarivo, Madagascar (G. Dobigny)

DOI: https://doi.org/10.3201/eid2901.221092

and did not enable identification of viruses at a finer specific level (*12*). In addition, these analyses usually lacked confirmatory assays (*13*). However, because of the high specificity of hantaviruses for their rodent hosts, positive serologic tests in rats could be ascribed to cross-reactions with SEOV or SEOV-like variants (*5*), as seen in Senegal (*12*,*13*). Of note, older serologic studies in Africa, including regions in West Africa, have detected antibodies against hantaviruses in the human general population and in febrile patients with putative hantavirus disease (*13*–*15*). Detecting putative hantavirus in febrile patients is a crucial public health issue in Africa, where fever of unknown etiology is very common. However, in the absence of differential diagnosis and further laboratory confirmation, we cannot be certain of the virus involved in these cases. We also cannot consider these initial observations exhaustive because of the lack of a proper epidemiologic approach and the limits of the methods used. Nonetheless, those reports might represent a primordial reflection of the health effects that hantavirus zoonoses could have in Africa.

Since 2006, a genus-reactive pan-hantavirus PCR has been available to search for new hantaviruses in small mammals (*16*,*17*). This PCR led to the discovery of the 2 molecularly characterized endemic hantaviruses in mammals in Africa: Sangassou virus in the African wood mouse (*Hylomyscus simus*) and Tanganya virus in the Therese's shrew (*Crocidura theresae*) (*13*,*16*,*17*). Since those discoveries, up to 10 indigenous hantaviruses have been identified in rodents, shrews, and even bats in Africa, making it the continent with the most recent scientific progress in hantavirus epizootiology and epidemiology (*10*). Recently, 2 studies using the pan-hantavirus PCR have molecularly assessed SEOV in rodents from southeastern Senegal (*18*) and southern Benin (*19*), confirming that SEOV circulates in West Africa and could be a cause of hantavirus disease in humans (Figure). In both cases, phylogenic analyses grouped the retrieved viral sequences with SEOV strains from Asia but from 2 different genetic lineages (*19*). Strains from Benin belonged to SEOV lineage 7, whereas lineages from Senegal belonged to SEOV lineage 3 or 4, depending on the genomic segment considered (Figure); this difference could indicate different introduction events in these 2 countries (*19*).

Role of Seaports and Maritime Traffic in Global SEOV Dissemination

Seaports have already been identified as potential entry points for hantavirus-infected brown rats, suggesting that brown rat–associated SEOV can be readily propagated worldwide through maritime

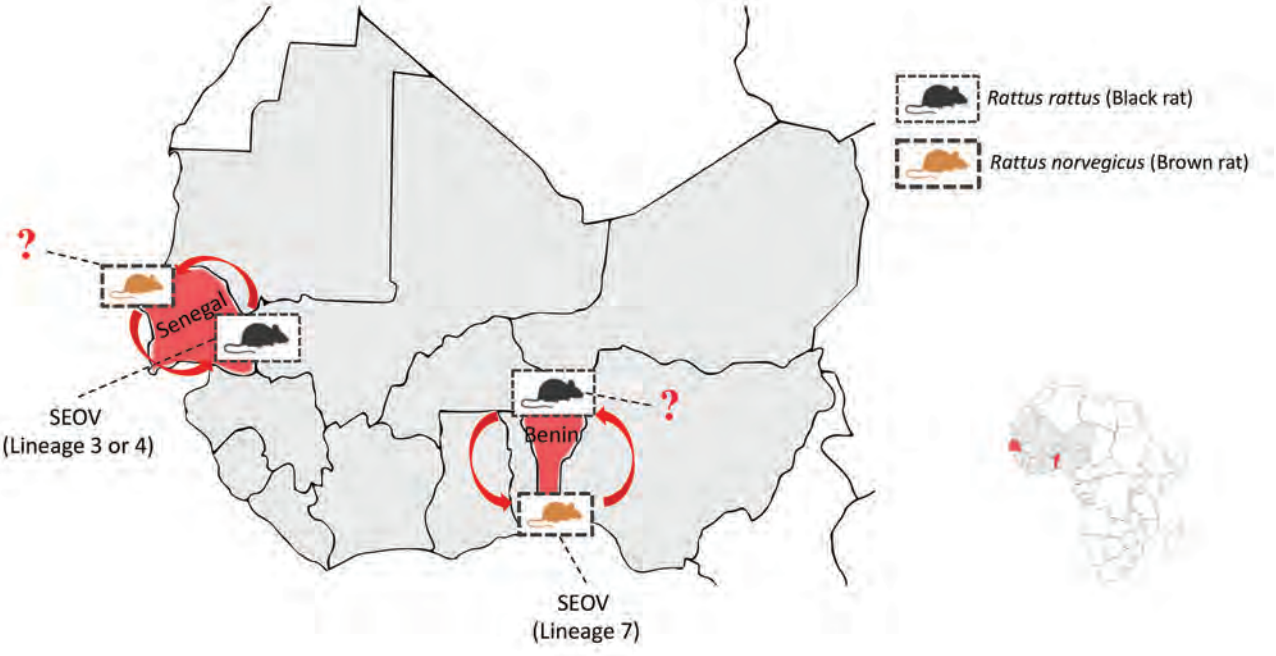

Figure. Seaports in which SEOV was detected in rats, West Africa. Detailed map shows localization of the 2 genetically characterized SEOV variants isolated from black rats (*Rattus rattus*) (*18*) and brown rats (*R. norvegicus*) (*19*). Red arrows indicate potential transmission between the rat species. Red question marks indicate current unknown SEOV infection status in the considered rat species. Inset shows the areas of interest on the continent of Africa. SEOV, Seoul orthohantavirus.

transportation systems (*20*–*22*). In Japan, during the 1960s, brown rats captured in the Tokyo seaport area were shown to have a higher seroprevalence for an HTNV-like agent (*5*). Since then, hantavirus has been detected in rats in other port areas in Asia, including China (*21*,*23*), and in Taiwan, where hantavirus antibody prevalence was much higher (20%) in rodents trapped in international seaports than in rural regions (≈5%), thus suggesting that hantavirus in Taiwan mainly originated from sea transportation (*24*). The role of seaports as the source of hantavirus was further supported by an inverse correlation between the seropositive rate of reservoir host species and the distance of small mammal sampling sites to the seaport (*21*). Of note, SEOV seroprevalence in brown rats from small islands closed to Taiwan was similar to that retrieved in seaports in Taiwan, and the SEOV lineage identified was genetically closely related to SEOV strains from Taiwan. In addition, since 1949, the only channels to trade or travel with those islands has been by boat or airplane to and from Taiwan, pointing again toward the critical role of ship-mediated transportation of rats (rats are more likely transported by boat) in disseminating SEOV in this region (*24*).

From this perspective, Africa is particularly exposed to future introduction events of rodentborne pathogens through maritime traffic due to the exponential increase of trade with the other continents. Increased maritime traffic potentially increases opportunities for ratborne pathogens, particularly SEOV, to expand their geographic range (*18*). Although one third of countries on the continent are landlocked, maritime trade constitutes Africa's main gateway to international trade with the global marketplace (*25*). Therefore, seaports in Africa can constitute a gateway for allochthonous rodentborne pathogens, notably from Europe and the Americas, the main regions with trading partners, but also from Asia, from which trade has been continuously increasing (*26*). Several rat species are well-known commensals to humans, among which brown rats live in close association with human infrastructure in many countries (*11*). This association could translate into the omnipresence of potential SEOV-carrying brown rats in human-made environments in Africa (*5*). In addition, brown rats can be numerous in seaports located within coastal cities (*27*,*28*), which provides opportunities for local SEOV infection among rats and port workers. Indeed, higher SEOV seroprevalence has been reported in workers in areas where seropositive urban rats were detected (*29*).

Ratborne Hantavirus Transportation and Spread Via Maritime Traffic

Ratborne hantavirus dissemination through maritime traffic is not a new phenomenon and probably has been occurring since human navigation for migration and trade, involuntarily transporting rodents aboard vessels (*22*). In Madagascar, molecular evidence showed circulation of the variant Anjozorobe virus (ANJZV), belonging to the Thailand hantavirus (THAIV) species, in black rats (*R. rattus*) and in the indigenous Major's tufted-tailed rat (*Eliurus majori*) (*30*). THAIV is phylogenetically close to but distinct from SEOV, but the 2 viruses share a recent common ancestor (*31*). THAIV is associated with the greater bandicoot rat (*Bandicota indica*) in Thailand (*31*). In addition, THAIV strains Serang and Jurong have been found circulating in Asian house rats (*R. tanezumi*) in Indonesia and Singapore and in Cambodia in *R. rattus* rats (*32*). Detection of the ANJZV variant in Madagascar, far from its most probable areas of origin in South and Southeast Asia, is likely the result of black rat importation into Madagascar through the Arabian Peninsula 2,000–3,000 years ago, when humans colonized the island during a period of vast trading activity in the Indian Ocean (*30*,*33*). Serologic indication of hantavirus circulation in humans also was recently demonstrated in a large national population-based study in Madagascar (*34*), confirming previous observations (*35*). In another study conducted on nearby Mayotte Island, a novel hantavirus, Mayotte virus (MAYOV), which clustered within the THAIV clade, was detected in 18% (29/160) of captured black rats (*36*). That finding also points to ship-transported virus by black rats from Southeast Asia via the Middle East during trade from Arabia thousands of years ago (*30*,*36*).

No available studies describe similar putative human-mediated scenarios for the introduction and spread of hantaviruses within continental Africa. However, SEOV was recently detected in invasive rats in Senegal and Benin (*18*,*19*), suggesting that human-mediated introductions have likely occurred.

Cross-Transmission from Brown Rats to Other Rodent Species

Although a strong virus–reservoir host specificity is globally accepted for hantaviruses, evidence of interspecies spillover among wild rodents exists, challenging the strict rodent–hantavirus coevolution and giving rise to fears of potential rodent host spectrum expansion (*37*). In Madagascar, the indigenous Major's tufted-tailed rat was found to be infected by the

ANJZV variant, pointing toward a spillover event among rodents from the Muroidea superfamily (*30*). In the same manner, spillover infection is the suspected cause of MAYOV and ANJZV acquisition by *R. rattus* rats from other hantavirus rodent reservoirs in Southeast Asia, such as *B. indica* for THAIV in Thailand and *R. tanezumi* for Jurong and Serang variants in Indonesia (*36*). Another study also showed that, although hantaviruses have preferred host species, spillover events can occur between black rats and domestic mice (*Mus musculus*) (*38*). Natural reassortment has already been documented for SEOV in brown rats and another hantavirus hosted by the striped field mouse (*Apodemus agrarius*) in Asia (*39*). Furthermore, the unambiguous detection of SEOV, both molecularly and serologically, in black rats from Senegal (*18*) shows that SEOV is not restricted to brown rats in Africa and can potentially jump to allied rat species via infected brown rats imported by ship (Figure). This hypothesis has not yet been investigated, but it could have major consequences for SEOV ecology and epidemiology on the continent. Indeed, the brown rat is currently expanding its range across the continent (*40*), which, by itself, might fuel SEOV dissemination in Africa. Even more, SEOV transmission and circulation in black rats could enhance geographic expansion because the *R. rattus* rat species was probably introduced centuries ago (*41*), is already widespread across the continent (*40*), and is still propagating because of its substantial invasive ability (*42*,*43*). When not dominated by other species, black rats are quite numerous in cities and live in close proximity to humans, including within households, especially in socioeconomically and environmentally degraded settlements where rat-to-human zoonotic spillover is possible (G. Dobigny et al., unpub. data, https://doi.org/10.5281/zenodo.6444777). Thus, if *R. rattus* rats are found to be a regular SEOV reservoir, the risk associated with this pathogenic but poorly documented virus in Africa could be even higher than is currently thought.

Discussion

Because of rapid economic development, environmental and climatic changes, and increased international trade, Africa urgently needs strengthened surveillance and timely rodent elimination in seaport areas, where rats can be numerous, to prevent transmission of rat-associated pathogens and potential disease outbreaks in humans (*22*,*44*). This strategy also represents an efficient way to limit the risk that newly introduced rodentborne viruses might disseminate further across the continent from seaports. To delineate the eco-epidemiology of hantaviruses and their associated risks in Africa, surveillance of viral genetic variability would provide valuable insights into pathogen transmission dynamics among animal reservoirs and the associated disease when human infection occurs. Low intrinsic genetic variability might reflect limited viral evolution and suggest recent colonization events from infected rats arriving via ships from a common source (*20*,*36*). This type of surveillance requires tools available on-site to amplify and characterize viral nucleic acid sequences from hantavirus-infected rodents or patients to unequivocally identify particular variants of SEOV or other hantaviruses, which is not possible with available serologic tests (*45*).

Surveillance in Africa should initially be directed to seaports and seaport workers, which represent the front lines for contamination by newly introduced viruses. However, surveillance is also needed inland because of passive dissemination of the rodent hosts (*22*,*46*), especially if SEOV has already jumped to more widely distributed rodent species. Urban environments might further increase the risk for disease emergence because of close daily contact between humans and rodents, especially rats (*47*; G. Dobigny et al., unpub. data).

No effective approved hantavirus diseases treatment is available, and whole-virus inactivated vaccines are only licensed for use in South Korea and China but have uncertain protective efficacies (*48*). In addition, only supportive care is available to patients with Seoul virus disease (*9*). Follow-up for rodent biologic invasion, particularly in seaports, is explicitly recommended by the World Health Organization International Health Regulations (2005) (*49*) and is critical for preventing future zoonotic emergence. Thus, seaports could play a role as sentinels of larger surveillance networks.

Conclusions

Because of associated risk for animal-to-human spillover of SEOV (*3*), prevention, detection, and healthcare personnel awareness of this often-misdiagnosed infection remain critical on the continent of Africa. Control of rats would require more effective and comprehensive collaboration between local authorities and the academic and research communities. This type of collaboration fits well with the World Health Organization 13th General Program of Work (*49*). Reducing the reservoir population by using a targeted pest management plan in areas where rodents are highly abundant and in frequent contact with humans could enable mitigation of rodent-related issues and the risk for human disease (K.R. Blasdell et al., unpub. data,

https://doi.org/10.1101/2021.03.18.436089). However, eradication of rat populations in areas of the most concern likely constitutes a more ambitious and unattainable goal and can paradoxically have contrary effects (*50*). Thus, a surveillance rather than riposte-based strategy, combined with medical staff training and implementation of on-site diagnostic methods (*13*), could reduce SEOV outbreak risk among humans in Africa.

This work was funded by The French National Research Program for Environmental and Occupational Health of Anses (ANSES-22-EST-090).

About the Author

Dr. Castel is a researcher in virology at Institut National de Recherche Pour l'Agriculture, l'Alimentation et l'Environnement, Paris, France. His research interests include using phylogenetic and phylogeographic approaches to analyze the diversity of hantaviruses and their evolutionary processes.

References

1. Meerburg BG, Singleton GR, Kijlstra A. Rodent-borne diseases and their risks for public health. Crit Rev Microbiol. 2009;35:221–70. https://doi.org/10.1080/10408410902989837
2. Colombe S, Jancloes M, Rivière A, Bertherat E. A new approach to rodent control to better protect human health: first international meeting of experts under the auspices of WHO and the Pan American Health Organization. Wkly Epidemiol Rec. 2019;17:197–203.
3. Grange ZL, Goldstein T, Johnson CK, Anthony S, Gilardi K, Daszak P, et al.; Expert panel; PREDICT Consortium; University of Edinburgh Epigroup members. Ranking the risk of animal-to-human spillover for newly discovered viruses. Proc Natl Acad Sci U S A. 2021;118:e2002324118. https://doi.org/10.1073/pnas.2002324118
4. Jonsson CB, Figueiredo LT, Vapalahti O. A global perspective on hantavirus ecology, epidemiology, and disease. Clin Microbiol Rev. 2010;23:412–41. https://doi.org/10.1128/CMR.00062-09
5. Clement J, LeDuc JW, Lloyd G, Reynes JM, McElhinney L, Van Ranst M, et al. Wild rats, laboratory rats, pet rats: global Seoul hantavirus disease revisited. Viruses. 2019;11:652. https://doi.org/10.3390/v11070652
6. Childs JE, Klein SL, Glass GE. A case study of two rodent-borne viruses: not always the same old suspects. Front Ecol Evol. 2019;7:35. https://doi.org/10.3389/fevo.2019.00035
7. Dupinay T, Pounder KC, Ayral F, Laaberki MH, Marston DA, Lacôte S, et al. Detection and genetic characterization of Seoul virus from commensal brown rats in France. Virol J. 2014;11:32. https://doi.org/10.1186/1743-422X-11-32
8. Clement J, LeDuc JW, McElhinney LM, Reynes JM, Van Ranst M, Calisher CH. Clinical characteristics of ratborne Seoul hantavirus disease. Emerg Infect Dis. 2019;25:387–8. https://doi.org/10.3201/eid2502.181643
9. US Centers for Disease Control and Prevention. FAQs: Seoul virus [cited 2022 Jul 1]. https://www.cdc.gov/hantavirus/outbreaks/seoul-virus/faqs-seoul-virus.html
10. Kruger DH, Figueiredo LT, Song JW, Klempa B. Hantaviruses—globally emerging pathogens. J Clin Virol. 2015;64:128–36. https://doi.org/10.1016/j.jcv.2014.08.033
11. Heyman P, Plyusnina A, Berny P, Cochez C, Artois M, Zizi M, et al. Seoul hantavirus in Europe: first demonstration of the virus genome in wild *Rattus norvegicus* captured in France. Eur J Clin Microbiol Infect Dis. 2004;23:711–7. https://doi.org/10.1007/s10096-004-1196-3
12. Diagne CA, Charbonnel N, Henttonen H, Sironen T, Brouat C. Serological survey of zoonotic viruses in invasive and native commensal rodents in Senegal, West Africa. Vector Borne Zoonotic Dis. 2017;17:730–3. https://doi.org/10.1089/vbz.2017.2135
13. Witkowski PT, Klempa B, Ithete NL, Auste B, Mfune JK, Hoveka J, et al. Hantaviruses in Africa. Virus Res. 2014; 187:34–42. https://doi.org/10.1016/j.virusres.2013.12.039
14. Gonzalez JP, McCormick JB, Baudon D, Gautun JP, Meunier DY, Dournon E, et al. Serological evidence for Hantaan-related virus in Africa. Lancet. 1984;2:1036–7. https://doi.org/10.1016/S0140-6736(84)91130-9
15. Witkowski PT, Leendertz SAJ, Auste B, Akoua-Koffi C, Schubert G, Klempa B, et al. Human seroprevalence indicating hantavirus infections in tropical rainforests of Côte d'Ivoire and Democratic Republic of Congo. Front Microbiol. 2015;6:518. https://doi.org/10.3389/fmicb.2015.00518
16. Klempa B, Fichet-Calvet E, Lecompte E, Auste B, Aniskin V, Meisel H, et al. Hantavirus in African wood mouse, Guinea. Emerg Infect Dis. 2006;12:838–40. https://doi.org/10.3201/eid1205.051487
17. Klempa B, Fichet-Calvet E, Lecompte E, Auste B, Aniskin V, Meisel H, et al. Novel hantavirus sequences in shrew, Guinea. Emerg Infect Dis. 2007;13:520–2. https://doi.org/10.3201/eid1303.061198
18. Diagne MM, Dieng I, Granjon L, Lucaccioni H, Sow A, Ndiaye O, et al. Seoul orthohantavirus in wild black rats, Senegal, 2012–2013. Emerg Infect Dis. 2020;26:2460–4. https://doi.org/10.3201/eid2610.201306
19. Castel G, Kant R, Badou S, Etougbétché J, Dossou HJ, Gauthier P, et al. Genetic characterization of Seoul virus in the seaport of Cotonou, Benin. Emerg Infect Dis. 2021;27:2704–6. https://doi.org/10.3201/eid2710.210268
20. Arikawa J, Yoshimatsu K, Kariwa H. Epidemiology and epizootiology of hantavirus infection in Japan. Jpn J Infect Dis. 2001;54:95–102.
21. Wu YW, Hsu EL, Lin TH, Huang JH, Chang SF, Pai HH. Seaport as a source of hantavirus: a study on isolated isles. Int J Environ Health Res. 2007;17:25–32. https://doi.org/10.1080/09603120601124280
22. Lin XD, Guo WP, Wang W, Zou Y, Hao ZY, Zhou DJ, et al. Migration of Norway rats resulted in the worldwide distribution of Seoul hantavirus today. J Virol. 2012;86:972–81. https://doi.org/10.1128/JVI.00725-11
23. Wang QW, Tao L, Lu SY, Zhu CQ, Ai LL, Luo Y, et al. Genetic and hosts characterization of hantaviruses in port areas in Hainan Province, P. R. China. PLoS One. 2022;17:e0264859. https://doi.org/10.1371/journal.pone.0264859
24. Chin C, Chiueh TS, Yang WC, Yang TH, Shih CM, Lin HT, et al. Hantavirus infection in Taiwan: the experience of a geographically unique area. J Med Virol. 2000;60:237–47. https://doi.org/10.1002/(SICI)1096-9071(200002)60:2<237::AID-JMV21>3.0.CO;2-B
25. Maritime trade and Africa. Press release. United Nations Conference on Trade and Development. 2018 Oct 3 [cited 2022 Jul 1]. https://unctad.org/press-material/maritime-trade-and-africa

26. Ducruet C, Tsubota K. Maritime networks of Africa and Asia. In: Olukoju A, Castillo Hidalgo D, editors. African seaports and maritime economics in historical perspective. Palgrave Studies in Maritime Economics. Geneva: Palgrave Macmillan; 2020. p. 202–18. https://doi.org/10.1007/978-3-030-41399-6_8
27. Voelckel J, Varieras G. The distribution of *R. norvegicus* and *R. rattus* species in Douala [in French]. Med Trop. 1959;19:456–9.
28. Dossou HJ, Le Guyader M, Gauthier P, Badou S, Etougbetche J, Houemenou G, et al. Fine-scale prevalence and genetic diversity of urban small mammal-borne pathogenic Leptospira in Africa: a spatiotemporal survey within Cotonou, Benin. Zoonoses Public Health. 2022;69:643–54. https://doi.org/10.1111/zph.12953
29. Lokugamage N, Kariwa H, Lokugamage K, Iwasa MA, Hagiya T, Yoshii K, et al. Epizootiological and epidemiological study of hantavirus infection in Japan. Microbiol Immunol. 2004;48:843–51. https://doi.org/10.1111/j.1348-0421.2004.tb03616.x
30. Reynes JM, Razafindralambo NK, Lacoste V, Olive MM, Barivelo TA, Soarimalala V, et al. Anjozorobe hantavirus, a new genetic variant of Thailand virus detected in rodents from Madagascar. Vector Borne Zoonotic Dis. 2014;14:212–9. https://doi.org/10.1089/vbz.2013.1359
31. Hugot JP, Plyusnina A, Herbreteau V, Nemirov K, Laakkonen J, Lundkvist A, et al. Genetic analysis of Thailand hantavirus in *Bandicota indica* trapped in Thailand. Virol J. 2006;3:72. https://doi.org/10.1186/1743-422X-3-72
32. Johansson P, Yap G, Low HT, Siew CC, Kek R, Ng LC, et al. Molecular characterization of two hantavirus strains from different rattus species in Singapore. Virol J. 2010;7:15. https://doi.org/10.1186/1743-422X-7-15
33. Brouat C, Tollenaere C, Estoup A, Loiseau A, Sommer S, Soanandrasana R, et al. Invasion genetics of a human commensal rodent: the black rat *Rattus rattus* in Madagascar. Mol Ecol. 2014;23:4153–67. https://doi.org/10.1111/mec.12848
34. Rabemananjara HA, Raharinosy V, Razafimahefa RM, Ravalohery JP, Rafisandratantsoa JT, Andriamandimby SF, et al. Human exposure to hantaviruses associated with rodents of the *Murinae* subfamily, Madagascar. Emerg Infect Dis. 2020;26:587–90. https://doi.org/10.3201/eid2603.190320
35. Rollin PE, Mathiot C, Nawrocka E, Ravaoalimalala VE, Coulanges P, Sureau P, et al. Hemorrhagic fever with renal syndrome in Madagascar. First seroepidemiologic survey of rat populations [in French]. Arch Inst Pasteur Madagascar. 1986;52:181–6.
36. Filippone C, Castel G, Murri S, Beaulieux F, Ermonval M, Jallet C, et al. Discovery of hantavirus circulating among *Rattus rattus* in French Mayotte Island, Indian Ocean. J Gen Virol. 2016;97:1060–5. https://doi.org/10.1099/jgv.0.000440
37. Fang LZ, Zhao L, Wen HL, Zhang ZT, Liu JW, He ST, et al. Reservoir host expansion of hantavirus, China. Emerg Infect Dis. 2015;21:170–1. https://doi.org/10.3201/eid2101.140960
38. Raharinosy V, Olive MM, Andriamiarimanana FM, Andriamandimby SF, Ravalohery JP, Andriamamonjy S, et al. Geographical distribution and relative risk of Anjozorobe virus (Thailand orthohantavirus) infection in black rats (*Rattus rattus*) in Madagascar. Virol J. 2018;15:83. https://doi.org/10.1186/s12985-018-0992-9
39. Zou Y, Hu J, Wang ZX, Wang DM, Yu C, Zhou JZ, et al. Genetic characterization of hantaviruses isolated from Guizhou, China: evidence for spillover and reassortment in nature. J Med Virol. 2008;80:1033–41. https://doi.org/10.1002/jmv.21149
40. Hima K, Houémenou G, Badou S, Garba M, Dossou H-J, Etougbétché J, et al. Native and invasive small mammals in urban habitats along the commercial axis connecting Benin and Niger, West Africa. Diversity (Basel). 2019;11:238. https://doi.org/10.3390/d11120238
41. Etougbétché J, Houémènou G, Dossou HJ, Badou S, Gauthier P, Abdou Karim IY, et al. Genetic diversity and origins of invasive black rats (*Rattus rattus*) in Benin, West Africa. J Vertebr Biol 2020;69:20014.1-1. https://doi.org/10.25225/jvb.20014
42. Berthier K, Garba M, Leblois R, Navascues M, Tatard C, Gauthier P, et al. Black rat invasion of inland Sahel: insights from interviews and population genetics in South-Western Niger. Biol J Linn Soc Lond. 2016;119:748–65. https://doi.org/10.1111/bij.12836
43. Konečný A, Estoup A, Duplantier JM, Bryja J, Bâ K, Galan M, et al. Invasion genetics of the introduced black rat (*Rattus rattus*) in Senegal, West Africa. Mol Ecol. 2013;22:286–300. https://doi.org/10.1111/mec.12112
44. Muylaert RL, Bovendorp RS, Sabino-Santos G Jr, Prist PR, Melo GL, Priante CF, et al. Hantavirus host assemblages and human disease in the Atlantic Forest. PLoS Negl Trop Dis. 2019;13:e0007655. https://doi.org/10.1371/journal.pntd.0007655
45. Klempa B, Koivogui L, Sylla O, Koulemou K, Auste B, Krüger DH, et al. Serological evidence of human hantavirus infections in Guinea, West Africa. J Infect Dis. 2010;201:1031–4. https://doi.org/10.1086/651169
46. Khan A, Khan M, Ullah S, Wei DQ. Hantavirus: the next pandemic we are waiting for? Interdiscip Sci. 2021;13:147–52. https://doi.org/10.1007/s12539-020-00413-4
47. Weinstein SB, Malanga KN, Agwanda B, Maldonado JE, Dearing MD. The secret social lives of African crested rats, *Lophiomys imhausi*. J Mammal. 2020;101:1680–91. https://doi.org/10.1093/jmammal/gyaa127
48. Liu R, Ma H, Shu J, Zhang Q, Han M, Liu Z, et al. Vaccines and therapeutics against hantaviruses. Front Microbiol. 2020;10:2989. https://doi.org/10.3389/fmicb.2019.02989
49. World Health Organization. International health regulations (2005), 3rd edition. Geneva: The Organization; 2016.
50. Murray MH, Sánchez CA. Urban rat exposure to anticoagulant rodenticides and zoonotic infection risk. Biol Lett. 2021;17:20210311. https://doi.org/10.1098/rsbl.2021.0311

Address for correspondence: Guillaume Castel, Centre de Biologie pour la Gestion des Populations, INRAE, 755 Avenue du campus Agropolis, 34988 Montferrier-sur-Lez CEDEX, France; email: guillaume.castel@inrae.fr

Risk for Severe Illness and Death among Pediatric Patients with Down Syndrome Hospitalized for COVID-19, Brazil

Char Leung, Li Su, Ana Cristina Simões-e-Silva,
Luisamanda Selle Arocha, Karina Mary de Paiva, Patricia Haas

Down syndrome is the most common human chromosomal disorder. Whether Down syndrome is a risk factor for severe COVID-19 outcomes in pediatric patients remains unclear, especially in low-to-middle income countries. We gathered data on patients <18 years of age with SARS-CoV-2 infection from a national registry in Brazil to assess the risk for severe outcomes among patients with Down syndrome. We included data from 14,684 hospitalized patients, 261 of whom had Down syndrome. After adjustments for sociodemographic and medical factors, patients with Down syndrome had 1.8 times higher odds of dying from COVID-19 (odds ratio 1.82, 95% CI 1.22–2.68) and 27% longer recovery times (hazard ratio 0.73, 95% CI 0.61–0.86) than patients without Down syndrome. We found Down syndrome was associated with increased risk for severe illness and death among COVID-19 patients. Guidelines for managing COVID-19 among pediatric patients with Down syndrome could improve outcomes for this population.

Described by John Langdon Down in the 19th Century, Down syndrome is a birth defect caused by a random error in cell division during meiosis that results in an additional full or partial copy of chromosome 21. Down syndrome is rare but is the most common chromosomal disorder; the global estimated birth prevalence is 14 cases/10,000 live births, and prevalence in Brazil is 4 cases/10,000 live births (*1*). The lower prevalence in Brazil might be because of the difference in the maternal age profile (*1*). Nevertheless, death among persons with Down syndrome in Brazil has increased in recent years, particularly among children (*2*). Socioeconomic and regional differences in the quality of and access to healthcare, particularly in the North and Northeast regions, might explain increased death rates (*2*,*3*). Furthermore, the government of Brazil has proposed healthcare guidelines for persons with Down syndrome, but compliance remains poor (*4*).

Down syndrome is characterized by anatomic abnormalities and intellectual disabilities. Persons with Down syndrome are more prone to chronic diseases, including visual impairment (prevalence 73%), thyroid disease (50%), congenital heart disease (25%), hypoacusis (27%), obesity (22%), osteoporosis (20%), and epilepsy (8%) (*5*). Because of immune disturbances, Down syndrome patients are more susceptible to respiratory tract infections and acute respiratory distress syndrome (ARDS) (*6*). Congenital heart defects and respiratory infections remain the most common causes of death and hospitalization among persons with Down syndrome (*7*,*8*). In children with Down syndrome, ≤80% of all hospitalizations and intensive care unit (ICU) admissions result from lower respiratory tract infections, and ≤29% of deaths are associated with pneumonia, influenza, and aspiration (*9*).

Patients with Down syndrome might be at higher risk for COVID-19–related death because they are more susceptible to respiratory failure, a major cause of death among COVID-19 patients. In addition, common underlying conditions among persons with Down syndrome, such as cardiovascular disease and obesity, have been identified as independent risk factors for COVID-19–related death (*10*). Despite these factors, studies of SARS-CoV-2 infection in children and adolescents with Down

Author affiliations: University of Leicester, Leicester, England, UK (C. Leung); University of Cambridge, Cambridge, England, UK (C. Leung, L. Su, A.C. Simões-e-Silva, L.S. Arocha); Universidade Federal de Minas Gerais, Belo Horizonte, Brazil (A.C. Simões-e-Silva); University of Cambridge, Cambridge (L. Selle Arocha); Universidade Federal de Santa Catarina, Florianopolis, Brazil (K.M. de Paiva, P. Haas)

DOI: https://doi.org/10.3201/eid2901.220530

syndrome remain rare, and findings are limited. One case–control study found low mortality rates in pediatric patients with COVID-19 overall in high and low-to-middle income countries, despite more severe COVID-19 clinical manifestations among patients with Down syndrome (*11*). The same study reported higher mortality rates for adults with Down syndrome than those without, but because of limitations of the data, the study did not find an association between pediatric Down syndrome and risks for COVID-19–related death (*11*).

To assess whether pediatric patients with Down syndrome are at higher risk for severe COVID-19 outcomes, we conducted a cohort study by using propensity score matching to reduce confounding from underlying conditions associated with Down syndrome. We used a nationwide database in Brazil to examine whether pediatric Down syndrome was associated with increased risk for severe COVID-19 outcomes among hospitalized patients.

Methods

Study Cohort

The study population included persons registered in the Severe Acute Respiratory Syndrome Database of Sistema de Informacao de Vigilancia Epidemiologica da Gripe (SIVEP-Gripe; https://painel-sivep-gripe.herokuapp.com), a nationwide database managed by the government of Brazil (*2*). SIVEP-Gripe was developed for severe acute respiratory syndrome surveillance related to influenza and other respiratory viruses during the influenza A(H1N1) pandemic in 2009. Patients who have a reportable disease and are admitted to public or private hospitals are registered in SIVEP-Gripe. When the 2020 pandemic began, COVID-19 was declared a reportable disease and incorporated into the surveillance network. SIVEP-Gripe is the primary source of information on COVID-19 hospitalizations and deaths in Brazil. Basic demographic and medical data were systematically registered in a predetermined form used for severe respiratory disease hospitalizations; data were verified by the medical practitioner at the point of care.

On November 26, 2021, we collected data on all COVID-19 cases registered in SIVEP-Gripe during March 5, 2020–November 22, 2021. We included cases in our study that met all these criteria: PCR positive for SARS-CoV-2; patient recovered or died; and patient was <18 years of age. We excluded data for patients who died of causes other than SARS-CoV-2 infection. We categorized patients as Down syndrome or non–Down syndrome, according to the SIVEP-Gripe database, where Down syndrome is reported by clinical providers on a standardized registry form.

Data Sources and Measurement

We collected covariate data from SIVEP-Gripe, including sociodemographic factors and clinical characteristics. These data were age, sex, clinical endpoint (discharge or death), time to recover (i.e., time from admission to discharge), ethnicity (Caucasian, Asian, Hispanic/African, or Indigenous), location by region, need for ventilation, ICU admission, vaccination (against influenza and SARS-CoV-2), use of antiviral drugs, and signs and symptoms (including asymptomatic). Data also included underlying conditions, such as cardiovascular, hematologic, liver, renal, pulmonary, and neurologic diseases; asthma; diabetes; immunocompromise; and obesity.

Patients self-identified sex and ethnicity. We included ethnicity to reflect racial disparities in healthcare access. Signs, symptoms, and underlying conditions referred to those noted at symptom onset or admission. Except for low oxygen saturation (<95%), other signs and symptoms were assessed by certified medical practitioners. We included these signs and symptoms because they are predictors of in-hospital COVID-19 death (*12*). Location referred to North, Northeast, Southeast, Center West, and South regions of Brazil, which we included to reduce bias due to geographic disparities in healthcare access. Other clinical covariates were recorded during the clinical course. Antiviral drugs referred to those used against influenza, such as oseltamivir and zanamivir. Respiratory viral infections were confirmed by PCR tests for influenza, respiratory syncytial virus, human parainfluenza virus, adenovirus, metapneumovirus, bocavirus, rhinovirus, enterovirus, and other coronaviruses that do not generally cause ARDS (namely NL63, OC43, 229E, and HKU1), but that should not be ignored in high-risk populations (*13*); thus, we included them in the analysis.

Not all variables had complete data. For missing data on signs, symptoms, or underlying conditions, we assumed the clinical condition to be absent, following the approach used in a previous study that analyzed the same database (*14*). To reduce age-related selection bias, we calculated age as the difference between the date of birth and the date of symptom onset, rather than the self-reported age. We considered cases without date of birth as missing data and excluded them.

Outcome and Comparison Group Definitions

The primary outcome was whether Down syndrome is associated with increased risk for in-hospital

death, measured by odds ratio (OR) for mortality. The secondary outcome was whether Down syndrome is associated with increased risk for severe illness, measured by hazard ratio (HR) for recovery. We adjusted both outcomes for demographic factors, underlying conditions other than Down syndrome, and intervention.

Statistical Analysis

To compare descriptive statistics between Down syndrome and non–Down syndrome cohorts, we used Mann-Whitney or Student *t*-tests for continuous variables, such as age and time to recovery, depending on the normality condition. We used Fisher exact rather than χ^2 tests for dichotomous variables because χ^2 is an approximate test. For the primary outcome, we calculated the OR for death by using a multivariable logistic regression model. For the secondary outcome, we calculated HR for time to recovery by using a multivariable Cox regression model. We assessed the assumption of proportional hazard by using Grambsch-Therneau test and modified the regression model to meet this assumption if the test result indicated any violations.

For both primary and secondary outcomes, we adopted the forward variable selection procedure for all regression models and used $p<0.1$ as the threshold and the expected (E) value for sensitivity analysis (*15*). In brief, E value is the minimum strength of association that an unmeasured confounder would need to have with both the case and the control group to fully explain away a specific exposure–outcome association, conditional on the covariates (*15*). Because signs, symptoms, ICU admission, and ventilation are mediators rather than confounders, we removed them from the regression analysis. We chose the Southeast region as the reference for the location variables because healthcare is generally more accessible in this region. We chose Hispanic/African as the reference for ethnicity because those ethnicities represent the largest ethnic group in the country. For the logistic regression model, we used the area under the receiver operating characteristic curve (AUC) to assess the goodness-of-fit. For the Cox regression model, we used the concordance index to assess the goodness-of-fit. We performed all calculations in R version 4.1.1 (The R Foundation for Statistical Computing, https://www.r-project.org) by using MatchIt and survival packages. We considered $p<0.05$ statistically significant.

Because some variables had missing data, we created an additional category for missing data in categorical variables that allowed for nonrandom missingness. For quantitative variables, we excluded cases with missing data from the corresponding statistical analysis because no reliable information was available for imputation. Neither Brazil nor the United Kingdom required ethics approval for this study because we used de-identified, publicly available data.

Results

A total of 2,812,965 cases were registered in the SIVEP-Gripe, of which 1,162,755 (41.3%) were PCR positive for SARS-CoV-2 (Figure 1). Among those patients, 17,018 (1.5%) were <18 years of age, 1,144,249 (98.4%) were ≥18 years of age, and 1,488 (0.1%) had missing age data. Among 17,018 patients <18 years of age, 261 (1.5%) had Down syndrome and 16,757 (98.5%) did not, 78 (0.5%) died of causes other than SARS-CoV-2 infection, and 2,256 (13.3%) had missing outcomes. Consequently, the study included a total of 14,684 (86.3%) cases that met all selection criteria and had COVID-19 diagnosed by PCR during March 5, 2020–November 22, 2021.

Among 14,684 patients in the study, 236 (1.6%) had Down syndrome and 14,448 (98.4%) did not (Table). The sample was well balanced for sex ($p = 0.237$) and median age ($p = 0.670$) between the 2 groups. We noted no significant difference in ethnicity among the cohort, for Asian ($p>0.999$) or Indigenous ($p>0.999$) persons, and for those missing data ($p = 0.238$). The in-hospital case-fatality rate for patients with Down syndrome was 23.7% and was 8.2% for patients without Down syndrome, and the difference was highly significant ($p<0.001$). The Down syndrome group also had a longer median time to recover (8.5 days vs. 5 days; $p<0.001$). Patients with Down syndrome had more signs and symptoms of severe COVID-19 clinical course than patients without Down syndrome, including dyspnea (59.8% vs. 48.9%; $p = 0.001$), low oxygen saturation (58.9% vs. 37.4%; $p<0.001$), and respiratory discomfort (59.8% vs. 45.8%; $p<0.001$). Not surprisingly, patients with Down syndrome were more prone to health conditions, most notably cardiovascular disease (35.6% vs. 3.5%; $p<0.001$) and immune disorders (6.78% vs. 3.55%; $p = 0.013$). Furthermore, patients with Down syndrome required more advanced healthcare, evidenced by the higher rates of ICU admission (47.5% vs. 27.0%; $p<0.001$) and mechanical ventilation (67.4% vs. 44.5%; $p<0.001$).

After the adjusting for demographic and clinical factors, multivariable logistic regression suggested that patients with Down syndrome had higher risk for in-hospital death (adjusted OR [aOR] 2.06, 95% CI 1.39–3.01) (Figure 2). Adjusted factors were cardiovascular diseases (aOR 3.04, 95% CI 2.38–3.87), neurologic diseases (aOR 3.23, 95% CI 2.62–3.96),

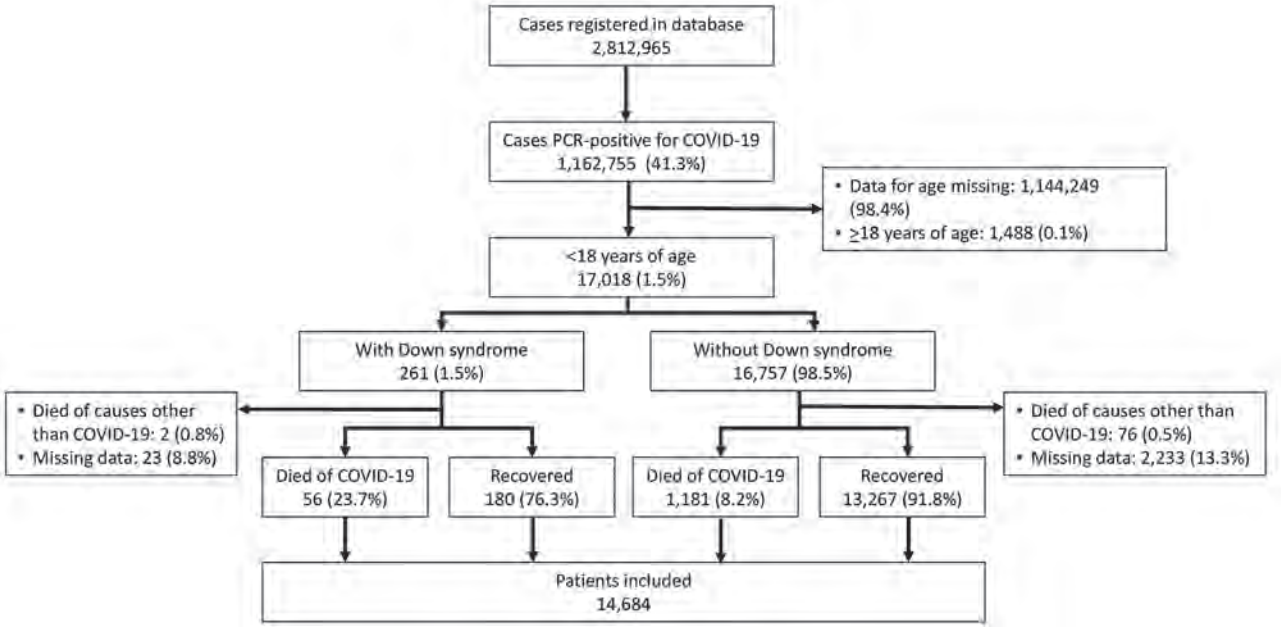

Figure 1. Flowchart of case inclusion in a study of risk for severe illness and death among pediatric patients with Down syndrome hospitalized for COVID-19, Brazil. We used publicly available data from COVID-19 cases registered in the Severe Acute Respiratory Syndrome Database of Sistema de Informacao de Vigilancia Epidemiologica da Gripe (SIVEP-Gripe; https://painel-sivep-gripe.herokuapp.com), a nationwide database managed by the government of Brazil.

renal diseases (aOR 1.90, 95% CI 1.29–3.01), liver diseases (aOR 4.15, 95% CI 2.24–7.53), and obesity (aOR 2.30, 95% CI 1.59–3.25).

The difference in the crude and adjusted OR for location and ethnicity variables might not reflect confounding effects because we calculated aOR by using a reference group, giving different interpretations. For example, the crude OR for North means that patients from that region had 2 times the odds of death compared with persons from other regions, whereas the aOR showed that patients in the North had ≈2.7 times the odds for death compared with persons in the Southeast region, the reference group.

The AUC was 0.75 (95% CI 0.73–0.75), indicative of accuracy. ORs related to COVID-19 death were usually ≈2 (*16*), close to the computed E values (Appendix Table 1, https://wwwnc.cdc.gov/EID/article/29/1/22-0503-App1.pdf). This result indicates fair robustness of our results for the influence of unmeasured confounders.

For time to recovery, we created Kaplan-Meier curves for patients with and without Down syndrome (Figure 3). The log-rank test suggested a difference in the 2 survival curves (p<0.001), indicating that patients with Down syndrome had a lower probability of recovery during the first month of hospitalization than patients without Down syndrome. Grambsch-Therneau test results showed that proportional hazard assumption of the multivariable Cox regression model was violated (p<0.001). We stratified the variables for age and Caucasian, based on p values from the Grambsch-Therneau test, and found p = 0.140 in the stratified model (Figure 4). After adjusting for demographic and clinical factors, patients with Down syndrome had 59% longer time to recovery (adjusted HR [aHR] 0.41, 95% CI 0.19–0.97). We also noted statistically significant associations between other underlying conditions and longer time to recovery. Patients with renal disease had 77% longer time to recovery (aHR 0.23, 95% CI 0.10–0.53), those with neurologic disease had 59% (adjusted HR 0.41, 95% CI 0.29–0.59) longer, those with hematologic disease had 57% (aHR 0.43, 95% CI 0.22–0.86) longer, and those with cardiovascular disease had 55% (aHR 0.45, 95% CI 0.32–0.64) longer.

The concordance index was 0.59 (95% CI 0.57–0.61), indicating that the Cox regression model was adequate. Adjusted HR of risk factors related to time to recovery in COVID-19 patients was usually 1.2–1.7 (*17*), smaller than most of the computed E values (Appendix Table 2), indicative of fair robustness of our results.

Discussion

After adjusting for demographic and medical factors, we found pediatric patients with Down syndrome hospitalized for COVID-19 had higher risk for severe

illness and death than those without Down syndrome. We observed higher mortality rates (23.7%) among Down syndrome patients than in a previous case–control study (*11*). In that study, the authors reported a 6.7% mortality rate among 328 children with Down syndrome from low-to-middle income countries (*11*), but their result might be prone to selection bias because all controls were from the United States. Mortality rates reported in that study might also be lower than we observed because of socioeconomic inequality and vulnerability in Brazil. Despite efforts to ensure access to health services for persons with disabilities (*18*), inequality in healthcare access continues in

Table 1. Characteristics of patients with and without Down syndrome in a study of risk for severe illness and death among pediatric patients hospitalized for COVID-19, Brazil*

Characteristics	No. participants		p value
	With Down syndrome, n = 236	Without Down syndrome, n = 14,448	
Median age, y (IQR)	3.4 (0.6–12.4)	3.6 (0.7–11.5)	0.670
Sex, %	N = 236	N = 14,440	
M	50.0	53.9	0.237
F	50.0	46.1	
Died, no. (%)	56 (23.7)	1,181 (8.2)	<0.001
Median time to recover, d (IQR)	8.5 (4.0–18.0), n =172	5.0 (3.0–10.0), n = 11,919	<0.001
Region, no. (%)			
North	17 (7.2)	907 (6.3)	0.501
Northeast	42 (17.8)	3,350 (23.2)	0.052
Southeast	100 (42.4)	6,908 (47.8)	0.101
Center West	23 (9.7)	1,330 (9.2)	0.734
South	54 (22.9)	1,953 (13.5)	<0.001
Ethnicity, no. (%)	n = 191	n = 11,210	
Caucasian	107 (56.0)	4,894 (43.7)	0.001
Asian	1 (0.5)	87 (0.8)	>0.999
Hispanic	82 (42.9)	6,150 (54.9)	0.001
Indigenous	1 (0.5)	79 (0.7)	>0.999
Missing	42 (19.1), n = 236	3,238 (22.4), n = 14,448	0.238
Signs and symptoms, no. (%)			
Asymptomatic	1 (0.4)	60 (0.4)	>0.999
Abdominal pain	13 (5.5)	883 (6.1)	0.891
Anosmia	2 (0.8)	304 (2.1)	0.248
Ageusia	1 (0.4)	297 (2.1)	0.097
Coryza	18 (8.1)	1,470 (10.2)	0.328
Cough	134 (56.8)	8,909 (61.7)	0.138
Diarrhea	48 (20.3)	1,979 (13.7)	0.006
Dyspnea	141 (59.7)	7,059 (48.9)	0.001
Fatigue	23 (9.7)	1,250 (8.7)	0.559
Fever	163 (69.1)	9,676 (67.0)	0.530
Headache	6 (2.5)	800 (5.5)	0.043
Myalgia	1 (0.4)	387 (2.7)	0.023
Oxygen saturation <95%	139 (58.9)	5,400 (37.4)	<0.001
Respiratory discomfort	141 (59.7)	6,612 (45.8)	<0.001
Sore throat	31 (13.1)	1,941 (13.4)	>0.999
Vomiting	41 (17.4)	2,447 (16.9)	0.861
Other symptoms	77 (32.6)	5,189 (35.9)	0.306
Underlying conditions, no. (%)			
Cardiovascular disease	84 (35.6)	505 (3.5)	<0.001
Hematologic disease	4 (1.7)	274 (1.9)	>0.999
Liver disease	2 (0.8)	68 (0.5)	0.311
Asthma	13 (5.5)	1,050 (7.3)	0.374
Diabetes	2 (0.8)	286 (2.0)	0.337
Neurologic disease	20 (8.5)	805 (5.6)	0.063
Pulmonary disease	11 (4.7)	301 (2.1)	0.018
Immunocompromised	16 (6.8)	513 (3.6)	0.013
Renal disease	6 (2.5)	189 (1.3)	0.137
Obesity	6 (2.5)	324 (2.2)	0.658
Intervention, no. (%)			
Antiviral against influenza	30 (12.7)	1,559 (10.8)	0.341
ICU admission	112 (47.5)	3,904 (27.0)	<0.001
Ventilation	159 (67.4)	6,426 44.5)	<0.001
Influenza vaccinate	18 (7.6)	981 (6.8)	0.601
COVID-19 vaccine	3 (1.3)	81 (0.6)	0.153

*ICU, intensive care unit.

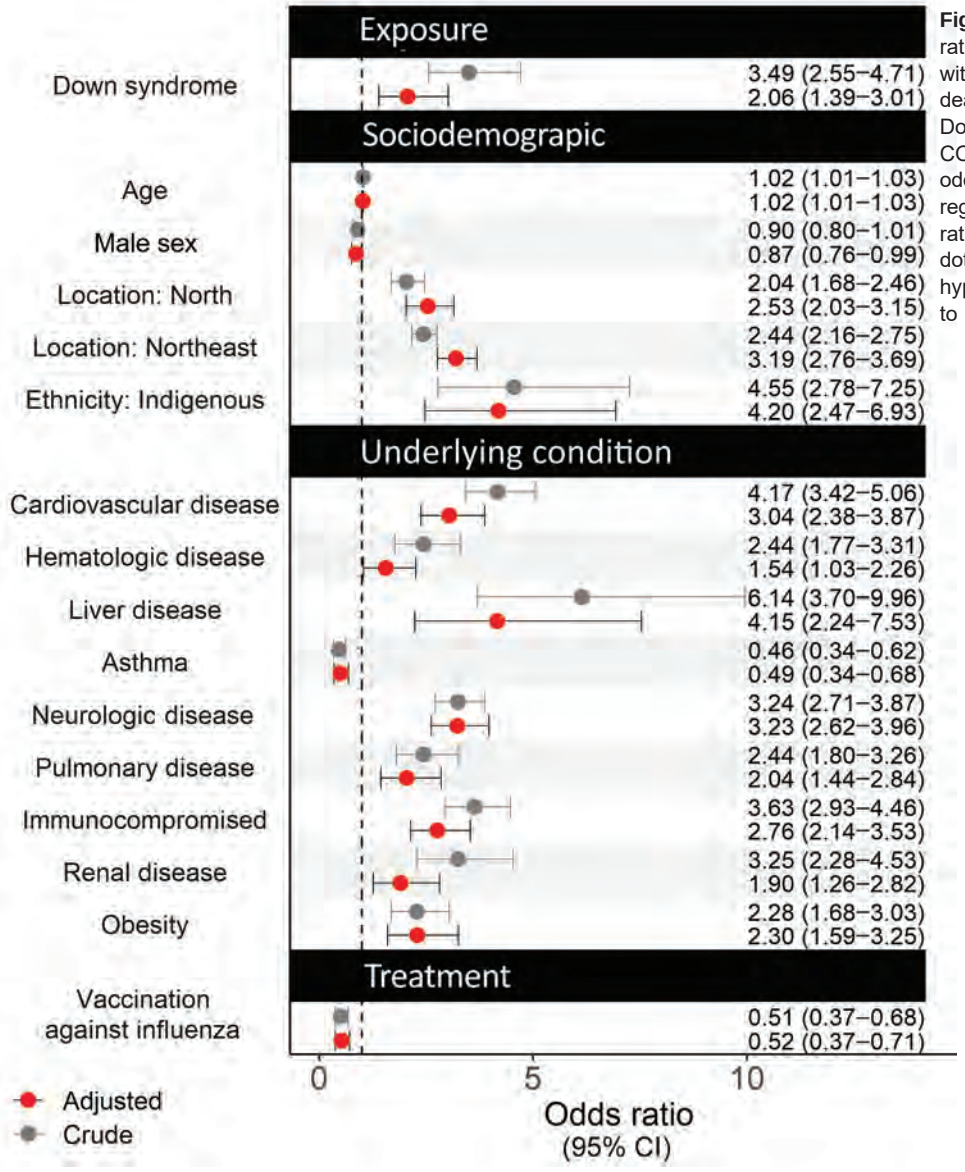

Figure 2. Crude and adjusted odds ratios for various factors associated with risk for severe illness and death among pediatric patients with Down syndrome hospitalized for COVID-19, Brazil. We calculated odds ratios by using logistic regression. Circles indicate odds ratios; error bars indicate 95% CI; dotted vertical line indicates the null hypothesis of odds ratio being equal to 1.

Brazil. We noted that pediatric Down syndrome patients hospitalized with COVID-19 in regions of Brazil with a low socioeconomic profile, such as the North and Northeast, had ≈3–4 times the odds for death and ≈30% longer time to recovery than those in the South region (Figures 2, 4). Furthermore, inequality in access to heart surgery to treat Down syndrome–related heart defects also might explain the higher in-hospital case-fatality rate observed in our study because cardiovascular disease is an independent risk factor for COVID-19–related in-hospital death. Even in southern Brazil, where healthcare is more accessible, recent literature indicates only one quarter of patients with Down syndrome have undergone heart surgery (*19*). Nevertheless, we found that Down syndrome was a risk factor for severe COVID-19 after we adjusted for cardiovascular disease; having undergone heart surgery implies the presence of cardiovascular disease.

Beyond Brazil, several factors specific to Latin America might explain why Down syndrome could be a risk factor for severe COVID-19 outcomes. First, quality healthcare might be out of reach for families of children with Down syndrome because they often are ostracized by the community due to religiously motivated social perceptions of Down syndrome. For instance, one study reported medical practitioners in Ecuador rarely diagnose Down syndrome in an empathetic manner (*20*), which can lead parents to distrust the healthcare system and discourage them from

seeking professional help. Second, some families lack the financial ability to access healthcare for COVID-19 even when they live in a geographic area where healthcare is accessible. Therefore, the increased risk for death related to the lack of healthcare might not reflect geographic variables in our study but instead might be associated with Down syndrome status. This problem does not only exist in Brazil; a sizeable portion of the population in Latin America has no access to any kind of health insurance (*21*). Third, Latin America remains one of the least vaccinated areas in the world; barely 30% of the population has been vaccinated against COVID-19 (*22*). Although Latin America has only 8.4% of the world's population, the region contributed 20% of confirmed global COVID-19 cases and 30% of deaths (*22*). Vaccination rate was low in the pediatric population in our study, and no information was available regarding differences in vaccination rates among children with and without Down syndrome. Finally, ICU admission and ventilation might be less available to children with Down syndrome in low-income countries such as Brazil.

Increased risk for severe illness and death among patients with COVID-19 and Down syndrome intensifies the burden of Down syndrome, which already has greater effects on society in Latin America because resources are scarce. Prenatal diagnostic testing is not affordable for many in Latin America; noninvasive prenatal testing costs 238% and amniocentesis costs 68% of the average monthly income in Brazil

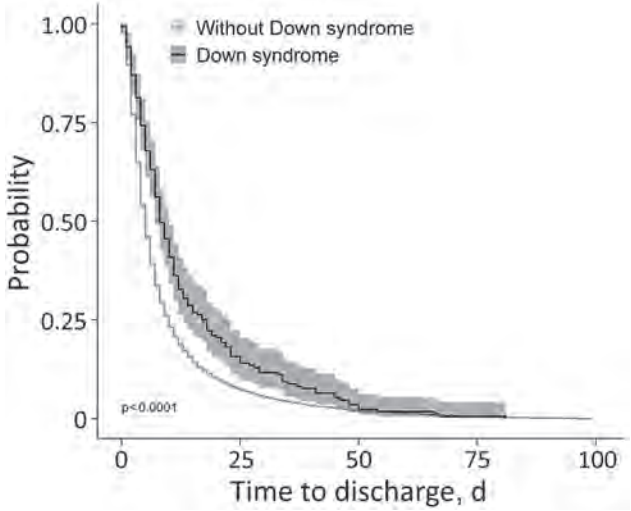

Figure 3. Kaplan-Meier curves for probability of recovery in a study of risk for severe illness and death among pediatric patients with Down syndrome hospitalized for COVID-19, Brazil. The log-rank test suggested a difference in the 2 survival curves (p<0.001), indicating that patients with Down syndrome had a lower probability of recovery during the first month of hospitalization than patients without Down syndrome. Gray shading around lines represents 95% CI.

(*23*). As of 2014, Paraguay had only 1 laboratory for genetic testing, but many samples were sent to Chile, Brazil, or Argentina for testing (*24*), further straining the resources in these countries.

No literature confirming a biological link between Down syndrome and COVID-19 outcomes is available. Because cytokine release syndrome is a leading cause of COVID-19 deaths, we speculate that increased interleukin-6 (IL-6) production in children with Down syndrome (*25*) could increase risk for death and that elevated IL-6 results from altered immune response to viral infection in patients with Down syndrome, as noted with influenza (*26*). We also hypothesize that patients with Down syndrome might be more susceptible to poor COVID-19 outcomes because the *TMPRSS2* gene, a serine protease for SARS-CoV-2 spike protein priming for viral host cell entry, is located on the *21q22.3* gene (*27*), a critical part of the Down syndrome region.

Several studies have reported on SARS-CoV-2 infection among Down syndrome patients, but those studies focused on the general population or adults. Nonetheless, those studies generally noted more severe COVID-19 in persons with Down syndrome, aligning with our work. One case series in Belgium reported on 5 adult patients, 43–62 years of age, with Down syndrome, 4 of whom had a severe clinical course; the other was asymptomatic (*28*). In a dual-center study comprising 7,246 COVID-19 patients, including 12 with Down syndrome, levels of inflammation markers, such as C-reactive protein and IL-6, were not much different between 12 patients with Down syndrome and 60 patients without, but the Down syndrome patients had more severe disease (*29*). Nevertheless, the sample size of that study is too small to refute the general belief that IL-6 is a prognostic biomarker for COVID-19. In a study conducted in Sweden, COVID-19 patients with Down syndrome (n = 85) had 1.8 times higher odds of COVID-19 diagnosis and 4.3 times higher odds of ICU admission (*30*). Based on a time-to-event analysis, a study on 8 million adults with SARS-CoV-2 infection reported a 10-fold increase in risk for COVID-19 related hospitalization and 4-fold increase in risk for death among patients with Down syndrome (*31*).

We reduced confounding in our study to enhance the robustness of the results. First, we included several variables, such as intervention and respiratory viral infections, that were not considered in other studies. We also included location variables to account for effects of geographic disparities in access to healthcare. Second, Down syndrome patients have underlying conditions that are also independent risk factors for

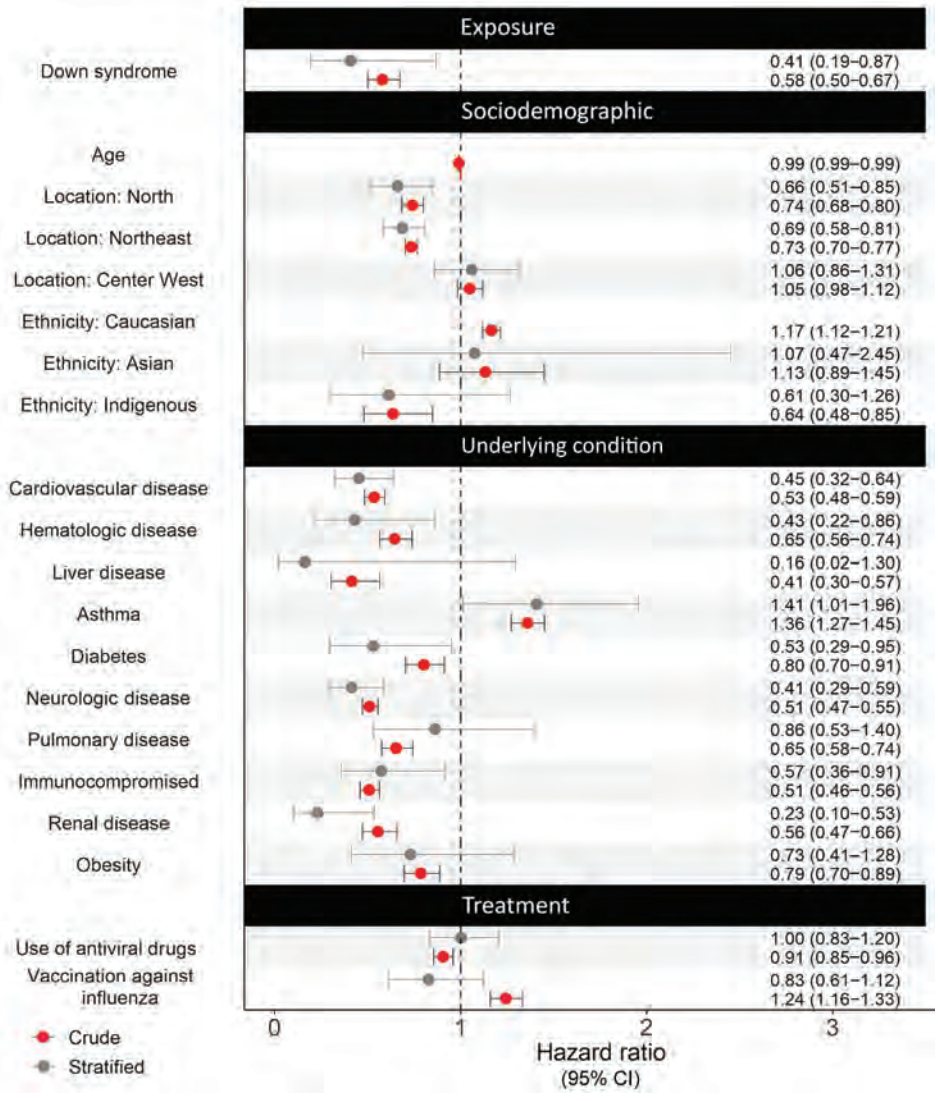

Figure 4. Crude and stratified hazard ratios for various factors associated with risk for severe illness and death among pediatric patients with Down syndrome hospitalized for COVID-19, Brazil. We calculated hazard ratios by using Cox regression. Circles indicate hazard ratio; error bars indicate 95% CI; dotted vertical line indicates the null hypothesis of hazard ratio being equal to 1.

COVID-19–related death. These conditions are strong confounders between Down syndrome and death, and between Down syndrome and time to recovery. We used a multivariable regression model to reduce confounding, plus we used propensity score matching to confirm the results. Finally, we included cases and controls from the same target population, which increases the level of evidence.

Limitations of this study include missing data, which usually arises in nationwide registries. Using a nationwide database implies large population coverage, but inaccurate data are inevitable. Nevertheless, we made every effort to verify data. Furthermore, we created an additional category for missing data in ethnicity, enabling nonrandom missingness. For missing data in the date of clinical endpoint, we observed many variables that had a statistically significant difference between groups with missing and available data included in the logistic and Cox regression models (Appendix Table 3). This partly accounts for random missingness by conditioning these variables in the regression models. Nonetheless, nonmissing randomness in the date of clinical endpoint remains a limitation. In addition to missing data, we only considered hospitalized cases, limiting the generalizability of our findings. Because predetermined forms were used to standardize the nationwide reporting, no information on clinical management for Down syndrome was available. However, those data are partly reflected in geographic variables that imply access to healthcare. Furthermore, no guidance or details were available on diagnosis of most underlying conditions, except for respiratory viral infections, which were confirmed by PCR; however, data on underlying conditions were registered and verified by certified medical practitioners. Finally, the sample size for the Down syndrome

group was small because Down syndrome is a rare disorder, and we only considered a subset of this population, children and adolescents.

In conclusion, our data showed that Down syndrome in children and adolescents is associated with increased risk for severe COVID-19 illness and death among hospitalized patients, even after adjusting for sociodemographic factors and clinical factors common in Down syndrome, such as cardiovascular diseases. Social stratification and the lack of resources at the national level might intensify the risk for severe COVID-19 outcomes among pediatric patients with Down syndrome. Guidelines for managing COVID-19 among Down syndrome patients could improve outcomes for this population.

Acknowledgments

This study was supported by the National Institute for Health and Care Research (NIHR) Applied Research Collaboration East Midlands and Leicester NIHR Biomedical Research Centre. The views expressed are those of the author(s) and not necessarily those of the NIHR or the Department of Health and Social Care.

C.L. conceptualized and designed the study, designed the data collection instruments, collected data, carried out the initial analyses, drafted the initial manuscript, and reviewed and revised the manuscript. L.S., A.C.S-e-S., and L.S.A. drafted the initial manuscript and reviewed and revised the manuscript for important intellectual content. K.M.P. and P.H. critically reviewed and revised the manuscript for important intellectual content. All authors approved the final manuscript as submitted and agree to be accountable for all aspects of the work.

About the Author

Dr. Leung is lecturer of medical statistics and epidemiology at University of Leicester, Leicester, United Kingdom. His main research interests are epidemiology of viral respiratory infections, such as COVID-19, influenza and common cold, and healthcare in Brazil.

References

1. Laignier MR, Lopes-Júnior LC, Santana RE, Leite FMC, Brancato CL. Down syndrome in Brazil: occurrence and associated factors. Int J Environ Res Public Health. 2021;18:11954. https://doi.org/10.3390/ijerph182211954
2. de Campos Gomes F, de Melo-Neto JS, Goloni-Bertollo EM, Pavarino ÉC. Trends and predictions for survival and mortality in individuals with Down syndrome in Brazil: a 21-year analysis. J Intellect Disabil Res. 2020;64:551–60. https://doi.org/10.1111/jir.12735
3. Szwarcwald CL, Souza Júnior PR, Marques AP, Almeida WD, Montilla DE. Inequalities in healthy life expectancy by Brazilian geographic regions: findings from the National Health Survey, 2013. Int J Equity Health. 2016;15:141. https://doi.org/10.1186/s12939-016-0432-7
4. Moriyama CH, Mustacchi Z, Pires S, Massetti T, da Silva T, Herrero D, et al. Functional skills and caregiver assistance of Brazilian children and adolescents with Down syndrome. NeuroRehabilitation. 2019;45:1–9. https://doi.org/10.3233/NRE-192763
5. Carfì A, Romano A, Zaccaria G, Villani ER, Manes Gravina E, Vetrano DL, et al. The burden of chronic disease, multimorbidity, and polypharmacy in adults with Down syndrome. Am J Med Genet A. 2020;182:1735–43. https://doi.org/10.1002/ajmg.a.61636
6. Colvin KL, Yeager ME. What people with Down syndrome can teach us about cardiopulmonary disease. Eur Respir Rev. 2017;26:160098. https://doi.org/10.1183/16000617.0098-2016
7. Blake JM, Estrada Gomez D, Skotko BG, Torres A, Santoro SL. Pneumonia and respiratory infection in Down syndrome: a 10-year cohort analysis of inpatient and outpatient encounters across the lifespan. Am J Med Genet A. 2021;185:2878–87. https://doi.org/10.1002/ajmg.a.62355
8. Kapoor S, Bhayana S, Singh A, Kishore J. Co-morbidities leading to mortality or hospitalization in children with Down syndrome and its effect on the quality of life of their parents. Indian J Pediatr. 2014;81:1302–6. https://doi.org/10.1007/s12098-014-1389-4
9. Verstegen RH, van Hout RW, de Vries E. Epidemiology of respiratory symptoms in children with Down syndrome: a nationwide prospective web-based parent-reported study. BMC Pediatr. 2014;14:103. https://doi.org/10.1186/1471-2431-14-103
10. Figliozzi S, Masci PG, Ahmadi N, Tondi L, Koutli E, Aimo A, et al. Predictors of adverse prognosis in COVID-19: a systematic review and meta-analysis. Eur J Clin Invest. 2020;50:e13362. https://doi.org/10.1111/eci.13362
11. Emes D, Hüls A, Baumer N, Dierssen M, Puri S, Russell L, et al.; on behalf of the Trisomy Research Society Covid-Initiative Study Group. COVID-19 in children with Down syndrome: data from the Trisomy 21 Research Society Survey. J Clin Med. 2021;10:5125. https://doi.org/10.3390/jcm10215125
12. Mesas AE, Cavero-Redondo I, Álvarez-Bueno C, Sarriá Cabrera MA, Maffei de Andrade S, Sequí-Dominguez I, et al. Predictors of in-hospital COVID-19 mortality: a comprehensive systematic review and meta-analysis exploring differences by age, sex and health conditions. PLoS One. 2020;15:e0241742. https://doi.org/10.1371/journal.pone.0241742
13. Dadashi M, Khaleghnejad S, Abedi Elkhichi P, Goudarzi M, Goudarzi H, Taghavi A, et al. COVID-19 and influenza co-infection: a systematic review and meta-analysis. Front Med (Lausanne). 2021;8:681469. https://doi.org/10.3389/fmed.2021.681469
14. Oliveira EA, Colosimo EA, Simões E Silva AC, Mak RH, Martelli DB, Silva LR, et al. Clinical characteristics and risk factors for death among hospitalised children and adolescents with COVID-19 in Brazil: an analysis of a nationwide database. Lancet Child Adolesc Health. 2021;5:559–68. https://doi.org/10.1016/S2352-4642(21)00134-6
15. VanderWeele TJ, Ding P. Sensitivity analysis in observational research: introducing the E-value. Ann Intern Med. 2017;167:268–74. https://doi.org/10.7326/M16-2607
16. Dessie ZG, Zewotir T. Mortality-related risk factors of COVID-19: a systematic review and meta-analysis of 42 studies and 423,117 patients. BMC Infect Dis. 2021;21:855. https://doi.org/10.1186/s12879-021-06536-3

17. Tolossa T, Wakuma B, Seyoum Gebre D, Merdassa Atomssa E, Getachew M, Fetensa G, et al. Time to recovery from COVID-19 and its predictors among patients admitted to treatment center of Wollega University Referral Hospital (WURH), Western Ethiopia: survival analysis of retrospective cohort study. PLoS One. 2021;16:e0252389. https://doi.org/10.1371/journal.pone.0252389
18. Ministério da Saúde (BR). Ordinance no. 793. Establishes the care network for persons with disabilities within the scope of the Unified Health System [in Portuguese]. Brasília: The Ministry; 2012 [cited 2021 Nov 26]. https://bvsms.saude.gov.br/bvs/saudelegis/gm/2012/prt0793_24_04_2012.html
19. Bermudez BE, Medeiros SL, Bermudez MB, Novadzki IM, Magdalena NI. Down syndrome: prevalence and distribution of congenital heart disease in Brazil. Sao Paulo Med J. 2015;133:521–4. https://doi.org/10.1590/1516-3180.2015.00710108
20. Huiracocha L, Almeida C, Huiracocha K, Arteaga J, Arteaga A, Blume S. Parenting children with Down syndrome: societal influences. J Child Health Care. 2017;21:488–97. https://doi.org/10.1177/1367493517727131
21. Allyse M, Minear MA, Berson E, Sridhar S, Rote M, Hung A, et al. Non-invasive prenatal testing: a review of international implementation and challenges. Int J Womens Health. 2015;7:113–26. https://doi.org/10.2147/IJWH.S67124
22. Economic Commission for Latin America and the Caribbean, Pan American Health Organization. The prolongation of the health crisis and its impact on health, the economy and social development. 2021 Oct 14 [cited 2022 Jan 10]. https://iris.paho.org/bitstream/handle/10665.2/54991/eclacpahoreport2021_eng.pdf
23. Chandrasekharan S, Minear MA, Hung A, Allyse M. Noninvasive prenatal testing goes global. Sci Transl Med. 2014;6:231fs15. https://doi.org/10.1126/scitranslmed.3008704
24. Ferreira CR, de Herreros MB. Medical genetics in Paraguay. Mol Genet Genomic Med. 2014;2:458–66. https://doi.org/10.1002/mgg3.119
25. Huggard D, Kelly L, Ryan E, McGrane F, Lagan N, Roche E, et al. Increased systemic inflammation in children with Down syndrome. Cytokine. 2020;127:154938. https://doi.org/10.1016/j.cyto.2019.154938
26. Broers CJ, Gemke RJ, Weijerman ME, van der Sluijs KF, van Furth AM. Increased pro-inflammatory cytokine production in Down syndrome children upon stimulation with live influenza A virus. J Clin Immunol. 2012;32:323–9. https://doi.org/10.1007/s10875-011-9625-4
27. Hou Y, Zhao J, Martin W, Kallianpur A, Chung MK, Jehi L, et al. New insights into genetic susceptibility of COVID-19: an ACE2 and TMPRSS2 polymorphism analysis. BMC Med. 2020;18:216. https://doi.org/10.1186/s12916-020-01673-z
28. De Cauwer H, Spaepen A. Are patients with Down syndrome vulnerable to life-threatening COVID-19? Acta Neurol Belg. 2021;121:685–7. https://doi.org/10.1007/s13760-020-01373-8
29. Malle L, Gao C, Hur C, Truong HQ, Bouvier NM, Percha B, et al. Individuals with Down syndrome hospitalized with COVID-19 have more severe disease. Genet Med. 2021;23:576–80. https://doi.org/10.1038/s41436-020-01004-w
30. Bergman J, Ballin M, Nordström A, Nordström P. Risk factors for COVID-19 diagnosis, hospitalization, and subsequent all-cause mortality in Sweden: a nationwide study. Eur J Epidemiol. 2021;36:287–98. https://doi.org/10.1007/s10654-021-00732-w
31. Clift AK, Coupland CAC, Keogh RH, Hemingway H, Hippisley-Cox J. COVID-19 mortality risk in Down syndrome: results from a cohort study of 8 million adults. Ann Intern Med. 2021;174:572–6. https://doi.org/10.7326/M20-4986

Address for correspondence: Char Leung, Department of Population Health Sciences, University of Leicester, University Road, Leicester LE1 7RH, England, UK; email: ltc.leung@leicester.ac.uk, ltcl2@medschl.cam.ac.uk

Molecular Tools for Early Detection of Invasive Malaria Vector *Anopheles stephensi* Mosquitoes

Om P. Singh, Taranjeet Kaur, Gunjan Sharma, Madhavinadha P. Kona, Shobhna Mishra, Neera Kapoor, Prashant K. Mallick

Reports of the expansion of the Asia malaria vector *Anopheles stephensi* mosquito into new geographic areas are increasing, which poses a threat to the elimination of urban malaria. Efficient surveillance of this vector in affected areas and early detection in new geographic areas is key to containing and controlling this species. To overcome the practical difficulties associated with the morphological identification of immature stages and adults of *An. stephensi* mosquitoes, we developed a species-specific PCR and a real-time PCR targeting a unique segment of the second internal transcribed spacer lacking homology to any other organism. Both PCRs can be used to identify *An. stephensi* mosquitoes individually or in pooled samples of mixed species, including when present in extremely low proportions (1:500). This study also reports a method for selective amplification and sequencing of partial ribosomal DNA from *An. stephensi* mosquitoes for their confirmation in pooled samples of mixed species.

Reports of the expansion of the malaria vector *Anopheles stephensi* mosquito (*1*–*6*) are increasing, intensifying the threat of urban malaria (*7*). The gradual southward expansion of this species has been recorded in India since the 1970s (*1*). The first occurrence of *An. stephensi* mosquito in Africa was reported as early as 1966 in a town in Egypt (*2*). During the past 2 decades, several reports of expansion of this species in the Horn of Africa, Sudan, Sri Lanka, and Lakshadweep (a union territory of India) have appeared (*1*–*6*). A high probability of presence within many urban cities across Africa has been predicted, which warrants prioritizing vector surveillance (*8*).

As a consequence of recent invasions of this vector species in several countries, the World Health Organization (WHO) recommended conducting active surveillance of *An. stephensi* mosquitoes in urban and periurban areas, in addition to routine surveillance in rural areas in the affected and surrounding geographic areas (*9*). However, identifying this species, a process that relies mainly on the morphologic characteristics of adult female mosquitoes, is often challenging. Sampling of adult *An. stephensi* mosquitoes from their resting habitats is difficult because they are secretive in their habits (*10*). WHO has recommended sampling immature *An. stephensi* mosquitoes from natural breeding habitats and rearing them in the laboratory until their emergence into adults to enable species identification (*9*). This practice is being adopted for sampling this species in regions of Africa (*4*,*5*,*11*), which is a time-consuming and labor-intensive process. Even freshly emerged adults have been reported to be misidentified as *An. gambiae* mosquitoes because of superficial resemblance (*11*).

Adult mosquito collection through light-trap or pyrethrum spray collections are alternative and popular methods of sampling *An. stephensi* mosquitoes, but identifying adults collected through such methods can be difficult because of the loss of morphologic characteristics critical for their correct identification. Therefore, developing highly specific PCR-based assays is crucial for identifying both larval and adult *An. stephensi* species collected by a variety of methods. Such diagnostics will be helpful to field technologists who are not familiar with the morphology of this species. Those assays can detect *An. stephensi* mosquitoes in a large pool of mosquitoes when their proportion is extremely low. Equally vital is developing a DNA sequencing strategy to confirm the presence of *An. stephensi* mosquitoes in such pools of mixed species. Such molecular tools will help detect invasions of *An. stephensi* mosquitoes early in new geographic areas where they are present in extremely low densities.

Author affiliations: National Institute of Malaria Research, New Delhi, India (O.P. Singh, T. Kaur, G. Sharma, M.P. Kona, S. Mishra, P.K. Mallick); Indira Gandhi National Open University, New Delhi (N. Kapoor)

DOI: https://doi.org/10.3201/eid2901.220786

Methods

Mosquito Samples

We obtained adult mosquitoes or their DNA samples belonging to a total of 17 anopheline and 3 culicine species from different parts of the world either from BEI Resources (https://www.beiresources.org) or locally (Appendix Table, https://wwwnc.cdc.gov/EID/article/29/1/22-0786-App1.pdf). Field-collected *An. stephensi* mosquitoes were processed for identifying biologic forms according to the methods described by Singh et al. (*10*).

DNA Isolation from Individual and Pooled Samples

We isolated DNA from individual specimens as well as pooled samples of mosquitoes to standardize PCR-based assays and their validation. We used pooled samples of different sizes, each consisting of a single *An. stephensi* mosquito and the rest *An. culicifacies* mosquitoes. We also used a pool of field-collected mosquitoes consisting of a single *An. stephensi* mosquito and other species.

We selected 2 commercial kits for DNA isolation. For DNA isolation from individual mosquitoes or smaller pool sizes, we used the DNeasy Blood and Tissue kit (QIAGEN, https://www.qiagen.com), recommended for ≥25 mg of tissue. For larger pools, we used DNAzol Reagent (ThermoFisher Scientific, https://www.thermofisher.com), recommended for 25–50 mg of tissue per milliliter of reagent. In addition, we isolated DNA from individual *An. stephensi* mosquitoes by boiling method.

DNeasy Blood and Tissue Kits

We isolated DNA from individual mosquitoes of some *Anopheles*, *Culex*, and *Aedes* species (Appendix Table) following the manufacturer's protocol and eluted in 200 μL elution buffer. We isolated DNA from smaller pools of III–IV instar larvae or adults, each containing a single *An. stephensi* mosquito and the rest *An. culicifacies* mosquitoes in different pool sizes (i.e., 2, 5, 10, 20, and 50). We also isolated DNA from the single leg of an *An. stephensi* mosquito, which was eluted in 50 μL of elution buffer.

DNAzol Reagent

We used DNAzol Reagent for DNA isolation from pools (i.e., 25, 100, and 500) of adult mosquitoes and pools of 100 larvae (III–IV instar), each containing 1 *An. stephensi* mosquito and the rest *An. culicifacies* mosquitoes. We directly homogenized pools of 25 and 100 mosquitoes in 1 mL of DNAzol reagent in a microcentrifuge tube. In the case of pools of 100 mosquitoes, we transferred 250 μL of the triturate to a separate microcentrifuge tube to make up a volume of 1 mL with DNAzol. We ground the pools of 500 mosquitoes in liquid nitrogen and transferred ≈25 mg of triturate in a microcentrifuge tube and homogenized in 1 mL of DNAzol reagent. We centrifuged all triturates at 10,000 × *g* for 10 min and transferred 500 μL of supernatant to a fresh 1.5-mL microcentrifuge tube, which we subjected to ethanol precipitation, washing, and solubilization of DNA following the vendor's protocol. We dissolved DNA in 200 μL of 8.0 mM NaOH. We also isolated DNA from a pool of 100 mosquitoes containing a single *An. stephensi* mosquito and field-collected (through hand-catch method) mosquitoes belonging to *An. culicifacies*, *An. subpictus*, *An. fluviatilis*, and *Culex quinquefasciatus.*

Boiling Method

We isolated DNA from 10 individual specimens of *An. stephensi* mosquitoes by the boiling method described by Sharma et al. (*13*). We either used the DNA isolated from this method immediately after isolation or preserved it at –20 °C for later use.

Selecting Target Sites for Designing Primers and Probes

We selected ribosomal DNA (rDNA) as a target site for developing diagnostics to identify *An. stephensi* mosquitoes, which are present in hundreds of copies in an individual and are highly conserved in a species because of homogenization of sequence through unequal crossing over and gene conversion, a process known as concerted evolution. We selected the internal transcribed spacer 2 (ITS2) rDNA, which is conserved within a species but highly variable across taxa, for designing *An. stephensi*–specific primers and probes. For designing *An. stephensi*–specific primers and probes, we conducted a homology search of ITS2 sequences of *An. stephensi* (*14*) through a nucleotide BLAST search (https://blast.ncbi.nlm.nih.gov/Blast.cgi). We optimized the search for blastn (somewhat similar sequences) and excluded the taxon *Anopheles stephensi* from the search. All 297 search returns belonged to the *Anopheles* mosquitoes, all belonging to the *Neocellia* series (subgenus *Cellia*); however, none of the returns showed homology to the last 122 bp segment of ITS2. We considered this region unique to *An. stephensi* mosquitoes and exploited this region for designing highly specific *An. stephensi*–specific primers and probes (Figure 1). For designing universal primers and a probe, we identified highly conserved regions from 5.8S and 28S rDNA (Figure 1) based on the alignment of sequences of anophelines available in the GenBank. To verify the specificity of each

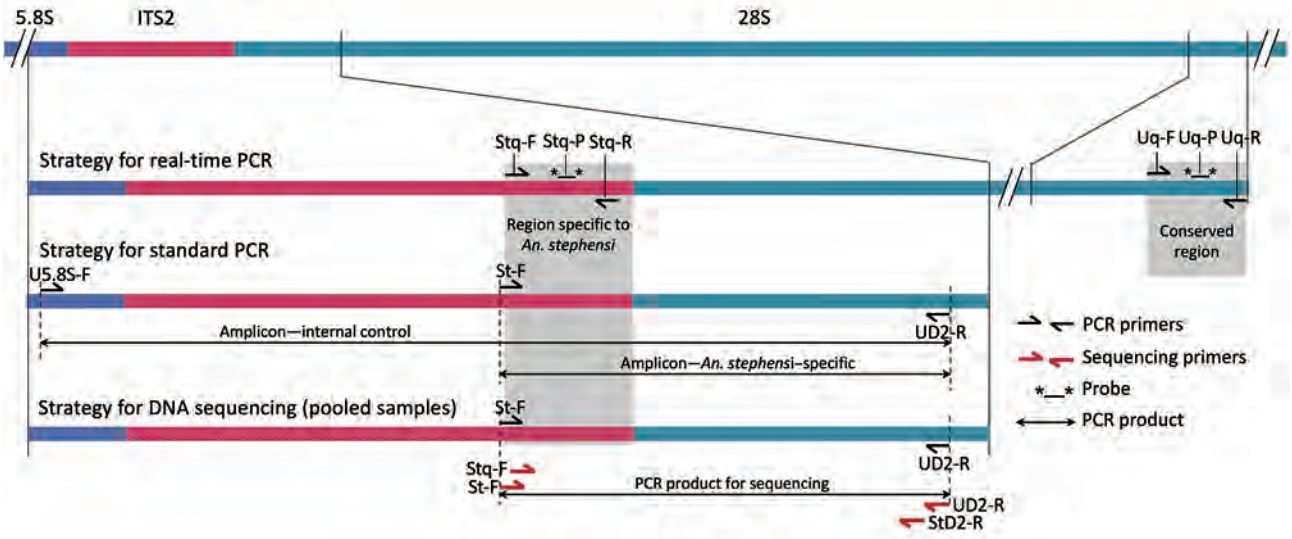

Figure 1. Schematic representation of PCR and sequencing strategies used for early detection of invasive malaria vector *Anopheles stephensi* mosquitoes

An. stephensi–specific primer and probe (Table 1), we performed a blastn search in silico, which ensured that none of the primers and probes matched rDNA sequences of any other mosquitoes.

Development of a Hydrolysis Real-Time PCR

For *An. stephensi*–specific hydrolysis real-time PCR, we designed 2 oligonucleotide primers, (Stq-F and Stq-R) and a hydrolysis probe (Stq-P) from the *An. stephensi*–specific ITS2 region (Table 1; Figure 1). For internal control (IC), we designed primers (Uq-F and Uq-R) and a hydrolysis probe (Uq-P) from a region of 28S-rDNA conserved in anophelines (Table 1; Figure 1). We performed real-time PCR in 10 µL of reaction mixture containing 0.4 µM each of Uq-F, Uq-R and Stq-F; 0.5µM of Stq-R; 0.2 µM of each probe (Stq-P and Uq-P); 1X QuantiFast Multiplex PCR kit (QIAGEN); and 1 µL of template DNA in Bio-Rad CFX96 Touch Real-Time PCR Detection System (https://www.bio-rad.com). The cyclic conditions were predenaturation at 95°C for 5 min, followed by 35 cycles, each with denaturation at 95°C for 10 s and annealing/extension at 60°C for 30 s. We scored the number of cycles required for the fluorescent signal to cross the threshold (cycle threshold [Ct] values) by using the software CFX Maestro (Bio-Rad) (Appendix Figure 1).

We evaluated PCR efficiencies of each hydrolysis probe assay by performing duplex real-time PCR assays in triplicate at 6 different concentrations, diluted serially by 10-fold. We performed the experiments on 2 samples of *An. stephensi* DNA with different DNA concentrations, 8.7 and 3.2 ng/µL (Figure 2). To determine the limit of detection (LOD), we conducted real-time PCR on the diluted DNA of *An. stephensi* mosquitoes with concentrations of 160 fg, 80 fg, 40 fg, and 20 fg, each with 12 replicates.

Development of Size-Diagnostic PCR

For a size-diagnostic PCR, we designed 3 primers: we designed the *An. stephensi*–specific forward primer (St-F) from the *An. stephensi*–specific region of ITS2 and designed 2 flanking universal primers from conserved 5.8S rDNA (U5.8S-F) and D2 domain of 28S rDNA (UD2-R). According to the strategy designed (Figure 1), an *An. stephensi*–specific diagnostic

Table 1. Sequences of primers and probes used in study of molecular tools for early detection of invasive malaria vector *Anopheles stephensi* mosquitoes

Name	Sequence, 5′ → 3′	Annealing specificity	Reference
Stq-F	TCTTTCCTCGCATCCAGTTG	*An. stephensi*	This study
Stq-R	CGGGAGAAGCGGTGATAAAT	*An. stephensi*	This study
Stq-P	/56-FAM/CGTGCTAAC/ZEN/CTCACTCACCCACAC/3IABKFQ/	*An. stephensi*	This study
Uq-F	GAGATTCCCTCTGTCCCTATCT	Universal	This study
Uq-R	AGCTCAACAGGGTCTTCTTTC	Universal	This study
Uq-P	/5HEX/TAGCGAAAC/ZEN/CACAGCCAAGGGAA/3IABKFQ/	Universal	This study
U5.8S-F	ATCACTCGGCTCATGGATCG	Universal	(*15*)
St-F	CGTATCTTTCCTCGCATCCA	*An. stephensi*	This study
UD2-R	GCACTATCAAGCAACACGACT	Universal	This study
StD2-R	GTCTGCCACCACAGTCCT	*An. stephensi*	This study

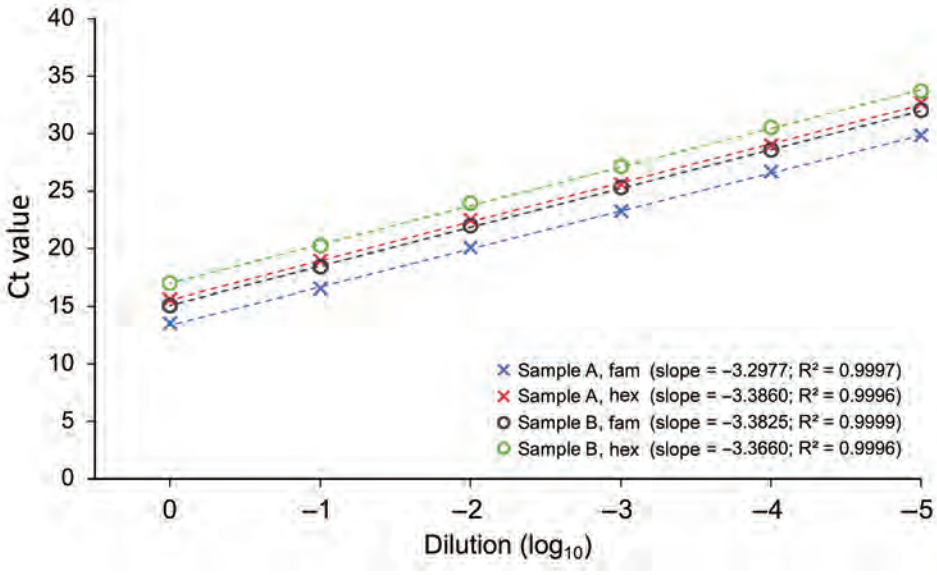

Figure 2. Standard curve showing correlation of Ct values against 10-fold serially diluted DNA samples of *Anopheles stephensi* mosquitoes (2 samples, A and B) in the duplex hydrolysis fluorescent probe assay. The slope of each line represents [–1/log_{10} (PCR efficiency)] for a hydrolysis probe assay. R^2 represents correlation coefficient of a slope. Ct, cycle threshold.

amplicon of 438 bp size will be formed by the primers St-F and D2-R, and a universal amplicon of varying sizes (>600 bp), depending upon the length of ITS2 in a particular species, will be formed by the primers 5.8S and D2-R. The universal amplicon will serve as an IC to rule out PCR failure.

Because of the competitive nature of primers in multiplex-PCR, we optimized 2 protocols of PCR on the basis of the number of mosquitoes in a pool. For individual mosquitoes or smaller pools, we conducted size-diagnostic PCR assays by using Hot Start Taq 2X Master Mix (New England Biolabs, https://www.neb.com) in a 20-μL reaction mixture containing 0.5 units of taq polymerase, 1.5 mM of $MgCl_2$, 0.25 μM of primer St-F, 0.25 μM of primer U5.8S-F, 0.375 μM of UD2-R, and 0.50 μL of DNA template (protocol-1). In another protocol (protocol-2), we reduced the concentration of primer U5.8S-F to 0.10 μM and increased the concentration of UD2-R to 0.50 μM for larger pools of mosquitoes (25–500). We also observed that the intensity of amplicon in size-diagnostic PCR with pools of mosquitoes (>25) could be improved by the dilution of template DNA. Therefore, the template DNA of larger pools of mosquitoes (>25) was further diluted by 1/10 before using it as template DNA for size-diagnostic PCR reactions to minimize the PCR inhibitors in PCR reactions. However, such dilution was not required for real-time PCR. Optimized thermal cycling conditions were an initial denaturation step at 95°C for 30 s, 30 cycles each with a denaturation step at 95°C for 30 s, annealing at 55°C for 30 s and extension at 68°C for 45 s, and final extension at 68°C for 7 min. Five μL of PCR product was run on 2% agarose gel and visualized in the gel documentation system.

DNA Sequencing Strategy for the Confirmation of PCR-Based Identification of *An. stephensi* Mosquitoes in Pooled Samples

We amplified *An. stephensi*–targeted amplicons from DNA isolated from pools of 100 (field-collected) and 500 mosquitoes, each pool containing a single *An. stephensi* mosquito, using primers St-F and UD2-R. We performed PCR by using Hot Start Taq 2X Master Mix in a 20 μL reaction mixture containing 0.25 μM of each primer. PCR conditions were similar to PCR protocol-1 but with extension time reduced to 30 s and number of cycles increased to 35. The amplified products were treated with Exo-Sap II, and sequence termination reactions were performed from both directions of strands using BigDye Terminator v3.1 Cycle Sequencing Kit (both ThermoFisher Scientific). The primers used for sequencing were the primers used for PCR amplification as well as the 2 internal primers (Stq-F and StD2-R) (Table 1; Figure 1). Both internal primers are specific to *An. stephensi* and were expected to provide a noise-free sequence by eliminating the possibility of sequencing nonspecific PCR product. The sequencing products were electrophoresed on an ABI Prism 3730xl (ThermoFisher Scientific).

Results

Real-time PCR

PCR efficiencies, as estimated based on Ct values of 6 serially diluted concentrations of DNA, were 97.5%–

101% for *An. stephensi*–diagnostic (Fam-labeled probe) PCR and 97.4%–98.2% for IC (Hex-labeled probe) PCR (Figure 2). The dynamic range of Ct values for real-time PCR for *An. stephensi*–specific PCR

Table 2. Results of hydrolysis real-time PCR and size-diagnostic PCR on individual and pooled mosquitoes for early detection of invasive malaria vector *Anopheles stephensi* mosquitoes*

Specimen type	DNA isolation method	Real-time PCR			Size-diagnostic PCR		
		No.	Ct values (*An. stephensi*)†	Ct values IC	No.	*An. stephensi*–specific band	IC band
Anophelines							
Neocellia series							
An. stephensi type	DNeasy	26	13.47–17.23	15.20–18.93	24	Positive	Positive
An. stephensi intermediate	DNeasy	2	14.75–15.60	15.39–16.06	2	Positive	Positive
An. stephensi var. *mysorensis*	DNeasy	1	14.54	15.01	1	Positive	Positive
An. stephensi strain STE2	DNeasy	1	14.85–15.25	16.06–16.51	2	Positive	Positive
An. stephensi type form	Boiling	10	15.17–17.41	15.97–18.05	-	Not done	Not done
An. stephensi type form, single leg	DNeasy	4	18.64–22.29	19.02–23.51	4	Positive	Positive
Pyretophorus series							
An. gambiae	DNeasy	3	Negative	14.58–17.32	3	Negative	Positive
An. quadrimaculatus	DNeasy	2	Negative	14.52–15.64	2	Negative	Positive
An. merus	DNeasy	2	Negative	15.22–15.35	2	Negative	Positive
An. subpictus form A	DNeasy	2	Negative	16.61–17.02	1	Negative	Positive
An. subpictus form A‡	Pre-isolated§	1	33.09	18.32		Negative	Positive
An. subpictus form B	Pre-isolated§	2	Negative	16.17–16.35	1	Negative	Positive
An. sundaicus cytoform D	Pre-isolated§	1	Negative	14.47	1	Negative	Positive
Albimanus series							
An. albimanus	DNeasy	2	Negative	16.21–16.58	1	Negative	Positive
Anopheles series							
An. freeborni	DNeasy	2	Negative	15.73–15.81	1	Negative	Positive
An. atroparvus	DNeasy	2	Negative	14.70–15.88	1	Negative	Positive
Neomyzomyia series							
An. dirus	DNeasy	2	Negative	17.34–18.01	1	Negative	Positive
An. farauti	DNeasy	2	Negative	19.09–19.48	1	Negative	Positive
Myzomyia series							
An. funestus	DNeasy	2	Negative	15.50–15.62	1	Negative	Positive
An. culicifacies species A	DNeasy	1	Negative	17.41	1	Negative	Positive
An. culicifacies species B	Pre-isolated§	1	Negative	17.48	1	Negative	Positive
An. fluviatilis species S	Pre-isolated§	1	Negative	16.61	1	Negative	Positive
An. fluviatilis species T	Pre-isolated§	1	Negative	17.02	1	Negative	Positive
Culicines							
Culex quinquefasciatus	DNeasy	3	Negative	16.58–19.20	2	Negative	Positive
Aedes albopictus	DNeasy	2	Negative	16.65–16.68	2	Negative	Positive
Ae. aegypti	DNeasy	2	Negative	18.96–19.20	2	Negative	Positive
Ae. aegypti‡	Pre-isolated§	1	32.95	20.97		Negative	Positive
Single *An. stephensi* individual pooled with *An. culicifacies*¶							
Adults (1/2)	DNeasy	1	17.06	18.31	1	Positive	Positive
Adults (1/5)	DNeasy	1	15.37	16.11	1	Positive	Positive
Adults (1/10)	DNeasy	1	15.77	15.30	1	Positive	Positive
Adults (1/20)	DNeasy	1	15.74	13.71	1	Positive	Positive
Adults (1/50)	DNeasy	1	15.43	11.43	1	Positive	Positive
Adults (1/25)	DNAzol	1	14.53	12.61	1	Positive	Positive
Adults (1/100)	DNAzol	1	16.37	11.27	1	Positive	Positive
Adults (1/500)	DNAzol	2	20.12–23.96	11.08–11.50	2	Positive	Positive
Larvae (1/2)	DNeasy	1	15.56	16.87	1	Positive	Positive
Larvae (1/5)	DNeasy	1	15.49	16.65	1	Positive	Positive
Larvae (1/10)	DNeasy	1	16.36	15.53	1	Positive	Positive
Larvae (1/20)	DNeasy	1	16.51	15.06	1	Positive	Positive
Larvae (1/50)	DNeasy	1	16.27	14.40	1	Positive	Positive
Larvae (1/100)	DNAzol	1	18.14	13.16	1	Positive	Positive
Single *An. stephensi* individual pooled with field collected mosquitoes (mixed mosquito-species)¶							
Adults (1/100)	DNAzol	1	17.61	11.70	1	Positive	Positive

*Ct, cycle threshold; IC, internal control.
†Ct value shown as Negative implies that no Ct value was scored within 35 cycles of reactions.
‡Contaminated with *An. stephensi* DNA.
§Preserved DNA isolated manually for other studies.
¶Denominator of numeric expression inside parenthesis indicate total number of mosquitoes in a pool.

was 13.5–32 and for IC-PCR was 15.5–33.5; the LOD was 40 fg of genomic DNA.

The real-time PCRs conducted on DNA isolated from individual *An. stephensi* mosquito samples, 19 different nontarget *Anopheles* mosquito species, and a single *An. stephensi* mosquito in different pool sizes were specific based on software-determined Ct value scored within 35 cycles of reactions, except in the case of 2 preisolated DNA (1 each of *Aedes aegypti* and *An. subpictus* mosquitoes) showing false positivity with late Ct values (>32) (Table 2). The 2 false-positive samples were contaminated with the *An. stephensi* mosquito DNA as revealed through *An. stephensi*–targeted sequencing (Appendix). Although primers and probe for IC were designed on the basis of anophelines' 28S rDNA sequences, they also worked on all 3 nonanopheline species tested (i.e., *Cx. quinquefasciatus*, *Ae. aegypti*, and *Ae. albopictus* mosquitoes). The real-time PCR also successfully identified *An. stephensi* mosquito from DNA samples isolated by boiling method and DNA isolated from a single leg of mosquitoes. The real-time PCR was sensitive to detecting a single *An. stephensi* mosquito in pools of 500 mosquitoes with low Ct values (<24) (Table 2). Rising of fluorescent signal was noticed with IC probe in some experiments only in negative controls after 30 cycles but not with *An. stephensi*–specific probe (Appendix Figure 1).

Size-Diagnostic PCR

We performed PCR protocol-1 on DNA samples isolated from individual *An. stephensi* mosquito samples, nontarget mosquitoes, and pooled samples of mixed species (≤50 mosquitoes), which provided desired amplicons. All *An. stephensi* mosquitoes were positive for *An. stephensi*–specific band (438 bp), and all other mosquito species were negative (Table 2; Figures 3, 4). All species exhibited amplification of an IC band of varying sizes (>600 bp). *Ae. aegypti* mosquitoes exhibited the smallest IC band (≈650 bp) because of the shortest length of ITS2 (200 bp). *An. funestus* and *An. dirus* mosquitoes exhibited the largest IC bands (>1 kb) because of longer ITS2 (700 bp). PCR protocol 1 successfully identified *An. stephensi* mosquitoes in all pooled samples of mixed species, where the *An. stephensi*–specific band was prominent in pools of ≤20 mosquitoes. We observed that the *An. stephensi* mosquito diagnostic band grew fainter as the concentration of *An. stephensi* mosquito DNA decreased in larger pools (Figure 3, panel A). Therefore, a different protocol (protocol 2) with different primer concentrations was adopted for larger pools. PCR protocol 2 successfully identified *An. stephensi* mosquitoes in pools of 25–500 mosquitoes and provided clearly visible *An. stephensi*–specific band in pools of ≤100 mosquitoes. On the basis of these results, we found PCR protocol-1 suitable for individual samples or smaller pools (up to 25) (Figure 3, panel A) and PCR protocol-2 suitable for larger pools (25–100 mosquitoes) (Figure 3, panels B and C).

Sequencing Results

An. stephensi–targeted DNA sequencing was successful with all 4 sequencing primers. The quality of DNA sequences generated from pooled mosquitoes was reasonably high (Appendix Figure 2). The output

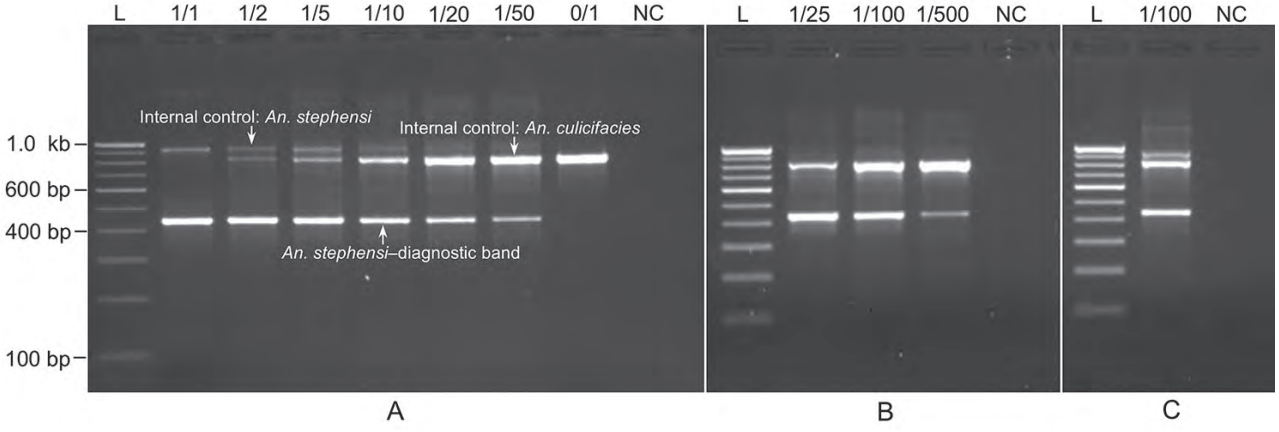

Figure 3. Gel photographs visualizing the result of PCRs specific to invasive malaria vector *Anopheles stephensi* mosquitoes. A) PCR protocol 1 on individual specimens and pools of *An. stephensi* and *An. culicifacies.* B) PCR protocol 2 on larger pools of *An. stephensi* and *An. culicifacies*. C) PCR protocol 2 on a pool of 100 mosquitoes containing a single *An. stephensi* mixed with other wild-caught anophelines (*An. culicifacies*, *An. fluviatilis*, *An. minimus*, and *An. subpictus*). The numerator of numeric expression shown on the top of each lane indicates number of *An. stephensi* in a pool, and denominator indicates size of mosquito-pool. L, 100-bp ladder; NC, negative control.

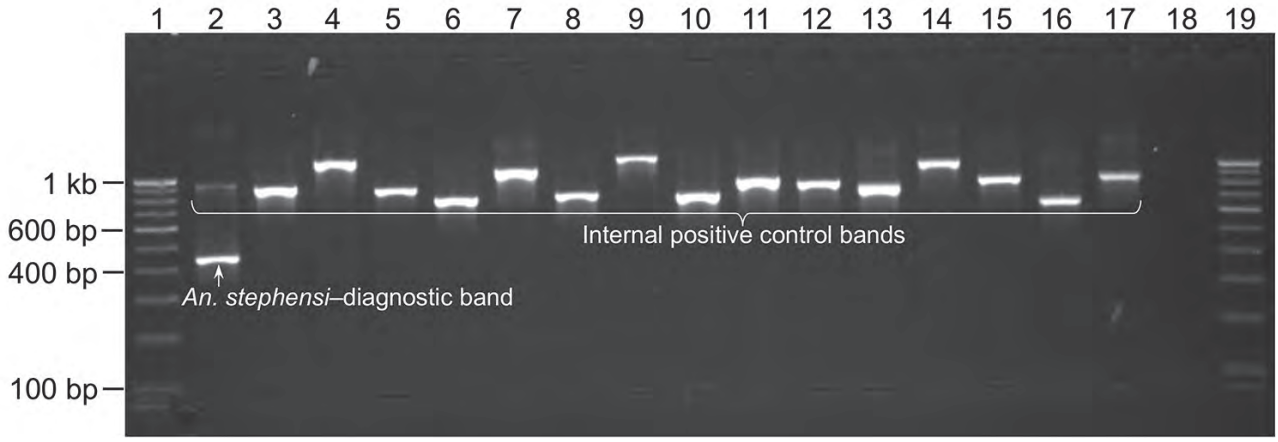

Figure 4. Gel photograph showing the result of PCR specific to invasive malaria vector *Anopheles stephensi* mosquitoes (protocol 1) on some individual mosquitoes belonging to the genus *Anopheles*, *Culex*, and *Aedes*. Lanes 1 and 19, 100-bp DNA ladder; 2, *An. stephensi*; 3, *An. gambiae*; 4, *An. dirus*; 5, *An. albimanus*; 6, *An. quadrimaculatus*; 7, *An. farauti;* 8, *An. freeborni*; 9, *An. funestus*; 10, *An. atroparvus*; 11, *An. merus*; 12, *An. fluviatilis* species T*;* 13, *Cx. quinquefasciatus;* 14, *An. subpictus* molecular form A; 15, *An. minimus* sensu strictu; 16, *Ae. aegypti*; 17, *Ae. albopictus*; 18, negative control.

sequences showed 100% similarity with *An. stephensi* mosquito sequences in a BLAST search. The second highest similarity was with *An. superpictus* mosquitoes, which demonstrated 94.88% similarity on the basis of only 73% coverage. The remaining 27% nucleotide sequence belonging to the ITS2 region did not show a match with any organism other than *An. stephensi* mosquitoes.

Discussion

The molecular methods developed in this study can identify and confirm *An. stephensi* mosquitoes individually or in a large pool of mixed mosquito species, which could enable screening of large numbers of samples collected through a variety of methods (such as light trap, pyrethrum spray collection, larval collection, etc.) with relatively limited effort and time. This method could help in early reporting of the presence of *An. stephensi* mosquitoes to concerned state health agencies and WHO.

In molecular diagnostics, we designed *An. stephensi*–specific primers and probes from a segment of ITS2 lacking homology to any other organisms for which the rDNA sequence database is available in the public domain, enabling the design of primers that are highly specific to *An. stephensi* mosquitoes and refractory to nonspecific annealing. However, this process does not preclude the possibility of any mosquito's sequence, as-yet unreported, having matching sequences with *An. stephensi*–specific primers or probes. Therefore, confirmatory DNA sequencing should be performed in new areas using the *An. stephensi*–specific primers suggested in this report.

In earlier studies, confirmation of this species was done through sequencing of ITS2 and mitochondrial DNA using universal primers, which cannot be used in pooled samples of mixed species. Moreover, Mishra et al. (*14*) have shown that direct DNA sequencing of ITS2 in the case of *An. stephensi* mosquitoes is not fruitful because of the presence of indel variants, which causes the collapse of a sequence starting from the indel position. The method proposed here for sequencing *An. stephensi* mosquitoes in a pooled sample was targeted to indel-free partial ITS2 (which lacks homology with any organism) and D1-D2 domains of 28S of rDNA, which are species-informative.

The real-time PCR developed in this study is for diagnostic purposes only and by no means intended for quantitative PCR (qPCR); qPCR is not reliable in the case of pooled mosquitoes belonging to different species because of interspecific variations in rDNA copy number (*16*) and body mass. However, the proportion of *An. stephensi* mosquitoes in a mosquito population, when present in extremely low density, can be obtained by the method used for the estimation of infection rates in hematophagous insects by estimating minimum infection rate or maximum-likelihood procedure (*17*) on the basis of the number of pools positive, methods frequently used for xenomonitoring.

LOD for the real-time PCR is considered a vital criterion for assessing the sensitivity of real-time PCR when the copy number of target nucleic acid is a limiting factor (e.g., detecting pathogens in an organism). However, LOD is not a limiting factor for the *An. stephensi*–specific diagnostic real-time PCR; rDNA is abundantly found in the organism because

of its high copy number. We observed in this study that LOD cannot be a limiting factor even when the proportion of target mosquitoes is 1/500 in a pooled sample or tested on DNA isolated from a single leg (Ct values <24). On the basis of our observations, we suggest a cutoff value of 30 for real-time PCR for more reliable results. Ct values above this threshold can be suspected to be DNA contamination which should be verified through DNA sequencing (Appendix). In this study, we observed false positivity for *An. stephensi* mosquitoes with late Ct values (>32) in 2 DNA samples (1 each of the *Ae. aegypti* and *An. subpictus* mosquito) because of the contamination of DNA from *An. stephensi* mosquitoes.

The diagnostic PCRs in this study were designed to identify *An. stephensi* mosquitoes in large pools of samples. However, pooling of a large number of samples can accumulate potential PCR inhibitors. The heme compound in the blood (*18*) and eye pigment in the head of an insect (*19*) are reported potential inhibitors. Although we did not observe inhibitory effect of pooling in the real-time PCR, we observed substantial inhibitory effect in a size-diagnostic PCR with a pool of ≥50 mosquitoes. In this study, we experienced an improvement in the intensity of the band in size-diagnostic PCR in such pools by diluting DNA.

Although we have successfully demonstrated identifying a single *An. stephensi* mosquito in pools of 500 mosquitoes, using a pool of up to 100 mosquitoes that can be ground in a single microcentrifuge tube during DNA isolation without the need for grinding by mortar and pestle is recommended. Grinding by using a mortar and pestle might increase the risk for carryover contamination. For confirmation of *An. stephensi* mosquitoes in pooled samples through Sanger sequencing, we suggest using internal primers (Stq-F and StD2-R, both of which are specific to *An. stephensi* mosquitoes) for sequence termination reactions as a precautionary measure. This step is critical to rule out sequencing of false-positive PCR products because of nonspecific annealing with unknown nontarget species, if any.

In conclusion, the molecular tools developed in this study can be used to identify and confirm *An. stephensi* mosquitoes, individually or in a pool of mixed mosquito species. This process will enable health authorities to detect early invasion of the species, especially in areas where it exists with low density.

Acknowledgment

We thank Kanwar Singh for mosquito collection, Priya and Vijay Kumar for DNA sequencing, and Abhinav Sinha for critical review of the manuscript.

The following reagents were obtained through BEI Resources, National Institute of Allergy and Infectious Diseases, National Institutes of Health: *An. gambiae*, strain G3, MRA-132K; *An. albimanus* strain STECLA, MRA-133K; *An. stephensi*, strain STE2, MRA-134K; *An. freeborni*, strain F-1, MRA-136K; *An. quadrimaculatus*, strain ORLANDO, MRA-137K; *An. dirus*, strain WRAIR2, MRA-700K; and *An. farauti*, strain FAR1, MRA-489K, all contributed by Mark Q. Benedict; *An. funestus*, strain FUMOZ, MRA-1027K, contributed by Maureen Coetzee; *An. merus*, strain OPHANSI, MRA-803B, contributed by Rajendra Maharaj; and *An. atroparvus*, strain EBRO, MRA-493B, contributed by Carlos Aranda and Mark Q. Benedict.

This research was supported by Science and Engineering Board (SERB), India. The dataset supporting the conclusions of this article is included within the article.

O.P.S. designed PCR strategies, analyzed data, and wrote the first draft of the manuscript; G.S., T.K., M.P.K., and P.K.M. performed laboratory experiments; P.K.M., S.M., and N.K. contributed to the manuscript. All authors approved the final version of the manuscript.

About the Author

Dr. Singh is a scientist at the National Institute of Malaria Research, New Delhi. His primary research interests include the molecular basis of insecticide resistance in disease vectors and developing molecular tools for vector surveillance.

References

1. Sharma SK, Hamzakoya KK. Geographical spread of *Anopheles stephensi* vector of urban malaria, and *Aedes aegypti*, vector of dengue/DHF, in the Arabian Sea Islands of Lakshadweep, India. Dengue Bulletin. 2001;25:88–91. WHO Regional Office for South-East Asia [cited 2020 Nov 24]. https://apps.who.int/iris/handle/10665/148798
2. Gad AM. *Anopheles stephensi* liston in Egypt, UAR. Mosq News. 1967;27:171–4.
3. Faulde MK, Rueda LM, Khaireh BA. First record of the Asian malaria vector *Anopheles stephensi* and its possible role in the resurgence of malaria in Djibouti, Horn of Africa. Acta Trop. 2014;139:39–43. https://doi.org/10.1016/j.actatropica.2014.06.016
4. Carter TE, Yared S, Gebresilassie A, Bonnell V, Damodaran L, Lopez K, et al. First detection of *Anopheles stephensi* Liston, 1901 (Diptera: culicidae) in Ethiopia using molecular and morphological approaches. Acta Trop. 2018;188:180–6. https://doi.org/10.1016/j.actatropica.2018.09.001
5. Balkew M, Mumba P, Dengela D, Yohannes G, Getachew D, Yared S, et al. Geographical distribution of *Anopheles stephensi* in eastern Ethiopia. Parasit Vectors. 2020;13:35. https://doi.org/10.1186/s13071-020-3904-y
6. Gayan Dharmasiri AG, Perera AY, Harishchandra J, Herath H, Aravindan K, Jayasooriya HTR, et al. First record of *Anopheles stephensi* in Sri Lanka: a potential challenge for prevention of malaria reintroduction.

Malar J. 2017;16:326. https://doi.org/10.1186/s12936-017-1977-7
7. Takken W, Lindsay S. Increased threat of urban malaria from *Anopheles stephensi* mosquitoes, Africa. Emerg Infect Dis. 2019;25:1431–3. https://doi.org/10.3201/eid2507.190301
8. Sinka ME, Pironon S, Massey NC, Longbottom J, Hemingway J, Moyes CL, et al. A new malaria vector in Africa: predicting the expansion range of *Anopheles stephensi* and identifying the urban populations at risk. Proc Natl Acad Sci U S A. 2020;117:24900–8. https://doi.org/10.1073/pnas.2003976117
9. World Health Organizaton. Vector alert: *Anopheles stephensi* invasion and spread. 2019. WHO reference number: WHO/HTM/GMP/2019.09 [cited 2020 Nov 24]. https://apps.who.int/iris/rest/bitstreams/1242915/retrieve
10. Christophers SR. The fauna of British India, including Ceylon and Burma. Diptera. 4. Family Culicidae, Tribe Anophelini. London: Taylor and Francis; 1933.
11. Ahmed A, Khogali R, Elnour MB, Nakao R, Salim B. Emergence of the invasive malaria vector *Anopheles stephensi* in Khartoum State, Central Sudan [Erratum in: Parasit Vectors. 2021;14:562]. Parasit Vectors. 2021;14:511. https://doi.org/10.1186/s13071-021-05026-4
12. Singh OP, Mishra S, Sharma G, Sindhania A, Kaur T, Sreehari U, et al. Evaluation of intron-1 of odorant-binding protein-1 of Anopheles stephensi as a marker for the identification of biological forms or putative sibling species. PLoS One. 2022;17:e0270760. https://doi.org/10.1371/journal.pone.0270760
13. Sharma G, Lather M, Singh OP. Variations in palpal ornamentation of *Anopheles fluviatilis* species T and U (Diptera: Culicidae) and their taxonomic consequence. Indian J Exp Biol. 2020;58:64–8. https://doi.org./10.56042/ijeb.v58i01.65321
14. Mishra S, Sharma G, Das MK, Pande V, Singh OP. Intragenomic sequence variations in the second internal transcribed spacer (ITS2) ribosomal DNA of the malaria vector *Anopheles stephensi.* PLoS One. 2021;16:e0253173. https://doi.org/10.1371/journal.pone.0253173
15. Manonmani A, Townson H, Adeniran T, Jambulingam P, Sahu S, Vijayakumar T. rDNA-ITS2 polymerase chain reaction assay for the sibling species of Anopheles fluviatilis. Acta Trop. 2001;78:3–9. https://doi.org/10.1016/S0001-706X(00)00154-6
16. Kumar A, Rai KS. Chromosomal localization and copy number of 18S + 28S ribosomal RNA genes in evolutionarily diverse mosquitoes (Diptera, Culicidae). Hereditas. 1990;113:277–89. https://doi.org/10.1111/j.1601-5223.1990.tb00094.x
17. Walter SD, Hildreth SW, Beaty BJ. Estimation of infection rates in population of organisms using pools of variable size. Am J Epidemiol. 1980;112:124–8. https://doi.org/10.1093/oxfordjournals.aje.a112961
18. Akane A, Matsubara K, Nakamura H, Takahashi S, Kimura K. Identification of the heme compound copurified with deoxyribonucleic acid (DNA) from bloodstains, a major inhibitor of polymerase chain reaction (PCR) amplification. J Forensic Sci. 1994;39:362–72. https://doi.org/10.1520/JFS13607J
19. Boncristiani H, Li J, Evans J, Pettis J, Chen Y. Scientific note on PCR inhibitors in the compound eyes of honey bees, *Apis mellifera.* Apidologie (Celle). 2011;42:457–60. https://doi.org/10.1007/s13592-011-0009-9

Address for correspondence: Om P. Singh, National Institute of Malaria Research, Sector 8, New Delhi-110077, India; email: singh@nimr.org.in; dr.opsingh@gmail.com

EID Podcast

Isolation Cocoon, May 2020—After Zhuangzi's Butterfly Dream

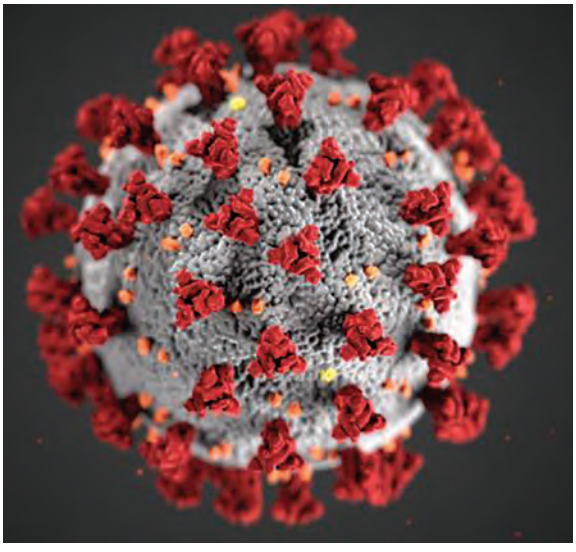

For many people, the prolonged period of social distancing during the coronavirus disease pandemic felt frightening, uncanny, or surreal.

For Ron Louie, the sensation was reminiscent of a moth taking refuge in its cocoon, slumbering in isolation as he waited for better days ahead.

In this EID podcast, Dr. Ron Louie, a clinical professor in Pediatrics Hematology-Oncology at the University of Washington in Seattle, reads and discusses his poem about the early days of the pandemic.

Visit our website to listen: https://go.usa.gov/x6W9A

EMERGING INFECTIOUS DISEASES®

Integrating Citizen Scientist Data into the Surveillance System for Avian Influenza Virus, Taiwan

Hong-Dar Isaac Wu, Ruey-Shing Lin, Wen-Han Hwang, Mei-Liang Huang, Bo-Jia Chen, Tseng-Chang Yen, Day-Yu Chao

The continuing circulation and reassortment with low-pathogenicity avian influenza Gs/Gd (goose/Guangdong/1996)-like avian influenza viruses (AIVs) has caused huge economic losses and raised public health concerns over the zoonotic potential. Virologic surveillance of wild birds has been suggested as part of a global AIV surveillance system. However, underreporting and biased selection of sampling sites has rendered gaining information about the transmission and evolution of highly pathogenic AIV problematic. We explored the use of the Citizen Scientist eBird database to elucidate the dynamic distribution of wild birds in Taiwan and their potential for AIV exchange with domestic poultry. Through the 2-stage analytical framework, we associated nonignorable risk with 10 species of wild birds with ≥100 significant positive results. We generated a risk map, which served as the guide for highly pathogenic AIV surveillance. Our methodologic blueprint has the potential to be incorporated into the global AIV surveillance system of wild birds.

Mapping the interface risk between wild birds and poultry requires information of wild bird distribution and migration patterns. Bird band recovery or global positioning system (GPS) tracking data are used for spatial risk mapping. Recently, citizen science data has become an increasingly valuable source for addressing a wide range of ecologic research questions. With this study, we provided the analytical framework of using eBird, a Citizen Scientist database (https://www.citizenscience.gov), to elucidate the dynamic distribution of wild birds and their potential for avian influenza virus (AIV) exchange with domestic poultry. We generated a risk map that can be integrated into the current AIV surveillance system, enabling strategic allocation of limited resources for spatially targeted virologic surveillance. The coding source, the open terrestrial environmental dataset, and eBird dataset are fully available at http://aiv.nchu.edu.tw.

AIV is an influenza A virus that belongs to the Orthomyxoviridae family. AIVs have been identified in a wide variety of species of wild and domestic birds, but their natural reservoir is wild waterbirds of the orders Anseriformes and Charadriiformes (e.g., ducks, geese, swans, and shorebirds). Wild waterbirds maintain a diverse group of low-pathogenicity avian influenza A viruses (LPAIVs), which cause limited illness in these host species (*1*). On the contrary, highly pathogenic influenza A viruses (HPAIVs), characterized by mortality of gallinaceous poultry, are limited to H5 or H7 subtypes and continue to cause illness and death in poultry worldwide (*2*,*3*). Periodically, human infections associated with HPAIV have been detected (*4*). In particular, the Eurasian (goose/Guangdong/1996 [Gs/Gd]) lineage has substantially affected global epizootic outbreaks of highly pathogenic avian influenza (HPAI), which have become enzootic in some areas and involve multiple waves of influenza with genetically distinct virus clades and subclades (*5*). Wild geese and ducks may form the bridge for AIV transmission between wild and domestic birds, which are kept alongside each other, creating the opportunity for genetic mixing of HPAIVs and LPAIVs when they infect the same bird concomitantly. Such genetic mixing promotes bidirectional virus exchange between wild and domestic birds for the continued adaptation of Gs/Gd HPAIVs in wild bird hosts and long-distance spread to new geographic regions along the flyway (*6*–*8*). Information about where wild and domestic birds can

Author affiliations: National Chung Hsing University, Taichung, Taiwan (H.-D.I. Wu, W.-H. Hwang, M.-L. Huang, B.-J. Chen, T.-C. Yen, D.-Y. Chao); Taiwan Endemic Species Research Institute, Jiji Town, Taiwan (R.S. Lin)

DOI: https://doi.org/10.3201/eid2901.220659

potentially interact on the landscape can help identify areas where disease transmission may be more likely to occur, useful for risk management and control measures. Such regions could become focal areas for surveillance and prevention (*9*).

The first step of mapping the interface risk requires information of wild bird distribution and migration patterns; however, obtaining such information is difficult. Without empirical data, previous studies implemented simulations or mathematical modeling for spatial risk mapping (*10*–*13*). Meanwhile, bird migration routes can be acquired from the bird band recovery (*14*) or GPS tracking data (*15*), but only a limited number of wild birds can be tracked and analyzed. Citizen science data are valuable for addressing a wide range of ecologic research questions, and the scope and volume of available data have rapidly increased globally (*16*). However, data from large-scale citizen science projects typically present a number of challenges that can inhibit robust ecologic inferences, including species bias, spatial bias, varied efforts, and varied observer skills (*17*–*19*). When using citizen science data, it is imperative to carefully consider the data processing and analytical procedures required to appropriately address the bias and variation.

Since 2015, Taiwan, which is on the East Asian Flyway of bird migration, has been affected by HPAI H5 virus clade 2.3.4.4, resulting in tremendous economic loss (*20*,*21*). In this study, we established an analytical framework (Figure 1) using citizen science data, eBird (*22*), to map the interface risk between wild birds and poultry flocks and to shed light on the underlying mechanism of AIV transmission in Taiwan. Our risk map presents a quantitative evaluation of the risk for AIV exchange at the interface between poultry flocks and wild birds, thereby enabling strategic allocation of limited resources for spatial targeting surveillance for AIV in wild birds and poultry.

Materials and Methods

Datasets and Software

We obtained bird-sighting records from the eBird Citizen Science database, the world's largest citizen science program, providing fine-scale occurrence data of bird species (*23*). The reporting system is based on checklists (*22*), whereby the observer provides a list of birds detected, GPS location, sampling effort (whether all detected species are reported), sampling duration, sampling protocol (e.g., stationary point, travel, and banding and distance traveled in the case of traveling protocol), starting time of the sampling event, and number of observers. We used the eBird Taiwan dataset focusing on the records from January 2015 through June 2020. The Taiwan Endemic Species Research Institute, Council of Agriculture, Taiwan, established an open terrestrial environmental dataset with 1-km high resolution spanning 5-decade periods during 1970–2020 and used it to predict occupancy probability of the selected wild bird species (*24*). This dataset contains 100 variables, including 9 land-cover types (e.g., farmland, forest, or wetland), 8 topographies (e.g., latitude or slope), 79 climates (e.g., monthly average temperature or rainfall), and 4 other variables (e.g., traffic or length of roads). From the Council of Agriculture, Taiwan, we obtained the

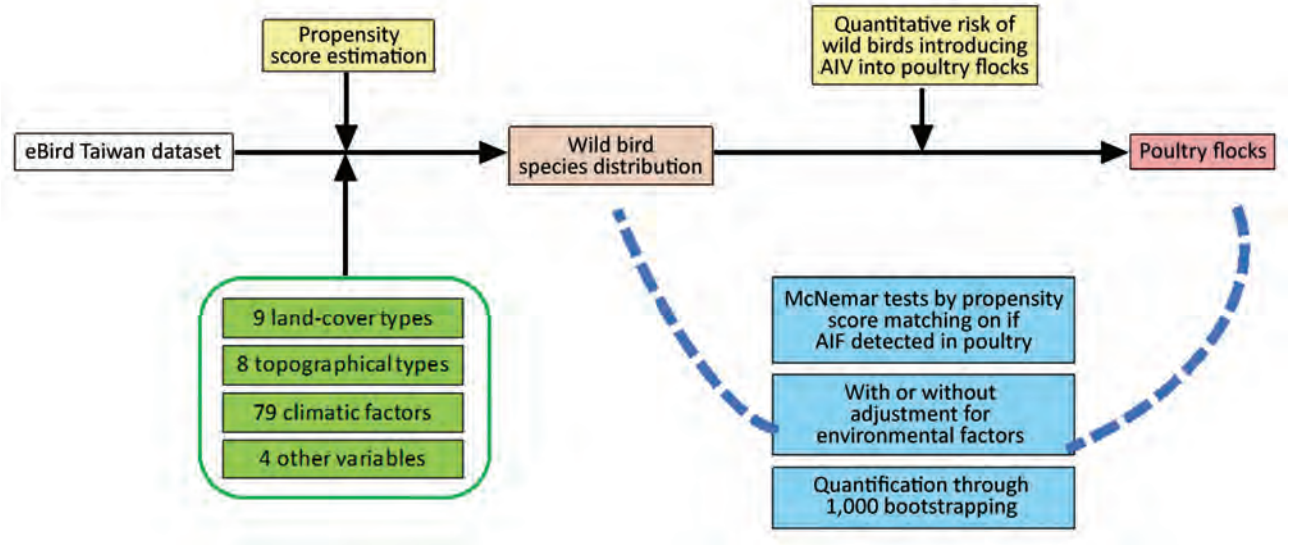

Figure 1. Framework of the analyses performed to map the risk of wild birds introducing avian influenza virus (AIV) into poultry farms for study of integrating citizen scientist data into the surveillance system for avian influenza virus, Taiwan.

complete poultry farm census dataset, established in 2017 and based on an islandwide survey that used remote satellite imaging technology conducted by the Taiwan Agriculture Research Institute. The poultry farm outbreaks dataset was obtained from the surveillance system established by the Bureau of Animal and Plant Health Inspection and Quarantine, Taiwan, as described previously (*20*,*25*). During 2015–2017, a total of 1,223 poultry farm outbreaks were reported and laboratory confirmed in Taiwan (1,003 outbreak poultry farms in 2015, 38 in 2016, and 182 in 2017).

We partitioned Taiwan into 4,762 squares, each 3 × 3 km, consisting of 306 grids, covering the coastline for follow-up spatial modeling. We performed all graphs and statistics in R software (The R Foundation for Statistical Computing, https://www.R-project.org) and produced maps by using QGIS (https://www.qgis.org). The packages used in R can be found from coding sources provided at http://aiv.nchu.edu.tw/Open_data.html.

Spatial Exploration

To explore the spatial relationship of land-cover types or wild bird distribution, we subjected the area of each land-cover type or propensity score from each grid estimated for individual wild bird species from the wild bird species distribution map to principal component analysis and t-distributed stochastic neighbor embedding (tSNE) analysis. The tSNE analysis is a modern dimension reduction method that uses an iterative algorithm to visualize the high-dimensional data in 2 dimensions while also revealing some global structures (i.e., clusters) (*26*).

Wild Bird Species Distribution Map

To investigate the risk for AIV exchange at the interface between poultry flocks and wild birds, we first mapped the potential distribution of the wild bird species (Figure 1). All spatial models are based on partitions, which generated 4,762 grids, 3 × 3 km each. To eliminate spatial counting bias in eBird data, we applied a set of autoregressive logistic models to the eBird Taiwan dataset to estimate the occupancy probability of the distribution of each species of wild bird in each spatial grid (*27*) (Appendix 1, https://wwwnc.cdc.gov/EID/article/29/1/22-0659-App1.pdf). Because multicollinearity might be present, to improve the stability of regression estimation, we used the elastic net method for variable selection. If the zero-inflated Poisson model did not fit the data well, we used the zero-inflated negative binomial regression model instead (*28*,*29*). Last, we used the occupancy probability of each bird species for individual grids to generate the distribution map for individual bird species. The estimated probability of occupancy is the propensity score, which we used for the matched-pair design (*30*).

Risk Mapping at the Interface of Wild Birds and Poultry

A fundamental problem with mapping the risk for AIV transmission at the interface between wild birds and poultry is the difficulty of quantifying the amount of contact between them. Hence, we measured relative spatial risk on a 3-km × 3-km grid by matching on the propensity score the occupancy probability (P_m) of each bird species. The tolerance of matching criterion is $P_m \times 10\%$, which means if the case grid has its estimated score , the matched control should have a score lying within the tolerance interval ($P_{m,l}$,$P_{m,u}$), in which $P_{m,l} = 0.90$ and $P_{m,u} = \min(1.10, 1)$. We considered the approach of matched-pair design, in which the case grid contains ≥1 poultry farm outbreak and the control grid contains poultry farms with no outbreaks during 2015–2017. Because the species of wild bird is both itself a risk factor as well as a confounder, propensity scores for each species with respect to all other species are matched out. By this manner, we estimated the partial effect of that particular species, possibly with adjustment for environmental and terrestrial factors. The association was measured by the McNemar χ^2 statistic on 1 degree of freedom. Because there could be many candidate controls for each case grid, we performed 1,000 bootstrapped resamplings to produce 1,000 -realizations under the null hypothesis that the specific species of bird has no association with the outbreaks. We report the bootstrap results using the notations N_{pa} = number of positive associations in 1,000 replicates and N_{sp} = number of significant positive associations in those N_{pa} experiments (Table). The proportion of N_{sp} can be interpreted as parallel to the concept of p value, if the complement of ($1 - N_{sp}/1{,}000$) is taken. The proportion of $N_{sp}/1{,}000$ reflects the strength against the null hypothesis; higher values imply stronger evidence. However, we did not adopt a strict criterion for statistical significance; that is, we did not require p to be <0.05 (Appendix 1). We used the proportion of N_{sp} as the probability of AIV being introduced by the wild birds into poultry farms or vice versa.

After matched-pair McNemar analysis, we used only the bird species with positive association to depict a risk map of AIV exchange at the interface between poultry flocks and wild birds. The risk, defined as an infection probability (R_j) of grid j, can be estimated by an additive-multiplicative risk model (Appendix 1).

Table. Risk for avian influenza virus transmission from wild birds to poultry, with and without adjustments for environmental and terrestrial factors*

Wild bird species		Without adjustment		With adjustment	
Scientific name	Common name	N_{pa}	N_{sp} (in N_{pa})	N_{pa}	N_{sp}
Calidris subminuta	Long-toed stint	998	544	1,000	784(A)
Chroicocephalus ridibundus	Black-headed gull	1,000	896	1,000	482
Tachybaptus ruficollis	Little grebe	976	116	998	402
Gallinago gallinago	Common snipe	944	87	991	191
Anas acuta	Pintail duck	916	18	980	174
Pluvialis fulva	Pacific golden plover	987	171	993	157
Himantopus himantopus	Black-winged stilt	968	138	816	27
Sternula albifrons	Little tern	999	416	964	9
Hirundo rustica	House swallow	956	119	X	X
Bubulcus ibis	Cattle egret	972	188	X	X

*N_{pa}, no. positive associations in 1,000 replicates; N_{sp}, no. significant positive associations in the N_{pa} experiments.

Results

We report all grids with bird-sighting records for 2015–2020 (Figure 2, panel A). There are no records for central grids of Taiwan because they are high-mountain areas and are not easily accessible by bird sighters. Because poultry farms are not distributed in the high-mountain areas (Figure 2, panels B, C), such sparse data did not affect our follow-up analysis.

Occupancy probability was estimated by zero-inflated Poisson model (Figure 3, panel B). The distribution of the predicted occupancy probability is consistent with the bird-sighting distribution from the observer records (Figure 3, panel A) and highly overlaps with the wetland land-cover type (Figure 3, panel C). Distribution maps for all 68 species of wild bird are shown at http://aiv.nchu.edu.tw/migrating_species.html. Among the 68 species, 66 selected for this study can be well modeled for their occupancy probabilities by using a zero-inflated Poisson model.

The major land-cover type in Taiwan is forest, which comprises 55.8% of the total area of Taiwan's main island, and <0.1% of the area is poultry farms (Figure 4, panel A). On the contrary, <2.5% of main island area is covered by bush, wetland, and bare land, which are the main land-cover types for poultry farming. Water bodies cover only 1.19% of the island but also contain 3.27% of the area for poultry farming, mainly Anseriformes, such as ducks and geese. Because the estimated occupancy probability of wild bird species is based on 4,762 grids, 3-km × 3-km, generated for the whole island, many grids are made of mixed land-cover types (Figure 4, panel B). To explore the relationship of wild bird distribution with land-cover type, the estimated occupancy probabilities, also referred to as propensity scores, of 68 different species of

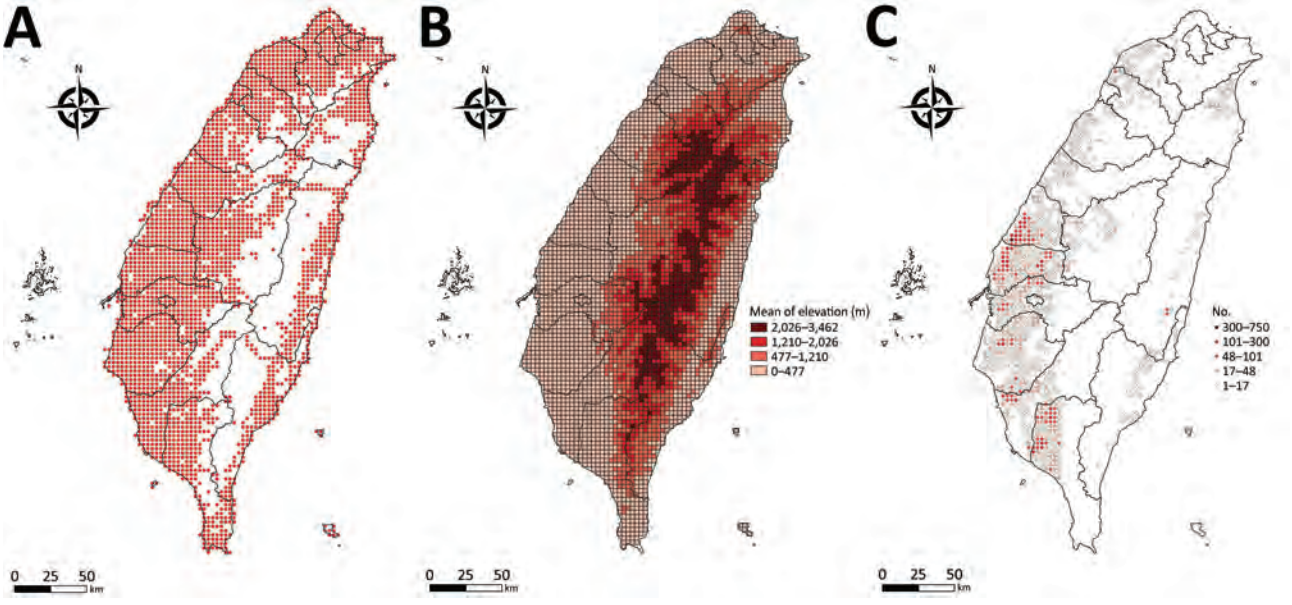

Figure 2. Distribution maps for study of integrating citizen scientist data into the surveillance system for avian influenza virus, Taiwan. A) The 3-km × 3-km grid with bird-sighting records based on Taiwan eBird dataset during 2015–2020; B) average altitude based on Taiwan open terrestrial environmental dataset; C) poultry farm census data for Taiwan.

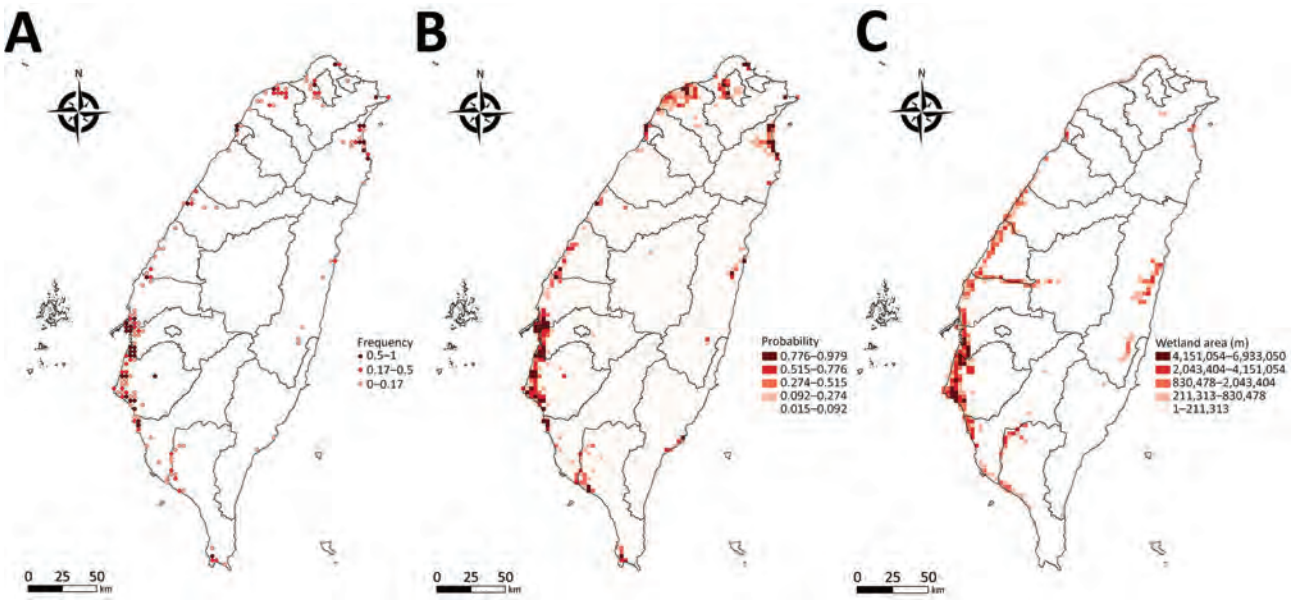

Figure 3. Distribution maps of pintail duck (*Anas acuta*) for study of integrating citizen scientist data into the surveillance system for avian influenza virus, Taiwan. A) True observation frequency from Taiwan eBird dataset; B) occupancy probability estimated by zero-inflated Poisson model; C) distribution map of wetland, based on the land-cover type from the Taiwan open terrestrial environmental dataset.

wild bird were also subjected to principal component analysis and tSNE. The results showed that various wild birds were distributed in different ecologic environments, including forest and bodies of water, for which probabilities for AIV exchange between poultry farms and wild birds might differ (Figure 4, panel C).

In the second stage of our analysis, we performed propensity score matching with bootstrapping to precisely map the probability of AIV exchange between poultry flocks and wild birds. By doing so, we treated environmental factors as confounders and included them for the purpose of multivariate adjustment. Through propensity score matching with the probability of wild bird appearance, the significance of poultry farm outbreaks caused by HPAIV could be examined by bootstrapped resampling scheme based on randomness in selecting case–control matched pairs. There were nonignorable species with ≥100 significant results among the 1,000 bootstrapped realizations of the McNemar statistic (Table 1). Four species of wild bird, including the long-toed stint, black-headed gull, little grebe, and pacific golden plover, were highly correlated with the HPAIV outbreaks on poultry farms, with or without adjustment. The wild bird species that can be viewed as being significant when environmental factors were considered, is the long-toed stint, with a p value of 0.216 (1 – 0.784) (Table 1). On the other hand, if environmental factors were not considered, the black-headed gull shows a highly significant association (p = 1–0.896 = 0.104).

Discussion

The continuing circulation and reassortment of Gs/Gd-like HPAIV with LPAIV has caused huge economic losses and raised public health concerns because of its zoonotic potential (*31*). Virologic surveillance of wild birds has been suggested as part of a global AIV surveillance system (*32*,*33*) and could directly benefit human and animal health through knowledge of how avian influenza virus genes flow among different hosts and how factors that drive AIV prevalence in wild birds enable virus spillover, emergence, and maintenance. However, problems with understanding the transmission and evolution of HPAIV include underreporting, biased selection of sampling sites, and limiting AIV surveillance to wild bird carcasses (*34*). The risk map generated in this study (Figure 5) can be used for, but is not limited to, educational purposes of the government to communicate with stakeholders to increase their biosecurity of poultry farms; a sustained cost-effective AIV surveillance program that promotes sampling site selections, thereby enabling limited resources to be strategically allocated for early detection of changing AIV dynamics in reservoir populations to support public health and pandemic preparedness (*35*); and a quantitative assessment of the risk of introducing AIV from wild birds into poultry flocks as well as the possible transmission of AIVs between wild bird populations affected by bird behavior, age structures of populations, and detailed migration routes.

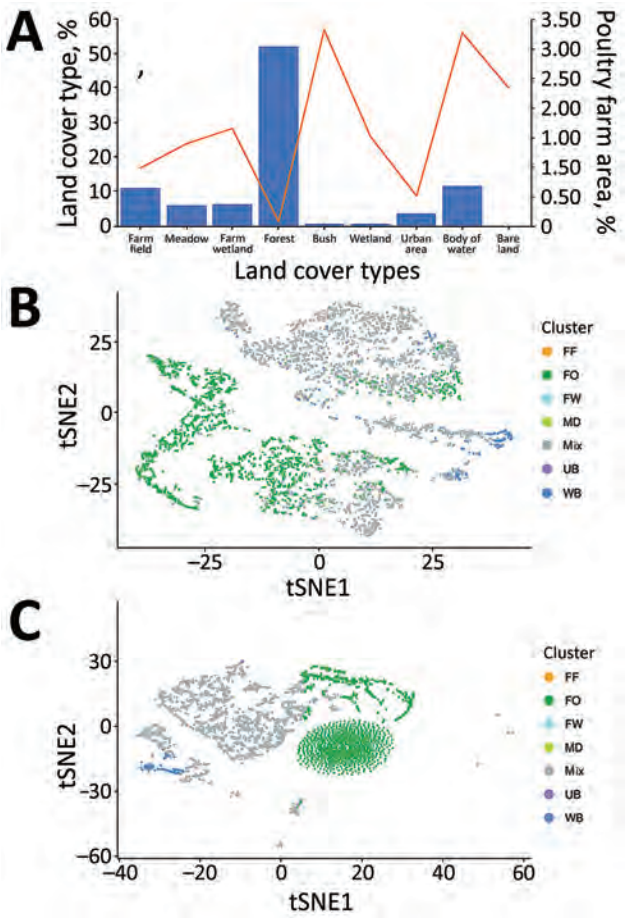

Figure 4. Land cover and bird distribution data for study of integrating citizen scientist data into the surveillance system for avian influenza virus, Taiwan. A) Percentages of 9 land-cover types in the total area of Taiwan main island (bars), area of poultry farms in the total area of indicated land-cover types (line). B, C) The clustering pattern of the area of each land-cover type (B) and the propensity score for each bird species from 3,764 grids partitioned by 3-km × 3-km squares of the main island of Taiwan (C), are based on principal component analysis and tSNE dimension reduction. Clusters are colored by the land-cover type as shown in panel A. For 4,762 grids, if 1 specific land-cover type is composed of >90% in the grid, such grid will be regarded as such specific land-cover type. Otherwise, it will be labeled as the mixed land-cover type. The labels of clusters in panels B and C are consistent with those in panel A. FF, farm field; FO, forest; FW, farm wetland; MD, meadow; mix, mixed land-cover types; tSNE, t-distributed stochastic neighbor embedding; UB, urban; WB, water body.

Pathogens that cross the interface between diverse populations, such as wildlife and livestock or animals and humans, pose particular challenges to developing effective and efficient surveillance and control measures. AIVs can spread globally among wild birds, poultry, and humans, with potentially devastating effects. The Citizen Science project eBird, which collects large volumes of data across broad spatial and temporal dimensions, provides a great opportunity for investigating how wild birds contribute to this spread. However, citizen science data often suffer from bias arising from bird sighters' viewing preferences, convenience (for bird sighting and travel planning), incentives (if any), and others. It may even come from the process of data recording and reporting. Although different analytical approaches for minimizing the bias have been published (*36*–*38*), our study used a high-quality inventory filtering procedure by constraining aspects of the observation process (e.g., the duration of observation and records of bird species sighting by ignoring the counts of birds on the checklists to remove potential sources of variation and facilitate subsequent analysis). Furthermore, birds are observed mostly during the day, and wild birds may forage near waterfowl poultry farms during the night (*39*). Such foraging flight distance is relatively short (e.g., the median for pintail ducks marked with satellite transmitters is within 3 km) and is covered by the size of the grids here (C.-C. Chen, National Pingtung University of Science and Technology, pers. comm., 2022 Jul 1).

Another layer of bias in using the eBird dataset comes from the accessibility of bird sighting by the observers. Because the locations for bird sighting are highly influenced by the proximity to the road accessible by the observers, the distribution of bird-sighting records cannot fully reflect the ecologic distribution of the wild birds. However, the main difficulty with building a unified regression model to map the ecologic distribution of wild birds and using the eBird dataset is the number of variables from the open terrestrial environmental dataset. In our study, the numbers of bird species and environmental variables both exceed 100. Therefore, we focused on 1 species at a time but kept all other variables as confounders. The elastic net regularization method was first used as a unified machine learning algorithm to generate parsimonious models for estimating potential risk maps (*40*). The elastic net regularization method is a compromise between ridge regression and lasso regression. To avoid complexity, we modeled only the presence or absence of individual bird species in each grid by using a conditional autoregressive logistic model, taking spatial autocorrelations into account.

Wild waterfowl are known reservoirs for LPAIV and potentially HPAIV because of the global evolution and circulation of Gs/GD-derived clade 2.3.4.4 (*41*), which resulted in a new era of AIV surveillance requiring identification of critical interfaces between wild birds and poultry on the landscape for potential interspecies transmission and virus evolution. Although such estimates can be extrapolated from

active poultry surveillance, as suggested by previous studies (*42*–*44*), accurately determining the likelihood (or potency) of the exchange of AIV at the interface between poultry flocks and wild birds is difficult because of incomplete active surveillance and a lack of biosecurity information for individual farms. In this study, we performed propensity score matching with bootstrapping by ensuring the randomness of case–control pair selections for estimating probability (*45*). By doing so, environmental factors were seen as confounders for which further adjustment can be made. We identified 10 nonignorable species of wild bird with ≥100 significant results among the 1,000 bootstrapped realizations of the McNemar statistic (Table 1). Among them, 4 wild bird species, including the long-toed stint, black-headed gull, little grebe, and pacific golden plover, were highly correlated with the introduction of HPAIV into poultry farms, with or without adjustment (Table 1). Those 4 species are mainly wintering birds; their preferred habitats are wetland or farmland. In particular, based on GISAID (https://www.gisaid.org), there are extensive records of LPAI in black-headed gull, little grebe, and pacific golden plover, which increases their chances of transmitting AIV into poultry farms as shown for the bootstrapping results (Table 1). Although the p values are not high, note that the term "p value" used here represents a concept of significance level based on bootstrapped samples, rather than the 0.05 level of significance criterion traditionally pursued in statistics.

The key limitation of our study is the lack of detailed information contributing to between-farm AIV transmission. Such information includes bridge bird species on or near poultry farms, transportation vehicles, or other farm animals (e.g., rats feeding on bird carcasses). It is also evident that different AIV subtypes and pathotypes can vary according to the epidemiology and prevalence of wild birds (*46*). For example, the following can interfere with significance results in McNemar tests: spatiotemporal variation in between-farm transmission by wild birds, species age structure, behaviors including roosting/breeding sites, AIV susceptibility, and AIV pathology. Although phylogenetic analysis of HPAIV from individual outbreak poultry farms could reveal between-farm transmission events, we, unfortunately, had no access to sequence data of outbreak viruses. We also selected 36 different nonmigratory wild birds and followed the same analytical frameworks as those for migratory birds. The results suggested that 4 nonmigratory wild bird species, including the black bulbul, black-headed munia, red collared dove, and common moorhen, could potentially serve as bridging species for introducing AIV into poultry farms (Appendix 2 Table 2, https://wwwnc.cdc.gov/EID/article/29/1/22-0659-App2.pdf), although other bridging species could also play major roles. Furthermore, increased occurrence of HPAI in wild birds resulted in disease and death of fairly large numbers of birds (>10,000 individuals) and affected diverse species (*47*). Mortality data for birds, especially nonmigratory species, could be indicators for

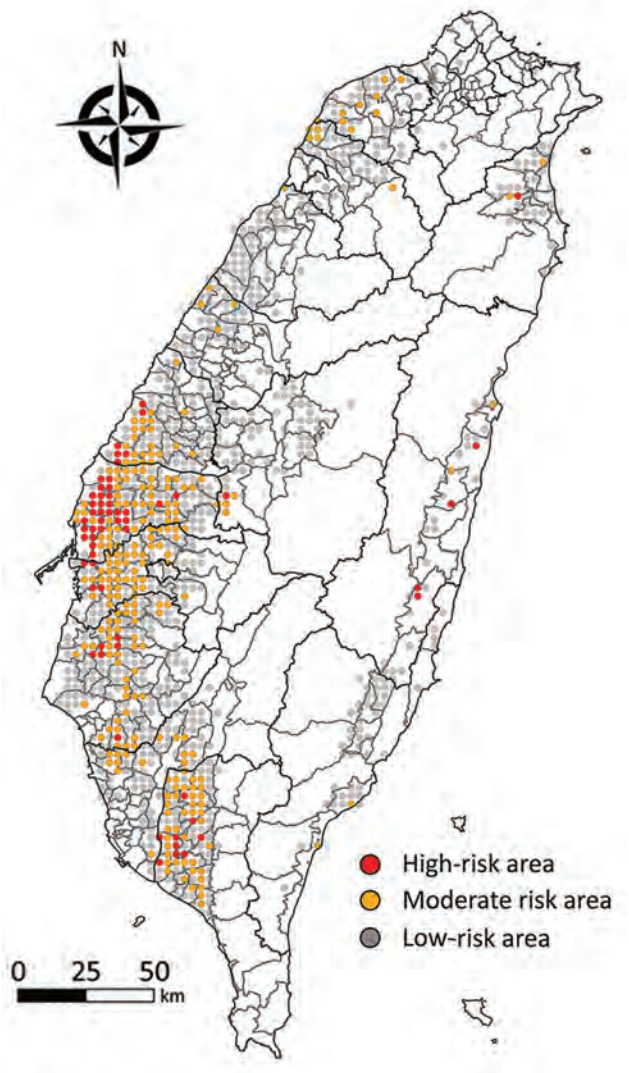

Figure 5. Risk maps showing risk of poultry farm acquiring avian influenza virus infection from migratory wild birds, from study of integrating citizen scientist data into the surveillance system for avian influenza virus, Taiwan. Each dot represents each 3-km × 3-km grid. Red dots represent the high-risk area with probability calculated based on 10 bird species with high risk of transmitting avian influenza virus into poultry farms (Table). Orange dots represent the middle-risk area, with bird species with ≥1 positive McNemar test result. Gray dots represent the low-risk area with bird species having no positive or negative McNemar test results.

HPAIV transmission and could be incorporated into spatiotemporal data analysis together with other genetic or bird behavior data in the future (*25*).

In summary, information about the spatial distribution of wild birds and how they exchange AIV with poultry, as well as the related risks, has the potential to benefit surveillance, pandemic preparedness, and prevention plans. However, poor availability of data presents challenges. The integration of citizen science data, such as eBird, into the surveillance system is underappreciated, and the workflow developed in our study can be applied in other countries for AIV surveillance in wild bird site selections to increase the breadth of virus strain coverage and knowledge of gene flow of AIV among wild birds.

Acknowledgment

We express our deepest appreciation to A.Y. Chang and W.J. Chen for advice with regard to the eBird dataset. We thank Lydia Wang for English editing of the manuscript and Zheng-Fu Liu and Yong-Sheng Zhuang for their help with statistical computation.

Mountain Jade Scholar Charles W. Tu for provided funding from the ENABLE center of National Chung-Hsing University. The work is also funded by the Bureau of Animal and Plant Health Inspection and Quarantine (110AS-5.5.3-BQ-B1(2)). The funding source of this study had no role in the study design, data collection, data analysis, data interpretation, or writing of the report. The corresponding author had full access to all data in the study and final responsibility for the decision to submit for publication.

The authors declare no conflict of interest of any form that might be perceived to influence the results or discussion reported in this paper.

About the Author

Dr. Wu is an associate professor of statistics in the Department of Applied Mathematics and Institute of Statistics, National Chung Hsing University, Taichung, Taiwan. His research interests include spatial statistics and modeling, epidemiologic study design, and big data analytics.

References

1. Yoon SW, Webby RJ, Webster RG. Evolution and ecology of influenza A viruses. Curr Top Microbiol Immunol. 2014;385:359–75. https://doi.org/10.1007/82_2014_396
2. Lee DH, Criado MF, Swayne DE. Pathobiological origins and evolutionary history of highly pathogenic avian influenza viruses. Cold Spring Harb Perspect Med. 2021;11:a038679. https://doi.org/10.1101/cshperspect.a038679
3. Briand F-X, Niqueux E, Schmitz A, Martenot C, Cherbonnel M, Massin P, et al. Highly pathogenic avian influenza A(H5N8) virus spread by short- and long-range transmission, France, 2016–17. Emerg Infect Dis. 2021;27:508–16. https://doi.org/10.3201/eid2702.202920
4. Li YT, Linster M, Mendenhall IH, Su YCF, Smith GJD. Avian influenza viruses in humans: lessons from past outbreaks. Br Med Bull. 2019;132:81–95. https://doi.org/10.1093/bmb/ldz036
5. Smith GJ, Donis RO; World Health Organization/World Organisation for Animal Health/Food and Agriculture Organization (WHO/OIE/FAO) H5 Evolution Working Group. Nomenclature updates resulting from the evolution of avian influenza A(H5) virus clades 2.1.3.2a, 2.2.1, and 2.3.4 during 2013–2014. Influenza Other Respir Viruses. 2015;9:271–6. https://doi.org/10.1111/irv.12324
6. Lee DH, Bertran K, Kwon JH, Swayne DE. Evolution, global spread, and pathogenicity of highly pathogenic avian influenza H5Nx clade 2.3.4.4. J Vet Sci. 2017;18(S1):269–80. https://doi.org/10.4142/jvs.2017.18.S1.269
7. Lycett SJ, Pohlmann A, Staubach C, Caliendo V, Woolhouse M, Beer M, et al.; Global Consortium for H5N8 and Related Influenza Viruses. Genesis and spread of multiple reassortants during the 2016/2017 H5 avian influenza epidemic in Eurasia. Proc Natl Acad Sci U S A. 2020; 117:20814–25. https://doi.org/10.1073/pnas.2001813117
8. Global Consortium for H5N8 and Related Influenza Viruses. Role for migratory wild birds in the global spread of avian influenza H5N8. Science. 2016;354:213–7. https://doi.org/10.1126/science.aaf8852
9. Poulson RL, Brown JD. Wild bird surveillance for avian influenza virus. Methods Mol Biol. 2020;2123:93–112. https://doi.org/10.1007/978-1-0716-0346-8_8
10. Prosser DJ, Hungerford LL, Erwin RM, Ottinger MA, Takekawa JY, Newman SH, et al. Spatial modeling of wild bird risk factors for highly pathogenic A(H5N1) avian influenza virus transmission. Avian Dis. 2016;60 (Suppl):329–36. https://doi.org/10.1637/11125-050615-Reg
11. Hill A, Gillings S, Berriman A, Brouwer A, Breed AC, Snow L, et al. Quantifying the spatial risk of avian influenza introduction into British poultry by wild birds. Sci Rep. 2019;9:19973. https://doi.org/10.1038/s41598-019-56165-9
12. Prosser DJ, Hungerford LL, Erwin RM, Ottinger MA, Takekawa JY, Ellis EC. Mapping avian influenza transmission risk at the interface of domestic poultry and wild birds. Front Public Health. 2013;1:28. https://doi.org/10.3389/fpubh.2013.00028
13. La Sala LF, Burgos JM, Blanco DE, Stevens KB, Fernández AR, Capobianco G, et al. Spatial modelling for low pathogenicity avian influenza virus at the interface of wild birds and backyard poultry. Transbound Emerg Dis. 2019;66:1493–505. https://doi.org/10.1111/tbed.13136
14. Franklin AB, Bevins SN, Ellis JW, Miller RS, Shriner SA, Root JJ, et al. Predicting the initial spread of novel Asian origin influenza A viruses in the continental USA by wild waterfowl. Transbound Emerg Dis. 2019;66:705–14. https://doi.org/10.1111/tbed.13070
15. Tian H, Zhou S, Dong L, Van Boeckel TP, Cui Y, Newman SH, et al. Avian influenza H5N1 viral and bird migration networks in Asia. Proc Natl Acad Sci U S A. 2015;112:172–7. https://doi.org/10.1073/pnas.1405216112
16. Wood C, Sullivan B, Iliff M, Fink D, Kelling S. eBird: engaging birders in science and conservation. PLoS Biol. 2011;9:e1001220. https://doi.org/10.1371/journal.pbio.1001220
17. Callaghan CT, Nakagawa S, Cornwell WK. Global abundance estimates for 9,700 bird species. Proc Natl Acad

Sci U S A. 2021;118:e2023170118. https://doi.org/10.1073/pnas.2023170118
18. Kelling S, Johnston A, Hochachka WM, Iliff M, Fink D, Gerbracht J, et al. Can observation skills of citizen scientists be estimated using species accumulation curves? PLoS One. 2015;10:e0139600. https://doi.org/10.1371/journal.pone.0139600
19. Boakes EH, Gliozzo G, Seymour V, Harvey M, Smith C, Roy DB, et al. Patterns of contribution to citizen science biodiversity projects increase understanding of volunteers' recording behaviour. Sci Rep. 2016;6:33051. https://doi.org/10.1038/srep33051
20. Liang W-S, He Y-C, Wu H-D, Li Y-T, Shih T-H, Kao G-S, et al. Ecological factors associated with persistent circulation of multiple highly pathogenic avian influenza viruses among poultry farms in Taiwan during 2015-17. PLoS One. 2020;15:e0236581. https://doi.org/10.1371/journal.pone.0236581
21. Lee MS, Chen LH, Chen YP, Liu YP, Li WC, Lin YL, et al. Highly pathogenic avian influenza viruses H5N2, H5N3, and H5N8 in Taiwan in 2015. Vet Microbiol. 2016;187:50–7. https://doi.org/10.1016/j.vetmic.2016.03.012
22. Sullivan BL, Aycrigg JL, Barry JH, Bonney RE, Bruns N, Cooper CB, et al. The eBird enterprise: an integrated approach to development and application of citizen science. Biol Conserv. 2014;169:31–40. https://doi.org/10.1016/j.biocon.2013.11.003
23. Sullivan BL, Wood CL, Iliff MJ, Bonney RE, Fink D, Kelling S. eBird: a citizen-based bird observation network in the biological sciences. Biol Conserv. 2009;142:2282–92. https://doi.org/10.1016/j.biocon.2009.05.006
24. Chen WJ, Lo CC, Tsai FA, Chang AY. Using open data to establish a multi-temporal and terrestrial environmental dataset of Taiwan [in Chinese]. Taiwan Journal of Biodiversity. 2020;22:13–44.
25. Wu H-D I, Chao D-Y. Two-stage algorithms for visually exploring spatio-temporal clustering of avian influenza virus outbreaks in poultry farms. Sci Rep. 2021;11:22553. https://doi.org/10.1038/s41598-021-01207-4
26. Van der Maaten L, Hinton G. Visualizing data using t-SNE. Journal of Machine Learning Research. 2008;9:2579–605.
27. Anselin L. Spatial econometrics: methods and models. Dordrecht: Kluwer Academic Publishers. 1988.
28. Lord D, Washington SP, Ivan JN. Poisson, Poisson-gamma and zero-inflated regression models of motor vehicle crashes: balancing statistical fit and theory. Accid Anal Prev. 2005;37:35–46. https://doi.org/10.1016/j.aap.2004.02.004
29. Lambert D. Zero-inflated Poisson regression, with an application to defects in manufacturing. Technometrics. 1992;34:1–14. https://doi.org/10.2307/1269547
30. Rosenbaum PR, Rubin DB. The central role of the propensity score in observational studies for causal effects. Biometrika. 1983;70:41–55. https://doi.org/10.1093/biomet/70.1.41
31. Yamaji R, Saad MD, Davis CT, Swayne DE, Wang D, Wong FYK, et al. Pandemic potential of highly pathogenic avian influenza clade 2.3.4.4 A(H5) viruses. Rev Med Virol. 2020;30:e2099. https://doi.org/10.1002/rmv.2099
32. Machalaba CC, Elwood SE, Forcella S, Smith KM, Hamilton K, Jebara KB, et al. Global avian influenza surveillance in wild birds: a strategy to capture viral diversity. Emerg Infect Dis. 2015;21:e1–7. https://doi.org/10.3201/eid2104.141415
33. Verhagen JH, Fouchier RAM, Lewis N. Highly pathogenic avian influenza viruses at the wild-domestic bird interface in Europe: future directions for research and surveillance. Viruses. 2021;13:212. https://doi.org/10.3390/v13020212
34. Olsen B, Munster VJ, Wallensten A, Waldenström J, Osterhaus AD, Fouchier RAM. Global patterns of influenza A virus in wild birds. Science. 2006;312:384–8. https://doi.org/10.1126/science.1122438
35. Cheng MC, Lee MS, Ho YH, Chyi WL, Wang CH. Avian influenza monitoring in migrating birds in Taiwan during 1998–2007. Avian Dis. 2010;54:109–14. https://doi.org/10.1637/8960-061709-Reg.1
36. Xue Y, Davies I, Fink D, Wood C, Gomes CP. Avicaching: a two-stage game for bias reduction in citizen science. In: Proceedings of the 15th International Conference on Autonomous Agents and Multiagent Systems; 2016 May 9–13; Singapore. p. 776–85.
37. Chen D, Gomes CP. Bias reduction via end-to-end shift learning: application to citizen science. Proc Conf AAAI Artif Intell. 2019;33:493–500. https://doi.org/10.1609/aaai.v33i01.3301493
38. Troudet J, Grandcolas P, Blin A, Vignes-Lebbe R, Legendre F. Taxonomic bias in biodiversity data and societal preferences. Sci Rep. 2017;7:9132. https://doi.org/10.1038/s41598-017-09084-6
39. Elbers ARW, Gonzales JL. Quantification of visits of wild fauna to a commercial free-range layer farm in the Netherlands located in an avian influenza hot-spot area assessed by video-camera monitoring. Transbound Emerg Dis. 2020;67:661–77. https://doi.org/10.1111/tbed.13382
40. Zou H, Hastie T. Regularization and variable selection via the elastic net. J R Stat Soc B. 2005;67:301–20. https://doi.org/10.1111/j.1467-9868.2005.00503.x
41. He G, Ming L, Li X, Song Y, Tang L, Ma M, et al. Genetically divergent highly pathogenic avian influenza A(H5N8) viruses in wild birds, eastern China. Emerg Infect Dis. 2021;27:2940–3. https://doi.org/10.3201/eid2711.204893
42. Gonzales JL, Stegeman JA, Koch G, de Wit SJ, Elbers ARW. Rate of introduction of a low pathogenic avian influenza virus infection in different poultry production sectors in the Netherlands. Influenza Other Respir Viruses. 2013;7:6–10. https://doi.org/10.1111/j.1750-2659.2012.00348.x
43. Bouwstra R, Gonzales JL, de Wit S, Stahl J, Fouchier RAM, Elbers ARW. Risk for low pathogenicity avian influenza virus on poultry farms, the Netherlands, 2007-2013. Emerg Infect Dis. 2017;23:1510–6. https://doi.org/10.3201/eid2309.170276
44. Gonzales JL, Pritz-Verschuren S, Bouwstra R, Wiegel J, Elbers ARW, Beerens N. Seasonal risk of low pathogenic avian influenza virus introductions into free-range layer farms in the Netherlands. Transbound Emerg Dis. 2021;68:127–36. https://doi.org/10.1111/tbed.13649
45. Efron B. Bootstrap methods: another look at the jackknife. Ann Stat. 1979;7:1–26. https://doi.org/10.1214/aos/1176344552
46. Li Y-T, Chen C-C, Chang A-M, Chao D-Y, Smith GJ. Co-circulation of both low and highly pathogenic avian influenza H5 viruses in current poultry epidemics in Taiwan. Virus Evolution. 2020;6:veaa037.
47. Ramey AM, Hill NJ, DeLiberto TJ, Gibbs SEJ, Hopkins MC, Lang AS, et al. Highly pathogenic avian influenza is an emerging disease threat to wild birds in North America. J Wildl Manage. 2022;86:e22171. https://doi.org/10.1002/jwmg.22171

Address for correspondence: Day-Yu Chao, Graduate Institute of Microbiology and Public Health, College of Veterinary Medicine, National Chung-Hsing University, Taichung 402, Taiwan; email: dychao@nchu.edu.tw

Widespread Exposure to Mosquitoborne California Serogroup Viruses in Caribou, Arctic Fox, Red Fox, and Polar Bears, Canada

Kayla J. Buhler, Antonia Dibernardo, Nicholas W. Pilfold, N. Jane Harms, Heather Fenton, Suzanne Carriere, Allicia Kelly, Helen Schwantje, Xavier Fernandez Aguilar, Lisa-Marie Leclerc, Geraldine G. Gouin, Nicholas J. Lunn, Evan S. Richardson, David McGeachy, Émilie Bouchard, Adrián Hernández Ortiz, Gustaf Samelius, L. Robbin Lindsay, Michael A. Drebot, Patricia Gaffney, Patrick Leighton, Ray Alisauskas, Emily Jenkins

Northern Canada is warming at 3 times the global rate. Changing diversity and distribution of vectors and pathogens is an increasing health concern. California serogroup (CSG) viruses are mosquitoborne arboviruses; wildlife reservoirs in northern ecosystems have not been identified. We detected CSG virus antibodies in 63% (95% CI 58%–67%) of caribou (n = 517), 4% (95% CI 2%–7%) of Arctic foxes (n = 297), 12% (95% CI 6%–21%) of red foxes (n = 77), and 28% (95% CI 24%–33%) of polar bears (n = 377). Sex, age, and summer temperatures were positively associated with polar bear exposure; location, year, and ecotype were associated with caribou exposure. Exposure was highest in boreal caribou and increased from baseline in polar bears after warmer summers. CSG virus exposure of wildlife is linked to climate change in northern Canada and sustained surveillance might be used to measure human health risks.

Annual temperatures in the circumpolar Arctic are rising at 2–3 times the global average, reducing ecologic barriers for arthropod reproduction and fueling shifts in insect diversity and distribution (*1*,*2*). The northward advancement of the tree line and a 50%–60% increase in Arctic precipitation over the past 20 years provide a favorable environment for arthropod emergence (*3*,*4*). Consequently, arboviruses are a growing wildlife and public health concern in the Arctic. Limited information exists on the diversity of arboviruses in Arctic ecosystems, and few studies have identified hosts in sylvatic transmission cycles.

California serogroup (CSG) viruses are antigenically and genetically related emerging vectorborne pathogens of the genus *Orthobunyavirus* that are found throughout North America and are associated with febrile illness and cases of neuroinvasive disease in humans (*5*). Pathogenic strains include La Crosse, Jamestown Canyon (JCV), California encephalitis, snowshoe hare (SSHV), Chatanga, and Inkoo viruses (*6*). Both JCV and SSHV have been identified as causes of arbovirus-associated neurologic diseases in North America (*7*). CSG viruses are transmitted through mosquitoes (*Aedes*, *Culiseta*, and *Anopheles* spp.), maintained by transovarial vector transmission,

Author affiliations: University of Saskatchewan, Saskatoon, Saskatchewan, Canada (K.J. Buhler, É. Bouchard, A. Hernández Ortiz, R. Alisauskas, E. Jenkins); National Microbiology Laboratory Branch, Winnipeg, Manitoba, Canada (A. Dibernardo, L.R. Lindsay, M.A. Drebot); San Diego Zoo Wildlife Alliance, Escondido, California, USA (N.W. Pilfold, P. Gaffney); Government of Yukon, Whitehorse, Yukon, Canada (N.J. Harms); Ross University School of Veterinary Medicine, Basseterre, St. Kitts and Nevis (H. Fenton); Government of the Northwest Territories, Yellowknife, Northwest Territories, Canada (H. Fenton, S. Carriere, A. Kelly); Government of British Columbia, Nanaimo, British Columbia, Canada (H. Schwantje); University of Calgary, Calgary, Alberta, Canada (X. Fernandez Aguilar); Government of Nunavut, Kugluktuk, Nunavut, Canada (L.-M. Leclerc); Makivik Corporation, Kuujjuaq, Québec, Canada (G.G. Gouin); Environment and Climate Change Canada, Edmonton, Alberta, Canada (N.J. Lunn, D. McGeachy); Environment and Climate Change Canada, Winnipeg (E.S. Richardson); Snow Leopard Trust, Seattle, Washington, USA (G. Sameilus); Université de Montréal, Saint-Hyacinthe, Québec (É. Bouchard, P. Leighton)

DOI: https://doi.org/10.3201/eid2901.220154

and circulate in a wide range of vertebrate hosts (*5*,*8*). Since 2006, documented human exposure to CSG viruses has steadily increased in Canada as serologic tests have become available, although infections are still likely underdiagnosed (*5*).

Studies on CSG virus ecology and epidemiology have primarily focused on southern Canada and the contiguous United States. However, recent cases of human exposure in Alaska and the province of Manitoba, Canada have been reported (*9*,*10*), indicating that those viruses exist in northern ecosystems. Human encephalitis in Canada, while rare, has generally been linked to JCV and SSHV serotypes (*5*). Furthermore, we recently detected JCV and SSHV in *Aedes* sp. mosquitoes and biting midges collected in northern Québec (*11*), further confirming circulation of CSG viruses in northern vectors. Potential reservoirs in southern Canada and the United States are cervids for JCV and rodents and lagomorphs for SSHV (*5*). We assessed potential reservoir and sentinel hosts in northern Canada by surveying caribou, rodents and shrews, and carnivores for CSG virus antibodies or RNA across a broad geographic range and identified biologic and ecologic factors associated with exposure.

Materials and Methods

Study Area

We collected samples in Yukon, Northwest Territories (NT), Nunavut, Quebec, Manitoba, and British Columbia (BC), Canada (Figure). The study areas comprised tundra, boreal, and mountain ecosystems.

Sample Collection

We collected blood from hunter-harvested migratory tundra and boreal caribou (*Rangifer tarandus*) in Nunavik (2018, Tasiujaq and Umiujaq, n = 53) and Nunavut (2016, Bathurst Inlet, n = 19). We collected serum samples from caribou live-captured for radio collaring in Yukon (2017–2019, n = 152), BC (2018–2019, n = 20), NT (2010–2019, n = 219) and Nunavut (2019, Kugluktuk, n = 10; 2018, Bathurst Inlet, n = 44) (Figure). We determined sex but not age for caribou.

We collected blood from Arctic and red fox carcasses harvested for fur by licensed trappers in the NT (2018–2019, Inuvik, Sachs Harbour, and Ulukhaktok, n = 72), Nunavut (2019–2021, Cambridge Bay and Gjoa Haven, n = 85), Nunavik (2019–2021, Inukjuak and Tasiujaq, n = 20), and southern Quebec (2016–2017, n = 61). We collected serum samples from Arctic

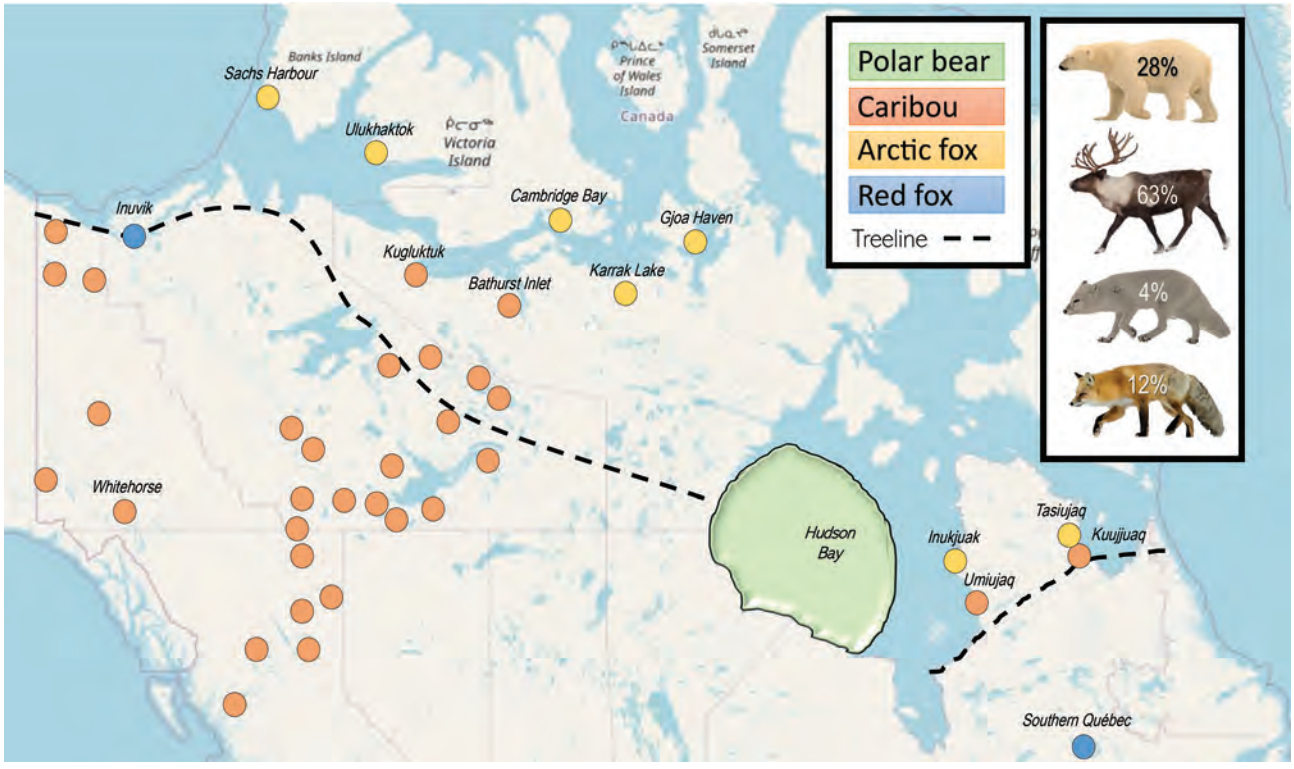

Figure. Distribution of animals in study of widespread exposure to mosquitoborne California serogroup viruses in caribou, Arctic fox, red fox, and polar bears, Canada. The green region is the mean on-ice home range of polar bears according to adult female movement (*12*). Locations of caribou include both capture/release and hunter-harvested samples. Dashed line indicates the tree line.

foxes trapped alive at Karrak Lake, Nunavut (2014–2018, n = 108) and Cambridge Bay, Nunavut (2021, n = 28) (*13*). We determined sex of the animals and estimated ages according to a tooth condition index (*14*).

Serum samples were collected from live-captured adult polar bears (n = 377) as part of a long-term study of the western Hudson Bay population during 1986–1989, 1995–1998, and 2015–2017 (*15*,*16*). Sex was determined, and age was estimated by extracting a vestigial premolar tooth and counting cementum annuli (*17*,*18*).

We collected tissues (instead of blood because of their small size) from rodents and shrews lethally trapped on line transects in the NT during the summers of 2017, 2018, and 2019 (n = 496). We also collected samples at Karrak Lake, Nunavut, during the summers of 2018 and 2019 (n = 9).

Serology

We stored blood (from carcasses) and serum samples (from live captures) at –20°C until processing. Serologic methods were performed as previously described (*19*). In brief, we detected SSHV and JCV IgM in samples from foxes, caribou, and bears by using a competitive ELISA (cELISA). We measured optical densities at 450 nm, and samples with an inhibition value >30% were considered seropositive. Because this approach was originally developed for serum samples, we compared a positive caribou serum sample diluted in heart blood (1:2) and the same serum sample diluted in blocking buffer (1:2) to identify potential inhibitory effects of whole blood. The dilution in heart blood resulted in 15% loss of inhibition, indicating that whole blood likely underestimates IgM prevalence.

After performing cELISAs, we sent subsets of positive caribou (n = 18) and fox (n = 4) serum samples to the National Microbiology Laboratory in Winnipeg for plaque reduction neutralization tests (PRNTs) to determine exposures to different viruses within the serogroup (*20*). We only conducted differential testing of this subset of animals because of resource limitations arising from the SARS-CoV-2 pandemic. Samples were considered positive for CSG viruses if neutralizing antibody titers were ≥1:20. A 4-fold increase in titer was used to determine antibody specificity to a single CSG virus versus previous exposures to multiple viruses.

RNA Extraction and Reverse Transcription PCR for CSG Viruses

We stored tissues from rodents at –20°C until RNA was extracted from a pooled sample of liver, lung, spleen, and kidney for each animal by using the RNeasy Mini Kit (QIAGEN, https://www.qiagen.com). We performed real-time reverse transcription PCR on extracted RNA samples by using the primers CE-NC-F1 (5′-GTGTTTTATGATGTCGCATCA-3′) and CE-NC-R1(5′-CATATACCCTGCATCAGGATCAA-3′) for SSHV and CE-NC-F2 (5′-GTTTTCTATGATGATGCATCC-3′) and CE-NC-R2 (5′-CACAAACCCTGCATCTGGATCAA-3′) for JCV. The probe for both SSHV and JCV was CE-NC (Fam-CAGGTGCAAATGGA-MGB; Integrated DNA Technologies, https://www.idtdna.com). We performed PCR under the following conditions: 50°C for 5 min, 95° for 20 s, then 45 cycles of 95°C for 3 s and 60°C for 30 s. A 20 μL reaction mixture was used containing 5 μL TaqMan Fast Virus 1-Step Master Mix (Thermo Fisher Scientific, https://www.thermofisher.com), 9.4 μL H_2O, 0.1 μl of each primer (100 μmol/L), 0.2 μL of probe (25 μmol/L), and 5 μL of template. Positive controls were gBlock gene fragments (Integrated DNA Technologies) from the small segment of SSHV and JCV isolates reported in GenBank (accession nos. MK352486.1 and MN135989.1).

Statistical Analysis

We calculated sample prevalence and 95% CIs by using EpiTools epidemiologic calculators (*21*). We used multiple linear regression to model seropositivity with fixed effect variables 1/0 (positive/negative) as the dependent variables and region, year, age, species, and sex as predictor variables for fox data. We also used multiple linear regression to predict seropositivity (1/0) according to region, year, ecotype, and sex (but not age) for caribou. We classified regions as provinces or territories (BC, Yukon, NT, Nunavut, and Quebec) and ecotypes as migratory tundra, mountain, and boreal. The Leaf River caribou herd in Quebec was classified as migratory tundra caribou during this study, although they are often grouped as woodland forest-tundra caribou.

We also examined co-exposures to CSG viruses and 7 pathogens previously documented in the same polar bears (*18*) by using Pearson χ^2 tests. Because of the long timeline for polar bear sample collection, we related seroprevalence (1/0) in polar bears to biologic and climatic factors (Table 1) by using binomial (logit link function) generalized linear mixed models and the same constrained set of a priori models for each pathogen as described previously (*18*). In brief, we evaluated sets of biologic and climatic variables separately and identified top factors by using Akaike information criterion corrected for small sample size and weight of the model ≥0.60. To

Table 1. Covariates used to model the likelihood of California serogroup virus seropositivity in adult polar bears of western Hudson Bay, Canada, 1986–2017, in study of widespread exposure to mosquitoborne California serogroup viruses in caribou, Arctic fox, red fox, and polar bears*

Variables	Range	Description (reference)
Biologic		
Age, y	5–31	Age of polar bear according to tooth histology (*17*)
Sex	1/0#	Field determination with females as reference category
Poor condition†	1/0#	Polar bears rated 1 or 2 on 5-point body condition index (*22*)
Good condition†	1/0#	Polar bears rated 4 or 5 on 5-point body condition index (*22*)
Weight, kg‡	136–602	Calculated weight (*23*) matched to temporal equations for WHB
Conflict§	1/0#	Polar bears captured by Manitoba Conservation in Churchill, MB (*24*) before sample collection
Climatic¶		
Ice free, d	110–152	No. days sea ice concentration was <15% as determined by SSM/I (*25*), within 95% MCP estimate of polar bear home range (*12*)
Summer temperature, °C	7.8–10.8	Mean air temperature, June–September, measured at Churchill airport, MB (*26*)
Summer precipitation, mm	169.0–310.6	Total precipitation, June–September, measured at Churchill airport, MB (*26*)
Winter temperature, °C	–30.0 to –24.9	Mean minimum air temperature, December–March, measured at Churchill airport, MB (*26*)
Annual temperature, °C	–7.4 to –5.2	Mean annual air temperature measured at Churchill airport, MB (*26*)
Annual precipitation, mm	344.7–507.8	Total annual precipitation measured at Churchill Airport, MB (*26*)

*This table was published previously (*18*). MB, Manitoba; MCP, minimum complex polygon; SSM/I, special sensor microwave/imager; WHB, western Hudson Bay.
†The 5-point body condition index was dummy-coded with an average score of 3 forming the reference category.
‡Mean weight centered within sex before modeling.
§Bears with a history of capture as part of the Polar Bear Alert Program prior to sampling.
¶All climate variables measured the year before serum sample collection.
#Multiple linear regression was used to model seropositivity with fixed effect variables 1/0 (positive/negative) as dependent variables.

assess the comparative influence of biologic and climatic factors on CSG virus exposure, we combined top biologic and climatic factors into 1 model and used log-likelihood ratio tests to examine model improvement (reported as χ^2).

We performed analyses by using SPSS Statistics 28 (IBM, https://www.ibm.com) for caribou and foxes and R software version 3.3.3 (The R Project for Statistical Computing, https://www.r-project.org) for polar bears. We reported all variances with 95% CIs, and α was set to 0.05 for significance. We considered all animals sampled multiple times during the study (bears, n = 40; Arctic foxes, n = 12; Caribou; n = 52) positive if a single blood sample tested positive. We did not include subsequent results from positive animals in the analyses because duration of virus antibody production is not well understood.

Results

Prevalence

Mean seroprevalence was 63% (95% CI 58%–67%, n = 517) for caribou, 4% (95% CI 2%–7%, n = 297) for Arctic foxes, 12% (95% CI 6%–21%, n = 77) for red foxes, and 28% (95% CI 24%–33%, n = 377) for polar bears (Table 2). The prevalence for bears varied significantly between time periods (χ^2 = 9.98, degrees of freedom [d.f.] = 2, p = 0.007); a significant increase in positive cases was observed between the mid-1980s and mid-1990s (χ^2 = 9.78, d.f. = 1, p = 0.002). Seropositivity in the mid-2010s did not significantly differ from either the mid-1980s (χ^2 = 1.55, d.f. = 1, p = 0.213) or mid-1990s (χ^2 = 2.71, d.f. = 1, p = 0.100) (Table 3). Polar bears sampled repeatedly (3 during 1995–1998 and 2 during 2015–2017) had positive titers that decreased below the cELISA threshold in subsequent sampling. Three of those bears were sampled again 1 year after initial positive samples, indicating that virus antibodies were short-lived (inhibition values were 38%, 45%, and 94% the year before). The other 2 bears were sampled 18–19 years after initial positive samples.

Estimated seroprevalence varied between regions for caribou and foxes; the highest prevalence was observed in the NT (83%, n = 219) and Nunavut (80%, n = 73) for caribou and in Nunavik for red foxes (20%, n = 10) and Arctic foxes (30%, n = 10) (Table 2). Boreal caribou (87%, n = 172) were exposed more often than migratory tundra (48%; n = 243) or mountain caribou (59%, n = 87) (Table 4). By PRNT, 18 positive cELISA samples from caribou in the NT had a positive titer ≥1:20 for JCV. We observed an SSHV titer of 1:40 in 4 caribou, 2 of which had a JCV titer of 1:160 and 1:320, indicating exposure to JCV. Furthermore, PRNT of 4 positive fox samples (3 from Nunavut and 1 from Quebec) indicated exposure to JCV.

Of the caribou that were repeatedly sampled during 2016–2018 (n = 52), 3 animals had titers that dropped below the cELISA cutoff value between winter and the following spring. Conversely, 3 animals seroconverted during the same time frame (inhibition values between 31%–43%). We did not detect viral RNA by PCR in samples from 349 red

Table 2. Prevalence of California serogroup viruses in wildlife in Canada, 2017, in study of widespread exposure to mosquitoborne California serogroup viruses in caribou, Arctic fox, red fox, and polar bears*

Species	Sample size	Test	Total prevalence, % (no./total)	Location	Regional prevalence, % (95% CI) (no./total)	Prevalence, serum, % (no./total)	Prevalence, whole blood, % (no./total)
Caribou	517	cELISA	63 (324/517)	BC	45 (26–66) (9/20)	45	NA
				Yukon	45 (37–53) (68/152)	45	NA
				NT	83 (78–88) (182/219)	83	NA
				Nunavut	80 (69–87) (58/73)	91 (49/54)	47 (9/19)
				Nunavik	13 (7–25) (7/53)	NA	13
Arctic fox	297	cELISA	4 (11/297)	NT	0 (0–6) (0/66)	NA	0
				Nunavut	4 (2–7) (8/221)	5 (7/136)	1 (1/85)
				Nunavik	30 (11–60) (3/10)	NA	30
Red fox	77	cELISA	12 (9/77)	NT	0 (0–39) (0/6)	NA	0
				Nunavik	20 (6–51) (2/10)	NA	20
				South QC	12 (6–22) (7/61)	NA	12
Polar bear	377	cELISA	28 (107/377)	Manitoba	28 (24–33)	28	NA
Red-backed vole	349	qPCR	0	NT	0 (0–1)	NA	NA
Meadow vole	20	qPCR	0	NT	0 (0–16)	NA	NA
Deer mouse	68	qPCR	0	NT	0 (0–5)	NA	NA
Collared lemming	9	qPCR	0	Nunavut	0 (0–30)	NA	NA
Shrew, unidentified	59	qPCR	0	NT	0 (0–6)	NA	NA

*BC, British Columbia; MB, Manitoba; NA, not applicable; NT, Northwest Territories; QC, Québec; qPCR; quantitative PCR; cELISA, competitive ELISA.

backed voles (*Myodes rutilus*), 20 meadow voles (*Microtus pennsylvanicus*), 68 deer mice (*Peromyscus maniculatus*), 9 collared lemmings (*Dicrostonyx groenlandicus*), and 59 shrews (species unidentified).

Biologic, Ecologic, and Climatic Factors

We did not detect substantial co-occurrence between CSG viruses and 7 other pathogens previously examined in the same polar bears (*18*). Both biologic and climatic factors influenced polar bear exposure to CSG viruses. Adult female polar bears were 2.6 (95% CI 1.6–4.2) times more likely to be seropositive than adult male polar bears. Age was negatively correlated with seropositivity, although the 95% CI included zero (β = −0.04, 95% CI –0.04 to 0.0). Polar bears previously captured in the town of Churchill, Manitoba, were 3.4 (95% CI 1.8–6.4) times less likely to be seropositive for CSG viruses. Summer temperature in the preceding year (corrected Akaike information criterion, weight of model = 0.97) was a top climatic factor in the model, and warmer summer air temperatures were positively correlated with polar bear exposure to CSG viruses (β = 0.78, 95% CI 0.47–1.09). Inclusion of biologic and climatic factors in the same model significantly improved model fit (χ^2 = 29.0, d.f. = 3, p<0.001) (Appendix Table 1, https://wwwnc.cdc.gov/EID/article/29/1/22-0154-App1.pdf).

Biologic factors did not influence fox exposure to CSG viruses; however, location was significantly associated with seroprevalence (β = −0.2, p<0.05) and was highest in foxes in the eastern Arctic (R^2 = 0.06, d.f. = 5, p<0.05). For caribou, location was also significantly associated with exposure (β = −0.6, p<0.001); the highest prevalence was observed in Nunavut and NT. In addition, ecotype (β = 0.3, p<0.001) and year (β = −0.2, p<0.001) were significant variables in the model (R^2 = 0.22, d.f. = 4, p<0.001); the highest exposures occurred in 2010 (94%) and 2012 (93%) in the boreal woodland ecotype (Table 4).

Discussion

This study demonstrates widespread exposure to mosquitoborne viruses in wildlife across northern Canada. Caribou were most often exposed to CSG viruses (likely JCV) with seroprevalence ≥80% in the NT and Nunavut. The high prevalence, along with identification of cervids as reservoir hosts in temperate regions, suggests that caribou might serve as reservoirs and sentinels for JCV (*27*). Caribou congregate in herds and are particularly vulnerable to arthropod bites during calving when they are sedentary (*28*). Thus, we expected higher rates of CSG virus exposure in caribou than in polar bears that spend a considerable amount of time on sea ice or foxes that

Table 3. Seroprevalence of California serogroup viruses in the western Hudson Bay polar bear population during 3 periods in study of widespread exposure to mosquitoborne California serogroup viruses in caribou, Arctic fox, red fox, and polar bears, Canada*

Years	Sample size	Prevalence, % (95% CI)	No. males	Prevalence, % (no.)	No. females	Prevalence, % (no.)
1986–1989	142	21 (13–26)	67	18 (12)	70	23 (16)
1995–1998	149	36 (28–44)	73	23 (17)	76	47 (36)
2015–2017	100	27 (19–36)	47	17 (8)	53	36 (19)

*Repeat samples from bears were counted individually if bears were sampled between periods. Only one sampling was counted if bears were sampled multiple times within the same period. Sex was not determined for 5 bears.

Table 4. Prevalence of California serogroup viruses within caribou ecotypes and herds/study areas across Canada in study of widespread exposure to mosquitoborne California serogroup viruses in caribou, Arctic fox, red fox, and polar bears*

Ecotype	Prevalence, % (95% CI) (no./total)	Herd or study area	Capture location	Prevalence, % (95% CI) (no./total)
Migratory tundra caribou	48 (42–54) (116/243)	Beverly	NT	83 (55–95) (10/12)
		Bluenose East	NT	60 (36–80) (9/15)
		Bathurst	NT	77 (50–92) (10/13)
		Dolphin and Union	Nunavut	80 (69–87) (58/73)
		Porcupine	Yukon	24 (15–35) (17/72)
		Forty Mile	Yukon	100 (57–100) (5/5)
		Leaf River	Nunavik, QC	13 (7–25) (7/53)
Mountain woodland caribou	59 (48–68) (51/87)	Heart River	Yukon	78 (58–90) (18/23)
		Ibex	Yukon	38 (14–69) (3/8)
		Clear Creek	Yukon	70 (48–86) (14/20)
		Carcross	Yukon	43 (25–64) (9/21)
		Tay River	Yukon	50 (10–91) (1/2)
		Laberge	Yukon	100 (21–100) (1/1)
		Pink Mountain	BC	67 (21–94) (2/3)
		Muskwa	BC	24 (5–70) (1/4)
		Kennedy Siding	BC	50 (10–91) (1/2)
		Itcha-Ilgachuz	BC	0 (0–79) (0/1)
		Chase	BC	0 (0–79) (0/1)
		Quinette	BC	100 (21–100) (1/1)
Boreal woodland caribou	87 (81–91) (149/172)	Chinchaga	BC	50 (10–91) (1/2)
		Snake-Sahtaneh	BC	100 (21–100) (1/1)
		Maxhamish	BC	0 (0–79) (0/1)
		Calendar	BC	100 (21–100) (1/1)
		North Deh Cho	NT	92 (78–97) (33/36)
		South Deh Cho	NT	89 (74–95) (31/35)
		Pine Point-Buffalo Lake	NT	97 (85–99) (34/35)
		Hay River Lowlands	NT	78 (61–89) (25/32)
		Mackenzie	NT	79 (62–90) (23/29)

*Ecotype data were not available for 13 caribou; herd/study area data were not available for 15 caribou. BC, British Columbia; NT, Northwest Territories; QC, Québec.

have a smaller body size and are nocturnally active (*29*,*30*). Sampling location (province/territory) was associated with exposure, and high seroprevalence in caribou in central and western Arctic regions contrasted with 13% seroprevalence in the eastern Arctic (Nunavik, Quebec). This result reflects a difference in virus prevalence, although the use of whole blood from harvested animals in the eastern Arctic likely underestimated seroprevalence, especially in the migratory tundra ecotype. Noticeable differences in prevalence were also observed between whole blood and serum samples from caribou in Nunavut (Table 2), indicating that whole blood is likely not an ideal sample for the cELISA.

Canada's changing climate might play a role in CSG virus seroprevalence. The western Arctic region in Canada is warming more rapidly than the eastern Arctic region of Canada and the rest of the world (*2*). Warming temperatures have been linked to changes in mosquito diversity, density, distribution, and host-seeking behaviors (*31*,*32*). For example, rising temperatures can increase mosquito development and survival and bring mosquitoes into phenologic synchrony with caribou, providing opportunities for pathogen transmission (*31*). Increases in precipitation might also influence regional differences in vector abundance and competence. Normalized precipitation increased 30% from 1948 to 2012 in the Arctic region of Canada (*33*), especially in Nunavut, thereby increasing the abundance of larval development sites for mosquito vectors (*2*,*34*). Sampling year also influenced caribou exposure. Therefore, future long-term studies should investigate associations between climate and temporal patterns of exposure in caribou, as we did for polar bears.

Ecotype was the final factor that was associated with caribou exposure. Boreal caribou had greater exposure than those in other ecotypes (87%; Table 4). Boreal caribou remain in treed environments year-round, whereas tundra and mountain caribou migrate to tundra and alpine habitats during the summer months (*35*,*36*). Warmer temperatures at lower altitudes and lower windspeeds in treed environments might increase exposure to insect bites (*37*). Climate change has been linked to the northward advancement of the tree line, which might increase exposure to CSG viruses for caribou populations in the future (*4*). These factors, along with differences in the distribution and diversity of mosquito species and their vector competence, might all contribute to observed variations in seroprevalence among caribou and might also correlate with risk for human exposure.

In foxes, overall CSG virus seroprevalence was much lower than for caribou, likely because of lower exposure to mosquitoes (smaller body size, nocturnal activity) (*30*). Region was associated with exposure in foxes. However, contrary to the results from caribou, the highest seroprevalence for foxes was in northern Quebec (30% for Arctic fox and 20% for red fox). This result might reflect a difference in viral serotype in foxes. Caution is warranted when interpreting these results because the sample size in this region was small (n = 10 for each species) and only samples from 4 foxes were successfully tested by using PRNTs, which revealed exposure to JCV. Increasing the number of fox samples tested with cELISA and PRNT would help identify what CSG viruses are present in northern Quebec.

Archived serum samples from western Hudson Bay polar bears provided a unique opportunity to monitor changes in exposure to CSG viruses and other pathogens (*18*) over time in one of the most rapidly warming Arctic regions in Canada. Exposure to CSG viruses in polar bears increased between 1986–1989 and 1995–1998 but did not continue to increase during 2015–2017 (Table 3). We found a strong positive association between air temperatures in the previous summer and virus exposure. Warmer air temperatures during summer when bears are on land likely increased the abundance of mosquitoes and bite exposures, especially in peatland ecosystems that are not moisture limited, overwhelming the influence of other climatic factors on CSG virus exposure. Summer air temperature and ice-free days did not increase from 1995–1998 to 2015–2017 (Appendix Table 2), which might explain the lack of continued increase in exposure to CSG viruses. However, because sea ice breakup in western Hudson Bay has been occurring ≈5–6 days earlier per decade (*15*,*29*) and temperatures continue to rise, polar bear exposures to vectorborne pathogens, including CSG viruses, will likely increase.

Summer segregation of polar bears by age and sex might partly explain why female and younger adult bears had higher CSG virus exposure. Hudson Bay is ice-free during the summer and fall, forcing polar bears onshore for 3–4 months; pregnant females are forced onshore for 8 months (*38*–*40*). While onshore, adult males are typically found in drier coastal areas, whereas adult females with cubs and pregnant females travel inland (*39*). The inland area consists of peatlands that are underlain by continuous permafrost resulting in poor drainage and extensive bogs and fens (*41*,*42*). Dens are constructed in peat deposits near water sources (*41*–*44*). Thus, proximity to stagnant water likely accounts for increased exposure of females and young bears to mosquito bites. Our study design limited the analysis to adult polar bears, and the age effect might have been more pronounced with the inclusion of younger animals.

Polar bears that were captured in Churchill were less likely to be exposed to CSG viruses, which is congruent with patterns of exposure to *Francisella tularensis* previously described (*18*). Similar to CSG viruses, the life cycle of *F. tularensis* involves transmission by biting insects (*45*). Churchill is on the Hudson Bay coast, and polar bears previously captured in town might be more likely to inhabit coastal areas that have reduced exposure to biting insects than polar bears found farther inland. These results suggest that persons in coastal regions of the Arctic have lower risk for arboviral exposure than those who live or travel inland.

Rodents and lagomorphs are theorized reservoirs for SSHV (*5*). However, all rodent samples tested during this study were negative for SSHV RNA, possibly caused by the short viremia duration typically associated with arboviral infections or by sample storage. For example, white-tailed deer (*Odocoileus virginianus*) had detectable JCV in the blood for only 2–4 days after inoculation (*27*). Thus, antibody rather than virus detection might be more practical for CSG virus surveillance, and hosts with larger blood volume (such as hares) might be better suited as sentinels for SSHV surveillance. However, serologic methods also introduce challenges. Results from repeatedly sampled caribou and polar bears suggest that antibodies might be relatively short-lived. In addition, 3 caribou seroconverted over winter, which suggests that false positives are possible.

All caribou samples from the NT tested by using PRNT had neutralizing antibodies against JCV, which was expected because white-tailed deer have been suggested as reservoir hosts for JCV in the United States and Canada (*46*,*47*). In Quebec, areas with moderate densities of white-tailed deer were associated with greater risk for human JCV seropositivity (*48*). Although exposure to JCV was expected, 4 caribou from the NT also had antibodies against SSHV, suggesting serologic cross-reactivity or exposure to both viruses.

Climate change, along with a deep cultural relationship between Indigenous persons and wildlife, suggests that northern Canada is an ideal location to study the effects of environmental variability on diseases that affect both human and animal health (*49*). This study demonstrated widespread distribution and regional differences in exposure to CSG viruses in wildlife of northern Canada across multiple ecosystems, highlighting the benefit of monitoring wildlife as

sentinels for human disease risk. We identified high CSG virus seroprevalence in caribou populations, some of which are declining across northern Canada, emphasizing the need to determine whether caribou are reservoir hosts and whether JCV affects health and fecundity of these animals. Our finding of increased CSG virus seroprevalence in polar bears over time demonstrates the utility of comparing prevalence of climate sensitive diseases against baseline values for species known to be affected by rapid climate change (*18*,*50*). We identified summer air temperature as a key factor influencing polar bear exposure to CSG viruses, suggesting that infections will likely become more prevalent as the climate continues to change. Our study provides preliminary data for future surveillance of mosquitoborne viruses and highlights the need for continued studies to decipher the transmission dynamics of vectorborne diseases in regions experiencing substantial climate change. Future sustained surveillance of CSG and other arboviruses would provide additional information to measure health risks for humans and wildlife of conservation significance.

Acknowledgments

We thank the Hunters and Trappers Organization in Kugluktuk, regional and local Nunavimmi Umajulivijiit Katujaqatigininga (LNUK and RNUK), Makivik Corporation, Nunavik Research Centre, Faculté de Médecine Vétérinaire and Centre québécois sur la santé des animaux sauvages (CQSAS), Hunters and Trappers Organization in Cambridge Bay (Ekaluktutiak), Gjoa Haven (Oksoktok); Jack Skillings, Matilde Tomaselli, Dana Kellett; Susan Kutz and her laboratory team, especially Angie Schneider and James Wang, Marsha Branigan, Christine Menno, Verna Pokiak, Ève Lamontagne, Judy Williams, Kyle Russell, Kelsey Russell, Mike Suitor, Martin Keinzler, Maud Henaff; regional staff and the BC Wildlife Health program; staff and graduate students who collected polar bear samples as part of Environment and Climate Change Canada's long-term research; Ian Stirling, Andrew Derocher, Dennis Andriashek, Bruce Rideout, Megan Owen, Megan Jones, and Courtney Loomer and Brooks Waitt for assistance with sample collection and storage, permit acquisition, or laboratory analyses.

Fox, rodent, and caribou work was supported by NSERC Discovery Grant and Northern Research Supplement (nos. NRS-2018-517969, RGPIN-2018-04900, and RGPIN-04171-2014), Weston Family Foundation, Northern Scientific Training Program, ArcticNet, Irving Maritime Shipbuilding/Nunavut Arctic College, and Polar Knowledge Canada (grant nos. NST-1718-0012 and NST-1718-0015). The long-term research at Karrak Lake, Nunavut, has been supported by Polar Continental Shelf Project, Central and Mississippi Flyway Councils, Canadian Wildlife Service, and Wildlife Research Division of Environment and Climate Change. Funding for caribou work was also provided by the Government of Yukon, Environment Climate Change Canada, and Parks Canada. Polar bear testing was funded by the McBeth Foundation. Financial and logistic support for fieldwork was provided by the Canadian Association of Zoos and Aquariums, Churchill Northern Studies Centre, Canadian Wildlife Federation, Care for the Wild International, Earth Rangers Foundation, Hauser Bears, the Isdell Family Foundation, Manitoba Sustainable Development, Natural Sciences and Engineering Research Council of Canada, Parks Canada Agency, Polar Bears International, Quark Expeditions, Schad Foundation, Wildlife Media Inc., and World Wildlife Fund (Canada).

Fox research was approved by the Government of Nunavut (permit nos. 2014-029, 2015-019, 2016-015, 2017-009, 2018-014, and 2019-03) and University of Saskatchewan Animal Research Ethics Board (approval nos. 20090159 and 19990029). Rodent trapping in Nunavut was approved under Government of Nunavut wildlife permits (nos. 2018-013 and 2019-016) and University of Saskatchewan Animal Research Ethics Board (approval no. 2011-0030 and 2019-0021). Rodent and shrew trapping in the NT was approved under permit NWTWCC 2021-001 (live-trapping) and NWTWCC 2021-002 (snap-trapping). Polar bear research was approved under Government of Manitoba wildlife research permits (nos. SAR14010 and SAR20663), Parks Canada Agency wildlife research and collection permits (nos. WAP-2014-17039 and WAP-2017-26059), and Environment and Climate Change Canada Western and Northern Animal Care Committee protocol approvals (nos. 15NL01, 16NL01, and 17NL01). BC caribou samples were collected under Wildlife Act permits (nos. FJ14-93094, FJ18-421458, FJ19-426636, FJ21-618702, and PG17-284065). Yukon caribou samples were also collected under the Wildlife Act (exemption for Yukon Government staff) and protocols were approved by the Yukon Government Wildlife Care Committee. All animal use adhered to the Canadian Council on Animal Care guidelines for humane animal use (https://ccac.ca/en/standards/guidelines).

About the Author

Ms. Buhler is a PhD candidate at the University of Saskatchewan. Her research interests include the epidemiology and ecology of zoonotic pathogens and focuses on vectorborne pathogen transmission in wildlife across northern ecosystems.

References

1. Hoberg EP, Brooks DR. Evolution in action: climate change, biodiversity dynamics and emerging infectious disease. Philos Trans R Soc Lond B Biol Sci. 2015;370:20130553. https://doi.org/10.1098/rstb.2013.0553
2. Zhang X, Flato G, Kirchmeier-Young M, Vincent L, Wan H, Wang X, et al. Changes in temperature and precipitation across Canada. In: Bush E, Lemmen DS, editors. Canada's changing climate report. Ottawa (ON, Canada): Government of Canada; 2019. p. 112–93.
3. Bintanja R. The impact of Arctic warming on increased rainfall. Sci Rep. 2018;8:16001. https://doi.org/10.1038/s41598-018-34450-3
4. Grace J, Berninger F, Nagy L. Impacts of climate change on the tree line. Ann Bot. 2002;90:537–44. https://doi.org/10.1093/aob/mcf222
5. Drebot MA. Emerging mosquito-borne bunyaviruses in Canada. Can Commun Dis Rep. 2015;41:117–23. https://doi.org/10.14745/ccdr.v41i06a01
6. Hughes HR, Lanciotti RS, Blair CD, Lambert AJ. Full genomic characterization of California serogroup viruses, genus *Orthobunyavirus*, family Peribunyaviridae including phylogenetic relationships. Virology. 2017;512:201–10. https://doi.org/10.1016/j.virol.2017.09.022
7. Meier-Stephenson V, Langley JM, Drebot M, Artsob H. Encephalitis in the summer: a case of snowshoe hare (California serogroup) virus infection in Nova Scotia. Can Commun Dis Rep. 2007;33:23–6.
8. LeDuc JW. Epidemiology and ecology of the California serogroup viruses. Am J Trop Med Hyg. 1987;37:60S–8S. https://doi.org/10.4269/ajtmh.1987.37.60S
9. Vosoughi R, Walkty A, Drebot MA, Kadkhoda K. Jamestown Canyon virus meningoencephalitis mimicking migraine with aura in a resident of Manitoba. CMAJ. 2018;190:E262–4. https://doi.org/10.1503/cmaj.170940
10. Miernyk KM, Bruden D, Parkinson AJ, Hurlburt D, Klejka J, Berner J, et al. Human seroprevalence to 11 zoonotic pathogens in the U.S. Arctic, Alaska. Vector Borne Zoonotic Dis. 2019;19:563–75. https://doi.org/10.1089/vbz.2018.2390
11. Villeneuve CA, Buhler KJ, Iranpour M, Avard E, Dibernardo A, Fenton H, et al. New records of California serogroup viruses in Aedes mosquitoes and first detection in simulioidae flies from Northern Canada and Alaska. Polar Biol. 2021;44:1911–5. https://doi.org/10.1007/s00300-021-02921-5
12. McCall AG, Derocher AE, Lunn NJ. Home range distribution of polar bears in western Hudson Bay. Polar Biol. 2015;38:343–55. https://doi.org/10.1007/s00300-014-1590-y
13. Buhler KJ, Maggi RG, Gailius J, Galloway TD, Chilton NB, Alisauskas RT, et al. Hopping species and borders: detection of Bartonella spp. in avian nest fleas and arctic foxes from Nunavut, Canada. Parasit Vectors. 2020;13:469. https://doi.org/10.1186/s13071-020-04344-3
14. Chevallier C, Gauthier G, Berteaux D. Age estimation of live arctic foxes Vulpes lagopus based on teeth condition. Wildlife Biol. 2017;2017:1–6. https://doi.org/10.2981/wlb.00304
15. Lunn NJ, Servanty S, Regehr EV, Converse SJ, Richardson E, Stirling I. Demography of an apex predator at the edge of its range: impacts of changing sea ice on polar bears in Hudson Bay. Ecol Appl. 2016;26:1302–20. https://doi.org/10.1890/15-1256
16. Stirling I, Spencer C, Andriashek D. Immobilization of polar bears (*Ursus maritimus*) with Telazol in the Canadian Arctic. J Wildl Dis. 1989;25:159–68. https://doi.org/10.7589/0090-3558-25.2.159
17. Calvert W, Ramsay MA. Evaluation of age determination of polar bears by counts of cementum growth layer groups. Ursus. 1998;10:449–53.
18. Pilfold NW, Richardson ES, Ellis J, Jenkins E, Scandrett WB, Hernández-Ortiz A, et al. Long-term increases in pathogen seroprevalence in polar bears (*Ursus maritimus*) influenced by climate change. Glob Change Biol. 2021;27:4481–97. https://doi.org/10.1111/gcb.15537
19. Rocheleau JP, Michel P, Lindsay LR, Drebot M, Dibernardo A, Ogden NH, et al. Emerging arboviruses in Quebec, Canada: assessing public health risk by serology in humans, horses and pet dogs. Epidemiol Infect. 2017;145:2940–8. https://doi.org/10.1017/S0950268817002205
20. Beaty BJ, Calisher CH, Shope RS. Arboviruses. In: Schmidt NJ, Emmons RW, editors. Diagnostic procedures for viral, rickettsial and chlamydial Infections. Washington: American Public Health Association; 1989. p. 797–856.
21. Sergeant ESG. Epitools epidemiological calculators. Ausvet, 2019 [cited 2021 Aug 15]. https://epitools.ausvet.com.au
22. Stirling I, Thiemann GW, Richardson E. Quantitative support for a subjective fatness index for immobilized polar bears. J Wildl Manage. 2008;72:568–74. https://doi.org/10.2193/2007-123
23. Thiemann GW, Lunn NJ, Richardson ES, Andriashek DS. Temporal change in the morphometry–body mass relationship of polar bears. J Wildl Manage. 2011;75:580–7. https://doi.org/10.1002/jwmg.112
24. Towns L, Derocher AE, Stirling I, Lunn NJ, Hedman D. Spatial and temporal patterns of problem polar bears in Churchill, Manitoba. Polar Biol. 2009;32:1529–37. https://doi.org/10.1007/s00300-009-0653-y
25. Cavalieri DJ, Parkinson CL, Gloersen P, Zwally HJ. Sea ice concentrations from Nimbus-7 SMMR and DMSP SSM/I-SSMIS passive microwave data, version 1. Boulder (CO): NASA National Snow and Ice Data Center Distributed Active Archive Center; 1996. https://doi.org/10.5067/8GQ8LZQVL0VL
26. Government of Canada. Historical Data. National Climate Data and Information Archive [cited 2020 Feb 23]. https://climate.weather.gc.ca/historical_data/search_historic_data_e.html
27. Watts DM, Tammariello RF, Dalrymple JM, Eldridge BF, Russell PK, Top FH Jr. Experimental infection of vertebrates of the Pocomoke Cypress Swamp, Maryland with Keystone and Jamestown Canyon viruses. Am J Trop Med Hyg. 1979;28:344–50. https://doi.org/10.4269/ajtmh.1979.28.344
28. Corbet PS, Downe AER. Natural hosts of mosquitoes in northern Ellesmere Island. Arctic. 1966;19:153–61. https://doi.org/10.14430/arctic3422
29. Castro de la Guardia L, Myers PG, Derocher AE, Lunn NJ, Terwisscha van Scheltinga AD. Sea ice cycle in western Hudson Bay, Canada, from a polar bear perspective. Mar Ecol Prog Ser. 2017;564:225–33. https://doi.org/10.3354/meps11964
30. Audet AM, Robbins CB, Larivière S. *Alopex lagopus*. Mammalian Species. 2002;713:1–10. https://doi.org/10.1644/1545-1410(2002)713<0001:AL>2.0.CO;2
31. Culler LE, Ayres MP, Virginia RA. In a warmer Arctic, mosquitoes avoid increased mortality from predators by growing faster. Proc Biol Sci. 2015;282:20151549. https://doi.org/10.1098/rspb.2015.1549
32. Corbet PS, Danks HV. Egg-laying habits of mosquitoes in the high Arctic. Mosquito News. 1975;35:8–14.
33. Vincent LA, Zhang X, Brown RD, Feng Y, Mekis E, Milewska EJ, et al. Observed trends in Canada's climate and influence of low-frequency variability modes.

J Clim. 2015;28:4545–60. https://doi.org/10.1175/JCLI-D-14-00697.1
34. Ogden NH, Lindsay LR, Ludwig A, Morse AP, Zheng H, Zhu H. Weather-based forecasting of mosquito-borne disease outbreaks in Canada. Can Commun Dis Rep. 2019;45:127–32. https://doi.org/10.14745/ccdr.v45i05a03
35. Seip DR, Cichowski DB. Population ecology of caribou in British Columbia. Rangifer. 1996;16:73–80. https://doi.org/10.7557/2.16.4.1223
36. Bergerud AT. Caribou. In: Davis DE, editor. CRC handbook of census methods for terrestrial vertebrates, 1st ed. Boca Raton (LA): CRC Press; 1982. p. 268–270
37. Downes CM, Theberge JB, Smith SM. The influence of insects on the distribution, microhabitat choice, and behaviour of the Burwash caribou herd. Can J Zool. 1986;64:622–9. https://doi.org/10.1139/z86-092
38. Stirling I, Jonkel C, Smith P, Robertson R, Cross D. The ecology of the polar bear (*Ursus maritimus*) along the western coast of Hudson Bay. Canadian Wildlife Service, occasional paper no. 33, 1977 [cited 2021 Oct 20]. https://publications.gc.ca/collections/collection_2018/eccc/CW69-1-33-eng.pdf
39. Derocher AE, Stirling I. Distribution of polar bears (*Ursus maritimus*) during the ice-free period in western Hudson Bay. Can J Zool. 1990;68:1395–403. https://doi.org/10.1139/z90-208
40. Peacock E, Derocher AE, Lunn NJ, Obbard ME. Polar bear ecology and management in Hudson Bay in the face of climate change. In: Ferguson SH, Loseto LL, Mallory ML, editors. A little less Arctic. Dordrecht (the Netherlands): Springer-Verlag; 2010. p. 93–116.
41. Ritchie JC. The vegetation of northern Manitoba. V. Establishing the major zonation. Arctic. 1960;13:210–29. https://doi.org/10.14430/arctic3703
42. Brook RK. Structure and dynamics of the vegetation in Wapusk National Park and the Cape Churchill Wildlife Management Area of Manitoba, community and landscape scales [master's thesis]. Winnipeg (MN, Canada): University of Manitoba; 2001.
43. Clark DA, Stirling I, Calvert W. Distribution, characteristics, and use of earth dens and related excavations by polar bears on the western Hudson Bay lowlands. Arctic. 1997;50:158–66. https://doi.org/10.14430/arctic1098
44. Richardson E, Stirling I, Hik DS. Polar bear (*Ursus maritimus*) maternity denning habitat in western Hudson Bay: a bottom-up approach to resource selection functions. Can J Zool. 2005;83:860–70. https://doi.org/10.1139/z05-075
45. Feldman KA. Tularemia. J Am Vet Med Assoc. 2003;222:725–30. https://doi.org/10.2460/javma.2003.222.725
46. Hollis-Etter KM, Montgomery RA, Etter DR, Anchor CL, Chelsvig JE, Warner RE, et al. Environmental conditions for Jamestown Canyon virus correlated with population-level resource selection by white-tailed deer in a suburban landscape. PLoS One. 2019;14:e0223582. https://doi.org/10.1371/journal.pone.0223582
47. Patriquin G, Drebot M, Cole T, Lindsay R, Schleihauf E, Johnston BL, et al. High seroprevalence of Jamestown Canyon virus among deer and humans, Nova Scotia, Canada. Emerg Infect Dis. 2018;24:118–21. https://doi.org/10.3201/eid2401.170484
48. Rocheleau JP, Michel P, Lindsay LR, Drebot M, Dibernardo A, Ogden NH, et al. Risk factors associated with seropositivity to California serogroup viruses in humans and pet dogs, Quebec, Canada. Epidemiol Infect. 2018;146:1167–76. https://doi.org/10.1017/S0950268818001000
49. Dudley JP, Hoberg EP, Jenkins EJ, Parkinson AJ. Climate change in the North American Arctic: a One Health perspective. Ecohealth. 2015;12:713–25. https://doi.org/10.1007/s10393-015-1036-1
50. Fuglei E, Ims RA. Global warming and effects on the Arctic fox. Sci Prog. 2008;91:175–91. https://doi.org/10.3184/003685008X327468

Address for correspondence: Kayla J. Buhler, Department of Veterinary Microbiology, Western College of Veterinary Medicine, 52 Campus Dr, Saskatoon, SK S7N 5B4, Canada; email: kab048@mail.usask.ca

Genomic Confirmation of *Borrelia garinii*, United States

Natalie Rudenko, Maryna Golovchenko, Ales Horak, Libor Grubhoffer, Emmanuel F. Mongodin,[1] Claire M. Fraser, Weigang Qiu, Benjamin J. Luft, Richard G. Morgan, Sherwood R. Casjens, Steven E. Schutzer

Lyme disease is a multisystem disorder primarily caused by *Borrelia burgdorferi* sensu lato. However, *B. garinii*, which has been identified on islands off the coast of Newfoundland and Labrador, Canada, is a cause of Lyme disease in Eurasia. We report isolation and whole-genome nucleotide sequencing of a *B. garinii* isolate from a cotton mouse (*Peromyscus gossypinus*) in South Carolina, USA. We identified a second *B. garinii* isolate from the same repository. Phylogenetic analysis does not associate these isolates with the previously described isolates of *B. garinii* from Canada.

Lyme disease is a multisystem disorder caused by infection with bacteria of the *Borrelia burgdorferi* sensu lato species complex. Three members of this complex, *B. burgdorferi* sensu stricto, *B. garinii*, and *B. afzelii*, are responsible for most cases of Lyme disease worldwide (*1*,*2*). *B. burgdorferi* s.l. is the only one of these 3 species that is found widely in North America, although *B. garinii* has been identified on islands off the coast of Newfoundland and Labrador, Canada (*3*–*5*).

We describe the isolation and genome sequencing characterization of a South Carolina *B. garinii* isolate from a repository of strains from rodent hosts and tick vectors in the southeastern United States that had been identified as *B. burgdorferi* s.l. A second *B. garinii* isolate from the same *B. burgdorferi* s.l. strain repository was identified on the basis of multilocus sequence typing (MLST). Phylogenetic analysis showed that these 2 strains from the southeastern United States were most closely related to a group of *B. garinii* isolates from Europe but were not derived from strains from Canada, or vice versa (*3*).

Author affiliations: Institute of Parasitology, Biology Centre Czech Academy of Sciences, Ceske Budejovice, Czech Republic (N. Rudenko, M. Golovchenko, A. Horak, L. Grubhoffer); University of Maryland School of Medicine, Baltimore, Maryland, USA (E.F. Mongodin, C.M. Fraser); Hunter College of the City University of New York, New York, New York, USA (W. Qiu); Stony Brook University, Stony Brook, New York, USA (B.J. Luft); New England Biolabs, Ipswich, Massachusetts, USA (R.G. Morgan); University of Utah, Salt Lake City, Utah, USA (S.R. Casjens); Rutgers New Jersey Medical School, Newark, New Jersey, USA (S.E. Schutzer)

DOI: https://doi.org/10.3201/eid2901.220930

Methods

Sources, Cultivation, and Analyses of *Borrelia* spp.

The 2 *Borrelia* isolates described were isolated from ear biopsy specimens from a cotton mouse (*Peromyscus gossypinus*) (SCCH-7) trapped in Charleston County, South Carolina, in 1995 and from an eastern woodrat (*Neotoma floridana*) (SCGH-19) trapped in Georgetown County, South Carolina, in 1996 (Appendix, https://wwwnc.cdc.gov/EID/article/29/1/22-0930-App1.pdf) (*6*). We performed *Borrelia* culture in Barbour-Stoenner-Kelly H medium, DNA purification, and PCR analyses as described (*7*). We detected *B. burgdorferi* s.l. in samples by amplification of the 5S-23S intergenic region (*8*) (Appendix) by using species-specific PCR and primers designed on the basis of the *ospA* gene, which confirmed the presence of multiple spirochete species (*9*). Cultures in which *B. garinii* was confirmed were plated on solid medium, and clonal single colonies were isolated according to a modified protocol (*10*) (Appendix).

Whole-Genome Sequencing and Genome Assembly

We performed whole-genome sequencing by using the Pacific Biosciences Sequel II system (https://www.pacb.com). We performed genome assembly by using the Genome Assembly tool in PacBio SMRTLink version 10.2 and 150 Mb of the HiFi reads >5 kb (Appendix).

Nucleotide Sequence Accession Numbers

Sequences have been deposited in GenBank. The genome assembly of SCCH-7 has been deposited

[1]Current affiliation: National Institutes of Health, Bethesda, Maryland, USA.

in GenBank under BioProject PRJNA431102 and BioSample accession no. SAMN26226110 (Appendix). Nucleotide sequences of 8 housekeeping genes (*clpA*, *clpX*, *nifS*, *pepX*, *pyrG*, *recG*, *rplB*, and *uvrA*) of SCCH-7 and SCGT-19 have been deposited in GenBank under accession nos. KP795353–60 (SCCH-7) and KT285873–80 (SCGT-19). The MLST sequences have also been deposited into the PubMLST database (https://pubmlst.org) under allele numbers assigned to unique loci (SCCH-7, *clpX* allele no. 272 and *uvrA* allele no. 278; SCGT-19, *clpA* allele no. 311 and *clpX* gene allele no. 273). Unique sequence type (ST) numbers in the PubMLST database are 1049 for SCCH-7 and 1050 for SCGT-19.

Sequence Analysis

We performed MLST analysis of 8 housekeeping genes (*clpA*, *clpX*, *nifS*, *pepX*, *pyrG*, *recG*, *rplB*, and *uvrA*) of both isolates (SCCH-7 and SCGT-19) and whole-genome sequencing of strain SCCH-7 on DNA isolated at passage 6 as described (*11*). The maximum-likelihood phylogeny of *B. garinii* strains from a concatenated dataset of the 8 housekeeping loci sequences (184 total isolates, 4,791 nt) was inferred in RaxML (https://raxml-ng.vital-it.ch) under the generalized time reversible plus Γ4 model (Appendix). We performed phylogeographic analysis of diffusion on discrete space as implemented in BEAST (*12*) under the constant-size coalescent tree prior, and symmetric substitution model with Bayesian stochastic search variable selection enforced (Appendix). To compare sequences for the entire chromosome, we aligned the SCCH-7 chromosomal sequence with the 2 published chromosomal sequences of strain 20047 by using NUCMER (*13*). We derived a phylogenetic tree by using IQTREE (*14*) with default parameters from an MLST alignment of 34 *B. garinii* isolates most closely related to the 2 isolates from the United States.

Results

B. garinii from Rodents in South Carolina

The 2 *B. garinii* isolates we report were cultured from ear biopsy samples of a cotton mouse (*Peromyscus gossypinus*) (isolate SCCH-7) and an eastern woodrat (*Neotoma floridana*) (isolate SCGT-19); both were trapped in South Carolina (*6*). Those cultures were part of a southeastern United States collection of ≈300 *Borrelia* isolates that were obtained during 1991–1999 in Missouri, Georgia, Florida, Texas, and South Carolina and housed in the James H. Oliver, Jr., Institute of Arthropodology and Parasitology, Georgia Southern University (Statesboro, Georgia, USA). Multiple *Borrelia* species in numerous cultures of this collection, often present as co-infections, were reported in earlier investigations, including *B. andersonii* (*15*–*18*), *B. burgdorferi* s.s. (*6*,*15*,*19*), *B. bissettiae* (*15*–*18*), *B. carolinensis* (*7*,*20*), *B. americana* (*21*), and a previously undescribed isolate from Texas, TXW-1 (*16*–*18*).

We confirmed *B. burgdorferi* s.l. in cultures by PCR amplification of total DNA with a 5S-23S rRNA set of primers (*8*). We identified the *B. burgdorferi* s.l. species present by cloning the total PCR products into the pCR4-TOPO TA vector and sequencing individual recombinants. We observed sequences with high similarity to *B. garinii* from 5 cultures. We then plated those cultures on solid medium to obtain single colonies and chose pure clonal cultures of *B. garinii* SCCH-7 clone 138 and SCGT-19 clone 19 from 2 of the cultures for further study.

Whole-Genome Sequence of *B. garinii* Isolate SCCH-7

We determined the whole-genome sequence of isolate SCCH-7 by single-molecule real-time PacBio methods (Appendix). Similar to other *B. burgdorferi* sensu lato genomes (*22*–*24*), the SCCH-7 genome contains a linear chromosome and several linear plasmids (lp) and circular (cp) plasmids. SCCH-7 carries lp17, lp28–7, lp32–10, lp36, and lp54 and cp26, cp32–3, and cp32–6 (*25*). Plasmid SCCH-7 sequences are typical of known *B. garinii* genomes and are similar to those of *B. garinii* strain 20047, although strain 20047 carries an lp28–4 plasmid that is lacking in SCCH-7. The SCCH-7 genome is 1,161,212 bp (chromosome 906,106 bp, linear plasmids 168,083 bp, and circular plasmids 87,023 bp). Because the linear chromosome and plasmid sequences include all telomeres, this genome joins *B. burgdorferi* B31 and *B. mayonii* MN14–1539 genomes in being truly complete (*26*–*28*). The SCCH-7 chromosome differs from that of *B. garinii* strain 20047 by only 2 single-nucleotide variations (SNVs) and 2 short insertion/deletions from the sequence in accession no. CP028861 and by 8 SNVs and 4 short indels from the sequence in CP018744 (those 2 20047 chromosomal sequences were produced by 2 independent research groups, those of S. Bontemps-Gallo and G. Margos, Bioproject PRJNA224116). The 20047 plasmids were described briefly by Casjens et al. (*24*). This whole-genome sequence unambiguously demonstrates that SCCH-7 is a *B. garinii* isolate.

Phylogenetic Analysis

B. garinii isolates from North America have been previously reported on coastal islands in the Atlantic Ocean in eastern Canada (*3*–*5*,*29*). To investigate

whether the South Carolina isolates might have originated from these islands in Canada or vice versa, and to clarify the relationship of SCCH-7 and SCGT-19 with other *B. garinii* isolates, we amplified by using PCR and determined SCGT-19 sequences for the 8 genes (Appendix) previously used in MLST analyses of *B. burgdorferi* sensu lato isolates. We then extracted those sequences from the SCCH-7 and 20047 whole-genome sequences.

We compiled a phylogenetic tree (Appendix Figure 1) of the MLST data from isolates in this branch of the *B. burgdorferi* s.l. species and a maximum-likelihood (RAxML) tree (Figure) of the MLST sequences that includes isolates SCCH-7 and SCGT-19 and the 178 other isolates available from the closely related species *B. garinii* and *B. bavariensis*, as well as 5 isolates of *B. turdi* as an outgroup (Appendix Table 1). Apart from 1 unusual isolate from European Russia

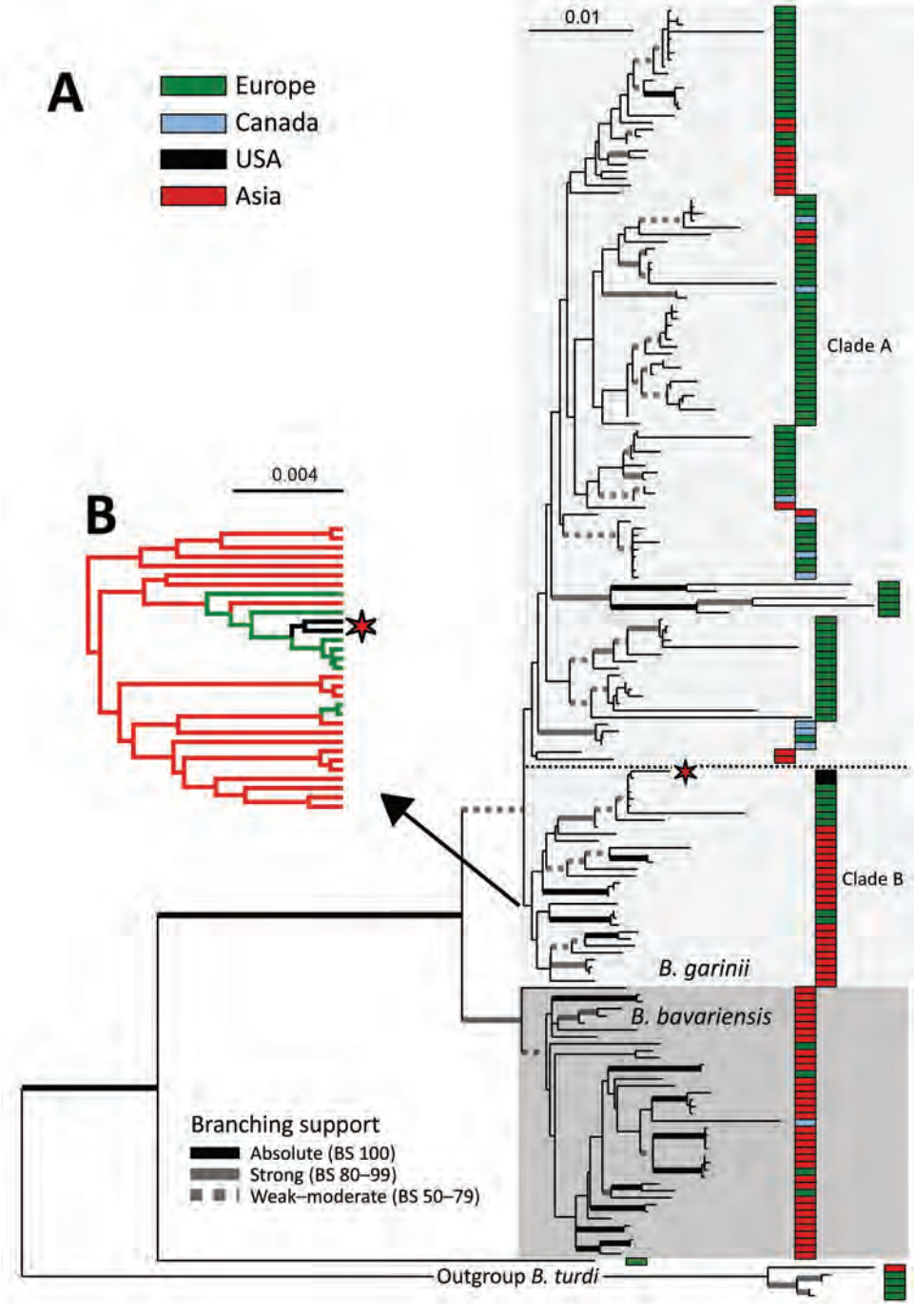

Figure. Maximum-likelihood phylogeny of *Borrelia garinii/B. bavariensis*. A) Maximum-likelihood phylogeny of *B. garinii/B. bavariensis* rooted with *B. turdi*. Topology is based on analysis of the partitioned dataset of 8 multilocus sequence typing genotyping loci s) under the generalized time reversible plus Γ4 model (for each partition) in RAxML 8 (https://cme.h-its.org/exelixis/web/software/raxml). The final alignment comprises 184 taxa and 4,791-nt positions. Thickened branches indicate branching support as estimated by nonparametric bootstrap analysis based on 1,000 replicates in RAxML 8. For better readability, support is categorized according to the scheme shown at the bottom of the tree. Isolates were clustered into 7 categories according to their geographic origin, which is color-coded according the scheme in the upper right part of the tree on the topology. The position of 2 US isolates is indicated by an asterisk. B) Subset of results phylogeographic analysis of diffusion on the discrete space showing the estimated geographic origin of the inner branches for the ancestral clade of *B. garinii* from Asia. Full topology is shown in Appendix Figure 2, panel B (https://wwwnc.cdc.gov/EID/article/29/1/22-0390-App1.pdf), and full details on the methods used are provided in the Appendix. Scale bars indicate nucleotide substitutions per site. BS, branching support.

(pubMLST ID:2488 Om16-103-Iapr) that is a sister branch to all the other isolates, the remaining 178 isolates form 2 clades that agree with previously defined *B. bavariensis* (39 isolates) and *B. garinii* (139 isolates) species (Figure) (*30*). The *B. bavariensis* group contains 4 isolates from Europe and 1 isolate from Canada, interspersed among most isolates from Asia, suggesting, on the basis of maximum parsimony, that this group is an ancestrally clade from Asia that has had several independent introgressions into Europe (*31*).

The *B. garinii* clade is split into 2 major clades. The larger one (clade A, 108 isolates) comprises 76 isolates from Europe, 13 from continental Asia, 2 from Japan, 9 from Canada (Newfoundland and Labrador), and 8 from Iceland that are mostly distributed within this branch without apparent clustering by geographic origins. The smaller *B. garinii* clade (clade B, 31 isolates) contains 21 isolates from continental Asia and Japan, 8 from Europe, and the 2 described here from the United States. The 2 United States isolates form a nested subclade with 5 strains of European origin in clade B (Figure, panel B). Also, the *B. garinii* from Canada are members of clade A (Figure) and are not closely related to the United States isolates.

To shed more light on the possible origin of the 2 United States isolates and the evolutionary history of *B. garinii* in general, we performed phylogeographic analysis of diffusion in discrete space as implemented in BEAST (Appendix). This Bayesian method infers the ancestral state at each node of a given discrete trait (in this case, the geographic origin of the strain). The resulting tree topology (Appendix Figure 2, panel A), as inferred under the Coalescence (https://www2.unil.ch/popgen/softwares/quantinemo/coalescence.html) constant size model, separated the isolates into several groups. The *B. bavariensis* clade and clade B, whose composition corresponds to the MLST topology (Figure), are both predicted to originate in Asia. The 2 United States isolates (Figure) are in clade B and nested among a few sequences from Europe (Appendix Figure 2). The isolates from Europe are split into 3 clades (A1, A2, and A3), the first of which (A1) is found at the base of the whole *B. bavariensis*/*B. garinii* portion of the tree. Clade A1 is composed of 5 divergent *B. garinii* isolates from Slovakia separated from all other isolates from Europe and the *B. bavariensis* isolates. The ancestral clade from Asia (clade B) (Figure; Appendix Figure 2, panel A) is nested within clade A1 and clade A2, which were both predicted to have origins in Europe. The terminal position of strains from Europe in the ancestral clade from Asia (clade B) suggests a secondary, more recent introduction into Europe from Asia. Thus, ancestral reconstruction with BEAST suggested frequent historical and recent migration events of *B. bavarensis* and *B. garinii* species within Eurasia.

The affiliation of United States isolates with Europe and the broader *B. garinii* ancestral clade from Asia (clade B) is consistently present in both trees (Figure; Appendix Figure 2, panel A) and is supported by phylogeographic reconstruction using the Bayesian stochastic search variable selection algorithm (*33*,*34*). However, because of the large single number of isolates and relatively low number of phylogenetic-informative positions (i.e., high sequence similarity), the bootstrap support of inner branches was not high. Therefore, we tested the independent evolutionary history of isolates from the United States and Canada by using the approximately unbiased topology test (*35*). First, we force-constrained the monophyly of the 2 United States isolates with each of the 9 isolates from Canada; we then used RAxML to reoptimize the general topology. We then compared the per-site log-likelihood scores of those alternative topologies with the original MLST topology (Figure) by using the approximately unbiased in CONSEL (*36*). The resulting p values, ranging from 1.48×10^{-36} to 1.9×10^{-2} (Appendix Table 2), support the rejection of a common origin of *B. garinii* from Canada and the United States. We conclude that, in contrast to the isolates from Canada, which might have been introduced there from Europe or Iceland by seabirds and ticks associated with them (*37*), *B. garinii* from the southeastern United States are a part of ancestral lineage from East Asia that might have arrived in the United States from Europe.

Chromosomal Relationships with Closely Related *B. garinii* Genomes

A maximum-likelihood tree of 32 closely related *B. garinii* genomes based on 8 housekeeping loci (Appendix Figure 3) shows that the 2 isolates from the United States cluster with a few isolates from Europe, which, by tree topology, were probably associated with an ancestor from Asia (Figure). We compiled all sequence differences at the 8 housekeeping loci among the strains that are most closely related to the 2 isolates from the United States (Appendix Table 3). The genome-derived MLST SCCH-7 sequence and 2 independent 20047 MLST sequences are nearly identical. The reported 20047 MSLT sequence has 2 differences in the *recG* gene compared with the 3 whole-genome sequences, probably caused by sequencing errors. Those sequence identities strongly support a non-Canada origin, specifically a recent Europe origin, of United States isolate SCCH-7.

In contrast to SCCH-7, strain SCGT-19 shows a distinct MLST haplotype defined by 16 SNVs and 1 short indel (Appendix Table 3). The SCGT-19 versions of some of these SNVs and the indel are found in other *B. garinii* strains from Japan and Europe, suggesting that they are unlikely to be sequencing errors. Furthermore, consecutive runs of SNVs at the *clpA* and *clpX* loci strongly indicate that their origins are caused by recombination and not de novo mutation. The differences between SCCH-7 and SCGT-19 suggests that a migration or importation of *B. garinii* from Eurasia to the United States might have consisted of multiple strains of a source population.

Discussion

Our results provide strong evidence that *B. garinii* has been present in rodents in South Carolina, although its current status there is not known. Specifically, 5 samples we tested were positive for *B. garinii*, and from 2 independent *B. garinii* cultures, we propagated and analyzed, SCCH-7 clone 138 and SCCH-19 clone 19.

MLST analyses of both isolates and whole-genome sequencing of SCCH-7 showed that these isolates are not closely related to *B. garinii* strains from Canada; however, they are closely related to a subset of Eurasian isolates. How and when *B. garinii* arrived in South Carolina remains unknown. There were no reported Lyme disease outbreaks in the southeastern United States in humans at the time the strains were deposited in the repository or during the subsequent 2 decades. This finding minimizes the urgency for an immediate new search for *B. garinii* in this region. Nonetheless, clinical vigilance for *B. garinii* in humans in this region seems warranted.

Acknowledgments

We thank all former members of the James Oliver, Jr. Institute of Arthropodology and Parasitology, Statesboro, GA, for contributing to establishment of the southeastern spirochete collection during 1991–1999, and Xiaohua Yang for her contributions in culturing the microbes.

This study was supported in part by grants AI110820 (C.M.F.) and AI139782 (W.Q.) from the National Institute of Allergy and Infectious Diseases, National Institutes of Health; by grants NV-19-05-00191 from the Ministry of Health of the Czech Republic (N.R and M.G.) and 21-26209S from the Czech Grant Agency (A.H.); the Institute of Parasitology, Biology Centre, Czech Academy of Sciences (N.R., M.G., A.H., and L.G.); the Institute for Genomic Sciences (C.M.F. and E.F.M.), New England BioLabs (R.G.M.); and the Steven and Alexandra Cohen Foundation and the Global Lyme Alliance (B.J.L.).

About the Author

Dr. Rudenko is a senior research scientist at the Institute of Parasitology, Biology Centre Czech Academy of Sciences, Ceske Budejovice, Czech Republic. Her primary research interests include spirochetes from the *B. burgdorferi* sensu lato complex, and ecologic, epidemiologic, and molecular aspects of Lyme disease.

References

1. Radolf JD, Caimano MJ, Stevenson B, Hu LT. Of ticks, mice and men: understanding the dual-host lifestyle of Lyme disease spirochaetes. Nat Rev Microbiol. 2012; 10:87–99. https://doi.org/10.1038/nrmicro2714
2. Piesman J, Schwan TG. Ecology of borreliae and their arthropod vectors. In: Samuels DS, Radolf JD, editors. *Borrelia*: molecular biology, host interaction, and pathogenesis.Norfolk (UK): Caister Academic; 2010. p. 251–78.
3. Smith RP Jr, Muzaffar SB, Lavers J, Lacombe EH, Cahill BK, Lubelczyk CB, et al. *Borrelia garinii* in seabird ticks (*Ixodes uriae*), Atlantic Coast, North America. Emerg Infect Dis. 2006;12:1909–12. https://doi.org/10.3201/eid1212.060448
4. Munro HJ, Ogden NH, Lindsay LR, Robertson GJ, Whitney H, Lang AS. Evidence for *Borrelia bavariensis* infections of *Ixodes uriae* within seabird colonies of the North Atlantic Ocean. Appl Environ Microbiol. 2017;83:e01087–17. https://doi.org/10.1128/AEM.01087-17
5. Baggs EM, Stack SH, Finney-Crawley JR, Simon NP. *Peromyscus maniculatus*, a possible reservoir host of *Borrelia garinii* from the Gannet Islands off Newfoundland and Labrador. J Parasitol. 2011;97:792–4. https://doi.org/10.1645/GE-2548.1
6. Oliver JH Jr, Clark KL, Chandler FW Jr, Tao L, James AM, Banks CW, et al. Isolation, cultivation, and characterization of *Borrelia burgdorferi* from rodents and ticks in the Charleston area of South Carolina. J Clin Microbiol. 2000;38:120–4. https://doi.org/10.1128/JCM.38.1.120-124.2000
7. Rudenko N, Golovchenko M, Grubhoffer L, Oliver JH Jr. *Borrelia carolinensis* sp. nov., a new (14th) member of the *Borrelia burgdorferi* sensu lato complex from the southeastern region of the United States. J Clin Microbiol. 2009a;47:134–41. https://doi.org/10.1128/JCM.01183-08
8. Postic D, Assous MV, Grimont PA, Baranton G. Diversity of *Borrelia burgdorferi* sensu lato evidenced by restriction fragment length polymorphism of rrf (5S)-rrl (23S) intergenic spacer amplicons. Int J Syst Bacteriol. 1994;44:743–52. https://doi.org/10.1099/00207713-44-4-743
9. Demaerschalck I, Ben Messaoud A, De Kesel M, Hoyois B, Lobet Y, Hoet P, et al. Simultaneous presence of different *Borrelia burgdorferi* genospecies in biological fluids of Lyme disease patients. J Clin Microbiol. 1995;33:602–8. https://doi.org/10.1128/jcm.33.3.602-608.1995
10. Rosa PA, Hogan D. Colony formation by *Borrelia burgdorferi* in solid medium: clonal analysis of *osp* locus variants. In: Proceedings of the 1st International Conference on Tick-Borne Pathogens at the Host-Vector Interface: An Agenda for Research; 1992 Sep 15–18. St. Paul (MN): University of Minnesota; 1992. p. 95–103.
11. Margos G, Gatewood AG, Aanensen DM, Hanincová K, Terekhova D, Vollmer SA, et al. MLST of housekeeping genes captures geographic population structure and suggests a European origin of *Borrelia burgdorferi*. Proc Natl

Acad Sci U S A. 2008;105:8730–5. https://doi.org/10.1073/pnas.0800323105
12. Camacho C, Coulouris G, Avagyan V, Ma N, Papadopoulos J, Bealer K, et al. BLAST+: architecture and applications. BMC Bioinformatics. 2009;10:421. https://doi.org/10.1186/1471-2105-10-421
13. Marçais G, Delcher AL, Phillippy AM, Coston R, Salzberg SL, Zimin A. MUMmer4: a fast and versatile genome alignment system. PLOS Comput Biol. 2018;14:e1005944. https://doi.org/10.1371/journal.pcbi.1005944
14. Nguyen L-T, Schmidt HA, von Haeseler A, Minh BQ. IQ-TREE: a fast and effective stochastic algorithm for estimating maximum-likelihood phylogenies. Mol Biol Evol. 2015;32:268–74. https://doi.org/10.1093/molbev/msu300
15. Oliver JH Jr, Lin T, Gao L, Clark KL, Banks CW, Durden LA, et al. An enzootic transmission cycle of Lyme borreliosis spirochetes in the southeastern United States. Proc Natl Acad Sci U S A. 2003;100:11642–5. https://doi.org/10.1073/pnas.1434553100
16. Lin T, Oliver JH Jr, Gao L, Kollars TM Jr, Clark KL. Genetic heterogeneity of *Borrelia burgdorferi* sensu lato in the southern United States based on restriction fragment length polymorphism and sequence analysis. J Clin Microbiol. 2001;39:2500–7. https://doi.org/10.1128/JCM.39.7.2500-2507.2001
17. Lin T, Oliver JH Jr, Gao L. Genetic diversity of the outer surface protein C gene of southern *Borrelia* isolates and its possible epidemiological, clinical, and pathogenetic implications. J Clin Microbiol. 2002;40:2572–83. https://doi.org/10.1128/JCM.40.7.2572-2583.2002
18. Lin T, Oliver JH Jr, Gao L. Comparative analysis of *Borrelia* isolates from southeastern USA based on randomly amplified polymorphic DNA fingerprint and 16S ribosomal gene sequence analyses. FEMS Microbiol Lett. 2003;228:249–57. https://doi.org/10.1016/S0378-1097(03)00763-8
19. Rudenko N, Golovchenko M, Hönig V, Mallátová N, Krbková L, Mikulásek P, et al. Detection of *Borrelia burgdorferi* sensu stricto *ospC* alleles associated with human lyme borreliosis worldwide in non-human-biting tick *Ixodes affinis* and rodent hosts in Southeastern United States. Appl Environ Microbiol. 2013;79:1444–53. https://doi.org/10.1128/AEM.02749-12
20. Rudenko N, Golovchenko M, Grubhoffer L, Oliver JH Jr. *Borrelia carolinensis* sp. nov., a novel species of the *Borrelia burgdorferi* sensu lato complex isolated from rodents and a tick from the south-eastern USA. Int J Syst Evol Microbiol. 2011;61:381–3. https://doi.org/10.1099/ijs.0.021436-0
21. Rudenko N, Golovchenko M, Lin T, Gao L, Grubhoffer L, Oliver JH Jr. Delineation of a new species of the *Borrelia burgdorferi* sensu lato complex, *Borrelia americana* sp. nov. J Clin Microbiol. 2009b;47:3875–80. https://doi.org/10.1128/JCM.01050-09
22. Casjens SR, Mongodin EF, Qiu WG, Dunn JJ, Luft BJ, Fraser-Liggett CM, et al. Whole-genome sequences of two *Borrelia afzelii* and two *Borrelia garinii* Lyme disease agent isolates. J Bacteriol. 2011;193:6995–6. https://doi.org/10.1128/JB.05951-11
23. Mongodin EF, Casjens SR, Bruno JF, Xu Y, Drabek EF, Riley DR, et al. Inter- and intra-specific pan-genomes of *Borrelia burgdorferi* sensu lato: genome stability and adaptive radiation. BMC Genomics. 2013;14:693. https://doi.org/10.1186/1471-2164-14-693
24. Casjens SR, Di L, Akther S, Mongodin EF, Luft BJ, Schutzer SE, et al. Primordial origin and diversification of plasmids in Lyme disease agent bacteria. BMC Genomics. 2018;19:218. https://doi.org/10.1186/s12864-018-4597-x
25. Casjens S, Eggers C, Schwartz I. Comparative genomics of *Borrelia*. In: Samuels DS, Radolf JD, editors. *Borrelia*: molecular biology, host interaction and pathogenesis. Norwich (UK): Horizon Scientific Press; 2010. p. 26–52.
26. Fraser CM, Casjens S, Huang WM, Sutton GG, Clayton R, Lathigra R, et al. Genomic sequence of a Lyme disease spirochaete, *Borrelia burgdorferi*. Nature. 1997;390:580–6. https://doi.org/10.1038/37551
27. Tourand Y, Deneke J, Moriarty TJ, Chaconas G. Characterization and *in vitro* reaction properties of 19 unique hairpin telomeres from the linear plasmids of the Lyme disease spirochete. J Biol Chem. 2009;284:7264–72. https://doi.org/10.1074/jbc.M808918200
28. Kingry LC, Batra D, Replogle A, Rowe LA, Pritt BS, Petersen JM. Whole genome sequence and comparative genomics of the novel Lyme borreliosis causing pathogen, *Borrelia mayonii*. PLoS One. 2016;11:e0168994. https://doi.org/10.1371/journal.pone.0168994
29. Comstedt P, Jakobsson T, Bergström S. Global ecology and epidemiology of *Borrelia garinii* spirochetes. Infect Ecol Epidemiol. 2011;1:9545. https://doi.org/10.3402/iee.v1i0.9545
30. Takano A, Nakao M, Masuzawa T, Takada N, Yano Y, Ishiguro F, et al. Multilocus sequence typing implicates rodents as the main reservoir host of human-pathogenic *Borrelia garinii* in Japan. J Clin Microbiol. 2011;49:2035–9. https://doi.org/10.1128/JCM.02544-10
31. Gatzmann F, Metzler D, Krebs S, Blum H, Sing A, Takano A, et al. NGS population genetics analyses reveal divergent evolution of a Lyme Borreliosis agent in Europe and Asia. Ticks Tick Borne Dis. 2015;6:344–51. https://doi.org/10.1016/j.ttbdis.2015.02.008
32. Suchard MA, Lemey P, Baele G, Ayres DL, Drummond AJ, Rambaut A. Bayesian phylogenetic and phylodynamic data integration using BEAST 1.10. Virus Evol. 2018;4:vey016. https://doi.org/10.1093/ve/vey016
33. Drummond AJ, Suchard MA, Xie D, Rambaut A. Bayesian phylogenetics with BEAUti and the BEAST 1.7. Mol Biol Evol. 2012;29:1969–73. https://doi.org/10.1093/molbev/mss075
34. Lemey P, Rambaut A, Drummond AJ, Suchard MA. Bayesian phylogeography finds its roots. PLOS Comput Biol. 2009;5:e1000520. https://doi.org/10.1371/journal.pcbi.1000520
35. Shimodaira H. An approximately unbiased test of phylogenetic tree selection. Syst Biol. 2002;51:492–508. https://doi.org/10.1080/10635150290069913
36. Shimodaira H, Hasegawa M. CONSEL: for assessing the confidence of phylogenetic tree selection. Bioinformatics. 2001;17:1246–7. https://doi.org/10.1093/bioinformatics/17.12.1246
37. Muzaffar SB, Smith RP Jr, Jones IL, Lavers J, Lacombe EH, Cahill BK, et al. Trans-Atlantic movement of the spirochete *Borrelia garinii*: the role of ticks and their seabird hosts. In: Paul E, editor. Emerging avian disease. Studies in Avian Biology, Volume 42. Berkeley (CA): University of California Press; 2012. p. 23–30.

Address for correspondence: Natalie Rudenko, Biology Centre, Czech Academy of Sciences, Institute of Parasitology, Branisovska 31, 37005, Ceske Budejovice, Czech Republic; email: natasha@paru.cas.cz

Seroepidemiology and Carriage of Diphtheria in Epidemic-Prone Area and Implications for Vaccination Policy, Vietnam

Noriko Kitamura, Thanh T. Hoan, Hung M. Do, The A. Dao, Lien T. Le, Thao T.T. Le, Thuy T.T. Doan, Thuong N. Chau, Hoi T. Dinh, Masaaki Iwaki, Mitsutoshi Senoh, Androulla Efstraciou, Nen M. Ho, Duc M. Pham, Duc-Anh Dang, Michiko Toizumi, Paul Fine, Hung T. Do, Lay-Myint Yoshida

In 2019, a community-based, cross-sectional carriage survey and a seroprevalence survey of 1,216 persons 1–55 years of age were conducted in rural Vietnam to investigate the mechanism of diphtheria outbreaks. Seroprevalence was further compared with that of an urban area that had no cases reported for the past decade. Carriage prevalence was 1.4%. The highest prevalence, 4.5%, was observed for children 1–5 years of age. Twenty-seven asymptomatic *Coerynebacterium diphtheriae* carriers were identified; 9 carriers had *tox* gene–bearing strains, and 3 had nontoxigenic *tox* gene–bearing strains. Child malnutrition was associated with low levels of diphtheria toxoid IgG, which might have subsequently increased child carriage prevalence. Different immunity patterns in the 2 populations suggested that the low immunity among children caused by low vaccination coverage increased transmission, resulting in symptomatic infections at school-going age, when vaccine-induced immunity waned most. A school-entry booster dose and improved infant vaccination coverage are recommended to control transmissions.

Diphtheria is an infectious disease caused by toxigenic strains of *Corynebacterium diphtheriae, C. ulcerans*, and, rarely, *C. pseudotuberculosis* (*1*–*3*). Although the diphtheria toxoid vaccine contributed to a decrease in the number of diphtheria cases globally, the disease remains a threat to public health, particularly in South and Southeast Asia (*4*,*5*).

Currently, the World Health Organization recommends 3 primary doses of the diphtheria–tetanus–pertussis (DTP) vaccine in young infants (i.e., at 6, 10, and 14 weeks of age), followed by 3 booster doses at 12–23 months, 4–7 years, and 9–15 years of age, to protect all age groups. Nevertheless, many low- and middle-income countries have not introduced all booster doses.

The Vietnamese Ministry of Health (MOH) first introduced DTP in 1981, targeting infants 2, 3, and 4 months of age. A booster dose targeting children 18 months of age was introduced during 2011 (*6*). Because of efforts in vaccination, reported diphtheria cases in Vietnam decreased to nearly zero by 2010. However, several small diphtheria outbreaks in remote districts in central and western Vietnam have been observed since 2013 (*7*).

Supplemental immunization activities (SIAs), in which vaccination is delivered to all targeted persons regardless of their previous vaccination history, were conducted in the areas surrounding Quang Ngai Province when diphtheria cases were identified during 2013–2019 (*8*). However, most of the population of Quang Ngai Province has not been covered by SIAs as of October 2019. According to the national surveillance program, Quang Ngai Province reported 2 laboratory-confirmed cases in 2017–2018 and 47 in 2019–2020, among an estimated population of 1,231,697 (*9*). Among these cases, 36 (73%) cases were in school-age children (6–17 years of age). Among confirmed cases, 3 (6%) were fatal.

Although national administrative coverage of 3 doses of DTP among infants has been maintained

Author affiliations: London School of Hygiene and Tropical Medicine, London, UK (N. Kitamura, P. Fine); Nagasaki University, Nagasaki, Japan (N. Kitamura, M. Toizumi, L.-M. Yoshida); Pasteur Institute in Nha Trang, Nha Trang, Vietnam (T.T. Hoan, H.M. Do, T.A. Dao, L.T. Le, T.T.T. Le, T.T.T. Doan, H.T. Do); Quang Ngai Provincial Health Services, Quang Ngai, Vietnam (T.N. Chau, H.T. Dinh, N.M. Ho, D.M. Pham); National Institute of Infectious Diseases, Tokyo, Japan (M. Iwaki, M. Senoh); National Institute of Hygiene and Epidemiology, Hanoi, Vietnam (D.-A. Dang); UK Health Security Agency, London (A. Efstraciou)

DOI: https://doi.org/10.3201/eid2901.220975

above 90% in Vietnam since 1994 (excluding 2002 and 2013), subnational coverage has not always been high (*10*). In addition, although low vaccination coverage in localized spots appeared to cause diphtheria outbreaks, the immune profile of the population in these areas is unknown (*4*). The World Health Organization suggests including adults in SIAs to control diphtheria outbreaks because adults might also be susceptible. However, no specific age groups are recommended because epidemiologic characteristics differ by country (*2*).

Asymptomatic carriers play a major role in transmission dynamics, but details of the carrier stage in affected areas are largely unknown because the proportion of healthy carriers who carry toxigenic and nontoxigenic strains has not been investigated in Southeast Asia (*11*,*12*). Moreover, host factors that govern carriage status have not been elucidated.

This study aimed primarily to measure the carriage prevalence of *Corynebacterium* species in the respiratory tract in areas in which outbreaks occurred and to assess potential risk factors for carriage. The second aim was to measure the age-stratified serologic immune profile against diphtheria toxin to help to identify the mechanism of the recent outbreaks and target the most appropriate age groups for SIA. Reflecting a previous study suggesting that low antibody levels increased the risk for being a carrier (*13*), this study also examined the factors that contributed to low immunity among persons. The third aim was to compare the immune profile patterns in areas in which cases have been reported and not reported to discuss the current DTP schedule in Vietnam.

Methods

Study Site

Two districts, Tay Tra and Son Ha in Quang Ngai Province, were selected as a study area because 3 diphtheria cases were identified there during January–September 2019, and no SIAs had been implemented (Figure 1). Two communes in the Son Ha District were excluded because a mop-up vaccination campaign of DTP was conducted in those communities during 2018. The estimated population of the 2 study districts was 99,121 in 2019 (*9*). Health access is limited in this area because of the mountainous topography.

Study Design and Sampling Method

We conducted a community-based cross-sectional survey in October 2019. We stratified age into 4 groups, 1–5, 6–17, 18–40, and 41–55 years of age; children attend primary through high school between

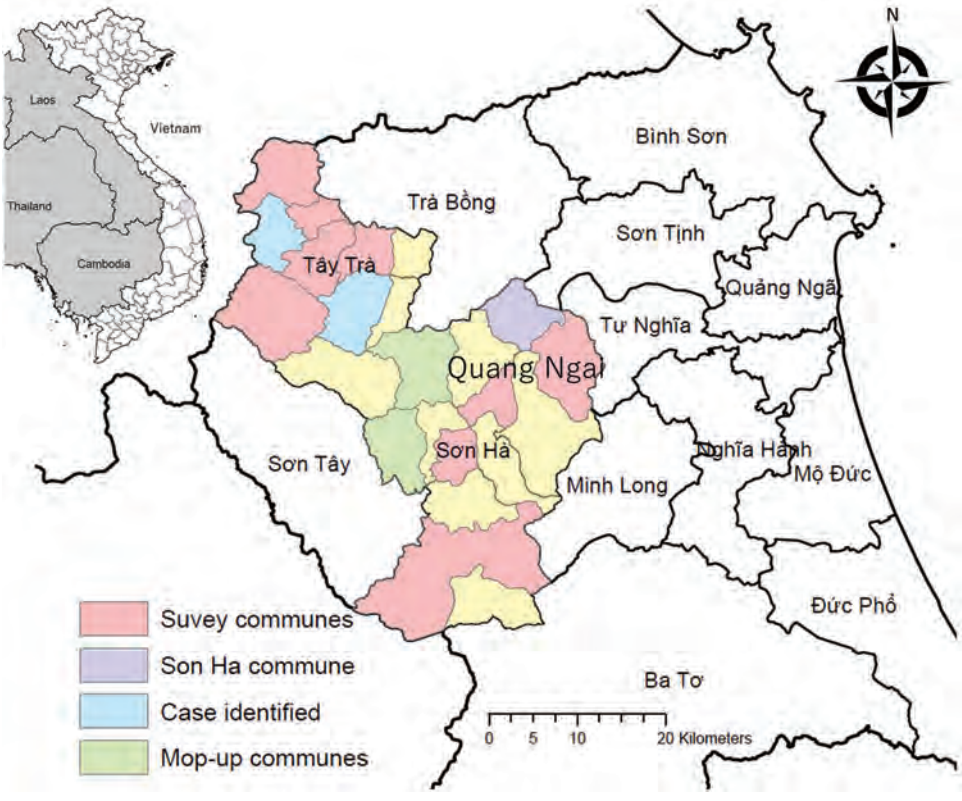

Figure 1. Study areas and locations where the cases were identified before and during diphtheria study in Tay Tra and Son Ha districts in Quang Ngai Province, Vietnam. Red and purple indicate 10 communes selected for this study. Blue and purple indicate 1 laboratory-confirmed diphtheria case reported during January–September 2019 in each of these communes. Purple (Son Ha commune) indicates 12 confirmed cases reported in this commune within 1 month from the survey date, October 2019. Green indicates 2 communes excluded from the selection process of this study because a mop-up vaccine campaign was conducted in 2018. Inset map shows location of the study area in Vietnam.

the ages of 6 and 17 years in Vietnam. On the basis of previously obtained age-stratified seroprevalence in Vietnam (*14*,*15*), the required sample size for each age stratum was estimated to be 350, 400, 400, and 350, respectively, with 10% precision, a 3.5 design effect, and an 80% response rate.

We conducted multistage cluster sampling. In each district, we sampled 5 communes by population proportion to size and selected 3 villages from each commune by simple random sampling. A total of 30 villages were selected (Figure 1). Because the average household size in Vietnam is 4 persons (*16*), we selected 15 households in each village and 450 households to recruit 1,500 persons. We oversampled households that had children 1–5 years of age to recruit a higher proportion of the sample size than the original population.

Data and Sample Collection and Ethics

Local healthcare workers visited homes of participants to invite them to participate in the survey. Written informed consent was obtained from each participant or guardian. The survey teams interviewed each participant by using a standardized questionnaire and collected sociodemographic information. Based on previously reported risk factors for diphtheria infection or carriage of *C. diphtheriae*, age, vaccination history, seropositivity (diphtheria toxoid IgG titer ≥0.1 IU/mL), bed-sharing, school attendance, staying in school dormitories, household size, frequency of bathing or handwashing, having livestock or companion animals, diphtheria toxoid IgG level, and mid-upper arm circumference (MUAC) were assessed for their association with carriage of *Corynebacterium* species (*13*,*17*–*21*). MUAC was used as a measure of the nutritional status of children 1–5 years of age. We collected vaccination history for children ≤10 years of age from either the vaccination card of the participant or the vaccine registration book at the respective community health centers in their residence area.

We collected dried blood spots (DBS) by using venipuncture or fingerprick onto 903 protein saver cards (#Z761575; Whatman, https://www.cytivalifesciences.com/en/us/about-us/our-brands/whatman) and stored them at −80°C according to the procedure of the Centers for Disease Control and Prevention (*22*,*23*). We collected throat swab specimens and stored them in Amies medium and collected nasopharyngeal swab specimens and stored them in skim milk, tryptone, glucose, and glycerin medium (*3*). All collected samples were stored at the Institut Pasteur Institute in Nha Trang and stored at −80°C until testing. Ethics approval was obtained from the ethical review boards of the Pasteur Institute in Nha Trang, MOH Vietnam, Nagasaki University, and the London School of Hygiene and Tropical Medicine (1775/IPN-DT, 1046/K2DT-KHCN, Nagasaki University Institutional Review Board approval no. 191226228, LSHTM ethics reference no. 17518).

Microbiological Tests

We cultured collected swab specimens on tellurite-containing agar medium in a 35°C incubator for 24–48 hours (*3*). If black colonies grew, we initially tested them by Gram stain to identify gram-positive bacilli (*3*). We used the API Coryne Test (bioMérieux, https://www.biomerieux.com) to identify species

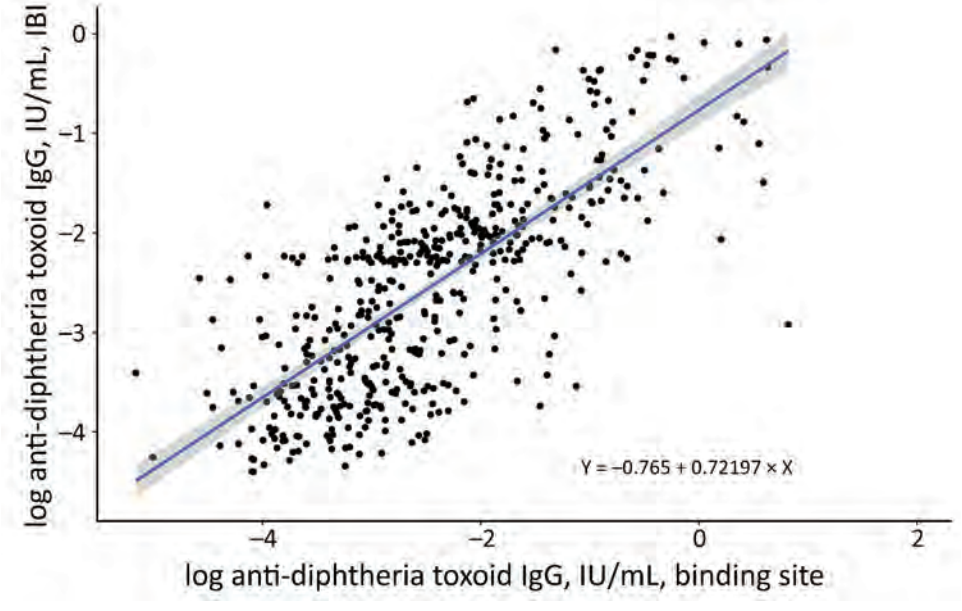

Figure 2. Best-fitted linear regression line (blue line) comparing log-transformed IgG concentrations measured by Binding Site and IBL ELISAs. Shaded region indicates 95% CI.

Table 1. Sociodemographic characteristics of participants and households in Tay Tra and Son Ha District in survey, Quang Ngai Province, Vietnam, 2019*

Individual data	All, n = 1,216	Tay Tra, n = 604	Son Ha, n = 612	p value
Age, y				
≤5	269 (22)	125 (21)	144 (24)	0.45†
6–17	322 (26)	171 (28)	151 (25)	
18–40	523 (43)	258 (43)	265 (43)	
40–55	102 (8)	50 (8)	52 (8)	
Sex				
M	615 (51)	309 (51)	306 (50)	0.69†
F	601 (49)	295 (49)	306 (50)	
Ethnic group				
Co	487 (40)	486 (80)	1 (0.2)	<0.01†
Hre	531 (44)	0 (0)	531 (87)	
K'Dong	110 (9)	105 (17)	5 (1)	
Kinh	79 (6)	5 (1)	74 (12)	
Other	9 (1)	8 (1)	1 (0.2)	
≥18 years old	All, n = 625	Tay Tra, n = 308	Son Ha, n = 317	
Occupation				
Farmer	569 (91)	278 (90)	291 (92)	0.50†
Other	56 (9)	30 (10)	26 (8)	
≤10 years old	All, n = 464	Tay Tra, n = 231	Son Ha, n = 233	
Confirmed vaccination history				
BCG	361 (78)	165 (71)	196 (84)	<0.01†
DTP1	347 (75)	165 (71)	182 (78)	0.12†
DTP3	343 (74)	163 (71)	180 (77)	0.12†
DTP4	198 (43)	90 (39)	108 (46)	0.13†
Measles	350 (75)	160 (69)	190 (82)	0.02†
MUAC, cm	All, n = 235	Tay Tra, n = 111	Son Ha, n = 124	
Mean (SD)	14.7 (1.3)	14.6 (1.4)	14.8 (1.2)	0.20‡
Household data	All, n = 458	Tay Tra, n = 252	Son Ha, n = 206	
Toilet facility	323 (71)	215 (85)	108 (52)	<0.01§
Water source				
Well	168 (37)	2 (1)	166 (81)	<0.01§
River	249 (54)	247 (98)	32 (16)	<0.01§
Energy source				
Gas	95 (21)	22 (9)	73 (35)	<0.01§
Bio fuel	358 (78)	226 (90)	132 (64)	<0.01§

*Values are no. (%) except as indicated. BCG, *Mycobacterium bovis* Bacillus Calmette–Guérin; DTP, diphtheria–tetanus–pertussis; MUAC, mid-upper arm circumference.
†By χ^2 test.
‡By t-test.
§By χ^2 test or Fisher exact test.

and biovars for each subculture (*3*). We tested subcultures for expression of the diphtheria toxin by using the modified Elek test (*24*).

We conducted quadruplex, real-time, reverse transcription PCR (qRT-PCR) directly on throat swab specimens and aliquots of skim milk, tryptone, glucose, and glycerin medium to identify *C.diphtheriae*, *C.ulcerans*, or *C. pseudotuberculosis* and the diphtheria toxin gene according to published methods (*3*,*25*). DNA was extracted by using the QIAmp DNA Extraction Kit (QIAGEN, https://www.qiagen.com) (*26*). Primers and probes targeted 2 *rpoB* genes, the *tox* gene, and the green fluorescent protein gene (*gfp*), which we used as internal positive controls.

Diphtheria Toxoid Serologic Assay

We measured diphtheria toxoid IgG levels by using a commercially available ELISA Kit (Binding Site, https://www.bindingsite.com) according to the manufacturer's protocol. We punched out a DBS with a 6-mm hole punch and stored in Eppendorf tubes, then eluted DBS with 500 μL elution buffer and incubated overnight at 4°C. We then used the supernatant of the eluted solution for the ELISA (*27*–*30*). We defined an IgG level ≥0.1 IU/mL, an international standard cutoff value, as seropositive (*31*,*32*).

Comparison of Seroprevalence in 2 Areas with or without Reported Cases

This study compared seroprevalence in an epidemic-prone area (Quang Ngai Province) and a nonepidemic area in Vietnam. Regarding the nonepidemic area, Nha Trang (city) in Khanh Hoa Province was selected because the population is well-vaccinated and has not reported any diphtheria cases since 2013. Moreover, the age-stratified seroprevalence data among persons 1–55 years of age were investigated in Nha Trang during 2017 (*15*). Therefore, we compared the

immunity pattern of the population in Quang Ngai Province with that for Nha Trang.

We used 2 different ELISAs for measuring diphtheria toxoid IgG: the Binding Site ELISA for the study in Quang Ngai and the IBL ELISA (https://www.ibl-international.com) for the study in Nha Trang. First, we tested 546 subsets of the samples collected in Quang Ngai by using 2 ELISA kits in parallel and compared the 2 results by using linear regression analysis. On the basis of the best-fitted line, we converted the log-transformed IgG value measured by the Binding Site test to the value of IBL by using the equation Y(log IgG IBL) = −0.7652 + 0.72197X (log IgG Binding Site) (Figure 2).

We recalculated seroprevalence for Quang Ngai by using the converted IgG concentration and stratified seroprevalence into 5 age groups of 1–5, 6–15, 16–25, 26–35, and 36–55 years. We compared age-stratified seroprevalence and 95% CIs in Quang Ngai and Nha Trang.

Statistical Analysis

We measured carriage prevalence and seroprevalence by using 95%s CIs after being weighted by population size. We summarized sociodemographic information on the participants by districts. We examined differences in characteristics of the districts by using the χ^2 test or t-test.

We used the Fisher exact test or *t*-test to examine the association between carriage status and each risk factor. We conducted multivariate logistic regression to confirm whether carriage status was associated with young persons or persons who had low levels of IgG. Because nutrition is a critical element for immunoresponse, we conducted multivariate linear regression to explore the association between immunity level (natural log-transformed IgG) and nutrition status (MUAC) of a person with adjustment for age. We conducted statistical analyses by using Stata 15 (*33*).

Results

We recruited 1,216 persons from 458 households. Of those, 269 (22%) were 1–5 years of age, 322 (26%) 6–17 years of age, 523 (43%) 18–40 years of age, and 102 (8%) 41–55 years of age; 615 (51%) were male and 601 (49%) female. Of children ≤10 years of age, 75% had received ≥1 dose, 74% had received 3 doses, and 43% had received 4 doses of DTP (DTP1, DTP3, and DTP4). There was no statistical difference in DTP3 or DTP4 coverage between the 2 districts. No participants recalled any symptom or diagnosis of diphtheria in the past. Nobody had received DTP or tetanus–diphtheria vaccine because of injuries or involvement in the recent SIAs. Eighty percent of participants in Tay Tra District were in the Co ethnic group, and 87% of participants in Son Ha District were in the Hre ethnic group. The major ethnic group in Vietnam, the Kinh, accounted for only small proportions in the 2 districts. Most (91%) of the adult participants were farmers (Table 1).

Overall weighted carriage prevalence of *Corynebacterium* species was 1.4% (95% CI 0.4%–5.3%), and the prevalence of the *tox* gene–bearing strain was 0.5% (95% CI 0.0%–4.7%). Age-stratified carriage prevalence levels were 4.5% for those 1–5 years of age, 2.5% for 6–17 years of age, 1.0% for 18–40 years of age, and 0.0% for 41–55 years of age. Overall weighted seroprevalence of diphtheria toxoid IgG (≥0.1 IU/mL) in

Table 2. Age-stratified carriage prevalence of *Corynebacterium diphtheriae* and seroprevalence of diphtheria toxoid IgG in 2 districts, Quang Ngai Province, Vietnam*

Group	Mean ± SD age, y	Total	Seroprevalence, no. (%, 95% CI)	Carriage prevalence, no. (%, 95% CI)
Age group, y				
≤5	3.2 ± 1.36	269	108 (39.5 22.7–59.2)	12 (4.50, 3.7–5.5)
6–17	10.1 ± 3.17	332	120 (36.7 29.4–44.6)	10 (2.5, 0.1–47.5)
18–40	29.5 ± 5.61	513	283 (55.3 42.8–67.1)	5 (1.0, 0.6–1.7)
41–55	46.3 ± 4.30	102	64 (62.9, 60.9–64.8)	0
Total	20.0 ± 14.3	1,216	575 (51.4, 3.6–59.1)	27 (1.4, 0.4–5.4)
District				
Tay Tra, by age group, y				
≤5	3.1 ± 1.42	125	41 (32.8, 25.1–41.5)	6 (4.8, 2.2–10.3)
6–17	9.9 ± 3.09	171	59 (34.5, 27.8–41.9)	0
18–40	29.7 ± 5.19	258	152 (58.9, 52.8–64.8)	3 (1.2, 0.4–3.5)
41–55	46.4 ± 4.69	50	31 (62.0, 47.9–74.3)	0
Total	20.0 ± 14.2	604	283 (50.6, 33.6–67.5)	9 (0.9, 0.2–3.7)
Son Ha, by age group, y				
≤5	3.2 ± 1.31	144	67 (46.5, 38.5–54.7)	6 (4.2, 1.9–9.0)
6–17	10.4 ± 3.25	151	61 (40.4, 32.9–48.4)	10 (6.6, 3.6–11.9)
18–40	29.4 ± 6.04	265	131 (49.4, 43.4–55.4)	2 (0.8, 0.2–0.3)
41–55	46.2 ± 3.94	52	33 (63.5, 49.7–75.3)	0
Total	20.0 ± 14.4	612	292 (52.4, 39.1–65.3)	18 (2.0, 0.3–11.0)

*Seroprevalence and carriage prevalence were weighted for overall groups. IgG cutoff ≥0.1 IU/mL.

Table 3. Geographical distribution, characteristics, and vaccination history of 27 carriers of *Corynebacterium diphtheriae*, Vietnam*

Patient no.	District	Commune	Village	HH ID no.	Age, y/sex	*tox* gene	Biovar	Elek test result	Vaccine status, no. doses	DTP3 coverage, % (95% CI)
1	Tay Tra	Tra Phong	Tra Nga	305	25/M	–	*gravis*	–	NA	60 (35–81)
2		Tra Thanh	Thon Mon	818	23/M	–	NA	NA	NA	76 (1–91)
3†		Tra Lanh	Tra Luong	1003	40/F	–	*mitis*	–	NA	64 (34–86)
4		Tra Xinh	Tra Kem	1401	5/F	–	NA	NA	4	85 (55–96)
5				1404	2/F	–	NA	NA	4	
6				1407	4/F	–	NA	NA	4	
7			Tra Veo	1501	3/F	–	mitis	–	4	63 (38–82)
8					5/F	–	mitis	–	4	
9				1505	2/F	+	mitis	–	4	
10	Son Ha	Son Ha	Deo Ron	1607	10/F	+	NA	NA	0	71 (44–89)
11					3/F	–	*mitis*	–	3	
12					2/F	+	NA	NA	4	
13			Dong Reng	1704	9/M	–	NA	NA	0	40 (19–65)
14				1707	14/M	+	*mitis*	+	NA	
15			Ha Bac	1807	9/M	+	NA	NA	0	71 (46–87)
16				1811	7/F	+	*mitis*	+	4	
17					10/M	+	*mitis*	–	3	
18				1812	10/M	+	*mitis*	–	3	
19					4/M	–	*mitis*	–	0	
20		Son Giang	Lang Ri	2314	10/F	–	*mitis*	–	0	94 (68–99)
21			Ta Dinh	2406	28/M	–	*gravis*	–	NA	93 (63–99)
22					25/F	+	*gravis*	+	NA	
23				2409	3/M	–	*gravis*	–	4	
24		Son Ky	Lang Re	2505	7/F	–	NA	NA	4	88 (61–97)
25		Son Hai	Lang Trang	3004	7/F	–	*gravis*	–	3	80 (57–92)
26				3011	2/F	–	NA	NA	3	
27				3012	5/F	–	*gravis*	–	3	

*DTP3 coverage was the coverage at the village level where carriers were living. DTP, diphtheria–tetanus–pertussis; HH, household; ID, identification; NA, not available; –, negative; +, positive.
†For patient 3, *C.diphtheriae* was identified from a nasopharyngeal swab specimen and a throat swab specimen. Others were identified only from nasopharyngeal swab specimens.

the study area was 51% (95% CI 44%–59%). Age-stratified seroprevalence levels were 40% for those 1–5 years of age, 37% for 6–17 years of age, 55% for 18–40 years of age, and 63% for 41–55 years of age (Table 2).

We identified 27 carriers of *C. diphtheriae* by qRT-PCR. Among identified carriers, 17 (63%) were female (10 1–5 years of age) and 10 (37%) male (2 1–5 years of age). Sixteen carriers had received ≥3 doses of DTP. *C. diphtheriae* was isolated by culture from 17 of 27 qRT-PCR–positive samples. Eleven samples were biovar *mitis,* and 6 were biovar *gravis*. Swab specimens from 9 of the 27 carriers (33%) were *tox* gene positive by qRT-PCR, but only 6 specimens were successfully recovered by isolation. From those 6 isolates, diphtheria toxin expression was confirmed in 3 isolates by using the modified Elek test (2 biovar *mitis* and 1 biovar *gravis*). The remaining 3 isolates did not express diphtheria toxin and were thus *tox* gene–bearing nontoxigenic strains (NTTB). All 3 belonged to biovar *mitis* (Table 3).

We identified 27 carriers from 21 households located in 8 communes. Ten of 27 lived in a commune known as the Son Ha commune. Of 21 households, >1 carriers were identified in 5 households. Four households had 2 carriers, and 1 household had 3 carriers (Table 3).

We found strong evidence that age and IgG level were associated with carriage status (Table 4). Young children were likely to be carriers, after adjusting for IgG levels. High IgG levels were unexpectedly associated with carriers after adjusting for age. Multivariate linear regression analysis showed that smaller MUAC was associated with low IgG levels after adjusting for age, although MUAC was not associated with carriage status (Tables 4, 5).

The overall seroprevalence was higher for Quang Ngai (47%, 95% CI 45%–50%) than for Nha Trang (26%, 95% CI 20%–32%). The seroprevalence among children 1–5 years of age was lower in Quang Ngai (36%, 95% CI 31%–42%) than in Nha Trang (68%, 95% CI 67%–69%), and the seroprevalence among children 6–15 years of age in Quang Ngai (34%, 95% CI 29%–40%) was higher than in Nha Trang (7%, 95% CI 4%–11%) (Table 6; Figure 3).

Discussion

We conducted this study to investigate the potential mechanisms underlying the recent outbreaks of diphtheria in Vietnam and to recommend a reasonable outbreak response and vaccination strategy. This study described community-based *C. diphtheriae* carriage

prevalence in a diphtheria epidemic-prone area and assessed potential risk factors for carrier status and low immunity among persons. We also highlighted the difference in population immunity between the diphtheria epidemic-prone and nonepidemic areas.

The carriage prevalence, especially the prevalence of toxigenic strains, in the study population was much higher than that reported recently in Europe. According to a multicountry study conducted in Europe during 2007–2008, the prevalence of toxigenic strain in 8 countries in Europe was 0% (*34*). Toxigenic strains were isolated only in Latvia (0.08%) and Lithuania (0.07%), which had >1,500 cases and 112 cases reported, respectively, since 1994 (*35*,*36*). The prevalence of nontoxigenic strain was reported as 0.4% in Turkey in the same study (*34*). In our study, carriage prevalence was highest in the youngest age group and decreased by age. In Italy, 0.15% of healthy children 6–14 years of age carried a nontoxigenic strain in the early 2000s (*37*). In Indonesia, the prevalence of a toxigenic strain was reported as 3% among children 1–15 years of age during the outbreak in 2012 (*38*). Based on these findings, the long-running child vaccination program in Europe appears to have reduced carriage prevalence, especially the carriage prevalence of toxigenic strains. Conversely, toxigenic strains were still identified in countries in which symptomatic cases have been reported in the past 10 years. In addition, the current carriage prevalence in this study was similar to the situation in the United Kingdom during 1971 (1.2%) (*39*). If one considers that introduction of DTP in the United Kingdom was

Table 4. Associations between *Corynebacterium diphtheriae* carriage and potential risk factors, Vietnam*

Risk factor	Carriage, no. (%)		p value†
	Total	Tested	
Age group, y			
≤5	12 (4.5)	257 (95.5)	<0.01
6–17	10 (3.1)	314 (96.9)	
18–40	5 (1.0)	518 (99.0)	
41–55	0	102 (100.0)	
Sex			
M	10 (1.6)	605 (98.4)	0.198
F	17 (2.8)	584 (97.2)	
DTP1 ≤10 years			
0 doses	5 (4.5)	107 (95.5)	>0.99
≥1 dose	16 (4.5)	336 (95.5)	
DTP3 ≤10 years			
<3 doses	5 (4.3)	111 (95.7)	>0.99
≥3 doses	16 (4.6)	332 (95.4)	
Diphtheria antibody, IU/mL			
<0.1	11 (1.7)	630 (98.3)	0.24
≥0.1	16 (2.8)	559 (97.2)	
School			
Not attended	17 (1.8)	906 (98.2)	0.12
Attended	6 (2.1)	283 (97.9)	
Dormitory			
Not staying	23 (2.2)	1,035 (97.8)	0.77
Staying	4 (2.5)	154 (97.5)	
Sharing bed			
Yes	4 (2.7)	143 (97.3)	0.56
No	23 (2.2)	1,037 (97.8)	
Household size, no, persons			
≤4	13 (2.2)	585 (97.8)	>0.99
>4	14 (2.3)	604 (97.7)	
Bathing, times/day			
<1	0	72 (100.0)	0.40
≥1	27 (2.4)	1,117 (97.6)	
Handwashing, times/day			
<3	4 (1.6)	247 (98.4)	0.11
≥3	18 (3.9)	445 (96.1)	
Livestock or pet animal			
No	24 (2.7)	866 (97.3)	0.08
Yes	3 (0.9)	323 (99.1)	
Category	Positive	Negative	p value by t-test
MUAC, cm, mean (SD)	15.0 (1.77)	14.8 (1.33)	0.16
Age, y, mean (SD)	7 (9.7)	20 (14.3)	<0.01
log-transformed IgG level, mean (SD)	–1.4 (2.1)	–2.2 (1.2)	<0.01

*DTP, diphtheria–tetanus–pertussis; MUAC, mid-upper arm circumference.
†By Fisher exact test except as indicated.

Table 5. Associations between *Corynebacterium diphtheriae* carriage and diphtheria toxoid IgG levels adjusted for age assessed by logistic regression and between IgG levels and mid-upper arm circumference adjusted for age by linear regression, Vietnam*

Association between carriage status and IgG	Crude odds ratio 95% CI)	p value	Adjusted odds ratio (95% CI)	p value
log-transformed IgG level	1.49 (1.15–1.93)	<0.01	1.49 (1.17–1.90)	<0.01
Age, y	0.94 (0.90–0.97)	<0.01	0.94 (0.90–0.97)	<0.01
Association between IgG and MUAC	Crude coefficient	p value	Adjusted coefficient	p value
MUAC, cm	0.01 (–0.01 to 0.02)	0.43	0.02 (0.00–0.03)	0.014
Age, y	–0.21 (–0.34 to –0.08)	<0.01	–0.31 (–0.45 to –0.16)	<0.01

*MUAC, mid-upper arm circumference.

during 1941, forty years earlier than in Vietnam, vaccination coverage might be required to be adequate in the next few decades to reduce the carriage prevalence of toxigenic strain in Vietnam. The high prevalence of toxigenic strain indicates that more cases might be observed if the population remains susceptible. Twelve additional laboratory-confirmed cases were identified within 1 month from the survey date in Son Ha commune in which the highest carriage prevalence was observed.

Nine (33%) of 27 carriers harbored *tox* gene–bearing strains. The remaining 18 were nontoxigenic strains, which rarely cause invasive diseases (*40*,*41*). Conversely, nontoxigenic strains were often suggested to play a major role in maintaining the transmission of *C. diphtheriae* among human hosts (*12*,*42*). Nontoxigenic strains could be converted to toxigenic ones by lysogenization with a specific temperate bacteriophage. Lysogenic conversions might occur in nontoxigenic strains in carriers, and the converted strains might infect others (*43*). Multilocus sequence typing of the identified strains from carriers and cases in this study might provide evidence to indicate that this conversion might have occurred in this community.

For 9 *tox* gene–bearing strains, all 3 healthy carriers who had a nontoxigenic *tox* gene–bearing (NTTB) strain have received 3 doses of DTP, which supports that NTTB strains are increasingly identified in Europe because of vaccine pressure (*11*,*44*). The current vaccine does not protect persons from NTTB strains (*45*). Although it is unlikely that NTTB strains will be an immediate threat in Vietnam, it might be necessary to monitor NTTB strains as a potential cause of disease in the future.

We found that carriers were concentrated in specific households and communities. This observation was consistent with household transmission being the main route of *C. diphtheriae* transmission in the prevaccination era (*46*). Once diphtheria appears in a household or specific community, transmissions might continue if persons in neighboring areas are not well vaccinated (*43*).

We found no association between carrier status and bed-sharing, staying at the school dormitory, or less frequent bathing, but several other studies have identified those as risk factors for infection (*17*–*21*). A small number of carriers might be a reason that we could not identify the association; biologic characteristics, such as age or individual immunity level, might have been played a greater role than social factors. At an aggregated level, carriage prevalence was negatively associated with seroprevalence against diphtheria. However, we could not identify the association between carrier status and low IgG level at an individual level, probably because of natural boosting of immunity after being a carrier. Because this study was cross-sectional, we could not prove the chronological change in immunity and carriage status for an individual directly.

We confirmed the lowest seroprevalence was in persons 6–17 years old (37%) because it was expected from the previous findings that most of the laboratory-confirmed cases were of school-going age (*7*). In addition, the seroprevalence was similarly low among children 1–5 years of age (40%), which might occur because of low DTP3 coverage and the waning of vaccine-derived immunity. Another potential reason is that the seroconversion rate after DTP vaccination might have been low because of host factors, such as malnutrition or external factors, such as suboptimum cold chains. In Quang Ngai Province, it was reported that 5.7% of children ≤5 years of age were wasted, and 25.5% were stunted in 2013 (*47*). Because small MUAC was associated with low levels of diphtheria toxoid

Table 6. Associations between *Corynebacterium diphtheriae* carriage and age group in 2 districts, Vietnam

Age, y	Na Trang, % (95% CI)	Qung Ngi, % (95% CI)
1–5	68 (67–69)	36 (31–42)
6–10	7 (4–9)	34 (29–40)
16–25	12 (7–19)	39 (31–46)
25–36	33 (27–40)	50 (47–56)
36–55	28 (17–43)	54 (47–60)
Total	26 (20–32)	42 (39–46)

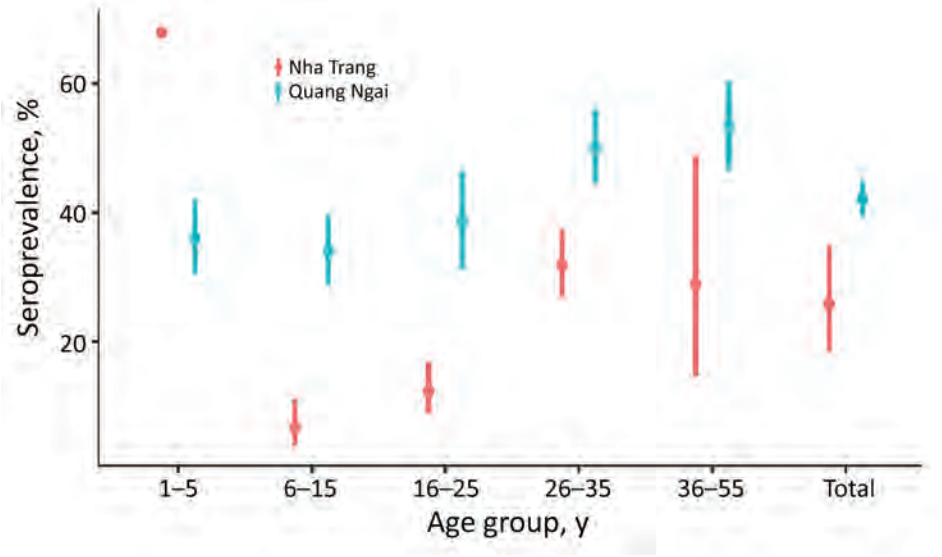

Figure 3. Comparison of the age-stratified seroprevalence, the proportion of persons who had diphtheria toxoid antibody ≥0.1 IU/mL, between Quang Ngai Province and Nha Trang City (15), Vietnam. Seroprevalence of Quang Ngai was not weighted by population for this comparison. Nha Trang is a well-vaccinated community that has had no reported diphtheria cases since 2013. Error bars indicate 95% CIs.

IgG, poor nutrition status might be associated with low immunoresponse in persons.

The age-stratified seroprevalence for Quang Ngai Province compared with that for Nha Trang provided insights of waning and acquired immunity. The seroprevalence among persons 1–5 years of age in Quang Ngai was lower than that in Nha Trang, most likely because of the low vaccination coverage in Quang Ngai. Conversely, the seroprevalence among those 6–15 years of age in Quang Ngai was higher than that in Nha Trang, potentially reflecting the continuous natural exposure in Quang Ngai. This observation indicates that the low immunity among children 1–5 years of age led to ongoing transmission, resulting in high seroprevalence among those ≥6–15 years of age in Quang Ngai than in Nha Trang. The same observation was found in a seroprevalence survey in Indonesia during 2012 (*38*).

This study compared the IgG levels measured in DBS and serum. Schou et al. reported a good correlation for diphtheria serum DBS (*28*). In addition, we compared the diphtheria antibody levels measured by using the same ELISA kit (IBL) for serum samples and DBS by using 96 samples collected in Vietnam. We found high sensitivity (0.91) and specificity (0.92) of seropositive of age, when vaccine-induced immunity showed the greatest decrease. Persons >17 years of age were more protected than young age groups, probably by naturally acquired immunity. Nevertheless, 50% of the population >17 years of age were susceptible, which explains why all age groups have been recently affected by diphtheria (*4*). A school-entry booster dose will be recommended to prevent future cases because the infant immunization program appeared to create low immunity in school age children (*15*). Conversely, low immunity in preschool age children would be another reason for the recent epidemic in Quang Ngai Province. Therefore, improving routine infant vaccination coverage will be essential to control diphtheria.

Based on the low seroprevalence in the age groups 1–5 and 6–17 years of age, SIAs would be most effective if they targeted the population 1–17 years of age. The Vietnamese MOH so far included the population 1–40 years of age a target of diphtheria SIAs, but SIAs in Indonesia, Bangladesh, and Haiti targeted children 1–14 years of age (*48*–*50*). In Vietnam, targeting the population of 18–40 years of age could be beneficial because 50% of this age group was susceptible. Also, we should also be aware that SIAs would not stop transmission in a short time once transmission has started in susceptible populations.

This study found that 1.4% of the population were healthy carriers of *C. diphtheriae*. Two-thirds of them harbored nontoxigenic strains, which could be transmitted among human hosts asymptomatically. A school-entry booster dose and improved infant vaccination coverage are recommended to stop current *C.diphtheriae* transmission in Vietnam. SIAs targeting persons 1–17 years of age will be efficient as an outbreak response.

Acknowledgments

We thank the staff at the Institut Pasteur in Nha Trang, Vietnam, and Quang Ngai Provincial Health Services for conducting the field survey; persons for participating in the study and surveys; Norman K. Fry and David Litt for providing support and advice; and Ryo Kinoshita for providing support with English language editing.

This study was supported the Nagasaki University WISE Program (Nagasaki University Doctoral Program for World-Leading Innovative and Smart Education for Global Health, KENKYU SHIDO KEIHI Research Grant); the Japan Program for Infectious Diseases Research and Infrastructure; the Japan Agency for Medical Research and Development (grant JP21wm0125006]; and JSPS KAKENHI (grant JP20K18905).

About the Author

Dr. Kitamura is a physician and research degree student at the London School of Hygiene and Tropical Medicine, London, UK, and Nagasaki University, Nagasaki, Japan. Her primary research interest is outbreak response in Asia and Africa.

References

1. Christie AB, editor. Infectious diseases: epidemiology and clinical practice. 4th ed. Edinburgh: Churchill Livingstone; 1987.
2. World Health Organization. Surveillance standards for vaccine-preventable diseases. 2nd ed. Geneva: World Health Organization, Licence: CC BY-NC-SA 3.0 IGO; 2018 [cited 2022 Oct 31]. https://apps.who.int/iris/handle/10665/275754
3. World Health Organization. WHO laboratory manual for the diagnosis of diphtheria and ther related infections. Geneva: The Organization; 2021.
4. Clarke KE, MacNeil A, Hadler S, Scott C, Tiwari TS, Cherian T. Global epidemiology of diphtheria, 2000–2017. Emerg Infect Dis. 2019;25:1834–42. https://doi.org/10.3201/eid2510.190271
5. World Health Organization. Diphtheria vaccine: WHO position paper, August 2017. Recommendations. Vaccine. 2018;36:199–201. https://doi.org/10.1016/j.vaccine.2017.08.024
6. Vietnam Ministry of Health. 25 years of expanded program of immunization in Vietnam [in Vietnamese]. The Ministry: Hanoi; 2012.
7. Kitamura N, Le TTT, Le LT, Nguyen LD, Dao AT, Hoang TT, et al. Diphtheria outbreaks in schools in Central Highland Districts, Vietnam, 2015–2018. Emerg Infect Dis. 2020;26:596–600. https://doi.org/10.3201/eid2603.191027
8. World Health Organization. Essential programme on immunization 2022 [cited 2022 Oct 31]. https://www.who.int/teams/immunization-vaccines-and-biologicals/essential-programme-on-immunization/implementation/immunization-campaigns
9. Completed results of the 2019 Viet Nam population and housing census. Hanoi: General Statistics Office, Vietnam; 2019.
10. World Health Organization. Diphtheria tetanus toxoid and pertussis (DTP) vaccination coverage [cited 2022 Oct 31]. https://immunizationdata.who.int/pages/coverage/DTP.html
11. Hoskisson PA. Microbe profile. *Corynebacterium diphtheriae*: an old foe always ready to seize opportunity. Microbiology (Reading). 2018;164:865–7. https://doi.org/10.1099/mic.0.000627
12. Sangal V, Hoskisson PA. Evolution, epidemiology and diversity of *Corynebacterium diphtheriae*: new perspectives on an old foe. Infect Genet Evol. 2016;43:364–70. https://doi.org/10.1016/j.meegid.2016.06.024
13. Bergamini M, Fabrizi P, Pagani S, Grilli A, Severini R, Contini C. Evidence of increased carriage of *Corynebacterium* spp. in healthy individuals with low antibody titres against diphtheria toxoid. Epidemiol Infect. 2000;125:105–12. https://doi.org/10.1017/S0950268899004331
14. Le VB, Nguyen TL, Pham TD, Le VT. Evaluation of antibody responses to diphtheria among persons aged 6–25 years after tetanus-diphtheria (Td) vaccine immunization in Kon Plong District, Kon Tum Province, from May 2016 to March 2017. Vietnam Journal of Preventive Medicine. 2017;8:465–7.
15. Kitamura N, Le LT, Le TT, Nguyen HT, Edwards T, Madaniyazi L, et al. The seroprevalence, waning rate, and protective duration of anti-diphtheria toxoid IgG antibody in Nha Trang, Vietnam. Int J Infect Dis. 2022;116:273–80. https://doi.org/10.1016/j.ijid.2022.01.025
16. General Statistics Office and UNICEF. Viet Nam multiple indicator cluster survey 2014, Final report. Ha Noi, Viet Nam; 2015 [cited 2022 Nov 1]. https://mics.unicef.org/news_entries/2
17. Quick ML, Sutter RW, Kobaidze K, Malakmadze N, Nakashidze R, Murvanidze S, et al. Risk factors for diphtheria: a prospective case-control study in the Republic of Georgia, 1995-1996. J Infect Dis. 2000;181(Suppl 1):S121–9. https://doi.org/10.1086/315563
18. Husada D, Primayani D, Kartina L, Puspitasari D, Basuki PS, Moedjito I. Risk factors for diphtheria during the outbreak in Indonesia. Am J Trop Med Hyg. 2018;99(Suppl.):147.
19. Suhendri MR, Ghazali PL. The determinant of diphtheria outbreak in Cirebon, Indonesia. Trans R Soc Trop Med Hyg. 2019;113(Suppl.):S277.
20. Muhamad Ramdan I, Susanti R, Ifroh RH, Noviasty R. Risk factors for diphtheria outbreak in children aged 1–10 years in East Kalimantan Province, Indonesia. F1000 Res. 2018;7:1625. https://doi.org/10.12688/f1000research.16433.1
21. Murakami H, Phuong NM, Thang HV, Chau NV, Giao PN, Tho ND. Endemic diphtheria in Ho Chi Minh City; Viet Nam: a matched case–control study to identify risk factors of incidence. Vaccine. 2010;28:8141–6. https://doi.org/10.1016/j.vaccine.2010.09.088
22. Guthrie R. The origin of newborn screening. Screening. 1992;1:5–15. https://doi.org/10.1016/0925-6164(92)90025-Z
23. Hannon WH. Blood collection on filter paper for neonatal screening programs: approved standard. NCCLS; 1997. [cited 2022 Nov 1]. https://clsi.org/media/1493/nbs01a6_sample.pdf
24. Engler KH, Glushkevich T, Mazurova IK, George RC, Efstratiou A. A modified Elek test for detection of toxigenic corynebacteria in the diagnostic laboratory. J Clin Microbiol. 1997;35:495–8. https://doi.org/10.1128/jcm.35.2.495-498.1997
25. De Zoysa A, Efstratiou A, Mann G, Harrison TG, Fry NK. Development, validation and implementation of a quadruplex real-time PCR assay for identification of potentially toxigenic corynebacteria. J Med Microbiol. 2016;65:1521–7. https://doi.org/10.1099/jmm.0.000382
26. Nakao H, Popovic T. Development of a direct PCR assay for detection of the diphtheria toxin gene. J Clin Microbiol. 1997;35:1651–5. https://doi.org/10.1128/jcm.35.7.1651-1655.1997
27. Phetsouvanh R, Blacksell SD, Jenjaroen K, Day NP, Newton PN. Comparison of indirect immunofluorescence assays for diagnosis of scrub typhus and murine typhus using venous blood and finger prick filter paper blood spots. Am J Trop Med Hyg. 2009;80:837–40. https://doi.org/10.4269/ajtmh.2009.80.837

28. Schou C, Simonsen O, Heron I. Determination of tetanus and diphtheria antitoxin content in dried samples of capillary blood: a convenient method applied to infants. Scand J Infect Dis. 1987;19:445–51. https://doi.org/10.3109/00365548709021677
29. Kattenberg JH, Erhart A, Truong MH, Rovira-Vallbona E, Vu KA, Nguyen TH, et al. Characterization of *Plasmodium falciparum* and *Plasmodium vivax* recent exposure in an area of significantly decreased transmission intensity in central Vietnam. Malar J. 2018;17:180. https://doi.org/10.1186/s12936-018-2326-1
30. Mirchamsy H, Nazari F, Stellman C, Esterabady H. The use of dried whole blood absorbed on filter-paper for the evaluation of diphtheria and tetanus antitoxins in mass surveys. Bull World Health Organ. 1968;38:665–71.
31. Di Giovine P, Pinto A, Olander RM, Sesardic D, Stickings P, Berbers G, et al. External quality assessment for the determination of diphtheria antitoxin in human serum. Clin Vaccine Immunol. 2010;17:1282–90. https://doi.org/10.1128/CVI.00096-10
32. von Hunolstein C, Ralli L, Pinto A, Stickings P, Efstratiou A, Czumbel I, et al. Relevance and criticality in an external quality assessment for the determination of diphtheria antitoxin. J Immunol Clin Res. 2014;2:1022.
33. Stata Corp. Stata Statistical Software: Release 15. College Station (TX): StataCorp LLC.; 2017.
34. Wagner KS, White JM, Neal S, Crowcroft NS, Kuprevičiene N, Paberza R, et al.; Members of the Diphtheria Surveillance Network. Screening for *Corynebacterium diphtheriae* and *Corynebacterium ulcerans* in patients with upper respiratory tract infections 2007–2008: a multicentre European study. Clin Microbiol Infect. 2011;17:519–25. https://doi.org/10.1111/j.1469-0691.2010.03269.x
35. Kantsone I, Lucenko I, Perevoscikovs J. More than 20 years after re-emerging in the 1990s, diphtheria remains a public health problem in Latvia. Euro Surveill. 2016;21:30414. https://doi.org/10.2807/1560-7917.ES.2016.21.48.30414
36. World Health Organization. Diphtheria reported cases and incidence [cited 2022 Nov 1]. https://immunizationdata.who.int/pages/incidence/diphtheria.html
37. Bergamini M, Bonanni P, Cocchioni M, Dedonno A, Gabutti G, Giammanco G, et al. Low prevalence of *Corynebacterium diphtheriae* carriers in Italian schoolchildren. J Prev Med Hyg. 2005;46:139–44.
38. Hughes GJ, Mikhail AF, Husada D, Irawan E, Kafatos G, Bracebridge S, et al. Seroprevalence and determinants of immunity to diphtheria for children living in two districts of contrasting incidence during an outbreak in East Java, Indonesia. Pediatr Infect Dis J. 2015;34:1152–6. https://doi.org/10.1097/INF.0000000000000846
39. Butterworht A, Abbott JD, Simmons LE, Ironside AG, Mandal BK, Williams RF, et al. Diphtheria in the Manchester area 1967–1971. Lancet. 1974;2:1558–61. https://doi.org/10.1016/S0140-6736(74)90296-7
40. Funke G, Altwegg M, Frommelt L, von Graevenitz A. Emergence of related nontoxigenic *Corynebacterium diphtheriae* biotype mitis strains in Western Europe. Emerg Infect Dis. 1999;5:477–80. https://doi.org/10.3201/eid0503.990326
41. Tiwari T, Wharton M. Vaccines. In: Plotkin SA, Orenstein W, Offit P, editors. Plotkin's vaccines, 7th ed. Philadephia: W.B. Saunders Co; 2018.
42. Groman N, Cianciotto N, Bjorn M, Rabin M. Detection and expression of DNA homologous to the *tox* gene in nontoxinogenic isolates of *Corynebacterium diphtheriae*. Infect Immun. 1983;42:48–56. https://doi.org/10.1128/iai.42.1.48-56.1983
43. Pappenheimer AM. Diphtheria. New York: Elsevier Inc; 1984. p. 1–36.
44. Zakikhany K, Neal S, Efstratiou A. Emergence and molecular characterisation of non-toxigenic *tox* gene–bearing *Corynebacterium diphtheriae* biovar mitis in the United Kingdom, 2003-2012. Euro Surveill. 2014;19:20819. https://doi.org/10.2807/1560-7917.ES2014.19.22.20819
45. Hacker E, Antunes CA, Mattos-Guaraldi AL, Burkovski A, Tauch A. *Corynebacterium ulcerans*, an emerging human pathogen. Future Microbiol. 2016;11:1191–208. https://doi.org/10.2217/fmb-2016-0085
46. Crum FS. A statistical study of diphtheria. Am J Public Health (N Y). 1917;7:445–77. https://doi.org/10.2105/AJPH.7.5.445-a
47. Viet Nam National Institute of Nutrition. UNICEF, Alive & Thrive. Nutrition surveillance profiles 2013. Ha Noi, Viet Nam; 2014 [cited 2022 Nov 1]. https://www.aliveandthrive.org/sites/default/files/attachments/Sample-IYCF-Surveillance-Data_Viet-Nam.pdf
48. Harapan H, Anwar S, Dimiati H, Hayati Z, Mudatsir M. Diphtheria outbreak in Indonesia, 2017: an outbreak of an ancient and vaccine-preventable disease in the third millennium. Clin Epidemiol Global Health Journal Translated Name Clinical Epidemiology and Global Health. 2019;7:261–2. https://doi.org/10.1016/j.cegh.2018.03.007
49. Feldstein LR, Bennett SD, Estivariz CF, Cooley GM, Weil L, Billah MM, et al. Vaccination coverage survey and seroprevalence among forcibly displaced Rohingya children, Cox's Bazar, Bangladesh, 2018: a cross-sectional study. PLoS Med. 2020;17:e1003071. https://doi.org/10.1371/journal.pmed.1003071
50. Pan American Health Organization. Haiti launches campaign to vaccinate over 2 million children against diphtheria, with PAHO support 2018 [cited 2022 Oct 31]. https://www.paho.org/en/news/10-4-2018-haiti-launches-campaign-vaccinate-over-2-million-children-against-diphtheria-paho

Address for correspondence: Noriko Kitamura, Department of Infectious Disease Epidemiology, London School of Hygiene and Tropical Medicine, Keppel St, London WC1E 7HT, UK; email: noriko.kitamura@lshtm.ac.uk

Akkermansia muciniphila Associated with Improved Linear Growth among Young Children, Democratic Republic of the Congo

Christine Marie George, Alves Birindwa, Shan Li, Camille Williams, Jennifer Kuhl, Elizabeth Thomas, Ruthly François, Amani Sanvura Presence, Bisimwa Rusanga Jean Claude, Patrick Mirindi, Lucien Bisimwa, Jamie Perin, O. Colin Stine

To investigate the association between enteric pathogens, fecal microbes, and child growth, we conducted a prospective cohort study of 236 children <5 years of age in rural eastern Democratic Republic of the Congo. We analyzed baseline fecal specimens by quantitative PCR and measured child height and weight at baseline and growth at a 6-month follow-up. At baseline, 66% (156/236) of children had ≥3 pathogens in their feces. We observed larger increases in height-for-age-z-scores from baseline to the 6-month follow-up among children with *Akkermansia muciniphila* in their feces (coefficient 0.02 [95% CI 0.0001–0.04]; p = 0.04). Children with *Cryptosporidium* in their feces had larger declines in weight-for-height/length z-scores from baseline to the 6-month follow-up (coefficient –0.03 [95% CI –0.05 to –0.005]; p = 0.02). Our study showed high prevalence of enteric pathogens among this pediatric cohort and suggests *A. muciniphila* can potentially serve as a probiotic to improve child growth.

An estimated 500,000 deaths globally are attributed to diarrheal diseases each year among children <5 years of age (*1*). Enteric pathogens infecting the intestinal tract can cause diarrhea and reduce a child's ability to absorb nutrients, even when infections are asymptomatic, resulting in malnutrition and impaired growth (*2*,*3*). Globally, in 2021, a total of 149 million children <5 years of age were estimated to be stunted in growth (*4*). Enteric diseases can have long-lasting effects; studies have found that early childhood enteric infections leading to unmet energetic demands for adequate brain development can result in adverse cognitive developmental outcomes later in life (*5*–*7*). In the Democratic Republic of the Congo (DRC), an estimated 45 million diarrheal episodes occur each year, contributing to 10% of deaths among children <5 years of age; 43% of children in this age group are estimated to have stunted growth (*8*–*10*).

A recent study found that the presence of *Akkermansia muciniphila,* a commensal microorganism, in child fecal samples was associated with significantly less diarrhea and greater linear growth measured using height-for-age (HAZ) z-scores (Almeida et al., unpub data). We conducted this cross-sectional study as part of the Global Enteric Multicenter Study (GEMS) conducted in Mali, Kenya, Gambia, and Bangladesh. Additional prospective studies are needed, however, to investigate the association between *A. muciniphila* and child growth. *Lactobacillus* spp. have also been shown protective against enteric infections and associated with healthy gut microbiota composition (*11*–*13*). In a multicountry study, the presence of *L. salivarius* was associated with less *Shigella*-attributed diarrhea (*14*). Laboratory studies have found that *L. salivarius* can improve growth in animals (*15*), but no study has investigated this association in humans.

The Reducing Enteropathy, Undernutrition, and Contamination in the Environment (REDUCE) study focuses on identifying pathways of exposure to fecal pathogens that are significant contributors to diarrheal diseases for young children in the DRC, and on developing and evaluating scalable interventions to reduce fecal contamination from these pathways.

Johns Hopkins Bloomberg School of Public Health Department of International Health, Baltimore, Maryland, USA, and Bukavu, Democratic Republic of the Congo (C.M. George, A. Birindwa, C. Williams, J. Kuhl, E. Thomas, R. François, A.S. Presence, B.R. Jean Claude, L. Bisimwa, J. Perin); University of Maryland School of Medicine Department of Epidemiology and Public Health, Baltimore (S. Li, O.C. Stine); Food for the Hungry, Washington DC, USA, and Bukavu (P. Mirindi)

DOI: https://doi.org/10.3201/eid2811.212118

Our primary objective in conducting this prospective cohort study was to determine whether the presence and quantity of enteric microorganisms, including *L. salivarius* and *A. muciniphila,* in feces was significantly associated with growth in young children in rural DRC. We hypothesized that the enteric pathogens *Giardia*, *Shigella*, *Cryptosporidium* spp., and *Campylobacter jejuni* would impair child growth by increasing intestinal inflammation and reducing nutrient absorption. Conversely, we hypothesized that *L. salivarius* and *A. muciniphila* would improve child growth by reducing intestinal inflammation and facilitating nutrient absorption.

Methods

Study Design

We conducted this prospective cohort study of 236 children <5 years of age in rural Walungu Territory in South Kivu Province, DRC as part of the REDUCE program. The study was part of a larger USAID/Bureau for Humanitarian Assistance–funded Development Food Security Activities (DFSA) awarded with the goal of improving food and nutrition security and economic wellbeing in vulnerable households in South Kivu and Tanganyika provinces in DRC. We enrolled participants during June 2018–January 2019 and conducted 6-month follow-up visits in households during December 2018–August 2019. The number of samples for analysis was determined on the basis of the number of participants with baseline fecal samples and child growth data. We included in the analysis data from all children meeting these criteria who were <5 years of age at follow-up with ≥5 months of surveillance data from baseline to follow-up. Caregivers were administered a questionnaire at baseline to obtain information on demographic factors. Informed consent was obtained from a parent or guardian of all study participants. Study procedures were approved by the research ethics review committees of the University of Kinshasa (protocol 043-2017) and the Johns Hopkins Bloomberg School of Public Health (protocol 8057).

At baseline, caregivers were provided DNase/RNase-free feces cups and a cooler box with an icepack for collecting and storing feces specimens from children <5 years of age during home visits. Research assistants then transported fecal samples within 6 hours of collection to the microbiology laboratory at the Catholic University of Bukavu in Bukavu, DRC, where samples were stored in liquid nitrogen. Research assistants with training in standardized anthropometry measured children's weight 1 time and height or length 3 times at baseline and 6-month follow-up. We measured length for children ≤23 months and height for children 24–59 months of age. We used these measurements to calculate z-scores according to World Health Organization (WHO) child growth standards (*16*): height-for-age (HAZ), weight-for-age (WAZ), and weight-for-height/length z-scores (WHLZ).

Laboratory Analysis

Fecal samples were transported on dry ice in temperature-controlled shipping containers to the Enteric Microbiology Laboratory at the University of Maryland School of Medicine in Baltimore, Maryland, USA, and stored in a freezer at −80° C until analysis. We isolated DNA from frozen fecal samples using a modified procedure that included bead-beating steps and an adapted QIAGEN QIAamp (https://www.qiagen.com) DNA stool extraction procedure (*17*). We measured concentration of DNA using a Nanodrop spectrophotometer (ThermoFisher Scientific, https://www.thermofisher.com). We analyzed DNA for *Shigella* spp., ETEC, *C. jejuni*, *G. intestinalis*, and *Cryptosporidium* spp. by quantitative PCR (qPCR) using primers published elsewhere (*18*,*19*) and SYBR Green. In addition, we analyzed 2 commensal bacteria, *A. muciniphila* (forward primer TCCATCATGAGCCTGTCCGA and reverse primer ACGAGCACCAGAATGATCAG) and *L. salivarius* (forward primer TTATCATTTTAGGCGTCTGGA and reverse primer ATGGGAGACTTGGTTGGATG). We determined gene copies in the specimens by quantification using a standard curve based on dilutions of purified total genomic DNA isolated by QIAGEN column for each 96-well plate (*14*). We combined the DNA concentration, qPCR measurement, and standard curve to estimate the number of gene copies per 100 ng of total fecal DNA. We set ≥1 copy/100 ng DNA as the cutoff to define the presence of an enteric microorganism, using methods published elsewhere (*20*,*21*).

Statistical Analysis

To assess the association between enteric microorganisms and measures of child growth, we performed analyses in linear regression models using generalized estimating equations to account for clustering at the household level and to approximate 95% CIs; we recorded changes in HAZ, WAZ, and WHLZ from baseline to the 6-month follow-up as outcomes and presence and quantities of enteric microorganisms as predictors. We adjusted models to account for caregiver formal education (household education), number of persons in the household (household size), household wall type (housing type), breastfeeding

(exclusive, any, or none), and animal-source food intake (nutritional status measured using a structured dietary questionnaire on foods consumed in the 24 hours before sampling). We included household education because previous studies had found association between this variable and child growth (*22*,*23*). We included household wall type as a measure of socioeconomic status of the household, which has been associated with child growth (*24*). We included household size as a measure of crowding, which has been associated with food insecurity and delayed growth in young children (*24*–*26*). We included breastfeeding because of studies demonstrating association between this variable and improved child growth and reduced diarrheal diseases (*27*,*28*). We included animal-source food intake because of association between this variable and child growth (*29*,*30*). To assess factors associated with the presence of *A. muciniphila*, we performed analyses on linear regression models using generalized estimating equations to account for clustering at the household level and to approximate 95% CIs, using presence of *A. muciniphila* as the outcome and factors such as age and sex as predictors. We compared children with and without anthropometric data at the 6-month follow-up using a χ^2 test and performed analyses in SAS version 9.4 software (SAS Institute Inc., https://www.sas.com).

Results

We obtained baseline fecal samples and anthropometric measurements for 236 children. Median (±SD) baseline age for participants was 2 ±1 years (range 0.08–5.00 years) (Table 1). Girls accounted for 52% (153/236) of participants; 71% (167/236) resided in a household with ≥1 persons with any level of formal education. Caregivers reported 54% (127/236) of children had any or exclusive breastfeeding in the 24 hours before sampling; 30% (8/27) of children <6 months of age were exclusively breastfed. Other variables among participating children included 69% (163/236) consuming animal-source food in the 24 hours before sampling. For wall materials, 60% (153/236) of participants resided in households with mud walls, 4% (9/236) wood, 5% (12/236) concrete, 6% (13/236) wood and mud, 5% (12/236) biomass, 2% (5/236) brick, and 7% (16/236) wood and concrete.

We excluded 43 children in our cohort study from analyses because we did not have 6-month follow-up anthropometric measurements for them. We found no significant ($p<0.05$) differences for any enteric microorganism or demographic factors at baseline between children with or without anthropometric data at 6-month follow-up. At baseline, 95% (224/236) of children had *Giardia*, 54% (127/236) *C. jejuni*, 35% (83/236) *Shigella*, 5% (11/236) *Cryptosporidium*, 70% (166/236) *A. muciniphila*, and 31% (73/236) *L. salivarius* (Table 2). Median copies per 100 ng DNA (range) was 197 (0–2,258,242) for *Giardia,* 1.5 (0–4,724,251) for *C. jejuni*, 0 (0–35,687,711) for *Shigella*, 19 (0–3,290,838) for *Cryptosporidium* spp., 15 (0–17,730,754) for *A. muciniphila*, and 0 (0–1,556) for *L. salivarius*. Median ±SD pathogens in feces was 3 ±1 (range 0–5). For the number of pathogens, 2% (5/236) of children

Table 1. Baseline demographic characteristics for participants in prospective cohort study of enteric microbes and child growth among young children, Democratic Republic of the Congo*

Characteristic	Value
Children <5 y of age	236
Baseline age, y, median ±SD (range)	1.5 ±1.2 (0.08–4.6)
Sex	
F	122 (52)
M	114 (48)
Household wall type	
Mud walls	153 (66)
Wood walls	9 (4)
Concrete walls	12 (5)
Wood and mud walls	13 (6)
Biomass walls	12 (5)
Brick walls	12 (5)
Wood and concrete walls	5 (2)
Other	16 (7)
Household member with any formal education	167 (71)
Household size, median ±SD (range)	6 ±2.4 (2–17)
Baseline growth measurements, z-score, median ±SD (range)	
Height for age	−2.0 ±1.6 (−5.7 to 5.9)
Weight for height	0.4 ±1.4 (−4.8 to 5.2)
Weight for age	−0.7 ±1.3 (−4.7 to 3.0)

*Values are no. (%) children except as indicated.

Table 2. Type and number of enteric pathogens and commensal microbes in feces samples from participants in prospective cohort study of enteric microbes and child growth among young children, Democratic Republic of the Congo

Category	No. (%)	Median ±SD (range)
Participants with >1 pathogen in feces, n = 236	73 (89)	3 ±1 (0–5)
Pathogen type		
Giardia	224 (95)	197 ±170,042 (0–2,258,242)
Shigella	83 (35)	0 ±2,937,024 (0–35,687,711)
Cryptosporidium	11 (5)	0 ±214,213 (0–3,290,838)
Campylobacter jejuni	127 (54)	1.5 ±487,706 (0–4,724,251)
No. pathogens		
None	10 (4)	
1	58 (25)	
2	118 (50)	
3	49 (20)	
4	1 (1)	
Commensal microbes		
Akkermansia muciniphila	166 (70)	15 ± 1,196,734 (0–17,730,754)
Lactobacillus salivarius	73 (31)	0 ± 151 (0–1,556)

had zero, 9% (21/236) had one, 23% (54/236) had two, 47% (110/236) had three, 19% had four, and 1 child had five.

We observed larger increases in HAZ, 0.34 HAZ coefficient (95% CI 0.2–0.67; p = 0.04), from baseline to 6-month follow-up for children with *A. muciniphila* detected in their feces at baseline compared with those who did not (Table 3). When we included *A. muciniphila* as a continuous outcome (log transformed) in the model, HAZ coefficient was also significantly higher, 0.02 (95% CI 0.0001–0.04; p = 0.04). Children with versus without *Cryptosporidium* spp. in their feces had larger declines in WHLZ, −0.03 WHLZ coefficient (95% CI −0.05 to −0.005; p = 0.02). We observed no other significant associations between enteric pathogens or microbes and child growth. Including caregiver-reported child antibiotic usage in our models did not significantly change our observed associations. Older children had significantly higher *A. muciniphila* in feces (p <0.05) (Appendix Table 1), whereas children <2 years of age had a significantly higher number of enteric pathogens in their feces (p = 0.046) (Appendix Table 2).

Discussion

In this prospective cohort study conducted in rural eastern DRC, we found that *A. muciniphila* was associated with improved linear growth in young children, *Cryptosporidium* was associated with impaired growth, and two thirds of children had a high prevalence (≥3) of enteric pathogens in their feces. Children with *Cryptosporidium* in their feces, as measured by WHLZ, grew more poorly as the abundance of the pathogen increased. In contrast, *A. muciniphila* in feces was associated with improved linear growth. This promising finding suggests that *A. muciniphila* may have the potential to serve a probiotic role to help improve growth in young children; however, experimental studies must first be conducted to prove this potential benefit. Children are most susceptible to linear growth faltering during the first 2 years of life (*31*), and effective interventions are urgently needed to improve child health during this critical window of development.

Our finding that *A. muciniphila* was associated with improvements in linear growth is consistent with a recent cross-sectional study among children in GEMS, which found that children who had *A. muciniphila* in their feces had higher HAZ than did children who did not (Almeida et al., unpub. data). Previous studies in adult populations have found *A. muciniphila* more abundant in healthy persons compared with those with inflammatory bowel disease (*32*). *A. muciniphila* resides in the intestinal mucin, which may serve as its carbon source (*33*). We hypothesize that *A. muciniphila* impacts the gut mucosal barrier through reducing intestinal inflammation. Our results, however, do not imply causality, and our study is not a substitute for a randomized clinical trial. Low *A. muciniphila* presence may be a marker of pathogenic processes, such as increased intestinal inflammation, contributing to poor child growth, but the microbe itself may not be directly influencing child growth. Mechanistic studies are needed to further investigate our observed association between *A. muciniphila* and child growth.

Findings from human and animal studies suggest that *A. muciniphila* is a highly promising probiotic (*34*). Oral *A. muciniphila* supplementation improved clinical responses to immune checkpoint inhibitors targeting the PD-1/PD-L1 (programmed death-1/programmed death ligand-1) axis in animal studies (*35*), and *A. muciniphila* reduced biomarkers of liver dysfunction and inflammation among persons who were overweight or obese (*36*); however, no studies have investigated its effect on child growth or diarrhea. Rhubarb extract has been shown

to promote *A. muciniphila* abundance (*34*) and might therefore serve as a potential natural source of *A. muciniphila*. Future mechanistic studies are needed to determine if A. muciniphila is associated with decreased enteric inflammation and systemic inflammation. Experimental studies are also needed to investigate our observed association between *A. muciniphila* and child growth in other global settings to determine whether this commensal microbe can be used as a potential therapeutic agent to improve child growth.

Cryptosporidium is a protozoan parasite that infects the small intestine, resulting in damage to the intestinal epithelium walls, and causes an estimated 44 million diarrheal episodes globally each year, 9 million in sub-Saharan Africa (*37*,*38*). This intestinal damage can reduce nutrient absorption and barrier function and lead to a disorder named environmental enteropathy, associated with impaired linear growth in young children (*39*,*40*). *Cryptosporidium* is zoonotic in origin and can be spread through cattle and also through fecal–oral transmission (*41*). Consistent with our findings, a recent meta-analysis found that *Cryptosporidium* was associated with declines in WHLZ (*37*). Future studies are needed to determine the predominant *Cryptosporidium* transmission pathways for patients in our study setting in eastern DRC.

Nearly all (98%) children in our study had ≥1 enteric pathogen in their feces, and 89% had >1. A recent study of hospitalized diarrhea patients (children and adults) at a cholera treatment center in Uvira, South Kivu, DRC, found that 50% of girls and 68% of boys 1–15 years of age had >1 pathogen in their feces, a lower percentage than in our study (*42*). However, this difference is likely because the Uvira study included children older than the children <5 years of age comprising our study cohort; older persons typically have fewer enteric pathogens. The most common enteric pathogen in the Uvira study was *Cryptosporidium,* experienced by 28% of participants.

Among our study's limitations, we analyzed feces specimens only at baseline, which prevented us from investigating risk factors for subsequent enteric infections or determining the prevalence of enteric infections among our study population over time. Second, we did not perform an in-depth analysis of a larger panel of enteric pathogens from the gut microbiome, which might have provided further information about potential pathways by which enteric microbes affect child growth (*43*). Third, we did not collect information on the HIV status of children. Persons with HIV are at higher risk for *Cryptosporidium* infections (*44*). Fourth, we did not adjust for multiple comparison; however, all significant findings were in the hypothesized direction. Fifth, we did not have data on diarrhea for all study children; future studies should apply model-derived quantitative cut-points to investigate causes of diarrhea in children (*18*). Finally, our small sample size did not support subgroup analyses by age, which would have been particularly useful for children during the first 2 years of life when they are most susceptible to growth faltering. Future studies should involve larger sample sizes to investigate data by age strata.

Among our study's strengths, we collected anthropometric data at baseline and 6-month follow-up,

Table 3. Associations between enteric pathogens and anthropometric measurements for participants in study of *Akkermansia muciniphila* association with improved linear growth among young children, Democratic Republic of the Congo*

Category	Change from baseline to 6-month follow-up, coefficient (95% CI)		
	Height-for-age z-score	Weight-for height/ length z-score	Weight-for-age z-score
Pathogen or microbe, presence vs. absence			
No. pathogens	0.08 (–0.05 to 0.21)	–0.01 (–0.15 to 0.14)	0.06 (–0.04 to 0.15)
Giardia	0.27 (–0.25 to 0.80)	–0.13 (–0.84 to 0.58)	0.02 (–0.36 to 0.41)
Shigella	0.01 (–0.30 to 0.33)	0.11 (–0.20 to 0.42)	0.03 (–0.21 to 0.27)
Cryptosporidium	0.37 (–0.08 to 0.81)	–0.41 (–0.83 to 0.0008)	0.00 (–0.38 to 0.37)
ETEC	0.11 (–0.19 to 0.42)	–0.26 (–0.60 to 0.09)	0.04 (–0.27 to 0.34)
Campylobacter jejuni	0.09 (–0.15 to 0.34)	0.11 (–0.17 to 0.40)	0.16 (–0.05 to 0.37)
Akkermansia muciniphila	0.34 (0.02–0.67)	–0.04 (–0.37 to 0.28)	0.23 (–0.01 to 0.47)
Lactobacillus salivarius	–0.12 (–0.40 to 0.17)	–0.01 (–0.29 to 0.27)	–0.03 (–0.26 to 0.19)
Pathogen or microbe, log transformed presence vs. absence			
Giardia	0.01 (–0.02 to 0.04)	–0.01 (–0.04 to 0.03)	0.0005 (–0.02 to 0.02)
Shigella	0.0007 (–0.02 to 0.02)	0.01 (–0.01 to 0.03)	0.01 (–0.01 to 0.02)
Cryptosporidium	0.02 (–0.01 to 0.05)	–0.03 (–0.05 to 0.005)	–0.01 (–0.03 to 0.02)
ETEC	–0.01 (–0.03 to 0.01)	0.0004 (–0.02 to 0.02)	0.003 (–0.01 to 0.02)
Campylobacter jejuni	0.004 (–0.01 to 0.02)	0.002 (–0.02 to 0.02)	0.01 (–0.01 to 0.02)
Akkermansia muciniphila	0.02 (0.001 to 0.04)	–0.01 (–0.03 to 0.01)	0.01 (–0.01 to 0.02)
Lactobacillus salivarius	–0.01 (–0.04 to 0.02)	0.00 (–0.03 to 0.03)	–0.001 (–0.02 to 0.02)

*Models adjusted for wall type, household educational level, number of persons in the household, animal source food, and breastfeeding. ETEC, enterotoxigenic *Escherichia coli*.

using a prospective design that enabled us to assess relationships between enteric infections at baseline and subsequent changes in child growth over time. Second, in addition to enteric pathogens, we included data on commensal microbes, specifically *A. muciniphila* and *L. salivarius*, which could serve as potential therapeutic interventions to promote subsequent child growth. Most studies have focused only on enteric pathogens in child feces. Third, we used qPCR and a bead beating step. qPCR detects enteric microbes at lower concentrations (i.e., qPCR has a higher sensitivity than traditional culture methods [*14*,*45*]). The bead beating step releases more DNA and higher quality DNA than other methods for microbial DNA (*11*,*21*).

In our community-based prospective cohort study, young children had a high burden of enteric pathogens in eastern DRC. We found Cryptosporidium in feces was associated with growth faltering, further evidence to support the role of enteric pathogens on child growth in a sub-Saharan Africa setting and highlighting the need for interventions to reduce pediatric exposure to fecal pathogens. Our results also show that A. muciniphila was associated with improved linear growth in young children, illustrating the potential of this enteric microbe to serve as a therapeutic intervention for this high-risk population and suggesting pathways for future research globally.

Acknowledgments

We thank the US Agency for International Development (USAID) Bureau for Humanitarian Assistance and Sarah Bauler, Nicole Coglianese, Phil Moses and Amagana Togo at Food for the Hungry for their support. We also thank all the study participants and the research supervisors and assistants who were crucial to successfully implementing this study: Willy Mapendano, Eric-Yves Iragi, Pascal Tezangi, Blessing Muderhwa, Manu Kabiyo, Fraterne Luhiriri, Wivine Ntumba, Julienne Rushago, Pacifique Kitumaini, Freddy Endelea, Claudia Bazilerhe, Jean Claude Lunye Lunye, Adolophine F. Rugusha, Gisele N. Kasanzike, Brigitte Munyerenkana, Jessy T. Mukulikire, Dieudonné Cibinda, Jean Basimage, and Siloé Barhuze. These persons were supported by funding from USAID and declare no conflicts of interest.

This material is based in part upon work supported by the USAID Bureau for Humanitarian Assistance under a Development Food Security Activity, led by Food for the Hungry in the Sud Kivu and Tanganyika provinces of DRC (cooperative Agreement AID-FFP-A-16-00010).

Dr. George is an infectious disease epidemiologist and environmental engineer. Her research focuses on developing and evaluating community and healthcare facility–based water, sanitation, and hygiene interventions to reduce infections in low- and middle-income countries and low-resource settings globally.

References

1. Troeger CE, Khalil IA, Blacker BF, Biehl MH, Albertson SB, Zimsen SRM, et al.; GBD 2017 Diarrhoeal Disease Collaborators. Quantifying risks and interventions that have affected the burden of diarrhoea among children younger than 5 years: an analysis of the Global Burden of Disease Study 2017. Lancet Infect Dis. 2020;20:37–59. https://doi.org/10.1016/S1473-3099(19)30401-3
2. Humphrey JH. Child undernutrition, tropical enteropathy, toilets, and handwashing. Lancet. 2009;374:1032–5. https://doi.org/10.1016/S0140-6736(09)60950-8
3. George CM, Burrowes V, Perin J, Oldja L, Biswas S, Sack D, et al. Enteric infections in young children are associated with environmental enteropathy and impaired growth. Trop Med Int Health. 2018;23:26–33. https://doi.org/10.1111/tmi.13002
4. World Health Organization. Levels and trends in child malnutrition: UNICEF/WHO/The World Bank Group joint child malnutrition estimates: key findings of the 2020 edition [cited 2021 Oct 12]. https://www.who.int/publications/i/item/9789240003576
5. Prado EL, Dewey KG. Nutrition and brain development in early life. Nutr Rev. 2014;72:267–84. https://doi.org/10.1111/nure.12102
6. Berkman DS, Lescano AG, Gilman RH, Lopez SL, Black MM. Effects of stunting, diarrhoeal disease, and parasitic infection during infancy on cognition in late childhood: a follow-up study. Lancet. 2002;359:564–71. https://doi.org/10.1016/S0140-6736(02)07744-9
7. Walker SP, Chang SM, Powell CA, Simonoff E, Grantham-McGregor SM. Early childhood stunting is associated with poor psychological functioning in late adolescence and effects are reduced by psychosocial stimulation. J Nutr. 2007;137:2464–9. https://doi.org/10.1093/jn/137.11.2464
8. UNICEF. Child and adolescent health: diarrhoeal disease [cited 2021 Oct 12]. https://data.unicef.org/topic/child-health/diarrhoeal-disease</eref>
9. Diarrhoeal Diseases Collaborators GBD; GBD Diarrhoeal Diseases Collaborators. Estimates of global, regional, and national morbidity, mortality, and aetiologies of diarrhoeal diseases: a systematic analysis for the Global Burden of Disease Study 2015. Lancet Infect Dis. 2017;17:909–48. https://doi.org/10.1016/S1473-3099(17)30276-1
10. Democratic Republic of Congo: demographic and health survey 2013-14: key findings. (English) [cited 2021 Oct 12]. https://dhsprogram.com/pubs/pdf/SR218/SR218.e.pdf
11. Lindsay B, Oundo J, Hossain MA, Antonio M, Tamboura B, Walker AW, et al. Microbiota that affect risk for shigellosis in children in low-income countries. Emerg Infect Dis. 2015;21:242–50. https://doi.org/10.3201/eid2101.140795
12. Corr SC, Li Y, Riedel CU, O'Toole PW, Hill C, Gahan CG. Bacteriocin production as a mechanism for the antiinfective activity of *Lactobacillus salivarius* UCC118. Proc Natl Acad Sci U S A. 2007;104:7617–21. https://doi.org/10.1073/pnas.0700440104
13. Guandalini S. Probiotics for children with diarrhea: an update. J Clin Gastroenterol. 2008;42(Suppl 2):S53–7. https://doi.org/10.1097/MCG.0b013e3181674087
14. Lindsay B, Ochieng JB, Ikumapayi UN, Toure A, Ahmed D, Li S, et al. Quantitative PCR for detection of *Shigella*

improves ascertainment of *Shigella* burden in children with moderate-to-severe diarrhea in low-income countries. J Clin Microbiol. 2013;51:1740–6. https://doi.org/10.1128/JCM.02713-12
15. Sayan H, Assavacheep P, Angkanaporn K, Assavacheep A. Effect of *Lactobacillus salivarius* on growth performance, diarrhea incidence, fecal bacterial population and intestinal morphology of suckling pigs challenged with F4+ enterotoxigenic *Escherichia coli.* Asian-Australas J Anim Sci. 2018;31:1308–14. https://doi.org/10.5713/ajas.17.0746
16. de Onis M, Onyango AW. WHO child growth standards. Lancet. 2008;371:204. https://doi.org/10.1016/S0140-6736(08)60131-2
17. Black RE, Allen LH, Bhutta ZA, Caulfield LE, de Onis M, Ezzati M, et al.; Maternal and Child Undernutrition Study Group. Maternal and child undernutrition: global and regional exposures and health consequences. Lancet. 2008;371:243–60. https://doi.org/10.1016/S0140-6736(07)61690-0
18. Liu J, Platts-Mills JA, Juma J, Kabir F, Nkeze J, Okoi C, et al. Use of quantitative molecular diagnostic methods to identify causes of diarrhoea in children: a reanalysis of the GEMS case-control study. Lancet. 2016;388:1291–301. https://doi.org/10.1016/S0140-6736(16)31529-X
19. Vu DT, Sethabutr O, Von Seidlein L, Tran VT, Do GC, Bui TC, et al. Detection of *Shigella* by a PCR assay targeting the ipaH gene suggests increased prevalence of shigellosis in Nha Trang, Vietnam. J Clin Microbiol. 2004;42:2031–5. https://doi.org/10.1128/JCM.42.5.2031-2035.2004
20. Lindsay BR, Chakraborty S, Harro C, Li S, Nataro JP, Sommerfelt H, et al. Quantitative PCR and culture evaluation for enterotoxigenic *Escherichia coli* (*ETEC*) associated diarrhea in volunteers. FEMS Microbiol Lett. 2014;352:25–31. https://doi.org/10.1111/1574-6968.12362
21. Pop M, Paulson JN, Chakraborty S, Astrovskaya I, Lindsay BR, Li S, et al. Individual-specific changes in the human gut microbiota after challenge with enterotoxigenic *Escherichia coli* and subsequent ciprofloxacin treatment. BMC Genomics. 2016;17:440. https://doi.org/10.1186/s12864-016-2777-0
22. Boyle MH, Racine Y, Georgiades K, Snelling D, Hong S, Omariba W, et al. The influence of economic development level, household wealth and maternal education on child health in the developing world. Soc Sci Med. 2006;63:2242–54. https://doi.org/10.1016/j.socscimed.2006.04.034
23. Wamani H, Astrøm AN, Peterson S, Tumwine JK, Tylleskär T. Predictors of poor anthropometric status among children under 2 years of age in rural Uganda. Public Health Nutr. 2006;9:320–6. https://doi.org/10.1079/PHN2006854
24. Tusting LS, Gething PW, Gibson HS, Greenwood B, Knudsen J, Lindsay SW, et al. Housing and child health in sub-Saharan Africa: A cross-sectional analysis. PLoS Med. 2020;17:e1003055. https://doi.org/10.1371/journal.pmed.1003055
25. Haines A, Bruce N, Cairncross S, Davies M, Greenland K, Hiscox A, et al. Promoting health and advancing development through improved housing in low-income settings. J Urban Health. 2013;90:810–31. https://doi.org/10.1007/s11524-012-9773-8
26. Ruiz-Castell M, Muckle G, Dewailly É, Jacobson JL, Jacobson SW, Ayotte P, et al. Household crowding and food insecurity among Inuit families with school-aged children in the Canadian Arctic. Am J Public Health. 2015;105:e122–32. https://doi.org/10.2105/AJPH.2014.302290
27. Onyango AW, Esrey SA, Kramer MS. Continued breastfeeding and child growth in the second year of life: a prospective cohort study in western Kenya. Lancet. 1999;354:2041–5. https://doi.org/10.1016/S0140-6736(99)02168-6
28. Lamberti LM, Fischer Walker CL, Noiman A, Victora C, Black RE. Breastfeeding and the risk for diarrhea morbidity and mortality. BMC Public Health. 2011;11(Suppl 3):S15. https://doi.org/10.1186/1471-2458-11-S3-S15
29. Grillenberger M, Neumann CG, Murphy SP, Bwibo NO, Weiss RE, Jiang L, et al. Intake of micronutrients high in animal-source foods is associated with better growth in rural Kenyan school children. Br J Nutr. 2006;95:379–90. https://doi.org/10.1079/BJN20051641
30. Kaimila Y, Divala O, Agapova SE, Stephenson KB, Thakwalakwa C, Trehan I, et al. Consumption of animal-source protein is associated with improved height-for-age z scores in rural Malawian children aged 12–36 months. Nutrients. 2019;11:480. https://doi.org/10.3390/nu11020480
31. Victora CG, de Onis M, Hallal PC, Blössner M, Shrimpton R. Worldwide timing of growth faltering: revisiting implications for interventions. Pediatrics. 2010;125:e473–80. https://doi.org/10.1542/peds.2009-1519
32. Derrien M, Belzer C, de Vos WM. *Akkermansia muciniphila* and its role in regulating host functions. Microb Pathog. 2017;106:171–81. https://doi.org/10.1016/j.micpath.2016.02.005
33. Derrien M, Vaughan EE, Plugge CM, de Vos WM. *Akkermansia muciniphila* gen. nov., sp. nov., a human intestinal mucin-degrading bacterium. Int J Syst Evol Microbiol. 2004;54:1469–76. https://doi.org/10.1099/ijs.0.02873-0
34. Zhou K. Strategies to promote abundance of *Akkermansia muciniphila*, an emerging probiotics in the gut, evidence from dietary intervention studies. J Funct Foods. 2017;33:194–201. https://doi.org/10.1016/j.jff.2017.03.045
35. Routy B, Le Chatelier E, Derosa L, Duong CPM, Alou MT, Daillère R, et al. Gut microbiome influences efficacy of PD-1-based immunotherapy against epithelial tumors. Science. 2018;359:91–7. https://doi.org/10.1126/science.aan3706
36. Depommier C, Everard A, Druart C, Plovier H, Van Hul M, Vieira-Silva S, et al. Supplementation with *Akkermansia muciniphila* in overweight and obese human volunteers: a proof-of-concept exploratory study. Nat Med. 2019;25:1096–103. https://doi.org/10.1038/s41591-019-0495-2
37. Khalil IA, Troeger C, Rao PC, Blacker BF, Brown A, Brewer TG, et al. Morbidity, mortality, and long-term consequences associated with diarrhoea from *Cryptosporidium* infection in children younger than 5 years: a meta-analyses study. Lancet Glob Health. 2018;6:e758–68. https://doi.org/10.1016/S2214-109X(18)30283-3
38. Kirkpatrick BD, Daniels MM, Jean SS, Pape JW, Karp C, Littenberg B, et al. Cryptosporidiosis stimulates an inflammatory intestinal response in malnourished Haitian children. J Infect Dis. 2002;186:94–101. https://doi.org/10.1086/341296
39. Bouzid M, Hunter PR, Chalmers RM, Tyler KM. *Cryptosporidium* pathogenicity and virulence. Clin Microbiol Rev. 2013;26:115–34. https://doi.org/10.1128/CMR.00076-12
40. Kosek M, Haque R, Lima A, Babji S, Shrestha S, Qureshi S, et al. Fecal markers of intestinal inflammation and permeability associated with the subsequent acquisition of linear growth deficits in infants. Am J Trop Med Hyg. 2013;88:390–6. https://doi.org/10.4269/ajtmh.2012.12-0549
41. Xiao L, Feng Y. Zoonotic cryptosporidiosis. FEMS Immunol Med Microbiol. 2008;52:309–23. https://doi.org/10.1111/j.1574-695X.2008.00377.x

42. Williams C, Cumming O, Grignard L, Rumedeka BB, Saidi JM, Grint D, et al. Prevalence and diversity of enteric pathogens among cholera treatment centre patients with acute diarrhea in Uvira, Democratic Republic of Congo. BMC Infect Dis. 2020;20:741. https://doi.org/10.1186/s12879-020-05454-0
43. Bagamian KH, Anderson JD IV, Muhib F, Cumming O, Laytner LA, Wierzba TF, et al. Heterogeneity in enterotoxigenic *Escherichia coli* and shigella infections in children under 5 years of age from 11 African countries: a subnational approach quantifying risk, mortality, morbidity, and stunting. Lancet Glob Health. 2020;8:e101–12. https://doi.org/10.1016/S2214-109X(19)30456-5
44. Pieniazek NJ, Bornay-Llinares FJ, Slemenda SB, da Silva AJ, Moura IN, Arrowood MJ, et al. New cryptosporidium genotypes in HIV-infected persons. Emerg Infect Dis. 1999;5:444–9. https://doi.org/10.3201/eid0503.990318
45. Platts-Mills JA, Babji S, Bodhidatta L, Gratz J, Haque R, Havt A, et al.; MAL-ED Network Investigators. Pathogen-specific burdens of community diarrhoea in developing countries: a multisite birth cohort study (MAL-ED). Lancet Glob Health. 2015;3:e564–75. https://doi.org/10.1016/S2214-109X(15)00151-5

Address for correspondence: Christine Marie George, Department of International Health, Program in Global Disease Epidemiology and Control, Johns Hopkins, Bloomberg School of Public Health, 615 N Wolfe St, Rm E5535, Baltimore, MD 21205-2103, USA; email: cgeorg19@jhu.edu

etymologia revisited

Nipah Virus

[ne´-pə vī´-rəs]

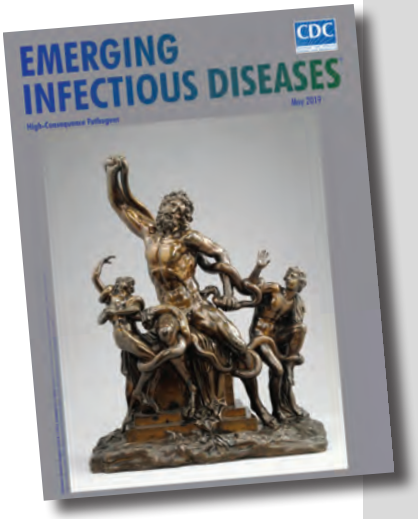

Originally published in May 2019

In 1994, a newly described virus, initially called equine morbillivirus, killed 13 horses and a trainer in Hendra, a suburb of Brisbane, Australia. The reservoir was subsequently identified as flying foxes, bats of the genus *Pteropus* (Greek pteron ["wing"] + *pous* ["foot"]). In 1999, scientists investigated reports of febrile encephalitis and respiratory illness among workers exposed to pigs in Malaysia and Singapore. (The pigs were believed to have consumed partially eaten fruit discarded by bats.)

The causative agent was determined to be closely related to Hendra virus and was later named for the Malaysian village of Kampung Sungai Nipah. The 2 viruses were combined into the genus *Henipavirus*, in the family *Paramyxoviridae*. Three additional species of *Henipavirus*—Cedar virus, Ghanaian bat virus, and Mojiang virus—have since been described, but none is known to cause human disease. Outbreaks of Nipah virus occur almost annually in India and Bangladesh, but *Pteropus* bats can be found throughout the tropics and subtropics, and henipaviruses have been isolated from them in Central and South America, Asia, Oceania, and East Africa.

Sources:

1. Centers for Disease Control and Prevention. Outbreak of Hendra-like virus—Malaysia and Singapore, 1998–1999. MMWR Morb Mortal Wkly Rep. 1999;48:265–9.
2. Selvey LA, Wells RM, McCormack JG, Ansford AJ, Murray K, Rogers RJ, et al. Infection of humans and horses by a newly described morbillivirus. Med J Aust. 1995;162:642–5.

https://wwwnc.cdc.gov/eid/article/25/5/et-2505_article

High SARS-CoV-2 Seroprevalence after Second COVID-19 Wave (October 2020–April 2021), Democratic Republic of the Congo

Yannick Munyeku-Bazitama, Gervais T. Folefack, Marc K. Yambayamba, Paul M. Tshiminyi, Benito M. Kazenza, John O. Otshudiema, Noe Tondri Guinko, Moreau D. Umba, Anastasie Mulumba, Lionel K. Baketana, Patrick K. Mukadi, Chris Smith, Jean-Jacques Muyembe-Tamfum, Steve Ahuka-Mundeke, Sheila Makiala-Mandanda

Serologic surveys are important tools for estimating the true burden of COVID-19 in a given population. After the first wave of SARS-CoV-2 infections, a household-based survey conducted in Kinshasa, Democratic Republic of the Congo, estimated ≥292 infections going undiagnosed for every laboratory-confirmed case. To ascertain the cumulative population exposure in Kinshasa after the second wave of COVID-19, we conducted a prospective population-based cross-sectional study using a highly sensitive and specific ELISA kit. The survey included 2,560 consenting persons from 585 households; 55% were female and 45% male. The overall population-weighted, test kit–adjusted SARS-CoV-2 seroprevalence was 76.5% (95% CI 74.5%–78.5%). The seroprevalence was 4-fold higher than during the first wave, and positivity was associated with age, household average monthly income, and level of education. Evidence generated from this population-based survey can inform COVID-19 response, especially vaccination campaign strategies in the context of vaccine shortages and hesitancy.

Two years after the first detected case of COVID-19 in Kinshasa, Democratic Republic of the Congo (DRC), the country experienced 4 subsequent waves of the virus, with peaks in June 2020 and January, June, and December 2021 (*1*). As observed across countries in Africa, the second wave in DRC was severe compared with the first wave in terms of disease incidence and associated deaths, partly because of lightening of stringent public health countermeasures implemented during the first wave, including international travel restrictions, and the spread of SARS-CoV-2 Beta variant (B.1.351) from southern Africa countries (*2*,*3*). By March 6, 2021, a total of 26,468 laboratory-confirmed cases were reported, including 712 virus-related deaths and 132,929 tests performed; Kinshasa accounted for nearly 75% of all reported cases (*1*).

The true burden of COVID-19 in Kinshasa is likely underestimated because PCR testing is conducted mainly on symptomatic persons meeting the case definition, omitting a large portion of persons who become infected with SARS-CoV-2 but are either asymptomatic or paucisymptomatic. Limited testing facilities throughout Africa, combined with the population's underutilization of healthcare services, further widened the gap between the number of actual infections and detected cases (*2*,*4*). On the basis of data from a previously conducted household-based survey in Kinshasa after the first wave, we reported an infection-to-case ratio of 292:1 and a prevalence of 16.6% (*5*). The survey underscored the critical role of serologic surveys as complementary tools to routine testing results for guiding public health interventions.

Author affiliations: Hokkaido University, Sapporo, Japan (Y. Munyeku-Bazitama); Université de Kinshasa, Kinshasa (Y. Munyeku-Bazitama, M.K. Yambayamba, B.M. Kazenza, P.K. Mukadi, J.-J. Muyembe-Tamfum, S. Ahuka-Mundeke, S. Makiala-Mandanda); Institut National de Recherche Biomédicale, Kinshasa, Democratic Republic of the Congo (Y. Munyeku-Bazitama, P.M. Tshiminyi, L.K. Baketana, P.K. Mukadi, J.-J. Muyembe-Tamfum, S. Ahuka-Mundeke, S. Makiala-Mandanda); Organisation Mondiale de la Santé, Kinshasa (G.T. Folefack, J.O. Otshudiema, N. Tondri Guinko, M.D. Umba, A. Mulumba); Nagasaki University, Japan (P.K. Mukadi, C. Smith); London School of Hygiene and Tropical Medicine, London, UK (C. Smith)

DOI: http://doi.org/10.3201/eid2901.221009

Serologic surveys reveal the extent of infection within a given population and provide timely estimates on such key indicators as attack rate, mortality rate, and deaths, thus guiding public health actions and the development of evidence-based strategies (*6*). In the DRC particularly, natural infection immunity is more likely to outpace vaccine-induced immunization because vaccine rollout is hindered by factors such as vaccine hesitancy, low vaccine availability, and low vaccine coverage rates (*7*,*8*). Evidence is needed, therefore, to guide overall public health response, particularly vaccination strategies aimed at optimizing the use and delivery of available vaccines. We describe a population-based SARS-CoV-2 serosurvey conducted in Kinshasa after the second wave (October 2020–April 2021) of the COVID-19 epidemic to ascertain the cumulative population exposure.

Methods

Study Design and Population

We conducted a prospective population-based, cross-sectional study in Kinshasa on March 6–14, 2021, as part of the World Health Organization's global framework for SARS-CoV-2 seroepidemiologic investigations (i.e., Unity Studies) (*9*). Kinshasa is the capital of the DRC and has an estimated population of 15 million, representing ≈15% of the population. Kinshasa is divided into 35 health districts, comprising 380 health areas.

We used a multistage, cluster sampling procedure to select study participants from a population spanning all 35 health districts of Kinshasa (Figure 1). We randomly selected 3 health areas within each health district by using probability sampling proportional to the size. After listing all streets or villages in each health area, we randomly selected 1 to 2 streets or villages within each area. We then listed all households in the selected streets or villages and systematically selected an average of 5 households from each health area. We determined eligible participants as persons of all ages who stayed in Kinshasa 2 weeks before the survey and had no contraindications to venipuncture. We obtained written informed consent from adults (participants ≥18 years of age) and emancipated minors, parental consent for participants <18 years, and assent for participants 10–17 years of age. The ethics committee of the Kinshasa School of Public Health reviewed the study (ESP/CE/81B/2020), and the study was

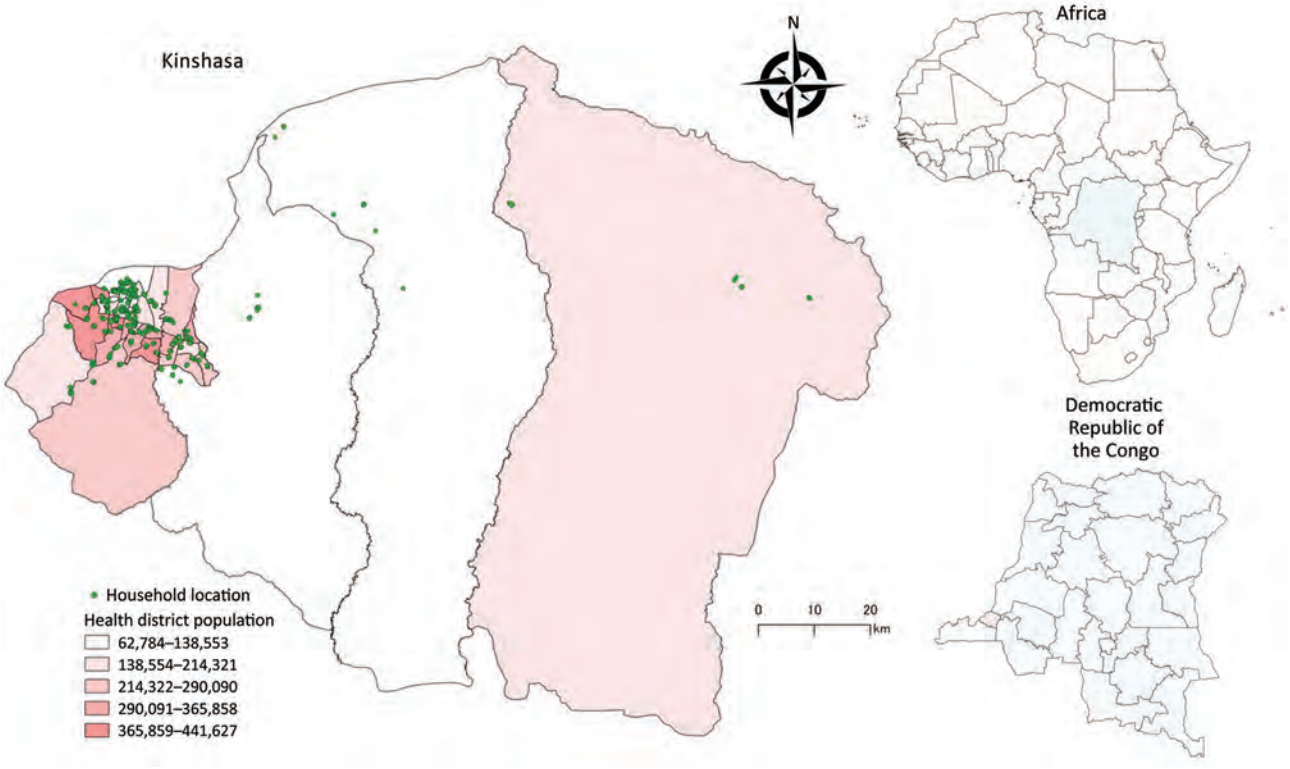

Figure 1. Study area for prospective, population-based, cross-sectional study to ascertain the cumulative population SARS-CoV-2 exposure in Kinshasa, Democratic Republic of the Congo, after the second wave of SARS-CoV-2. Inset maps show location of Kinshasa in Democratic Republic of the Congo (pink shading) and Democratic Republic of the Congo in Africa (blue shading).

aligned with the World Health Organization's Unity Studies' master protocol.

Sample Size Calculation

We calculated the sample size based on the hypothesis of an expected seroprevalence of 20%, with a precision of 3%, a design effect of 2.2, and a nonresponse rate of 30%. We determined that ≥2,146 participants needed to be recruited.

Data Collection

We presented a structured, pretested questionnaire to participants on an electronic tablet equipped with a mobile data-gathering application (Epicollect 5; Imperial College, London, https://www.imperial.ac.uk). The questionnaire covered questions regarding sociodemographic characteristics, medical history (with emphasis on COVID-19, hypertension [blood pressure ≥140/90 mm Hg], stroke, pulmonary disease, diabetes, chronic kidney disease, cancer, and obesity), alcohol and tobacco intake, SARS-CoV-2–related practices, and exposures to SARS-CoV-2. Exposures to SARS-CoV-2 comprised a previous SARS-CoV-2 infection, known contact with persons having suspected or laboratory-confirmed SARS-CoV-2 infection, and a history of travel to an affected province or country 2 weeks before the survey. We provided all participants with face masks and hand sanitizers and encouraged them to practice physical and social distancing.

Blood Collection and SARS-CoV-2 Antibody Detection

We collected 3–5 mL of venous blood samples from eligible participants in red-topped plain tubes, which were transported at 4°C in cool boxes to the National Institute of Biomedical Research in Kinshasa the same day. At the institute, we processed blood specimens to obtain serum, aliquoted the serum in 2-mL cryotubes, and stored the tubes at –20°C for subsequent analyses.

We used the Wantai SARS-CoV-2 ELISA kit (Beijing Wantai Biologic Pharmacy Enterprise Co, Ltd, https://bjwtbp.en.ec21.com) to detect anti-spike IgG and IgM in a single replicate, according to the manufacturer's instructions. We used known SARS-CoV-2–positive and SARS-CoV-2–negative samples as controls. We included prepandemic samples collected as part of measles surveillance, which tested negative for the measles virus serology (Appendix Figure 1). We considered a sample positive if the absorbance-to-cutoff ratio was ≥1.1. In the case of borderline results, we reran the test in duplicate and considered 2 matching results to be the final result.

The Wantai SARS-CoV-2 Total Antibodies ELISA kit has a sensitivity of 94.4% and a specificity of 100% (*10*). It detects whole antibodies against the receptor-binding domain (RBD) within the S1 subunit of the spike protein. The RBD represents approximately one third of the S1 subunit and is highly variable between SARS-CoV-2 and other betacoronaviruses (*11*). In this way, the Wantai SARS-CoV-2 Total Antibodies ELISA kit does not present cross-reactions with other coronaviruses that cause the common cold (i.e., OC43, HKU1, NL63, 229E). Besides providing high sensitivity and specificity, the Wantai kit offers dual detection of IgG and IgM, making the test kit useful in the very early phase of the disease course and in situations where the proportion of SARS-CoV-2 infections with asymptomatic or mild forms is prevalent; that is, when IgG synthesis is absent or low, and IgM is more likely to be abundantly synthesized and detected (*11*–*13*). The test kit also detects antibodies in most COVID-19 cases where the order of IgM-IgG seroconversion might not always be observed. In addition, antibodies directed against the RBD of the spike protein are strongly correlated with virus neutralization (*11*). The Wantai kit therefore can be helpful and informative as part of serologic surveys in gauging protective immunity in a general population.

Statistical Analyses

We extracted data from the Epicollect 5 server, converted those results into a comma-separated values file, and transferred that information to Stata 15.1 (StataCorp LLC, https://www.stata.com) for analysis. We employed the svyset command to account for the survey design. We weighted estimates to reflect the population parameters. We used proportions with corresponding 95% CIs to summarize categorical variables and the mean or the median with standard deviation or interquartile range to summarize continuous variables. We used the Pearson χ^2 test to assess the difference in seroprevalence between groups and the multivariable logistic regression to assess the association between SARS-CoV-2 seropositivity and key exposures. Finally, we corrected the seroprevalence to account for test kit performance as described elsewhere (*14*).

Results

A total of 597 households were selected from 105 health areas (clusters), of which 585 (97.9%) agreed to participate in the survey. From the selected households, 2,681 persons were surveyed, of whom 2,601 (97%) were present on the survey dates. From the 2,601 eligible persons, only 2,560 (98.4%)

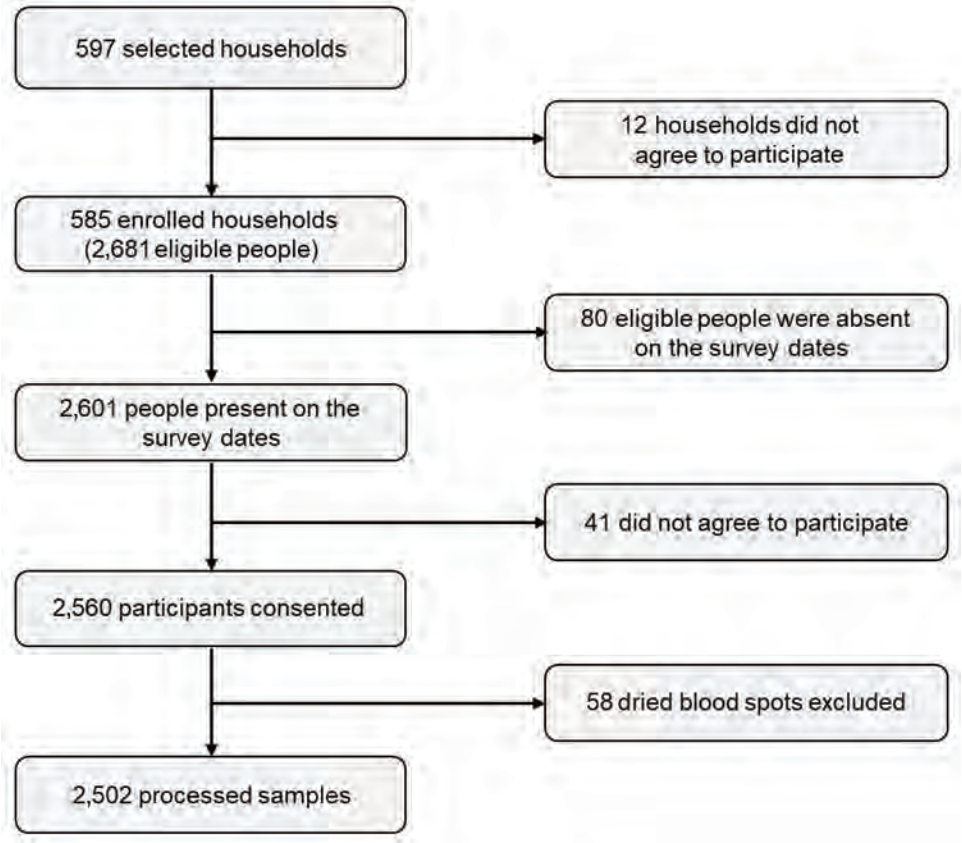

Figure 2. Flowchart of participants and household inclusion for prospective, population-based, cross-sectional study to ascertain the cumulative population SARS-CoV-2 exposure in Kinshasa, Democratic Republic of the Congo, after the second wave of SARS-CoV-2.

consented to be interviewed and provided blood samples. Of the 2,560 blood samples, 58 dried blood spots were excluded. We successfully processed 2,502 (97.7%) samples, including 26 (1%) samples with borderline results that were not included in the analysis (Figure 2).

Of the 2,560 eligible participants, 1,412 (55.2%) were female and 1,148 (44.8%) were male. Most participants (1,787, 69.8%) were from health districts located in the western part of Kinshasa (Table 1). The median age was 30 years (interquartile range 18–46 years). Persons 20–29 years of age were the most represented (511/2,560, 19.9%), followed by those 30–39 years of age (409, 15.9%). The median size of the household was 7 (interquartile range of 6–9). Six households in 10 (349/585, 59.6%) reported an average monthly income of $51–$250 (US dollars), whereas nearly one quarter (145/585) reported an average monthly income of $1–$50. Most participants (1,209/2,560, 47.2%) had junior-high school education level, and 3.0% (77) had no formal education (Table 1).

Regarding COVID-19 prevention measures, 37.9% (971/2,560) of participants reported washing their hands ≥6 times/day; another one fifth reported washing their hands daily (481 reported 1×/d, 535 reported 2×/d). More than one quarter of participants reported wearing a face mask frequently (659, 25.7%), but nearly one quarter reported rarely wearing a face mask (623, 24.3%). Most participants were nonsmokers (2,410, 94.1%) and 67.2% (1,721) reported no alcohol consumption (Table 1).

One in 2 participants reported ≥1 symptom indicative of COVID-19; fever was mentioned most frequently (713, 27.8%), followed by headache (627, 24.5%), chills (423, 16.5%), fatigue (409, 15.9%), and cough (400, 15.6%), (Table 2). Only 12.0% (308) of participants reported ≥1 comorbidity, with hypertension (166, 6.5%) and obesity (96, 3.7%) being the most reported. Most participants reported no contact with a laboratory-confirmed COVID-19 case (2,493, 97.4%) (Table 2).

The overall population-weighted SARS-CoV-2 seroprevalence was 72.2% (95% CI 69.8–4.4%) (Appendix Table 2). The seroprevalence was slightly higher, although not significantly, among female than male participants (73.8% vs. 70.1%; p = 0.146), and significantly higher in the western health districts of Kinshasa than in the eastern (74.3% vs. 68.3%; p = 0.021) (Appendix Table 1). Two health districts on either side of Kinshasa had the highest seroprevalence: Barumbu (88.4%, 95% CI 74.9%–95.1%) and

Masina 2 (88.6%, 95% CI 77.1%–94.8%) (Appendix Table 2). Similarly, higher seroprevalence was found among participants 40–49 years of age (78.6%, 95% CI 72.9%–83.3%), those with university education (84.0%, 95% CI 69.9%–92.2%), and those who declared washing hands 5–6 times a day (76.8%, 95% CI 71.9%–81.0%) (Appendix Table 1). Most households (94.2%, 551/585) had ≥1 seropositive member; median was 3 positive members (Appendix Table 3, Figures 2, 3). After adjusting for the laboratory test kit performance, the overall seroprevalence increased from 72.2% (95% CI 69.8%–74.4%) to 76.5% (95% CI 74.5%–78.5%).

Participants living in households with an average monthly income of $51–$250 had 42% increased odds of SARS-CoV-2 infection compared with participants from a household with an average monthly income of $1–$50 (crude OR 1.42, 95% CI 1.12–1.80) (Table 3). In contrast, participants from households with an average monthly income of >$1,000 were 88% less likely to be infected with SARS-CoV-2 (crude OR 0.12, 95% CI 0.04–0.36). The likelihood of SARS-CoV-2 infection tended to increase with increasing education level and age. Participants with university-level education were ≥3 times more likely to be infected with SARS-CoV-2 than those without formal education (crude OR 3.73, 95% CI 1.10–12.67) (Table 3).

On multivariable analysis, after adjusting for sex, age, and geographic area, an association emerged between SARS-CoV-2 infection and the 5–9-year age group (adjusted OR 0.38, 95% CI 0.15–0.96) and the 10–14-year age group (adjusted OR 0.33, 95% CI 0.12–0.91) (Table 3). SARS-CoV-2 infection remained associated with average household monthly income, especially for a household earning >$1,000 (adjusted OR 0.12, 95% CI 0.04–0.33). The association with education level remained and became stronger in effect size and statistical significance, especially for participants with university-level education (adjusted OR 4.33, 95% CI 2.36–17.18) (Table 3).

Discussion

We conducted this population-based serologic survey at the end of the second wave (October 2020–April 2021) of COVID-19 in Kinshasa, DRC, before vaccination became available. As such, our results provide evidence of the cumulative exposure to SARS-CoV-2 among this population.

Our results show that, 1 year after detecting the first COVID-19 case, ≥3 out of 4 persons (76.5%) had been infected with SARS-CoV-2. This high seroprevalence indicates sustained community transmission in Kinshasa. Considering the Kinshasa population of 15 million in March 2021 (*15*), we estimate 11.5 million SARS-CoV-2 infections had occurred by March 6, 2021, but only 19,831 confirmed cases were reported (1 PCR-confirmed case for nearly 580 estimated infections). During the same period, 3,325 COVID-19 cases were active, and <100 hospitalizations occurred in COVID-19 treatment centers. Factors such as the younger age of the population, the predominance of

Table 1. Sociodemographic and behavioral Characteristics of 2,560 study participants in a study to ascertain cumulative SARS-CoV-2 exposure in Kinshasa, Democratic Republic of the Congo, after the second COVID-19 wave*

Variables	Value
Sex	
F	1,412 (55.2)
M	1,148 (44.8)
Geographic area	
Western	1,787 (69.8)
Eastern	773 (30.2)
Median age, y (IQR)	30 (18–46)
Age group, y	
0–4	40 (1.6)
5–9	175 (6.8)
10–14	260 (10.2)
15–19	265 (10.4)
20–29	511 (19.9)
30–39	409 (15.9)
40–49	359 (14.0)
50–59	269 (10.5)
60–69	186 (7.3)
70–79	71 (2.8)
≥80	15 (0.6)
Household size, median (IQR)	7 (6–9)
Household average monthly income, US $	
1–50	634 (24.7)
51–250	1,525 (59.6)
251–500	340 (13.3)
501–1,000	56 (2.2)
>1,000	5 (0.2)
Education	
No formal education	77 (3.0)
Primary	473 (18.5)
Junior-high school	1,209 (47.2)
Secondary, vocational	268 (10.5)
Higher, vocational	46 (1.8)
University	487 (19.0)
Daily hand washing frequency	
<1 time	481 (18.8)
1–2 times	535 (20.9)
3–4 times	377 (14.7)
5–6 times	196 (7.7)
>6 times	971 (37.9)
Face mask wearing	
Never	422 (16.5)
Rarely	623 (24.3)
Sometimes	496 (19.4)
Often	659 (25.7)
Always	360 (14.1)
Alcohol intake	
N	1,721 (67.2)
Y	839 (32.8)
Tobacco intake	
N	2,410 (94.1)
Y	150 (5.9)

*Values are no. (%) except as indicated. IQR, interquartile range.

Table 2 Clinical characteristics of 2,560 study participants in a study to ascertain cumulative SARS-CoV-2 exposure in Kinshasa, Democratic Republic of the Congo, after the second COVID-19 wave*

Variables	Value
Symptoms suggestive of COVID-19 2 weeks before survey	
N	1,280 (50.0)
Y	1,280 (50.0)
Fever	713 (27.8)
Headaches	627 (24.5)
Chills	423 (16.5)
Fatigue	409 (15.9)
Coughing	400 (15.6)
Runny nose	369 (14.4)
Myalgia	363 (14.2)
Abdominal pain	214 (8.4)
Sore throat	134 (5.2)
Nausea	132 (5.2)
Diarrhea	125 (4.9)
Anosmia/ageusia	83 (3.2)
Chest pain	73 (2.9)
Dyspnea	57 (2.2)
Median (IQR) no. symptoms	3 (1–4)
Comorbidity	
N	2,252 (88.0)
Y	308 (12.0)
Hypertension	
N	2,394 (93.5)
Y	166 (6.5)
Stroke	
N	2,540 (99.2)
Y	20 (0.8)
Asthma	
N	2,521 (98.5)
Y	39 (1.5)
Diabetes mellitus	
N	2,532 (98.9)
Y	28 (1.1)
Kidney injury	
N	2,553 (99.7)
Y	7 (0.3)
Cancer	
N	2,554 (99.8)
Y	6 (0.2)
Obesity	
N	2,464 (96.3)
Y	96 (3.7)
Pregnancy†	
N	1,371 (97.1)
Y	41 (2.9)
Contact with a laboratory-confirmed case	
N	2,493 (97.4)
Y	67 (2.6)

*Values are no. (%) except as indicated. IQR interquartile range.
†Only women were considered for pregnancy.

mild and asymptomatic cases self-managed in the community, poor testing capacities, and low healthcare utilization might explain the discrepancies between reported cases, the actual number of infections, and the number of moderately or severely ill hospitalized persons.

The population-weighted and test kit–adjusted seroprevalence of 76.5% was nearly 4 times higher than that reported after the first wave (16.6%), reflecting an extensive community transmission after the lightening of lockdown measures, including the travel ban implemented during the first wave (*5*). Lower seroprevalence estimates were reported in Bangladesh (63.1%), Mali (58.5%), India (54.2%), Zimbabwe (53.0%), Kenya (44.2%), and Sierra Leone (2.6%) during similar periods (*16*–*22*). The characteristics of the test kit used and the variability in exposure levels across countries might explain differences in seroprevalence estimates. In our study and that of Bangladesh, an ELISA-based test detecting total antibodies against the RBD of the spike protein was used (*10*,*16*). Studies from Zimbabwe and India used serologic assays, targeting IgGs directed against the nucleocapsid protein, which are known to wane faster over time than those directed against the spike protein (*18*,*19*,*23*). Studies from Mali and Kenya used serologic tests that only targeted anti-spike IgG, thus missing newly infected persons who could bear anti-spike IgM rather than IgG (*17*,*20*). The Sierra Leone study used a lateral flow assay that targets both anti-spike IgM and IgG but is less sensitive than ELISA (*22*). Female participants were nearly 20% more likely to be infected than male participants, but the difference was not statistically significant. Similar results have been reported from other sub-Saharan Africa countries (*24*,*25*). As reported after the first wave of the COVID-19 epidemic in the DRC, the seroprevalence was not statistically different between western and eastern health districts of Kinshasa on multivariable analysis, although more cases were reported in western health districts (*5*). In our study, we observed a trend of increasing seroprevalence with age. This trend is consistent with other reports from Africa and Asia, which found higher exposures among participants 39–59 years of age (*16*,*17*,*20*,*22*). In addition, our results suggest that the second wave was characterized by similar infection rates for all age groups (*5*).

The risk for SARS-CoV-2 infection increased with average monthly household income up to $500 before decreasing dramatically, especially among households with incomes of ≥$1,000. Household income was associated with SARS-CoV-2 infection, and higher incomes reduced the risk for infection in households (*26*). The discrepancy in our study can be explained by respondent bias, because household income was assessed based on household heads' responses rather than owned assets. Participants with a university education were more likely to be infected (84%), and having a university-level education was associated with a 4-fold increase in the risk for infection. A study from Portugal reported that a lower level of education was a critical risk

factor for SARS-CoV-2 transmission compared with tertiary education (*27*). Higher levels of education are usually associated with better job opportunities and higher income and, thus, better living conditions and compliance with individual and collective protective measures. Conversely, a higher level of education and better employment may be associated with higher mobility and complex interactions with potentially infected persons, increasing the odds of infection.

Our study has several strengths, such as the robust sampling frame, which provided a large and representative sample size that included all 35 health districts of Kinshasa, and the high response rate among households (97.9%) and participants (98.4%). However, we were unable to perform a neutralizing antibody test on positive samples to ascertain protective immunity. In addition, there might have been respondent bias because we relied on self-reporting for variables such as comorbidities, household income, face mask wearing, daily hand washing, alcohol intake, and tobacco use. The stigma associated with COVID-19 might have played a role in underreporting critical information, as exemplified by the lower proportion (2.6%) of participants who reported a known contact with a laboratory-confirmed case. Finally, we collected clinical symptoms by interviewing participants, and there might have been recall bias, especially for symptoms that occurred more than 2 weeks prior to the survey.

Table 3. Sociodemographic and behavioral characteristics associated with SARS-CoV-2 infection in a study to ascertain cumulative SARS-CoV-2 exposure in Kinshasa, Democratic Republic of the Congo, after the second COVID-19 wave*

Characteristic	Total no.	Seropositive, no. (%)	Crude OR (95% CI)	Adjusted OR (95% CI)
Sex				
F	1,369	1,005 (73.8)	Referent	Referent
M	1,107	780 (70.1)	0.83 (0.64–1.07)	0.83 (0.62–1.06)
Geographic area				
Western	1,724	1,291 (74.3)	Referent	Referent
Eastern	752	494 (68.3)	0.74 (0.58–0.95)	0.81 (0.61–1.07)
Age, y				
0–4	32	22 (70.8)	Referent	Referent
5–9	165	98 (60.2)	0.62 (0.29–1.33)	0.38 (0.15–0.96)
10–14	255	163 (61.8)	0.66 (0.28–1.55)	0.33 (0.12–0.91)
15–19	258	187 (72.4)	1.08 (0.51–2.27)	0.40 (0.15 –1.06)
20–29	497	364 (72.7)	1.10 (0.53–2.26)	0.39 (0.14–1.04)
30–39	393	295 (74.8)	1.22 (0.57–2.62)	0.42 (0.15–1.18)
40–49	349	272 (78.6)	1.51 (0.71–3.19)	0.52 (0.19–1.44)
50–59	265	194 (74.0)	1.17 (0.53–2.63)	0.40 (0.15–1.08)
60–69	179	131 (73.4)	1.14 (0.54–2.39)	0.41 (0.16–1.03)
70–79	69	51 (76.6)	1.35 (0.51–3.56)	0.63 (0.24–1.68)
≥80	14	8 (65.5)	0.78 (0.23–2.63)	0.39 (0.09–1.61)
Household average monthly income, US $				
1–50	602	386 (66.8)	Referent	Referent
51–250	1,471	1,099 (74.2)	1.42 (1.12–1.80)	1.22 (0.94–1.59)
251–500	335	259 (75.3)	1.50 (0.98–2.33)	1.16 (0.73–1.82)
501–1,000	53	35 (65.2)	0.93 (0.46–1.85)	0.81 (0.41–1.57)
>1,000	5	1 (20.0)	0.12 (0.04–0.36)	0.12 (0.04–0.33)
Education				
No formal education	66	41 (58.4)	Referent	Referent
Primary	457	281 (62.2)	1.17 (0.56–2.44)	1.73 (0.72–4.17)
Junior-high school	396	273 (69.7)	1.63 (0.82–3.24)	2.15 (0.88–5.23)
High school	782	595 (74.6)	2.09 (1.04–4.17)	2.44 (1.02–5.86)
Secondary, (vocational	263	203 (78.6)	2.61 (1.23–5.52)	3.02 (1.22–7.48)
Higher, vocational	46	37 (76.2)	2.28 (1.07–4.83)	2.75 (1.06–7.14)
University	466	355 (84.0)	3.73 (1.10–2.67)	4.33 (2.36–17.18)
Daily hand washing frequency				
<1 time	466	297 (64.1)	Referent	Referent
1–2 times	516	389 (75.4)	1.72 (1.18–2.50)	1.43 (0.89–2.31)
3–4 times	362	248 (66.1)	1.09 (0.73–1.62)	0.91 (0.59–1.41)
5–6 times	190	143 (76.8)	1.85 (1.30–2.64)	1.41 (0.85–2.36)
>6 times	942	708 (74.8)	1.66 (1.20–2.31)	1.47 (0.92–2.36)
Face mask wearing				
Never	398	247 (63.6)	Referent	Referent
Rarely	611	440 (71.6)	1.43 (0.96–2.14)	1.14 (0.66–1.96)
Sometimes	478	363 (74.8)	1.69 (1.19–2.41)	1.29 (0.80–2.07)
Often	640	477 (74.5)	1.66 (1.15–2.39)	1.22 (0.73–2.03)
Always	349	258 (74.1)	1.63 (0.96–2.76)	0.99 (0.51–1.96)

*OR, odds ratio.

In conclusion, our data suggest an extensive transmission of SARS-CoV-2 during the second COVID-19 wave in Kinshasa, resulting in a higher seroprevalence. Evidence generated from this population-based survey is critical to adjusting the COVID-19 response and especially vaccination campaign strategies in the context of vaccine scarcity and hesitancy, when a large proportion of potential vaccinees have been naturally exposed to SARS-CoV-2. The emergence and global spread of SARS-CoV-2 variants of concern, with their potential to resist neutralizing antibodies developed after natural infection, and antibodies waning could hamper the putative protective immunity. Serosurveillance coupled with neutralization tests and genomic surveillance of SARS-CoV-2 variants is needed to adjust the COVID-19 response plan in the DRC, including vaccination strategies, as the pandemic evolves.

Acknowledgments

The authors would like to thank all participants and are grateful to the Division Provinciale de Santé de Kinshasa, the 35 Health districts (Zone de Santé), and 105 health areas (Aires de Santé) for their assistance with community mobilization and samples collection. The authors are also grateful to Manda Jun, Elias Mbuyi, Carmel Matondo, Esthera Muhangi, and the 175 field investigators for their valuable contribution to data acquisition and field logistics.

This work was funded by the World Health Organization.

About the Author

Dr. Yannick Munyeku-Bazitama is a researcher at the Virology Department of the National Institute of Biomedical Research (French acronym INRB) in Kinshasa, DRC, and a PhD student at Hokkaido University International Institute for Zoonosis Control. His research interests include the epidemiology of infectious and tropical diseases.

References

1. World Health Organization. The Democratic Republic of Congo: WHO coronavirus disease (COVID-19) dashboard with vaccination data [cited 2021 Dec 27]. https://covid19.who.int/region/afro/country/cd
2. Salyer SJ, Maeda J, Sembuche S, Kebede Y, Tshangela A, Moussif M, et al. The first and second waves of the COVID-19 pandemic in Africa: a cross-sectional study. Lancet. 2021;397:1265–75. https://doi.org/10.1016/S0140-6736(21)00632-2
3. Wilkinson E, Giovanetti M, Tegally H, San JE, Lessells R, Cuadros D, et al. A year of genomic surveillance reveals how the SARS-CoV-2 pandemic unfolded in Africa. Science. 2021;374:423–31. https://doi.org/10.1126/science.abj4336
4. Chitungo I, Dzobo M, Hlongwa M, Dzinamarira T. COVID-19: Unpacking the low number of cases in Africa. Public Health Pract (Oxf). 2020;1:100038. https://doi.org/10.1016/j.puhip.2020.100038
5. Nkuba AN, Makiala SM, Guichet E, Tshiminyi PM, Bazitama YM, Yambayamba MK, et al. High prevalence of anti-severe acute respiratory syndrome coronavirus 2 (anti-SARS-CoV-2) antibodies after the first wave of coronavirus disease 2019 (COVID-19) in Kinshasa, Democratic Republic of the Congo: Results of a cross-sectional household-based survey. Clin Infect Dis. 2022;74:882–90. https://doi.org/10.1093/cid/ciab515
6. Murhekar MV, Clapham H. COVID-19 serosurveys for public health decision making. Lancet Glob Health. 2021;9:e559–60. https://doi.org/10.1016/S2214-109X(21)00057-7
7. Ditekemena JD, Nkamba DM, Mutwadi A, Mavoko HM, Siewe Fodjo JN, Luhata C, et al. COVID-19 vaccine acceptance in the Democratic Republic of Congo: a cross-sectional survey. Vaccines (Basel). 2021;9:153. https://doi.org/10.3390/vaccines9020153
8. Nachega JB, Sam-Agudu NA, Masekela R, van der Zalm MM, Nsanzimana S, Condo J, et al. Addressing challenges to rolling out COVID-19 vaccines in African countries. Lancet Glob Health. 2021;9:e746–8. https://doi.org/10.1016/S2214-109X(21)00097-8
9. World Health Organization. Population-based age-stratified seroepidemiological investigation protocol for COVID-19 virus infection, 17 March 2020. World Health Organization; 2020 [cited 2021 Aug 9]. https://apps.who.int/iris/handle/10665/331656
10. Wantai SARS-CoV-2 Manual Diagnostic Kits: COVID-19 serology and molecular tests [cited 2021 Aug 9]. https://www.ystwt.cn/covid-19
11. Mohit E, Rostami Z, Vahidi H. A comparative review of immunoassays for COVID-19 detection. Expert Rev Clin Immunol. 2021;17:573–99. https://doi.org/10.1080/1744666X.2021.1908886
12. Brochot E, Demey B, Handala L, François C, Duverlie G, Castelain S. Comparison of different serological assays for SARS-CoV-2 in real life. J Clin Virol. 2020;130:104569. https://doi.org/10.1016/j.jcv.2020.104569
13. Hanssen DAT, Slaats M, Mulder M, Savelkoul PHM, van Loo IHM. Evaluation of 18 commercial serological assays for the detection of antibodies against SARS-CoV-2 in paired serum samples. Eur J Clin Microbiol Infect Dis. 2021;40:1695–703. https://doi.org/10.1007/s10096-021-04220-7
14. Sempos CT, Tian L. Adjusting coronavirus prevalence estimates for laboratory test kit error. Am J Epidemiol. 2021;190:109–15. https://doi.org/10.1093/aje/kwaa174
15. Kinshasa, Democratic Republic of the Congo Population. Population Stat 2022 [cited 2022 Sep 25]. https://population-stat.com/democratic-republic-of-the-congo/kinshasa
16. Bhuiyan TR, Hulse JD, Hegde ST, Akhtar M, Islam T, Khan ZH, et al. SARS-CoV-2 seroprevalence before Delta variant surge, Chattogram, Bangladesh, March–June 2021. Emerg Infect Dis. 2022;28:429–31. https://doi.org/10.3201/eid2802.211689
17. Sagara I, Woodford J, Kone M, Assadou MH, Katile A, Attaher O, et al. Rapidly increasing SARS-CoV-2 seroprevalence and limited clinical disease in three Malian communities: a prospective cohort study. Clin Infect Dis. 2022;3:1030–8. https://doi.org/10.1093/cid/ciab589
18. Laxmaiah A, Rao NM, Arlappa N, Babu J, Kumar PU, Singh P, et al. SARS-CoV-2 seroprevalence in the city of Hyderabad, India in early 2021. IJID Reg. 2022;2:1–7. https://doi.org/10.1016/j.ijregi.2021.10.009

19. Fryatt A, Simms V, Bandason T, Redzo N, Olaru ID, Ndhlovu CE, et al. Community SARS-CoV-2 seroprevalence before and after the second wave of SARS-CoV-2 infection in Harare, Zimbabwe. EClinicalMedicine. 2021;41:101172. https://doi.org/10.1016/j.eclinm.2021.101172
20. Uyoga S, Adetifa IMO, Otiende M, Yegon C, Agweyu A, Warimwe GM, et al. Prevalence of SARS-CoV-2 antibodies from a national serosurveillance of Kenyan blood donors, January–March 2021. JAMA. 2021;326:1436–8. https://doi.org/10.1001/jama.2021.15265
21. Lei R, Qiu R. A strategy to prevent and control zoonoses? Hastings Cent Rep. 2020;50:73–4. https://doi.org/10.1002/hast.1142
22. Barrie MB, Lakoh S, Kelly JD, Kanu JS, Squire JS, Koroma Z, et al. SARS-CoV-2 antibody prevalence in Sierra Leone, March 2021: a cross-sectional, nationally representative, age-stratified serosurvey. BMJ Glob Health. 2021;6:e007271. https://doi.org/10.1136/bmjgh-2021-007271
23. Ripperger TJ, Uhrlaub JL, Watanabe M, Wong R, Castaneda Y, Pizzato HA, et al. Orthogonal SARS-CoV-2 serological assays enable surveillance of low-prevalence communities and reveal durable humoral immunity. Immunity. 2020;53:925–933.e4. https://doi.org/10.1016/j.immuni.2020.10.004
24. Kleynhans J, Tempia S, Wolter N, von Gottberg A, Bhiman JN, Buys A, et al.; PHIRST-C Group. PHIRST-C Group. SARS-CoV-2 seroprevalence in a rural and urban household cohort during first and second waves of infections, South Africa, July 2020–March 2021. Emerg Infect Dis. 2021;27:3020–9. https://doi.org/10.3201/eid2712.211465
25. Mulenga LB, Hines JZ, Fwoloshi S, Chirwa L, Siwingwa M, Yingst S, et al. Prevalence of SARS-CoV-2 in six districts in Zambia in July, 2020: a cross-sectional cluster sample survey. Lancet Glob Health. 2021;9:e773–81. https://doi.org/10.1016/S2214-109X(21)00053-X
26. Allan-Blitz L-T, Goldbeck C, Hertlein F, Turner I, Klausner JD. Association of lower socioeconomic status and SARS-CoV-2 positivity in Los Angeles, California. J Prev Med Public Health. 2021;54:161–5. https://doi.org/10.3961/jpmph.21.126
27. Leite A, Leão T, Soares P, Severo M, Moniz M, Lucas R, et al. A case-control study of contextual factors for SARS-CoV-2 transmission. Front Public Health. 2021;9:772782. https://doi.org/10.3389/fpubh.2021.772782

Address for correspondence: Sheila Makiala-Mandanda, Institut National de Recherche Biomédicale, 5345 Avenue de la Démocratie (Ex Des Huileries), Kinshasa-Gombe, Democratic Republic of the Congo; email: shemakiala@yahoo.fr

Originally published in June 2020

Scrapie

[skra'pe]

Scrapie is a fatal neurodegenerative disease of sheep and goats that was the first of a group of spongiform encephalopathies to be reported (1732 in England) and the first whose transmissibility was demonstrated by Cuille and Chelle in 1936. The name resulted because most affected sheep develop pruritis and compulsively scratch their hides against fixed objects. Like other transmissible spongiform encephalopathies, scrapie is associated with an alteration in conformation of a normal neural cell glycoprotein, the prion protein. The scrapie agent was first described as a prion (and the term coined) by Stanley Prusiner in 1982, work for which he received the Nobel Prize in 1997.

Sources:

1. Brown P, Bradley R. 1755 and all that: a historical primer of transmissible spongiform encephalopathy. BMJ. 1998;317:1688–92.
2. Cuillé J, Chelle PL. The so-called "trembling" disease of sheep: is it inoculable? [in French]. Comptes Rendus de l'Académie Sciences. 1936;203:1552.
3. Laplanche J-L, Hunter N, Shinagawa M, Williams E. Scrapie, chronic wasting disease, and transmissible mink encephalopathy. In: Prusiner SB, editor. Prion biology and diseases. Cold Spring Harbor (NY): Cold Spring Harbor Laboratory Press; 1999. p. 393–429.
4. Prusiner SB. Novel proteinaceous infectious particles cause scrapie. Science. 1982;216:136–44.

https//wwwnc.cdc.gov/eid/article/26/6/et-2606_article

Human Immunity and Susceptibility to Influenza A(H3) Viruses of Avian, Equine, and Swine Origin

Elien Vandoorn, Wojciech Stadejek, Isabel Leroux-Roels, Geert Leroux-Roels, Anna Parys, Kristien Van Reeth

Influenza A viruses (IAVs) of subtype H3 that infect humans are antigenically divergent from those of birds, horses, and swine. Human immunity against these viruses might be limited, implying potential pandemic risk. To determine human risk, we selected 4 avian, 1 equine, and 3 swine IAVs representing major H3 lineages. We tested serum collected during 2017–2018 from 286 persons in Belgium for hemagglutination inhibiting antibodies and virus neutralizing antibodies against those animal-origin IAVs and tested replication in human airway epithelia. Seroprevalence rates for circulating IAVs from swine in North America were ≥51%, swine in Europe 7%–37%, and birds and equids ≤12%. Replication was efficient for cluster IAVs from swine in North America and IAVs from swine in Europe, intermediate for IAVs from horses and poultry, and absent for IAVs from wild birds and a novel human-like swine IAV in North America. Public health risk may be highest for swine H3 IAVs.

Influenza A viruses (IAVs) of the H3 subtype are endemic to humans, swine, and wild birds; they also cause outbreaks in horses and are often detected in domestic birds. An H3 IAV that crosses the species barrier from animals to humans can result in a pandemic if the virus carries a hemagglutinin (HA) against which humans lack protective antibodies and the virus readily replicates in and spreads among humans. For example, in 1968, transmission of an IAV with an avian-origin H3 HA to humans caused the influenza A(H3N2) pandemic (*1*).

The natural IAV reservoir is considered to be wild waterfowl, but transmission to domestic poultry is frequent. Avian H3 IAVs are classified as Eurasian and North American lineages, although the HA of these viruses is antigenically closely related (*2*,*3*). In contrast, after being introduced to humans in 1968, the HA of human H3 IAVs quickly drifted away from that of the avian precursor IAV. Consequently, contemporary human H3 IAVs are antigenically divergent from those in birds (*2*). Similarly, avian H3 IAVs were introduced into horses in the 1960s, after which their HA antigenically drifted. That evolution was, however, different and slower than for human H3 IAVs (*4*). Equine H3 IAVs of Florida clade 1 (FC1) are currently predominant (*5*). All swine H3 IAVs derived their HA from human IAVs.

H3 IAVs from swine in Europe originated from a human IAV that circulated in the late 1970s. Of the 2 major lineages cocirculating in North America, cluster IV-A was derived from human IAVs from the late 1990s and novel human-like swine H3 IAVs from human IAVs from the early 2010s (*6*). H3 IAVs undergo slower antigenic drift in swine than in humans. Consequently, persons born after the swine viruses' human ancestor IAV had circulated are unlikely to have cross-reactive antibodies against the swine H3 IAVs. Therefore, with time, human population immunity against swine H3 IAVs decreases, increasing the pandemic risk (*7*–*10*).

The infectious potential of swine H3 IAVs for humans is evident from >400 recorded zoonotic infections in the United States caused by North American cluster IV-A or novel human-like H3 swine IAVs. Four zoonotic infections with H3 IAVs from swine in Europe have also been reported (*6*,*11*–*13*). H3 IAVs from equids can infect humans under experimental conditions, but there are no confirmed cases of natural transmission (*14*). Animal H3 IAVs might, however, become more adapted to humans by accumulating mutations in their viral proteins, reassortment of gene segments with IAVs of different species, or both (*6*,*15*). Avian H3 IAVs can infect humans directly or via an intermediate host, such as poultry or swine (*2*,*15*). In 2019, an H3N1 IAV that

Author affiliations: Ghent University, Merelbeke, Belgium (E. Vandoorn, W. Stadejek, A. Parys, K. Van Reeth); Ghent University and Ghent University Hospital, Ghent, Belgium (I. Leroux-Roels, G. Leroux-Roels)

DOI: https://doi.org/10.3201/eid2901.220943

originated from wild birds caused outbreaks at 82 poultry farms in Belgium and 3 in France without infecting humans but was unusually virulent for poultry (*16*). In 2022, two zoonotic infections with avian H3N8 IAVs were reported (*17*).

H3 IAVs continue to evolve in each host species. Therefore, frequent re-evaluation of human seroprevalence and replication potential in humans for circulating animal H3 IAVs is recommended. Serum hemagglutination inhibiting (HI) and virus neutralizing (VN) antibodies correlate with protection. Thus, prevalence of such antibodies against animal H3 IAVs in persons of different age groups can be used to estimate the public health risk (*18*). Recent seroprevalence studies are available for H3 IAVs from swine in North America, but studies in Europe were conducted with samples and IAVs collected before 2011 (*7*–*10*,*19*). Studies for H3 IAVs from birds and equids are generally lacking, except for a few small-scale studies with historic IAV strains (*20*–*24*). The infectivity of animal H3 IAVs in humans was previously evaluated with mammalian models, outdated IAV strains, or both (*15*,*25*–*29*). To help evaluate the public health risk posed by different animal H3 IAVs, we analyzed serum samples collected from persons of different age groups in Belgium for prevalence and titers of HI and VN antibodies against all major circulating swine, avian, and equine H3 IAV lineages. We also assessed the replicative capacity of selected IAVs in human airway epithelia. The Commission for Medical Ethics of the Ghent University Hospital approved the study (approval no. 2017/834).

Materials and Methods

Human Serum and Tissue Samples

During August 2017–January 2018, we selected 286 serum samples from immunocompetent persons in Belgium born during 1921–2017 who had unknown influenza infection or vaccination history. The male:female ratio was ≈1:1, and we used ≈3 samples per birth year.

From Epithelix Sàrl (https://www.epithelix.com), we purchased human airway epithelia (MucilAir) reconstituted from primary cells of biopsy samples from 6 donors (Table 1). We maintained the tissues at the air–liquid interface with MucilAir culture medium (Epithelix) according to the manufacturer's instructions.

Viruses

IAVs for seroreactivity and replication studies included representatives of major H3 lineages circulating in wild birds (mlOH18, mlBE18), horses (eqCH18), and swine (swG17, swIN16, swMO15); the avian H3N1 IAV that caused outbreaks in poultry in Belgium in 2019 (chG19); the 1968 human pandemic virus (HK68); and the presumed avian ancestor IAV of HK68 (dkUK63) (Table 2; Figure 1, panel A). We used epidemiologic data to select major H3 lineages (*5*,*30*–*32*). We selected test viruses on the basis of antigenic relatedness and amino acid homology to currently circulating IAVs of each lineage available in GenBank.

The major target of neutralizing antibodies is HA1. We downloaded the viruses' HA1 nucleotide sequences from GenBank and translated them to amino acids. We aligned sequences with the MUSCLE algorithm (https://www.ebi.ac.uk/Tools/msa/muscle) and constructed maximum-likelihood trees by using the Jones-Taylor-Thornton model and the nearest-neighbor-interchange heuristic method in MEGA7 (https://www.megasoftware.net) (*33*). We determined numbers of identical amino acids in presumed antigenic sites (*34*) and percentages of amino acid homology between test viruses by using MEGA7 and R version 3.5.3 (The R Foundation for Statistical Computing, https://www.r-project.org).

We received avian IAVs from the Flemish Institute for Biotechnology (Flanders, Belgium) and Ohio State University (Columbus, Ohio, USA), equine IAVs from St. Jude Children's Research Hospital (Memphis, Tennessee, USA), North American swine IAVs from the US Department of Agriculture–Agricultural Research Service (Bethesda, Maryland, USA), and the human IAV from Philipps University Marburg (Marburg, Germany). Viruses for serologic assays and inoculation of MucilAir tissues were grown in MDCK cells; only avian and equine viruses for HI assays were propagated in allantoic cavities of 10-day-old embryonated chicken eggs; and all underwent ≤4 passages.

Serologic Assays

HI and VN assays for antibodies against each test virus were performed according to standard procedures (*35*). We performed HI assays with 1% horse erythrocytes for avian and equine IAVs and 0.5% turkey erythrocytes for human and swine IAVs. Antibody titers represent the reciprocal of the highest serum dilution showing complete hemagglutination inhibition of 4 hemagglutinating units of virus (HI) or 50% neutralization of 100 tissue culture infective doses ($TCID_{50}$) of virus (VN). Starting dilutions were 1:20 in HI and 1:10 in VN. We considered a titer of ≥40 to be positive.

Table 1. Characteristics of MucilAir donors and tissues used for study of human susceptibility to influenza A(H3) viruses of avian, equine, and swine origin*

Donor ID	Donor no.	Age, y/sex	Ethnicity	Smoking status	Tissue type	Age of ALI at inoculation, wk	TEER ± SD, $\Omega.cm^2$†
ND1	MD0738	32/F	Caucasian	Nonsmoker	Nasal	11	774 ± 27
ND2	MD0436	46/M	Caucasian	Unknown	Nasal	11	1,256 ± 15
ND3	MD0722	61/M	Unknown	Unknown	Nasal	11	611 ± 27
BD1	MD0802	55/F	African	Nonsmoker	Bronchial	9	669 ± 32
BD2	MD0670	15/M	Caucasian	Nonsmoker	Bronchial	11	477 ± 23
BD3	MD0810	52/F	Hispanic	Nonsmoker	Bronchial	11	424 ± 24

*MucilAir, Epithelix Sàrl (https://www.epithelix.com). ALI, air–liquid interface; ID, identifier; TEER, transepithelial electrical resistance.
†Average and SD on the basis of 12 values as mentioned in the certificate of analysis provided by the manufacturer, Epithelix.

Virus Replication Kinetics

To standardize the amount of mucus, we washed the apical side of fully differentiated MucilAir tissues (1/donor/condition) 1 time with culture medium. Three days later, we inoculated the tissues apically with 250 µL of medium (mock inoculation) or IAV at multiplicity of infection 0.01 $TCID_{50}$. After incubating the samples for 1 hour at 34°C and 5% CO_2, we removed the inoculum and washed the apical side of the tissues 1 time. At 0–4 days postinoculation (dpi), we measured transepithelial electrical resistance (TEER) with a Millicell-ERS2 Voltohmmeter (Merck KGaA, https://www.merckmillipore.com) and took samples for virus titration. For titration, we added 250 µL medium apically, allowed it to equilibrate for 30 min at 34°C, and collected it. We determined $TCID_{50}$ titers of inocula and samples by titration on MDCK monolayers, which 5 days later underwent immunocytochemical staining of IAV nucleoprotein, as previously described (*36*); the start dilution was 1:2.

Statistical Analyses

We used log_2-transformed antibody titers to calculate geometric mean titers (GMTs) and 95% CIs against each virus for samples from persons each birth decade. We used log_{10}-transformed virus titers to calculate the area under the curve (AUC) for each virus in each MucilAir tissue. Samples that tested negative were assigned a titer of half the detection limit (HI 10, VN 5, virus titration 0.65 $TCID_{50}$/mL). We used Kruskal-Wallis and Mann-Whitney U tests to compare antibody titers between viruses for a certain age group or between age groups for a certain virus. We used the same tests to compare AUCs between viruses for a certain tissue or between tissues for a certain virus. We compared proportions of positive samples by using Fisher exact tests. We determined Spearman correlation coefficients (CCs) between HI titers or between VN titers against different viruses by using nonstratified data. For serologic data, we applied the Bonferroni adjustment of the p values and considered adjusted $p<0.05$ significant. For AUCs, we considered $p\leq0.1$ significant. We performed all analyses with R version 3.5.3.

Results

Genetic Relatedness Between Test Viruses

For seroreactivity and replication studies in humans, we selected 9 H3 IAVs from humans, birds, horses, and swine. Their genetic relatedness was determined on the basis of HA1 amino acid sequence homology (Table 3; Figure 1). Human virus HK68 was closely related to the avian IAVs, showing 93%–96% homology and 32–34/40 identical amino acids in presumed antigenic sites. HK68 and avian IAVs were ≤83% homologous with recent equine and swine IAVs. Swine IAVs shared 24–26 aa in antigenic sites with HK68 and

Table 2. IAV H3 strains used for study of human immunity and susceptibility to influenza A(H3) viruses of avian, equine, and swine origin*

Virus strain	Abbreviation	Subtype	Host	H3 lineage	H3 GenBank accession no.
A/duck/Ukraine/1/63	dkUK63	H3N8	Duck	Eurasian avian	HE802062
A/mallard/Ohio/18OS1219/2018	mlOH18	H3N8	Mallard	American avian	MN431078
A/*Anas platyrhynchos*/Belgium/7827/2018	mlBE18	H3N8	Mallard	Eurasian avian	MT407033
A/chicken/Belgium-Gent/136/2019	chG19	H3N1	Chicken	Eurasian avian	OP417305
A/equine/Chile/EQCL003/2018	eqCH18	H3N8	Horse	Equine Florida clade 1	OP467551
A/Hong Kong/1/68	HK68	H3N2	Human	Human pandemic	CY044261
A/swine/Gent/48/2017	swG17	H3N2	Pig	European swine	OP415564
A/swine/Indiana/A01729047/2016	swIN16	H3N2	Pig	N. Am. cluster IV-A swine	KU598305
A/swine/Missouri/A01840724/2015	swMO15	H3N2	Pig	N. Am. novel human-like swine	KP901306

*Horizontal rules represent grouping of IAVs isolated from similar host species; groups of host species are ordered chronologically according to the first detection of H3 IAVs in each of those species, and viruses of each species are ordered chronologically according to the time point at which the corresponding lineages first arose. IAV, influenza A virus; N. Am., North American.

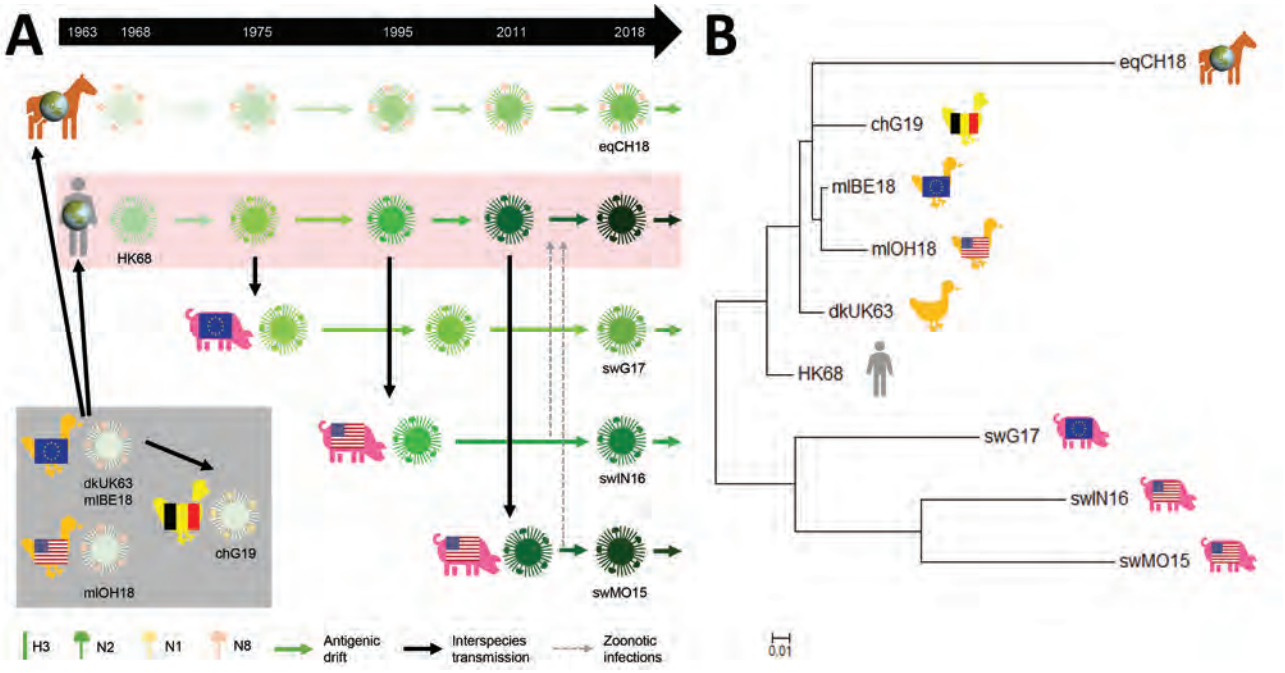

Figure 1. Epidemiologic and phylogenetic relationship between avian, equine, human, and swine influenza A test viruses. A) Schematic positioning of the test viruses in the influenza A(H3) virus epidemiology. B) Maximum-likelihood neighbor-joining phylogenetic tree of the hemagglutinin 1 of the test viruses. Complete isolate names are provided in Table 2. Scale bar indicates amino acid substitutions per site.

17–23 aa with avian IAVs. Equine and swine IAVs were most distantly related; homology was ≤78% and 18–21 amino acids in antigenic sites. Whereas all avian IAVs were closely related, swine IAVs were antigenically distant from each other.

Seroreactivity against HK68

When we tested human serum samples for antibodies against HK68 to evaluate potential exposure to this virus, we found that, overall, 51% were seropositive for HK68 in HI and 40% in VN assays (Figures 2, 3). Seroprevalence and GMTs were higher for persons born before 1977 (71% in HI, 65% in VN, GMTs ≥51) than for persons born during 1977–2017 (25% in HI, 6% in VN, GMTs ≤18; p<0.001) (Tables 4, 5). Seroreactivity was highest in those born during 1947–1966 and lowest in those born during 1997–2017.

Seroreactivity against Avian H3 IAVs

DkUK63 is the presumed avian ancestor IAV of HK68. MlOH18 and mlBE18 represent North American and Eurasian lineage H3 IAVs currently circulating in wild birds. For these IAVs, ≤10% were seropositive in HI and ≤12% in VN (Figures 2, 3). Differences in

Table 3. Percentage amino acid homology (lower left) and number of identical amino acids out of 40 aa in presumed antigenic sites (upper right) (*34*) between hemagglutinin 1 of the H3 influenza A viruses used for study of human immunity and susceptibility to influenza A(H3) viruses of avian, equine, and swine origin*

	Avian				Equine	Human	Swine		
	dkUK63	mlOH18	mlBE18	chG19	eqCH18	HK68†	swG17	swIN16	swMO15
Virus strain	Eurasian	American	Eurasian	Eurasian	FC1	Pandemic	European	N. Am.	N. Am.
dkUK63		37	36	36	24	33	22	20	18
mlOH18	93.9		39	37	25	34	22	18	18
mlBE18	96.7	95.1		38	26	34	21	18	17
chG19	94.5	91.5	95.1		26	32	22	20	17
eqCH18	82.1	80.9	82.4	80.5		24	21	20	18
HK68	95.7	92.7	95.7	93.0	82.1		23	18	18
swG17	81.4	81.1	82.1	80.8	77.9	83.4		22	22
swIN16	80.8	78.7	80.8	80.8	73.2	81.4	79.4		26
swMO15	79.6	77.5	79.0	77.8	71.4	79.9	79.2	82.9	

*Viruses are ordered according to host species and chronologically according to the emergence of each of the influenza A virus lineages in these species. Blank cells indicate crossover points between comparisons. Complete isolate names are provided in Table 2. FC1, Florida clade 1; N. Am., North American.
†Human influenza A virus that no longer circulates.

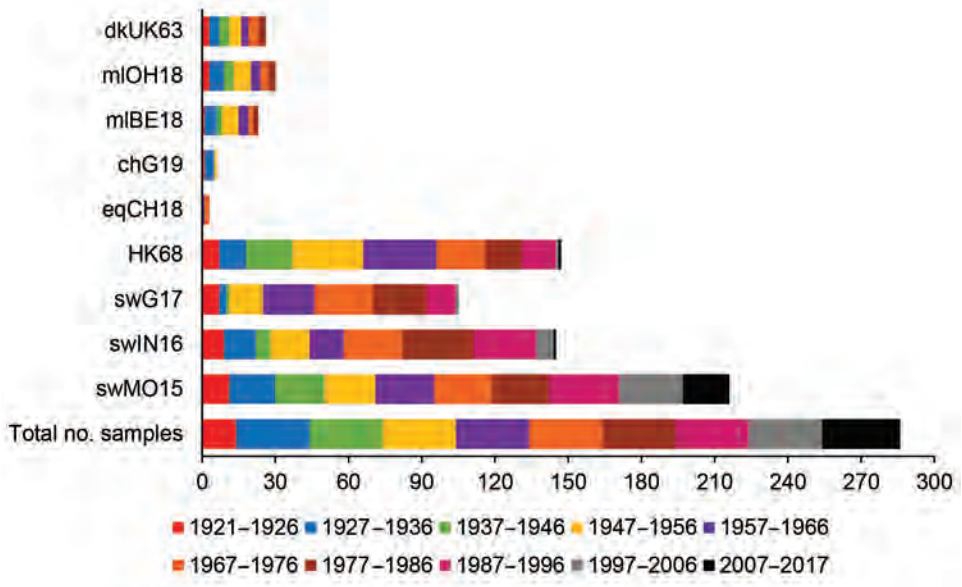

Figure 2. Number of positive human serum samples in the hemagglutination inhibition assay (titer ≥40) for each test virus compared with the total number of samples tested per birth cohort. Birth cohorts are represented by colors. A total of 286 serum samples collected during August 2017–January 2018 from immunocompetent persons in Belgium were tested. Complete isolate names are provided in Table 2.

seroprevalence rates between the 3 IAVs for each age group or between age groups for each IAV were not significant, except VN seroprevalence for mlBE18 of persons born during 1947–1956 (9%) and those born during 2007–2017 (0%; p<0.04). GMTs were <20 for all age groups, and no HI or VN antibodies against the 3 IAVs of wild birds were detected in persons born during 1997–2017 (Tables 4, 5).

ChG19 represents the avian H3N1 IAV that caused outbreaks in poultry in Belgium during 2019. Overall seroprevalence rates for chG19 were 2% in HI and 1% in VN (Figures 2, 3), and differences in seroprevalence rates between age groups were not significant. GMTs were below the detection limit for all age groups and no antibodies against chG19 were detected in persons born during 1987–2017 (Tables 4, 5).

Seroreactivity Against Equine H3 IAVs

The predominant H3 IAVs in horses belong to FC1, represented by eqCH18. Only 1% of all serum samples tested positive against eqCH18 in HI and 3% in VN (Figures 2, 3). GMTs were below the detection limit for all age groups (Tables 4, 5). Seroreactivity against eqCH18 did not differ significantly between age groups.

Seroreactivity against Swine H3 IAVs

SwG17 represents contemporary H3 IAVs in swine in Europe. Of all persons tested, 37% were seropositive

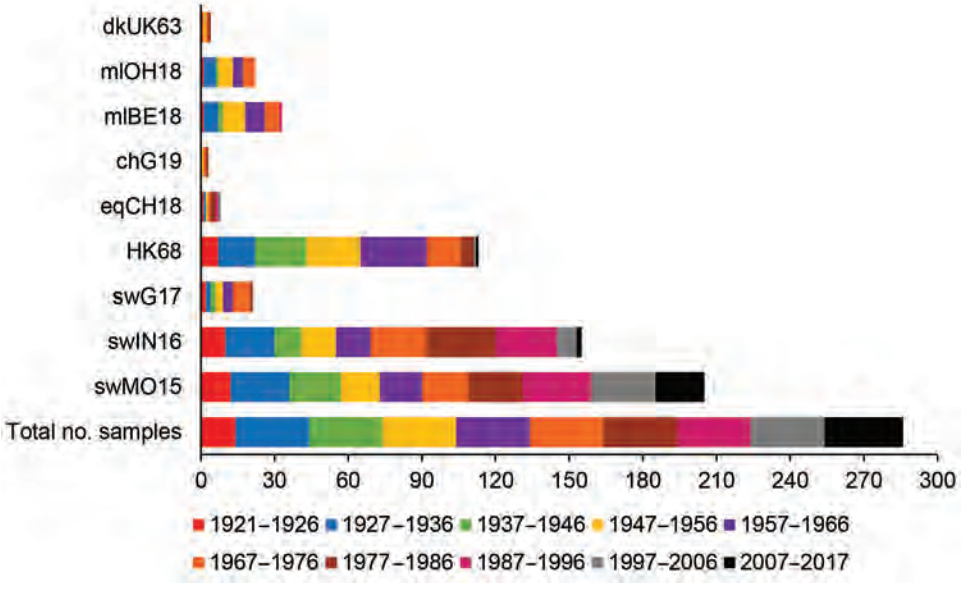

Figure 3. Number of positive human serum samples in the virus neutralization assay (titer ≥40) for each test virus compared with the total number of samples tested per birth cohort. Birth cohorts are represented by colors. A total of 286 serum samples collected during August 2017–January 2018 from immunocompetent persons in Belgium were tested. Complete isolate names are provided in Table 2.

Table 4. Geometric mean of hemagglutination inhibition antibody titers against H3 influenza A viruses of different species in different age groups, Belgium, 2017–2018*

Birth year range (age, y)†	No.	Avian				Equine	Human	Swine		
		dkUK63	mlOH18	mlBE18	chG19	eqCH18	HK68‡	swG17	swIN16	swMO15
		Eurasian	Am.	Eurasian	Eurasian	FC1	Pandemic	European	N. Am.	N. Am.
1921–1926	14	16	16	13	12	10	30	23	42	80
(96–91)		(10–25)	(10–23)	(10–19)	(10–16)	(10–10)	(17–52)	(14–38)	(24–75)	(29–219)
1927–1936	30	15	16	14	13	10	26	14	25	59
(90–81)		(12–19)	(12–21)	(11–16)	(10–16)	(10–11)	(20–35)	(11–18)	(17–36)	(35–99)
1937–1946	30	13	15	13	11	10	37	12	16	52
(80–71)		(11–16)	(12–19)	(11–15)	(10–12)	(10–10)	(27–51)	(11–14)	(12–22)	(32–83)
1947–1956	30	15	18	16	11	10	180	29	30	59
(70–61)		(12–19)	(14–23)	(12–21)	(10–13)	(10–10)	(128–252)	(21–39)	(20–43)	(39–91)
1957–1966	30	13	16	16	11	11	327	44	31	58
(60–51)		(11–16)	(13–20)	(13–20)	(10–12)	(10–13)	(249–432)	(30–63)	(22–44)	(40–83)
1967–1976	30	14	14	12	10	12	80	58	61	78
(50–41)		(11–18)	(11–17)	(10–15)	(10–11)	(10–15)	(43–150)	(40–83)	(40–91)	(49–124)
1977–1986	30	13	13	11	10	10	32	45	146	98
(40–31)		(10–17)	(10–15)	(10–14)	(10–11)	(10–11)	(21–50)	(34–58)	(105–202)	(60–162)
1987–1996	30	10	10	10	10	10	30	25	139	254
(30–21)		(10–11)	(10–10)	(10–10)	(10–10)	(10–10)	(21–42)	(18–35)	(87–224)	(170–380)
1997–2006	30	10	10	10	10	10	10	11	19	101
(20–11)		(10–10)	(10–10)	(10–10)	(10–10)	(10–10)	(10–12)	(10–13)	(14–26)	(64–158)
2007–2017	32	10	10	10	10	10	11	11	11	37
(10–0)		(10–10)	(10–10)	(10–10)	(10–10)	(10–10)	(10–12)	(10–13)	(10–13)	(25–54)
1921–2017	286	13	13	12	11	10	42	23	36	75
(96–0)		(12–13)	(12–14)	(12–13)	(10–11)	(10–11)	(36–49)	(21–26)	(31–42)	(64–87)

*Values represent geometric mean hemagglutination inhibition titers (95% CI). Viruses are ordered according to host species and chronologically according to the emergence of each of the influenza A virus lineages in these species. Complete isolate names are provided in Table 2. Am., American; FC1, Florida clade 1; N. Am., North American.
†Age at the end of 2017.
‡Human influenza A virus that no longer circulates.

for swG17 in HI and 7% in VN (Figures 2, 3). Seroprevalence rates and GMTs were higher among persons born before 1997 (HI 46%, VN 9%, GMTs ≥28) than among persons born during 1997–2017 (HI 2%, VN 0%, GMTs ≤11; p<0.02) and peaked among those born during 1967–1976 (Tables 4, 5).

The 2 predominant H3 IAV lineages currently circulating among swine in North America are North American cluster IV-A (represented by swIN16) and novel human-like swine IAVs (represented by swMO15). At least half of all serum samples tested positive for swIN16, 51% in HI and 54% in VN (Figures 2, 3). Seroprevalence rates and GMTs were higher among persons born before 1997 (61% in HI, 65% in VN, GMTs ≥46) than for those born during 1997–2017 (13% in HI, 16% in VN, GMTs ≤14; p<0.001) and peaked among persons born during 1977–1986 (Tables 4, 5).

Overall seroprevalence rates for swMO15 were 76% in HI and 72% in VN (Figures 2, 3). At least 50% of persons in each age group were positive in both HI and VN, with GMTs of ≥35 (Tables 4, 5). Seroreactivity was highest for persons born during 1987–1996, and significant differences in seroprevalence were found only between those in this group and those born during 2006–2017 in HI (97% vs. 59%; p = 0.02) and those born during 1947–1956 in VN (93% vs. 53%; p = 0.04). Seroreactivity was higher against IAVs of the swine H3 lineages that were more recently introduced to swine and peaked among persons born shortly before these introductions.

Correlations between Antibody Titers against Different H3 IAVs

Antibody titers against avian IAVs were highly correlated (CC = 0.39–0.85 in HI, CC = 0.47–0.85 in VN) (Table 6). Titers against HK68 were highly correlated with those against IAVs of wild birds (CC = 0.45–0.50 in HI, CC = 0.48–0.72 in VN). CCs between titers against other epidemiologically related IAVs of different species (dkUK63 and eqCH18, HK68 and swG17) were lower (CC = 0.28–0.58 in HI, CC = 0.22–0.29 in VN). Titers against different swine IAVs showed variable CCs (0.35–0.61 in HI and 0.14–0.50 in VN [the first value of which is not significant]).

Replication Kinetics of H3 IAVs in Human Airway Epithelia

Human HK68 virus replicated to titers of up to 9.6 $\log_{10}$ $TCID_{50}$/mL in all human airway epithelia except that of ND2 (Figure 4). Similar high titers of cluster IV-A H3 IAV swIN16 from swine in North America and swG17 from swine in Europe were detected in all nasal tissues and tissues of BD1 (Figure 4). Replication of these 3 IAVs peaked at 2–4 dpi and generally caused irreversible tissue damage, indicated by a decrease in TEER to values of <100 $\Omega.cm^2$ (*37*) (Figure 5).

Table 5. Geometric mean of virus neutralization antibody titers against H3 influenza A viruses of different species in different age groups of the human population, 2017–2018, Belgium*

Birth year range (age, y)†	No.	Avian				Equine	Human	Swine		
		dkUK63	mlOH18	mlBE18	chG19	eqCH18	HK68‡	swG17	swIN16	swMO15
		Eurasian	Am.	Eurasian	Eurasian	FC1	Pandemic	European	N. Am.	N. Am.
1921–1926	14	7	10	8	6	7	30	10	104	116
(96–91)		(5–9)	(7–15)	(6–12)	(5–7)	(5–10)	(12–72)	(5–19)	(44–247)	(38–351)
1927–1936	30	6	12	12	6	7	43	9	60	105
(90–81)		(5–7)	(9–18)	(8–17)	(5–7)	(5–8)	(27–68)	(6–11)	(34–106)	(62–176)
1937–1946	30	5	9	10	5	6	48	9	33	79
(80–71)		(5–6)	(7–12)	(7–14)	(5–6)	(5–6)	(32–72)	(6–12)	(21–53)	(46–137)
1947–1956	30	7	14	15	6	7	69	8	31	35
(70–61)		(5–9)	(10–21)	(11–22)	(5–7)	(5–9)	(44–110)	(6–11)	(18–52)	(20–60)
1957–1966	30	6	15	19	7	6	100	12	28	37
(60–51)		(5–7)	(11–20)	(13–27)	(5–9)	(5–6)	(72–138)	(8–16)	(17–47)	(24–56)
1967–1976	30	7	11	12	6	6	31	18	94	60
(50–41)		(5–9)	(8–17)	(8–17)	(5–7)	(5–7)	(17–55)	(13–25)	(56–157)	(35–103)
1977–1986	30	6	7	6	5	8	9	9	285	84
(40–31)		(5–7)	(6–8)	(5–7)	(5–6)	(6–10)	(6–13)	(7–12)	(175–462)	(45–154)
1987–1996	30	5	6	5	5	6	6	7	219	225
(30–21)		(5–5)	(5–6)	(5–6)	(5–5)	(5–7)	(5–6)	(6–8)	(129–372)	(156–323)
1997–2006	30	5	5	5	5	5	5	6	18	163
(20–11)		(5–5)	(5–5)	(5–5)	(5–5)	(5–6)	(5–6)	(5–7)	(11–29)	(96–275)
2007–2017	32	5	5	5	5	6	6	6	8	40
(10–0)		(5–5)	(5–5)	(5–5)	(5–5)	(5–7)	(5–7)	(5–6)	(6–10)	(24–67)
1921–2017	286	6	9	9	6	6	21	9	49	77
(96–0)		(5–6)	(8–10)	(8–10)	(5–6)	(6–7)	(18–25)	(8–9)	(40–60)	(64–91)

*Values represent geometric mean virus neutralization titers (95% CI). Viruses are ordered according to host species and chronologically according to the emergence of each of the influenza A virus lineages in these species. Complete isolate names are provided in Table 2. Am., American; FC1, Florida clade 1; N. Am., North American.
†Age at the end of 2017.
‡Human influenza A virus that no longer circulates.

Equine IAV eqCH18 replicated efficiently in tissues of ND1, BD1, and BD3 without considerably affecting TEER (Figures 4, 5). Peak titers were detected at 3–4 dpi and were 1.5–2.7 $\log_{10}$ $TCID_{50}$/mL lower than those for HK68, swIN16, and swG17.

ChG19 isolated from poultry replicated to titers of up to 3.9 $\log_{10}$ $TCID_{50}$/mL in bronchial tissue of BD3 without affecting TEER (Figures 4, 5). ChG19 was also detectable in tissues of ND1 and BD1 at 4 dpi.

For the 3 IAVs of wild birds and North American novel human-like swine IAV swMO15, no virus was detectable in any of the tissues except dkUK63, mlOH18, and mlB18 had titers of <2.2 $\log_{10}$ $TCID_{50}$/mL at 4 dpi in tissues of ND1 and BD1, and an swMO15 titer of 3.0 $\log_{10}$ $TCID_{50}$/mL was detected at 2 dpi in the tissue of ND2 (Figures 4, 5). Because of large donor-to-donor variation, only a few differences in virus replication AUCs were significant ($p \leq 0.1$). In nasal tissues, AUCs were significantly higher for swG17 and swIN16 than for all avian IAVs and swMO15. In bronchial tissues, AUCs were significantly higher for HK68 than for all avian IAVs, eqCH18, and swMO15.

Discussion

Antibody titers against animal H3 IAVs in serum samples from humans in Belgium depended on the virus

Table 6. Spearman correlation coefficients between hemagglutination inhibition antibody titers against influenza A(H3) viruses of different species (upper right) and between virus neutralization antibody titers against H3 influenza A viruses of different species (lower left)*

	Avian				Equine	Human	Swine		
	dkUK63	mlOH18	mlBE18	chG19	eqCH18	HK68†	swG17	swIN16	swMO15
Virus strain	Eurasian	American	Eurasian	Eurasian	FC1	Pandemic	European	N. Am.	N. Am.
dkUK63		0.76	0.73	0.39	0.28	0.45	0.27	NS	NS
mlOH18	0.49		0.85	0.45	0.28	0.49	0.27	NS	NS
mlBE18	0.49	0.85		0.46	0.33	0.50	0.28	NS	NS
chG19	0.55	0.47	0.49		0.25	0.22	NS	NS	NS
eqCH18	0.22	NS	NS	0.27		0.27	0.21	NS	NS
HK68	0.48	0.66	0.72	0.44	NS		0.58	0.26	NS
swG17	NS	0.25	0.28	0.22	NS	0.29		0.61	0.35
swIN16	NS	NS	NS	NS	NS	NS	0.38		0.60
swMO15	NS	NS	NS	NS	NS	NS	NS	0.50	

*Viruses are ordered according to host species and chronologically according to the emergence of each of the influenza A virus (IAV) lineages in these species. Blank cells indicate crossover points between comparisons. Complete isolate names are provided in Table 2. FC1, Florida clade 1; N. Am., North American; NS, not significant.
†Human IAV that no longer circulates.

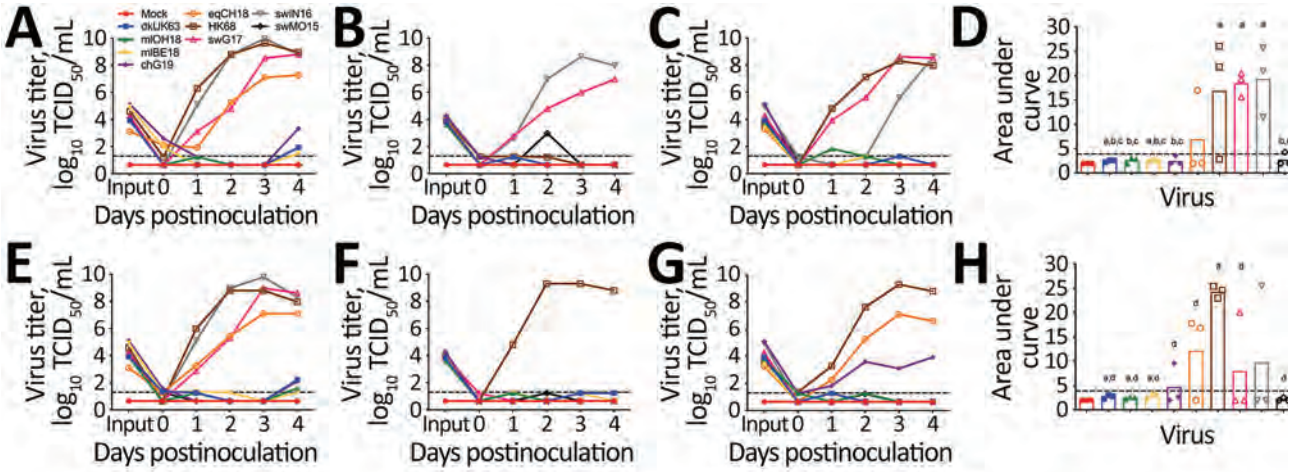

Figure 4. Replication kinetics of influenza A(H3) viruses of different species in human airway epithelia (MucilAir; Epithelix Sàrl, https://www.epithelix.com). Tissues were infected with viruses at a multiplicity of infection of 0.01 $TCID_{50}$, and supernatants were collected at different days postinfection for virus titration in MDCK cells. A–C) Virus replication in nasal tissue of donors ND1 (A), ND2 (B), and ND3 (C). D) Virus yield in nasal tissues. E–G) Virus replication in bronchial tissue of donors BD1 (E), BD2 (F), and BD3 (G). H) Virus yield in bronchial tissues. Virus yield in panels D and H was determined by calculating the area under the curve at 1–4 dpi; letters indicate significant differences ($p \leq 0.1$): mock (a), swG17 (b), swIN16 (c), or HK68 (d). Black dashed lines represent detection limit. Complete isolate names are provided in Table 2. $TCID_{50}$, 50% tissue culture infectious dose.

strain and the person's birth year. Overall seroprevalence rates were high (≥51%) for IAVs from swine in North America, intermediate (7%–37%) for IAVs from swine in Europe, and low (≤12%) for IAVs from birds and equids. Seroreactivity against swine IAVs was highest among persons born during 1967–1996, and seroactivity against almost all IAVs was lowest among the youngest persons, born during 1997–2017. These results are consistent with findings of previous studies with other, often older, swine IAV strains and studies that tested only a low number of serum samples from adults against historic avian or equine IAVs (*7*–*10*,*19*–*24*,*31*,*38*). Cluster IV-A IAVs from swine in North America and H3 IAVs from swine in Europe replicated efficiently in human airway epithelia, whereas replication was intermediate for H3 IAVs of

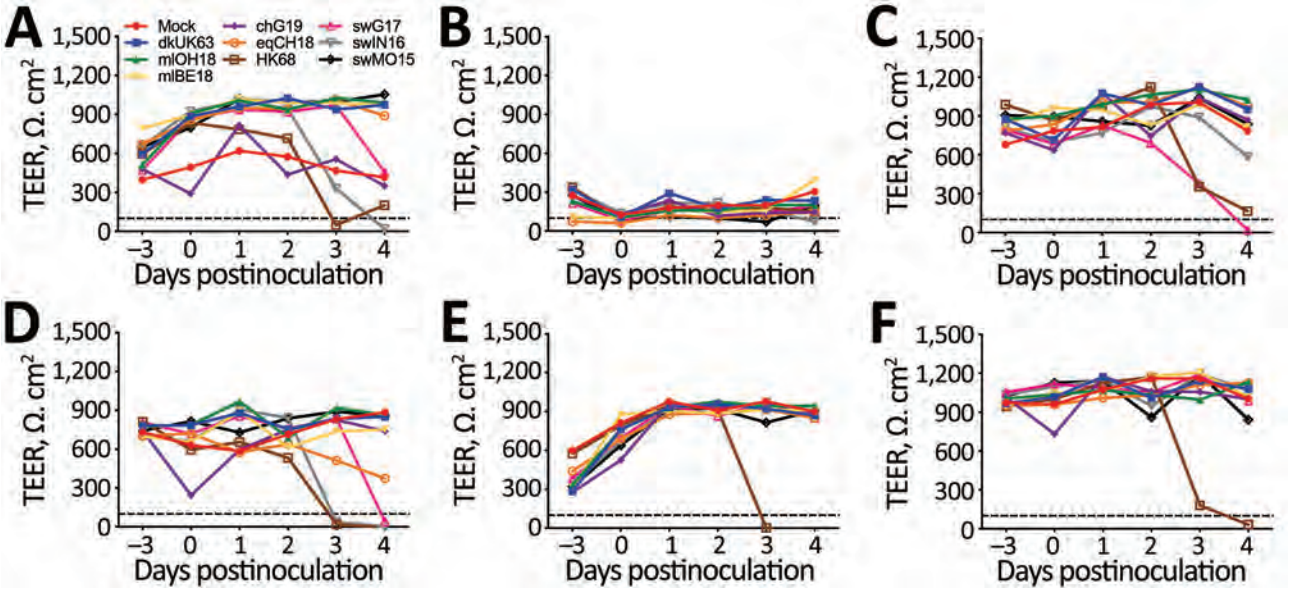

Figure 5. TEER of human airway epithelia (MucilAir; Epithelix Sàrl, https://www.epithelix.com) at different days postinfection with influenza A(H3) viruses of different species at a multiplicity of infection of 0.01 50% tissue culture infective dose. TEER is shown for nasal tissue of donors ND1 (A), ND2 (B), and ND3 (C) and for bronchial tissue of donors BD1 (E), BD2 (F), and BD3 (G). Black dashed lines represent the TEER below which tissue integrity is irreversibly lost (*37*). Complete isolate names are provided in Table 2. TEER, transepithelial electrical resistance.

horses and poultry, and minimal for H3 IAVs of wild birds and a North American novel human-like swine H3 IAV. Our results for cluster IV-A IAVs from swine in North America and IAVs from swine in Europe are consistent with previous findings in differentiated human (tracheo)bronchial epithelial cells (*25*,*27*). However, 1 study also reported efficient replication of a zoonotic novel human-like IAV from swine in North America (*27*). A previous study with historic strains detected substantial replication of avian H3 IAVs, whereas an equine H3 IAV did not replicate (*25*). Discrepancies between our findings and previous findings can result from the use of different cell systems and variation in the genetic background of human cell donors or IAV strains (*39*,*40*).

Antibody titers against swine H3 IAVs reflect cross-reactive titers against human ancestor IAVs. Antibodies against human ancestor IAVs can be deduced from the theory of antigenic seniority: humans are likely to have antibodies against human IAVs that circulated after their birth, with peak titers against IAVs encountered early in life (*41*), confirmed by our results for HK68. Our findings, together with those of previous studies showing similar seroreactivity against older swine H3 IAVs and their human ancestor IAV (*7*,*9*,*10*), suggest slow antigenic drift of H3 HA in swine and indicate swine as a reservoir for historic human IAVs. We estimate that HA1 amino acid homology between our swine test viruses and their human ancestor is 87%–93%, with 29–32 identical amino acids in antigenic sites (Figure 6). Although the HA1 sequences of the avian H3 IAVs were more closely related to that of human virus HK68, cross-reactive serum antibody titers were minimal. Accordingly, ferret serum against human H3 IAVs showed low cross-reactivity with avian H3 IAVs (*42*), which might be caused by a few key amino acid differences between HK68 and avian H3 IAVs. Compared with all avian IAVs, HK68 has 4 mutations in antigenic sites, of which N145S might be of particular relevance. This mutation mediated antigenic cluster transitions for swine and human H3 IAVs (*43*,*44*). Furthermore, higher HA glycosylation of human IAVs might mask certain epitopes shared with avian IAVs, preventing humans from raising antibodies against these epitopes. For example, glycosylation at positions 122, 133, and 144 masks epitopes in antigenic site A. In contrast, HA glycosylation patterns for swine IAVs and for the human ancestor IAV are similar (*45*). For equine H3 IAVs, the lack of cross-reactive antibodies can be explained by the closer relatedness to avian than to human IAVs and substantial antigenic drift in horses after the introduction from the avian reservoir (*2*,*3*).

Seroprevalence rates of ≤12% for avian and equine H3 IAVs suggest that these IAVs pose a high pandemic risk. Comparable seroprevalences of 2%–19% against the 2009 pandemic influenza A(H1N1) virus were detected right before the pandemic started (*46*). However, more efficient replication of H3 IAVs of swine in human respiratory tissues as opposed to those of birds or horses suggests that swine pose the highest risk for introduction of H3 IAVs to humans. Indeed, 434 human infections with cluster IV-A and novel human-like H3 IAVs from swine in North America and 4 infections with H3 IAVs from swine in Europe have been reported (*11*–*13*), whereas only 2 zoonotic infections with avian H3 IAVs and no zoonotic infections with equine H3 IAVs have been reported. Swine IAVs are derived from past human IAVs, which can explain their higher potential to infect humans. Swine IAVs prefer human-type α-2,6 sialic acid receptors, whereas avian and equine IAVs prefer avian-type α-2,3 receptors. Human cells also support polymerase activity of swine but not avian IAVs (*47*). In addition, humans frequently encounter dense swine populations and, unlike for horses and poultry, H3 IAVs are

	Antigenic site A									Antigenic site B															Antigenic site C									Antigenic site D						Antigenic site E				
	133	137	140	141	142	143	144	145	146	155	156	157	158	159	160	185	186	187	188	189	193	51	52	53	276	277	278	279	280	201	205	207	208	217	220	61	62	78	81	83
dkUK63	N	S	K	R	G	P	A	N	G	T	K	S	E	S	A	P	S	T	N	Q	N	I	C	N	T	C	I	S	E	R	S	R	R	I	R	G	R	V	N	T
mlOH18	.	.	.	.	.	.	.	.	.	.	.	.	G	.	.	.	.	.	.	.	S	.	.	.	.	.	.	.	.	.	.	.	.	.	.	.	.	.	D	.
mlBE18	.	G	.	.	.	.	.	.	.	.	.	.	G	.	.	.	.	.	.	.	S	.	.	.	.	.	.	.	.	.	.	.	.	.	.	.	.	.	D	.
chG19	.	G	.	.	.	.	.	.	.	.	.	.	G	.	.	.	.	.	D	.	.	.	.	.	.	.	.	.	.	.	.	.	.	.	.	.	.	.	D	.
eqCH18	.	G	.	.	.	S	.	D	S	.	.	.	G	.	S	.	.	S	T	.	K	.	.	.	I	.	V	.	.	.	.	K	.	.	.	.	K	A	Y	N
HK68	.	N	.	.	.	.	G	S	.	.	.	.	G	.	T	.	.	.	.	.	S	.	.	.	.	.	.	.	.	.	.	.	.	.	.	.	I	.	.	.
VI75	.	N	.	.	.	.	D	I	.	Y	.	.	G	.	T	.	.	.	D	K	D	.	.	.	.	.	S	.	.	K	.	K	.	V	.	.	I	G	.	K
swG17	.	.	.	.	.	L	N	K	S	Y	.	.	G	N	T	.	.	.	D	K	D	.	.	K	.	.	N	.	.	K	.	K	.	.	.	.	A	G	.	R
NC95	D	Y	.	.	.	S	V	K	S	H	.	L	.	Y	K	.	.	.	D	S	S	.	.	D	N	.	N	.	.	.	.	K	.	.	.	.	K	G	.	E
swIN16	D	Y	R	.	.	S	V	.	S	Y	N	L	N	Y	K	.	.	.	D	K	.	.	.	.	E	.	N	.	.	.	.	K	.	.	.	.	K	D	.	K
VI11	.	.	I	.	R	S	N	.	S	.	H	L	N	F	K	.	G	.	D	K	F	.	.	D	K	.	N	.	.	.	.	K	.	.	.	.	E	G	.	K
swMO15	D	.	.	.	R	S	S	K	S	.	H	L	N	F	K	.	A	.	D	K	S	.	.	.	K	.	N	.	A	.	.	K	.	.	.	.	E	G	.	K

Figure 6. Amino acids at presumed antigenic sites of the hemagglutinin 1 (*34*) of the influenza A(H3) viruses used in this study and their presumed ancestor viruses. Dots indicate that the amino acid is the same as that for dkUK63. Gray indicates the presumed human ancestor viruses of swG17 (A/Victoria/3/75 [VI75]), swIN16 (A/Nanchang/933/95 [NC95]), and swMO15 (A/Victoria/361/2011 [VI11]), which were not included as test viruses in this study. Complete isolate names are provided in Table 2.

endemic among swine. Because zoonotic infections generally result from close contact with infected animals, swine IAVs are also more likely than IAVs of horses or birds to be transmitted to humans (*48*). On the basis of the seroprevalence rates of ≥30% for persons >16 years of age, swine H3 IAVs are considered a lower pandemic risk (*18*). They do, however, pose a zoonotic risk to the youngest persons who lack cross-reactive antibodies, which can explain why most human infections with swine H3 IAVs occurred in persons <18 years of age (*11*–*13*). Our results suggest that population immunity will wane over time and that the human population will sooner become fully susceptible to H3 IAVs from swine in Europe than to H3 IAVs from swine in North America.

We estimated the infection potential of animal H3 IAVs in humans on the basis of their replicative capacity in nasal and bronchial MucilAir tissues. However, adaptive and some innate immune responses that are not represented in this model might cause more restricted replication of swine, equine, or avian H3 IAVs in vivo. Also, in vitro experiments in differentiated human airway epithelia will, in the best case, reflect only replication efficiency in a single person and are in no way indicative of airborne transmission between humans (*49*).

In conclusion, our results stress the need to closely monitor circulating H3 IAVs in different animal species and to frequently evaluate humans for antibodies against these IAVs. This need applies especially to H3 IAVs of swine, which seem to pose the highest zoonotic risk.

Acknowledgments

We thank Nele Dennequin and Melanie Bauwens for excellent technical assistance and Xavier Saelens for critical reading of the manuscript.

This study was financed by the Belgian Federal Service for Public Health, Food Chain Safety and Environment (grant no. RF 16/6305 EVAFLU); by Ghent University Research Fund Bijzonder OnderzoeksFonds (grant no. 01D02017); and by the European Union Horizon 2020 Research Innovation Programme (grant no. 727922 DELTA-FLU).

About the Author

Ms. Vandoorn was a PhD student at the Laboratory of Virology, Faculty of Veterinary Medicine, Ghent University, during the period of the study. Her principal research interests are the pandemic potential of swine influenza A viruses and broadly protective vaccination strategies for influenza A viruses.

References

1. Fang R, Min Jou W, Huylebroeck D, Devos R, Fiers W. Complete structure of A/duck/Ukraine/63 influenza hemagglutinin gene: animal virus as progenitor of human H3 Hong Kong 1968 influenza hemagglutinin. Cell. 1981;25:315–23. https://doi.org/10.1016/0092-8674(81)90049-0
2. Bailey E, Long LP, Zhao N, Hall JS, Baroch JA, Nolting J, et al. Antigenic characterization of H3 subtypes of avian influenza A viruses from North America. Avian Dis. 2016;60(Suppl):346–53. https://doi.org/10.1637/11086-041015-RegR
3. Pu J, Liu QF, Xia YJ, Fan YL, Brown EG, Tian FL, et al. Genetic analysis of H3 subtype influenza viruses isolated from domestic ducks in northern China during 2004–2005. Virus Genes. 2009;38:136–42. https://doi.org/10.1007/s11262-008-0300-7
4. Woodward A, Rash AS, Medcalf E, Bryant NA, Elton DM. Using epidemics to map H3 equine influenza virus determinants of antigenicity. Virology. 2015;481:187–98. https://doi.org/10.1016/j.virol.2015.02.027
5. World Organisation for Animal Health. OIE expert surveillance panel on equine influenza vaccine composition. 2020 Apr 16 [cited 2021 Aug 27]. https://oiebulletin.fr/?officiel=08-4-2-2020-1-panel
6. Anderson TK, Chang J, Arendsee ZW, Venkatesh D, Souza CK, Kimble JB, et al. Swine influenza A viruses and the tangled relationship with humans. Cold Spring Harb Perspect Med. 2021;11:a038737. https://doi.org/10.1101/cshperspect.a038737
7. Qiu Y, Muller CP, Van Reeth K. Lower seroreactivity to European than to North American H3N2 swine influenza viruses in humans, Luxembourg, 2010. Euro Surveill. 2015;20:25–33. https://doi.org/10.2807/1560-7917.ES2015.20.13.21078
8. Lorbach JN, Fitzgerald T, Nolan C, Nolting JM, Treanor JJ, Topham DJ, et al. Gaps in serologic immunity against contemporary swine-origin influenza A viruses among healthy individuals in the United States. Viruses. 2021;13:127. https://doi.org/10.3390/v13010127
9. Krumbholz A, Lange J, Dürrwald R, Walther M, Müller TH, Kühnel D, et al. Prevalence of antibodies to European porcine influenza viruses in humans living in high pig density areas of Germany. Med Microbiol Immunol (Berl). 2014;203:13–24. https://doi.org/10.1007/s00430-013-0309-y
10. Hoschler K, Thompson C, Casas I, Ellis J, Galiano M, Andrews N, et al. Population susceptibility to North American and Eurasian swine influenza viruses in England, at three time points between 2004 and 2011. Euro Surveill. 2013;18:20578. https://doi.org/10.2807/1560-7917.ES2013.18.36.20578
11. US Centers for Disease Control and Prevention. Novel influenza A virus infections [cited 2021 Nov 21]. https://gis.cdc.gov/grasp/fluview/Novel_Influenza.html
12. Freidl GS, Meijer A, de Bruin E, de Nardi M, Munoz O, Capua I, et al.; FLURISK Consortium. Influenza at the animal-human interface: a review of the literature for virological evidence of human infection with swine or avian influenza viruses other than A(H5N1). Euro Surveill. 2014;19:20793. https://doi.org/10.2807/1560-7917.ES2014.19.18.20793
13. Piralla A, Moreno A, Orlandi ME, Percivalle E, Chiapponi C, Vezzoli F, et al.; Influenza Surveillance Study Group. Swine influenza A(H3N2) virus infection in immunocompromised man, Italy, 2014. Emerg Infect Dis. 2015;21:1189–91. https://doi.org/10.3201/eid2107.140981

14. Xie T, Anderson BD, Daramragchaa U, Chuluunbaatar M, Gray GC. A review of evidence that equine influenza viruses are zoonotic. Pathogens. 2016;5:3–10. https://doi.org/10.3390/pathogens5030050
15. Baz M, Paskel M, Matsuoka Y, Zengel J, Cheng X, Jin H, et al. Replication and immunogenicity of swine, equine, and avian H3 subtype influenza viruses in mice and ferrets. J Virol. 2013;87:6901–10. https://doi.org/10.1128/JVI.03520-12
16. Steensels M, Gelaude P, Van Borm S, Van Den Berg T, Cargnel M, Roupie V, et al. Atypical pathogenicity of avian influenza (H3N1) virus involved in outbreak, Belgium, 2019. Emerg Infect Dis. 2020;26:1899–903. https://doi.org/10.3201/eid2608.191338
17. Tan X, Yan X, Liu Y, Wu Y, Liu JY, Mu M, et al. A case of human infection by H3N8 influenza virus. Emerg Microbes Infect. 2022;11:2214–7. https://doi.org/10.1080/22221751.2022.2117097
18. World Health Organization. Tool for Influenza Pandemic Risk Assessment (TIPRA) version 1. 2016 May [cited 2021 Sept 28]. https://apps.who.int/iris/handle/10665/250130
19. Fragaszy E, Ishola DA, Brown IH, Enstone J, Nguyen-Van-Tam JS, Simons R, et al.; Flu Watch Group; Combating Swine Influenza (COSI) Consortium. Increased risk of A(H1N1)pdm09 influenza infection in UK pig industry workers compared to a general population cohort. Influenza Other Respir Viruses. 2016;10:291–300. https://doi.org/10.1111/irv.12364
20. Sikkema RS, Freidl GS, de Bruin E, Koopmans M. Weighing serological evidence of human exposure to animal influenza viruses - a literature review. Euro Surveill. 2016;21:30388. https://doi.org/10.2807/1560-7917.ES.2016.21.44.30388
21. Zhou N, He S, Zhang T, Zou W, Shu L, Sharp GB, et al. Influenza infection in humans and pigs in southeastern China. Arch Virol. 1996;141:649–61. https://doi.org/10.1007/BF01718323
22. Burnell FJ, Holmes MA, Roiko AH, Lowe JB, Heil GL, White SK, et al. Little evidence of human infection with equine influenza during the 2007 epizootic, Queensland, Australia. J Clin Virol. 2014;59:100–3. https://doi.org/10.1016/j.jcv.2013.11.011
23. Khurelbaatar N, Krueger WS, Heil GL, Darmaa B, Ulziimaa D, Tserennorov D, et al. Little evidence of avian or equine influenza virus infection among a cohort of Mongolian adults with animal exposures, 2010-2011. PLoS One. 2014;9:e85616. https://doi.org/10.1371/journal.pone.0085616
24. Larson KR, Heil GL, Chambers TM, Capuano A, White SK, Gray GC. Serological evidence of equine influenza infections among persons with horse exposure, Iowa. J Clin Virol. 2015;67:78–83. https://doi.org/10.1016/j.jcv.2015.04.009
25. Ilyushina NA, Ikizler MR, Kawaoka Y, Rudenko LG, Treanor JJ, Subbarao K, et al. Comparative study of influenza virus replication in MDCK cells and in primary cells derived from adenoids and airway epithelium. J Virol. 2012;86:11725–34. https://doi.org/10.1128/JVI.01477-12
26. Shin DL, Yang W, Peng JY, Sawatsky B, von Messling V, Herrler G, et al. Avian influenza A virus infects swine airway epithelial cells without prior adaptation. Viruses. 2020;12:589. https://doi.org/10.3390/v12060589
27. Sun X, Pulit-Penaloza JA, Belser JA, Pappas C, Pearce MB, Brock N, et al. Pathogenesis and transmission of genetically diverse swine-origin H3N2 variant influenza A viruses from multiple lineages isolated in the United States, 2011–2016. J Virol. 2018;92:e00665–18. https://doi.org/10.1128/JVI.00665-18
28. Driskell EA, Jones CA, Stallknecht DE, Howerth EW, Tompkins SM. Avian influenza virus isolates from wild birds replicate and cause disease in a mouse model of infection. Virology. 2010;399:280–9. https://doi.org/10.1016/j.virol.2010.01.005
29. Solórzano A, Foni E, Córdoba L, Baratelli M, Razzuoli E, Bilato D, et al. Cross-species infectivity of H3N8 influenza virus in an experimental infection in swine. J Virol. 2015;89:11190–202. https://doi.org/10.1128/JVI.01509-15
30. Walia RR, Anderson TK, Vincent AL. Regional patterns of genetic diversity in swine influenza A viruses in the United States from 2010 to 2016. Influenza Other Respir Viruses. 2019;13:262–73. https://doi.org/10.1111/irv.12559
31. Henritzi D, Petric PP, Lewis NS, Graaf A, Pessia A, Starick E, et al. Surveillance of European domestic pig populations identifies an emerging reservoir of potentially zoonotic swine influenza A viruses. Cell Host Microbe. 2020;28:614–627.e6. https://doi.org/10.1016/j.chom.2020.07.006
32. Choi JG, Kang HM, Kim MC, Paek MR, Kim HR, Kim BS, et al. Genetic relationship of H3 subtype avian influenza viruses isolated from domestic ducks and wild birds in Korea and their pathogenic potential in chickens and ducks. Vet Microbiol. 2012;155:147–57. https://doi.org/10.1016/j.vetmic.2011.08.028
33. Kumar S, Stecher G, Tamura K. MEGA7: Molecular Evolutionary Genetics Analysis version 7.0 for bigger datasets. Mol Biol Evol. 2016;33:1870–4. https://doi.org/10.1093/molbev/msw054
34. Rajão DS, Gauger PC, Anderson TK, Lewis NS, Abente EJ, Killian ML, et al. Novel reassortant human-like H3N2 and H3N1 influenza A viruses detected in pigs are virulent and antigenically distinct from swine viruses endemic to the United States. J Virol. 2015;89:11213–22. https://doi.org/10.1128/JVI.01675-15
35. Van Reeth K, Gregory V, Hay A, Pensaert M. Protection against a European H1N2 swine influenza virus in pigs previously infected with H1N1 and/or H3N2 subtypes. Vaccine. 2003;21:1375–81. https://doi.org/10.1016/S0264-410X(02)00688-6
36. Van Poucke SG, Nicholls JM, Nauwynck HJ, Van Reeth K. Replication of avian, human and swine influenza viruses in porcine respiratory explants and association with sialic acid distribution. Virol J. 2010;7:38. https://doi.org/10.1186/1743-422X-7-38
37. Boda B, Benaoudia S, Huang S, Bonfante R, Wiszniewski L, Tseligka ED, et al. Antiviral drug screening by assessing epithelial functions and innate immune responses in human 3D airway epithelium model. Antiviral Res. 2018;156:72–9. https://doi.org/10.1016/j.antiviral.2018.06.007
38. Liu F, Levine MZ. Heterologous antibody responses conferred by A(H3N2) variant and seasonal influenza vaccination against newly emerged 2016–2018 A(H3N2) variant viruses in healthy persons. Clin Infect Dis. 2020;71:3061–70. https://doi.org/10.1093/cid/ciz1203
39. Ciminski K, Chase GP, Beer M, Schwemmle M. Influenza A viruses: understanding human host determinants. Trends Mol Med. 2021;27:104–12. https://doi.org/10.1016/j.molmed.2020.09.014
40. Stewart CE, Torr EE, Mohd Jamili NH, Bosquillon C, Sayers I. Evaluation of differentiated human bronchial epithelial cell culture systems for asthma research. J Allergy (Cairo). 2012;2012:943982.
41. Fonville JM, Wilks SH, James SL, Fox A, Ventresca M, Aban M, et al. Antibody landscapes after influenza virus infection or vaccination. Science. 2014;346:996–1000. https://doi.org/10.1126/science.1256427

42. Guan L, Shi J, Kong X, Ma S, Zhang Y, Yin X, et al. H3N2 avian influenza viruses detected in live poultry markets in China bind to human-type receptors and transmit in guinea pigs and ferrets. Emerg Microbes Infect. 2019;8:1280–90. https://doi.org/10.1080/22221751.2019.1660590
43. Smith DJ, Lapedes AS, de Jong JC, Bestebroer TM, Rimmelzwaan GF, Osterhaus AD, et al. Mapping the antigenic and genetic evolution of influenza virus. Science. 2004;305:371–6. https://doi.org/10.1126/science.1097211
44. de Jong JC, Smith DJ, Lapedes AS, Donatelli I, Campitelli L, Barigazzi G, et al. Antigenic and genetic evolution of swine influenza A (H3N2) viruses in Europe. J Virol. 2007;81:4315–22. https://doi.org/10.1128/JVI.02458-06
45. Tharakaraman K, Raman R, Stebbins NW, Viswanathan K, Sasisekharan V, Sasisekharan R. Antigenically intact hemagglutinin in circulating avian and swine influenza viruses and potential for H3N2 pandemic. Sci Rep. 2013;3:1822. https://doi.org/10.1038/srep01822
46. Broberg E, Nicoll A, Amato-Gauci A. Seroprevalence to influenza A(H1N1) 2009 virus—where are we? Clin Vaccine Immunol. 2011;18:1205–12. https://doi.org/10.1128/CVI.05072-11
47. Long JS, Mistry B, Haslam SM, Barclay WS. Host and viral determinants of influenza A virus species specificity. Nat Rev Microbiol. 2019;17:67–81. https://doi.org/10.1038/s41579-018-0115-z
48. Borkenhagen LK, Salman MD, Ma MJ, Gray GC. Animal influenza virus infections in humans: a commentary. Int J Infect Dis. 2019;88:113–9. https://doi.org/10.1016/j.ijid.2019.08.002
49. Sorrell EM, Schrauwen EJA, Linster M, De Graaf M, Herfst S, Fouchier RAM. Predicting 'airborne' influenza viruses: (trans-) mission impossible? Curr Opin Virol. 2011;1:635–42. https://doi.org/10.1016/j.coviro.2011.07.003

Address for correspondence: Kristien Van Reeth, Laboratory of Virology, Faculty of Veterinary Medicine, Ghent University, Salisburylaan 133, 9820 Merelbeke, Belgium; email: kristien.vanreeth@ugent.be

etymologia revisited

Coronavirus

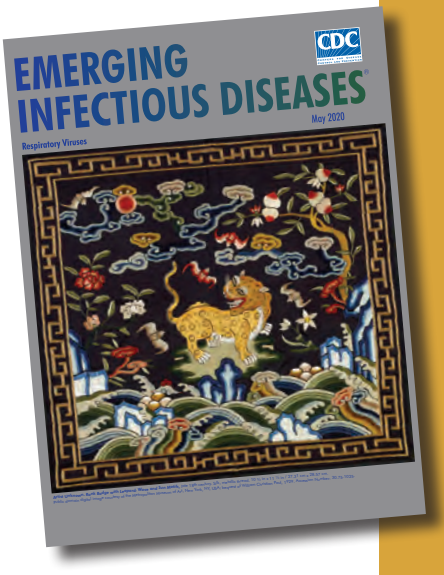

Originally published in May 2020

The first coronavirus, avian infectious bronchitis virus, was discovered in 1937 by Fred Beaudette and Charles Hudson. In 1967, June Almeida and David Tyrrell performed electron microscopy on specimens from cultures of viruses known to cause colds in humans and identified particles that resembled avian infectious bronchitis virus. Almeida coined the term "coronavirus," from the Latin *corona* ("crown"), because the glycoprotein spikes of these viruses created an image similar to a solar corona. Strains that infect humans generally cause mild symptoms. However, more recently, animal coronaviruses have caused outbreaks of severe respiratory disease in humans, including severe acute respiratory syndrome (SARS), Middle East respiratory syndrome (MERS), and 2019 novel coronavirus disease (COVID-19).

Sources:

1. Almeida JD, Tyrrell DA. The morphology of three previously uncharacterized human respiratory viruses that grow in organ culture. J Gen Virol. 1967;1:175–8. https://doi.org/10.1099/0022-1317-1-2-175
2. Beaudette FR, Hudson CB. Cultivation of the virus of infectious bronchitis. J Am Vet Med Assoc. 1937;90:51–8.
3. Estola T. Coronaviruses, a new group of animal RNA viruses. Avian Dis. 1970;14:330–6. https://doi.org/10.2307/1588476
4. Groupe V. Demonstration of an interference phenomenon associated with infectious bronchitis virus of chickens. J Bacteriol. 1949;58:23–32. https://doi.org/10.1128/JB.58.1.23-32.1949

https://wwwnc.cdc.gov/eid/article/26/5/et-2605_article

Genomic Epidemiology Linking Nonendemic Coccidioidomycosis to Travel

Juan Monroy-Nieto, Lalitha Gade, Kaitlin Benedict, Kizee A. Etienne, Anastasia P. Litvintseva, Jolene R. Bowers, David M. Engelthaler, Nancy A. Chow

Coccidioidomycosis is a fungal infection endemic to hot, arid regions of the western United States, northern Mexico, and parts of Central and South America. Sporadic cases outside these regions are likely travel-associated; alternatively, an infection could be acquired in as-yet unidentified newly endemic locales. A previous study of cases in nonendemic regions with patient self-reported travel history suggested that infections were acquired during travel to endemic regions. We sequenced 19 *Coccidioides* isolates from patients with known travel histories from that earlier investigation and performed phylogenetic analysis to identify the locations of potential source populations. Our results show that those isolates were phylogenetically linked to *Coccidioides* subpopulations naturally occurring in 1 of the reported travel locales, confirming that these cases were likely acquired during travel to endemic regions. Our findings demonstrate that genomic analysis is a useful tool for investigating travel-related coccidioidomycosis.

Coccidioides immitis and *C. posadasii*, the etiologic agents of coccidioidomycosis, also known as Valley fever, are environmental filamentous fungi with distinct geographic ranges in the western United States, northern Mexico, and parts of Central and South America (*1*,*2*). In 2015, *C. immitis* was discovered in Washington, USA (*3*). That discovery highlighted the importance of using molecular detection methods (*3*,*4*) and enhanced efforts to study *Coccidioides* spp. outside traditionally identified endemic areas. Finding that *Coccidioides* might exist outside its previously established endemic regions supports the hypothesis that the geographic range of this pathogen may be changing (*5*).

Author affiliations: Translational Genomics Research Institute, Pathogen and Microbiome Division, Flagstaff, Arizona, USA (J. Monroy-Nieto, J.R. Bowers, D.M. Engelthaler); Centers for Disease Control and Prevention, Atlanta, Georgia, USA (L. Gade, K. Benedict, K. Etienne, A.P. Litvintseva, N.A. Chow)

DOI: https://doi.org/10.3201/eid2901.220771

In recent years, genomic analyses of this pathogenic genus uncovered strong phylogeographic structure and delineated populations associated with specific geographic regions, findings that expand previous work based on immunological studies (*6*) and molecular studies using traditional, less-discerning methods (*7*). *C. immitis* is found primarily in California and Washington, *C. posadasii* in Arizona, Texas, Mexico, and Central and South America (*8*). Within species, population structure has been characterized, separating the Washington isolates from other *C. immitis* strains (*3*,*9*) and dividing *C. posadasii* into several differentiated phylogeographic clades (*10*), including the Arizona and Texas/Mexico/South America (TX/MX/SA) clades, and a more recently delimited Guatemala/Venezuela clade (*11*). Although no phenotypic distinction between these groups has been associated with disease outcome, the genetic differences and population structures among these clades represent considerable assets for molecular epidemiology and enable tracking of the origins of infections.

Coccidioides spp. can infect several species of mammals, including humans. Both immunocompromised and immunocompetent persons can develop coccidioidomycosis by inhaling airborne propagules from disturbed soil (*2*). In human hosts, symptoms range from inconsequential to self-limited and often protracted respiratory illness to chronic pulmonary disorders and, in rare cases, disseminated systemic infections (*12*,*13*). In the United States, >10,000 new cases/year have been reported to public health authorities in recent years, mainly in Arizona and California (*13*,*14*). Those states are also thought to be the source of most travel-related infections, as confirmed by the results of enhanced surveillance from 2016 describing clinical and epidemiologic characteristics of reported cases from 14 coccidioidomycosis nonendemic states (*12*). In that study, most patients had either traveled to coccidioidomycosis-endemic regions

during the 4 months before symptom onset or visited or previously resided in an endemic region at some point during their lifetimes. Previous studies (*3*,*15*) have shown that isolates can be traced to their place of origin by applying current understanding of *Coccidioides* phylogeography to the increasing number of publicly available genomes. We determined to further investigate the isolates from cases described in the 2016 enhanced surveillance by using genomic epidemiology to empirically evaluate the original findings and identify likely origins of coccidioidomycosis cases in nonendemic regions.

Methods

Sample Descriptions

We included 174 genomes (104 *C. posadasii* and 70 *C. immitis*) in this study (Appendix 1, https://wwwnc.cdc.gov/EID/article/29/1/22-0771-App1.xlsx). For the study, we processed 72 (41%) at the reference laboratory of the Mycotic Diseases Branch, Division of Foodborne, Waterborne, and Environmental Diseases, National Center for Emerging and Zoonotic Infectious Diseases, Centers for Disease Control and Prevention; 53 of the isolates were collected for routine fungal reference testing and 19 (16 *C. posadasii*, 3 *C. immitis*) as part of the enhanced surveillance study (*12*). For the routinely collected set, we received limited metadata, such as geographic region of collection, location where the infection was acquired, and patient travel history. The enhanced survey set included this same information, collected from interviews as described in the original publication (*12*); in brief, patients were asked about history of travel to any endemic area within 4 months before disease onset. Some samples sent from health departments in different jurisdictions we subsequently determined to be duplicates of multiple isolates (B17635, B14131, B15145) from the same patient. Those genomes were presented as unique clonal leaves to illustrate that they corresponded to multiple physical specimens and genome libraries of the same strain. Additional whole-genome sequences downloaded from the National Center for Biotechnology Information (NCBI) Sequence Read Archive (SRA) amounted to 102 (59% of the total) additional public samples included in our analyses; those sequences had been deposited under BioProjects PRJNA245906 (*3*), PRJNA472461 (*9*), PRJNA274372 (*10*), PRJNA438145 (*11*), and PRJNA46299 (*16*).

For the complete dataset, data for 144/174 (83%) isolates were from clinical cases of coccidioidomycosis, 11 (6%) environmental samples from previous studies (*3*,*10*) or reference testing, and 1 veterinary sample; 18 (10%) did not have this information available. Patient location, defined as where the *Coccidioides* sample was collected and its associated case reported, was known for 172 (99%) of the samples. Most of the variety of regional locations were in US states: 43 (25%) in Washington, 32 (18%) in Arizona, 29 (17%) in Oregon, 14 (8%) in California, and 11 (6%) in Michigan. An additional 10 (6%) locations were in Mexico, 7 (4%) in Venezuela, and 28 (16%) in other regions. We collected all 19 patient samples in the enhanced surveillance effort (*12*) from nonendemic areas.

DNA Extraction and Genome Sequencing

We grew all isolates on brain-heart infusion agar at 25°C for 10 days, extracted high molecular genomic DNA using the DNeasy Blood and Tissue kit (QIAGEN, https://www.qiagen.com) according to manufacturer recommendations, and confirmed isolates by sequencing the internal transcribed spacer 2 region of the rDNA. We stored genomic DNA at −20°C for future use. We constructed and barcoded genomic libraries using NEBNext Ultra DNA Library Prep kit for Illumina (New England Biolabs, https://www.neb.com), following manufacturer instructions. We sequenced libraries on either the Illumina HiSeq 2500 platform (https://www.illumina.com) using the HiSeq Rapid SBS Kit v2 500 cycles or the Illumina MiSeq platform using the MiSeq Reagent Kit v2 500 cycles, generating paired reads 250 bp in length. We deposited read data to the National Center for Biotechnology Information Sequence Read Archive, bundling the read files under Bioproject PRJNA808058.

Phylogenomic Analyses

Using the genomic sequence data from the selected isolates and publicly available genomes (Appendix 1), high-confidence single-nucleotide polymorphisms (SNPs) were identified with the Northern Arizona SNP Pipeline (NASP) v1.2.0, a genome analysis tool (*17*). For read data, we performed quality trimming for flanking regions with an average quality score <20 using BBduk version 38.26 from BBtools (https://www.sourceforge.net/projects/bbmap). Subsequently, in NASP, we used Burrows-Wheeler aligner (https://bio-bwa.sourceforge.net) to align reads to reference genomes: RMSCC3488 (GCA_000150055.1) for *C. posadasii* and RS (GCA_000149335.2) for *C. immitis* (*18*). We identified SNPs with GATK's UnifiedGenotyper (*3*,*7*,*19*). We analyzed previously assembled genomes as described elsewhere (*17*). NASP filtered out SNPs where ≥1 sample had <10× coverage or <90% concordance among the aligned reads and loci masked in the reference duplicated using MUMmer

(*20*). We used the remaining high-certainty genomic SNPs to reconstruct phylogenies using maximum-likelihood inference using the best scoring fit models, transversion plus ascertainment bias correction plus R5 for *C. posadasii* and transition model 3 plus ascertainment bias correction plus R5 for *C. immitis*, after conducting a full search of all available models in IQTREE (*21*) with 1,000 ultrafast bootstraps. We rooted trees by the next basal branch using the genome for *Uncinocarpus reesii* 1704 (GCA_000003515.2) as an outgroup. We used the ggtree plotting library (*22*) to generate tree figures.

Results

We performed separate phylogenetic analyses for samples of each species. Most (n = 99, 95%) *C. posadasii* samples clustered with 5 clades: Phoenix, Tucson 1, Tucson 2, TX/MX/SA, and Guatemala/Venezuela (Figure 1). *C. immitis* samples clustered mainly with the Washington clade (Figure 2). We also identified 7 geographic regions to categorize travel history locations: endemic southwestern United States (*C. immitis* and *C. posadasii*), endemic TX/MX/SA, suspected endemic northwestern United States (*C. immitis* and *C. posadasii*), endemic Caribbean, nonendemic United States, and Asia.

Of the 19 *Coccidioides* spp. isolates from travel-related cases from the enhanced surveillance study, 16 (84%) were *C. posadasii* and 3 (16%) were *C. immitis*. Of the 16 *C. posadasii* isolates, 13 (81%) clustered with isolates from the endemic southwestern United States region, consistent with reported patient travel to Arizona, and 1 with the TX/MX/SA group from a patient who had traveled to Texas. Isolates from the remaining 2 travel-related cases clustered with an outgroup to the TX/MX/SA clade not previously reconstructed, whose southwest United States geographic distribution has not been resolved. That outgroup included isolates collected from cases in Nevada and New Mexico, US states with some recognized endemicity, and a single isolate from a case with unknown history in Washington. Isolate B11866 was collected in Wisconsin from a patient who reported having traveled to Mexico or Arizona. Isolate B12226 was collected in Michigan, and the patient reported travel to only 1 endemic area, within the Phoenix metropolitan area in Arizona.

The 3 travel-related cases caused by *C. immitis* all had samples nested within the clades linked to California, another geographic region reported by patients in their travel histories (Figure 2). Two cases had isolates, B12220 and B12526, that clustered with 28 isolates collected in the suspected endemic northwestern United States region but nested within the Californian clade (Figure 2), which was consistent with the case-patients' reported travel histories. The isolate associated with the third *C. immitis* genome, which also clustered within the California clade, was recovered in Wisconsin from a patient who had traveled to several endemic regions throughout the southwestern United States.

Discussion

Coccidioides spp. fungi have long been thought to be limited to the southwestern United States, northern Mexico, and parts of Central and South America. Endemicity has been determined by case epidemiology, population-based skin test surveys, and, of note, from direct environmental detection (*23*). However, detection of *Coccidioides* spp. in the states of Utah in 2014 (*24*) and Washington in 2015 (*4*), as well as genomic analyses demonstrating *C. immitis* in Washington as a distinct clade (*9*,*10*), challenged our knowledge of this pathogen's true geographic distribution. Previous public health enhanced surveillance for coccidioidomycosis in nonendemic states showed that most cases were more likely attributed to travel than to local acquisition (*12*). The phylogeographic analysis of genome sequences from our epidemiology study corroborated those findings. Most of these isolates were from specific populations of *Coccidioides* spp. in regions known to be endemic to which case-patients had traveled.

We had detailed travel histories for all patients isolates from the 19 travel-related cases. Of 2 patients diagnosed in Michigan, one, associated with isolate B12399 (*C. posadasii* Phoenix clade), had not traveled to any known endemic area in the previous 10 years, and the other, associated with B11877 (*C. posadasii* Tucson 1 clade), had not traveled to any endemic area for 4 years, time periods longer than those usually queried on travel histories used to determine the risk of coccidioidomycosis. Those 2 cases from our study exemplify how travel to endemic areas might remain a risk factor for the disease even after several years. Therefore, healthcare providers should consider patients' lifetime travel histories when diagnosing illnesses, especially among patients potentially immunocompromised by coexisting medical conditions.

Genomic analysis offers an opportunity to address several unanswered epidemiologic questions about coccidioidomycosis. Clarifying the biogeographic distribution of *Coccidioides* spp. (*8*) was a necessary outcome of these studies. A case associated with clinical isolate B12226 was reported in Michigan, in which the case-patient had a travel history to

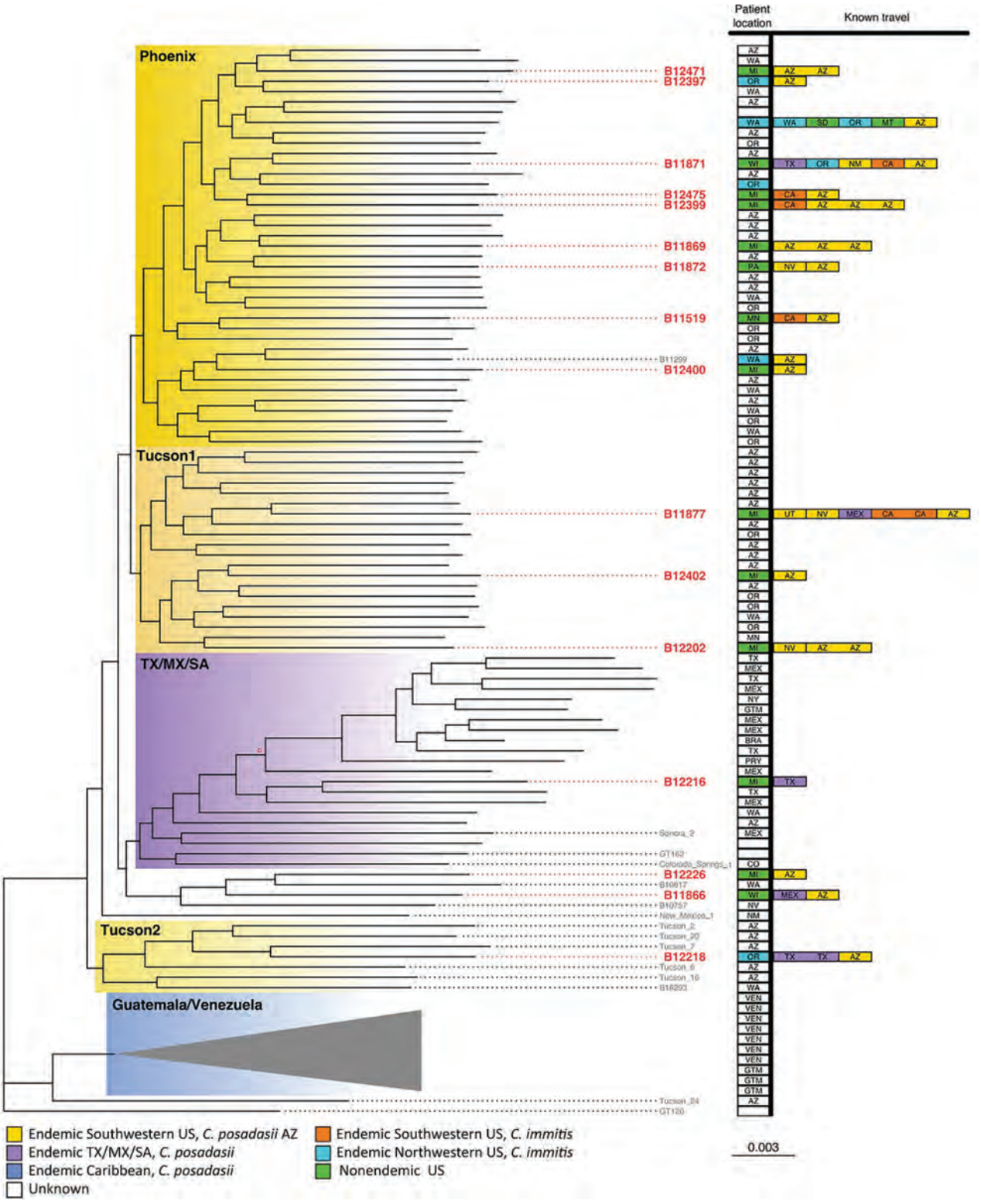

Figure 1. Summarized maximum-likelihood phylogenetic tree for *Coccidioides posadasii* isolates from study of genomic epidemiology linking nonendemic coccidioidomycosis to travel and reference isolates. Each recognized phylogeographic clade is highlighted with a colored gradient labeled in its top right corner. Samples with travel history are presented with locations of isolation and all known patient travel, with colors for the geographic regions. Red bold tip labels indicate samples sequenced for this study; other samples are included when including travel history or otherwise mentioned in the main text.

Arizona. However, unexpectedly, this genome clustered in the tree with a set of leaves neighboring the TX/MX/SA clade. Contrary to what would be expected based on reported travel history, this adjacent group is not part of the Arizona subpopulations. The topology and bootstrapping support for this

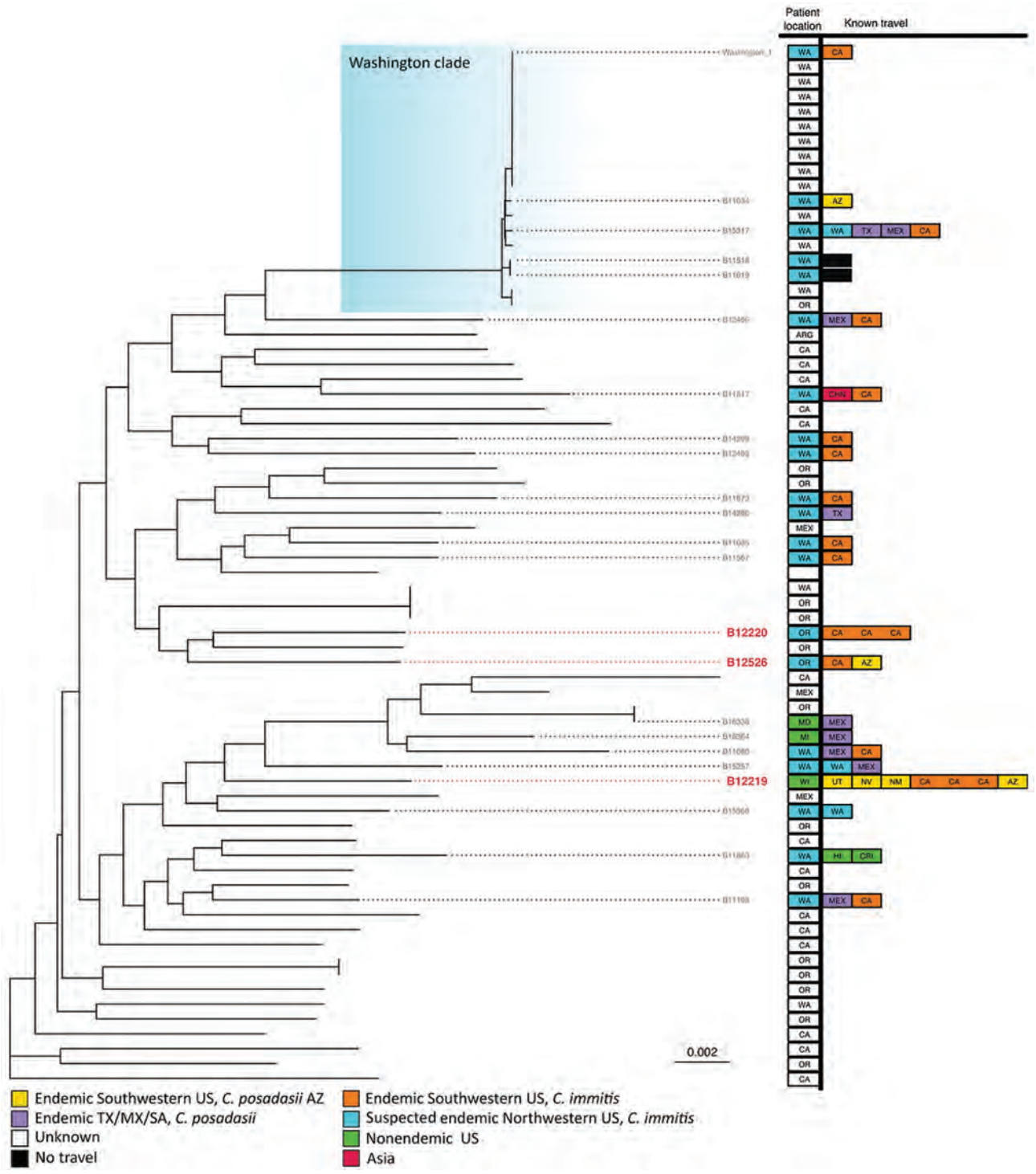

Figure 2. Summarized maximum-likelihood phylogenetic tree for *Coccidioides immitis* isolates from study of genomic epidemiology linking nonendemic coccidioidomycosis to travel and reference isolates. Each recognized phylogeographic clade is highlighted with a colored gradient labeled in its top right corner. Samples with travel history are presented with locations of isolation and all known patient travel, with colors for the geographic regions. Red bold tip labels indicate samples sequenced for this study; other samples are included when including travel history or otherwise mentioned in the main text.

neighboring Arizona clade suggest that it is a sibling subpopulation to the TX/MX/SA clade that has remained undersampled and thus not reconstructed until now. Bootstrap values in unabridged phylogenic trees (Appendix 2, https://wwwnc.cdc.gov/EID/article/29/1/22-0771-App2.pdf) show that the geographic origin of the Arizona clade remains unclear; the provenance of other clinical isolates in that branch includes New Mexico and Nevada, which obfuscates its probable geographic distribution. Sequencing both isolates from local patients with no travel history or environmental isolates belonging to this clade could help delineate the geographic borders of this subpopulation of *C. posadasii*. This gap in our understanding could potentially hinder the methodology that enabled this study because isolates in this group could not be traced unambiguously to their expected origins. This technique will most likely improve as more *Coccidioides* genomes are sequenced and population genomic efforts continue.

Conducting genomic sequencing more routinely could shed light on important clinical questions such as how long the infection can remain dormant before it reactivates and causes disease. Clinical cases of coccidioidomycosis have often been thought to represent relapses of previous infections; however, lack of documentation and difficulty tracking individual patients hindered this determination. Some reports of relapse indicate initial infections dating back several decades (*25*) and many patients in the 2016 enhanced surveillance study had a self-reported previous history of the illness (*12*). By procuring isolates during different instances of illness in the same patient, whole-genome sequencing could provide definitive evidence of the origin of the infection in each case, helping to resolve this longstanding clinical question.

More widespread phylogenetic typing platforms would greatly benefit epidemiologic efforts to understand *Coccidioides* spp. from a public health perspective. Increasingly available, whole-genome sequencing provides a reliable method for assigning pathogens to phylogenetic clades, enabling detection of the causes of outbreaks with unparalleled resolution. For our study, whole-genome sequencing provided information needed to resolve additional *Coccidioides* spp. population structure and enable further research into its pathogenicity.

Currently, a handful of isolates have remained challenging to assign to specific clades because of long terminal branches and low bootstrap support for leaf nodes in phylogenetic trees of *Coccidioides* genomes. Different analyses have not consistently placed *C. posadasii* isolates Sonora 2, Tucson 2, and Tucson 6 within the same clades (*10*,*26*). The long branches that separate any 2 genomes may result in long-branch attraction, making reconstruction of phylogenies highly contingent on the sampling selection and phylogenetic reconstruction algorithm and resulting in errors in tree topology (*27*) or uncertainty in assigning isolates (e.g., GT162, Colorado_springs_1). Our reconstruction of the *C. posadasii* species tree illustrates an ancestral lineage, here labeled Tucson 2, bearing similarities to the clade AZ clade I (*11*,*26*), but the Tucson and Arizona clades differ in their topological relations to other clades and the member isolates they contain. Those distinctions might become visible because of the increased genetic context provided by whole-genome sequencing to resolve phylogenetic relationships. Support for this lineage was present in previously published studies (*10*,*11*) that showed several of the isolates in this branch having admixture compositions different from those of the rest of the AZ and the TX/MX/SA clades.

The retrospective nature of this study limited our ability to review charts to acquire additional information of interest, including evidence of possible long-term infections. Our reliance on patients' missing or self-reported, possibly incomplete, travel histories limited information linked to location, especially for isolates collected outside of enhanced surveillance. Even though some patients included limited travel information, it could not be used with the same certainty as travel information collected systematically. Specifically, most isolates submitted from Oregon lacked patient travel information. Because most Oregon patients in this study were residents of the Portland metropolitan area, which has a humid, temperate climate not known to support endemic *Coccidioides* spp. population, those infections were likely acquired during travel. This conclusion, although based on extrapolation, does not conflict with other conclusions drawn in our study. Other irregularities in collection included 3 instances in which multiple isolates from the same patient were submitted, including 2 cases in which isolates were submitted independently by Oregon and Washington public health laboratories because the patient was diagnosed in one state but resided in the other. As indicated in the methods, we included all genomes that were sequenced separately. Clonal leaves are not expected results for coccidiomycosis cases and should be revised to identify collection irregularities. Such challenges require transversal solutions to capture, collect, and transmit information that might facilitate public health, clinical, and research efforts.

Despite challenges to reconstructing the population structure of *Coccidioides* spp., we were able to reliably correlate phylogeography and patient travel history in most cases of infection with these fungi. Further isolation and sequencing may better inform epidemiology and improve our understanding of the phylogeography of the *Coccidioides* species and their spatially linked lineages. Our results strengthen previous findings and underscore the importance of travel considerations when studying and diagnosing coccidiomycosis inside and outside known *Coccidioides*-endemic areas.

Acknowledgments

We thank state and local public health departments for conducting patient interviews and sending patient isolates to CDC. We also thank the Office of Advanced Molecular Detection, National Center for Emerging and Zoonotic Infectious Diseases, at CDC.

About the Author

Mr. Monroy-Nieto is an associate bioinformatician trained as an industrial microbiologist whose work with the Pathogen and Microbiome Division of the Translational Genomics Research Institute is focused on genomics, phylogenetics, and epidemiology of human fungal pathogens.

References

1. Ashraf N, Kubat RC, Poplin V, Adenis AA, Denning DW, Wright L, et al. Re-drawing the maps for endemic mycoses. Mycopathologia. 2020;185:843–65. https://doi.org/10.1007/s11046-020-00431-2
2. Kollath DR, Miller KJ, Barker BM. The mysterious desert dwellers: *Coccidioides immitis* and *Coccidioides posadasii*, causative fungal agents of coccidioidomycosis. Virulence. 2019;10:222–33. https://doi.org/10.1080/21505594.2019.1589363
3. Litvintseva AP, Marsden-Haug N, Hurst S, Hill H, Gade L, Driebe EM, et al. Valley fever: finding new places for an old disease: *Coccidioides immitis* found in Washington State soil associated with recent human infection. Clin Infect Dis. 2015;60:e1–3. https://doi.org/10.1093/cid/ciu681
4. Bowers JR, Parise KL, Kelley EJ, Lemmer D, Schupp JM, Driebe EM, et al. Direct detection of *Coccidioides* from Arizona soils using CocciENV, a highly sensitive and specific real-time PCR assay. Med Mycol. 2019;57:246–55. https://doi.org/10.1093/mmy/myy007
5. Gorris ME, Treseder KK, Zender CS, Randerson JT. Expansion of coccidioidomycosis endemic regions in the United States in response to climate change. Geohealth. 2019;3:308–27. https://doi.org/10.1029/2019GH000209
6. Edwards PQ, Palmer CE. Prevalence of sensitivity to coccidioidin, with special reference to specific and nonspecific reactions to coccidioidin and to histoplasmin. Dis Chest. 1957;31:35–60. https://doi.org/10.1378/chest.31.1.35
7. Koufopanou V, Burt A, Taylor JW. Concordance of gene genealogies reveals reproductive isolation in the pathogenic fungus *Coccidioides immitis*. Proc Natl Acad Sci U S A. 1997;94:5478–82. https://doi.org/10.1073/pnas.94.10.5478
8. Barker BM, Litvintseva AP, Riquelme M, Vargas-Gastélum L. *Coccidioides* ecology and genomics. Med Mycol. 2019;57(Supplement_1):S21–9. https://doi.org/10.1093/mmy/myy051
9. Oltean HN, Etienne KA, Roe CC, Gade L, McCotter OZ, Engelthaler DM, et al. Utility of whole-genome sequencing to ascertain locally acquired cases of coccidioidomycosis, Washington, USA. Emerg Infect Dis. 2019;25:501–6. https://doi.org/10.3201/eid2503.181155
10. Engelthaler DM, Roe CC, Hepp CM, Teixeira M, Driebe EM, Schupp JM, et al. Local population structure and patterns of Western Hemisphere dispersal for *Coccidioides* spp., the fungal cause of valley fever. MBio. 2016;7:e00550–16. https://doi.org/10.1128/mBio.00550-16
11. Teixeira MM, Alvarado P, Roe CC, Thompson GR III, Patané JSL, Sahl JW, et al. Population structure and genetic diversity among isolates of *Coccidioides posadasii* in Venezuela and surrounding regions. MBio. 2019;10:e01976-19. https://doi.org/10.1128/mBio.01976-19
12. Benedict K, Ireland M, Weinberg MP, Gruninger RJ, Weigand J, Chen L, et al. Enhanced surveillance for coccidioidomycosis, 14 US states, 2016. Emerg Infect Dis. 2018;24:1444–52. https://doi.org/10.3201/eid2408.171595
13. McCotter OZ, Benedict K, Engelthaler DM, Komatsu K, Lucas KD, Mohle-Boetani JC, et al. Update on the epidemiology of coccidioidomycosis in the United States. Med Mycol. 2019;57(Supplement_1):S30–40. https://doi.org/10.1093/mmy/myy095
14. Centers for Disease Control and Prevention. Valley fever (coccidioidomycosis) statistics. 2020 [cited 2021 May 31]. https://www.cdc.gov/fungal/diseases/coccidioidomycosis/statistics.html
15. Barker BM, Rajan S, De Melo Teixeira M, Sewnarine M, Roe C, Engelthaler DM, et al. Coccidioidal meningitis in New York traced to Texas by fungal genomic analysis. Clin Infect Dis. 2019;69:1060–2. https://doi.org/10.1093/cid/ciz052
16. Neafsey DE, Barker BM, Sharpton TJ, Stajich JE, Park DJ, Whiston E, et al. Population genomic sequencing of *Coccidioides* fungi reveals recent hybridization and transposon control. Genome Res. 2010;20:938–46. https://doi.org/10.1101/gr.103911.109
17. Sahl JW, Lemmer D, Travis J, Schupp JM, Gillece JD, Aziz M, et al. NASP: an accurate, rapid method for the identification of SNPs in WGS datasets that supports flexible input and output formats. Microb Genom. 2016;2:e000074. https://doi.org/10.1099/mgen.0.000074
18. Li H, Durbin R. Fast and accurate short read alignment with Burrows-Wheeler transform. Bioinformatics. 2009;25:1754–60. https://doi.org/10.1093/bioinformatics/btp324
19. McKenna A, Hanna M, Banks E, Sivachenko A, Cibulskis K, Kernytsky A, et al. The Genome Analysis Toolkit: a MapReduce framework for analyzing next-generation DNA sequencing data. Genome Res. 2010;20:1297–303. https://doi.org/10.1101/gr.107524.110
20. Marçais G, Delcher AL, Phillippy AM, Coston R, Salzberg SL, Zimin A. MUMmer4: a fast and versatile genome alignment system. PLOS Comput Biol. 2018;14:e1005944. https://doi.org/10.1371/journal.pcbi.1005944
21. Nguyen LT, Schmidt HA, von Haeseler A, Minh BQ. IQ-TREE: a fast and effective stochastic algorithm for estimating maximum-likelihood phylogenies. Mol Biol Evol. 2015;32:268–74. https://doi.org/10.1093/molbev/msu300

22. Yu G, Smith DK, Zhu H, Guan Y, Lam TT. GGTREE: an R package for visualization and annotation of phylogenetic trees with their covariates and other associated data. Methods Ecol Evol. 2017;8:28–36. https://doi.org/10.1111/2041-210X.12628
23. Ampel NM. Coccidioidomycosis: changing concepts and knowledge gaps. J Fungi (Basel). 2020;6:354. https://doi.org/10.3390/jof6040354
24. Johnson SM, Carlson EL, Fisher FS, Pappagianis D. Demonstration of *Coccidioides immitis* and *Coccidioides posadasii* DNA in soil samples collected from Dinosaur National Monument, Utah. Med Mycol. 2014;52:610–7. https://doi.org/10.1093/mmy/myu004
25. Gardner PG, Fuller EW Jr. Fatal relapse of coccidioidomycosis ten years after treatment with amphotericin B. N Engl J Med. 1969;281:950–2. https://doi.org/10.1056/NEJM196910232811709
26. de Melo Teixeira M, Lang BF, Matute DR, Stajich JE, Barker BM. Mitochondrial genomes of the human pathogens *Coccidioides immitis* and *Coccidioides posadasii*. G3(Bethesda). 2021;11:jkab132.
27. Philippe H, Zhou Y, Brinkmann H, Rodrigue N, Delsuc F. Heterotachy and long-branch attraction in phylogenetics. BMC Evol Biol. 2005;5:50. https://doi.org/10.1186/1471-2148-5-50

Address for correspondence: Nancy A. Chow, Centers for Disease Control and Prevention, 1600 Clifton Rd NE, Mailstop H17-2, Atlanta, GA 30329-4027, USA; email: yln3@cdc.gov

EID journal

Want to stay updated on the latest news in *Emerging Infectious Diseases*? Let us connect you to the world of global health. Discover groundbreaking research studies, pictures, podcasts, and more by following us on Twitter at @CDC_EIDjournal.

Risk for Severe COVID-19 Outcomes among Persons with Intellectual Disabilities, the Netherlands

Monique C.J. Koks-Leensen, Bianca W.M. Schalk, Esther J. Bakker-van Gijssel, Aura Timen, Masha E. Nägele, Milou van den Bemd, Geraline L. Leusink, Maarten Cuypers, Jenneken Naaldenberg

The COVID-19 pandemic has disproportionately affected persons in long-term care, who often experience health disparities. To delineate the COVID-19 disease burden among persons with intellectual disabilities, we prospectively collected data from 36 care facilities for 3 pandemic waves during March 2020–May 2021. We included outcomes for 2,586 clients with PCR-confirmed SARS-CoV-2 infection, among whom 161 had severe illness and 99 died. During the first 2 pandemic waves, infection among persons with intellectual disabilities reflected patterns observed in the general population, but case-fatality rates for persons with intellectual disabilities were 3.5 times higher and were elevated among those ≥40 years of age. Severe outcomes were associated with older age, having Down syndrome, and having ≥1 concurrent condition. Our study highlights the disproportionate COVID-19 disease burden among persons with intellectual disabilities and the need for disability-inclusive research and policymaking to inform disease surveillance and public health policies for this population.

The global COVID-19 pandemic has had a disproportionate effect on persons in long-term care (*1*), particularly persons with intellectual disabilities (*2*). Persons with intellectual disabilities experience many limitations in adaptive behavior and intellectual functioning that occur before adulthood (*3*). Consequently, their ability to understand and adhere to restrictive measures is impaired. Social distancing is challenging for persons with intellectual disabilities living in group homes or during close contact when receiving care (*4*–*8*). In addition, genetic syndromes that cause intellectual disabilities, such as Down syndrome, might contribute to the susceptibility to and severity of COVID-19 (*7*–*12*). Persons with intellectual disabilities often have concurrent conditions, such as diabetes, cardiovascular problems, and being overweight (body mass index [BMI] ≥25 kg/m^2) (*10*,*13*–*16*); they also are at increased risk for death from respiratory problems (*17*). Furthermore, COVID-19 pandemic risks can exacerbate health disparities among persons with intellectual disabilities (*2*,*18*).

Previous studies have shown substantially higher COVID-19 case rates, more hospital admissions, and higher case-fatality rates (CFRs) for persons with intellectual disabilities than for the general population, but those studies included relatively small sample sizes or were conducted during distinct periods of the pandemic (*6*,*9*–*11*,*19*–*22*). Besides the identified risk factors, intellectual disability also appeared to be an independent risk factor for severe COVID-19 outcomes, although the extent to which disability severity contributes is still unclear (*9*,*12*,*19*,*20*). Similarly, whereas pathogenicity of post–COVID-19 conditions is still emerging, specific characteristics among persons with intellectual disabilities and persistent post–COVID-19 symptoms are potentially unrecognized and unclear (*23*).

Because population surveillance for COVID-19 does not include information about disabilities, complete and integrated information about this vulnerable subgroup is lacking and potentially contributing to growing health disparities. To delineate specific factors driving excess risks for persons with intellectual disabilities infected with SARS-CoV-2, more information on the dynamic course of the outbreak, risk

Author affiliations: Radboud Institute for Health Sciences, Nijmegen, the Netherlands (M.C.J. Koks-Leensen, B.W.M. Schalk, E.J. Bakker–van Gijssel, A. Timen, M.E. Nägele, M. van den Bemd, G.L. Leusink, M. Cuypers, J. Naaldenberg); Siza, Arnhem, the Netherlands (E.J. Bakker-van Gijssel); Maastricht University Medical Center, Maastricht, the Netherlands (G.L. Leusink)

DOI: https://doi.org/10.3201/eid2901.221346

factors such as concurrent conditions, and population health in the local context is urgently needed.

We used data from a prospective nationwide registry on persons with intellectual disabilities and COVID-19 in long-term care in the Netherlands to provide comprehensive insight into the COVID-19 disease burden among this population. We aimed to examine characteristics of persons with intellectual disabilities and COVID-19, stratified by outcome severity; describe the course of SARS-CoV-2 infection and death in persons with intellectual disabilities across the initial 3 COVID-19 pandemic waves; and explore associations between severe outcomes and patient characteristics.

Methods

Design and Setting

We conducted an observational registry-based prospective study by collecting data on residents and outpatients with suspected COVID-19 from long-term care organizations in the Netherlands. The registry was a joint initiative of specialized intellectual disabilities physicians, researchers, and the Ministry of Health, Welfare, and Sport of the Netherlands to establish an adequate basis for policy and practice decision making regarding COVID-19 among persons with intellectual disabilities. We invited all 170 member organizations of Vereniging Gehandicaptenzorg Nederland, the association for disability care in the Netherlands, to participate; we also opened participation to nonmember organizations. In all, 36 organizations across the Netherlands participated, serving ≈60% of the estimated 115,000 clients with intellectual disabilities in long-term care (*24*). We considered the organizations geographically representative, which was necessary to adequately compare with general population data considering differences in regional spread of SARS-CoV-2. The registry was open from March 24, 2020–September 1, 2021. We collected and included data from cases that occurred during March 24, 2020–June 1, 2021, and facilities could enter follow-up data until September 1, 2021. The Medical Research Ethics Committee of Radboud University Medical Center approved the study without need for informed consent because this was a minimal risk study with de-identified data (reference no. 2020-6509).

Data Collection and Outcome Measures

Each participating location was granted access to an online registration system (Castor, https://www.castoredc.com). For each patient with intellectual disabilities suspected of COVID-19, participating organizations completed a questionnaire concerning demographic characteristics (age, sex, residential status), medical history (etiology and severity level of disability, concurrent conditions, and medications), and test status. For patients with COVID-19 confirmed by a positive PCR test, we obtained additional information regarding the need for oxygen therapy, hospital admission, and whether the patient died. Questions had a categorical or dichotomous answering scale, with an option to add free text when other was selected in a category (Appendix, https://wwwnc.cdc.gov/EID/article/29/1/22-1346-App1.pdf).

This study only included patients with a COVID-19 diagnosis, which we defined as a positive SARS-CoV-2 PCR test result during the study period. Our primary outcomes were serious COVID-19 illness or death within 4 weeks of COVID-19 diagnosis. We defined serious illness as a need for oxygen therapy, considered or actual hospital admission for COVID-19, or both. We assumed mild COVID-19 disease for all patients who did not experience severe illness or death. We registered reinfections by updating entries for patients after a record was opened, providing additional test data, and adding information for the COVID-19 case. However, we only included the first confirmed infection for each patient in this study. We retrieved comparator data for the general population of the Netherlands during the study period from publicly available data of the Rijksinstituut voor Volksgezondheid en Milieu (RIVM), the National Institute for Public Health and the Environment, which is responsible for population monitoring of COVID-19 in the Netherlands (*25*).

Wave Definition

In response to the different COVID-19 waves, testing and preventive regulations changed over the course of the pandemic. For comparability, we followed the same start and end dates per wave, which RIVM identified on the basis of SARS-CoV-2 infections in the general population. Wave I ran from epidemiologic week 11, 2020 through week 25, 2020; wave II ran from week 26, 2020, through week 4, 2021; and wave III ran from weeks 5 through 21, 2021 (*26*). We assigned patients in our study to a pandemic wave on the basis of reported date of positive PCR test. For cases missing PCR testing dates, we used the date of reported illness onset instead.

Statistical Methods

For descriptive characteristics, we used frequency and percentage or median and interquartile range (IQR) for the entire study population and stratified

characteristics by outcomes as mild illness, severe illness, or death. We excluded patients with missing information on both test date and first date of illness from comparison between waves because we could not assign them to a specific wave. We separately calculated the CFR per wave by sex and age group (0–17 years, 18–39 years, 40–69 years, and ≥70 years) by using the number of reported deaths as numerator and the total number of confirmed infections as denominator. We also calculated rates for serious illness and mild illness by dividing the number of serious or mild cases by the total number confirmed infections in the study population per wave. We used the same calculations to compare illness and death rates for general population data for the same strata.

To examine associations between demographic characteristics and concurrent conditions (dependent factors) and severe COVID-19 illness and death as outcomes, we conducted logistic regression modeling. In a first step, we assessed effects of sex, age, disability level, Down syndrome, and concurrent conditions by using a univariable model for each separate outcome measure to assess relevant variables for multivariate analysis and considered $p<0.10$ statistically significant. We combined all variables with a significant univariate association in the multivariable model. We conducted stepwise backward logistic regression with a significance level for removing variables of 0.10 (p value out) from the full model and for re-entering variables as 0.05 (p value in). We calculated the odds ratio (OR) and 95% CI for potential risk factors for severe outcomes. We used receiver operating characteristic area under the curve (AUC) to evaluate predictive performance of the multivariable models. AUC uses a combination of sensitivity and specificity of model predictions and actual cases of severe illness or death, to assess predictive performance. An AUC of 0.50 indicates no predictive ability, and higher values correspond to better performance. We assessed adequate model fit by using Hosmer-Lemeshow goodness-of-fit tests on both multivariable models and accepted cases in which $p>0.05$. We used 2-sided statistical tests for all calculations and considered $p<0.05$ statistically significant. We tested for collinearity among all independent variables by using the variance inflation factor (VIF) and retained covariates for each final analysis that had a VIF <5. We conducted all statistical analyses in SPSS Statistics 25.0 (IBM, https://www.ibm.com).

Results

Data for 9,163 persons with intellectual disabilities suspected of COVID-19 were entered into the registry, of which 2,586 (28.2%) had a PCR-confirmed SARS-CoV-2 infection. For 161 (6.2%) of these patients, severe illness was reported, and 99 (3.8%) patients died after their SARS-CoV-2 infection.

Characteristics of Persons with Intellectual Disabilities and COVID-19

We assessed demographic and health condition characteristics of 2,586 persons with intellectual disabilities and COVID-19, including their illness outcomes (Table 1). The median age was 51 (IQR 34–62) years, most (58.5%, n = 1,476) patients were men, and most (79.9%, n = 2,067) lived in group homes. Disability severity had equal representation, and 176 (6.8%) patients had Down syndrome. Among all included patients, 1,101 (42.6%) had concurrent conditions. The most prevalent conditions were being overweight (26.2%, n = 678), epilepsy (10.4%, n = 268), hypertension (7.5%, n = 195), diabetes (5.8%, n = 151), and chronic heart disease (4.6%, n = 120).

Patients with severe illness and those who died were older than others in the entire sample. The median age of persons with severe illness was 61 (IQR 52–67.5) years, and for those who died, median age was 68 (IQR 61–76) years. Those subgroups also included higher percentages of patients with Down syndrome, 12.4% (n = 20) of patients with severe illness and 15.2% (n = 15) of patients who died. In addition, approximately two thirds of patients who had severe illness (61.5%, n = 99) or who died (59.6%, n = 59) had concurrent conditions, compared with only 40.5% (n = 943) of patients who had mild illness (Table 1).

Infections and Outcomes Per Wave

The first wave of COVID-19 included 335 patients with intellectual disabilities, the second wave 1,927 patients, and the third wave 268 patients (Table 2). The pattern in weekly infections among persons with intellectual disabilities followed similar patterns as those for the general population for the first 2 waves and declined with the start of the vaccination campaign during the third wave (Figure 1). During the first wave, 17.1% (n = 57) of patients were ≥70 years of age, which is more than in subsequent waves: 11.6% (n = 221) in the second wave and 11.7% (n = 31) in the third wave. COVID-19 among younger persons, those 0–39 years of age, increased from 1.8% (n = 6) in the first wave to 6.4% (n = 17) in the third wave for those aged 0–17 years and from 20.4% (n = 68) in the first wave to 28.9% (n = 77) in the third wave for those 18–39 years of age (Table 2).

Severe illness was highest during the first wave (13.7%, n = 46) and was comparable during the second (5.1%, n = 99) and third (5.2%, n = 14) waves. In all

Table 1. Characteristics and outcomes for 2,586 persons included in a study of risk for severe COVID-19 outcomes among persons with intellectual disabilities, the Netherlands*

Characteristics	Mild illness, n = 2,326	Severe illness, n = 161	Died, n = 99†	Total, n = 2,586
Sex, no. (%), n = 2,525				
M	1,315 (58.0)	103 (64.0)	58 (59.2)	1,476 (58.5)
F	951 (42.0)	58 (36.0)	40 (40.8)	1,049 (41.5)
Median age, y (IQR), n = 2,519	49 (32.0–61.0)	61 (52.0–67.5)	68 (61.0–76.0)	51 (34–62)
Age groups, no. (%), n = 2,519				
0–17 y	81 (3.6)	0	1 (1.0)	82 (3.3)
18–39 y	721 (31.9)	16 (9.9)	2 (2.0)	739 (29.3)
40–49 y	330 (14.6)	16 (9.9)	4 (4.0)	350 (13.9)
50–59 y	491 (21.7)	44 (27.3)	16 (16.2)	551 (21.9)
60–69 y	399 (17.7)	57 (35.4)	32 (32.3)	488 (19.4)
≥70 y	237 (10.5)	28 (17.4)	44 (44.4)	309 (12.3)
Long term care type, no. (%)				
Group home	1,853 (79.7)	132 (82.0)	82 (82.8)	2,067 (79.9)
Independent living	349 (15.0)	28 (17.4)	16 (16.2)	393 (15.2)
Other or unknown	124 (5.3)	1 (0.6)	1 (1.0)	126 (4.9)
Disability level, no. (%), n = 2,468				
Borderline to mild	632 (28.5)	49 (31.2)	18 (18.9)	699 (28.3)
Moderate	798 (36.0)	47 (29.9)	42 (44.2)	887 (35.9)
Severe to profound	786 (35.5)	61 (38.9)	35 (36.8)	882 (35.7)
Disability etiology, no. (%)				
Down syndrome	141 (6.1)	20 (12.4)	15 (15.2)	176 (6.8)
No. concurrent conditions (%)				
None reported	1,383 (59.5)	62 (38.5)	40 (40.4)	1,485 (57.4)
1 reported	650 (27.9)	54 (33.5)	31 (31.3)	735 (28.4)
>1 reported	293 (12.6)	45 (28.0)	28 (28.3)	366 (14.2)
Concurrent conditions, no. (%)				
Diabetes	117 (5.0)	19 (11.8)	15 (15.2)	151 (5.8)
Hypertension	159 (6.8)	20 (12.4)	16 (16.2)	195 (7.5)
Heart disease	95 (4.1)	11 (6.8)	14 (14.1)	120 (4.6)
Lung disease; asthma, COPD, or both	57 (2.5)	13 (8.1)	9 (9.1)	79 (3.1)
Epilepsy	229 (9.8)	25 (15.5)	14 (14.1)	268 (10.4)
Overweight, body mass index ≥25 kg/m^2	587 (25.2)	67 (41.6)	24 (24.2)	678 (26.2)

*All persons included in the study had intellectual disabilities and tested positive for SARS-CoV-2 by PCR. Category totals do not always add up to column totals because of missing responses; percentages are based on variable totals per category. COPD, chronic obstructive pulmonary disease; IQR, interquartile range.
†Case-fatality ratio 3.8%.

3 waves, rates of severe illness were highest (71.4%–73.9%) among patients 40–69 years of age (Table 2).

CFR decreased from 14.6% during the first wave to 2.2% during the second wave and 2.6% in the third wave. Across all 3 waves, the CFR was 3.8% among our study cohort, whereas overall CFR was only 1.1% in the general population of the Netherlands (*25*). Among persons with intellectual disabilities, a substantial number of deaths occurred among persons between 40–69 years of age, whereas death in the general population was concentrated among persons ≥70 years of age (Figure 2).

Factors Associated with Severe COVID-19 Illness and Death

In multivariable analysis, we found that severe illness was more likely for patients with Down syndrome (OR 2.6, 95% CI 1.5–4.3) and for patients with several concurrent conditions, including lung diseases (OR 3.5, 95% CI 1.8–6.7), diabetes mellitus (OR 1.8, 95% CI 1.0–3.0), epilepsy (OR 1.8, 95% CI 1.1–2.8), or who were overweight (OR 1.8, 95% CI 1.3–2.5) (Table 3). Age was also substantially associated with severe COVID-19 illness and risks increased with increasing age (OR 1.04, 95% CI 1.03–1.05).

We performed similar logistic regressions for COVID-19–related deaths (Table 4). Increased risk of COVID-19 death was associated with increasing age (OR 1.1, 95% CI 1.1–1.1), and having Down syndrome (OR 5.6, 95% CI 2.9–10.6), lung disease (OR 4.6, 95% CI 2.0–10.7), or heart disease (OR 2.3, 95% CI 1.2–4.5).

Discussion

We report outcomes of a nationwide prospective COVID-19 registry of persons with intellectual disabilities in long-term care in the Netherlands during March 2020–May 2021. This registry provided a large dataset of COVID-19–positive patients with intellectual disabilities collected during 15 consecutive months of the pandemic. In addition to national surveillance data about the general population, this prospective registry generated detailed insights into COVID-19 disease and risk factors among the subpopulation of persons with intellectual disabilities.

COVID-19 among persons with intellectual disabilities followed similar epidemiologic wave patterns as those for the general population for the first 2 pandemic waves in the Netherlands, indicating the difficulty of protecting vulnerable subpopulations from generic contamination routes. The observed third wave of COVID-19 in persons with intellectual disabilities was less pronounced, which could be an indication of COVID-19 vaccine effectiveness in this subpopulation. Large-scale vaccination roll-out in the Netherlands started at the onset of the third wave and prioritized persons with intellectual disabilities along with other risk groups. Despite the rather similar epidemiologic pattern of COVID-19 in the general population and in persons with intellectual disabilities, pronounced differences were seen in the clinical course of the disease and its outcomes.

In our study population, we found the COVID-19 CFR was >3 times higher for persons with intellectual disabilities than for the general population of the Netherlands at a given time (*25*). In contrast to the general population, most deaths among persons with intellectual disabilities occurred at relatively young ages (40–69 vs. ≥70 years of age). Those findings are consistent with reports from the United Kingdom (*12*,*19*,*21*), Canada (*11*), and the United States (*4*,*9*,*10*,*20*), which implies that age-related thresholds applied to the general population in protective policies require adjustment when applied to the intellectual disability population.

In line with previous findings, patients with severe COVID-19 outcomes in our registry were older, more frequently had Down syndrome, and had a larger percentage reporting ≥1 concurrent condition compared with patients facing mild illness. In addition to studies reporting effects of intellectual disability

Table 2. Outcomes per COVID-19 wave among persons included in a study of risk for severe COVID-19 outcomes among persons with intellectual disabilities, the Netherlands*

Outcomes	Wave I, March–June 2020	Wave II, July 2020–January 2021	Wave III, February–May 2021
Total COVID-19 infections	335	1,927	268
Sex, no. (%)			
M	178 (53.1)	1,138 (59.5)	153 (57.1)
F	157 (46.9)	776 (40.5)	115 (42.9)
Infections per age group, no. (%)			
0–17 y	6 (1.8)	58 (3.0)	17 (6.4)
18–39 y	68 (20.4)	593 (31.0)	77 (28.9)
40–69 y	202 (60.7)	1,039 (54.4)	141 (53.0)
≥70 y	57 (17.1)	221 (11.6)	31 (11.7)
Mild illness, no. (%)†	240 (71.6)	1,785 (92.6)	247 (92.2)
Sex, no. (%)			
M	126 (52.5)	1,039 (58.6)	144 (58.3)
F	114 (47.5)	733 (41.4)	103 (41.7)
Infections per age group, no. (%)			
0–17 y	6 (2.5)	57 (3.2)	17 (6.9)
18–39 y	64 (26.9)	579 (32.7)	77 (31.4)
40–69 y	139 (58.4)	948 (53.6)	128 (52.2)
≥70 y	29 (12.2)	185 (10.5)	23 (9.4)
Severe illness, no. (%)	46 (13.7)	99 (5.1)	14 (5.2)
Sex, no. (%)			
M	27 (58.7)	68 (68.7)	7 (50.0)
F	19 (41.3)	31 (31.3)	7 (50.0)
Infections per age group, no. (%)			
0–17 y	0	0	0
18–39 y	3 (6.5)	13 (13.1)	0
40–69 y	34 (73.9)	71 (71.7)	10 (71.4)
≥70 y	9 (19.6)	15 (15.2)	4 (28.6)
No. deaths (case-fatality ratio)‡	49 (14.6)	43 (2.2)	7 (2.6)
Sex, no. (%)			
M	25 (52.1)	31 (72.1)	2 (28.6)
F	23 (47.9)	12 (27.9)	5 (71.4)
Deaths per age group, no. (%)			
0–17 y	0	1 (2.3)	0
18–39 y	1 (2.0)	1 (2.3)	0
40–69 y	29 (59.2)	20 (46.5)	3 (42.9)
≥70 y	19 (38.8)	21 (48.8)	4 (57.1)

*Because of missing data for some responses, values might not add up to 100%. For missing SARS-CoV-2 testing date, we used reported date of illness onset instead. In total, 56 patients had no date information and could not be assigned to a specific wave, of which 54 reported mild illness and 2 reported severe illness.
†Missing data for sex, n = 13, and age, n = 20.
‡Missing data for sex, n = 1.

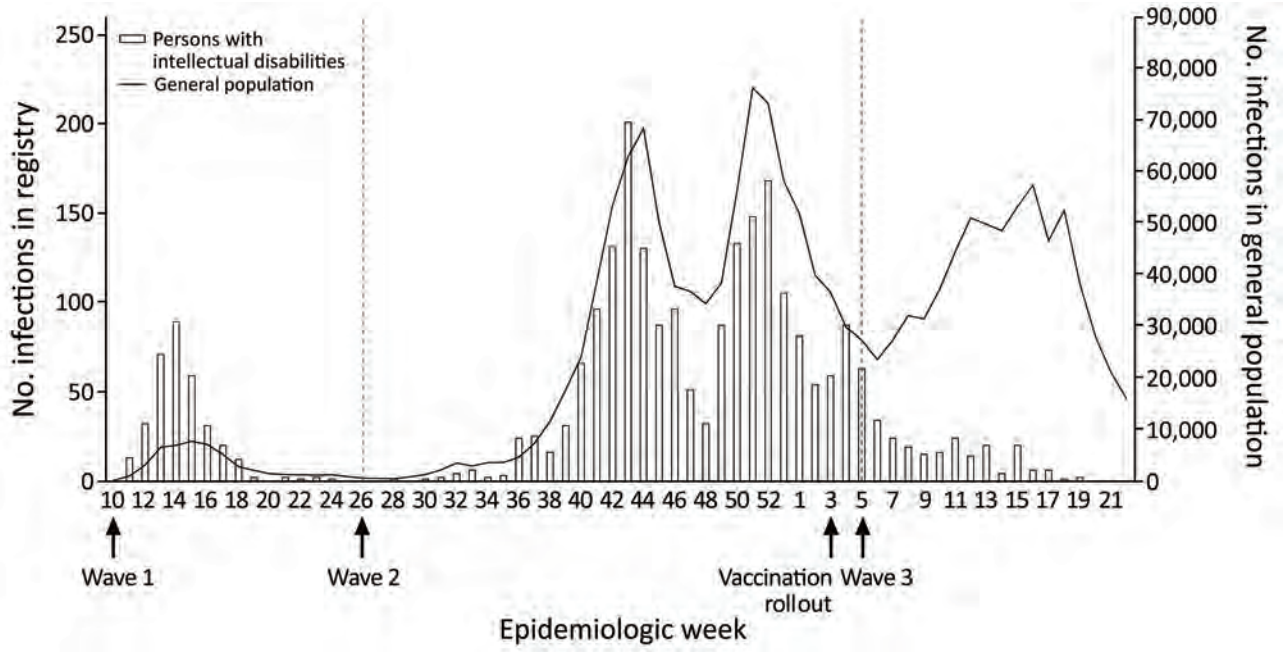

Figure 1. Weekly number of COVID-19 infections among persons with intellectual disabilities and the general population, the Netherlands, March 2020–May 2021. Graph shows epidemiologic weeks during 3 pandemic waves in the Netherlands: wave I, March–June 2020; wave II, July 2020–January 2021; and wave III, February–May 2021. The registry included 2,586 persons with intellectual disabilities in long-term care. Scales for the y-axes differ substantially to underscore patterns.

level as a risk factor (*12*,*16*), we did not find notable effects associated with disability severity. Our results indicate that several conditions were associated with risk for severe illness and death; chronic heart disease and lung diseases (asthma, COPD, or both) were significantly associated with COVID-19–related deaths ($p<0.001$), and having diabetes, epilepsy, or lung disease or being overweight increased risk for severe COVID-19 illness. One previous study also identified heart disease as a risk factor for COVID-19–related death among persons with intellectual disabilities (*10*). Other concurrent conditions we included in our analyses did not show statistically significant associations with COVID-19 death in our within-group analyses, although conditions such as diabetes, epilepsy, and being overweight are generally reported to be risk

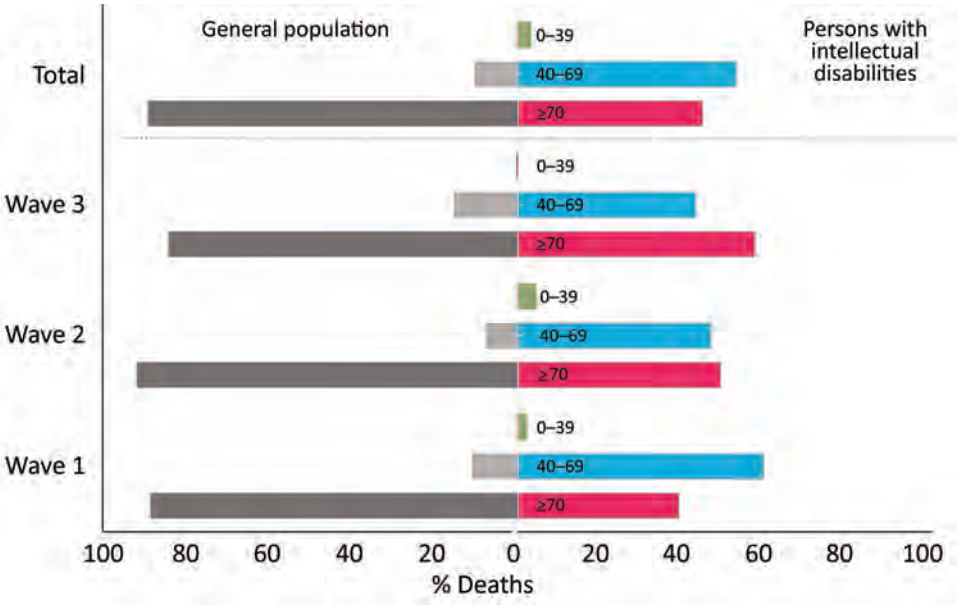

Figure 2. Distribution of COVID-19 deaths across age groups among persons with intellectual disabilities and the general population during 3 pandemic waves, the Netherlands. Wave I was March–June 2020; wave II, July 2020–January 2021; and wave III, February–May 2021. Information on 2,586 persons with intellectual disabilities was collected from long-term care organizations that care for this population.

Table 3. Univariable and multivariable logistic regression for severe illness by characteristics among 161 persons with intellectual disabilities and COVID-19, the Netherlands*

	Univariable		Multivariable†	
Characteristics	Odds ratio (95% CI)	p value	Odds ratio (95% CI)	p value
Sex				
M	1.3 (0.9–1.8)	0.14	ND	NA
F	Referent			
Age	1.04 (1.0–1.1)	<0.001	1.04 (1.03–1.05)	<0.001
Disability level				
Borderline to mild	Referent			
Moderate	1.0 (0.7–1.5)	0.99	ND	NA
Severe to profound	1.3 (0.9–2.0)	0.19	ND	NA
Etiology				
Down syndrome	2.2 (1.3–3.6)	0.002	2.6 (1.5–4.3)	<0.001
Concurrent conditions				
Diabetes	2.5 (1.5–4.2)	<0.001	1.8 (1.0–3.0)	0.04
Hypertension	1.9 (1.2–3.2)	0.009	ND	NA
Heart disease	1.7 (0.9–3.3)	0.10	ND	NA
Lung disease	3.5 (1.9–6.5)	<0.001	3.5 (1.8–6.7)	<0.001
Epilepsy	1.7 (1.1–2.6)	0.02	1.8 (1.1–2.8)	0.02
Overweight, BMI ≥25 kg/m^2	2.1 (1.5–2.9)	<0.001	1.8 (1.3–2.5)	<0.001

*Because of nonresponses for some patient data among 2,586 persons included in the study, these data reflect missing values for sex, n = 60; age n = 67; and disability level, n = 114. BMI, body mass index; NA, not applicable; ND, not done.
†Variables with p<0.1 in univariable analyses were included in multivariate logistic regression analysis. Because we used stepwise backward selection, we removed nonsignificant variables from the multivariable model and we could not provide estimates. The area under the curve was 0.731 (95% CI 0.691–0.770; p<0.001). We used Hosmer-Lemeshow goodness-of-fit test to assess the model fit for logistic regression and considered p>0.05 nonsignificant. Variance inflation factor (VIF) diagnostics indicated no evidence of collinearity (all VIF<1.2) among variables in final model.

factors for COVID-19–related death, hospitalization, or both, and were relatively common in our entire sample of SARS-CoV-2–positive patients (*19*,*20*,*27*). However, clinicians should recognize the associations between underlying health conditions and severe COVID-19 outcomes reported here to ensure that persons with intellectual disabilities and concurrent conditions receive appropriate medical care.

Future efforts to protect persons with intellectual disabilities in long-term care settings from adverse outcomes during this pandemic and future pandemics need to balance between protection and effects of implemented measures and restrictions, accounting for vulnerabilities and increased disease burden among this population. Accurate data to support decision making are then required. An example of

Table 4. Univariable and multivariable logistic regression by characteristics among 99 persons with intellectual disabilities who died of COVID-19, the Netherlands*

	Univariable		Multivariable†	
Characteristics	Odds ratio (95% CI)	p value	Odds ratio (95% CI)	p value
Sex				
M	1.0 (0.7–1.6)	0.82	ND	
F	Referent			
Age	1.1 (1.1–1.1)	<0.001	1.09 (1.07–1.12)	<0.001
Disability level‡				
Borderline to mild	Referent			
Moderate	0.5 (0.3–0.9)	0.03	ND	NA
Severe to profound	0.6 (0.4–1.1)	0.13	ND	NA
Disability etiology‡				
Down syndrome	2.86 (1.6–4.9)	0.001	5.6 (2.9–10.6)	<0.001
Concurrent conditions				
Diabetes	3.4 (1.9–6.0)	<0.001	ND	NA
Hypertension	2.6 (1.5–4.6)	0.001	ND	NA
Heart disease	3.9 (2.1–7.1)	<0.001	2.3 (1.2–4.5)	0.01
Lung disease	4.0 (1.9–8.3)	<0.001	4.6 (2.0–10.7)	<0.001
Epilepsy	1.5 (0.8–2.7)	0.17	ND	NA
Overweight, BMI ≥25 kg/m^2	0.9 (0.6–1.5)	0.82	ND	NA

*Because of nonresponses for some patient data among 2,586 persons included in the study, these data reflect missing values for sex, n = 60; age n = 67; and disability level, n = 114. BMI, body mass index; NA, not applicable; ND, not done.
†Variables with p<0.1 in univariable analyses were included in multivariate logistic regression analysis. Because we used stepwise backward selection, we removed nonsignificant variables from the multivariable model and we could not provide estimates. The area under the curve was 0.844 (95% CI 0.808–0.880; p<0.001). We used Hosmer-Lemeshow goodness-of-fit test to assess the model fit for logistic regression and considered p>0.05 nonsignificant. Variance inflation factor (VIF) diagnostics indicated no evidence of collinearity (all VIF<1.2) among variables in final model.
‡Both the variable disability level and the variable etiology concern the level of intellectual disability. To avoid interdependency, we only included etiology in the multivariable model, because this variable shows a stronger univariable relationship and had no missing values.

policy implications of our national registry is that it provided supportive evidence to prioritize vaccination for persons with intellectual disabilities in the Netherlands. Large-scale vaccination rollout started earlier for persons with intellectual disabilities than for the general population, resulting in less severe SARS-CoV-2 infections and consecutive gradual relaxations of socially restrictive measures in this population.

A strength of our study is collection of specific data from a representative sample of long-term care providers in the Netherlands that could not be retrieved from other sources. Of note, our registry was affected by changes in testing protocols. During the first wave, testing was available only under certain conditions for symptomatic patients, resulting in an overrepresentation of severe cases and a higher CFR among both groups.

However, one consequence of our registration method was that it did not provide information about the total population of persons with intellectual disabilities to which reported COVID-19 cases related. Therefore, we could not estimate the incidence of infections and death for the intellectual disability population at large, and we only had complete information to calculate CFRs within our sample. Furthermore, we observed no effect from residential status, probably because our data collection method focused on intellectual disability care facilities providing long-term care, which predominantly comprises residential care. The prevalence of some other risk factors was too low to include in analyses and obtain a complete profile of all potentially relevant risk factors. Although we had a large registry and total study population of persons with intellectual disabilities and COVID-19, the numbers of observations for some of the variables in our multivariable logistic models were low. Because OR and 95% CI provide a clear direction of the observed associations, we do not assume the small sample size substantially influenced our results.

To gain more accurate insights into risks associated with concurrent conditions, research incorporating control groups of persons without intellectual disabilities and without COVID-19 is needed to enable comparisons between groups. Finally, potential selection bias cannot be excluded because of a greater perceived relevance of reporting severe cases. Our study comprised the initial 3 pandemic waves and did not enable long-term follow-up to quantify the occurrence of post–COVID-19 syndromes. Long-term follow-up studies in persons with intellectual disabilities could provide further insights.

The findings from our prospective registry-based data provide critical information about risk factors and health disparities among persons with intellectual disabilities obscured in national surveillance data. In addition, the results contribute to the disability-inclusive response in research, policy, and practice that is currently called upon and will be needed in future pandemics. We collected specific information directly from care providers to demonstrate COVID-19 disease burden and factors affecting disease progression within the persons with intellectual disabilities group. Our data show persons with intellectual disabilities are a risk group that requires dedicated monitoring and evidence-based policies. Epidemiologic evidence of the COVID-19 disease burden among persons with intellectual disabilities is essential for addressing knowledge gaps and informing adequate policymaking. Our results highlight the specific need for attention to this group in policymaking to prevent growing inequities and provide quality care during pandemics.

Acknowledgments

We thank all the intellectual disability care organizations that participated in this registry for their commitment to accurately registering all cases in our database during an ongoing pandemic. We also thank the Academic Collaborative Sterker op Eigen Benen, the Vereniging Gehandicaptenzorg Nederland, and the Ministry of Health, Welfare, and Sport for their collaboration in this project.

This study was supported by grants from the Netherlands Organization for Health Research and Development (ZonMw grant no. 641001100) and the Dutch Ministry of Health, Welfare, and Sport (grant no. 329574).

About the Author

Dr. Koks-Leensen is a biomedical health scientist with the intellectual disabilities and health research group of the Department of Primary and Community Care at Radboud University Medical Center, Nijmegen, the Netherlands. Her primary research interest is health of persons with intellectual disabilities, including the impact of COVID-19 in the population of persons with mild disabilities.

References

1. Danis K, Fonteneau L, Georges S, Daniau C, Bernard-Stoecklin S, Domegan L, et al.; ECDC Public Health Emergency Team. High impact of COVID-19 in long-term care facilities, suggestion for monitoring in the EU/EEA, May 2020. Euro Surveill. 2020;25:2000956. https://doi.org/10.2807/1560-7917.es.2020.25.22.2000956
2. Courtenay K, Perera B. COVID-19 and people with intellectual disability: impacts of a pandemic. Ir J Psychol Med. 2020;37:231–6. https://doi.org/10.1017/ipm.2020.45
3. Schalock RL, Luckasson R, Tassé MJ. Intellectual disability: definition, classification, and systems of supports, 12th ed.

Silver Spring (MD); American Association on Intellectual and Developmental Disabilities; 2021.
4. Landes SD, Turk MA, Wong AWWA. COVID-19 outcomes among people with intellectual and developmental disability in California: The importance of type of residence and skilled nursing care needs. Disabil Health J. 2021;14:101051. https://doi.org/10.1016/j.dhjo.2020.101051
5. Hansford R, Ouellette-Kuntz H, Martin L. Short Report: The influence of congregate setting on positive COVID-19 tests among a high-risk sample of adults with intellectual and developmental disability in Ontario. Res Dev Disabil. 2022;122:104178. https://doi.org/10.1016/j.ridd.2022.104178
6. Landes SD, Turk MA, Formica MK, McDonald KE, Stevens JD. COVID-19 outcomes among people with intellectual and developmental disability living in residential group homes in New York State. Disabil Health J. 2020;13:100969. https://doi.org/10.1016/j.dhjo.2020.100969
7. Majithia M, Ribeiro SP. COVID-19 and Down syndrome: the spark in the fuel. Nat Rev Immunol. 2022;22:404–5. https://doi.org/10.1038/s41577-022-00745-w
8. Clift AK, Coupland CAC, Keogh RH, Hemingway H, Hippisley-Cox J. COVID-19 mortality risk in Down syndrome: results from a cohort study of 8 million adults. Ann Intern Med. 2021;174:572–6. https://doi.org/10.7326/M20-4986
9. Koyama AK, Koumans EH, Sircar K, Lavery A, Hsu J, Ryerson AB, et al. Severe outcomes, readmission, and length of stay among COVID-19 patients with intellectual and developmental disabilities. Int J Infect Dis. 2022;116:328–30. https://doi.org/10.1016/j.ijid.2022.01.038
10. Landes SD, Turk MA, Damiani MR, Proctor P, Baier S. Risk factors associated with COVID-19 outcomes among people with intellectual and developmental disabilities receiving residential services. JAMA Netw Open. 2021;4:e2112862. https://doi.org/10.1001/jamanetworkopen.2021.12862
11. Lunsky Y, Durbin A, Balogh R, Lin E, Palma L, Plumptre L. COVID-19 positivity rates, hospitalizations and mortality of adults with and without intellectual and developmental disabilities in Ontario, Canada. Disabil Health J. 2022;15:101174. https://doi.org/10.1016/j.dhjo.2021.101174
12. Williamson EJ, McDonald HI, Bhaskaran K, Walker AJ, Bacon S, Davy S, et al. Risks of covid-19 hospital admission and death for people with learning disability: population based cohort study using the OpenSAFELY platform. BMJ. 2021;374:n1592. https://doi.org/10.1136/bmj.n1592
13. Flygare Wallén E, Ljunggren G, Carlsson AC, Pettersson D, Wändell P. High prevalence of diabetes mellitus, hypertension and obesity among persons with a recorded diagnosis of intellectual disability or autism spectrum disorder. J Intellect Disabil Res. 2018;62:269–80. https://doi.org/10.1111/jir.12462
14. van den Bemd M, Schalk BWM, Bischoff EWMA, Cuypers M, Leusink GL. Chronic diseases and comorbidities in adults with and without intellectual disabilities: comparative cross-sectional study in Dutch general practice. Fam Pract. 2022;20220517:cmac042. https://doi.org/10.1093/fampra/cmac042
15. Horvath RA, Suto Z, Cseke B, Schranz D, Darnai G, Kovacs N, et al. Epilepsy is overrepresented among young people who died from COVID-19: analysis of nationwide mortality data in Hungary. Seizure. 2022;94:136–41. https://doi.org/10.1016/j.seizure.2021.11.013
16. Perera B, Laugharne R, Henley W, Zabel A, Lamb K, Branford D, et al. COVID-19 deaths in people with intellectual disability in the UK and Ireland: descriptive study. BJPsych Open. 2020;6:e123. https://doi.org/10.1192/bjo.2020.102
17. Cuypers M, Schalk BWM, Koks-Leensen MCJ, Nägele ME, Bakker-van Gijssel EJ, Naaldenberg J, et al. Mortality of people with intellectual disabilities during the 2017/2018 influenza epidemic in the Netherlands: potential implications for the COVID-19 pandemic. J Intellect Disabil Res. 2020;64:482–8. https://doi.org/10.1111/jir.12739
18. Krahn GL, Hammond L, Turner A. A cascade of disparities: health and health care access for people with intellectual disabilities. Ment Retard Dev Disabil Res Rev. 2006;12:70–82. https://doi.org/10.1002/mrdd.20098
19. Clift AK, Coupland CAC, Keogh RH, Diaz-Ordaz K, Williamson E, Harrison EM, et al. Living risk prediction algorithm (QCOVID) for risk of hospital admission and mortality from coronavirus 19 in adults: national derivation and validation cohort study. BMJ. 2020;371:m3731. https://doi.org/10.1136/bmj.m3731
20. Gleason J, Ross W, Fossi A, Blonsky H, Tobias J, Stephens M. The devastating impact of Covid-19 on individuals with intellectual disabilities in the United States. NEJM Catal. 2021;2:1–12. https://doi.org/10.1056/CAT.21.0051
21. Henderson A, Fleming M, Cooper SA, Pell JP, Melville C, Mackay DF, et al. COVID-19 infection and outcomes in a population-based cohort of 17,203 adults with intellectual disabilities compared with the general population. J Epidemiol Community Health. 2022;76:550–5. https://doi.org/10.1136/jech-2021-218192
22. Turk MA, Landes SD, Formica MK, Goss KD. Intellectual and developmental disability and COVID-19 case-fatality trends: TriNetX analysis. Disabil Health J. 2020;13:100942. https://doi.org/10.1016/j.dhjo.2020.100942
23. Shankar R, Perera B, Roy A, Courtenay K, Laugharne R, Sivan M. Post-COVID syndrome and adults with intellectual disability: another vulnerable population forgotten? Br J Psychiatry. 2022;1–3:1–3. https://doi.org/10.1192/bjp.2022.89
24. Statistics Netherlands. Persons eligible for ID care 2020 [cited 2021 Jul 15]. https://www.monitorlangdurigezorg.nl/kerncijfers/indicatie
25. Rijksinstituut voor Volksgezondheid en Milieu (RIVM). Dataset: COVID-19 numbers per municipality per publication date [in Dutch]. Bilthoven: RIVM; 2021.
26. Rijksinstituut voor Volksgezondheid en Milieu. Coronavirus, COVID-19 [in Dutch] [cited 2021 July 15]. https://www.rivm.nl/en/coronavirus-covid-19
27. Joy M, Hobbs FR, Bernal JL, Sherlock J, Amirthalingam G, McGagh D, et al. Excess mortality in the first COVID pandemic peak: cross-sectional analyses of the impact of age, sex, ethnicity, household size, and long-term conditions in people of known SARS-CoV-2 status in England. Br J Gen Pract. 2020;70:e890–8. https://doi.org/10.3399/bjgp20X713393

Address for correspondence: Monique Koks-Leensen, Radboud University Medical Center, Radboud Institute for Health Sciences, Department of Primary and Community Care–Intellectual Disabilities and Health, PO Box 9101, 6500 HB, Nijmegen, the Netherlands; email: Monique.Koks-Leensen@radboudumc.nl

Effects of Second Dose of SARS-CoV-2 Vaccination on Household Transmission, England

Asad Zaidi, Ross Harris, Jennifer Hall, Sarah Woodhall, Nick Andrews, Kevin Dunbar, Jamie Lopez-Bernal, Gavin Dabrera

A single SARS-CoV-2 vaccine dose reduces onward transmission from case-patients. We assessed the potential effects of receiving 2 doses on household transmission for case-patients in England and their household contacts. We used stratified Cox regression models to calculate hazard ratios (HRs) for contacts becoming secondary case-patients, comparing contacts of 2-dose vaccinated and unvaccinated index case-patients. We controlled for age, sex, and vaccination status of case-patients and contacts, as well as region, household composition, and relative socioeconomic condition based on household location. During the Alpha-dominant period, HRs were 0.19 (0.13–0.28) for contacts of 2-dose BNT162b2-vaccinated case-patients and 0.54 (0.41–0.69) for contacts of 2-dose Ch4dOx1-vaccinated case-patients; during the Delta-dominant period, HRs were higher, 0.74 (0.72–0.76) for BNT162b2 and 1.06 (1.04–1.08) for Ch4dOx1. Reduction of onward transmission was lower for index case-patients who tested positive ≥2 months after the second dose of either vaccine.

Observational studies conducted in several countries including Qatar (*1*) and the United Kingdom (*2*) have demonstrated that SARS-CoV-2 vaccination provides protection against symptomatic infection, hospitalization, and death. The role of SARS-CoV-2 vaccination in preventing transmission from persons with confirmed infection to others has also been demonstrated previously using household contacts as a high-risk exposure group (*3*,*4*). Previous work conducted in England in early 2021 using the Household Transmission Evaluation Dataset (HOSTED) identified reduced odds of infection among unvaccinated household contacts of vaccinated cases compared with those for unvaccinated household contacts of unvaccinated cases (*3*). We studied the period in which the interval between vaccine doses for adults was as long as 12 weeks when the national program could focus on rapidly establishing maximum single-dose coverage for the population (*5*). Consequently, most adults had received 1 dose of vaccine and the available information was insufficient to investigate whether additional doses of vaccine might yield further benefits in reducing transmission. In that period, the Alpha variant emerged and rapidly became the dominant SARS-CoV-2 variant in England; household transmission was greater than that of previously circulating SARS-CoV-2 (*6*). Since then, the epidemiologic situation has changed significantly with the emergence of new variants, the expansion of the national vaccine rollout program and subsequent increase in population coverage of second and booster doses, and changes to public health measures. Those factors all underline the need for further investigation and analysis. The objective of our study was to expand our initial assessment of the effect of SARS-CoV-2 vaccine on transmission to household contacts to include 2 doses of vaccine and incorporate the period dominated by the Delta variant.

Methods

Dataset Creation

The creation of the routine HOSTED dataset has been described in detail (*3*,*7*). In brief, test-confirmed cases of COVID-19 in England are reported to national laboratory surveillance systems (*8*). During the period studied, the widely used assays were the reverse transcription PCR (RT-PCR) and the lateral flow device (LFD) test; national requirements to confirm a positive LFD test with a RT-PCR test and the presence of

Author affiliations: COVID-19 Vaccines and Epidemiology Division—UK Health Security Agency, London, UK (A. Zaidi, J. Hall, S. Woodhall, G. Dabrera); Statistics, Modelling, and Economics Department—UK Health Security Agency (R. Harris, N. Andrews); Institute for Women's Health, University College, London (J. Hall); Immunisation and Countermeasures Division—UK Health Security Agency (K. Dunbar, J. Lopez-Bernal)

DOI: https://doi.org/10.3201/eid2901.220996

a negative confirmatory RT-PCR removed the initial positive tests from the data. Reported cases are linked to a Unique Property Reference Number (UPRN) via healthcare records associated with their National Health Service (NHS) number. The UPRN is an identifier allocated to each dwelling in England and can be used to assess property class (residential, commercial, etc.) and property type (flat, semi-detached, terraced, etc.). The cases' UPRNs are then used to extract data on persons who share the same residence and may or may not themselves be cases.

Because the aim of our analysis was to estimate effects on transmission within the most common residential household groupings, we included only residential dwellings that had 2–10 residents in the dataset. We excluded single-resident households, households with >10 residents, and known institutional settings such as care homes and prisons.

We linked the HOSTED dataset with data from the National Immunisation Management System (*9*) in England to obtain information for all persons within the cohort on the dates and types of COVID-19 vaccination doses administered. The final dataset included specimen dates of cases; individual-level sociodemographic data for case-patients and those listed as residing alongside case-patients, including age and sex; household-level sociodemographic data such as Index of Multiple Deprivation (IMD), household size, and property type; individual-level outcome information on hospitalizations and deaths; and individual-level vaccination information on the date and type (ChAdOx1 [AstraZeneca, https://www.astrazeneca.com], BNT162b2 [Pfizer-BioNTech, https://www.pfizer.com], or mRNA-1273 [Moderna, https://www.modernatx.com]) of first and second doses for all vaccinated persons in the dataset.

Definitions

Using the chronology of specimen dates within each household, we defined index cases as the earliest case of test-confirmed COVID-19 for a household. We defined household contacts as all persons registered to live at the same UPRN as each index case of COVID-19. We defined secondary cases as a known household contact of an index case who had a positive SARS-CoV-2 test with a specimen date 2–14 days after the specimen date of the index case.

We included contacts of index cases with a specimen date of February 1, 2021–September 13, 2021 in the analysis. We excluded households in which transmission patterns were likely different from household transmission in the community: households in which the index case was tested in the UK's Pillar 1 system, which historically consists predominantly of hospital-based testing; households in which the index case was <16 years of age and ineligible for vaccination during the period studied; households with vulnerable residents who were vaccinated before the general rollout in the United Kingdom (January 4, 2021); and households with multiple index cases or co-primary cases.

We restricted our analysis to index cases and contacts with a clearly-defined vaccination status: unvaccinated persons who had not received any vaccine before the index case date and fully vaccinated persons who had received 2 doses of vaccine, the second dose ≥14 days before the index case date. Thus, we excluded all persons with 1 dose or other partial protection from the vaccine-related analysis, although we counted them in the definition of household size and composition variables. The period of study preceded the rollout of booster doses for the population by age criteria, which began in September 2021 for adults in risk groups and those ≥50 years of age and opened to all adults in November 2021.

Statistical Analysis

We analyzed data in a time-to-event framework with household contacts at risk of being a secondary case 2–14 days after the specimen date of the index case. The main variable of interest was the vaccination status of the index case; we calculated adjusted hazard ratios for contacts of index cases who had received 2 vaccine doses versus contacts of unvaccinated index cases.

We fitted stratified Cox regression models with age of index case, age of contact, household type/size, region, and vaccination status of contact as strata variables. We adjusted for week of index case specimen date, deprivation (IMD quintile), sex of index case, and sex of contact. We fitted models separately to each calendar month of data, February–September 2021, and in 2 broad periods, Alpha-dominant (February–May 2021) and Delta-dominant (June–September 2021).

We conducted 2 sensitivity analyses. The first included unvaccinated contacts only, as in previous analyses (*3*), to enable us to compare our findings with earlier estimates. The second excluded any persons (index cases or contacts) still unvaccinated as of September 13, 2021, when all the adult population would have been eligible and had the opportunity to be vaccinated, to exclude potential biases in case ascertainment for this group. We also obtained estimates from an unstratified cohort model, and included these strata variables as adjustment variables in the model.

In addition, we extended the base model to consider effect modification by dose interval, time since vaccination, and age. First, we divided the interval between first and second doses in the index case into 3 categories: <6 weeks, 6–10 weeks, and >10 weeks. We defined time since vaccination by 30-day categories (<30 days, 30–59, 60–89, 90–119, 120–149, and ≥150 days from second dose of index case vaccination to index case date) and compared vaccine transmission effects by both calendar time and time since vaccination. Finally, we considered the effect of age by estimating a separate vaccination transmission effect for each age group. We assessed extensions to the model via likelihood ratio tests.

Results

The initial dataset comprised 1,779,448 index cases from 1,535,288 unique households, and 4,110,051 contacts. For those households in which transmission patterns were likely different from household transmission in the community, and to maintain comparability to the earlier analysis, we applied exclusions in 2 steps, first at the household level, and then at the individual level. For the first step we applied overlapping criteria, excluding households with index cases in children (n = 1,265,196 persons), with residents tested in pillar 1 (n = 99,627), with co-primary index cases (n = 785,669), and with residents who were vaccinated ahead of the national rollout (before January 2021; n = 194,160), leaving 1,035,271 index cases or households and 2,818,017 contacts. For the second step, we excluded persons with indeterminate vaccine status, after which there were 606,720 index cases and 1,440,269 contacts in the analysis dataset. Characteristics of contacts excluded through specific criteria compared with those excluded for indeterminate vaccination status of household members were similar in age, IMD, and geography (Appendix Table 1, https://wwwnc.cdc.gov/EID/article/29/1/22-0996-App1.pdf); the main difference appeared to be an increased proportion of secondary cases in households with multiple index cases.

The median age of index cases was 35 (IQR 25–50) years, and of contacts, 32 (IQR 13–52) years. We restricted index cases to those ≥16 years of age and eligible for vaccination, whereas we included all contacts. The proportion of female participants was 50.5% in index cases and 49.4% in contacts. We included 122,423 (8.5%) secondary cases among contacts (Appendix Table 2). During February–May 2021, proportions of secondary cases were highest in household contacts of unvaccinated index cases. However, proportions increased in contacts of index cases vaccinated with ChAdOx1 and BNT162b2 vaccines over time. From June onwards, these were highest among contacts of index cases who had received ChAdOx1 vaccine. Proportions of secondary cases among contacts of index cases receiving mRNA-1273 vaccine were consistently low, although data were sparse.

We estimated a strong protective effect for ChAdOx1 vaccine (HR 0.54, 95% CI 0.41–0.69) (Table) and a very strong effect for BNT162b2 vaccine (HR 0.19, 95% CI 0.13–0.28) in the February–May period, which persisted under different inclusion criteria and models. However, we estimated that in June–September the ChAdOx1 vaccine had minimal effect except in model D (Table), which included only unvaccinated contacts, and the protective effect of BNT162b2 vaccine was attenuated (HR 0.74, 95% CI 0.72–0.76). Estimates for mRNA-1273 vaccine, for which there were data only in June–September, were strongly protective.

We estimated the effect of index case vaccination over time and according to time since index case vaccination (Figure). For BNT162b2 vaccine, we noted strong protective effects up to 2 months after the index case was vaccinated, but hazard ratios were attenuated toward the null from 2–3 and 3–4 months after vaccination, particularly in August and September. The pattern of decreasing effect with time since index case vaccination was less clear for ChAdOx1 vaccine; we estimated little protective effect even soon after vaccination from June onwards. Estimates crossed the null to indicate an apparent increased risk of being a

Table. Adjusted hazard ratios for household contacts of persons with COVID becoming a secondary case by inclusion criteria for different models

		Analysis model HR (95% CI)				
Period	Vaccine	A, never vaccinated	B, not vaccinated before index case	C, vaccinated after index case	D, unvaccinated contacts only	E, cohort
Feb-May	ChAdOx1	0.54 (0.41–0.69)	0.50 (0.38–0.64)	0.50 (0.38–0.65)	0.48 (0.37–0.64)	0.53 (0.43–0.66)
	BNT162b2	0.19 (0.13–0.28)	0.18 (0.12–0.26)	0.18 (0.12–0.26)	0.14 (0.09–0.23)	0.19 (0.13–0.26)
Jun-Sep	ChAdOx1	1.06 (1.04–1.08)	1.06 (1.04–1.08)	0.94 (0.88–1.00)	0.84 (0.76–0.92)	1.08 (1.06–1.10)
	BNT162b2	0.74 (0.72–0.76)	0.74 (0.73–0.76)	0.66 (0.62–0.71)	0.56 (0.51–0.62)	0.76 (0.74–0.78)
	mRNA-1273	0.36 (0.29–0.45)	0.36 (0.29–0.45)	0.31 (0.25–0.39)	0.30 (0.22–0.40)	0.38 0.30–0.47)

*For models A–D, we used a stratified Cox model with adjustment, and different inclusion criteria for contacts and of the baseline group of contacts of unvaccinated index cases. Model E has the same inclusion criteria as model A, but uses a cohort model with all covariates entered as adjustment variables, rather than stratification. HR, hazard ratio.

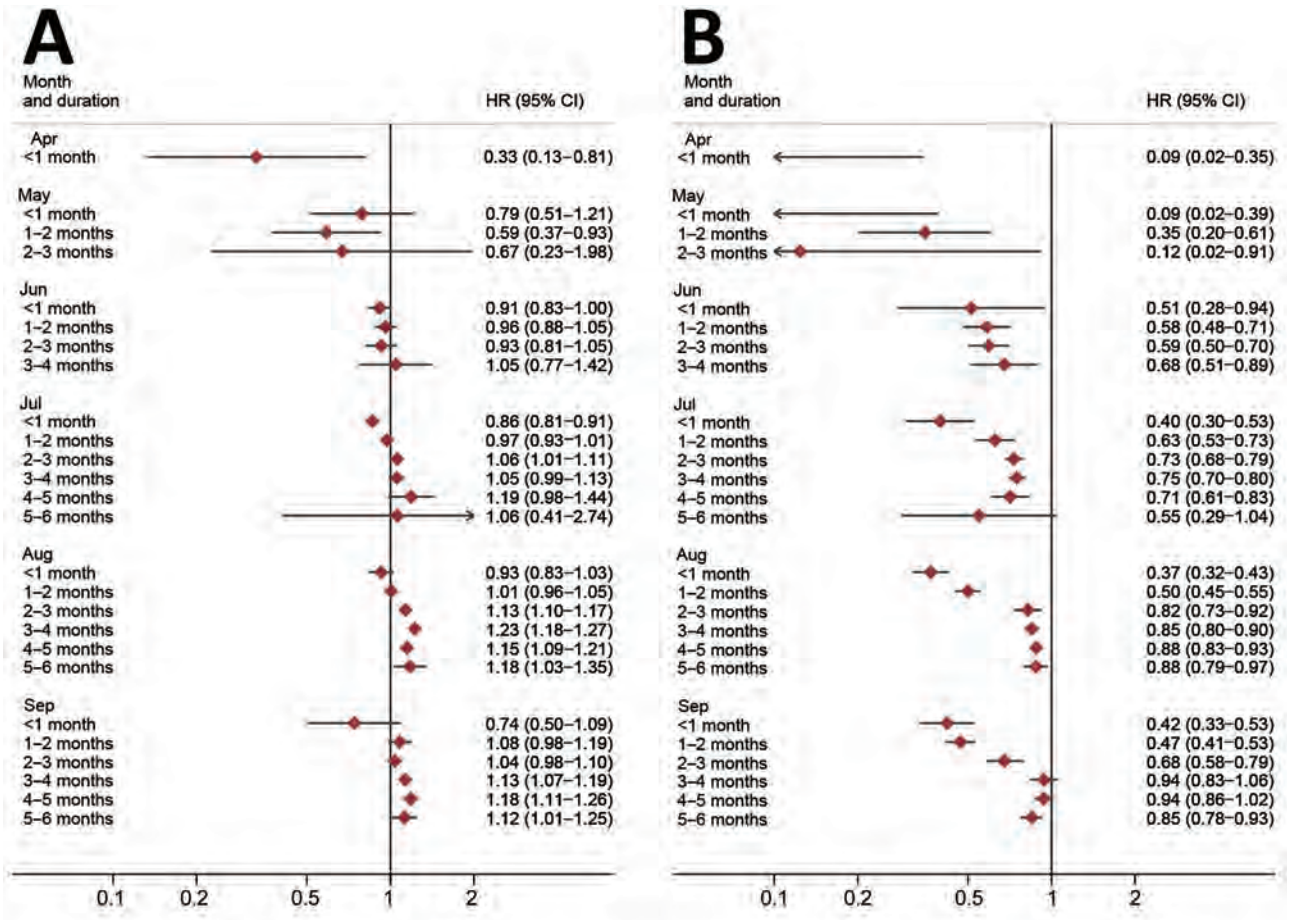

Figure. Adjusted hazard ratios for household contacts of COVID patients becoming secondary cases by calendar time and time since vaccination of the index case. A) Data for contacts of index cases who had ChAdOx1 vaccine (AstraZeneca, https://www.astrazeneca.com). B) Data for contacts of index cases who had BNT162b2 vaccine (Pfizer-BioNTech, https://www.pfizer.com). HR, hazard ratio.

secondary case in August–September for contacts of index cases who had received ChAdOx1 vaccine, compared with contacts of unvaccinated index cases.

Discussion

This analysis provides evidence that persons who have received ≥2 doses of vaccine ≥14 days before testing positive for SARS-CoV-2 infection had a reduced likelihood for onward transmission to household contacts in February–May 2021, the period in which Alpha variant was dominant. Of note, this reduction was smaller for BNT162b2 vaccine and all but disappeared for ChAdOx1 vaccine during the subsequent June–September 2021 period, when the Delta variant dominated England. ChAdOx1 vaccine showed reduction in onward transmission only in household contacts who were completely unvaccinated. This is consistent with observations of reduced vaccine effectiveness against symptomatic disease for confirmed cases of Delta infection compared with Alpha (*2*,*10*–*12*).

mRNA-1273 vaccine played a smaller role in the initial vaccination rollout of primary courses, so we could only analyze the effects of the vaccine during the latter half of the study period. However, we noted a large and sustained reduction in household transmission in addition to the direct protection of the vaccines in preventing index cases initially and therefore potential for transmission. We also demonstrated a differential reduction in the likelihood of household transmission that is based on the type of vaccine. During the period of Delta dominance, mRNA-1273 vaccine had the greatest association with reduced likelihood of household transmission, followed by BNT162b2 vaccine and then ChAdOx1 vaccine. This finding was consistent with observations of higher vaccine effectiveness with mRNA-1273 and BNT162b2 vaccines compared with ChAdOx1 vaccine for the prevention of symptomatic infection in confirmed Delta variant infections (*2*). This triangulation with observations from other analyses of protection

from disease (*2*) provides further evidence of a differential effect by vaccine for Delta variant cases.

Our work supplements the growing body of evidence related to waning of vaccine-driven protection. Previous analyses have shown reduced protection of persons from symptomatic infection (*10*,*11*). Our findings support another dimension to the waning effectiveness of vaccines: an attenuation in the reduction of onward transmission from index cases vaccinated with Ch4dOx1 and BNT162b2 vaccines to their household contacts (*13*). We observed this effect for vaccinated index cases who tested positive for COVID-19 ≥2 months after receiving their second dose. Hazard ratios for becoming a secondary case increased among household contacts of those case-patients, compared with the contacts of index cases who had a shorter interval between their vaccination and confirmed infection. The protective effect against onward transmission conferred by ChAdOx1 vaccine was initially smaller than that for BNT162b2 vaccine and diminished to no effect as time since second dose increased. The protective effect conferred by BNT162b2 vaccine, despite also reducing over time, did not fully disappear. Waning among index cases receiving mRNA-1273 vaccine could not be analyzed in this way because this vaccine was rolled out later in England.

This waning effect was more consistently observed from July 2021 onward, before which the effect was present but less apparent. Early July 2021 demarcates the transition between periods of Alpha and Delta variant dominance in England, suggesting a potential intrinsic difference between the variants and related protection from the vaccine (*13*).

Because vaccination programs have evolved internationally to provide boosters to vulnerable groups, we may observe a temporary reversal of the waning protection against onward transmission from cases to others. However, this effect requires further evaluation; factors such as time interval between doses, prevalent variants, and vaccine types could all influence any potentially observed effects. Such evaluation would be informative for future assessments of the overall effects of booster programs and therefore influence decision making.

The HOSTED analysis benefits from its very large number of cases and their contacts obtained from data for all reported test-confirmed cases in England; the dataset provides substantial sample sizes that enable large-scale monitoring of secondary infections without specialized data collection. In addition, we conducted several sensitivity analyses, which produced consistent and convergent results. However, the tradeoff is that passive surveillance systems are reliant on testing behaviors instead of targeted case-finding. In passive surveillance, chains of onward household transmission may be missed where contacts did not test, and the secondary attack rate would be underestimated as a result. These missed chains of transmission would be disproportionately present in households where access to testing is lower because of circumstance or choice. This result might explain our observation that contacts of index cases vaccinated with ChAdOx1 with a vaccination-infection interval of ≥3 months since their second dose had an apparent increase in risk compared with contacts of unvaccinated index cases in August–September 2021. Although vaccination might not reduce onward transmission, increased infectivity caused by vaccination does not appear biologically plausible. This increased risk for infection in the contacts of vaccinated index cases likely indicates differential case ascertainment or risk behaviors between vaccinated and unvaccinated groups, demonstrating a limitation of passive surveillance data.

Without specialized data collection, we were limited by the lack of information on symptoms and case severity, both of which may affect the likelihood of onward transmission (*14*). As such, our analyses treated all test-confirmed infections uniformly; the granularity that symptom and severity data provide could have highlighted subpopulations for which the vaccine-induced reduction of household transmission was more or less noticeable than for the overall population.

The logic underpinning how cases in a household are classified as index or secondary cases is rooted in the intervals between specimen dates, an approach already established in published analyses. However, the use of symptom onset dates may be more optimal, with symptom onset dates potentially being less affected by behavior and health service access than specimen collection dates.

In conclusion, receipt of 2 doses of mRNA vaccines among index cases reduced transmission to unvaccinated household contacts during a period in which the Delta variant dominated, compared with the Alpha-dominant periods, during which a single dose of mRNA or ChAdOx1 vaccine provided equivalent reductions in transmission. We also observed waning of this protective effect over time since the last dose of vaccine administered. These findings highlight the potential variation in protection from vaccines in relation to transmission effects that are caused by emerging variants and waning protection, and the importance of monitoring the effects of these factors for future SARS-CoV-2 vaccine strategies.

Acknowledgments

We thank the Second Generation Surveillance System Team at UKHSA, especially Anne-Marie O'Connell and Daniel West, and our collaborators at NHS Digital, particularly Heather Pinches, Phillip Bowker, and Paul Ellingham, without whom the HOSTED dataset would not exist. We also thank the COVID-19 Vaccine Effectiveness Working Group for preliminary input into this analysis.

About the Author

Mr. Zaidi is an epidemiologist with the UK Health Security Agency. His primary interest is in surveillance systems for respiratory and emerging infectious diseases.

References

1. Abu-Raddad LJ, Chemaitelly H, Butt AA; National Study Group for COVID-19 Vaccination. Effectiveness of the BNT162b2 COVID-19 vaccine against the B.1.1.7 and B.1.351 variants. N Engl J Med. 2021;385:187–9. https://doi.org/10.1056/NEJMc2104974
2. Lopez Bernal J, Andrews N, Gower C, Gallagher E, Simmons R, Thelwall S, et al. Effectiveness of COVID-19 vaccines against the B.1.617.2 (Delta) variant. N Engl J Med. 2021;385:585–94. https://doi.org/10.1056/NEJMoa2108891
3. Harris RJ, Hall JA, Zaidi A, Andrews NJ, Dunbar JK, Dabrera G. Effect of vaccination on household transmission of SARS-CoV-2 in England. N Engl J Med. 2021;385:759–60. https://doi.org/10.1056/NEJMc2107717
4. Hart WS, Miller E, Andrews NJ, Waight P, Maini PK, Funk S, et al. Generation time of the alpha and delta SARS-CoV-2 variants: an epidemiological analysis. Lancet Infect Dis. 2022;22:603–10. https://doi.org/10.1016/S1473-3099(22)00001-9
5. Joint Committee on Vaccination and Immunisation. Advice on priority groups for COVID-19 vaccination, 30 December 2020. 2020 [cited 23 May 2022]. https://www.gov.uk/government/publications/priority-groups-for-coronavirus-covid-19-vaccination-advice-from-the-jcvi-30-december-2020/joint-committee-on-vaccination-and-immunisation-advice-on-priority-groups-for-covid-19-vaccination-30-december-2020
6. Chudasama DY, Flannagan J, Collin SM, Charlett A, Twohig KA, Lamagni T, et al. Household clustering of SARS-CoV-2 variant of concern B.1.1.7 (VOC-202012-01) in England. J Infect. 2021;83:e26–8. https://doi.org/10.1016/j.jinf.2021.04.029
7. Hall JA, Harris RJ, Zaidi A, Woodhall SC, Dabrera G, Dunbar JK. HOSTED-England's Household Transmission Evaluation Dataset: preliminary findings from a novel passive surveillance system of COVID-19. Int J Epidemiol. 2021;50:743–52. https://doi.org/10.1093/ije/dyab057
8. Clare T, Twohig KA, O'Connell A-M, Dabrera G. Timeliness and completeness of laboratory-based surveillance of COVID-19 cases in England. Public Health. 2021;194:163–6. https://doi.org/10.1016/j.puhe.2021.03.012
9. Tessier E, Rai Y, Clarke E, Lakhani A, Tsang C, Makwana A, et al. Characteristics associated with COVID-19 vaccine uptake among adults aged 50 years and above in England (8 December 2020–17 May 2021): a population-level observational study. BMJ Open. 2022;12:e055278. https://doi.org/10.1136/bmjopen-2021-055278
10. Chemaitelly H, Tang P, Hasan MR, AlMukdad S, Yassine HM, Benslimane FM, et al. Waning of BNT162b2 vaccine protection against SARS-CoV-2 infection in Qatar. N Engl J Med. 2021;385:e83. https://doi.org/10.1056/NEJMoa2114114
11. Singanayagam A, Hakki S, Dunning J, Madon KJ, Crone MA, Koycheva A, et al. Community transmission and viral load kinetics of the SARS-CoV-2 Delta (B.1.617.2) variant in vaccinated and unvaccinated individuals in the UK: a prospective, longitudinal, cohort study. Lancet Infect Dis. 2021;21:183–95. https://doi.org/10.1016/S1473-3099(21)00648-4
12. Lopez Bernal J, Andrews N, Gower C, Robertson C, Stowe J, Tessier E, et al. Effectiveness of the Pfizer-BioNTech and Oxford-AstraZeneca vaccines on COVID-19–related symptoms, hospital admissions, and mortality in older adults in England: test negative case–control study. BMJ. 2021;373:n1088. https://doi.org/10.1136/bmj.n1088
13. Eyre DW, Taylor D, Purver M, Chapman D, Fowler T, Pouwels KB, et al. Effect of COVID-19 vaccination on transmission of Alpha and Delta variants. N Engl J Med. 2022;386:744–56. https://doi.org/10.1056/NEJMoa2116597
14. Jajou R, Mutsaers-van Oudheusden A, Verweij JJ, Rietveld A, Murk JL. SARS-CoV-2 transmitters have more than three times higher viral loads than non-transmitters - Practical use of viral load for disease control. J Clin Virol. 2022;150-151:105131. https://doi.org/10.1016/j.jcv.2022.105131

Address for correspondence: Gavin Dabrera, COVID-19 Vaccines and Epidemiology Division, UK Health Security Agency, Colindale, 61 Colindale Ave, London NW9 5EQ, UK; email: feedback.c19epi@ukhsa.gov.uk

COVID-19 Booster Dose Vaccination Coverage and Factors Associated with Booster Vaccination among Adults, United States, March 2022

Peng-jun Lu, Anup Srivastav, Kushagra Vashist, Carla L. Black, Jennifer L. Kriss, Mei-Chuan Hung, Lu Meng, Tianyi Zhou, David Yankey, Nina B. Masters, Hannah E. Fast, Hilda Razzaghi, James A. Singleton

The Centers for Disease Control and Prevention recommends a COVID-19 vaccine booster dose for all persons ≥18 years of age. We analyzed data from the National Immunization Survey–Adult COVID Module collected during February 27–March 26, 2022 to assess COVID-19 booster dose vaccination coverage among adults. We used multivariable logistic regression analysis to assess factors associated with vaccination. COVID-19 booster dose coverage among fully vaccinated adults increased from 25.7% in November 2021 to 63.4% in March 2022. Coverage was lower among non-Hispanic Black (52.7%), and Hispanic (55.5%) than non-Hispanic White adults (67.7%). Coverage was 67.4% among essential healthcare personnel, 62.2% among adults who had a disability, and 69.9% among adults who had medical conditions. Booster dose coverage was not optimal, and disparities by race/ethnicity and other factors are apparent in coverage uptake. Tailored strategies are needed to educate the public and reduce disparities in COVID-19 vaccination coverage.

A COVID-19 vaccine booster dose is intended to boost the immune system for better, long-lasting protection when the primary vaccine response decreases over time. Studies have shown that a booster increased the immune response in trial participants who completed a Pfizer-BioNTech (https://www.pfizer.com) or Moderna (https://www.modernatx.com) primary series 6 months earlier or who received a Johnson & Johnson/Janssen (https://www.jnj.com) single-dose vaccine 2 months earlier (*1*,*2*).

With an increased immune response, booster doses provide additional protection against both Delta and Omicron variants for clinical COVID-19 emergency department visits and hospitalization even for those persons who have received an initial vaccine series (*1*,*3*). For example, the mRNA vaccine effectiveness (VE) against emergency room visits during the period of Delta predominance was 76%–86% after the second initial dose and 94% after a booster dose; estimates of VE during Omicron variant predominance were 38%–52% after the second initial dose and 82% after a booster dose. VE against hospitalizations during the period of Delta predominance was 81%–90% after the second initial dose and 94% after a booster dose, and estimates of VE for during Omicron variant predominance were 57%–81% after the second initial dose and 90% after a booster dose (*3*).

The Centers for Diseases Control and Prevention (CDC) first recommended booster doses for select populations in September 2021 and on November 29, 2021, recommended that all persons ≥18 years of age should get a booster dose when eligible (*1*,*2*). By March 2022, approximately 84% of American adults were fully vaccinated with the COVID-19 primary vaccine series; primary vaccine series completion rates varied by some social–demographic characteristics (*4*). Receiving a COVID-19 booster dose is useful both to prevent COVID-19-related illness and death and slow the spread of COVID-19 in the United States. The objective of this study was to assess COVID-19 booster dose vaccination coverage by demographics and behaviors and experiences

Author affiliations: Centers for Disease Control and Prevention, Atlanta, Georgia, USA (P.-j. Lu, A. Srivastav, K. Vashist, C.L. Black, J.L. Kriss, M.-C. Hung, L. Meng, T. Zhou, D. Yankey, N.B. Masters, H.E. Fast, H. Razzaghi, J.A. Singleton); Leidos Inc., Atlanta (A. Srivastav, M.-C. Hung, T. Zhou); Oak Ridge Institute for Science and Education, Oak Ridge, Tennessee, USA (K. Vashist)

DOI: https://doi.org/10.3201/eid2901.221151

toward vaccination among fully vaccinated adults by using data from the National Immunization Survey–Adult COVID Module (NIS-ACM) (*5*).

Methods

We collected the NIS-ACM data used in this report by telephone interview among adults ≥18 years of age by using a random-digit–dialed sample of cell telephone numbers.

Data were collected during February 27–March 26, 2022. Trend analysis was based on data collected during October 31, 2021–March 26, 2022. Booster dose was defined as receipt of a third dose of COVID-19 vaccine after completion of a 2-dose primary mRNA COVID-19 vaccine series for adults who are not immunocompromised or a fourth dose of COVID-19 vaccine after completion of a 3-dose mRNA COVID-19 vaccine series for adults who reported being immunocompromised. For respondents whose initial vaccine was a Janssen/Johnson & Johnson vaccine, booster dose was defined as receipt of a second dose of the vaccine after completion of a single-dose primary vaccine series for adults who are not immunocompromised or a third dose of Janssen vaccine after completion of 2-dose series for adults who reported being immunocompromised (*1*,*2*). Receipt of a booster dose of COVID-19 vaccine was based on responses to the questions, "Have you received at least one dose of a COVID-19 vaccine?," "Which brand of COVID-19 vaccine did you receive for your first dose?," "How many doses of a COVID-19 vaccine have you received?," and self-reported health conditions that may put respondents at higher risk for COVID-19 (including immunocompromised status).

Survey questions also collected information on vaccine confidence, behaviors, and experiences, such as being concerned about getting COVID-19, thinking COVID-19 vaccines are safe, believing COVID-19 vaccines are useful for protection from COVID-19, whether friends or family were vaccinated, and whether the respondent had difficulty getting a COVID-19 vaccine (e.g., difficulty getting an appointment online, knowing where to get vaccinated, getting to vaccination sites). Information on demographic characteristics, health insurance status, reported medical conditions, previous diagnosis of COVID-19, disability status, frontline/essential work status, provider recommendation of a COVID-19 vaccine, and work/school COVID-19 vaccination requirement were also collected (*6*). Questions regarding vaccine confidence, behaviors, and experiences did not specifically address booster doses. Analytic datasets were created for approximate months of data collection, and we used data from 5 data collection periods (November 2021, collected during October 31–November 27; December 2021, collected during November 28–December 31; January 2022, collected during January 2–January 29; February 2022, collected during January 30–February 26; and March 2022, collected during February 27–March 26) for these analyses. The response rates for the 5 monthly datasets ranged from 21.4% to 22.0%, and the total sample sizes for the 5 periods were 39,508, 68,612, 62,693, 58,488, and 63,072, respectively.

We stratified COVID-19 booster dose vaccination coverage by using demographic characteristics and vaccine confidence, behaviors, and experiences. Race/ethnicity was classified as non-Hispanic White, non-Hispanic Black, Hispanic, non-Hispanic Asian, non-Hispanic American Indian/Alaska Native, non-Hispanic Native Hawaiian/Pacific Islander, or other/multiple races. Urbanicity status was derived based on the centroid of the postal code of residence, categorized as metropolitan statistical area (MSA) principal city, MSA nonprincipal city, or non-MSA. Social vulnerability index (SVI) was categorized as low, moderate, or high based on county of residence (CDC/Agency for Toxic Substances and Disease Registry) by using tertiles of SVI score (*7*).

We analyzed data by using SAS version 9.4 (https://www.sas.com) and SUDAAN version 11.0.1 (https://www.rti.org). We weighted all percentages to represent the noninstitutionalized US adult population and calibrated survey weights by age and sex to state-level vaccine administration data reported to CDC as of the middle of the monthly data collection period (*6*). We conducted multivariable logistic regression analysis and predictive marginals to assess factors associated with receipt of a booster dose among adults and generated the unadjusted prevalence ratio (PR) and the adjusted prevalence ratio (aPR) from regression models. We used PR to assess association instead of odds ratio [OR] in our analysis because PR is a more direct measure of effect than OR, and when outcomes are not rare, as with most of vaccination coverage analysis, the OR tends to present an exaggerated measure of effect compared with the PR. We used t-tests to determine differences between groups with statistical significance at $p<0.05$ and for linear trends over months. This activity was reviewed by CDC and was conducted consistent with applicable federal law and CDC policy (45 C.F.R. part 46.102(l)(2), 21 C.F.R. part 56; 42 U.S.C. §241(d); 5 U.S.C. §552a; 44 U.S.C. §3501).

Results

COVID-19 booster dose coverage among fully vaccinated adults ≥18 years of age increased from 25.7%

in November 2021 to 63.4% in March 2022 (p<0.05 by test for trend) (Figure). Coverage in mid-March 2022 among those 50–64 years of age (66.4%) and ≥65 years of age (79.5%) was higher than among those 18–49 years of age (53.6%) (Table 1, https://wwwnc.cdc.gov/EID/article/29/1/22-1151-T1.htm). By mid-March 2022, booster dose coverage was 52.8% among all adults ≥18 years of age (including unvaccinated adults in the denominator), and coverage among those 50–64 years of age (58.5%) and ≥65 years of age (77.0%) was higher than among those 18–49 years of age (40.6%).

Among fully vaccinated adults ≥18 years of age, booster dose coverage in mid-March 2022 was lower among Native Hawaiian/Pacific Islander (45.4%), Black (52.7%), Other/multiple races (54.1%), Hispanic (55.5%), and American Indian/Alaska Native (56.6%) than among White adults (67.7%); Asian adults had the highest coverage (74.6%) (p<0.05) (Table 1). Booster dose coverage was higher among all healthcare personnel (HCP) ≥18 years of age and among school and childcare workers 18–49 years of age than for other essential workers (Table 1).

Coverage was higher for adults who had reported medical conditions (69.9%) than in adults who did not have these conditions (60.4%). In addition, women and those who lived above the poverty level, had some college or higher education, had health insurance, and had received a vaccine other than COVID-19 in the past 2 years had higher booster vaccination coverage than did the respective reference groups (Table 1). Adults living in a moderate or high SVI county and those who had a previous COVID-19 infection had lower booster dose vaccination coverage than did the respective reference groups. Adults with disability had lower booster dose vaccination coverage than did adults without disability across age groups (18–49, 50–64, and ≥65 years of age) (Table 1). Furthermore, compared with the respective reference groups, booster dose coverage was higher among adults who reported they were concerned about getting COVID-19 (70.1% vs. 58.1%), thought the vaccine was safe (71.8% vs. 39.8%), and thought the vaccine was useful for protection from COVID-19 (67.8% vs. 22.8%). In addition, reporting little or no difficulty getting a COVID-19 vaccine was associated with decreased booster vaccination (Table 1).

In the multivariable model adjusted for demographic variables, characteristics independently associated with increased booster vaccination were older age, Asian race, household income ≥$75,000, some college or higher education, being insured, having received any vaccine that was not a COVID-19 vaccine in the past 2 years, and having reported medical conditions (Table 2, https://wwwnc.cdc.gov/EID/article/29/1/22-1151-T2.htm). In addition, for occupational categories, being an HCP, school/childcare worker, or other frontline worker, or not being an essential worker, was associated with increased booster vaccination compared with being in the category of other essential worker. Non-Hispanic Black adults, those living in a high SVI county, those living in non-MSAs, those with a disability, and those with a previous COVID-19 infection had decreased booster vaccination. For the multivariable model including demographic and behavioral variables, demographic characteristics independently associated with booster vaccination were similar to those for the model adjusted for demographic variables only. In addition, being concerned about getting COVID-19, believing the vaccine is safe, believing the vaccine is useful for protection, and having many or almost all friends and family vaccinated were independently associated with increased booster vaccination. Reporting a little

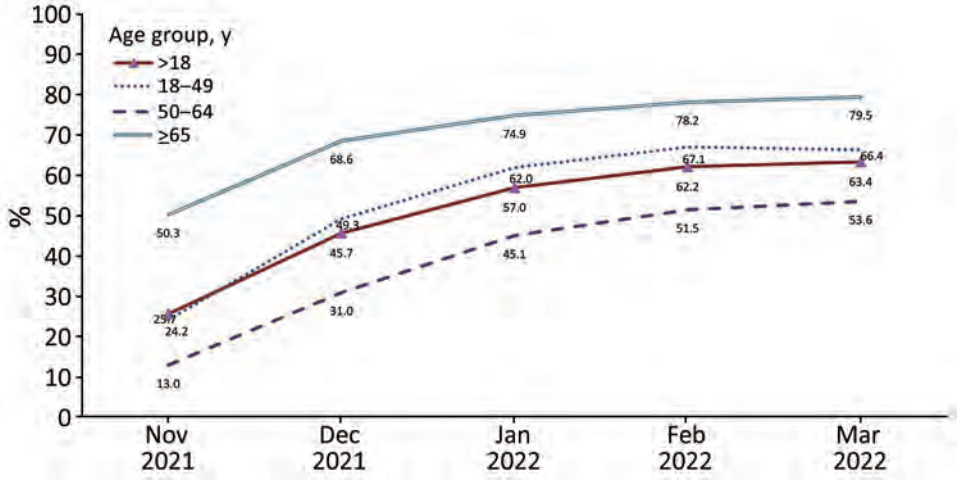

Figure. Trends in COVID-19 booster dose vaccination coverage among fully vaccinated adults, by age group, National Immunization Survey–Adult COVID Module, United States, November 2021–March 2022.

or no difficulty getting a COVID-19 vaccine was independently associated with decreased booster vaccination (Table 2).

Among adults ≥18 years of age who were fully vaccinated but did not receive a booster dose, prevalence of provider recommendation of COVID-19 vaccine was 47.9%, and prevalence was higher among adults 50–64 years of age (50.7%) than among adults 18–49 years (46.5%). Overall, 36.8% reported "being concerned about getting COVID-19," 60.6% reported "thinking the vaccine is safe," 80.5% reported "believing COVID-19 vaccine is important for protection from infection," 77.6% reported "most or almost all friends or family were vaccinated," and 31.9% reported "work or school requires COVID-19 vaccine" (Table 3). Among fully vaccinated adults who did not receive a booster dose, ≈4%–10% of adults reported difficulties in getting a COVID-19 vaccine (e.g., difficulty getting vaccinated [9.9%], difficulty getting an appointment online [9.5%], difficulty knowing where to get vaccinated [5.3%], and difficulty getting to vaccination sites [4.2%]) (Table 3).

Discussion

By March 2022, a total of 84% of American adults were fully vaccinated with the COVID-19 primary vaccine series, according to the NIS-ACM (*7*). Booster dose coverage among fully vaccinated adults ≥18 years of age was 63.4% in March 2022. Overall, ≈53% of the adult population have both received the primary series and ≥1 booster vaccination. Disparities by race/ethnicity and other factors are apparent in booster dose uptake. Healthcare providers can educate and encourage everyone to receive a booster dose when they are eligible. Targeted strategies are needed to reduce disparities in COVID-19 vaccination coverage toward reducing disparities in COVID-19.

Booster dose vaccine uptake was most strongly associated with confidence in the need for getting vaccinated, confidence in vaccine safety, and concern about getting COVID-19. Although persons were presumably amenable to getting the primary vaccine series, ≈39% of fully vaccinated adults who did not receive a booster dose did not believe COVID-19 vaccines were completely safe, and 20% did not believe they were useful for protection against COVID-19. Most fully vaccinated adults who did not receive a booster (63%) were not concerned about getting COVID-19, especially younger adults. Higher levels of concern about COVID-19 and positive attitudes toward vaccination among adults might contribute to uptake of booster dose vaccination. To further improve vaccine uptake, more innovative approaches are needed to improve vaccine confidence.

In addition, we found that reporting of family and friends being vaccinated was associated with booster dose vaccination uptake. This finding indicated the useful role of social processes for increasing vaccination (*8,9*). Community healthcare workers can educate the community about the vaccines, text persons to let them know of vaccine eligibility, use public media or social media, and encourage vaccinated

Table 3. Characteristics of persons who were fully vaccinated but did not receive booster dose vaccination, National Immunization Survey-Adult COVID Module, February 27–March 26, 2022*

Characteristic	Persons ≥18 y of age, n = 16,790	Persons 18–49 y of age, n = 9,378	Persons 50–64 y of age, n = 4,394	Persons ≥65 y of age, n = 2,767
Confidence, behavior, experience, provider recommendation, and requirement for adults fully vaccinated but who did not receive booster dose†				
Concerned about getting COVID-19, strongly or moderately	36.8 (35.3–38.4)	34.1 (32.2–36.1)	41.6 (38.4–44.9)‡	41.1 (37.2–45.2)‡
Thinks COVID-19 vaccine is safe, completely or mostly	60.6 (59.0–62.1)	60.5 (58.4–62.5)	59.5 (56.2–62.6)	64.4 (60.4–68.3)
Thinks COVID-19 vaccine is needed for protection, mostly or somewhat	80.5 (79.2–81.8)	78.9 (77.1–80.6)	82.5 (80.1–84.8)‡	84.4 (81.3–87.1)‡
Had friends/family who were vaccinated, almost all or many	77.6 (76.3–78.9)	78.6 (76.9–80.2)	76.6 (73.8–79.2)	74.4 (70.6–77.8)‡
Work or school requires COVID-19 vaccine	31.9 (30.4–33.4)	39.7 (37.7–41.7)	24.5 (21.8–27.4)‡	8.3 (6.3–10.8)‡
Provider recommendation of the COVID-19 vaccine	47.9 (46.3–49.4)	46.5 (44.5–48.5)	50.7 (47.4–53.9)‡	49.9 (45.9–54.0)
Difficulty for adults fully vaccinated but did not receive booster dose§				
Getting vaccinated, mostly or somewhat	9.9 (9.1–10.9)	9.5 (8.3–10.7)	11.2 (9.4–13.3)	9.6 (7.7–11.9)
Getting an appointment online	9.5 (8.6–10.5)	8.7 (7.6–9.8)	10.5 (8.7–12.7)	11.1 (8.6–14.2)
Not knowing where to get vaccinated	5.3 (4.7–6.1)	5.3 (4.4–6.3)	5.5 (4.3–7.0)	4.9 (3.7–6.5)
Getting to vaccination sites	4.2 (3.6–4.9)	4.3 (3.5–5.2)	4.0 (3.0–5.2)	3.9 (2.6–5.7)
Vaccination sites are not open at convenient times	5.1 (4.5– 5.7)	5.6 (4.8–6.7)	4.4 (3.5–5.5)	3.5 (2.6–4.6)‡

*Values are percentages (95% CIs). Percentages are weighted.
†Questions were asked about COVID-19 vaccination generally and not specifically about COVID-19 booster dose vaccination.
‡p<0.05 by t-test for comparisons with adults 18–49 y of age as the reference level.
§Questions were asked about difficulty getting a COVID-19 vaccination and did not ask specifically about difficulty getting a booster vaccine.

community members to share their own vaccination experiences with their unvaccinated friends and family as a means for improving COVID-19 vaccination coverage (*8*–*10*).

Our analysis did not find an association between increasing levels of difficulty accessing vaccine and lower booster dose vaccination coverage. This finding might be attributable to extensive efforts to reduce access barriers, including mobile vaccination sites, removing an insurance or identification requirement, and substantial community-led outreach (*11*–*13*). We found that persons who reported difficulty getting a COVID vaccine had higher booster dose coverage, a finding that might seem counterintuitive. However, our study assessed barriers to COVID-19 vaccination overall and not specifically for booster vaccines. Early adopters who sought vaccine at the beginning of the COVID-19 vaccination program when supply was scarce might have been more likely to experience barriers to vaccination. The finding that factors such as lower income and education were associated with lower booster uptake, even after controlling for attitudinal factors, suggests that barriers to access might remain. Among fully vaccinated adults who did not receive booster dose vaccination, ≈4%–10% of adults did report difficulties in getting a COVID-19 vaccine (e.g., difficulty getting vaccinated, getting an appointment online, knowing where to get vaccinated, or getting to vaccination sites). Understanding the barriers to vaccination can help identify strategies most likely to increase vaccine uptake. Many of these barriers could be further reduced by providing vaccination in the office of their usual medical provider (*14*,*15*). Reducing barriers to COVID-19 vaccination could further improve vaccination coverage among adults.

COVID-19 has disproportionately impacted racial and ethnic minority populations by illness, hospitalizations, and death in the United States (*16*,*17*). Although most disparities in primary COVID-19 vaccination had been eliminated by March 2022 (*7*), disparities in booster dose vaccination remain. Booster coverage was lower among all racial/ethnic groups except Asian compared with non-Hispanic White adults. Equitable vaccination can help to reduce illness-related disparities in minority groups. One study found that COVID-19 vaccine hesitancy decreased more rapidly among non-Hispanic Black than non-Hispanic White adults during December 2020–June 2021, indicating that lower coverage might be less likely the result of vaccine hesitancy than other factors (*18*). Several factors, including knowledge, attitudes, and beliefs about vaccines and barriers related to accessing vaccines and healthcare services, contribute to lower vaccination coverage in non-Hispanic Black adults and other minority groups (*18*–*21*). Tailored and community-led interventions, including postal code–level vaccination access planning and community engagement, have been shown to reduce inequities in COVID-19 vaccination by race and ethnicity (*10*,*22*,*23*). Vaccination programs could implement culturally and linguistically appropriate focused interventions among communities with lower vaccination coverage to reduce vaccination disparities.

COVID-19 booster dose vaccination coverage was particularly lower among adults living in poverty, with lower education, or without health insurance, and continued efforts are needed to reach these groups and reduce inequities (*24*–*26*). In addition, having a previous COVID-19 infection was independently associated with decreased booster vaccination. We did not assess when persons had COVID-19 in relation to the timing of the initial vaccination series or booster vaccination, but this finding might suggest that persons who have already had COVID-19 might believe that they are protected and do not need a booster. However, COVID-19 vaccines including booster doses have been shown to provide additional protection to persons who had previous infections (*27*), and all adults are recommended to receive a booster dose, regardless of previous infection with COVID-19.

Although we were unable to assess provider recommendation specifically for booster vaccination, studies have shown that a provider recommendation is highly associated with vaccine uptake (*8*,*25*,*28*). Findings from our study indicated that, among those who have not received a booster dose, >50% have not received a provider recommendation for any COVID-19 vaccine. Underuse of primary care services during the COVID-19 pandemic and some adults not having a primary physician for sick or preventive care (*29*) might have limited opportunities for providers to convey recommendations and communicate with patients the benefits of primary and booster dose vaccination and information on the safety and effectiveness of COVID-19 vaccination. Clinicians and healthcare providers, including pharmacists and allied health professionals, can get coaching, practice, and support from the broader healthcare organizations in which they are embedded, follow the Advisory Committee on Immunization Practices (ACIP) recommendations (*1*,*2*), recommend needed vaccinations, and encourage eligible persons to receive COVID-19 booster dose vaccination.

Findings from this study showed that booster dose vaccination coverage among adults 50–64 and

≥65 years of age was higher than among those 18–49 years of age, and this pattern remained the same after controlling for demographic and behavioral variables. The risk for severe illness from COVID-19 increases with age (*30*,*31*). Higher COVID-19 booster dose vaccination coverage among older adults might also have been caused by early recommendation from ACIP for this population (*1*,*2*). Booster dose coverage was higher among persons who had reported medical conditions but lower among persons who had disabilities. Higher COVID-19 booster dose vaccination coverage among adults who had reported medical conditions might also be caused by the early recommendation in September 2021 from ACIP and recognition of increased risk for severe COVID-19 in this population (*1*,*2*). One recent study indicated that adults who had disabilities experienced more difficulty in obtaining a COVID-19 vaccination than persons who did not have a disability (*26*). Healthcare providers can try to ensure that all persons receive COVID-19 vaccination if they are eligible, regardless of age. Reducing barriers to scheduling and making vaccination sites more accessible might help improve vaccination coverage among adults who have disabilities (*26*).

Results from our study showed that booster dose coverage was much higher among essential HCP than among other essential workers. Although primary series vaccination was >90% among HCP and those in the education sector and ≈80% for other frontline and essential workers (*7*), booster dose coverage was much lower, leaving populations that have frequent COVID-19 exposure possibly susceptible to disease. This finding could be caused by lack of requirements for vaccination and removal of programs such as onsite vaccination that were available for the initial vaccine series. In addition, other access programs for different populations were probably available for initial vaccines but not for boosters. Reinstating these more intensive access programs or putting vaccines in the hands of primary care providers could help increase booster dose coverage among this population.

Four limitations might be considered when interpreting these findings. First, NIS-ACM has a low response rate (≈22%). However, survey weights were calibrated to COVID-19 vaccine administration data to mitigate possible bias from incomplete sample frame, nonresponse, and misclassification of vaccination status. Second, COVID-19 vaccination was self-reported and might be subject to recall or social desirability bias. However, reliability of self-reported COVID-19 vaccination might be comparable with that of self-report of influenza vaccination, which has been shown to have a relatively high agreement with vaccination status ascertained from medical records (*32*,*33*). Third, provider recommendations or work/school requirements for COVID-19 vaccination, and vaccination access barriers were not specifically assessed for booster doses.

Booster dose coverage was not optimal, and disparities by race/ethnicity and other factors are apparent in booster dose uptake. Continual monitoring of booster dose vaccination will be helpful for developing tailored strategies to improve vaccination coverage, especially with the recent recommendation for adults to receive the updated COVID-19 boosters (*34*). The updated COVID-19 boosters are formulated to better protect against the most recently circulating COVID-19 variant. The immune response of the updated COVID-19 booster vaccine was superior to that of the previous booster vaccine, and the safety was similar as that of the previous booster vaccine (*35*). To maximize protection against COVID-19, both an increase in persons initiating and completing the primary series, and getting recommended boosters, is needed.

Targeted strategies are needed to improve booster dose vaccination coverage among adults. These strategies should include healthcare providers educating and encouraging everyone to receive a booster dose when they are eligible regardless of age and previous infection with COVID-19 (*8*–*10*) and provisions for consistent access to vaccines, vaccination incentives, onsite vaccination, and reminders (*14*,*15*). More innovative approaches should include improving confidence in vaccines, community healthcare workers encouraging vaccinated community members to share their own vaccination experiences with their unvaccinated friends and family (*14*,*15*), understanding barriers and reducing barriers to vaccination (*14*,*15*), and providing vaccination in the office of their usual medical provider (*14*,*15*). Vaccination programs are needed that implement culturally and linguistically appropriate focused interventions among communities with lower vaccination coverage (*8*–*10*,*14*,*15*,*26*,*36*) and encourage national, state, and local health departments, and community-based and faith-based organizations to implement a combination of strategies, which have been shown to be effective in improving booster dose coverage (*26*,*36*).

About the Author

Dr. Lu is a research scientist at the National Center for Immunization and Respiratory Diseases, Centers for Disease Control and Prevention, Atlanta, GA. His primary research interest is child and adult vaccination assessment.

References

1. Mbaeyi S, Oliver SE, Collins JP, Godfrey M, Goswami ND, Hadler SC, et al. The Advisory Committee on Immunization Practices' interim recommendations for additional primary and booster doses of COVID-19 vaccines—United States, 2021. MMWR Morb Mortal Wkly Rep. 2021;70:1545–52. https://doi.org/10.15585/mmwr.mm7044e2
2. Centers for Disease Control and Prevention. COVID-19 vaccine booster shots [cited 2022 Sep 17]. https://www.cdc.gov/coronavirus/2019-ncov/vaccines/booster-shot.html
3. Thompson MG, Natarajan K, Irving SA, Rowley EA, Griggs EP, Gaglani M, et al. Effectiveness of a third dose of mRNA vaccines against COVID-19-associated emergency department and urgent care encounters and hospitalizations among adults during periods of Delta and Omicron variant predominance: VISION Network, 10 States, August 2021–January 2022. MMWR Morb Mortal Wkly Rep. 2022;71:139–45. https://doi.org/10.15585/mmwr.mm7104e3
4. Centers for Disease Control and Prevention. COVID-19 vaccination coverage and vaccine confidence [cited 2022 Apr 1]. https://www.cdc.gov/vaccines/imz-managers/coverage/covidvaxview/interactive.html2022.
5. Centers for Disease Control and Prevention. National Immunization Surveys (NIS) [cited 2022 Sep 17]. https://www.cdc.gov/vaccines/imz-managers/nis/about.html#current-surveys
6. Centers for Disease Control and Prevention. CDC/ATSDR Social Vulnerability Index [cited 2022 Sep 17]. https://www.atsdr.cdc.gov/placeandhealth/svi/index.html
7. Centers for Disease Control and Prevention. COVID-19 vaccination trends in the United States, national and jurisdictional cited 2022 Sep 19]. https://data.cdc.gov/Vaccinations/COVID-19-Vaccinations-in-the-United-States-Jurisdi/unsk-b7fc
8. Agranov M, Elliott M, Ortoleva P. The importance of social norms against strategic effects: the case of COVID-19 vaccine uptake. Econ Lett. 2021;206:109979. https://doi.org/10.1016/j.econlet.2021.109979
9. Graupensperger S, Abdallah DA, Lee CM. Social norms and vaccine uptake: college students' COVID vaccination intentions, attitudes, and estimated peer norms and comparisons with influenza vaccine. Vaccine. 2021;39:2060–7. https://doi.org/10.1016/j.vaccine.2021.03.018
10. Centers for Disease Control and Prevention. COVID-19 vaccination field guide: 12 strategies for your community [cited 2022 Sep 19]. https://www.cdc.govvaccines/covid-19/vaccinate-with-confidence/community.html
11. Announces Health and Human Services. $143.5 million to expand community-based efforts to address barriers to COVID-19 vaccination [cited 2022 Sep 15]. https://www.hhs.gov/about/news/2021/11/10/hhs-announces-143-million-to-expand-community-based-covid-19-vaccination-efforts.html
12. Health and Human Services. What providers need to know about COVID-19 vaccine fees and reimbursements? [cited 2022 Sep 16]. https://www.hrsa.gov/sites/default/files/hrsa/coronavirus/provider-covid-vaccine-factsheet.pdf
13. Velasquez D, Gondi S, Lu R, Pissaris A, Martin A. GOTVax: A novel mobile Covid-19 vaccine program. NEJM Catalyst. 2021 [cited 2022 Sep 16]. https://catalyst.nejm.org/doi/full/10.1056/CAT.21.0174
14. Gordon NP, Hornbrook MC. Older adults' readiness to engage with eHealth patient education and self-care resources: a cross-sectional survey. BMC Health Serv Res. 2018;18:220. https://doi.org/10.1186/s12913-018-2986-0
15. Office of the Assistant Secretary for Planning and Evaluation. Characteristics of homebound older adults: potential barriers to accessing the COVID-19 vaccine issue brief [cited 2022 Sep 18]. https://aspe.hhs.gov/reports/characteristics-homebound-older-adults-potential-barriers-accessing-covid-19-vaccine-issue-brief
16. Price-Haywood EG, Burton J, Fort D, Seoane L. Hospitalization and mortality among Black patients and White patients with COVID-19. N Engl J Med. 2020;382:2534–43. https://doi.org/10.1056/NEJMsa2011686
17. Holmes L Jr, Enwere M, Williams J, Ogundele B, Chavan P, Piccoli T, et al. Black–White risk differentials in COVID-19 (SARS-COV2) transmission, mortality and case fatality in the United States: translational epidemiologic perspective and challenges. Int J Environ Res Public Health. 2020;17:4322. https://doi.org/10.3390/ijerph17124322
18. Padamsee TJ, Bond RM, Dixon GN, Hovick SR, Na K, Nisbet EC, et al. Changes in COVID-19 vaccine hesitancy among Black and White individuals in the US. JAMA Netw Open. 2022;5:e2144470. https://doi.org/10.1001/jamanetworkopen.2021.44470
19. Brewer LI, Ommerborn MJ, Nguyen AL, Clark CR. Structural inequities in seasonal influenza vaccination rates. BMC Public Health. 2021;21:1166. https://doi.org/10.1186/s12889-021-11179-9
20. Lindley MC, Wortley PM, Winston CA, Bardenheier BH. The role of attitudes in understanding disparities in adult influenza vaccination. Am J Prev Med. 2006;31:281–5. https://doi.org/10.1016/j.amepre.2006.06.025
21. Lu PJ, Santibanez TA, Williams WW, Zhang J, Ding H, Bryan L, et al.; Centers for Disease Control and Prevention (CDC). Surveillance of influenza vaccination coverage—United States, 2007–08 through 2011–12 influenza seasons. MMWR Surveill Summ. 2013;62:1–28.
22. Carson SL, Casillas A, Castellon-Lopez Y, Mansfield LN, Morris D, Barron J, et al. COVID-19 vaccine decision-making factors in racial and ethnic minority communities in Los Angeles, California. JAMA Netw Open. 2021;4:e2127582. https://doi.org/10.1001/jamanetworkopen.2021.27582
23. Schmidt H, Weintraub R, Williams MA, Miller K, Buttenheim A, Sadecki E, et al. Equitable allocation of COVID-19 vaccines in the United States. Nat Med. 2021;27:1298–307. https://doi.org/10.1038/s41591-021-01379-6
24. Lu PJ, Srivastav A, Amaya A, Dever JA, Roycroft J, Kurtz MS, et al. Association of provider recommendation and offer and influenza vaccination among adults aged ≥18 years, United States. Vaccine. 2018;36:890–8. https://doi.org/10.1016/j.vaccine.2017.12.016
25. Lu PJ, Hung MC, O'Halloran AC, Ding H, Srivastav A, Williams WW, et al. Seasonal influenza vaccination coverage trends among adult populations, U.S., 2010–2016. Am J Prev Med. 2019;57:458–69. https://doi.org/10.1016/j.amepre.2019.04.007
26. Ryerson AB, Rice CE, Hung MC, Patel SA, Weeks JD, Kriss JL, et al. Disparities in COVID-19 vaccination status, intent, and perceived access for noninstitutionalized adults, by disability status—National Immunization Survey Adult COVID Module, United States, May 30–June 26, 2021. MMWR Morb Mortal Wkly Rep. 2021;70:1365–71. https://doi.org/10.15585/mmwr.mm7039a2
27. Plumb ID, Feldstein LR, Barkley E, Posner AB, Bregman HS, Hagen MB, et al. Effectiveness of COVID-19 mRNA vaccination in preventing COVID-19-associated hospitalization among adults with previous SARS-CoV-2 infection, United States, June 2021–February 2022. MMWR Morb Mortal Wkly Rep. 2022;71:549–55. https://doi.org/10.15585/mmwr.mm7115e2
28. Nguyen KH, Yankey D, Lu PJ, Kriss JL, Brewer NT, Razzaghi H, et al. Report of health care provider

recommendation for COVID-19 vaccination among adults, by recipient COVID-19 vaccination status and attitudes, United States, April–September 2021. MMWR Morb Mortal Wkly Rep. 2021;70:1723–30. https://doi.org/10.15585/mmwr.mm7050a1
29. Czeisler ME, Marynak K, Clarke KE, Salah Z, Shakya I, Thierry JM, et al. Delay or avoidance of medical care because of COVID-19-related concerns, United States, June 2020. MMWR Morb Mortal Wkly Rep. 2020;69:1250–7. https://doi.org/10.15585/mmwr.mm6936a4
30. Kim L, Garg S, O'Halloran A, Whitaker M, Pham H, Anderson EJ, et al. Risk factors for intensive care unit admission and in-hospital mortality among hospitalized adults identified through the US coronavirus disease 2019 (COVID-19)–associated Hospitalization Surveillance Network (COVID-NET). Clin Infect Dis. 2021;72:e206–14. https://doi.org/10.1093/cid/ciaa1012
31. Centers for Disease Control and Prevention. COVID-19 risks and vaccine information for older adults [cited 2022 Mar 16]. https://www.cdc.gov/aging/covid19/covid19-older-adults.html
32. Rolnick SJ, Parker ED, Nordin JD, Hedblom BD, Wei F, Kerby T, et al. Self-report compared to electronic medical record across eight adult vaccines: do results vary by demographic factors? Vaccine. 2013;31:3928–35. https://doi.org/10.1016/j.vaccine.2013.06.041
33. King JP, McLean HQ, Belongia EA. Validation of self-reported influenza vaccination in the current and prior season. Influenza Other Respir Viruses. 2018;12:808–13. https://doi.org/10.1111/irv.12593
34. Centers for Disease Control and Prevention. CDC recommends the first updated COVID-19 booster [cited 2022 Sep 22]. https://www.cdc.gov/media/releases/2022/s0901-covid-19-booster.html
35. Chalkias S, Harper C, Vrbicky K, Walsh SR, Essink B, Brosz A, et al. A bivalent Omicron-containing booster vaccine against COVID-19. N Engl J Med. 2022;387:1279–91 https://doi.org/10.1056/NEJMoa2208343
36. Reitsma MB, Goldhaber-Fiebert JD, Salomon JA. Quantifying and benchmarking disparities in COVID-19 vaccination rates by race and ethnicity. JAMA Netw Open. 2021;4:e2130343. https://doi.org/10.1001/jamanetworkopen.2021.30343

Address for correspondence: Peng-jun Lu, Centers for Disease Control and Prevention, 1600 Clifton Rd NE, Mailstop H24-4, Atlanta, GA 30329-4027, USA; email: lhp8@cdc.gov

etymologia revisited

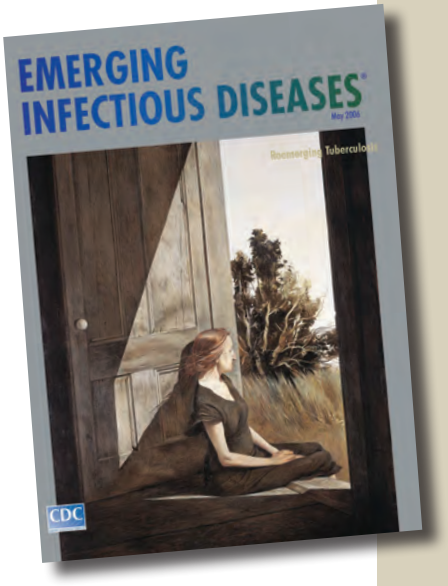

Originally published in May 2006

Tuberculosis
[too-ber''ku-lo'sis]

Any of the infectious diseases of humans or other animals caused by bacteria of the genus *Mycobacterium*. From the Latin *tuberculum*, "small swelling," the diminutive form of *tuber*, "lump." Tuberculosis has existed in humans since antiquity; it is believed to have originated with the first domestication of cattle. Evidence of tuberculosis has been shown in human skeletal remains and mummies from as early as 4000 BC. *Mycobacterium bovis* bacillus Calmette-Guérin has been successfully used to immunize humans since 1921, and treatment (rather than prevention) of tuberculosis has been possible since the introduction of streptomycin in 1946. Hopes of completely eliminating the disease, however, have been diminished since the rise of drug-resistant *M. tuberculosis* strains in the 1980s.

Source:

1. Dorland's illustrated medical dictionary. 30th ed. Philadelphia: Saunders; 2003; Merriam-Webster's collegiate dictionary. 11th ed. Springfield (MA): Merriam-Webster Incorporated; 2003; and http://www.wikipedia.org

https://wwwnc.cdc.gov/eid/article/12/5/et-1205_article

Pathologic and Immunohistochemical Evidence of Possible Francisellaceae among Aborted Ovine Fetuses, Uruguay

Federico Giannitti, Matías A. Dorsch, Carlos O. Schild, Rubén D. Caffarena, Karen Sverlow, Aníbal G. Armién, Franklin Riet-Correa

The only genus of the Francisellaceae family known to contain species pathogenic to mammals is *Francisella*, for which reported cases in the Southern Hemisphere have been limited to Australia. We describe severe necrotizing and inflammatory lesions and intralesional immunohistochemical identification of *Francisella* sp. lipopolysaccharide among aborted ovine fetuses in Uruguay.

The Francisellaceae family comprises gram-negative coccobacilli and 4 genera are currently recognized: *Francisella*, *Allofrancisella*, *Pseudofrancisella*, and *Cysteiniphilum* (*1*), of which only *Francisella* is of clinical relevance. *Francisella tularensis* is the most studied species because it causes tularemia, a highly transmissible, potentially life-threatening, zoonotic disease, also considered a potential bioterrorism agent (*2*,*3*).

Tularemia occurs over almost the entire Northern Hemisphere but is rarely reported in the Southern Hemisphere, where the only published cases have occurred in Australia (*4*–*7*). *F. tularensis* comprises 4 subspecies, *tularensis*, *holarctica*, *mediasiatica*, and *novicida*. *F. tularensis* subsp. *tularensis* occurs almost exclusively in North America and is responsible for 80%–90% of the tularemia cases, despite the co-existence of subspecies *holarctica*, which is the cause of most tularemia cases in Europe (*2*). The few cases of *F. tularensis* infection described in Australia were associated with *F. tularensis* subsp. *holarctica* and *novicida* (*4*–*6*). In the Americas, tularemia occurs in the United States, Mexico, and Canada (*2*,*8*), and no disease caused by *Francisella* spp. bacteria in mammals has been reported south of Mexico.

Although *F. tularensis* has a broad host range, sheep are the only livestock species affected by epizootics of tularemia and have been implicated in disease transmission to humans (*9*,*10*). We report a case of ovine abortion in Uruguay that raises concerns about the possible occurence of tularemia in South America.

The Study

In July 2015, two (≈1%) of ≈200 pastured sheep on a family farm in Colonia, Uruguay, aborted at ≈4 months of gestation. Autopsies on twin aborted fetuses (A and B) showed similar gross lesions (Table 1), consisting of severe multifocal widespread necrotizing hepatitis (Figure 1), and moderate fibrinous peritonitis and pericarditis. Samples of liver, adrenal gland, spleen, lung, heart, kidney, and brain tissues of both fetuses were fixed in formalin, then processed, embedded in paraffin, microtome-sectioned, and stained with hematoxylin and eosin. Histopathologic examination revealed severe acute multifocal random fibrinonecrotizing neutrophilic and histiocytic hepatitis (Figure 2, panel A), multifocal necrotizing and neutrophilic myocarditis, multifocal neutrophilic bronchiolitis and alveolitis, and multifocal fibrinous splenic capsulitis.

We processed formalin-fixed paraffin-embedded sections of liver from fetus B for immunohistochemistry to detect *Francisella* antigen (Appendix). We used tissue from a squirrel with culture- and PCR-confirmed *F. tularensis* septicemia as a positive control.

Author affiliations: Instituto Nacional de Investigación Agropecuaria, La Estanzuela, Colonia, Uruguay (F. Giannitti, M.A. Dorsch, C.O. Schild, R.D. Caffarena, F. Riet-Correa); University of California, Davis, California, USA (K. Sverlow, A.G. Armién); Universidade Federal da Bahia, Ondina, Salvador, Brazil (F. Riet-Correa)

DOI: https://doi.org/10.3201/eid2901.220698

Table 1. Autopsy findings in twin ovine fetuses with possible Francisellaceae infection, Uruguay

Autopsy findings	Fetus A	Fetus B
Crown-to-rump length	30 cm*	32 cm*
Sex	F	F
External aspects	Fully formed with complete wool, hair coat	Fully formed with complete wool, hair coat
Pulmonary aeration	Unexpanded, unventilated lungs†	Unexpanded, unventilated lungs†
Eponychium	Intact (uneroded) in all limbs†	Intact (uneroded) in all limbs†
Abomasum	No colostrum or milk curds†	No colostrum or milk curds†
Umbilical cord	Intact, wet, no hemorrhages or clots in umbilical vessels†	Intact, wet, no hemorrhages or clots in umbilical vessels†
Subcutaneous edema	Yes	No
Fibrinous peritonitis and pericarditis	Yes	Yes
Liver lesions	Enlarged liver with rounded edges, myriad discrete white to yellowish foci <2 mm in diameter disseminated throughout the hepatic parenchyma and visible from the capsular surface	Enlarged liver with rounded edges, myriad discrete white to yellowish foci <2 mm in diameter disseminated throughout the hepatic parenchyma and visible from the capsular surface
Placenta	Not available for examination	Not available for examination
Tissue autolysis	Moderate	Moderate

*Consistent with a gestational age of ≈4 mo.
†These findings suggest that the fetuses were dead at the time of expulsion (abortion).

We performed antigen retrieval in a decloaking chamber by using Antigen Decloaker citrate buffer (Biocare Medical, https://biocare.net). We applied a specific mouse monoclonal IgG3 raised against *F. tularensis* lipopolysaccharide, *F. tularensis* LPS Monoclonal Antibody (T14) (Thermo Fisher Scientific, https://www.thermofisher.com) as the primary antibody at 1:1,000 dilution. We used Mouse-on-Farma HRP-Polymer (Biocare Medical) and 3-amino-9-ethylcarbazole (Thermo Fisher Scientific) for antigen detection. For negative controls, we replaced *F. tularensis* monoclonal antibody with normal mouse IgG for both ovine and squirrel reactions.

Immunohistochemistry revealed strong abundant intralesional granular immunoreactivity in the necrotic foci of the fetal ovine liver, which was largely intracytoplasmic in infiltrating neutrophils and macrophages (Figure 2, panel B). We observed immunoreactivity in the positive control squirrel tissue but not in the negative controls. We conducted ancillary testing to rule out other ovine abortifacients (Table 2).

We postfixed formalin-fixed sections of liver from fetus B in modified Karnovsky's fixative, 1% osmium tetroxide, and 0.1 mol cacodylate buffer, then processed and embedded sections in resin for transmission electron microscopy. Despite suboptimal ultrastructural tissue preservation due to autolysis, intrahistiocytic and extracellular ≈0.7–1.7 μm gram-negative coccobacilli colocalized with the foci of necrotizing hepatitis.

The lack of historical reports of tularemia outside endemic areas of North America and Eurasia has been puzzling (*6*). Recently, tularemia emerged in Australia (*3*) and reemerged in the Northern Hemisphere (*7*). South America has been considered free of tularemia (*7*); a status that seems to be based solely on the lack of disease reporting. However, tularemia might have been undiagnosed because of limitations in disease surveillance systems in the region. No clinical disease

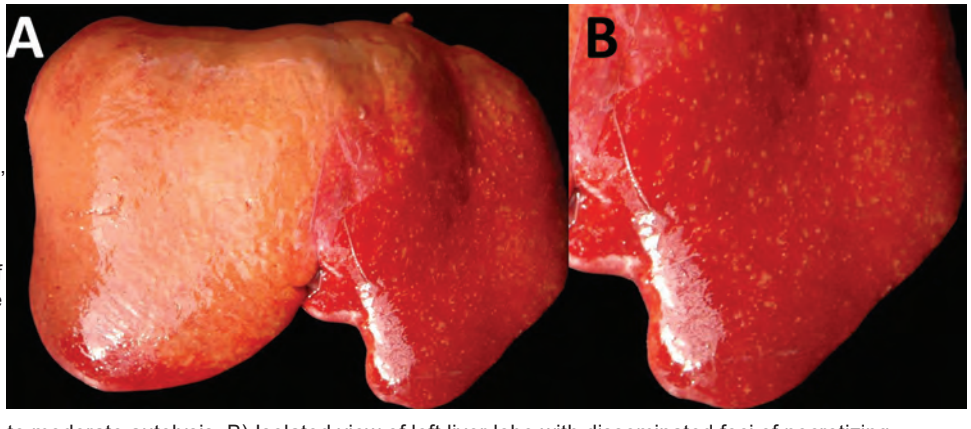

Figure 1. Diaphragmatic view of diseased liver from an aborted ovine fetus (fetus B) with possible Francisellaceae infection, Uruguay. A) Myriad discrete, white to yellowish, round, coalescing foci are visible, ranging from pinpoint to ≈2 mm in diameter, with a multifocal disseminated distribution in the hepatic parenchyma indicative of necrotizing hepatitis. Lesions are more visible in the left liver lobe (right side of the image) than the right liver lobe (left side of the image), in which the hepatic parenchyma is diffusely pale due to moderate autolysis. B) Isolated view of left liver lobe with disseminated foci of necrotizing hepatitis, which are characteristic in cases of tularemia.

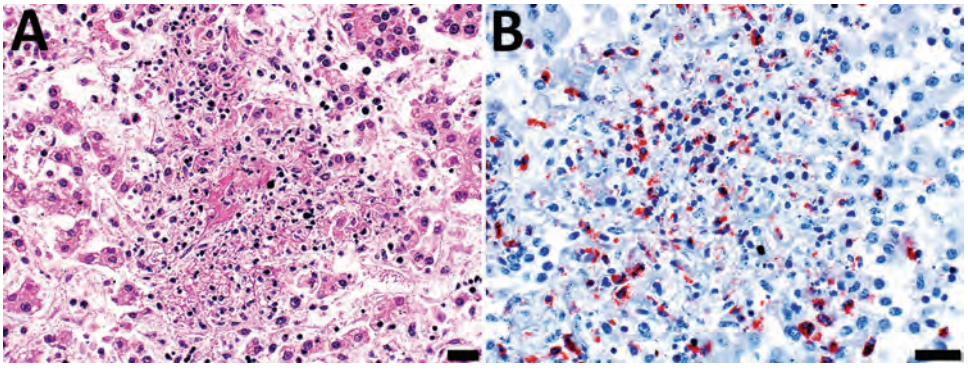

Figure 2. Microscopic images of diseased liver from an aborted ovine (fetus B) with possible Francisellaceae infection, Uruguay. A) Hematoxylin and eosin stain of section of liver. Hepatic histoarchitecture in center of image is effaced by eosinophilic karyorrhectic cellular debris (i.e., necrosis), fibrin exudate, and inflammatory cell infiltrates, mostly neutrophils and macrophages, evidence of severe necrotizing fibrinosuppurative hepatitis. Scale bar indicates 20 μm. B) Immunohistochemistry using a mouse monoclonal antibody raised against *F. tularensis* lipopolysaccharide and hematoxylin counterstain of section of liver shows abundant intralesional intracellular and extracellular immunoreactivity as a granular brownish-red precipitate (chromogen 3-amino-9-ethylcarbazole). Intracytoplasmic immunoreactivity was noted in infiltrating neutrophils and macrophages. Scale bar indicates 20 μm.

caused by *Francisella* spp. in mammals in the Americas south of Mexico has been described. Our results raise concerns about the possible occurence of tularemia in South America.

The abortifacient effects of *F. tularensis* in sheep have been described in the United States, and tularemia has been regarded as an overlooked syndrome in sheep (*9*). From a pathologic viewpoint, necrotic foci in the liver, spleen, or lungs in late term aborted ovine fetuses are characteristic of tularemia and should raise suspicion, although gross lesions can be absent even in cases with typical histologic inflammatory and necrotizing lesions (*9*). Contrary to most bacterial abortifacients of sheep (*11*), *F. tularensis* is not visible upon histopathologic examination of tissues stained with hematoxylin and eosin, Steiner silver, or Gram stains, even in tissues that have a high bacterial burden demonstrated by immunohistochemistry (*9*). The ultrastructural demonstration of intracellular gram-negative coccobacilli of the expected size in phagocytic and inflammatory cells in tissues with lesions, as in our case, aids in the diagnosis. Diagnostic investigation of any case of ovine abortion with fetal lesions indicating a bacterial etiology should include ancillary testing to identify *F. tularensis* and rule out other abortigenic pathogens (*11*).

The etiologic diagnosis in our case was reached by the immunohistochemical demonstration of abundant intralesional antigen by a specific monoclonal antibody raised against *F. tularensis* lipopolysaccharide. Immunohistochemistry has proven useful for identifying *F. tularensis* in diagnostic settings (*9*,*12*). *F. tularensis* lipopolysaccharide is a main specific antigen and virulence factor and differs from the lipopolysaccharide of other gram-negative bacteria (*13*). According to the manufacturer, the primary antibody we used for immunohistochemistry does not cross-react with *F. tularensis* subsp. *novicida*, *Yersinia pestis*, *Y. pseudotuberculosis*, *Y. enterocolitica*, *Vibrio cholerae*, *Escherichia coli*, *Salmonella enterica* serovar Typhimurium, *Brucella abortus*, *B. suis*, *B. ovis*, *B. melitensis*, or *B. neotomae*. We tested the immunohistochemistry in cases of abortion caused by *Campylobacter jejuni* and *C. fetus* but observed no cross-reactivity. Although cross-reaction with other members of Francisellaceae cannot be completely ruled out, *F. tularensis* is currently the only species of this family recognized as an ovine abortifacient. Definite species and subspecies identification requires bacterial isolation and DNA analysis, which we were unable to perform because the available specimens were unsuitable.

Sheep with tularemia have been implicated in disease transmission to sheep industry workers (*10*). In the case described here, the owners of the sheep lived on the farm and were in contact with the affected flock regularly; however, we do not know whether they had clinical signs consistent with tularemia.

Table 2. Ancillary testing performed in formalin-fixed paraffin-embedded sections of liver of aborted ovine fetus with possible Francisellaceae infection, Uruguay*

Tests	Results
Stains	
Steiner silver	No intralesional curved bacilli (i.e., *Campylobacter*) or spirochetes (i.e., *Leptospira*, *Flexispira*, *Helicobacter*) detected
Gomori's methenamine silver	No intralesional fungi detected
Gram	No intralesional bacteria detected
Immunohistochemistry	
Chlamydia spp.	Negative
Coxiella burnetii	Negative
Salmonella spp.	Negative
Listeria monocytogenes	Negative
Toxoplasma gondii	Negative

*All test results were validated using adequate positive/negative control tissues in each run.

The source of infection in this sheep remained unknown. However, *F. tularensis* has a broad animal reservoir, including arthropods, rodents, lagomorphs, and marsupials (*6*,*14*). Brown hares (*Lepus europaeus*), a species that plays a primary role in the ecology of tularemia in Europe (*12*), have been introduced to Uruguay and are frequently seen around the affected farm. In addition, *F. tularensis* can be transmitted by ticks, several of which, including *Amblyomma* spp., *Haemophysalis* spp., and *Ixodes* spp. ticks, are endemic in Uruguay. Of note, a gamma-proteobacterium related to *Francisella*-like organisms, but different from *F. tularensis*, was identified in Uruguay in *Amblyomma triste* ticks (*15*), the most prevalent tick species reported in human tick bites in the country.

Conclusions

We provide pathologic and immunohistochemical evidence of disease caused by a possible Francisellaceae member in sheep in Uruguay. Additional research is needed to isolate and speciate the pathogen and elucidate its regional epidemiology. Nonetheless, veterinarians, physicians, and public health officials should be aware of possible tularemia in South America.

Acknowledgments

We thank Yisell Perdomo for technical assistance with the histologic techniques.

This work was funded by research grant no. PL_27 N-23398 from the Instituto Nacional de Investigación Agropecuaria (INIA), Uruguay. M.A.D., R.D.C., and C.O.S. received financial support from INIA through graduate scholarships. R.D.C. also received financial support from the Agencia Nacional de Investigación e Innovación" (ANII), Uruguay, through a graduate scholarship.

About the Author

Dr. Giannitti is a principal investigator in veterinary pathology at the Instituto Nacional de Investigación Agropecuaria (INIA), La Estanzuela, Colonia, Uruguay. His primary research interests include the diagnostic investigation of naturally occurring diseases of livestock and wildlife and infectious abortifacients of ruminants.

References

1. Parte AC, Sardà Carbasse J, Meier-Kolthoff JP, Reimer LC, Göker M. List of Prokaryotic names with standing in nomenclature (LPSN) moves to the DSMZ. Int J Syst Evol Microbiol. 2020;70:5607–12 [cited 2022 Sep 21]. https://doi.org/10.1099/ijsem.0.004332
2. Colquhoum DJ, Larsson P, Duodu S, Forsman M. Chapter 14: the family *Francisellaceae*. In: Rosenberg E, DeLong EF, Lory S, Stackebrandt E, Thompson F, editors. The Prokaryotes gammaproteobacteria, 4th ed. New York: Springer; 2014. p. 287–314.
3. Maurin M. *Francisella tularensis* as a potential agent of bioterrorism? Expert Rev Anti Infect Ther. 2015;13:141–4. https://doi.org/10.1586/14787210.2015.986463
4. Whipp MJ, Davis JM, Lum G, de Boer J, Zhou Y, Bearden SW, et al. Characterization of a novicida-like subspecies of *Francisella tularensis* isolated in Australia. J Med Microbiol. 2003;52:839–42. https://doi.org/10.1099/jmm.0.05245-0
5. Jackson J, McGregor A, Cooley L, Ng J, Brown M, Ong CW, et al. *Francisella tularensis* subspecies *holarctica*, Tasmania, Australia, 2011. Emerg Infect Dis. 2012;18:1484–6. https://doi.org/10.3201/eid1809.111856
6. Eden JS, Rose K, Ng J, Shi M, Wang Q, Sintchenko V, et al. *Francisella tularensis* ssp. *holarctica* in ringtail possums, Australia. Emerg Infect Dis. 2017;23:1198–201. https://doi.org/10.3201/eid2307.161863
7. Yeni DK, Büyük F, Ashraf A, Shah MSUD. Tularemia: a re-emerging tick-borne infectious disease. Folia Microbiol (Praha). 2021;66:1–14. https://doi.org/10.1007/s12223-020-00827-z
8. Lupi O, Madkan V, Tyring SK. Tropical dermatology: bacterial tropical diseases. J Am Acad Dermatol. 2006;54:559–78. https://doi.org/10.1016/j.jaad.2005.03.066
9. O'Toole D, Williams ES, Woods LW, Mills K, Boerger-Fields A, Montgomery DL, et al. Tularemia in range sheep: an overlooked syndrome? J Vet Diagn Invest. 2008;20:508–13. https://doi.org/10.1177/104063870802000417
10. Jellison WL, Kohls GM. Tularemia in sheep and in sheep industry workers in western United States. Public Health Monogr. 1955;28:1–19. https://doi.org/10.5962/bhl.title.117381
11. Dorsch MA, Cantón GJ, Driemeier D, Anderson ML, Moeller RB, Giannitti F. Bacterial, protozoal and viral abortions in sheep and goats in South America: a review. Small Rumin Res. 2021;205:106547. https://doi.org/10.1016/j.smallrumres.2021.106547
12. Gyuranecz M, Szeredi L, Makrai L, Fodor L, Mészáros AR, Szépe B, et al. Tularemia of European brown hare (*Lepus europaeus*): a pathological, histopathological, and immunohistochemical study. Vet Pathol. 2010;47:958–63. https://doi.org/10.1177/0300985810369902
13. Okan NA, Kasper DL. The atypical lipopolysaccharide of *Francisella.* Carbohydr Res. 2013;378:79–83. https://doi.org/10.1016/j.carres.2013.06.015
14. Sjöstedt A. Tularemia: history, epidemiology, pathogen physiology, and clinical manifestations. Ann N Y Acad Sci. 2007;1105:1–29. https://doi.org/10.1196/annals.1409.009
15. Venzal JM, Estrada-Peña A, Portillo A, Mangold AJ, Castro O, de Souza CG, et al. Detection of Alpha and Gamma-Proteobacteria in *Amblyomma triste* (Acari: Ixodidae) from Uruguay. Exp Appl Acarol. 2008;44:49–56. https://doi.org/10.1007/s10493-007-9126-6

Address for correspondence: Federico Giannitti, Plataforma de Investigación en Salud Animal, Instituto Nacional de Investigación Agropecuaria, Rte no. 50, Km. no. 11, 70006 La Estanzuela, Colonia, Uruguay; email: fgiannitti@inia.org.uy

Bourbon Virus Transmission, New York, USA

Alan P. Dupuis II,[1] Melissa A. Prusinski,[1] Collin O'Connor, Joseph G. Maffei, Cheri A. Koetzner, Tela E. Zembsch, Steven D. Zink, Alexis L. White, Michael P. Santoriello, Christopher L. Romano, Guang Xu, Fumiko Ribbe, Scott R. Campbell, Stephen M. Rich, P. Bryon Backenson, Laura D. Kramer, Alexander T. Ciota

In July 2019, Bourbon virus RNA was detected in an *Amblyomma americanum* tick removed from a resident of Long Island, New York, USA. Tick infection and white-tailed deer (*Odocoileus virginianus*) serosurvey results demonstrate active transmission in New York, especially Suffolk County, emphasizing a need for surveillance anywhere *A. americanum* ticks are reported.

Bourbon virus (BRBV; genus *Thogotovirus*, family Orthomyxoviridae) is a suspected tickborne human pathogen isolated in 2014 from a patient residing in Bourbon County, Kansas, USA (*1*). BRBV is closely related to Oz virus, which was isolated from *Amblyomma testudinarium* ticks in Japan (*2*,*3*). Since the initial discovery of BRBV, human cases have been identified in Kansas, Missouri, and Oklahoma (*4*). The *Amblyomma americanum* lone star tick has been identified as the likely vector of BRBV transmission and maintenance (*5*,*6*). Small and medium-sized mammals and ground-dwelling birds such as wild turkeys (*Meleagris gallopavo*) are hosts for the immature ticks. Adults feed on large mammals, such as coyotes (*Canis latrans*) and white-tailed deer (*Odocoileus virginianus*). All 3 active developmental stages of the tick will bite humans (*7*). Virus detection in ticks and serologic evidence in mammalian hosts, including white-tailed deer, have been demonstrated in Missouri, Kansas, and North Carolina (*6*,*8*–*10*).

Author affiliations: New York State Department of Health, Slingerlands, New York, USA (A.P. Dupuis II, J.G. Maffei, C.A. Koetzner, S.D. Zink, L.D. Kramer, A.T. Ciota); New York State Department of Health, Albany, New York, USA (M.A. Prusinski, C. O'Connor, T.E. Zembsch, P.B. Backenson), Suffolk County Department of Health Services, Yaphank, New York, USA (A.L. White, M.P. Santoriello, C.L. Romano, S.R. Campbell); University of Massachusetts, Amherst, Massachusetts, USA (G. Xu, F. Ribbe, S.M. Rich); State University of New York at Albany School of Public Health, Albany (L.D. Kramer, A.T. Ciota)

DOI: https://doi.org/10.3201/eid2901.220283

The Study

In July 2019, New York State Department of Health (NYSDOH) epidemiologists were notified that BRBV RNA was detected in an individual, partially engorged female *A. americanum* tick removed from a Long Island, New York, resident. Comprehensive testing performed through the University of Massachusetts TickReport service (https://www.tickreport.com) revealed the tick was also positive for *Ehrlichia ewingii* bacteria. Notes on the tick submission form indicated the person was experiencing fever, chills, and fatigue; officials with NYSDOH and Suffolk County Department of Health Services (SCDHS) attempted to contact the resident for a follow-up investigation. No additional information was provided, and no blood samples were available to assess potential infection with BRBV.

In 2016, NYSDOH and SCDHS initiated active tick surveillance targeting *A. americanum* ticks for BRBV and Heartland virus (HRTV). HRTV-infected ticks and seropositive deer were detected on Long Island in 2018 and reported in 2021 (*11*). We used standardized flag sampling for the collection of host-seeking *A. americanum* ticks on public lands in Suffolk County. During 2016–2020, a total of 1,265 pools, representing 4,189 adults, 7,227 nymphs, and 97 larvae, tested negative for BRBV RNA by real-time reverse transcription PCR using an in-house multiplex assay to detect HRTV and BRBV (*11*). The BRBV primers for this assay were designed based on the St. Louis strain (GenBank accession no. MK453528) (*12*). During 2021, we expanded sampling for *A. americanum* ticks on Long Island to collect a greater number of ticks from more locations, and we modified molecular detection protocols to use BRBV-specific primers developed at TickReport (Table 1). We designed BRBV-specific primers based on the original virus strain deposited in GenBank (accession no. KU708254) (*13*). We collected a total of 1,058 pools, consisting of 4,406 adults

[1]These authors contributed equally to this article.

Table 1. Primer/probe sets for detection of Bourbon virus RNA in New York, NY, USA*

Name	Gene target	Sequence, 5′ → 3′
BRBV F†	Polymerase subunit, PB1	AACCGGCCAATAGGG
BRBV R	Polymerase subunit, PB1	TGCCAGTTGGGTAGC
BRBV PROBE_5Cy5		/5Cy5/ATGGAGCTG/TAO/CTTTCACTACC/3IAbRQSp/
Bourbon_virus_F1‡	Polymerase subunit, PB1	ATTGCTACTCCGTCCATGTTAGTAAG
Bourbon_virus_R1	Polymerase subunit, PB1	CCAGAACTTGGTAGACATTCCAATAAG
Bourbon_virus_P1_HEX probe		/5HEX/CCCTTGCTG/ZEN/CATCTTCCACCACTTTCACAA/3IABkFQ/

*BRBV, Bourbon virus; F, forward; P, probe; PB1, polymerase basic 1; R, reverse.
†Primer/probe set developed at Wadsworth Center, New York State Department of Health, based on Bourbon virus (St. Louis strain) (GenBank accession no. MK453528).
‡Primer/probe set developed at TickReport (https://www.tickreport) based on Bourbon virus (original strain) (GenBank accession no. KU708254)

(460 pools) and 9,972 nymphs (598 pools) from 12 sites in Suffolk County, New York. Pool sizes ranged from 1–10 adults and 5–20 nymphs. We detected BRBV RNA in 5 pools of unengorged nymphs. We collected positive pools at 1 site in Smithtown, New York (n = 3), on May 3, 2021, and 2 sites, 1 positive pool each, in Brookhaven, New York, on June 9 and July 8, 2021. We isolated infectious virus from all BRBV RNA-positive tick pools after incubation on Vero cells (ATCC, Manassas, VA, USA). We confirmed that the isolates were BRBV by real-time reverse transcription PCR.

Serologic testing of hunter-harvested white-tailed deer blood submitted for arbovirus serosurveys has been conducted in New York since 2007 using plaque reduction neutralization tests, as described (*14*). BRBV was included in these assays starting in 2019 for deer harvested in Suffolk County and the Hudson Valley Region and 2020 for deer harvested in central and western New York. We screened a total of 881 serum samples at 1:20 for the presence of neutralizing antibodies to BRBV (Table 2; Figure 1). We serially diluted samples testing positive for endpoint titers. Statewide, 37.7% of the deer were seropositive; 89.2% of the seropositive deer had titers >20. The seropositivity was 66.5% for deer harvested in Suffolk County (Table 2; Figures 1, 2). Seroprevalence was lower in western New York (3.8%), the Hudson Valley (1.7%), and central New York (1.2%). We did not detect BRBV neutralizing antibodies in 7 deer harvested in the northern New York region (Table 2; Figure 1). We tested *A. americanum* ticks (n = 1,641) collected from 145 deer harvested from Suffolk County for BRBV RNA; the virus was not detected.

Conclusion

Isolation of BRBV from the local tick population and high seropositivity in hunter-harvested white-tailed deer demonstrated active transmission throughout Suffolk County, New York, since 2019. In addition, serologic evidence suggests the virus is present in other regions of New York. Consistent with previous BRBV field studies and the recent discovery of a closely related virus transmitted by *Amblyomma* species ticks in Japan, *A. americanum* ticks were implicated in local transmission of BRBV (*2*,*6*). Tick minimal infection rates were 0%–0.77%. It is unclear whether the unengorged nymphs had acquired the virus as larvae feeding on viremic hosts, through cofeeding transmission, or transovarially. These routes of transmission have been demonstrated in laboratory studies (*5*). BRBV was not detected in adult ticks tested during surveillance despite high numbers collected. Considering the overlap of adult and nymphal tick activity on Long Island, future surveillance campaigns should study the effect of phenology on BRBV transmission.

Of interest, of the 5 BRBV positive pools detected by the TickReport primer set, 1 pool was positive with the primer set used during previous surveillance seasons despite similar assay limits of detection; this

Table 2. Plaque reduction neutralization test results for Bourbon virus in white-tailed deer specimen samples, New York, NY, USA

Region	Years sampled	No. samples	No. (%) positive
Northern New York	2020, 2021	7	0
Western New York	2020, 2021	132	5 (3.8)
Central New York	2019–2021	80	1 (1.2)
Hudson Valley	2019–2021	176	3 (1.7)
Long Island*	2019–2021	486	323 (66.5)
Brookhaven	2019–2021	291	199 (68.4)
Islip	2021	15	9 (60.0)
Riverhead	2019, 2020	3	1 (33.3)
Shelter Island	2019, 2020	140	85 (60.7)
Southampton	2019, 2020	4	4 (100.0)
Fire Island†	2020	33	25 (75.8)

*Townships are listed for Suffolk County, Long Island.
†Fire Island occupies 2 townships but is treated as a single entity for this study.

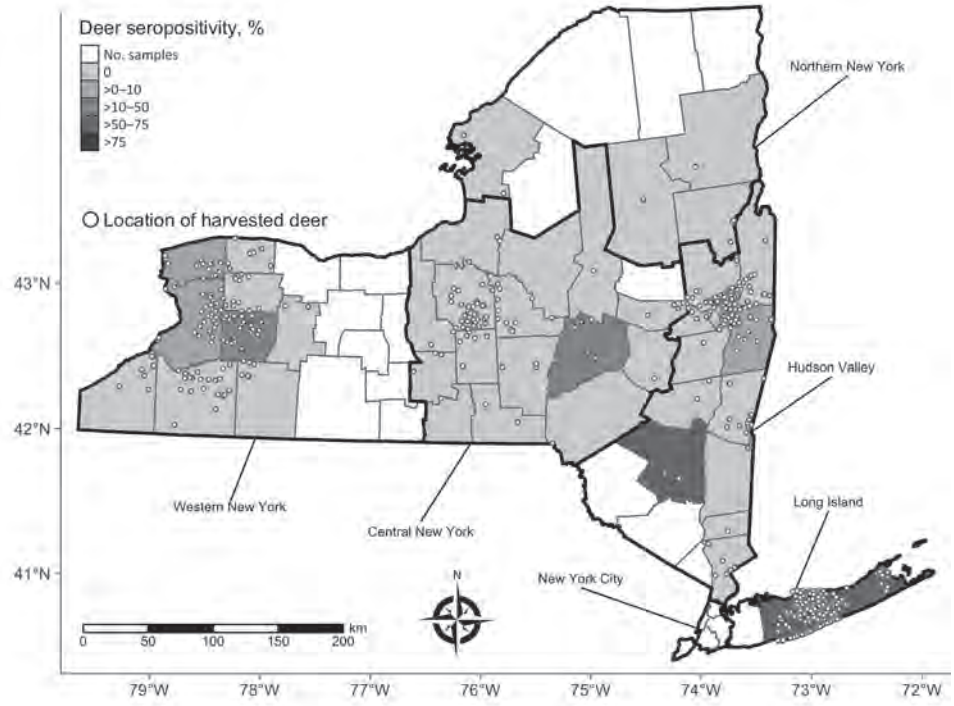

Figure 1. Sampling of hunter-harvested white-tailed deer blood and Bourbon virus seropositivity by county, New York, NY, USA. Locations (open circles) of harvested deer are randomly jittered within townships to avoid overplotting.

result suggested genetic differences in the primer target regions. We plan to conduct phylogenetic analyses and in-vitro growth characteristic studies.

White-tailed deer are a sensitive sentinel model for many arboviruses because of their overall abundance and distribution, small home ranges, and the frequency on which they are fed upon by ticks and other hematophagous arthropods (*14*,*15*). Seroprevalence in Suffolk County deer (66.5%) was higher than that reported in North Carolina deer (56%), but lower than deer harvested in Missouri (86%) (*8*,*9*). BRBV seroprevalence rates of white-tailed deer harvested from various areas in Suffolk County (Table 2) were similar to Oz virus seroprevalence rates (30.0%–73.7%) in wild sika deer (*Cervus nippon*) in Japan sampled from prefectures located near the initial detection of the virus (*3*). The lower seroprevalence in regions of New York outside of Long Island can be attributed to fewer established populations of *A. americanum* ticks or incidental transmission by bird-dispersed immatures originating from established regions. To date, no competent vertebrate host, including deer, has been implicated in BRBV amplification.

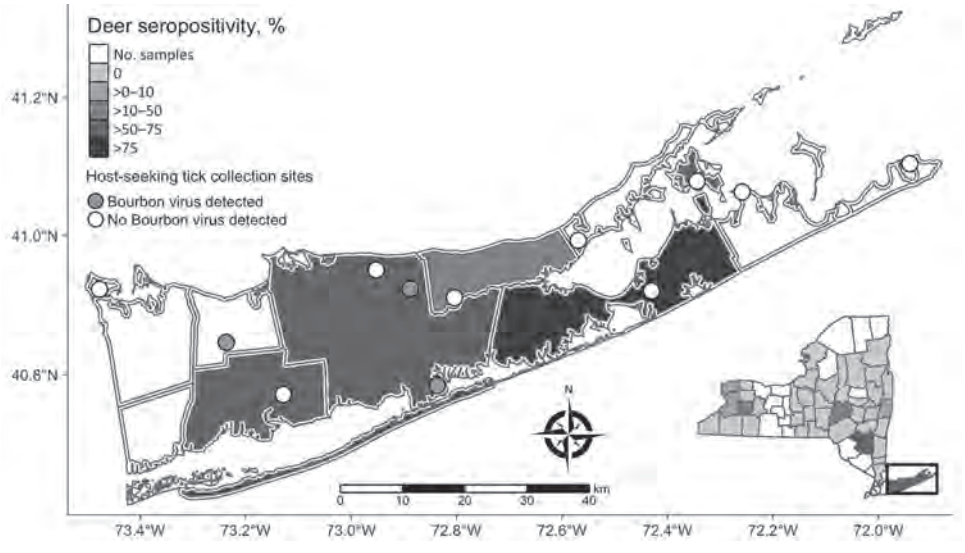

Figure 2. Suffolk County tick collection sites for study of Bourbon virus seropositivity, New York, NY, USA. Circles within townships indicate tick collection sites. Open circles are sites with no evidence of BRBV. Gray circles represent approximate locations of BRBV-positive tick pools. Shading indicates BRBV seroprevalence; darker shades represent higher rates. Inset map shows location of Suffolk County in New York.

Our findings emphasize the need to include emerging pathogens such as BRBV and HRTV in surveillance programs wherever lone star ticks are distributed. Clinicians outside of the midwestern United States should be aware of the potential for human disease. It is unclear if the symptoms of the person who removed the BRBV-positive tick were the result of potential infection with BRBV, *Ehrlichia ewingii*, or an unrelated etiology, because patient blood samples were not available. Considering the overlapping symptomologies of BRBV (fever, fatigue, loss of appetite, thrombocytopenia, and leukopenia) with other tickborne infections, including ehrlichiosis and Heartland virus disease, diagnosis is difficult without specific testing. Currently, testing is only available at the Centers for Disease Control and Prevention and a few state health laboratories. Providers should request BRBV and HRTV testing for patients with history of tick exposure or travel to regions where *A. americanum* ticks are reported and who are displaying clinical symptoms, including leukopenia and thrombocytopenia, that do not respond with antimicrobial treatment.

Acknowledgments

We thank Steve Young, Josh Dwyer, Julia Goldstein, Sean Reagan, Emalee Clark, Dylan Bartlett, Lauren Rose, Anna Perry, and Jessica Stout for assistance with tick surveillance, tick processing, and testing. We thank Beau Payne, Alexander Novarro, Jordan Raphael, and Kelsey Taylor for assistance with deer blood collections. Cells for serologic assays and media production were provided by the Wadsworth Center Media and Tissue Culture Core.

This publication was supported by cooperative agreement no. U01CK000509, funded by the Centers for Disease Control and Prevention and by the National Institutes of Health (no. R01AI142572).

About the Author

Mr. Dupuis is a research scientist at the Wadsworth Center, New York State Department of Health. His research interests include the role of the vertebrate host in the ecology of mosquitoborne and tickborne viruses.

References

1. Kosoy OI, Lambert AJ, Hawkinson DJ, Pastula DM, Goldsmith CS, Hunt DC, et al. Novel thogotovirus associated with febrile illness and death, United States, 2014. Emerg Infect Dis. 2015;21:760–4. https://doi.org/10.3201/eid2105.150150
2. Ejiri H, Lim CK, Isawa H, Fujita R, Murota K, Sato T, et al. Characterization of a novel thogotovirus isolated from *Amblyomma testudinarium* ticks in Ehime, Japan: a significant phylogenetic relationship to Bourbon virus. Virus Res. 2018;249:57–65. https://doi.org/10.1016/j.virusres.2018.03.004
3. Tran NTB, Shimoda H, Ishijima K, Yonemitsu K, Minami S, Kuroda Y, et al.; Supriyono. Zoonotic infection with Oz virus, a novel thogotovirus. Emerg Infect Dis. 2022;28:436–9. https://doi.org/10.3201/eid2802.211270
4. Fuchs J, Straub T, Seidl M, Kochs G. Essential role of interferon response in containing human pathogenic Bourbon virus. Emerg Infect Dis. 2019;25:1304–13. https://doi.org/10.3201/eid2507.181062
5. Godsey MS Jr, Rose D, Burkhalter KL, Breuner N, Bosco-Lauth AM, Kosoy OI, et al. Experimental infection of *Amblyomma americanum* (Acari: Ixodidae) with Bourbon virus (Orthomyxoviridae: Thogotovirus). J Med Entomol. 2021;58:873–9. https://doi.org/10.1093/jme/tjaa191
6. Savage HM, Burkhalter KL, Godsey MS Jr, Panella NA, Ashley DC, Nicholson WL, et al. Bourbon virus in field-collected ticks, Missouri, USA. Emerg Infect Dis. 2017;23:2017–22. https://doi.org/10.3201/eid2312.170532
7. Means RG, White DJ. New distribution records of *Amblyomma americanum* (L.) (Acari: Ixodidae) in New York State. J Vector Ecol. 1997;22:133–45.
8. Jackson KC, Gidlewski T, Root JJ, Bosco-Lauth AM, Lash RR, Harmon JR, et al. Bourbon virus in wild and domestic animals, Missouri, USA, 2012–2013. Emerg Infect Dis. 2019;25:1752–3. https://doi.org/10.3201/eid2509.181902
9. Komar N, Hamby N, Palamar MB, Staples JE, Williams C. Indirect evidence of Bourbon virus (*Thogotovirus*, *Orthomyxoviridae*) infection in North Carolina. N C Med J. 2020;81:214–5. https://doi.org/10.18043/ncm.81.3.214
10. Savage HM, Godsey MS Jr, Panella NA, Burkhalter KL, Manford J, Trevino-Garrison IC, et al. Surveillance for tick-borne viruses near the location of a fatal human case of Bourbon virus (family *Orthomyxoviridae*: genus *Thogotovirus*) in eastern Kansas, 2015. J Med Entomol. 2018;55:701–5. https://doi.org/10.1093/jme/tjx251
11. Dupuis AP II, Prusinski MA, O'Connor C, Maffei JG, Ngo KA, Koetzner CA, et al. Heartland virus transmission, Suffolk County, New York, USA. Emerg Infect Dis. 2021;27:3128–32. https://doi.org/10.3201/eid2712.211426
12. Bricker TL, Shafiuddin M, Gounder AP, Janowski AB, Zhao G, Williams GD, et al. Therapeutic efficacy of favipiravir against Bourbon virus in mice. PLoS Pathog. 2019;15:e1007790. https://doi.org/10.1371/journal.ppat.1007790
13. Lambert AJ, Velez JO, Brault AC, Calvert AE, Bell-Sakyi L, Bosco-Lauth AM, et al. Molecular, serological and in vitro culture-based characterization of Bourbon virus, a newly described human pathogen of the genus *Thogotovirus*. J Clin Virol. 2015;73:127–32. https://doi.org/10.1016/j.jcv.2015.10.021
14. Dupuis AP, Prusinski MA, Russell A, O'Connor C, Maffei JG, Oliver J, et al. Serologic survey of mosquito-borne viruses in hunter-harvested white-tailed deer (*Odocoileus virginianus*), New York state. Am J Trop Med Hyg. 2021;104:593–603. https://doi.org/10.4269/ajtmh.20-1090
15. Clarke LL, Ruder MG, Mead DG, Howerth EW. Heartland virus exposure in white-tailed deer in the southeastern United States, 2001–2015. Am J Trop Med Hyg. 2018;99:1346–9. https://doi.org/10.4269/ajtmh.18-0555

Address for correspondence: Alan P. Dupuis II, The Arbovirus Laboratory, New York State Department of Health, 5668 State Farm Rd, Slingerlands, NY 12159, USA; email: alan.dupuis@health.ny.gov

Genomic Microevolution of *Vibrio cholerae* O1, Lake Tanganyika Basin, Africa

Yaovi M.G. Hounmanou, Elisabeth Njamkepo, Jean Rauzier, Karin Gallandat, Aurélie Jeandron, Guyguy Kamwiziku, Klaudia Porten, Francisco Luquero, Aaron Aruna Abedi, Baron Bashige Rumedeka, Berthe Miwanda, Martin Michael, Placide Welo Okitayemba, Jaime Mufitini Saidi, Renaud Piarroux, François-Xavier Weill, Anders Dalsgaard, Marie-Laure Quilici

Africa's Lake Tanganyika basin is a cholera hotspot. During 2001–2020, *Vibrio cholerae* O1 isolates obtained from the Democratic Republic of the Congo side of the lake belonged to 2 of the 5 clades of the AFR10 sublineage. One clade became predominant after acquiring a *parC* mutation that decreased susceptibility to ciprofloxacin.

Cholera is an acute life-threatening diarrheal disease responsible for ≈4.3 million cases and 142,000 deaths annually worldwide (*1*). Excluding epidemic peaks in Haiti and Yemen (*2*,*3*), most cases of cholera originate from sub-Saharan Africa, predominantly the African Great Lakes Region (AGLR); specifically, the countries of the Lake Tanganyika basin (*4*). Many recurrent cholera outbreaks in the Democratic Republic of the Congo (DRC), Tanzania, Burundi, and Zambia have been linked to a common hotspot area around the Lake Tanganyika basin (*5*–*8*).

Author affiliations: University of Copenhagen, Frederiksberg, Denmark (Y.M.G. Hounmanou, A. Dalsgaard); Institut Pasteur, Université Paris Cité, Paris, France (E. Njamkepo, J. Rauzier, F.-X. Weill, M.-L. Quilici); London School of Hygiene and Tropical Medicine, London, UK (K. Gallandat, A. Jeandron); University of Kinshasa, Kinshasa, Democratic Republic of the Congo (G. Kamwiziku); Epicentre, Paris (K. Porten, F. Luquero); Ministry of Public Health, Kinshasa (A. Aruna Abedi, P. Welo Okitayemba); Ministry of Public Health, Uvira, Democratic Republic of the Congo (B. Bashige Rumedeka, J. Mufitini Saidi); Institut National de Recherche Biomédicale, Kinshasa (B. Miwanda); Sokoine University of Agriculture College of Veterinary Medicine and Biomedical Sciences, Morogoro, Tanzania (M. Michael); Sorbonne Université, Inserm UMR 1136, Assistance Publique-Hôpitaux de Paris, Hôpital Pitié-Salpêtrière, Paris (R. Piarroux)

DOI: https://doi.org/10.3201/eid2901.220641

By the end of 2018, the World Health Organization had noted a steady decline in cholera cases throughout the world, including the AGLR (*9*). Continuous genomic surveillance of circulating *Vibrio cholerae* bacteria strains is required to understand the transmission dynamics and genetic evolution of *V. cholerae* and potentially to guide prevention and response interventions to continue the trend toward decreasing case numbers, in line with the global cholera roadmap to 2030 (*10*). One lineage, seventh pandemic *V. cholerae* O1 El Tor (7PET), is responsible for the current pandemic, which began in 1961 (*11*); Africa was hit by 7PET in 1970 (*11*). During 1970–2014, ≥11 different 7PET sublineages were introduced from South Asia into Africa, and sublineage AFR10 (previously T10) replaced AFR5 (previously T5) in the AGLR in the late 1990s (*11*). Sublineage AFR13 (previously T13) was identified in East Africa (Tanzania, Uganda, Kenya) and Zimbabwe (*12*). We tracked the 7PET populations circulating in the Lake Tanganyika basin by studying recent *V. cholerae* O1 isolates collected in the region by conventional bacteriology and genomics and placing these genomes in a broader phylogenetic context to elucidate their evolutionary history.

The Study

We analyzed 96 *V. cholerae* O1 isolates collected during 2015–2020 in DRC (86 clinical isolates, including 39 collected in 2018–2020) and Tanzania (10 environmental isolates from fish and lake water) (Appendix 1, https://wwwnc.cdc.gov/EID/article/29/1/22-0641-App1.pdf; Appendix 2 Table 1, https://wwwnc.cdc.gov/EID/article/29/1/22-0641-App2.xlsx). We subjected the isolates to antimicrobial susceptibility testing, whole-genome sequencing, genomic characterization, and phylogenetic analyses, as previously

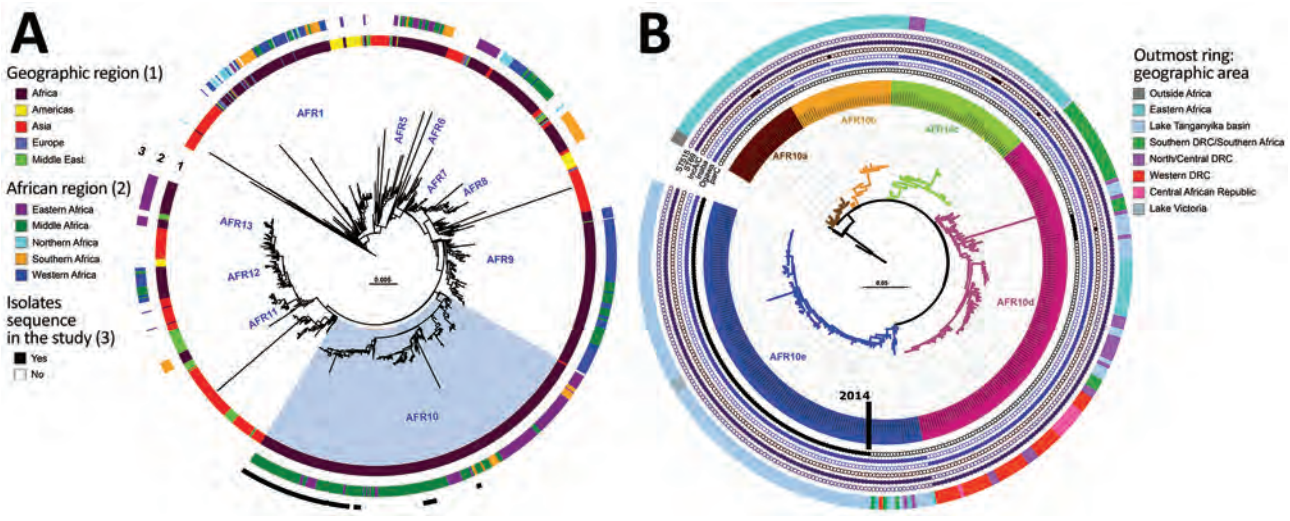

Figure 1. Phylogenomics of clinical and environmental *Vibrio cholerae* O1 El Tor isolates from the Lake Tanganyika basin, Africa. A) Maximum-likelihood phylogeny of 1,366 seventh pandemic *V. cholerae* O1 El Tor (7PET) genomes with strain A6 as the outgroup. The different sublineages introduced into Africa are indicated. Light blue indicates AFR10 sublineage. Rings 1 and 2 show geographic origin of isolates; ring 3 shows isolates sequenced in this study. B) Maximum-likelihood tree for 357 AFR10 isolates, with strain N16961 as an outgroup. The 5 clades are color-coded: AFR10a, brown; AFR10b, yellow; AFR10c, green; AFR10d, pink; and AFR10e, blue. The outermost ring indicates the geographic locations of the different isolates in the tree. Filled circles indicate the presence of ST69 or ST515, Ogawa and Inaba serotypes, IncA/C plasmid, and the S85L mutation in *par*C; open circles indicate their absence. MLST, multilocus sequence typing; ST, sequence type.

described (*11*,*12*) (Appendix 1). We performed a phylogenetic analysis of these genomes within a global collection of 1,366 7PET *V. cholerae* O1 genomes (Appendix 2 Table 2), including another 130 genomes from DRC collected during 1984–2017. We based the final maximum-likelihood phylogenetic tree on 10,352 single-nucleotide variants distributed over the nonrepetitive, nonrecombinant core genome (Figure 1, panel A).

Phylogenetic analysis of the 96 genomes of *V. cholerae* O1 isolates showed that all belonged to 7PET sublineage AFR10 (Figure 1, panel A). Within the limits of our sampling, sublineage AFR5, which circulated actively in the AGLR during the 1980s–1990s (*11*), appears to be extinct in the region, whereas sublineage AFR13, reported in 2015 in Uganda and Tanzania (*12*), has not yet spread to DRC. Since 1998, the endemicity of the AFR10 sublineage in the Tanganyika basin and surrounding countries has led to microevolution; an analysis of 357 AFR10 genomes from our global dataset revealed the presence of 5 clades, AFR10a–AFR10e (Figure 1, panel B; Appendix Figure 1). Clades AFR10a, AFR10b, and AFR10c were mostly associated with the eastern AGLR countries. The isolates of these clades were of sequence type (ST) 69 (Figure 1, panel B). Clades AFR10d and AFR10e predominated in DRC and the Lake Tanganyika basin. Clade AFR10d is of ST515, essentially Inaba serotype, and was widespread in DRC and neighboring countries (Figure 2, panel A), as previously reported (*13*). It was the only clade found in the Lake Kivu and Lake Edward basins. AFR10e strains are of ST69, Ogawa serotype, and were essentially restricted to the Lake Tanganyika basin, confirming previous findings (*13*). A further pangenome analysis of the AFR10 isolates revealed no clade-specific gain or loss of genes (Appendix Figure 2). AFR10e strains have gradually replaced AFR10d strains in the region since 2014; all *V. cholerae* O1 strains obtained from the Tanganyika basin by 2017, as well as those obtained from the lake itself in 2018 and 2019, were AFR10e strains (Figure 2 panel B). Epidemiologic studies identified cholera hotspots in the AGLR as a source of major countrywide outbreaks reaching the capital, Kinshasa, and the Atlantic coast, via the Congo River, in 2011, 2012, and 2016 (*5*). These outbreaks were caused primarily by clade AFR10d, which has a wider geographic distribution than clade AFR10e (Figure 2) (*14*).

One striking characteristic of AFR10e isolates was the presence of a mutation in the quinolone resistance–determining region of the topoisomerase IV subunit A gene, *parC* (S85L), that led to higher MIC values (0.25–0.38 mg/L) for ciprofloxacin. These isolates, which have a lower susceptibility

to ciprofloxacin than wild-type populations, would be classified as either resistant (MIC 0.38 mg/L) or susceptible (MIC 0.25 mg/L) in accordance with clinical breakpoints published by the European Committee on Antimicrobial Susceptibility Testing (https://www.eucast.org/clinical_breakpoints) in 2022, as inferred from the study of *Vibrio* strains and not Enterobacteriaceae strains. This *parC* mutation, sporadically reported in other AFR10 clades (Table; Figure 1, panel B; Appendix 2 Table 1), has been a distinctive characteristic of AFR10e isolates since 2014 (Figure 2, panel B). It was the second mutation affecting susceptibility to quinolones and fluroquinolones to be found in this AFR10e clade; the first was a mutation in the DNA gyrase subunit A gene, *gyrA* (S83I), present in all AFR10 isolates. This additional mutation does not seem to be associated with the specific use of fluoroquinolones for treating cholera outbreaks, because the antimicrobial drugs used for first-line cholera control in DRC are tetracyclines and macrolides, to which AFR10e isolates remain susceptible. Instead, the mutation may result from widespread self-medication with antimicrobials, a common practice in many sub-Saharan Africa countries including DRC (*15*).

All 96 isolates analyzed had known mutations of the *VC_0715* and *VC_A0637* genes conferring nitrofuran resistance (Table), consistent with previous findings (*2*). The isolates also carried the SXT/R391 genomic element ICE*Vch*Ind5, encoding resistance to streptomycin (*strAB*), sulfonamides (*sul2*), chloramphenicol (*flo*R), trimethoprim and the O/129 vibriostatic agent (*dfrA1*), and trimethoprim–sulfamethoxazole (*sul2* and *dfrA1*), with concordance between the phenotypic and genotypic data (Table; Appendix 2 Table 1).

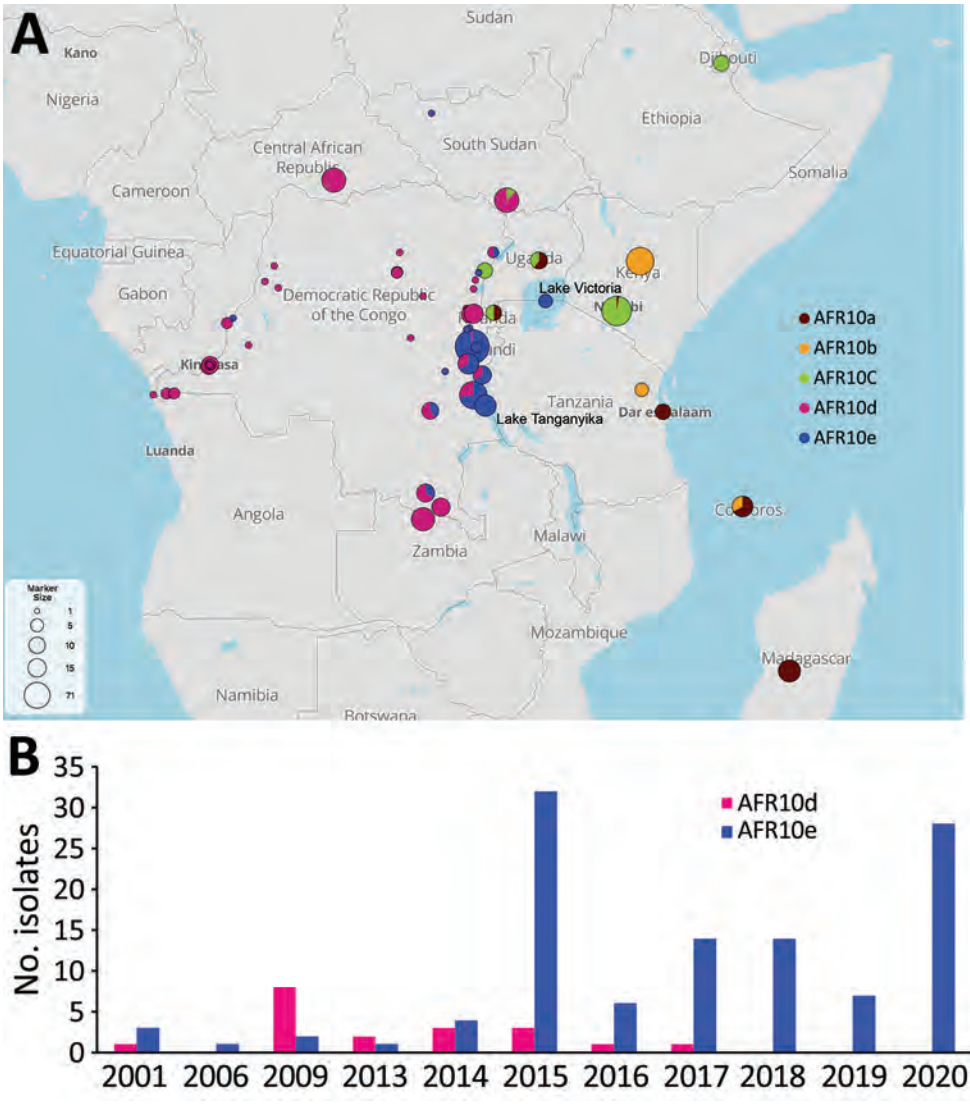

Figure 2. A) Spatiotemporal dynamics of the AFR10 clades of *Vibrio cholerae* O1 in the African Great Lakes Region, Africa, 1998–2020. Circle size indicates the number of isolates at the location concerned. The 5 AFR10 clades are color-coded: AFR10a, brown; AFR10b, yellow; AFR10c, green; AFR10d, pink; and AFR10e, blue. B) *V. cholerae* O1 isolates from the Lake Tanganyika basin. All AFR10 isolates from Bujumbura (Burundi), Kigoma (Tanzania) and the South-Kivu province (DRC) were considered to be Lake Tanganyika basin isolates.

Table. Characteristics of *Vibrio cholerae* O1 isolates from humans and the environment around Lake Tanganyika, Africa, 2015–2020*

Characteristic	2015	2016	2017	2018	2019	2020
No. isolates	26	7	14	14	7	28
AFR10 clade	AFR10d (1) AFR10e (25)	AFR10d (5) AFR10e (2)	AFR10e	AFR10e	AFR10e	AFR10e
Serotype	Inaba (1) Ogawa (25)	Inaba (5) Ogawa (2)	Ogawa	Ogawa	Ogawa	Ogawa
Source	Human	Human	Human	Human (10) Fish (2) Water (2)	Human (1) Fish (4) Water (2)	Human
MLST	ST515 (1) ST69 (25)	ST515 (5) ST69 (2)	ST69	ST69	ST69	ST69
Antimicrobial resistance determinants						
SXT/R391 element	ICE*Vch*Ind5	ICE*Vch*Ind5	ICE*Vch*Ind5†	ICE*Vch*Ind5	ICE*Vch*Ind5	ICE*Vch*Ind5
gyrA	S83I	S83I	S83I	S83I	S83I	S83I
parC	S85L	S85L (2), WT (5)	S85L	S85L	S85L	S85L
VC_0715	R169C	R169C	R169C	R169C	R169C	R169C
VC_A0637	Q5Stop	Q5Stop	Q5Stop	Q5Stop	Q5Stop	Q5Stop
AMR	AMR1‡ (26)	AMR1‡ (2) AMR2§ (5)	AMR1‡ (13) AMR3¶ (1)	AMR1 (14)‡	AMR1 (7)‡	AMR1 (28)‡

*Numbers in parentheses indicate number of isolates for each designation. AMR, antimicrobial resistance patterns; CIP, ciprofloxacin; DS, decreased susceptibility; FUR, nitrofurantoin; MLST, multilocus sequence typing; NAL, nalidixic acid; O129, cross-resistance to the vibriostatic agent O/129 and trimethoprim; PMB, polymyxin B; SSS, sulfonamides; ST, sequence type; STR, streptomycin; SXT, trimethoprim/sulfamethoxazole
†Deletion of the *strA*, *strB*, *floR*, and *sul2* genes in isolate CNRVC170308 (all isolates with intact ICE*Vch*Ind5 harbor the *strA*, *strB*, *dfrA1*, *floR*, and *sul2* resistance genes)
‡Resistance to STR, SSS, O129, SXT, FUR, PMB, NAL, and CIP^{DS}.
§Resistance to STR, SSS, O129, SXT, FUR, PMB, and NAL.
¶Resistance to O129, FUR, PMB, NAL, CIP^{DS}.

Conclusions

We found that the cholera outbreaks in the eastern part of DRC during 2001–2020 were caused by *V. cholerae* O1 sublineage AFR10, which was introduced into East Africa from South Asia in the late 1990s. The AFR13 sublineage was already reported in 2015 in Tanzania, including the city of Kigoma, located on the shore of Lake Tanganyika, but had not been detected in DRC as of 2022. The AFR10 isolates of this region belong principally to 2 clades, AFR10d (Inaba, ST515) and AFR10e (Ogawa, ST69). AFR10d was responsible for outbreaks reported in the western part of DRC in 2011–2017 and neighboring countries; AFR10e (Ogawa, ST69) was restricted to the Lake Tanganyika basin, in which reduced susceptibility to ciprofloxacin has been seen since 2014. Lake Tanganyika seems to serve as a transmission channel, favoring the establishment of AFR10e in local human populations. Further investigation, including studies of population movement, should reveal why AFR10e clade has remained within the Lake Tanganyika basin. The replacement of other clades by this antimicrobial-resistant clade in this area highlights the need for more systematic documentation of antimicrobial drug use and the implementation of adapted stewardship programs, particularly in outbreak responses. Overall, these findings highlight the need for continuous genomic surveillance and for coordinated communication between countries for effective interventions.

The International Foundation for Sciences funded the fieldwork for the isolation of environmental isolates (grant no. 1-2-A-6100-1). A.D.'s laboratory work is supported by core funding from the University of Copenhagen. The London School of Hygiene and Tropical Medicine study was cofunded by the French Agency for Development and the Veolia Foundation. The laboratory of F.-X.W. is part of the Integrative Biology of Emerging Infectious Diseases Laboratory of Excellence funded by the Government of France's "Investissement d'Avenir" programme (grant no. ANR-10-LABX-62-IBEID). The CNRVC is cofunded by Santé Publique France and the Institut Pasteur.

About the Author

Dr. Hounmanou is a postdoctoral fellow specializing in One Health at the University of Copenhagen. His primary research interests are microbial genomics, antimicrobial resistance, and routes of transmission between animals, humans, and bodies of water.

References

1. Weil AA, Ryan ET. Cholera: recent updates. Curr Opin Infect Dis. 2018;31:455–61. https://doi.org/10.1097/QCO.0000000000000474
2. Weill FX, Domman D, Njamkepo E, Almesbahi AA, Naji M, Nasher SS, et al. Genomic insights into the 2016–2017 cholera epidemic in Yemen. Nature. 2019;565:230–3. https://doi.org/10.1038/s41586-018-0818-3
3. Hendriksen RS, Price LB, Schupp JM, Gillece JD, Kaas RS, Engelthaler DM, et al. Population genetics of *Vibrio cholerae* from Nepal in 2010: evidence on the origin of the Haitian

outbreak. MBio. 2011;2:e00157-11. https://doi.org/10.1128/mBio.00157-11
4. Lessler J, Moore SM, Luquero FJ, McKay HS, Grais R, Henkens M, et al. Mapping the burden of cholera in sub-Saharan Africa and implications for control: an analysis of data across geographical scales. Lancet. 2018;391:1908–15 https://doi.org/10.1016/S0140-6736(17)33050-7
5. Ingelbeen B, Hendrickx D, Miwanda B, van der Sande MAB, Mossoko M, Vochten H, et al. Recurrent cholera outbreaks, Democratic Republic of the Congo, 2008–2017. Emerg Infect Dis. 2019;25:856–64. https://doi.org/10.3201/eid2505.181141
6. Hounmanou YMG, Mølbak K, Kähler J, Mdegela RH, Olsen JE, Dalsgaard A. Cholera hotspots and surveillance constraints contributing to recurrent epidemics in Tanzania. BMC Res Notes. 2019;12:664. https://doi.org/10.1186/s13104-019-4731-0
7. Debes AK, Shaffer AM, Ndikumana T, Liesse I, Ribaira E, Djumo C, et al. Cholera hot-spots and contextual factors in Burundi, planning for elimination. Trop Med Infect Dis. 2021;6:76. https://doi.org/10.3390/tropicalmed6020076
8. Mwaba J, Debes AK, Shea P, Mukonka V, Chewe O, Chisenga C, et al. Identification of cholera hotspots in Zambia: a spatiotemporal analysis of cholera data from 2008 to 2017. PLoS Negl Trop Dis. 2020;14:e0008227. https://doi.org/10.1371/journal.pntd.0008227
9. World Health Organization. Drop in cholera cases worldwide, as key endemic countries report gains in cholera control. 2019 [cited 2020 Apr 22]. https://www.who.int/news-room/detail/19-12-2019-drop-in-cholera-cases-worldwide-as-key-endemic-countries-report-gains-in-cholera-control
10. World Health Organization. Ending cholera. a global roadmap to 2030. 2017 [cited 2020 Apr 22]. https://www.gtfcc.org/wp-content/uploads/2019/10/gtfcc-ending-cholera-a-global-roadmap-to-2030.pdf
11. Weill FX, Domman D, Njamkepo E, Tarr C, Rauzier J, Fawal N, et al. Genomic history of the seventh pandemic of cholera in Africa. Science. 2017;358:785–9. https://doi.org/10.1126/science.aad5901
12. Hounmanou YMG, Leekitcharoenphon P, Kudirkiene E, Mdegela RH, Hendriksen RS, Olsen JE, et al. Genomic insights into *Vibrio cholerae* O1 responsible for cholera epidemics in Tanzania between 1993 and 2017. PLoS Negl Trop Dis. 2019;13:e0007934. https://doi.org/10.1371/journal.pntd.0007934
13. Irenge LM, Ambroise J, Mitangala PN, Bearzatto B, Kabangwa RKS, Durant JF, et al. Genomic analysis of pathogenic isolates of *Vibrio cholerae* from eastern Democratic Republic of the Congo (2014–2017). PLoS Negl Trop Dis. 2020;14:e0007642. https://doi.org/10.1371/journal.pntd.0007642
14. Breurec S, Franck T, Njamkepo E, Mbecko JR, Rauzier J, Sanke-Waïgana H, et al. Seventh Pandemic *Vibrio cholerae* O1 sublineages, Central African Republic. Emerg Infect Dis. 2021;27:262–6. https://doi.org/10.3201/eid2701.200375
15. Belachew SA, Hall L, Selvey LA. Non-prescription dispensing of antibiotic agents among community drug retail outlets in sub-Saharan African countries: a systematic review and meta-analysis. Antimicrob Resist Infect Control. 2021;10:13. https://doi.org/10.1186/s13756-020-00880-w

Address for correspondence: Marie-Laure Quilici, Institut Pasteur, Unité des Bactéries Pathogènes Entériques, 28 rue du Dr. Roux, 75724 Paris CEDEX 15, France; email: quilici@pasteur.fr

EID Podcast

Tracking *Bordetella pertussis*, Austria, 2018–20

Whooping cough is a reemerging, potentially deadly disease spread by a bacterium known as *Bordetella pertussis*. Fortunately, this respiratory infection is largely preventable with vaccination.

However, nature doesn't stay still, new antigenic variants of this bacterium are evolving and spreading.

In this EID podcast, Dr. Adriana Cabal Rosel, a public health microbiologist at the Austrian Agency for Health and Food Safety, describes a new surveillance system to track down these emerging variants in Austria.

Visit our website to listen: https://go.usa.gov/xshSV

EMERGING INFECTIOUS DISEASES®

Plasmodium falciparum *pfhrp2* and *pfhrp3* Gene Deletions in Malaria-Hyperendemic Region, South Sudan

Irene Molina-de la Fuente,[1] María José Sagrado Benito,[1] Laurence Flevaud, Janet Ousley, Harriet Akello Pasquale, Ahmed Julla, Abdirashid M. Abdi, Buai Tut Chol, Bakri Abubakr, Agustín Benito, Cristian Casademont, Carolina Nanclares, Pedro Berzosa

Pfhrp2 and *pfhrp3* gene deletions threaten the use of *Plasmodium falciparum* malaria rapid diagnostic tests globally. In South Sudan, deletion frequencies were 15.6% for *pfhrp2*, 20.0% for *pfhrp3*, and 7.5% for double deletions. Deletions were approximately twice as prevalent in monoclonal infections than in polyclonal infections.

Histidine-rich protein 2 (HRP2) is the primary target of the *Plasmodium falciparum* rapid diagnostic tests (RDT) that are a cornerstone of malaria control efforts in the high-burden, low-resource contexts in which malaria mortality is most acute (*1*). Increasing prevalence of *P. falciparum* parasites that do not express HRP2 or its paralogue histidine-rich protein 3 (encoded by the *pfhrp2* and *pfhrp3* genes) are affecting the accuracy of the RDTs. Infections with *pfhrp2* deletions are missed by HPR2-based RDTs much of the time; infections with double deletions (missing both *pfhrp2* and *pfhrp3* genes) are invisible to RDTs and create false-negative results. Because these deletions represent an existential threat to recent gains made in malaria control, the World Health Organization (WHO) has emphasized the critical need for surveillance (*2*).

Malaria is a leading cause of illness and death in South Sudan (*3*), where insufficient malaria prevention activities and a lack of access to healthcare combine dangerously. Despite the geographic and strategic importance of South Sudan in East and Central Africa, the only evidence of *pfhrp2* and *pfhrp3* deletions from the country come from a single report confirming their presence in 3 travelers to Australia (*4*). Accurate estimates of deletions could help responders delineate factors associated with deletions, predict future RDT needs, and clarify dynamics of false negativity rates in South Sudan overall.

In 2019, in collaboration with the South Sudanese Ministry of Health, Médecins Sans Frontières began a seasonal malaria chemoprophylaxis campaign combined with an assessment of molecular markers of antimalaria drug resistance in Yambio County, a malaria-endemic region of Western Equatoria State. We describe the frequency of *pfhrp2* and *pfhrp3* and double deletions in this clinical cohort, as well as the association between deletions, demographic factors, and infection characteristics in South Sudan. This study was approved by the internal ethics review board at Médecins Sans Frontières and by the South Sudan Research Ethics Committee. All participants provided informed consent.

The Study

We analyzed finger-prick blood samples collected in 9 villages in Yambio at the end of the malaria peak (January–February 2020) from persons ≥6 months of age with symptomatic malaria infection positively diagnosed by pan-pLDH–based RDT (CareStart

Author affiliations: Institute of Health Carlos III, Madrid, Spain (I. Molina-de la Fuente); Alcala University, Madrid (I.M. de la Fuente, A. Benito, P. Berzosa); Médecins Sans Frontières, Barcelona, Spain (M.J.S. Benito, L. Flevaud, C. Casademont, C. Nanclares); Médecins Sans Frontières, New York, New York, USA (J. Ousley); National Malaria Control Program, Ministry of Health, Juba, South Sudan (H.A. Pasquale, A. Julla); Médecins Sans Frontières, Juba (A.M. Abdi, B.T. Chol); Médecins Sans Frontières, Nairobi, Kenya (B. Abubakr); Centro de Investigación Biomedica en Red de Enfermedades Infecciosas, Madrid (A. Benito, P.J.B. Diaz)

DOI: https://doi.org/10.3201/eid2901.220775

[1]These authors contributed equally to this article.

Table 1. Frequency of *pfhrp2 and pfhrp3* deletion by geographic origin of samples, South Sudan*

Location	No isolates included	Overall *pfhrp2* deletion		Overall *pfhrp3* deletion	
		No.	Frequency, % (95% CI)	No.	Frequency, % (95% CI)
All sites	518	81	15.64 (12.62–19.06)	104	20.08 (16.71–23.79)
Kasia	50	6	12.00 (4.53–24.31)	11	22.00 (11.53–35.96)
Yambio State Hospital	44	13	29.55 (16.76–45.20)	18	40.91 (26.34–56.75)
Birisi	56	12	21.43 (11.59–34.44)	12	21.43 (11.59–34.44)
Bureangburu	62	7	11.29 (4.66–21.88)	7	11.29 (4.66–21.88)
Bakiwiri	58	6	10.34 (3.89–21.17)	7	12.07 (4.99–23.30)
Gitikiri	60	8	13.33 (5.94–24.59)	14	23.33 (13.38–36.04)
Nambia	70	14	20.00 (11.39–31.27)	12	17.14 (9.18–28.03)
Mamboi	51	5	9.80 (3.26–21.41)	7	13.73 (5.70–26.25)
Masumbu	67	10	14.93 (7.40–25.74)	15	22.39 (13.11–34.22)
p value by χ^2 test		0.108 (13.089)		0.014 (18.988)	

*Deletion frequency was calculated by dividing confirmed deletions by all confirmed *Plasmodium falciparum* samples included for analysis. *pfhrp2* and *pfhrp3* deletion frequency includes both single and double deletions. All analyses used a 95% CI and a p value of ≤0.05 for statistical significance.

Malaria PAN [pLDH] Ag RDT; Access Bio, https://accessbio.net). We performed malaria confirmation and speciation of 594 dried blood spot samples by multiplex PCR (*5*). Confirmed *P. falciparum* samples with high DNA quality (n = 518) underwent genotyping and molecular analysis for deletions in exon 2 of *pfhrp2* and *pfhrp3* (*5*) (Appendix, https://wwwnc.cdc.gov/EID/article/29/1/22-0775-App1.pdf). Demographic information was collected for all samples (Appendix). We defined multiplicity of infection (MOI) as the number of parasitic genotypes per infection and analyzed for a random subsample (n = 419) by amplifying *P. falciparum* merozoite surface protein 1 and 2 genes (*pfmsp1*, *pfmsp2*) (*6*). We defined

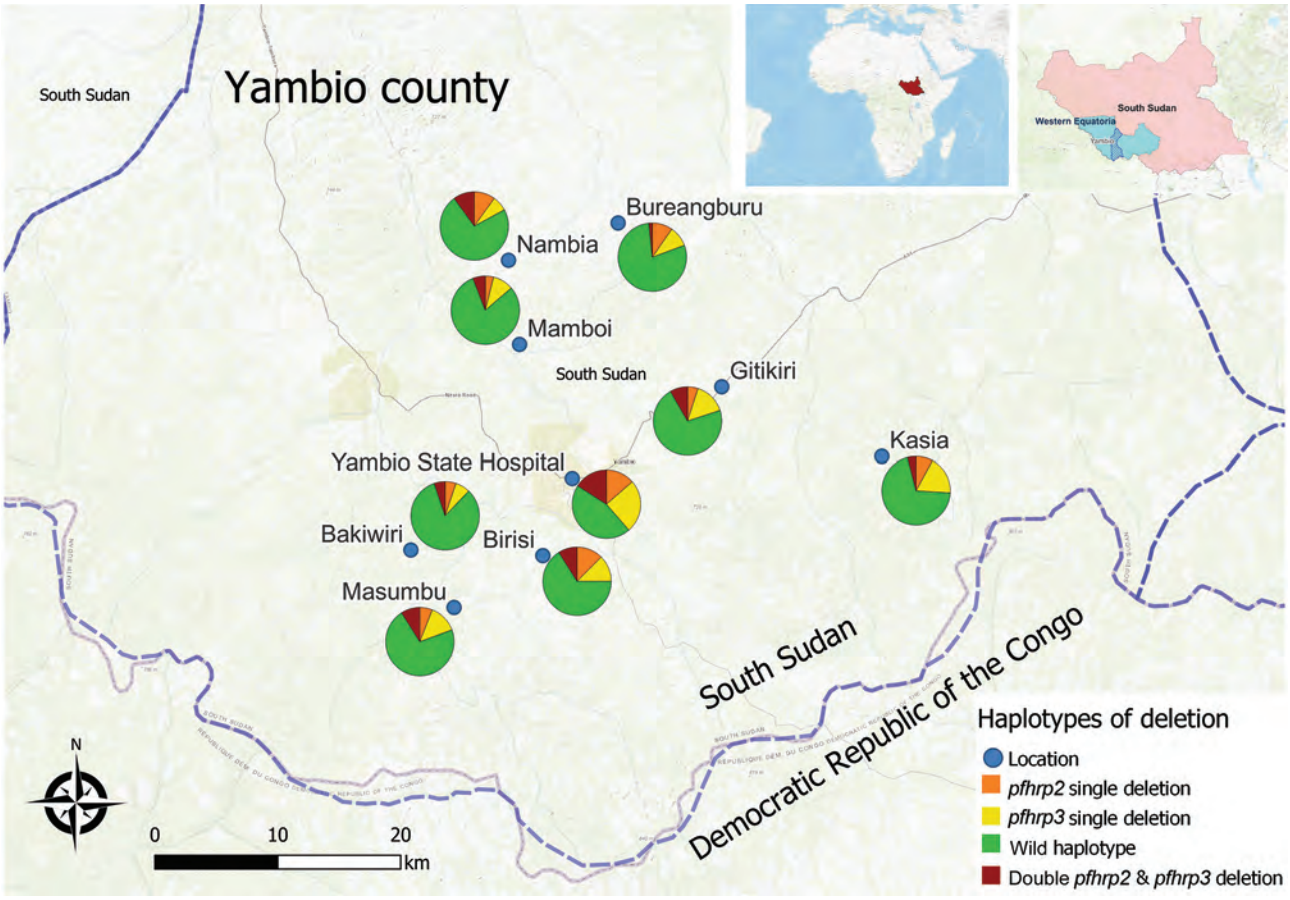

Figure 1. Frequencies of *Plasmodium falciparum* single and double *pfhrp2* and *pfhrp3* deletions in malaria-hyperendemic region, South Sudan. Color represents the type of deletion and proportion of each type of deletion and genotype. Open source QGIS software (https://www.qgis.org) was used to map sample collection locations. Inset map shows locations of the study area in South Sudan and of South Sudan in Africa.

Table 2. Association of age, sex, MOI, severity of infection, and previous seasonal malaria chemoprophylaxis with *pfhrp2* and *pfhrp3* deletions in malaria-hyperendemic region, South Sudan*

Characteristic	Total no.	*pfhrp2* deletion		*pfhrp3* deletion		*pfhrp2/3* double deletion		Wild-type	
		No.	Frequency, % (95% CI)	No.	Frequency, % (95% CI)	No.	Frequency, % (95% CI)	No.	Frequency, % (95% CI)
Age, y									
<5	159	28	17.61 (12.03–24.44)	29	18.24 (12.49–24.98)	14	8.81 (4.87–14.25)	117	73.58 (66.02–80.25)
5–14	196	24	12.24 (8.00–17.67)	30	15.31 (10.57–21.12)	10	5.10 (2.47–9.18)	152	77.55 (71.06–83.19)
>14	163	30	18.40 (12.77–25.21)	45	27.61 (20.90–35.14)	15	9.20 (5.24–14.72)	103	63.19 (55.29–70.60)
p value (χ^2)		0.238 (2.874)		0.012 (8.875)		0.261 (2.686)		0.009	
Sex									
F	271	44	16.24 (12.05–21.18)	60	22.14 (17.34–27.56)	24	8.86 (5.76–12.89)	191	70.48 (64.66–75.84)
M	247	37	14.98 (10.77–20.05)	44	17.81 (13.25–23.17)	15	6.07 (3.44–9.82)	181	73.79 (67.30–78.69)
p value (χ^2)		0.694 (0.154)		0.219 (1.507)		0.231 (1.438)		0.542	
MOI									
1: monoclonal	116	26	22.41 (15.19–31.09)	37	31.90 (23.55–41.19)	14	12.07 (6.76–19.42)	102	87.93 (80.58–93.24)
≥2: Polyclonal	303	43	14.29 (10.54–18.76)	46	15.28 (11.41–19.85)	15	4.98 (2.82–8.09)	288	95.05 (91.97–97.20)
p value (χ^2)		0.001 (9.881)		<0.001 (14.754)		0.010 (6.598)		0.019	
Severity									
Uncomplicated	472	68	14.41 (11.36–17.90)	82	17.37 (14.06–21.10)	31	6.57 (4.51–9.19)	359	73.56 (71.95–79.84)
Complicated	30	8	26.67 (12.28–45.89)	14	46.67 (28.34–65.67)	5	16.67 (5.64–34.72)	13	43.33 (25.46–62.57)
p value (χ^2)		0.087 (2.937)		<0.001 (14.031)		0.051 (3.819)		<0.001	
Seasonal malaria chemoprophylaxis for children <5 y									
Yes	137	24	17.52 (11.56–24.94)	22	16.06 (10.35–23.24)	11	8.03 (4.08–13.91)	102	74.45 (66.30–81.52)
Not	22	3	13.64 (2.91–34.91)	7	31.82 (13.86–54.87)	3	13.63 (2.91–34.91)	15	68.18 (45.13–86.14)
p value (χ^2)		0.652 (0.203)		0.075 (3.157)		0.742 (0.389)		0.720 (0.129)	

*Variables were considered categorical variables and the association between them and deletions were assessed using χ^2 testing. Deletions for *pfhrp2* and *pfhrp3* include both single and double deletions. All analyses used a 95% CI and a p value of ≤0.05 for statistical significance. MOI, multiplicity of infection.

monoclonal infection as the detection of a single PCR fragment for each locus and polyclonal infection as the detection of >1 PCR fragment for ≥1 locus.

Overall deletion frequency (including samples with both single and double deletions) among 518 genotyped PCR-positive samples was 15.6% for *pfhrp2* and 20.0% for *pfhrp3* (Table 1). Double deletions were found in 7.5% of isolates; patients at Yambio State Hospital had nearly twice the rate of double deletions (15.9%) as patients at all other sites (Figure 1). In 7/9 study sites, >10% of samples did not amplify *pfhrp2*; >5% of isolates were double-deleted in nearly half (4/10) of sites. *Pfhrp2* deletion rates in South Sudan were as high as or higher than the country's immediate neighbors, where reported deletion rates from specific sites have varied from 26% in Ethiopia to 19% in Kenya, 6% in the Democratic Republic of the Congo, 3% in Uganda, and <1% in Sudan (*7*–*11*).

Monoclonality was the only factor significantly associated with both *pfhrp2* and *pfhrp3* deletions and double deletions (Table 2). Even so, the frequency of deletion among polyclonal infections was higher than expected. Severe malaria cases exhibited significantly more *pfhrp3* and double deletions than uncomplicated infections. Patients >14 years of age were more likely to harbor deletions than were patients <5 and 5–14 years of age, although the difference was significant only for *pfhrp3* (Table 2).

Unequal deletion distribution between proximate geographic zones has been previously reported (*9*,*10*), and variability in double deletion rates by study site in Yambio was notable, suggesting possible hot spots. However, the higher rates seen at Yambio State Hospital could also be explained by its significantly higher proportion of monoclonal infections (Appendix). The small sample sizes at individual sites leave conclusions about hot spots unsettled, but they underscore the importance of realistic malaria control strategies targeted to the local molecular marker landscape.

We used a statistically significant multivariable logistic regression model for total MOI, infection severity, and patient age factors for *pfhrp2*, *pfhrp3* and double deletions (Figure 2). Age was the only significant predictor of *pfhrp2* deletions (after adjusting for MOI and severity of infection), whereas age, MOI, and clinical severity were all predictors for *pfhrp3* deletions. Only MOI was a significant predictor of double deletions (Appendix).

Most research surrounding the interaction between MOI and *pfhrp2* and *pfhrp3* deletions concludes that polyclonal infections mask deletions and lead to underestimates in deletion prevalence (*12*). Our results support this conclusion, finding lower MOI in Yambio associated with most deletions. In high-transmission settings, younger persons tend to have higher MOIs (*13*). We also found lower MOI and older patient age associated with deletions, contrasting with studies that have linked deletions to lower age but failed to consider MOI as a confounder (*9*).

In addition, the fitness-cost of deletions (the effects on the parasite after losing 1 of its proteins)

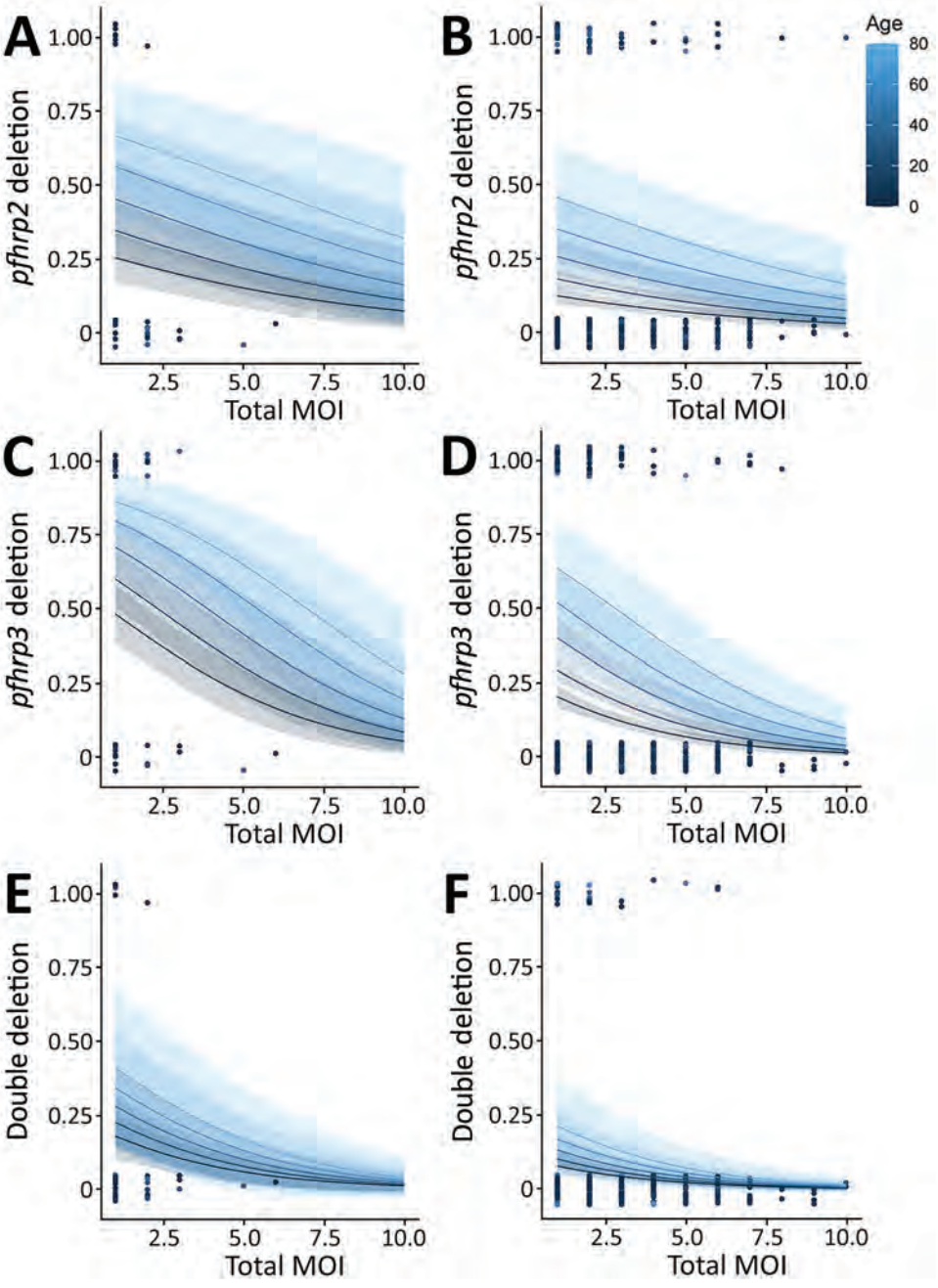

Figure 2. Multivariable regression model of *Plasmodium falciparum pfhrp2* deletions (A), *pfhrp3* deletions (B), and double deletions (C) in malaria-hyperendemic region, South Sudan. Panels A, C, and E indicate uncomplicated malaria; panels B, D, and F, severe malaria. The models combined 2 continuous variables: age of the patient, represented with different colors, and total MOI, represented in x-axis, with the binary response variable (presence of deletion). Probability of deletion (y-axis) was considered a binary outcome variable. The quality of the model was evaluated by the likelihood ratio method. The model was significant (p value<0.01) for *pfhrp2* and *pfhrp3* deletion and *pfhrp2* and *pfhrp3* double deletion. Each dot represents 1 sample. MOI, multiplicity of infection.

could be another way that age, disease severity, and deletion risk interact, because milder disease has previously been associated with *pfhrp2* deletion (*14*) and persons acquire immunity against *P. falciparum* as they age (*13*). In this area, our cohort breaks with consensus, finding deletions more commonly in complicated malaria patients. We believe this difference might reflect the difficulties of diagnosing febrile disease in South Sudan, where the signs of severe malaria might be caused by other undetected infections.

Sample collection in this study occurred at the end of the high-intensity malaria transmission season, when potentially high parasitic diversity but low prevalence could favor spread of gene-deleted organisms, making deletions easier to detect (*14*). When interpreting *pfhrp2* deletion surveillance, the transmission period should be considered (*9*,*15*).

This study was limited because it was a secondary analysis of a study of molecular markers of antimalarial drug resistance and did not follow WHO protocols for *pfhrp2* and *pfhrp3* deletion surveillance. Consequently, the precise prevalence of *pfhrp2* and *pfhrp3* gene deletions causing false-negative results on RDTs in South Sudan was not generated to assess whether it is within the 5% threshold established by WHO (*2*). We also exclusively used pan *p*-LDH RDT–positive samples, preventing us from evaluating the effects of deletions on malaria diagnoses.

Conclusions

Characterizing *pfhrp2* and *pfhrp3* deletions is critical to designing effective public health strategies for malaria control. This study describes these deletions in a clinical cohort in a country with little previous endemic evidence of *pfhrp2* and *pfhrp3* deletion. Monoclonal infections were a principal predictor of deletions. We identified high levels of single and double deletions of *pfhrp2* and *pfhrp3*, which if more widely present in this or other regions of South Sudan, could s eriously jeopardize HRP2-based RDT effectiveness moving forward. Future studies should be designed according to WHO protocol to produce precise estimates to measure the risk those deletions pose in South Sudan. Local variation in prevalence suggests the potential for deletion hotspots within the country and should be considered when designing malaria control strategies.

Acknowledgments

We thank the population in Yambio region for their participation. We also thank all the Médecins Sans Frontières, Ministry of Health, and partner staff involved in this project. We thank Luz Garcia, Vicenta González, and Rosario Gálvez for laboratory work with samples.

These data were previously presented in poster form at the Spanish Society of Tropical Medicine and International Health Conference in March 2022.

About the Author

Prof. Molina-de la Fuente is a PhD candidate at the University of Alcalá with Dr. Pedro Berzosa as PhD codirector. She is conducting research at the National Centre of Tropical Medicine at Institute of Health Carlos III in Spain on molecular and genomic epidemiology, malaria diagnosis evasion, and antimalaria drug resistance. Dr. Sagrado is the epidemiology adviser in Médecins Sans Frontières OCBA, where she conducts operational and clinical research in infectious and chronic diseases. She also has worked as an epidemiologist at the World Health Organization and the Spanish National Center of Epidemiology's Institute of Health Carlos III.

References

1. Rogier E, McCaffery JN, Nace D, Svigel SS, Assefa A, Hwang J, et al. *Plasmodium falciparum* pfhrp2 and pfhrp3 gene deletions from persons with symptomatic malaria infection in Ethiopia, Kenya, Madagascar, and Rwanda. Emerg Infect Dis. 2022;28:608–16. https://doi.org/10.3201/eid2803.211499
2. World Health Organization. Master protocol for surveillance of pfhrp2/3 deletions and biobanking to support future research [cited 2022 Dec 13]. https://apps.who.int/iris/bitstream/handle/10665/331197/9789240002050-eng.pdf
3. Republic of South Sudan Ministry of Health. Malaria Strategic Plan 2021 – 2025. 2020.
4. Prosser C, Gresty K, Ellis J, Meyer W, Anderson K, Lee R, et al. *Plasmodium falciparum* histidine-rich protein 2 and 3 gene deletions in strains from Nigeria, Sudan, and South Sudan. Emerg Infect Dis. 2021;27:471–9. https://doi.org/10.3201/eid2702.191410
5. Berzosa P, González V, Taravillo L, Mayor A, Romay-Barja M, García L, et al. First evidence of the deletion in the pfhrp2 and pfhrp3 genes in *Plasmodium falciparum* from Equatorial Guinea. Malar J. 2020;19:99. https://doi.org/10.1186/s12936-020-03178-9
6. Sondo P, Derra K, Rouamba T, Nakanabo Diallo S, Taconet P, Kazienga A, et al. Determinants of *Plasmodium falciparum* multiplicity of infection and genetic diversity in Burkina Faso. Parasit Vectors. 2020;13:427. https://doi.org/10.1186/s13071-020-04302-z
7. Feleke SM, Reichert EN, Mohammed H, Brhane BG, Mekete K, Mamo H, et al. *Plasmodium falciparum* is evolving to escape malaria rapid diagnostic tests in Ethiopia. Nat Microbiol. 2021;6:1289–99. https://doi.org/10.1038/s41564-021-00962-4
8. Beshir KB, Sepúlveda N, Bharmal J, Robinson A, Mwanguzi J, Busula AO, et al. *Plasmodium falciparum* parasites with histidine-rich protein 2 (pfhrp2) and pfhrp3 gene deletions in two endemic regions of Kenya. Sci Rep. 2017;7:14718. https://doi.org/10.1038/s41598-017-15031-2
9. Parr JB, Verity R, Doctor SM, Janko M, Carey-Ewend K, Turman BJ, et al. Pfhrp2-deleted *Plasmodium falciparum* parasites in the Democratic Republic of the Congo: a national cross-sectional survey. J Infect Dis. 2017;216:36–44.

10. Agaba BB, Anderson K, Gresty K, Prosser C, Smith D, Nankabirwa JI, et al. Molecular surveillance reveals the presence of pfhrp2 and pfhrp3 gene deletions in *Plasmodium falciparum* parasite populations in Uganda, 2017–2019. Malar J. 2020;19:300. https://doi.org/10.1186/s12936-020-03362-x
11. Boush M, Djibrine M, Mussa A, Talib M, Maki A, Mohammed A, et al. *Plasmodium falciparum* isolate with histidine-rich protein 2 gene deletion from Nyala City, Western Sudan. Sci Rep. 2020;10:12822.
12. Grignard L, Nolder D, Sepúlveda N, Berhane A, Mihreteab S, Kaaya R, et al. A novel multiplex qPCR assay for detection of *Plasmodium falciparum* with histidine-rich protein 2 and 3 (pfhrp2 and pfhrp3) deletions in polyclonal infections. EBioMedicine. 2020;55:102757. https://doi.org/10.1016/j.ebiom.2020.102757
13. Pinkevych M, Petravic J, Bereczky S, Rooth I, Färnert A, Davenport MP. Understanding the relationship between *Plasmodium falciparum* growth rate and multiplicity of infection. J Infect Dis. 2015;211:1121–7. https://doi.org/10.1093/infdis/jiu561
14. Watson OJ, Slater HC, Verity R, Parr JB, Mwandagalirwa MK, Tshefu A, et al. Modelling the drivers of the spread of *Plasmodium falciparum hrp2* gene deletions in sub-Saharan Africa. eLife. 2017;6:e25008. https://doi.org/10.7554/eLife.25008
15. Koita OA, Ndiaye J, Nwakanma D, Sangare L, Ndiaye D, Joof F. Seasonal changes in the frequency of false negative rapid diagnostic tests based on histidine rich protein 2 (HRP2). Am J Trop Med Hyg. 2013;80:1.

Address for correspondence: Maria Jose Sagrado Benito, Médecins Sans Frontières–Barcelona, Carrer de Zamora, 54, 08005 Barcelona, Spain; email: mariajose.sagrado@barcelona.msf.org

February 2022

Vectorborne Infections

- Viral Interference between Respiratory Viruses
- Novel Clinical Monitoring Approaches for Reemergence of Diphtheria Myocarditis, Vietnam
- Clinical and Laboratory Characteristics and Outcome of Illness Caused by Tick-Borne Encephalitis Virus without Central Nervous System Involvement
- Role of *Anopheles* Mosquitoes in Cache Valley Virus Lineage Displacement, New York, USA
- Invasive *Burkholderia cepacia* Complex Infections among Persons Who Inject Drugs, Hong Kong, China, 2016–2019
- Comparative Effectiveness of Coronavirus Vaccine in Preventing Breakthrough Infections among Vaccinated Persons Infected with Delta and Alpha Variants
- Effectiveness of mRNA BNT162b2 Vaccine 6 Months after Vaccination among Patients in Large Health Maintenance Organization, Israel
- Comparison of Complications after Coronavirus Disease and Seasonal Influenza, South Korea
- Epidemiology of Hospitalized Patients with Babesiosis, United States, 2010–2016
- Rapid Spread of Severe Fever with Thrombocytopenia Syndrome Virus by Parthenogenetic Asian Longhorned Ticks

- Wild Boars as Reservoir of Highly Virulent Clone of Hybrid Shiga Toxigenic and Enterotoxigenic *Escherichia coli* Responsible for Edema Disease, France
- Public Acceptance of and Willingness to Pay for Mosquito Control, Texas, USA
- Widespread Detection of Multiple Strains of Crimean-Congo Hemorrhagic Fever Virus in Ticks, Spain
- West Nile Virus Transmission by Solid Organ Transplantation and Considerations for Organ Donor Screening Practices, United States

- Serial Interval and Transmission Dynamics during SARS-CoV-2 Delta Variant Predominance, South Korea
- Postvaccination Multisystem Inflammatory Syndrome in Adult with No Evidence of Prior SARS-CoV-2 Infection
- Postmortem Surveillance for Ebola Virus Using OraQuick Ebola Rapid Diagnostic Tests, Eastern Democratic Republic of the Congo, 2019–2020
- SARS-CoV-2 Seroprevalence before Delta Variant Surge, Chattogram, Bangladesh, March–June 2021
- SARS-CoV-2 B.1.619 and B.1.620 Lineages, South Korea, 2021
- *Neisseria gonorrhoeae* FC428 Subclone, Vietnam, 2019–2020
- Zoonotic Infection with Oz Virus, a Novel Thogotovirus
- SARS-CoV-2 Cross-Reactivity in Prepandemic Serum from Rural Malaria-Infected Persons, Cambodia
- Tonate Virus and Fetal Abnormalities, French Guiana, 2019
- *Babesia crassa*–Like Human Infection Indicating Need for Adapted PCR Diagnosis of Babesiosis, France
- Clinical Features and Neurodevelopmental Outcomes for Infants with Perinatal Vertical Transmission of Zika Virus, Colombia

EMERGING INFECTIOUS DISEASES

To revisit the February 2022 issue, go to:
https://wwwnc.cdc.gov/eid/articles/issue/28/2/table-of-contents

Burden of Postinfectious Symptoms after Acute Dengue, Vietnam

Dong Thi Hoai Tam,[1] Hannah Clapham,[1] Elisabeth Giger, Nguyen Tan Thanh Kieu, Nguyen Tran Nam, Dinh Thi Tri Hong, Banh Thi Nuoi, Nguyen Thi Hong Cam, Nguyen Than Ha Quyen, Hugo C. Turner, Thomas Jaenisch, Cameron P. Simmons, Phung Khanh Lam, Bridget Wills

We assessed predominantly pediatric patients in Vietnam with dengue and other febrile illness 3 months after acute illness. Among dengue patients, 47% reported ≥1 postacute symptom. Most resolved by 3 months, but alopecia and vision problems often persisted. Our findings provide additional evidence on postacute dengue burden and confirm children are affected.

Dengue is a mosquitoborne viral infection found across much of the tropical and subtropical world. Most infections are asymptomatic or paucisymptomatic. Acute symptoms range from an influenza-like self-limited febrile illness to, in a small proportion of cases, severe and complicated disease that can prove fatal (*1*). In total, 4 dengue viral serotypes (DENV-1–4) exist; severe disease rarely occurs during the first exposure to any serotype (i.e., a primary infection) but is more likely to occur during a subsequent infection with a different serotype (i.e., a secondary infection).

The symptoms of acute dengue are generally understood to resolve after 1–2 weeks, but the potential for persistent or delayed symptoms has received increasing attention in recent years. However, few formal studies have been published, and these studies have reported a range of symptoms and frequencies (*2*–*8*). A recent review summarizing this literature showed a substantial proportion of persons experienced some kind of postacute symptoms; the proportion decreased over time after infection (*9*), and 24% reported notable fatigue (*4*).

Author affiliations: Oxford University Clinical Research Unit, Wellcome Trust Asia Programme, Ho Chi Minh City, Vietnam (D.T.H. Tam, E. Giger, N.T.T. Kieu, D.T.T. Hong, B.T. Nuoi, N.T.H. Cam, N.T.H. Quyen, P.K. Lam, B. Wills); University of Oxford, Oxford, England, UK (H. Clapham, B. Wills); National University of Singapore and National University Health System, Singapore (H. Clapham); City Children's Hospital, Ho Chi Minh City (N.T. Nam); Imperial College London, London, England, UK (H.C. Turner); Heidelberg University Hospital, Heidelberg, Germany (T. Jaenisch); Colorado School of Public Health, Aurora, Colorado, USA (T. Jaenisch); Monash University, Melbourne, Victoria, Australia (C,P. Simmons); University of Medicine and Pharmacy at Ho Chi Minh City, Ho Chi Minh City (K. Lam)

DOI: https://doi.org/10.3201/eid2901.220838

The Study

We report on postinfectious symptoms in 247 predominantly pediatric patients from Vietnam 3 months after an acute febrile illness; 200 of them had dengue (Appendix, https://wwwnc.cdc.gov/EID/article/29/1/22-0838-App1.pdf). After acute dengue, we observed a broad spectrum of postviral symptoms ranging from fatigue, joint pain, and muscle pain to vision problems and hair loss (Table). We report ≈8% patients experienced fatigue, consistent with a study in Singapore reporting 9% (*3*), but lower than the 24% in another Singapore study (*2*) and the 28% reported from Cuba (*4*). The Cuba study also reported headaches in 15% of patients compared with our estimate of 4%, whereas a recent study of 79 dengue-infected persons in Mexico indicated that 38% reported headaches in the second week after onset of fever, which dropped to 8% at 6–8 months (*10*). Our estimate of 47% of persons experiencing ≥1 symptom is higher than the 8.5% observed in Peru (*8*) but lower than the 65% experiencing ≥1 persistent symptom observed in Brazil (*6*). In general, the sample sizes were small in all studies, and the study methods or timeframes after infection differed.

Symptoms have previously been associated with older age, but in our study the only symptom observed to be more likely in adults than children was joint pain (Appendix Table 2). Other studies have noted a higher frequency of symptoms in female than male patients (*2*,*5*,*6*,*8*). We noted this difference for alopecia and joint pain only; few men (3%) experienced either of these symptoms compared with ≈30% of women (Appendix Table 3). As for most other

[1]These first authors contributed equally to this article.

Table. Number and percentage estimates of persons experiencing postacute symptoms after dengue or other febrile illness during the 3-month follow-up period, Vietnam

	Other febrile illness, n = 47		Dengue, n = 200	
Symptom	No.	% (95% CI)	No.	% (95% CI)
Alopecia	2	4.3 (0.5–14.5)	25	12.5 (8.3–17.9)
Tiredness	4	8.5 (2.4–20.4)	17	8.5 (5.0–13.3)
Resumed daily activities	47	100 (92.5–100)	200	100 (98.2–100)
Headaches	3	6.4 (1.3–17.5)	6	3.0 (1.1–6.4)
Muscle pain	0	0 (0.0–7.6)	3	1.5 (0.3–4.3)
Joint pain	2	4.3 (0.5–14.5)	3	1.5 (0.3–4.2)
Loss of appetite	2	4.3 (0.5–14.5)	3	1.5 (0.3–4.3)
Blurred vision	9	19.1 (9.2–33.3)	22	11.1 (7.0–16.2)
Rash	3	6.4 (1.3–17.5)	21	10.5 (6.6–15.6)
Sleep problem	2	4.3 (0.5–14.5)	9	4.5 (2.1–8.4)
Concentration problem	6	12.3 (4.8–25.7)	19	9.5 (5.8–14.4)
Little interest	1	2.1 (0.1–11.3)	1	0.5 (0.0–2.8)
Depressed	0	0 (0.0–7.6)	0	0 (0.0–1.8)
Other problems, including alopecia	3	6.4 (1.3–17.5)	32	16.0 (11.2–21.8)
Any symptom	22	47 (32.0–62.0)	92	46 (39.0–53.0)
Other acute illness	14	29.8 (17.3–44.9)	33	16.5 (11.6–22.4)

studies assessing the relationship between postinfectious symptoms and disease severity (*2*,*5*), we did not observe any relationship between symptoms after infection and disease severity during acute infection (Appendix Table 4). The numbers were small, but our study indicated worse symptoms (loss of appetite, blurred vision, and concentration problems) might be more likely after DENV-3 infection than infection with other serotypes (Appendix Table 4). This suggestion remained after controlling for disease severity and primary or secondary infection. Whether postacute symptoms vary by serotype is a possible line of future study.

The alopecia we report in our study (25/200 [13%] in dengue vs. 2/47 [4%] in other febrile illness [OFI]) has been observed previously, at a much lower rate in 1 study in Brazil (*7*) and at a similar rate in a recent study from Mexico (*10*). Alopecia after dengue has been noted in 1 case report (*11*). We identified alopecia in our study only in the category of other symptoms, and it was reported by patients without specific prompting, so this result is striking. Vision problems associated with dengue have previously been reported but mainly during the acute phase or soon afterwards (*12*,*13*). In our study, we saw that these symptoms can persist for several months or start much later after infection (Appendix Table 6), which was also seen in the recent study in Mexico (*10*). We found no association between specific symptoms during acute infection and afterwards (Appendix Table 5).

For many of the symptoms we report, occurrence rates were similar in the dengue and OFI groups (Table). Although the OFI group was relatively small and we do not have specific diagnoses for these persons, the data suggest that the late effects of dengue are not dissimilar to those experienced after other acute febrile illnesses. Our enrollment criteria and the fact that most patients recovered without additional therapy suggest a likely viral etiology; the pathogens causing disease in the control groups are likely to be quite variable between geographic locations, possibly explaining our lower rate of postacute consequences in the dengue group compared with the OFI groups in other studies (*3*,*8*).

Another potentially interesting observation was the lower rate of other illnesses experienced after the initial acute episode in the dengue group compared with the control group (33/200 [16.5%] vs. 14/47 [30%]) (Table). This lower rate might suggest some nonspecific immune modulation after dengue that is protective, or the rate in the other group could be higher than usual because of an effect of the other febrile illnesses.

Conclusions

Understanding the burden of postacute symptoms is key to calculating the overall disease burden of dengue (*14*). A recent review estimated that the economic cost of persistent symptoms after dengue in Mexico alone was US $22.6 million (2012 prices) (*9*). In those estimates, the authors assumed symptoms were only experienced in adults because they saw an increase in the proportion of persons experiencing symptoms with age. We clearly show that children also experience postacute symptoms. In countries such as Vietnam, where much of the acute disease occurs in children, including postacute consequences in this group might change burden estimates considerably. In the Global Burden of Disease 2013 Study, 44% of the estimated total number of disability-adjusted life-years (DALYs) lost because of dengue was attributed to persistent symptoms (*15*). In recent Global Burden of

Disease estimates, 8.5% of cases are assumed to experience acute consequences and are given a disability weight for chronic fatigue lasting for 6 months. In the context of our results, 8.5% might be a fairly realistic estimate; however, 100% of our patients had returned to work or normal daily life by 3 months postinfection. How accurately the infectious disease–postacute consequences disability weight currently being used represents the severity of postacute consequences is uncertain. We also observed that most symptoms lasted <1 month, suggesting 6 months is an overestimate of the duration of postacute consequences for this setting. This observation highlights the need for further research in this area because such burden calculations can influence public health priority-setting and funding decisions.

In summary, we have provided estimates of the proportion of dengue infections, mainly in children, that result in longer-term symptoms in a population in Vietnam. In addition to previously observed tiredness and joint pain, we have provided evidence for 2 longer-term symptoms, hair loss and vision problems. Further work in other settings should assess whether these symptoms are seen elsewhere. We also provide evidence that children experience long-term symptoms after dengue. This work is informative to the estimates of the burden of dengue and suggests additional information about the likely recovery path that could be given to patients when discharged after acute dengue.

This work was supported by the European Union's Seventh Framework Programme for research, technological development and demonstration (grant FP7-281803 IDAMS; http://www.idams.eu; publication reference number IDAMS: 57) as well as core grant support to the Oxford University Clinical Research Unit from Wellcome (grant code 106680/B/14/Z). H.C.T. acknowledges funding from the MRC Centre for Global Infectious Disease Analysis (reference MR/R015600/1), jointly funded by the UK Medical Research Council (MRC) and the UK Foreign, Commonwealth & Development Office (FCDO), under the MRC/FCDO Concordat agreement and is also part of the EDCTP2 programme supported by the European Union. iDSI is funded by the Bill and Melinda Gates Foundation [OPP1134345], the UK's Department for International Development, and the Rockefeller Foundation.

About the Author

Dr. Tam was until recently associate professor in the infectious diseases department of the University of Medicine at Ho Chi Minh City, Vietnam. Since retiring, she has continued her scientific research by contributing to many dengue clinical studies at the Oxford University Clinical Research Unit, Ho Chi Minh City. Dr. Clapham is an assistant professor who researches infectious disease dynamics at the Saw Swee Hock School of Public Health, National University of Singapore. Previously, she was head of the mathematical modelling group at the Oxford University Clinical Research Unit, Ho Chi Minh City.

References

1. Halstead SB. Dengue. Lancet. 2007;370:1644–52. https://doi.org/10.1016/S0140-6736(07)61687-0
2. Seet RCS, Quek AML, Lim ECH. Post-infectious fatigue syndrome in dengue infection. J Clin Virol. 2007;38:1–6. https://doi.org/10.1016/j.jcv.2006.10.011
3. Low JGH, Ooi E-E, Tolfvenstam T, Leo YS, Hibberd ML, Ng LC, et al. Early dengue infection and outcome study (EDEN)—study design and preliminary findings. Ann Acad Med Singap. 2006;35:783–9.
4. González D, Martínez R, Castro O, Serrano, T, Portela D, Vazquez S, et al. Evaluation of some clinical, humoral and imagenological parameters in patients of dengue haemorrhagic fever six months after acute illness. Dengue Bull. 2005;29:53–7.
5. García G, González N, Pérez AB, Sierra B, Aguirre E, Rizo D, et al. Long-term persistence of clinical symptoms in dengue-infected persons and its association with immunological disorders. Int J Infect Dis. 2011;15:e38–43. https://doi.org/10.1016/j.ijid.2010.09.008
6. Teixeira LAS, Lopes JSM. Martins AG da C, Campos FAB, Miranzi S de SC, Nascentes GAN. Persistence of dengue symptoms in patients in Uberaba, Minas Gerais State, Brazil [in Portuguese]. Cad Saude Publica. 2010;26:624–30. https://doi.org/10.1590/S0102-311X2010000300019
7. Tristão-Sá R, Kubelka CF, Zandonade E, Zagne SM, Rocha NS, Zagne LO, et al. Clinical and hepatic evaluation in adult dengue patients: a prospective two-month cohort study. Rev Soc Bras Med Trop. 2012;45:675–81. https://doi.org/10.1590/S0037-86822012000600004
8. Halsey ES, Williams M, Laguna-Torres VA, Vilcarromero S, Ocaña V, Kochel TJ, et al. Occurrence and correlates of symptom persistence following acute dengue fever in Peru. Am J Trop Med Hyg. 2014;90:449–56. https://doi.org/10.4269/ajtmh.13-0544
9. Tiga DC, Undurraga EA, Ramos-Castañeda J, Martínez-Vega RA, Tschampl CA, Shepard DS. Persistent symptoms of dengue: estimates of the incremental disease and economic burden in Mexico. Am J Trop Med Hyg. 2016;94:1085–9. https://doi.org/10.4269/ajtmh.15-0896
10. Tiga-Loza DC, Martínez-Vega RA, Undurraga EA, Tschampl CA, Shepard DS, Ramos-Castañeda J. Persistence of symptoms in dengue patients: a clinical cohort study. Trans R Soc Trop Med Hyg. 2021;114:355–364. https://doi.org/10.1093/trstmh/traa007
11. Hitani A, Yamaya W, To M, Kano I, Honda-Hosono N, Takasaki T, et al. A case of dengue fever and subsequent long-lasting depression accompanied by alopecia in a Japanese traveler returning from Bali, Indonesia [in Japanese]. Kansenshogaku Zasshi. 2015;89:279–82. https://doi.org/10.11150/kansenshogakuzasshi.89.279
12. Seet RCS, Quek AML, Lim ECH. Symptoms and risk factors of ocular complications following dengue infection. J Clin Virol. 2007;38:101–5. https://doi.org/10.1016/j.jcv.2006.11.002

13. Chee E, Sims JL, Jap A, Tan BH, Oh H, Chee S-P. Comparison of prevalence of dengue maculopathy during two epidemics with differing predominant serotypes. Am J Ophthalmol. 2009;148:910–3. https://doi.org/10.1016/j.ajo.2009.06.030
14. Hung TM, Wills B, Clapham HE, Yacoub S, Turner HC. The uncertainty surrounding the burden of post-acute consequences of dengue infection. Trends Parasitol. 2019;35:673–6. https://doi.org/10.1016/j.pt.2019.06.004
15. Global Burden of Disease Study 2013 Collaborators. Global, regional, and national incidence, prevalence, and years lived with disability for 301 acute and chronic diseases and injuries in 188 countries, 1990–2013: a systematic analysis for the Global Burden of Disease Study 2013. Lancet. 2015;386:743–800.

Address for correspondence: Hannah Clapham, Saw Swee Hock School of Public Health, National University of Singapore, MD1, 12 Science Dr 2, 117549, Singapore; email: hannah.clapham@nus.edu.sg

January 2022

Antimicrobial Resistance

- Outbreak of Mucormycosis in Coronavirus Disease Patients, Pune, India
- Severe Acute Respiratory Syndrome Coronavirus 2 and Respiratory Virus Sentinel Surveillance, California, USA, May 10, 2020–June 12, 2021
- Using the Acute Flaccid Paralysis Surveillance System to Identify Cases of Acute Flaccid Myelitis, Australia, 2000–2018
- Fungal Infections Caused by *Kazachstania* spp., Strasbourg, France, 2007–2020
- Multistate Outbreak of SARS-CoV-2 Infections, Including Vaccine Breakthrough Infections, Associated with Large Public Gatherings, United States
- Potential Association of Legionnaires' Disease with Hot Spring Water, Hot Springs National Park and Hot Springs, Arkansas, USA, 2018–2019
- Extensively Drug-Resistant Carbapenemase-Producing *Pseudomonas aeruginosa* and Medical Tourism from the United States to Mexico, 2018–2019
- Effects of Nonpharmaceutical COVID-19 Interventions on Pediatric Hospitalizations for Other Respiratory Virus Infections, Hong Kong
- Mask Effectiveness for Preventing Secondary Cases of COVID-19, Johnson County, Iowa, USA
- Transmission Dynamics of Large Coronavirus Disease Outbreak in Homeless Shelter, Chicago, Illinois, USA, 2020
- Risk Factors for SARS-CoV-2 Infection Among US Healthcare Personnel, May–December 2020

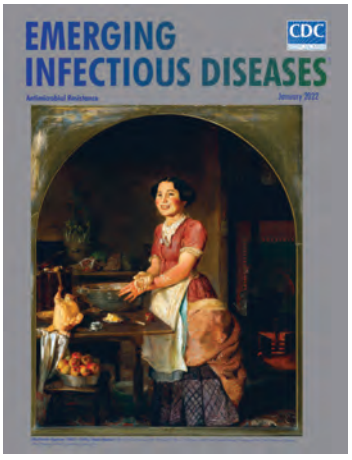

- Systematic Genomic and Clinical Analysis of Severe Acute Respiratory Syndrome Coronavirus 2 Reinfections and Recurrences Involving the Same Strain
- High-Level Quinolone-Resistant *Haemophilus haemolyticus* in Pediatric Patient with No History of Quinolone Exposure
- Global Genome Diversity and Recombination in *Mycoplasma pneumoniae*
- Invasive Multidrug-Resistant *emm*93.0 *Streptococcus pyogenes* Strain Harboring a Novel Genomic Island, Israel, 2017–2019
- Serotype Replacement after Introduction of 10-Valent and 13-Valent Pneumococcal Conjugate Vaccines in 10 Countries, Europe
- Effect on Antimicrobial Resistance of a Policy Restricting Over-the-Counter Antimicrobial Sales in a Large Metropolitan Area, São Paulo, Brazil
- New Sequence Types and Antimicrobial Drug–Resistant Strains of *Streptococcus suis* in Diseased Pigs, Italy, 2017–2019
- Coronavirus Disease Case Definitions, Diagnostic Testing Criteria, and Surveillance in 25 Countries with Highest Reported Case Counts
- Effect of Hepatitis E Virus RNA Universal Blood Donor Screening, Catalonia, Spain, 2017–2020
- *Streptococcus pneumoniae* Serotypes Associated with Death, South Africa, 2012–2018
- Coronavirus Disease Spread during Summer Vacation, Israel, 2020
- *Streptococcus gallolyticus* and Bacterial Endocarditis in Swine, United States, 2015–2020
- SARS-CoV-2 RNA Shedding in Semen and Oligozoospermia of Patient with Severe Coronavirus Disease 11 Weeks after Infection
- Melioidosis Manifesting as Chronic Femoral Osteomyelitis in Patient from Ghana
- Emergence of SARS-CoV-2 Delta Variant, Benin, May–July 2021
- *Salmonella* Serotypes Associated with Illnesses after Thanksgiving Holiday, United States, 1998–2018
- Use of Private Sector Workforce Respiratory Disease Short-Term Disability Claims to Assess SARS-CoV-2, Mexico, 2020
- Transfusion-Transmitted Hepatitis A Virus, France, 2018

EMERGING INFECTIOUS DISEASES®

To revisit the January 2022 issue, go to:
https://wwwnc.cdc.gov/eid/articles/issue/28/1/table-of-contents

Survey of West Nile and Banzi Viruses in Mosquitoes, South Africa, 2011–2018

Caitlin MacIntyre, Milehna Mara Guarido, Megan Amy Riddin, Todd Johnson, Leo Braack, Maarten Schrama, Erin Gorsich, Antonio Paulo Gouveia Almeida, Marietjie Venter

We collected >40,000 mosquitoes from 5 provinces in South Africa during 2011–2018 and screened for zoonotic flaviviruses. We detected West Nile virus in mosquitoes from conservation and periurban sites and potential new mosquito vectors; Banzi virus was rare. Our results suggest flavivirus transmission risks are increasing in South Africa.

Flaviviruses have been major emerging zoonotic pathogens in Africa within the past decade (*1*). In South Africa, West Nile virus (WNV) is the main flavivirus detected in animals and humans (*2*,*3*). Several other lesser-known flaviviruses were first described in South Africa but are understudied and potentially underreported, including Wesselsbron, Usutu, and Banzi (BANV) viruses (*4*). In South Africa, mosquito surveillance is not routinely performed and studies on flavivirus ecology are outdated (*5*). In this study, we aimed to update flavivirus vector epidemiology in northeastern provinces of South Africa through a large-scale ecologic survey.

The Study

We selected 15 sites (4 sentinel sites, 11 ad hoc sites) across 5 provinces in South Africa for mosquito collection according to recent cases of arboviral disease in humans and animals (*2*,*3*) (Figure 1). We established sentinel sites in Boschkop and Kyalami, both located in the Gauteng province (periurban sites), and Lapalala and Marakele, both located in the Limpopo province (conservation sites); collections were performed during 2011–2018 (Table 1). Opportunistic supplementary collections occurred at 10 ad hoc sites during 2015–2018 spanning 3 additional provinces that included urban, periurban, and conservation sites. We performed additional ad hoc collections during March–April 2017 in and around Kruger National Park (KNP) located within Limpopo and Mpumalanga provinces (periurban/conservation sites) (*6*). The methodologies for mosquito collection, identification, pooling, processing, flavivirus screening, and *COX1* gene sequencing have been previously described (*7*). To focus on months from midsummer to autumn in South Africa, when availability of mosquito breeding sites and vectorial capacity increases because of warmer and wetter weather conditions (*8*), we only screened mosquitoes collected during January–June. To submit sequences to GenBank, we generated *NS5* gene fragments >200 bp by using heminested PCR with 0.4 μmol/L each of forward primer (FU1, 5′-TACAACATGGGAAAGAGAGAA-3′) and reverse primer (CFD2, 5′-GTGTCCCAGCCGGCGGTGTCATCAGC-3′) and Platinum Taq DNA Polymerase (Thermo Fisher Scientific, https://www.thermofisher.com). For WNV positive pools, we performed reverse transcription PCR to amplify a 1,525 bp fragment of the WNV envelope protein gene for phylogenetic analysis (Appendix Table, https://wwwnc.cdc.gov/EID/article/29/1/22-0036-App1.pdf). We calculated the mosquito minimum infection rate (MIR) per site by using a standard formula: (number of positive pools/total number of individual mosquitoes tested) × 1000.

We collected a total of 66,299 mosquitoes belonging to 11 genera across 5 provinces in South Africa during 2011–2018 (Table 1; Appendix Figure 1). From those, we divided 40,731 female mosquitoes into 1,471 pools based on morphology, focusing on only 4 genera

Author affiliations: University of Pretoria, Pretoria, South Africa (C. MacIntyre, M.M. Guarido, M.A. Riddin, T. Johnson, L. Braack, M. Venter); Copperbelt University, Kitwe, Zambia (T. Johnson); Leiden University, Leiden, the Netherlands (M. Schrama); University of Warwick, Coventry, United Kingdom (E. Gorsich); NOVA University of Lisbon, Lisbon, Portugal (A.P.G. Almeida)

DOI: https://doi.org/10.3201/eid2901.220036

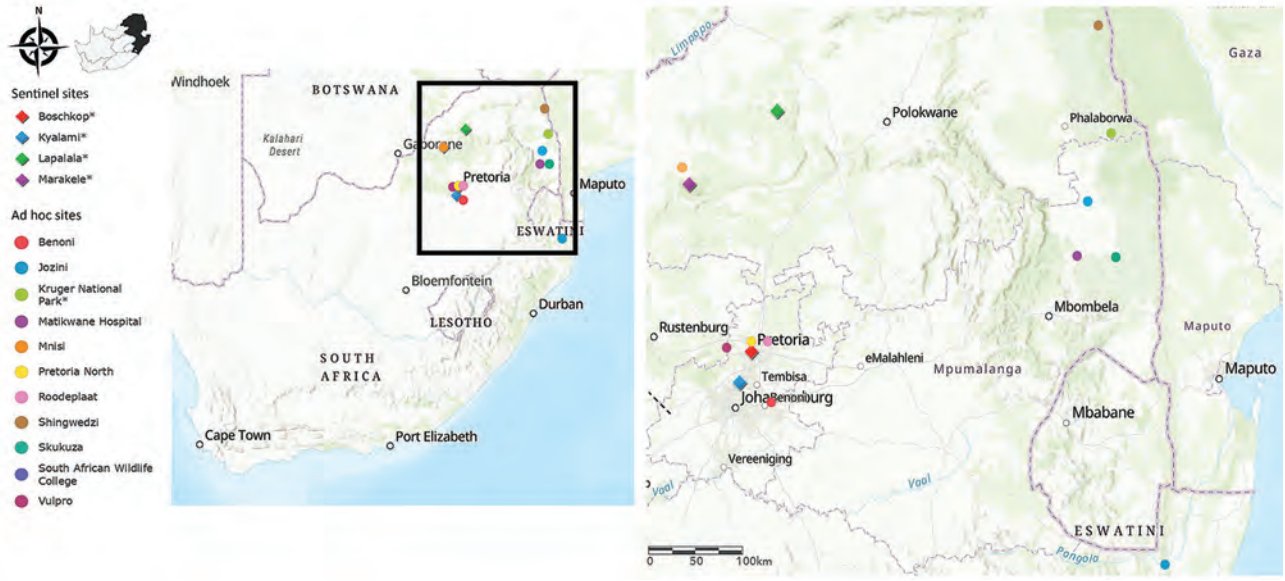

Figure 1. Sentinel and ad hoc mosquito collection sites across the northeastern region of South Africa in survey of West Nile and Banzi viruses in mosquitoes, South Africa, 2011–2018. Collection sites were selected according to recent cases of arboviral disease in humans and animals. Asterisks in the color-coded figure legend indicate sites where flaviviruses were identified in mosquitoes.

(*Culex*, *Mansonia*, *Anopheles*, and *Aedes*) and screened for flaviviruses. We detected WNV in 16 (1.09%) and BANV in 2 (0.14%) pools. We did not detect other zoonotic flaviviruses; however, insect-specific flaviviruses were detected and described elsewhere (*7*). WNV outbreaks can be expected once the MIR rises above 1 (*9*). We observed the highest MIRs in Kyalami (periurban site, MIR = 2.53), KNP (periurban/conservation site, MIR = 1.22), and Lapalala (conservation site, MIR = 1.01) (Table 2). Therefore, we identified those areas as higher risk sites for WNV outbreaks in humans and animals. These results correlated with areas where *Culex* spp. mosquitoes were the most abundant and where WNV cases were previously reported in humans and animals in South Africa (*3*,*10*).

Only 11 of 16 WNV-positive pools had partial *NS5* gene sequences of sufficient quality to perform maximum-likelihood analysis; we confirmed all 11 pools were WNV and also confirmed 2 BANV-positive pools (Figure 2; bootstrap value = 100 for both viruses). We observed high nucleotide similarity (94.62%–100.00%) between the identified WNV *NS5* gene sequences and those from previously identified, highly neuroinvasive strains from South Africa isolated from either equines or humans. We successfully amplified the 1,525 nt region of the envelope protein gene for 5 of 16 WNV-positive pools (Appendix Figure 2).

We performed *COX1* gene sequencing for 9 of 16 WNV-positive pools and confirmed morphologic identification of those mosquitoes as *Cx. univittatus* except for 1 pool collected in KNP that was identified by sequencing as *Cx. perexiguus* (Table 2; Appendix Figure 3), a mosquito species not known to be present in South Africa (*11*). This 1 pool might have contained a mix of both species, but Sanger sequencing was unable to distinguish between the 2 species. In addition, the *COX1* reference sequences for *Cx. perexiguus* mosquitoes obtained from online databases may not be accurate because this species has not been identified in South Africa. Recently, *COX1* gene amplification using universal primers followed by next-generation sequencing was shown to distinguish between species in mixed pools (*12*) and might be useful in future studies to resolve this ambiguity. Further studies are necessary to clarify the status of the *Cx. perexiguus* mosquitoes in South Africa. Most of the WNV-positive pools consisted of *Cx. univittatus*, *Cx. pipiens s.l.*, and *Cx. theileri* mosquitoes, which we collected in high abundance. This result reiterates the importance of these species as WNV vectors in South Africa (*5*). We identified *Cx. simpsoni*, *Cx. bitaeniorhynchus*, *An. gambiae* sensu lato, and *Cx. poicilipes* mosquitoes, none of which have been previously associated with WNV in South Africa, as new potential vectors for WNV by using *COX1* gene sequencing (*4*). Globally, from this list of species, only *Cx. poicilipes* mosquitoes from Senegal were found to be infected with WNV (*13*). Experimental studies have shown that the *Cx. bitaeniorhynchus* mosquito is a likely vector

Table 1. Total number of mosquitoes collected across sentinel and ad hoc sites in survey of West Nile and Banzi viruses in mosquitoes in South Africa during 2011–2018

Site	Site type	Province	Region type	Coordinates	No. mosquitoes collected	No. trapping events	Mean no. mosquitoes/trapping event
Boschkop	Sentinel	Gauteng	Peri-urban	−25.82786, 28.42047	4,790	353	12
Kyalami	Sentinel	Gauteng	Peri-urban	−25.99183, 28.02947	8,736	338	26
Lapalala	Sentinel	Limpopo	Conservation	−23.88458, 28.26953	16,675	568	29
Marakele	Sentinel	Limpopo	Conservation	−24.29364, 27.50325	13,347	487	24
Total nos., sentinel sites					43,548	1,746	23
Benoni	Ad hoc	Gauteng	Peri-urban	−26.10611, 28.36689	1,191	31	38
Jozini	Ad hoc	KwaZulu-Natal	Rural	−27.41258, 32.20647	10,954	47	233
Kruger National Park	Ad hoc	Limpopo, Mpumalanga	Conservation, peri-urban	−25.35384, 31.79936	2,440	30	58
Matikwane	Ad hoc	Mpumalanga	Urban	−24.98545, 31.236342	615	9	68
Mnisi	Ad hoc	Mpumalanga	Rural	−24.48206, 31.38583	5,549	171	32
Pretoria north	Ad hoc	Gauteng	Urban	−25.68663, 28.15895	219	23	12
Roodeplaat	Ad hoc	Gauteng	Peri-urban	−25.62075, 28.37136	298	15	20
Shingwedzi	Ad hoc	Limpopo	Conservation	−23.10819, 31.43628	457	13	35
Skukuza	Ad hoc	Mpumalanga	Conservation	−24.99633, 31.59189	482	15	32
Southern African Wildlife College	Ad hoc	Mpumalanga	Conservation	−24.53886, 31.33369	56	9	15
Vulpro	Ad hoc	Northwest	Peri-urban	−25.7112, 27.95322	490	12	41
Total nos., ad hoc sites					22,751	375	53

for WNV because this species was able to successfully transmit WNV (*14*). We were unable to genetically characterize the remaining 7 of 16 pools because of insufficient material for DNA extraction; we identified mosquitoes in those pools by morphologic characteristics.

Table 2. Detection of flaviviruses and their associated potential mosquito vectors in survey of West Nile and Banzi viruses in mosquitoes, South Africa, 2011–2018*

Site	Virus	Positive pool ID	No. mosquitoes†	Morphologic ID‡	Molecular ID§	MIR
Boschkop	WNV	GAU11MP26	2	*Culex pipiens* sensu lato	Not done	0.72
	WNV	GAU17MP72	33	*Cx. univittatus*	*Cx. univittatus*	
Kruger National Park	WNV	KNP17MP714	4	*Cx. simpsoni*	*Cx. simpsoni*	1.23
	WNV	KNP17MP718	36	*Cx. univittatus*	Cx *perexiguus*	
	WNV	KNP17MP720	1	*Cx. bitaeniorhynchus*	*Cx. bitaeniorhynchus*	
Kyalami	WNV	KYA11MP11	14	*Cx. univittatus*	Not done	2.53
	WNV	KYA11MP13	10	*Cx. pipiens s.l.*	Not done	
	WNV	KYA14MP133	10	*Cx. univittatus*	*Cx. univittatus*	
	WNV	KYA14MP134	19	*Cx. univittatus*	*Cx. univittatus*	
	WNV	KYA14MP115	5	*Cx. theileri*	*Cx. theileri*	
Lapalala	WNV	LAP13LP71	44	*Anopheles* spp.	Not done	1.01
	WNV	LAP13LP28	50	*Anopheles* spp.	Not done	
	WNV	LAP13LP22	50	*Aedes* spp.	Not done	
	WNV	LAP14MP394	2	*Cx. univittatus*	*Cx. univittatus*	
Marakele	WNV	MAR13MP77	50	*Cx. poicilipes*	Not done	0.33
	WNV	MAR15MP18	1	*An. gambiae s.l.*	*An. gambiae s.l.*	
Lapalala	BANV	LAP13MP25	49	*Cx.* spp.	*Cx. rubinotus*	0.83
	BANV	LAP13MP26	50	*Cx.* spp.	*Cx. annulioris*	

*BANV, Banzi virus; ID, identification; MIR, minimum infection rate; WNV, West Nile virus.
†Number of mosquitoes in each positive pool.
‡Species of mosquito identified by morphologic characteristics.
§Species of mosquito identified by sequencing the *COX1* gene.

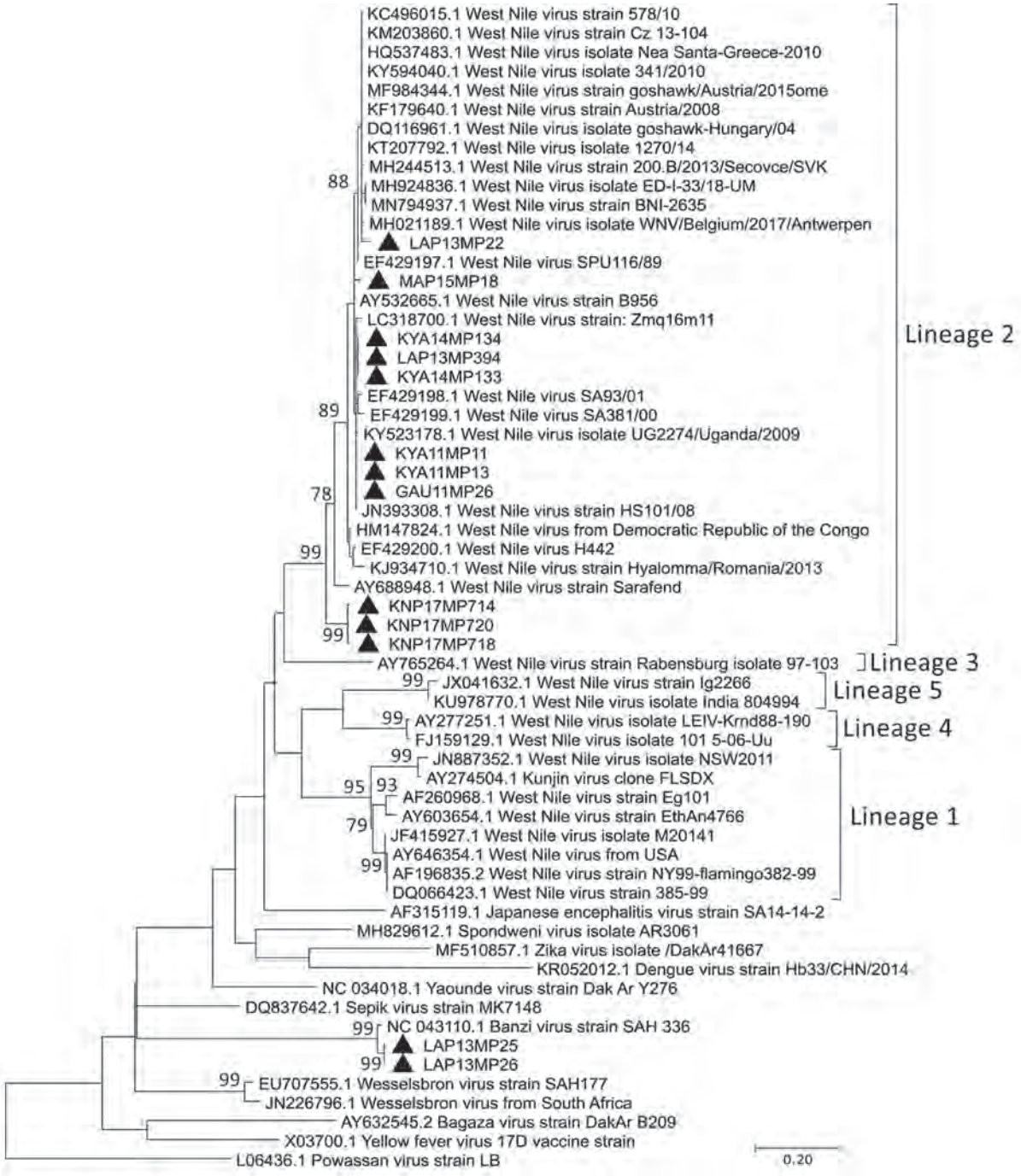

Figure 2. Phylogenetic analysis of flaviviruses using *NS5* gene sequences in survey of West Nile and Banzi viruses in mosquitoes, South Africa, 2011–2018. Maximum likelihood analysis was used to identify flaviviruses found in mosquitoes after partial sequencing of the flavivirus *NS5* gene region (226 nt, Kimura 2-parameter model plus gamma distribution plus proportion of invariable sites). Sequence data were edited by using CLC Main Workbench version 8.0.1 (QIAGEN, https://www.qiagen.com). Reference genomes were downloaded from GenBank. Multiple sequence alignments were created by using MAFFT (http://mafft.cbrc.jp/alignment/server/index.html) with default parameters. Phylogenetic analysis was performed by using MEGA X software (MEGA, https://www.megasoftware.net) with bootstrap support for network groupings calculated from 1,000 replicates. Bootstrap values (>70%) are displayed on branches. GenBank accession numbers for newly sequenced virus strains: OL411950 (KYA11MP13 isolate), OL411951 (GAU11MP26 isolate), OL411952 (KYA14MP133 isolate), OL411953 (KYA14MP134 isolate), OL411954 (LAP14MP394 isolate), OL411955 (MAR15MP18 isolate), OL411956 (LAP13MP22 isolate), OL411957 (KNP17MP714 isolate), OL411958 (KNP17MP720 isolate), OL411959 (KNP17MP718 isolate), OL411960 (KYA11MP11 isolate), OL411961 (LAP13MP25 isolate), and OL411962 (LAP13MP26 isolate). Solid black triangles are new viral sequences that were detected in mosquitoes in this study. Scale bar indicates nucleotide substitutions per site.

Detection of BANV in mosquito pools in South Africa has not been described since the late 1970s (*15*), and a lack of surveillance raises the question regarding the true incidence of this virus. Only the *Cx. rubinotus* mosquito is recognized as a vector for BANV (*15*). Despite unclear morphologic identification, we identified *Cx. rubinotus* and *Cx. annulioris* mosquitoes in the 2 BANV-positive pools through *COX1* gene sequencing (Table 2; Appendix Figure 3), which should be investigated further to confirm vector status.

Conclusions

The first limitation of our study is that we did not separate voucher specimens for mosquito species from the pools before homogenization. A voucher specimen is a mosquito species that is preserved and serves as a reference used to document identity. Second, identifications of mosquito species not previously associated with WNV infection are preliminary findings, and further investigation of vector competency is required.

Mosquito surveillance is not routinely performed for arboviruses in South Africa, and most studies were performed 40 years ago (*5*). In this study, 5 provinces were targeted for mosquito surveillance over a 7-year period. These investigations revealed a wide range of new potential vectors that require further investigation. Both WNV and BANV were identified in mosquitoes in periurban and conservation areas at the animal/human interface in South Africa, suggesting increasing circulation potential for those viruses between humans, wildlife, domestic animals, and avian species that are common in those areas.

Acknowledgments

We thank Lapalala Wilderness, Marataba Conservation, and South African National Parks for logistical assistance and permission to collect mosquitoes; Basil Brooke and Danny Govender for their contribution to the collection of the mosquitoes; all previous staff and students in the Zoonotic Arbo- and Respiratory virus program for their technical support; and Clarence Yah for his assistance in preparing the manuscript. A.P.G. Almeida has been a recipient of the Visiting Professor Programme of the University of Pretoria and acknowledges the Global Health and Tropical Medicine unit.

The study was funded in part by a cooperative agreement (no. 5 NU2GGH001874-02-00) with the US Centers for Disease Control and Prevention. The study was solely the responsibility of the authors and does not necessarily represent the official views of the US Centers for Disease Control and Prevention or US Department of Health and Human Services.

About the Author

Ms. MacIntyre is an MSc candidate in the Zoonotic Arbo- and Respiratory virus research group, Department of Medical Virology, at the University of Pretoria. Her research focuses on One Health investigations of West Nile virus in South Africa.

References

1. Hollidge BS, González-Scarano F, Soldan SS. Arboviral encephalitides: transmission, emergence, and pathogenesis. J Neuroimmune Pharmacol. 2010;5:428–42. https://doi.org/10.1007/s11481-010-9234-7x
2. Burt FJ, Grobbelaar AA, Leman PA, Anthony FS, Gibson GV, Swanepoel R. Phylogenetic relationships of southern African West Nile virus isolates. Emerg Infect Dis. 2002;8:820–6. https://doi.org/10.3201/eid0808.020027
3. Venter M, Pretorius M, Fuller JA, Botha E, Rakgotho M, Stivaktas V, et al. West Nile virus lineage 2 in horses and other animals with neurologic disease, South Africa, 2008–2015. Emerg Infect Dis. 2017;23:2060–4. https://doi.org/10.3201/eid2312.162078
4. Venter M. Assessing the zoonotic potential of arboviruses of African origin. Curr Opin Virol. 2018;28:74–84. https://doi.org/10.1016/j.coviro.2017.11.004
5. Jupp PG. The ecology of West Nile virus in South Africa and the occurrence of outbreaks in humans. Ann N Y Acad Sci. 2001;951:143–52. https://doi.org/10.1111/j.1749-6632.2001.tb02692.x
6. Gorsich EE, Beechler BR, van Bodegom PM, Govender D, Guarido MM, Venter M, et al. A comparative assessment of adult mosquito trapping methods to estimate spatial patterns of abundance and community composition in southern Africa. Parasit Vectors. 2019;12:462. https://doi.org/10.1186/s13071-019-3733-z
7. Guarido MM, Govender K, Riddin MA, Schrama M, Gorsich EE, Brooke BD, et al. Detection of insect-specific flaviviruses in mosquitoes (Diptera: *Culicidae*) in northeastern regions of South Africa. Viruses. 2021;13:2148. https://doi.org/10.3390/v13112148
8. Cornel AJ, Lee Y, Almeida APG, Johnson T, Mouatcho J, Venter M, et al. Mosquito community composition in South Africa and some neighboring countries. Parasit Vectors. 2018;11:331. https://doi.org/10.1186/s13071-018-2824-6
9. Bustamante DM, Lord CC. Sources of error in the estimation of mosquito infection rates used to assess risk of arbovirus transmission. Am J Trop Med Hyg. 2010;82:1172–84. https://doi.org/10.4269/ajtmh.2010.09-0323
10. Zaayman D, Venter M. West Nile virus neurologic disease in humans, South Africa, September 2008–May 2009. Emerg Infect Dis. 2012;18:2051–4. https://doi.org/10.3201/eid1812.111208
11. Mixão V, Bravo Barriga D, Parreira R, Novo MT, Sousa CA, Frontera E, et al. Comparative morphological and molecular analysis confirms the presence of the West Nile virus mosquito vector, *Culex univittatus*, in the Iberian Peninsula. Parasit Vectors. 2016;9:601. https://doi.org/10.1186/s13071-016-1877-7
12. Alkan C, Erisoz Kasap O, Alten B, de Lamballerie X, Charrel RN. Sandfly-borne phlebovirus isolations from Turkey: new insight into the sandfly fever Sicilian and sandfly fever Naples species. PLoS Negl Trop Dis. 2016;10:e0004519. https://doi.org/10.1371/journal.pntd.0004519

13. Hubálek Z, Halouzka J. West Nile fever—a reemerging mosquito-borne viral disease in Europe. Emerg Infect Dis. 1999;5:643–50. https://doi.org/10.3201/eid0505.990505
14. Ilkal MA, Mavale MS, Prasanna Y, Jacob PG, Geevarghese G, Banerjee K. Experimental studies on the vector potential of certain *Culex* species to West Nile virus. Indian J Med Res. 1997;106:225–8.
15. Jupp PG, McIntosh BM, Anderson D. *Culex* (*Eumelanomyia*) *rubinotus* Theobald as vector of Banzi, Germiston and Witwatersrand viruses. IV. Observations on the biology of *C. rubinotus*. J Med Entomol. 1976;12:647–51. https://doi.org/10.1093/jmedent/12.6.647

Address for correspondence: Marietjie Venter, Zoonotic Arbo- and Respiratory Virus Program, Centre for Viral Zoonosis, Department of Medical Virology, Pathology Building, Prinshof Campus South, University of Pretoria, Private Bag X323, Gezina 0031, South Africa; email: marietjie.venter@up.ac.za

May 2022

Viral Infections

- Invasive Group A *Streptococcus* Outbreaks Associated with Home Healthcare, England, 2018–2019
- Genomic Epidemiology of Global Carbapenemase-Producing *Escherichia coli*, 2015–2017
- Risk for Asymptomatic Household Transmission of *Clostridioides difficile* Infection Associated with Recently Hospitalized Family Members
- Estimating Relative Abundance of 2 SARS-CoV-2 Variants through Wastewater Surveillance at 2 Large Metropolitan Sites, United States
- Effectiveness of BNT162b2 Vaccine Booster against SARS-CoV-2 Infection and Breakthrough Complications, Israel
- Effects of Tick-Control Interventions on Tick Abundance, Human Encounters with Ticks, and Incidence of Tickborne Diseases in Residential Neighborhoods, New York, USA
- Pertactin-Deficient *Bordetella pertussis* with Unusual Mechanism of Pertactin Disruption, Spain, 1986–2018
- Determining Existing Human Population Immunity as Part of Assessing Influenza Pandemic Risk
- Disparities in First Dose COVID-19 Vaccination Coverage among Children 5–11 Years of Age, United States
- Multisystem Inflammatory Syndrome in Children after SARS-CoV-2 Vaccination
- Severe Multisystem Inflammatory Symptoms in 2 Adults after Short Interval between COVID-19 and Subsequent Vaccination

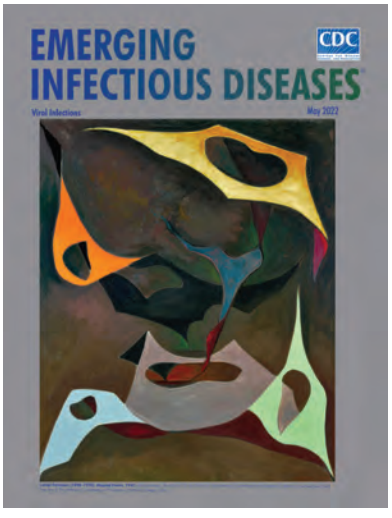

- Pathogens that Cause Illness Clinically Indistinguishable from Lassa Fever, Nigeria, 2018
- Duration of Infectious Virus Shedding by SARS-CoV-2 Omicron Variant–Infected Vaccinees
- Imported Monkeypox from International Traveler, Maryland, USA, 2021
- Intercontinental Movement of Highly Pathogenic Avian Influenza A(H5N1) Clade 2.3.4.4 Virus to the United States, 2021
- Rapid Replacement of SARS-CoV-2 Variants by Delta and Subsequent Arrival of Omicron, Uganda, 2021
- SARS-CoV-2 Antibody Prevalence and Population-Based Death Rates, Greater Omdurman, Sudan
- Cross-Variant Neutralizing Serum Activity after SARS-CoV-2 Breakthrough Infections
- Evidence of Prolonged Crimean-Congo Hemorrhagic Fever Virus Endemicity by Retrospective Serosurvey, Eastern Spain
- Lack of Evidence for Crimean–Congo Hemorrhagic Fever Virus in Ticks Collected from Animals, Corsica, France
- Highly Pathogenic Avian Influenza A(H5N8) Clade 2.3.4.4b Viruses in Satellite-Tracked Wild Ducks, Ningxia, China, 2020
- Novel Hendra Virus Variant Circulating in Black Flying Foxes and Grey-Headed Flying Foxes, Australia
- Increased COVID-19 Severity among Pregnant Patients Infected with SARS-CoV-2 Delta Variant, France
- Mathematical Modeling for Removing Border Entry and Quarantine Requirements for COVID-19, Vanuatu
- SARS-CoV-2 Seroprevalence after Third Wave of Infections, South Africa
- *Angiostrongylus cantonensis* in a Red Ruffed Lemur at a Zoo, Louisiana, USA
- Breast Milk as Route of Tick-Borne Encephalitis Virus Transmission from Mother to Infant
- *atpE* Mutation in *Mycobacterium tuberculosis* Not Always Predictive of Bedaquiline Treatment Failure
- Emerging Novel Reassortant Influenza A(H5N6) Viruses in Poultry and Humans, China, 2021
- *Mycobacterium lepromatosis* as Cause of Leprosy, Colombia
- Rare Case of Rickettsiosis Caused by *Rickettsia monacensis*, Portugal, 2021

EMERGING INFECTIOUS DISEASES®

To revisit the May 2022 issue, go to:
https://wwwnc.cdc.gov/eid/articles/issue/28/5/table-of-contents

Detection of Clade 2.3.4.4b Avian Influenza A(H5N8) Virus in Cambodia, 2021

Kimberly M. Edwards, Jurre Y. Siegers, Xiaoman Wei, Ammar Aziz, Yi-Mo Deng, Sokhoun Yann, Chan Bun, Seng Bunnary, Leonard Izzard, Makara Hak, Peter Thielen, Sothyra Tum, Frank Wong, Nicola S. Lewis, Joe James, Filip Claes, Ian G. Barr, Vijaykrishna Dhanasekaran,[1] Erik A Karlsson[1]

In late 2021, highly pathogenic avian influenza A(H5N8) clade 2.3.4.4b viruses were detected in domestic ducks in poultry markets in Cambodia. Surveillance, biosafety, and biosecurity efforts should be bolstered along the poultry value chain to limit spread and infection risk at the animal–human interface.

Since 2014, highly pathogenic avian influenza viruses (HPAIVs) with H5 hemagglutinin (HA) genes grouped in the genetic clade 2.3.4.4 have spread globally causing severe outbreaks in Africa, Europe, Asia, and most recently, North America (*1*). These viruses cause devastating outbreaks in poultry, rapidly evolve, and continuously reassort with other avian influenza viruses (AIVs), posing a threat to food security in many parts of the world and substantial zoonotic infection risk.

The Study

Since 2017, the Institut Pasteur du Cambodge and National Animal Health and Production Research Institute in Cambodia have partnered with the Food and Agriculture Organization of the United Nations to enhance ongoing longitudinal AIV surveillance in live bird markets and poultry storage facilities throughout Cambodia. This active surveillance reveals high levels of AIV circulation with ≈30%–50% of ducks and ≈20%–40% of chickens testing positive for various influenza A subtypes. Most detected HPAIVs were H5N1 HA clade 1 viruses during 2005–2014 and H5N1 HA clade 2.3.2.1c viruses since 2014; H5N6 clades 2.3.4.4g and 2.3.4.4h were detected sporadically during 2018–2020 (Appendix 1 Table 1, https://wwwnc.cdc.gov/EID/article/29/1/22-0934-App1.pdf). Other subtypes also circulate, including novel H7Nx low pathogenicity avian influenza viruses (LPAIVs) (*2*,*3*).

During active surveillance of live bird markets (National Ethics Committee for Health Research Approval no. 149/NECHR/2020) in late 2021, domestic ducks (*Anas platyrhynchos*) at Orussey (Phnom Penh, n = 1), Takmao (Kandal, n = 2), Chba Ampov (Phnom Penh, n = 1), and Takeo (Takeo, n = 1) tested positive for HPAIV H5 HA but negative for neuraminidase (NA) subtype N1 by real time reverse transcription PCR (RT-PCR). We determined these samples were the H5N8 subtype after further RT-PCR analysis (Appendix 1). Positive samples originated from Orussey and Chba Ampov markets during week 37, Takmao market during week 41, and Takeo market during week 46 of 2021 (Figure 1). Full genome sequencing on a GridION instrument (Oxford Nanopore Technologies, https://www.nanoporetech.com) confirmed these samples were HPAIV H5N8 and H5 HA clade 2.3.4.4b (*4*).

All H5N8 HA sequences from Cambodia encoded proteins with 2-4 amino acid differences

Author affiliations: University of Hong Kong, Hong Kong, China (K.M. Edwards, X. Wei, V. Dhanasekaran); Institut Pasteur du Cambodge, Phnom Penh, Cambodia (J.Y. Siegers, S. Yann, E.A. Karlsson); Peter Doherty Institute for Infection and Immunity, Melbourne, Victoria, Australia (A. Aziz, Y.-M. Deng, I.G. Barr); National Animal Health and Production Research Institute, Phnom Penh (C. Bun, S. Bunnary, S. Tum); Australian Center for Disease Preparedness, Geelong, Victoria, Australia (L. Izzard, F. Wong); Food and Agriculture Organization of the United Nations, Phnom Penh (M. Hak); Johns Hopkins University, Baltimore, Maryland, USA (P. Theilen); Royal Veterinary College, London, UK (N.S. Lewis, J. James); OIE/FAO International Reference Laboratory for Avian Influenza, Swine influenza and Newcastle Disease, Weybridge, UK (N.S. Lewis); Food and Agriculture Organization of the United Nations, Bangkok, Thailand (F. Claes)

DOI: https://doi.org/10.3201/eid2901.220934

[1]These authors contributed equally to this article.

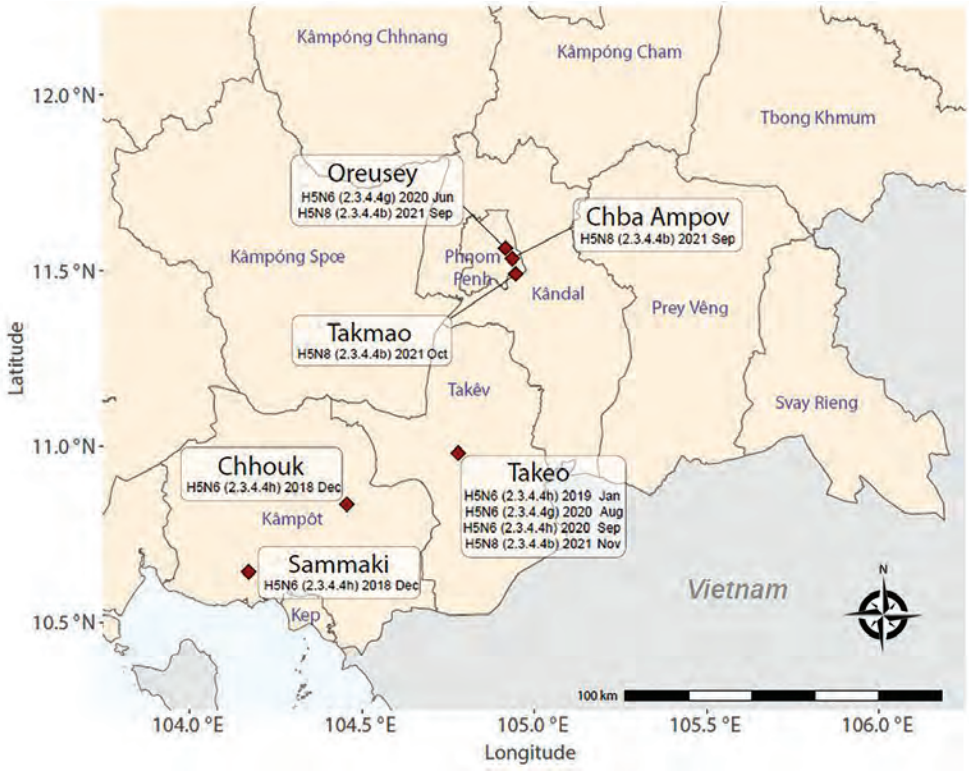

Figure 1. Location of live bird markets where highly pathogenic clade 2.3.4.4b avian influenza A(H5N8) viruses were detected in Cambodia during 2018–2021. The map shows where both H5N6 and H5N8 subtypes of avian influenza A were detected.

relative to the clade 2.3.4.4b candidate vaccine strain A/Astrakhan/3212/2020(H5N8) (Table 1). HA mutations T192I and H276N (according to the H3 numbering system) were shared across all H5N8 HA proteins, whereas A188V occurred in 2 sequences, and E273K, T312S, and I339K each occurred only once. Those mutations did not correlate with previously reported phenotypic traits. Consistent with other clade 2.3.4.4b HA proteins, H5N8 viruses from Cambodia retained the HPAIV cleavage site motif, REKRRKR|GLF. The NA sequences did not contain stalk deletions or markers of antiviral drug resistance. However, other genes encoded amino acid residues associated with increased replication capacity and mammalian pathogenicity, including V89, V292, D309, R389, and T598 in PB2; G622 in PB1; D30, M43, and A215 in M1; and S42 and M106 in NS proteins (*5*).

We performed hemagglutination inhibition assays to assess potential cross-reactivity among the 2.3.4.4b viruses isolated from ducks in Cambodia by using 2 key reference viruses: A/Astrakhan/3212/2020, the recommended candidate vaccine virus for clade 2.3.4.4.b; and A/domestic_duck/England/074477/2021, a recently identified clade 2.3.4.4b virus from poultry associated with human infection in the United Kingdom (*6*). H5N8 viruses from Cambodia with V188, I192 and N276 in HA showed good recognition by antiserum raised against A/Astrakhan/3212/2020. However, A/duck/Cambodia/f1PPOreu241D3/2021 (with I192 and N276, and K339 in HA) and A/duck/Cambodia/f6T241D4/2021 (with I192, K273, N276, S312 in HA) showed reduced recognition by the antiserum (Table 2).

Table 1. Amino acid mutations in hemagglutinin relative to the reference strain A/Astrakhan/3212/2020 in clade 2.3.4.4b avian influenza A(H5N8) viruses detected in Cambodia, 2021*

H5 clade 2.3.4.4b strain	HA amino acid position†					
	188	192	273	276	312	339
A/Astrakhan/3212/2020 (CVV)‡	A	T	E	H	N	I
A/duck/Cambodia/f6T241D4/2021		I	K	N	S	
A/duck/Cambodia/f4K241D3_C/2021	V	I		N		
A/duck/Cambodia/f4K241D4/2021	V	I		N		
A/duck/Cambodia/f1PPOreu241D3_C/2021		I		N		K
A/duck/Cambodia/f1PPChba241D6/2021		I		N		

*Blank cells indicate no mutation. HA, hemagglutinin.
†Amino acids were numbered according to the hemagglutinin H3 numbering system.
‡Candidate vaccine virus reference strain (GISAID accession no. EPI_ISL_1038924; https://www.gisaid.org).

Table 2. Hemagglutination inhibition titers of isolated virus strains in study of clade 2.3.4.4b avian influenza A(H5N8) virus detected in Cambodia, 2021*

Strain	Titer
A/duck/Cambodia/f1PPOreu241D3/2021	40
A/duck/Cambodia/f4K241D4/2021	80
A/duck/Cambodia/f4K241D3/2021	80
A/duck/Cambodia/f6T241D4/2021	40
A/domestic_duck/England/074477/2021	80
A/Astrakhan/3212/2020/2020 (CVV)†	160

*Hemagglutination inhibition titer using ferret antiserum against the reference virus strain A/Astrakhan/3212/2020.
†Candidate vaccine virus reference strain (GISAID accession no. EPI_ISL_1038924; https://www.gisaid.org).

The H5N8 viruses from Cambodia shared >95.7% nucleotide sequence homology across their genomes and formed distinct monophyletic lineages in maximum-likelihood phylogenies of several genes (bootstrap support was 100%, except for the matrix protein gene, which was 89%; Appendix Figure 1), implying circulation of a single virus strain ≥10 weeks from September to November 2021. The H5 HA gene was likely derived from H5N8 viruses that have caused widespread outbreaks in poultry and wild birds across Eurasia since early 2020 (*7*) (Figure 2). N8 NA gene segments were closest to that of HPAIV H5N8 detected in wild and domestic waterfowl in China and Korea during 2020–21, sharing most recent ancestry with NA of A/*Cygnus_columbianus*/Hubei/116/2020(H5N8) that was collected in November 2020 (Appendix Figure 1). Both the HA and MP gene segments were most closely related to

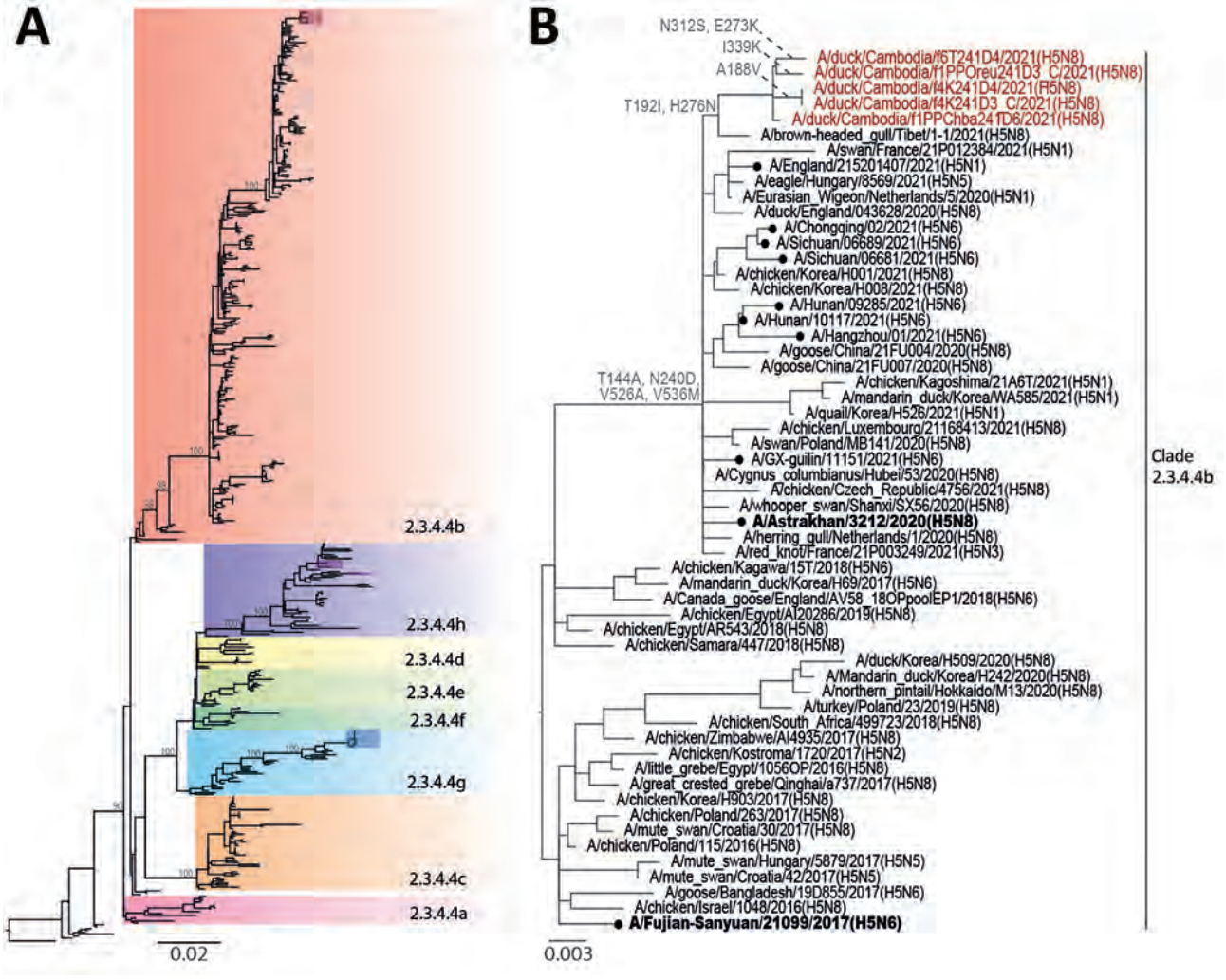

Figure 2. Phylogenetic analysis of the hemagglutinin genes of clade 2.3.4.4 avian influenza A(H5N8) viruses detected in Cambodia. Whole-genome sequencing of isolated viruses was performed and phylogenies were constructed using the maximum-likelihood method. A) Subclades of H5Nx clade 2.3.4.4. Recent isolates from Cambodia are shown in red, purple, and blue shaded boxes. B) Phylogeny of avian influenza A(H5N8) clade 2.3.4.4b isolates. Recent isolates from Cambodia are in red font and amino acid mutations are indicated at select nodes. Candidate vaccine viruses used as reference viruses are in bold font. Closed circles indicate cases of human infection with avian H5Nx viruses. Scale bars indicate nucleotide substitutions per site.

A/brown-headed gull/Tibet/1–1/2021(H5N8), collected in May 2021 (Figure 2, panel B; Appendix Figure 1). In contrast, the other gene segments encoding internal virus proteins were derived from LPAIV (Appendix Figure 1). PB2 and PB1 genes shared common ancestry with LPAIV detected in ducks in Vietnam in 2020. PA and NP genes shared recent common ancestry with LPAIV isolated in 2019 from wild ducks in Korea (PA gene) and China (NP gene). The NS protein gene was most similar to that of LPAIV from ducks in China in 2018. Overall, HPAIV H5Nx clade 2.3.4.4b showed evidence of extensive genetic reassortment with LPAIV found in wild waterfowl, which frequently spillover to and from domestic poultry.

In addition to various LPAIVs, multiple H5 subtypes and clades circulate in Cambodia (Appendix Table 1). H5N1 clade 2.3.2.1c viruses are detected regularly. H5N6 clade 2.3.4.4g viruses were found in Takeo and Orussey markets in chickens in 2019 and ducks in 2020, and H5N6 clade 2.3.4.4h viruses were detected sporadically in Kampot province in late 2018, Takeo province during 2019–2020, and Phnom Penh in 2020 (Figures 1, 2; Appendix Figures 2–5). Therefore, detection of H5N8 clade 2.3.4.4b viruses in these same markets is a major concern because further reassortment might occur. Since 2018, outbreaks of reassorted HPAIV H5Nx clade 2.3.4.4b with NA subtypes N8, N6, N1, N3, and N5 have increased in frequency (*8*). These viruses have disseminated intercontinentally across migratory flyways and regionally via poultry trade, often causing considerable economic losses. In 2021, H5Nx clade 2.3.4.4b viruses caused severe outbreaks in Europe, Africa, and Asia, particularly in wild birds in western China and in domestic poultry in Vietnam (*9*). Since January 2022, HPAIV H5N1 clade 2.3.4.4b has been detected in waterfowl, birds of prey, and poultry across North America (*10*).

H5Nx clade 2.3.4.4b viruses also pose a zoonotic risk to humans and other species. In February 2021, a total of 7 cases of asymptomatic human infections with HPAIV H5N8 clade 2.3.4.4b were reported in poultry farm workers in Russia following a poultry outbreak (*11*). H5N6 clade 2.3.4.4 viruses have caused 79 human infection cases (including 33 cases in 2021) in China with ≈32 deaths since 2014 and 1 case in Laos (*12*), and 3 cases of H5Nx were reported in Nigeria (*9*). HPAIV H5Nx clade 2.3.4.4 viruses have also been detected in domestic cats in China and Korea (*1*) and red foxes in The Netherlands (*1*), and serologic evidence exists for infection in swine (*13*). More recently, HPAIV H5N1 clade 2.3.4.4b containing HA genes closely related to A/Astrakhan/3212/2020 have caused human infections in the United Kingdom (*14*) and United States (*15*). HPAIV H5N1 clade 2.3.3.4b has not been detected in Cambodia.

Conclusions

Because of the global spread, economic impact, and zoonotic potential of HPAIV clade 2.3.4.4b viruses, active, longitudinal surveillance in live bird markets must be maintained in Cambodia, the Greater Mekong Subregion, and globally to monitor further introduction and reassortment events. In addition, surveillance of influenza-like illness needs to be maintained among persons in close contact with infected or deceased poultry. To combat the spread of HPAIV in Cambodia and other countries, viral monitoring, biosafety, and biosecurity efforts should be bolstered along the poultry value chain. Early warning and rapid control will limit infections at the animal–human interface to reduce potential pandemic risk.

Acknowledgments

We thank persons in the Virology Unit at Institut Pasteur du Cambodge (IPC) who provided technical expertise and analysis and fruitful discussions, including Viseth Srey Horm, Songha Tok, Phalla Y, Sonita Kol, Sarath Sin, Kim Lay Chea, and Veasna Duong; the support teams at IPC, including the drivers and facilities personnel who made these studies possible; all local teams, epidemiologists, veterinary officers, and other staff from the National Animal Health and Production Research Institute; Stephanie Meyer and Tom Lewis for their critical assistance in growing viral isolates and performing hemagglutination analysis, and the authors and originating and submitting laboratories of the sequences from the GISAID database (Appendix 2, https://wwwnc.cdc.gov/EID/article/29/1/22-0934-App2.xlsx).

Work at Institut Pasteur du Cambodge was supported by the Food and Agriculture Organization of the United Nations and funded by the United States Agency for International Development under the Emerging Pandemics Threats 2 (EPT-2) project. The Melbourne World Health Organization Collaborating Centre for Reference and Research on Influenza is supported by the Australian Government Department of Health.
The funders had no role in study design, data collection and analysis, decision to publish, or preparation of the manuscript.

About the Author

Mrs. Edwards serves as project manager for the Pathogen Evolution Laboratory in the School of Public Health at the University of Hong Kong. Her research focuses on the ecology, epidemiology, and evolution of infectious disease at the human–animal interface.

References

1. World Organisation for Animal Health (OIE). World animal health information system (OIE-WAHIS) [cited 2022 Sep 6]. https://wahis.oie.int
2. Karlsson EA, Horm SV, Tok S, Tum S, Kalpravidh W, Claes F, et al. Avian influenza virus detection, temporality and co-infection in poultry in Cambodian border provinces, 2017–2018. Emerg Microbes Infect. 2019;8:637–9. https://doi.org/10.1080/22221751.2019.1604085
3. Vijaykrishna D, Deng YM, Grau ML, Kay M, Suttie A, Horwood PF, et al. Emergence of influenza A(H7N4) virus, Cambodia. Emerg Infect Dis. 2019;25:1988–91. https://doi.org/10.3201/eid2510.190506
4. Thielen P. Influenza whole genome sequencing with integrated indexing on Oxford Nanopore platforms [cited 2022 Sep 6]. https://doi.org/10.17504/protocols.io.kxygxm7yzl8j/v1
5. Yamaji R, Saad MD, Davis CT, Swayne DE, Wang D, Wong FYK, et al. Pandemic potential of highly pathogenic avian influenza clade 2.3.4.4 A(H5) viruses. Rev Med Virol. 2020;30:e2099. https://doi.org/10.1002/rmv.2099
6. Oliver I, Roberts J, Brown CS, Byrne AM, Mellon D, Hansen RDE, et al. A case of avian influenza A(H5N1) in England, January 2022. Euro Surveill. 2022;27:2200061. https://doi.org/10.2807/1560-7917.ES.2022.27.5.2200061
7. Lewis NS, Banyard AC, Whittard E, Karibayev T, Al Kafagi T, Chvala I, et al. Emergence and spread of novel H5N8, H5N5 and H5N1 clade 2.3.4.4 highly pathogenic avian influenza in 2020. Emerg Microbes Infect. 2021;10:148–51. https://doi.org/10.1080/22221751.2021.1872355
8. Food and Agriculture Organization of the United Nations. EMPRES-i Global Animal Disease Information System [cited 2022 Sep 6]. https://empres-i.apps.fao.org/diseases
9. World Health Organization. Antigenic and genetic characteristics of zoonotic influenza A viruses and development of candidate vaccine viruses for pandemic preparedness. October 2021 [cited 2022 Sep 6]. https://apps.who.int/iris/handle/10665/347437
10. U.S. Department of Agriculture Animal and Plant Health Inspection Service. 2022 detections of highly pathogenic avian influenza in wild birds [cited 2022 Mar 15]. https://www.aphis.usda.gov/aphis/ourfocus/animalhealth/animal-disease-information/avian/avian-influenza/hpai-2022/2022-hpai-wild-birds
11. Pyankova OG, Susloparov IM, Moiseeva AA, Kolosova NP, Onkhonova GS, Danilenko AV, et al. Isolation of clade 2.3.4.4b A(H5N8), a highly pathogenic avian influenza virus, from a worker during an outbreak on a poultry farm, Russia, December 2020. Euro Surveill. 2021;26:2100439. https://doi.org/10.2807/1560-7917.ES.2021.26.24.2100439
12. World Health Organization. Avian influenza weekly update number 844. 2022 [cited 2022 May 22]. http://apps.who.int/iris/handle/10665/351652
13. Hervé S, Schmitz A, Briand F-X, Gorin S, Quéguiner S, Niqueux É, et al. Serological evidence of backyard pig exposure to highly pathogenic avian influenza H5N8 virus during 2016–2017 epizootic in France. Pathogens. 2021;10:621. https://doi.org/10.3390/pathogens10050621
14. UK Health Security Agency. Human case of avian flu detected in UK. 2022 [cited 2022 May 22]. https://www.gov.uk/government/news/human-case-of-avian-flu-detected-in-uk
15. Centers for Disease Control and Prevention. Reported human infections with avian influenza A viruses. 2022 [cited 2022 May 22]. https://www.cdc.gov/flu/avianflu/reported-human-infections.htm

Address for correspondence: Erik A. Karlsson, Institut Pasteur du Cambodge Virology Unit, 5 Monivong Blvd, PO Box 983, Phnom Penh, Cambodia; email: ekarlsson@pasteur-kh.org

Using Serum Specimens for Real-Time PCR-Based Diagnosis of Human Granulocytic Anaplasmosis, Canada

Carl Boodman, Courtney Loomer, Antonia Dibernardo, Todd Hatchette, Jason J. LeBlanc, Brooks Waitt, L. Robbin Lindsay

Whole blood is the optimal specimen for anaplasmosis diagnosis but might not be available in all cases. We PCR tested serum samples collected in Canada for *Anaplasma* serology and found 84.8%–95.8% sensitivity and 2.8 average cycle threshold elevation. Serum can be acceptable for detecting *Anaplasma* spp. when whole blood is unavailable.

Human granulocytic anaplasmosis (HGA) is a tickborne infection caused by the intracellular bacterium *Anaplasma phagocytophilum* (*1*), an emerging pathogen in North America (*2*–*5*). HGA can manifest as a subclinical infection; however, most symptomatic persons have fever, myalgia, and headache associated with thrombocytopenia, leukopenia, and elevated transaminase levels (*3*,*6*). Although uncommon, multiorgan failure and death occur predominantly in elderly and immunocompromised patients or when treatment is delayed (*7*,*8*). The manifestation of HGA as a nonspecific febrile illness can lead to lack of recognition, and delays in antimicrobial administration can cause illness and death (*9*,*10*). Early diagnosis is essential to avoid these preventable complications.

Laboratory diagnosis of HGA can be established by using microscopy, serology, or nucleic acid amplification test (NAAT) (*3*,*11*). Microscopy can be used to diagnose acute infections, but relies on experienced personnel to visualize intragranulocytic clusters or morulae in peripheral blood (*3*,*11*). Because morulae are present in only 25%–75% of cases, microscopy lacks sensitivity (*6*,*9*). Serology is more commonly used to diagnose HGA, relying primarily on indirect immunofluorescence assays (IFAs) (*7*,*9*). However, serologic tests are often negative during the first week of symptoms and require paired acute and convalescent serum samples ≥2 weeks apart to improve sensitivity (*8*–*10*). NAAT can be performed to detect *A. phagocytophilum* in whole blood or buffy coat and is the preferred test during the first 2 weeks of illness (*9*,*10*). However, most persons evaluated for tickborne infections have serum samples submitted as their primary specimen because serology is the standard diagnostic method for Lyme disease, the most common tickborne infection in North America. Unless anaplasmosis is considered when the patient is first seen, a whole blood specimen is rarely available. We used residual serum samples submitted for *Anaplasma* sp. serology in Canada to determine if serum samples could be an acceptable alternative to whole blood for the diagnosis of HGA by real-time PCR.

The Study

We tested 2 different serum specimen groups for *A. phagocytophilum* DNA. The first group consisted of serum samples from persons who were positive for *A. phagocytophilum* by using the NAAT of whole blood. The second group consisted of acute and convalescent serum samples (drawn ≥2 weeks apart) submitted to the National Microbiology Laboratory (Winnipeg, Manitoba) for *Anaplasma* serology during 2020–2021. The samples were anonymized, and the investigators were blinded to serology results. Ethics approval was not required because anonymized samples were evaluated for a quality improvement study.

Author affiliations: University of Manitoba, Winnipeg, Manitoba, Canada (C. Boodman); National Microbiology Laboratory, Winnipeg (C. Loomer, A. Dibernardo, B. Waitt, L.R. Lindsay); Dalhousie University and Nova Scotia Health, Halifax, Nova Scotia, Canada (T. Hatchette, J.J. LeBlanc)

DOI: https://doi.org/10.3201/eid2901.220988

We isolated DNA from 100 µL of serum by using DNeasy 96 kits (QIAGEN, https://www.qiagen.com) and eluted the DNA in 100 µL of elution buffer. We used carrier RNA (Applied Biosystems/Thermo Fisher Scientific, https://www.thermofisher.com) to improve recovery of low amounts of nucleic acids. We used T4 bacteriophage DNA as a positive extraction control. We amplified the *msp2* gene of *A. phagocytophilum* as previously described (*12*) by using 5 µL of template DNA in 30 µL reaction volumes containing TaqMan Universal Master Mix (Applied Biosystems). We performed amplifications on a ViiA7 system (Applied Biosystems) and thermocycling conditions were as follows: 2 min at 50°C, 10 min at 95°C, and 40 cycles of 95°C for 15 s and 60°C for 1 min. We included synthetic *A. phagocytophilum* DNA (Integrated DNA Technologies, https://www.idtdna.com) as a positive control and master mix without DNA as a negative control in each run. A sample was considered positive if cycle threshold (Ct) values were <40. We reextracted and retested positive samples to ensure reproducibility. Samples with repeated Ct values of <40 were considered positive. Positive samples with insufficient volume for reextraction were considered positive. We calculated averages and ranges from the initial extraction.

We used the semiquantitative Focus Diagnostics *A. phagocytophilum* IFA IgG kit (DiaSorin, https://www.diasorin.com), and IgG titers >1:64 indicated current or previous *A. phagocytophilum* infection (*13*). We defined seroconversion as a ≥4-fold increase in titer between acute and convalescent serum samples.

Of the 33 specimens from the first group of serum samples (Table 1), we collected 23 serum samples on the same day as whole blood and 10 serum samples on a different day. The maximum time between serum and whole blood sampling was 8 days. We collected whole blood samples before serum samples for 2 patients. PCR showed 28 (84.8%) serum samples were positive for *A. phagocytophilum* of which 6 (18.1%) had an IFA titer >1:64. The average Ct values were 27.6

Table 1. Comparison of PCR values for serum and whole blood samples in study using serum specimens for real-time PCR-based diagnosis of human granulocytic anaplasmosis, Canada*

Sample		Serum Ct values				Whole blood Ct values					
no.	IFA titer	Ct-I	Ct-R	Average†	Result	Ct-I	Ct-R	Average†	Result	ΔCt	Td‡
1	<1:64	19.9	NS	19.9	Positive	17.7	16.1	16.9	Positive	3	5
2	<1:64	21.8	NS	21.8	Positive	22	21.1	21.55	Positive	0.25	3
3	<1:64	22.8	21.8	22.3	Positive	22.1	21.5	21.8	Positive	0.5	0
4	<1:64	22.9	NS	22.9	Positive	18.5	17.9	18.2	Positive	4.7	0
5	<1:64	23	22.5	22.75	Positive	20.5	19.7	20.1	Positive	2.65	1
6	<1:64	23.3	22.1	22.7	Positive	19.1	18.1	18.6	Positive	4.1	1
7	<1:64	24.2	24.2	24.2	Positive	21.2	20.9	21.05	Positive	3.15	1
8	1:2048	25	25.8	25.4	Positive	22	21.9	21.95	Positive	3.45	0
9	<1:64	26.6	26	26.3	Positive	24.6	25.4	25	Positive	1.3	0
10	<1:64	26.6	25.6	26.1	Positive	23.2	23.5	23.35	Positive	2.75	0
11	1:512	27	NS	27	Positive	24.8	25.3	25.05	Positive	1.95	2
12	1:64	28	25.3	26.65	Positive	28.6	29.2	28.9	Positive	−2.25	0
13	<1:64	28.6	27.5	28.05	Positive	23	22.6	22.8	Positive	5.25	0
14	<1:64	28.8	28.1	28.45	Positive	33	33.3	33.15	Positive	−4.7	3
15	<1:64	29.2	28.3	28.75	Positive	27.7	27.1	27.4	Positive	1.35	0
16	1:2048	29.9	27.4	28.65	Positive	26.9	27	26.95	Positive	1.7	0
17	1:64	30	29.2	29.6	Positive	22	21.8	21.9	Positive	7.7	0
18	<1:64	31.7	31.7	31.7	Positive	30.5	30.2	30.35	Positive	1.35	0
19	<1:64	32.4	33.5	32.95	Positive	26.4	26.2	26.3	Positive	6.65	0
20	1:512	32.8	31.7	32.25	Positive	37	36.5	36.75	Positive	−4.5	8
21	<1:64	36.4	37.8	37.1	Positive	37.8	37.8	37.8	Positive	−0.7	0
22	<1:64	36.5	35.8	36.15	Positive	28.4	28.5	28.45	Positive	7.7	0
23	<1:64	36.7	36	36.35	Positive	32.5	32.7	32.6	Positive	3.75	0
24	<1:64	37.7	36.3	37	Positive	34	34	34	Positive	3	0
25	1:1024	37.8	37.4	37.6	Positive	32	32	32	Positive	5.6	0
26	1:256	38.2	38.3	38.25	Positive	25.1	24.8	24.95	Positive	13.3	−84
27	<1:64	38.3	40	39.15	Negative	37.2	37.6	37.4	Positive	1.75	0
28	<1:64	38.4	35.3	36.85	Positive	24.1	24.2	24.15	Positive	12.7	−4
29	<1:64	38.8	38.2	38.5	Positive	31.3	31.2	31.25	Positive	7.25	0
30	<1:64	40	38.3	39.15	Negative	38.9	39.5	39.2	Positive	−0.05	0
31	<1:64	40	40	40	Negative	35.3	36.7	36	Positive	4	0
32	1:64	40	40	40	Negative	33.4	32.9	33.15	Positive	6.85	0
33	<1:64	40	40	40	Negative	30.9	31.0	30.95	Positive	9.05	0

*Only Ct values <40 after repeat extraction were deemed positive. Ct, cycle threshold; Ct-I, Ct values for initial extraction; Ct-R, confirmatory Ct values for repeat extraction; ΔCt, difference between average serum Ct and average whole blood Ct; IFA, indirect immunofluorescence assay; NS, no sample remaining for repeat extraction; Td, time difference in days between serum sampling (earlier) and whole blood sampling (later).
†Average of Ct-I and Ct-R for each isolate.
‡Negative numbers indicate that whole blood was sampled before serum samples.

Table 2. Comparison between PCR-positive acute serum samples and paired convalescent serum samples in study using serum specimens for real-time PCR-based diagnosis of human granulocytic anaplasmosis, Canada*

Sample	Acute serum samples				Convalescent serum samples					
no.	IFA titer	Ct-I	Ct-R	PCR status	IFA	Ct-I	Ct-R	PCR status	Time, d†	Conversion‡
1	<1:64	23.7	24.7	Positive	1:128	40.0	NA	Negative	24	Yes
2	<1:64	24.3	NS	Positive	1:512	35.5	NS	Positive	33	Yes
3	<1:64	25.1	NS	Positive	<1:64	27.6	NS	Positive	42	No
4	<1:64	25.8	NS	Positive	1:1024	39.9	37.1	Positive	13	Yes
5	<1:64	26.8	NS	Positive	1:512	40.0	NA	Negative	56	Yes
6	1:64	28.0	25.3	Positive	1:256	40.0	NA	Negative	49	Yes
7	1:2048	28.2	30.4	Positive	1:2048	40.0	NA	Negative	12	No
8	<1:64	28.8	28.1	Positive	1:128	40.0	NA	Negative	21	Yes
9	<1:64	29.7	NS	Positive	<1:64	40.0	NA	Negative	39	No
10	1:1024	31.0	29.9	Positive	1:1024	40.0	NA	Negative	28	No
11	<1:64	31.2	31.4	Positive	<1:64	40.0	NA	Negative	0	No
12	<1:64	31.7	31.7	Positive	1:256	40.0	NA	Negative	51	Yes
13	1:1024	32.4	32.8	Positive	1:256	39.8	40.0	Negative	8	No
14	<1:64	32.4	33.4	Positive	1:256	40.0	NA	Negative	38	Yes
15	1:512	32.8	31.7	Positive	1:512	40.0	NA	Negative	27	No
16	<1:64	34.7	36.3	Positive	<1:64	40.0	NA	Negative	38	No
17	1:1024	35.6	36.3	Positive	1:512	40.0	NA	Negative	57	No
18	<1:64	36.1	37.8	Positive	1:64	40.0	NA	Negative	10	No
19	<1:64	37.5	36.8	Positive	1:256	40.0	NA	Negative	46	Yes

*Only Ct values <40 were deemed positive. Ct, cycle threshold; Ct-I, initial Ct values (in duplicate); Ct-R, confirmatory Ct values for repeat extraction; IFA, indirect immunofluorescence assay; NA, not applicable; NS, no sample remaining for repeat extraction.
†Time difference between acute and convalescent serum sampling.
‡Seroconversion was defined as ≥4-fold increase in IFA titer between acute and convalescent samples.

(range 17.7–39.5) for whole blood and 30.4 (range 19.9–38.8) for serum samples. Among 5 patients who had PCR-positive whole blood samples but PCR-negative serum samples, the average Ct was 35.1. All 10 serum specimens collected on a different day were PCR positive. We tested an additional 90 paired whole blood and serum samples, and the tests showed 95.8% sensitivity (Appendix Table 1, https://wwwnc.cdc.gov/EID/article/29/1/22-0988-App1.pdf).

Of 154 paired acute and convalescent serum samples submitted for *Anaplasma* serology, 19 (12.3%) acute specimens and 3 (1.9%) convalescent specimens were PCR positive (Table 2). Average Ct values were 30.3 (range 23.7–37.5) for acute samples and 34.3 (range 27.6–39.9) for convalescent samples. We did not observe seroconversion in 10 (52.6%) patients who had PCR-positive acute serum specimens.

Of the 154 paired acute and convalescent serum samples, 28 (18.2%) were serologically positive, but only 11 (7.1%) demonstrated seroconversion (Appendix Table 2). Titers increased from <1:64 to 1:64 in 3 paired samples, 13 samples demonstrated stable or decreasing titers, and 1 titer doubled. PCR of acute samples detected 9 of 11 (81.8%) patients who displayed seroconversion. PCR was negative using acute serum samples for 2 patients; those patient samples had initial IFA titers ≥1:1024, indicating either previous infection or delayed sampling. The sensitivity of serum-based PCR was 81.8%, and specificity was 93.0% compared with seroconversion (Appendix Table 3).

Conclusions

Because *A. phagocytophilum* occupies an intracellular niche, the prevailing dogma maintains that whole blood or buffy coat specimens are necessary for detection of *A. phagocytophilum* by PCR (*9*,*10*). Because serum is commonly obtained when tickborne infection is suspected, serum is a convenient PCR specimen to diagnosis HGA. Compared with whole blood, serum-based PCR has a sensitivity of 84.8%–95.8% and an average Ct elevation of 2.8.

PCR is superior to serology for diagnosing acute HGA (*10*). Few PCR-positive acute serum samples were associated with elevated IFA titers. PCR using acute serum samples resulted in a superior positivity rate (12.3%) than acute seroconversion measurements (7.1%). Acute serum specimens were 6.3 times more likely to be PCR positive than convalescent specimens, indicating the importance of early specimen collection when pursuing molecular diagnosis of HGA (*10*). The sensitivity of serum-based PCR was 81.8%. Although 81.8% sensitivity is comparable to the whole blood dataset, 10 patients with PCR-positive acute samples did not demonstrate acute seroconversion. Antimicrobial administration might have aborted or delayed seroconversion, which has been hypothesized in a previous study (*14*), although no clinical data exist to confirm this hypothesis. Similarly, 2 patients who had negative PCR results for acute serum samples ultimately had seroconversion. We did not have companion whole blood to determine whether those false negatives were the result

of decreased sensitivity of serum compared with whole blood or the acute serum was collected after the acute bacteremia stage. Many acute samples had titers greater than 1:512, which suggests those 2 samples were collected after acute bacteremia. Although whole blood remains the optimal specimen for PCR, this study demonstrates that reflex PCR testing of acute serum samples submitted for *A. phagocytophilum* serology might improve diagnostic sensitivity for acute HGA when whole blood is unavailable.

About the Author

Dr. Boodman specializes in infectious disease and medical microbiology and is currently pursuing another degree in the clinical investigator program at the University of Manitoba. His research interests focus on neglected infectious diseases, vectorborne infections, and the interplay between infectious disease and socioeconomic disparities.

References

1. Sanchez E, Vannier E, Wormser GP, Hu LT. Diagnosis, treatment, and prevention of Lyme disease, human granulocytic anaplasmosis, and babesiosis: a review. JAMA. 2016;315:1767–77. https://doi.org/10.1001/jama.2016.2884
2. Chase B, Bonnar P. A walk through the tall grass: a case of transaminitis, thrombocytopenia, and leukopenia resulting from an emerging zoonotic infection in Nova Scotia. J Assoc Med Microbiol Infect Dis Can. 2018;3:247–50. https://doi.org/10.3138/jammi.2018-08.07.2
3. Ismail N, Bloch KC, McBride JW. Human ehrlichiosis and anaplasmosis. Clin Lab Med. 2010;30:261–92. https://doi.org/10.1016/j.cll.2009.10.004
4. Nelder MP, Russell CB, Lindsay LR, Dibernardo A, Brandon NC, Pritchard J, et al. Recent emergence of *Anaplasma phagocytophilum* in Ontario, Canada: early serological and entomological indicators. Am J Trop Med Hyg. 2019;101:1249–58. https://doi.org/10.4269/ajtmh.19-0166
5. Manitoba Government. Manitoba annual tick-borne disease report, 2018 [cited 2022 Mar 5]. https://www.gov.mb.ca/health/publichealth/cdc/tickborne/docs/tbd_report2018.pdf
6. Aguero-Rosenfeld ME. Diagnosis of human granulocytic ehrlichiosis: state of the art. Vector Borne Zoonotic Dis. 2002;2:233–9. https://doi.org/10.1089/153036602321653815
7. Bakken JS, Aguero-Rosenfeld ME, Tilden RL, Wormser GP, Horowitz HW, Raffalli JT, et al. Serial measurements of hematologic counts during the active phase of human granulocytic ehrlichiosis. Clin Infect Dis. 2001;32:862–70. https://doi.org/10.1086/319350
8. Ismail N, McBride JW. Tick-borne emerging infections: ehrlichiosis and anaplasmosis. Clin Lab Med. 2017;37:317–40. https://doi.org/10.1016/j.cll.2017.01.006
9. Chapman AS, Bakken JS, Folk SM, Paddock CD, Bloch KC, Krusell A, et al.; Tickborne Rickettsial Diseases Working Group; CDC. Diagnosis and management of tickborne rickettsial diseases: Rocky Mountain spotted fever, ehrlichioses, and anaplasmosis—United States: a practical guide for physicians and other health-care and public health professionals. MMWR Recomm Rep. 2006;55:1–27.
10. Schotthoefer AM, Meece JK, Ivacic LC, Bertz PD, Zhang K, Weiler T, et al. Comparison of a real-time PCR method with serology and blood smear analysis for diagnosis of human anaplasmosis: importance of infection time course for optimal test utilization. J Clin Microbiol. 2013;51:2147–53. PubMed https://doi.org/10.1128/JCM.00347-13
11. Rodino KG, Theel ES, Pritt BS. Tick-borne diseases in the United States. Clin Chem. 2020;66:537–48. https://doi.org/10.1093/clinchem/hvaa040
12. Courtney JW, Kostelnik LM, Zeidner NS, Massung RF. Multiplex real-time PCR for detection of *Anaplasma phagocytophilum* and *Borrelia burgdorferi*. J Clin Microbiol. 2004;42:3164–8. https://doi.org/10.1128/JCM.42.7.3164-3168.2004
13. Government of Canada. Indirect immunofluorescent assay (IFA)—IgG. Detection of IgG antibodies to *Anaplasma phagocytophilum* by IFA [cited 2022 Mar 5]. https://cnphi.canada.ca/gts/reference-diagnostic-test/4168?labId=1019
14. Carpenter CF, Gandhi TK, Kong LK, Corey GR, Chen SM, Walker DH, et al. The incidence of ehrlichial and rickettsial infection in patients with unexplained fever and recent history of tick bite in central North Carolina. J Infect Dis. 1999;180:900–3. https://doi.org/10.1086/314954

Address for correspondence: Carl Boodman, Department of Medical Microbiology and Infectious Diseases, University of Manitoba, Room 543, Basic Medical Sciences Building, 745 Bannatyne Ave, Winnipeg, MB R3E 0J9, Canada; email: boodmanc@myumanitoba.ca

Photobacterium damselae subspecies *damselae* Pneumonia in Dead, Stranded Bottlenose Dolphin, Eastern Mediterranean Sea

Danny Morick, Shlomo E. Blum, Nadav Davidovich, Ziv Zemah-Shamir, Eyal Bigal, Peleg Itay, Assaf Rokney, Iris Nasie, Noa Feldman, Marcelo Flecker, Mia Roditi-Elasar, Kobi Aharoni, Yotam Zuriel, Natascha Wosnick, Dan Tchernov, Aviad P. Scheinin

Photobacterium damselae subspecies *damselae*, an abundant, generalist marine pathogen, has been reported in various cetaceans worldwide. We report a bottlenose dolphin in the eastern Mediterranean Sea that was found stranded and dead. The dolphin had a severe case of chronic suppurative pneumonia and splenic lymphoid depletion caused by this pathogen.

The common bottlenose dolphin (*Tursiops truncatus*) is perhaps the most common and widespread dolphin species in the Mediterranean Sea (*1*). *Photobacterium damselae* subspecies *damselae* is a pathogen that produces wound infections and hemorrhagic septicemia and high mortality rates and affects various marine animals, such as fish, mollusks, crustaceans, and cetaceans (*2*,*3*). Highly pathogenic *P. damselae* subsp. *damselae* isolates have 2 major virulence factors: the phospholipase D damselysin (Dly) and the pore-forming toxin phobalysin P (initially called $HlyA_{pl}$). Both toxins are encoded by the plasmid pPHDD1 and produce hemolytic and cytolytic activities in a synergistic manner (*4*). We report a bottlenose dolphin in the eastern Mediterranean Sea that was found stranded, dead, and had a severe case of chronic suppurative pneumonia and splenic lymphoid depletion caused by this pathogen.

Author affiliations: University of Haifa, Haifa, Israel (D. Morick, N. Davidovich, Z. Zemah-Shamir, E. Bigal, P. Itay, M. Roditi-Elasar, Y. Zuriel, D. Tchernov, A.P. Scheinin); Hong Kong Branch of Southern Marine Science and Engineering, Guangzhou, China (D. Morick, D. Tchernov); Kimron Veterinary Institute, Bet Dagan, Israel (S.E. Blum, M. Flecker); Israeli Veterinary Services, Bet Dagan (N. Davidovich); Ministry of Health, Jerusalem, Israel (A. Rokney, I. Nasie, N. Feldman); Hebrew University of Jerusalem, Rehovot, Israel (K. Aharoni); Universidade Federal do Paraná, Curitiba, Brazil (N. Wosnick)

DOI: https://doi.org/10.3201/eid2901.221345

The Study

On January 29, 2021, a bottlenose dolphin was found beached nearby Ashdod, Israel. The carcass underwent a postmortem examination based on a widely accepted protocol (*5*) with some modifications because the carcass was also sampled for several anatomic and physiologic studies. Samples of the spleen, liver, lung, kidney and brain were collected for quantitative PCR molecular detection of *Toxoplasma gondii* (*6*) and canine distemper virus (*7*), and for PCR detection of *Brucella* spp. (*8*). Samples of spleen and lung were fixed in 10% buffered formalin for routine histologic evaluation. Samples of lungs and fluid from the thoracic cavity were obtained by using sterile swabs for lung samples and sterile syringes and needles for fluid samples and inoculated onto tryptone soy agar, blood agar (5% sheep blood enriched tryptone soy agar), and MacConkey agar, and incubated for 24–48 h at 37°C. Confirmation of bacteria species was initially performed by using matrix-assisted laser desorption/ionization time-of-flight mass spectrometry according to the manufacturer's protocol (Autoflex; Bruker, https://www.bruker.com).

The dolphin weighed 200 kg, had a length of 263 cm, and was identified as a mature female that had a moderate nutritional status (*9*). At external examination, a deep bruise was observed on the front of the dorsal fin, and an old visible scar was observed on the right side of the chest, which might have been the result of an injury by a foreign body that might have instigated the inflammation within the lung, leading to pneumonia (Figure 1, panel A). No additional external signs of interaction with fishing gear were

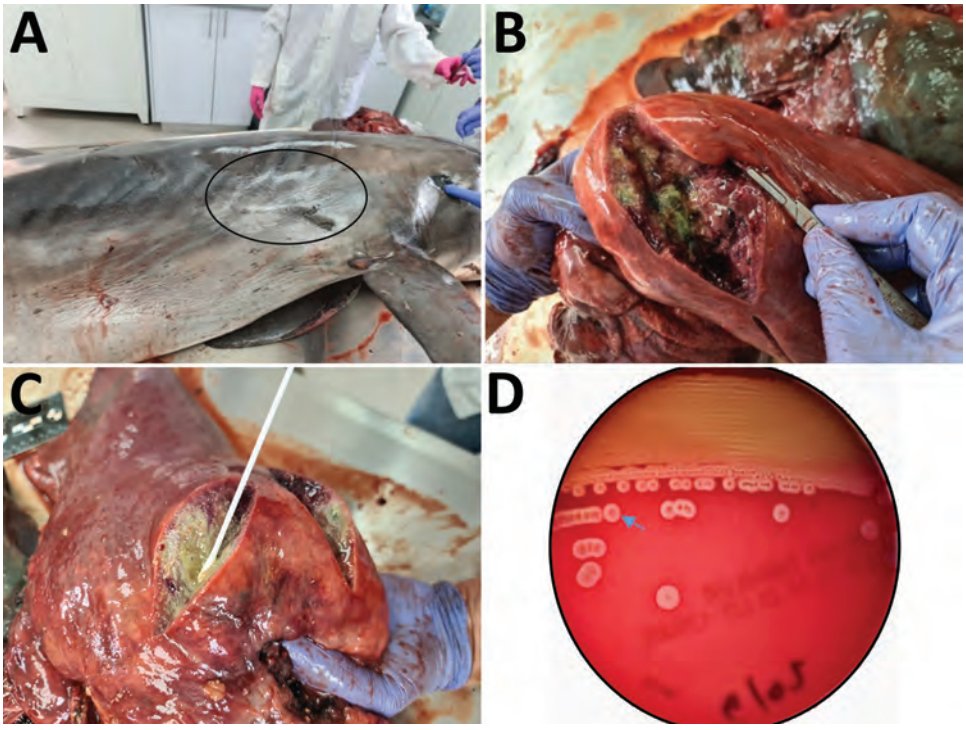

Figure 1. *Photobacterium damselae* subspecies *damselae* pneumonia in a bottlenose dolphin, eastern Mediterranean Sea. Gross pathologic examination of the dolphin (*Tursiops truncatus*) showed a scar (oval) at the right side of the chest (A) that might be a sign for a previous wound that initiated the infection (B, C). Four abscesses, 5–10 cm in diameter, filled with purulent fluid and necrotic debris were observed in the right lung of the animal. Hemolytic phenotype of the *P. damselae* subsp. *damselae* isolate on sheep blood agar (D) indicates the border of the halo of 1 colony (arrow). A weak hemolytic phenotype was observed after culturing isolate on blood agar plates for 24 h.

observed. The carcass was at stage 3 on the decomposition condition code scale (*5*). Internal examination indicated 4 large, firm nodules, 5–10 cm in diameter, replacing the cranial aspect of the right lung lobe. On cut sections, nodules were filled with purulent to caseous, thick, granular, green-tinged exudate surrounded by a dense fibrous capsule (abscess) (Figure 1, panels B, C). No other abnormalities were observed in all other internal organs.

Pure bacterial colonies of spherical or ovoid cocci, 1–2 μm in diameter, consistent with the genus *Photobacterium*, appeared on the blood agar plates at 48-hours postinoculation. Matrix-assisted laser desorption/ionization time-of-flight mass spectrometry confirmed the initial identification of *Photobacterium damselae*. The isolate was resistant to ampicillin and susceptible to gentamicin, sulfamethoxazole/trimethoprim, florfenicol, amikacin, and polymyxin B. The isolate also had intermediate susceptibility to amoxicillin/clavulanic acid; fluoroquinolones; and first-, second-, and third-generation cephalosporins.

The isolate species was also characterized and confirmed by using 16S rRNA gene primers and Sanger sequencing of the 800-nt PCR product. Whole-genome sequencing (WGS) was performed to obtain the allelic multilocus sequence typing (MLST) profile for sequence type determination and to analyze the presence of the 2 *P. damselae* subsp. *damselae* major virulence factor genes (*dly* and $hlyA_{pl}$).

We extracted DNA by using the QIAsymphony SP System and the QIAsymphony DNA Mini Kit (QIAGEN, https://www.qiagen.com), according to the manufacturer's recommendations. We prepared a DNA library by using the Nextera XT Library Preparation Kit (Illumina, https://www.illumina.com), followed by WGS using the Illumina MiSeq and a 250-bp paired-end read length. Reads were assembled by

Table 1. Similarity-based gene extraction of genes used in MLST scheme, including the obtained MLST allelic profile for *Photobacterium damselae* subspecies *damselae* pneumonia, in bottlenose dolphin, eastern Mediterranean Sea*

Gene	Identity,† %	Coverage, %	Reference length, bp	No. mismatches	No. open gaps	MLST allelic profiles
glpF	99.58	100.00	480	2	0	26
gyrB	97.58	100.00	537	13	0	27
metG	99.53	100.00	429	2	0	7
pntA	97.98	100.00	396	8	0	23
pyrC	98.42	100.00	507	8	0	31
toxR	93.32	99.74‡	387	23	1	35

*MLST, multilocus sequence typing.
†The percentage of identity to allele 1 sequence of each gene (taken from *P. damselae* subsp. *damselae* PubMLST database).
‡The *toxR* alleles length range is 372–390 bp (*10*). The *toxR* allele length of the isolate of this study is 390 bp, and the allele 1 reference length is 387 bp.

Table 2. PubMLST database of *Photobacterium damselae* subspecies *damselae* isolates from different marine animals, including a bottlenose dolphin in the eastern Mediterranean Sea*

Country	Host	Organ	Year							
			2010	2012	2013	2014	2015	2016	2021	NA
Australia	*Seriola lalandi*	Ot	2	0	0	0	4	2	0	0
Israel	*Tursiops truncatus*	Lu	0	0	0	0	0	0	1	0
Italy	*Caretta caretta*	Icc	0	0	3	0	0	0	0	0
	Delphinus delphis	Ot	0	0	1	0	0	0	0	0
	Physeter macrocephalus	Br	0	0	0	1	0	0	0	0
		Mf	0	0	0	1	0	0	0	0
		Sp	0	0	0	2	0	0	0	0
		Ut	0	0	0	1	0	0	0	0
	Stenella coeruleoalba	Br	0	0	14	3	0	0	0	0
		Icc	0	0	1	0	0	0	0	0
		In	0	0	3	0	0	0	0	0
		Jf	0	0	3	0	0	0	0	0
		Li	0	0	6	0	0	0	0	0
		Ln	0	0	2	0	0	0	0	0
		Lu	0	1	3	0	0	0	0	0
		Ot	0	0	3	0	0	0	0	0
		Sp	0	0	5	0	0	0	0	0
	Stenella spp.	Br	0	0	3	0	0	0	0	0
		In	0	0	1	0	0	0	0	0
		Li	0	0	1	0	0	0	0	0
		Ln	0	0	2	1	0	0	0	0
		Lu	0	0	1	1	0	0	0	0
		Sp	0	0	1	0	0	0	0	0
	Tursiops truncatus	Br	0	1	3	0	0	0	0	0
		Icc	0	0	1	1	0	0	0	0
		Lu	0	0	1	0	0	0	0	0
		Sp	0	0	1	0	0	0	0	0
		Un	0	0	0	1	0	0	0	0
Japan	*Labracoglossa argentiventris*	Ot	0	0	0	0	0	0	0	1
	Sardinops melanostictus	Ot	0	0	0	0	0	0	0	1
United States	*Carcharhinus plumbeus*	Li	0	0	0	0	0	0	0	1
	Chromis punctipinnis	Ot	0	0	0	0	0	0	0	1
		Total	2	2	59	12	4	2	1	4

*Database contained 86 isolates as of February 5, 2020 (https://pubmlst.org/organisms/photobacterium-damselae). Br, brain; Icc, intracardiac clot; In, intestine; Jf, joint fluid; Li, liver; Ln, lymph node; Lu, lung; Mf, mesenteric fluid; NA, no year data in PubMLST database; Ot, other; Sp, spleen; Un, unknown; Ut, uterus.

using the BioNumerics 8.0 Platform SPAdes 3.13.1 (Applied Maths, https://www.applied-maths.com).

The assembly was deposited to the pubMLST *P. damselae* database under identification no. 91. We obtained the allelic MLST profile by using the BioNumerics Sequence Extraction Tool (Applied Maths) and according to the *P. damselae* scheme based on 6 housekeeping genes (*glpF*, *gyrB*, *metG*, *pntA*, *pyrC*, and *toxR*) (*10*). This tool was also used for identification of virulence factor gene sequences *dly* (GenBank accession no. 9937366) and $hlyA_{pl}$ (GenBank accession no. ID 9937197). Hemolysis was tested by culturing the isolate on 5% sheep blood agar (#PD-005; Hylabs Ltd, https://www.hylabs.co.il) for 24 h at 37°C.

Identification of *P. damselae* subsp. *damselae* was supported and confirmed by molecular, phenotypic, and genomic characterization. The 16S rRNA sequence showed a similarity of 99.17% with other *P. damselae* subsp. *damselae* strains in GenBank. When tested for hemolysis, the isolate exhibited a weak hemolytic phenotype, producing narrow halos on sheep blood agar plate (Figure 1, panel D). This phenotype is typical of *P. damselae* subsp. *damselae* lacking the pPHDD1 plasmid and having the chromosomal PhlyC gene ($hlyA_{ch}$). WGS of the hemolytic genes *dly* and $hlyA_{pl}$ yielded only the *hlyA* sequence, which showed 99% identity to the $hlyA_{ch}$ sequences in GenBank.

The MLST allelic scheme extraction (Table 1) resulted in a new profile that was submitted to the isolate collection of the PubMLST *P. damselae* database as PDIN1, and was assigned a new sequence type (ST), ST63. Within the PubMLST database, most of the *P. damselae* subsp. *damselae* isolates (Table 2) originated from an unusual cetacean mortality event in Italy during 2013 (*11*). Neighbor-joining phylogenetic analysis suggested that the strain from Israel sequenced in this study was not strongly related to any other available ST and showed closest resemblance to isolate ST45 from a bottlenose dolphin from Italy (Appendix Figure, https://wwwnc.cdc.gov/EID/article/29/1/22-1345-App1.pdf).

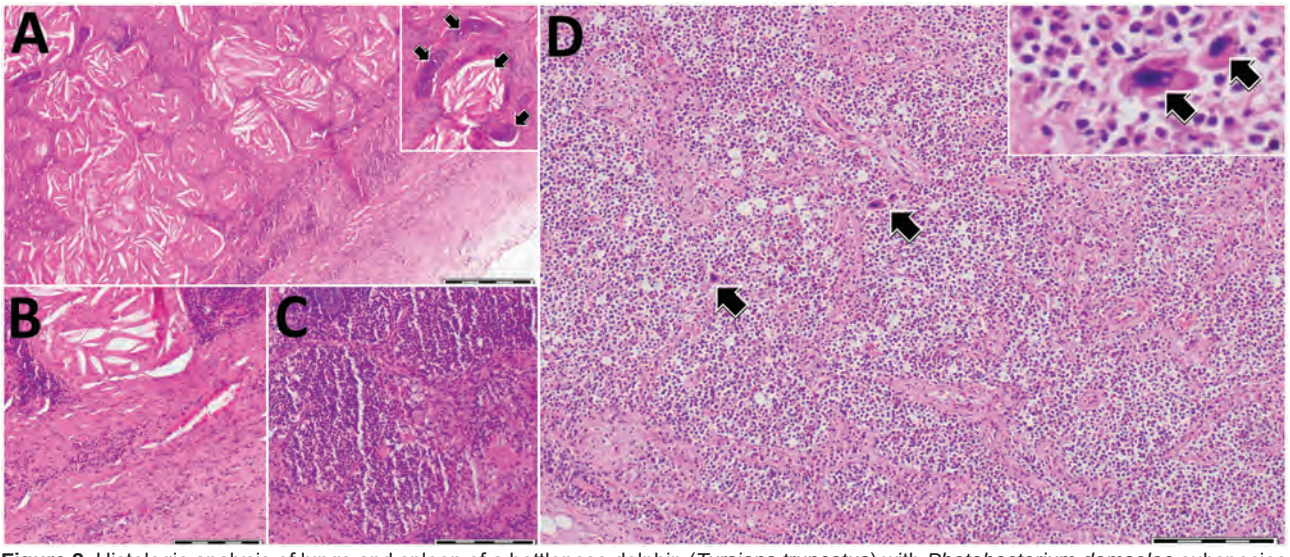

Figure 2. Histologic analysis of lungs and spleen of a bottlenose dolphin (*Tursiops truncatus*) with *Photobacterium damselae* subspecies *damselae* pneumonia, eastern Mediterranean Sea. A) Lung tissue showed a nodular structure covered by fibrous capsule (right bottom of figure panel) composed of numerous cholesterol clefts and areas of reactive fibrosis. Hyaline cartilage was observed, interpreted as bronchi and bronchioles. Inset, higher magnification showing an aggregate of cholesterol clefts and hyaline cartilage (arrow). B) Abundant fibrous lung tissue (lower right half) and cellular infiltrates were also observed. C) Different area of the lung parenchyma characterized by increased cellular infiltration. D) Spleen expressed an apparent contraction of the parenchyma showing diffuse cellularity, with only a few defined lymphoid follicles, as well as megakaryocytes (arrows) indicative of extramedullary hematopoiesis. Inset: higher magnification showing 2 adjacent megakaryocytes (arrow). Hematoxylin and eosin stained. Scale bars indicate 500 μm in panel A and 200 μm in panels B–D.

Results of molecular detection for *T. gondii*, canine distemper virus, and *Brucella* spp. were negative for all tested samples. Examination of lung tissue (Figure 2, panels A–C) showed a nodular structure covered by fibrous tissue composed of extensive cellular infiltration, numerous cholesterol clefts, and areas of reactive fibrosis. A second section of the lung showed extensive tissue lysis and concentric fibrosis of blood vessels. In part of the section, a locally extensive cellular infiltration was observed. An area of necrosis was accompanied by a neutrophilic inflammatory reaction and intralesional bacterial colonies. Two additional tissue sections showed diffuse solid fibrosis, multiple cholesterol clefts, and aggregations of leukocytes. Histopathologic analysis indicated an apparent contraction of the parenchyma with occasional lymphoid follicles and diffuse cellularity within the spleen (Figure 2, panel D), which were suggestive of extramedullary hematopoiesis. Morphologic features of both organs included severe chronic suppurative pneumonia and splenic lymphoid depletion, possibly resulting in extramedullary hematopoiesis in the spleen.

This strain caused severe chronic suppurative pneumonia in the absence of the *dly* gene. This result supports previous indications that this virulence factor is not essential for pathogenesis (*12*).

The antibacterial drug sensitivity test showed susceptibility of the isolate to drugs most frequently used in human and veterinary medicine in this region. Tests results for *T. gondii*, canine distemper virus, and *Brucella* spp. showed negative results, making *P. damselae* subsp. *damselae* the only culturable pathogen identified in the dolphin.

Conclusions

We report detection of *P. damselae* subsp. *damselae* in a bottlenose dolphin in the Mediterranean Sea. This report adds to the increasing baseline data regarding the health of these marine mammals and provides molecular information for a pathogen capable of infecting a large variety of animals in the marine environment, as well as humans.

This study was supported by the Southern Marine Science and Engineering Guangdong Laboratory (Guangzhou), Guangzhou, China (grant SMSEGL20SC02) and by the Kahn Foundation.

D.M., N.D., E.B., Y.Z., A.S., and K.A. contributed to field collections, necropsy procedure, and sample processing; Z.Z.S., A.R., I.N., D.T., N.W., P.I., and M.R.E. contributed to data processing, pathologic interpretation, and writing of the manuscript; and I.N., N.F., A.R., S.B., and M.F. performed bacterial isolation and molecular characterization. All authors participated in drafting the manuscript, contributed to writing the article, and approved the submitted version.

About the Author

Dr. Morick is a veterinarian, researcher, and head of the marine pathology laboratory at the Morris Kahn Marine Research Station, Haifa, Israel. His primary research interests are marine animals, pathogen emergence, disease transmission, aquatic animals, marine biology, marine ecology, and public health.

References

1. Bearzi G, Fortuna CM, Reeves RR. Ecology and conservation of common bottlenose dolphins *Tursiops truncatus* in the Mediterranean Sea. Mammal Rev. 2009;39:92–123. https://doi.org/10.1111/j.1365-2907.2008.00133.x
2. Rivas AJ, Lemos ML, Osorio CR. *Photobacterium damselae* subsp. *damselae*, a bacterium pathogenic for marine animals and humans. Front Microbiol. 2013;4:283. https://doi.org/10.3389/fmicb.2013.00283
3. Osorio CR, Vences A, Matanza XM, Terceti MS. *Photobacterium damselae* subsp. *damselae*, a generalist pathogen with unique virulence factors and high genetic diversity. J Bacteriol. 2018;200:e00002–00018. https://doi.org/10.1128/JB.00002-18
4. Rivas AJ, Balado M, Lemos ML, Osorio CR. The *Photobacterium damselae* subsp. *damselae* hemolysins damselysin and HlyA are encoded within a new virulence plasmid. Infect Immun. 2011;79:4617–27. https://doi.org/10.1128/IAI.05436-11
5. Geraci JR, Lounsbury VJ. Marine mammals ashore: a field guide for strandings. 2nd ed. National Aquarium in Baltimore. College Station (TX): Texas A&M University Press; 2005.
6. Bigal E, Morick D, Scheinin AP, Salant H, Berkowitz A, King R, et al. Detection of *Toxoplasma gondii* in three common bottlenose dolphins (*Tursiops truncatus*); a first description from the eastern Mediterranean Sea. Vet Parasitol. 2018;258:74–8. https://doi.org/10.1016/j.vetpar.2018.06.009
7. Elia G, Decaro N, Martella V, Cirone F, Lucente MS, Lorusso E, et al. Detection of canine distemper virus in dogs by real-time RT-PCR. J Virol Methods. 2006;136:171–6. https://doi.org/10.1016/j.jviromet.2006.05.004
8. Bardenstein S, Waner T, Etinger M, Even Tof B, Blum S, Bellaiche M, et al. First diagnosis of *Brucella canis* infection in dogs in Israel. Isr J Vet Med. 2021;76:12–8.
9. Sharir Y, Kerem D, Gol'din P, Spanier E. Small size in the common bottlenose dolphin *Tursiops truncatus* in the eastern Mediterranean: a possible case of Levantine nanism. Mar Ecol Prog Ser. 2011;438:241–51. https://doi.org/10.3354/meps09282
10. Alba P, Caprioli A, Cocumelli C, Ianzano A, Donati V, Scholl F, et al. A new multilocus sequence typing scheme and its application for the characterization of *Photobacterium damselae* subsp. *damselae* associated with mortality in cetaceans. Front Microbiol. 2016;7:1656. https://doi.org/10.3389/fmicb.2016.01656
11. Casalone C, Mazzariol S, Pautasso A, Di Guardo G, Di Nocera F, Lucifora G, et al. Cetacean strandings in Italy: an unusual mortality event along the Tyrrhenian Sea coast in 2013. Dis Aquat Organ. 2014;109:81–6. https://doi.org/10.3354/dao02726
12. Osorio CR, Romalde JL, Barja JL, Toranzo AE. Presence of phospholipase-D (*dly*) gene coding for damselysin production is not a pre-requisite for pathogenicity in *Photobacterium damselae* subsp. *damselae*. Microb Pathog. 2000;28:119–26. https://doi.org/10.1006/mpat.1999.0330

Address for correspondence: Danny Morick, Morris Kahn Marine Research Station, University of Haifa, Haifa 3498838, Israel; email: dmorick@univ.haifa.ac.il

Early Warning Surveillance for SARS-CoV-2 Omicron Variants, United Kingdom, November 2021–September 2022

Sarah Foulkes,[1] Edward J.M. Monk,[1] Dominic Sparkes, Nipunadi Hettiarachchi, Iain D. Milligan, Katie Munro, Andrew Taylor-Kerr, Naomi Platt, Anna Howells, Jerry Ye Aung Kyaw, Enemona Adaji, Eileen Gallagher, Jameel Khawam, Edgar Wellington, Lesley Price, David Crossman, Chris Norman, Elen de Lacy, Lisa Cromey, Diane Corrigan, Angie Lackenby, Paola Barbero, Busayo Elegunde, Maria Zambon, Meera A. Chand, Colin S. Brown, Jasmin Islam, Ana Atti, Susan Hopkins, Victoria J. Hall,[2] Michelle J. Cole[2]; the SIREN Study Group[3]

Since June 2020, the SARS-CoV-2 Immunity and Reinfection Evaluation (SIREN) study has conducted routine PCR testing in UK healthcare workers and sequenced PCR-positive samples. SIREN detected increases in infections and reinfections and detected Omicron subvariant emergence contemporaneous with national surveillance. SIREN methodology can be used for variant surveillance.

Since June 2020, the SARS-CoV-2 Immunity and Reinfection Evaluation (SIREN) Study has detected and investigated SARS-CoV-2 reinfections in the United Kingdom; after vaccine rollout, SIREN was adapted to monitor vaccine effectiveness (*1*–*5*). As the United Kingdom, like other countries, adapts to the postacute phase of the pandemic and reduced testing availability (*6*,*7*), SIREN has an ongoing function in national surveillance. SIREN informs the UK pandemic response by real-time monitoring of emerging variants and determining national rates of primary infection and reinfection. We describe SIREN's surveillance strategy and characterize emergence of Omicron subvariants during successive waves within the study.

Author affiliations: UK Health Security Agency, London, UK (S. Foulkes, E.J.M. Monk, D. Sparkes, N. Hettiarachchi, I.D. Milligan, K. Munro, A. Taylor-Kerr, N. Platt, A. Howells, J. Ye Aung Kyaw, E. Adaji, E. Gallagher, J. Khawam, E. Wellington, A. Lackenby, P. Barbero, B. Elegunde, M. Zambon, M.A. Chand, C.S. Brown, J. Islam, A. Atti, S. Hopkins, V. Hall, M.J. Cole); Royal Free London NHS Foundation Trust, London (I.D. Milligan); Glasgow Caledonian University, Glasgow, Scotland, UK (L. Price); Public Health Scotland Glasgow Office, Glasgow (L. Price); University of St. Andrews, St. Andrews, Scotland, UK (D. Crossman); Health and Care Research Wales, Cardiff, Wales, UK (C. Norman); Public Health Wales, Cardiff (E. de Lacy); Public Health Agency Northern Ireland, Belfast, Northern Ireland, UK (L. Cromey, D. Corrigan); Guy's and St. Thomas' NHS Foundation Trust, London (M.A. Chand); Royal Free Hospital, London (C.S. Brown); National Institute for Health Research Health Protection Research Unit in Healthcare Associated Infections and Antimicrobial Resistance, London (S. Hopkins, V.J. Hall)

DOI: https://doi.org/10.3201/eid2901.221293

The Study

SIREN is a large, multicenter, prospective cohort study of >44,000 UK healthcare workers from 135 secondary care health organizations. SIREN is led by the UK Health Security Agency in collaboration with Public Health Wales, Public Health Scotland, and the Public Health Agency Northern Ireland (*1*). Participants were initially followed for 12 months and had an option to extend to 24 months. Participants completed an initial enrollment survey regarding demographic and occupational data, then completed follow-up surveys every other week regarding symptoms, vaccination status, and occupational, household, and community SARS-CoV-2 exposures. Participants underwent PCR testing every 2 weeks and serologic testing monthly for the first

[1]These first authors contributed equally to this article.

[2]These authors contributed equally to this article.

[3]Additional SIREN Study Group members are listed at the end of this article.

12 months, then had quarterly serologic testing. We confirmed vaccination status through linkage to personal identifiable information in national vaccination registries (*1*). This study was approved the Berkshire Research Ethics Committee (approval no. IRAS ID 284460, REC reference no. 20/SC/0230) on May 22, 2020; the vaccine amendment was approved on January 12, 2021 (study registration no. ISRCTN11041050).

SIREN samples were processed according to local protocols. Data from sites were supplied through the national laboratory reporting systems and obtained through linkage to personal identifiers. SARS-CoV-2 testing records for all participants, including symptomatic PCR testing outside SIREN's protocol, were stored in the SIREN database (*1*).

When RNA load was sufficient, local SIREN teams referred PCR-positive samples for sequencing (*1*). An additional self-swab kit for centralized PCR testing and sequencing at the national reference laboratory in London was initially mailed to participants who had a new infection and a history of SARS-CoV-2 primary infection or COVID-19 vaccination. Since spring 2021, participants with a positive PCR, irrespective of previous infection and vaccination status, were mailed an additional self-swab kit when available, which maximized the opportunity to improve sequencing yields.

We defined primary infection as a PCR-positive test from a participant without laboratory evidence of prior infection, such as a positive PCR test or antibody positivity before first vaccination (*1*). We defined reinfection as 2 PCR-positive tests separated by ≥90 days; or before a participant was vaccinated, a PCR-positive test ≥28 days after first SARS-CoV-2 IgG detection.

Since June 2020, SIREN monthly infection rates show 6 distinct infection waves (Figure 1). These waves corresponded with wild-type SARS-CoV-2 and subsequent emergence of Alpha variant; Delta variant; and Omicron BA.1, BA.2, and BA.4/BA.5 subvariants. Those waves are consistent with national surveillance trends (*8*).

Infection rates during Omicron BA.1 and BA.2 subvariant dominance surpassed those observed in any previous wave (Figure 1). This dominance was most apparent for reinfection rates, which exceeded primary infection rates for the first time in December 2021 and peaked at 94.2 reinfections/1,000 participants tested in January 2022 (Figure 1). The study cohort was well characterized and highly vaccinated and had high rates of prior infections. Thus, SIREN data suggest infection-acquired and vaccine-acquired immunity were less protective against Omicron BA.1 subvariant infection.

Since May 2022, we have detected a sixth wave of SARS-CoV-2 infections in the SIREN cohort, and rates continue to increase across the United Kingdom. These findings coincide with emergence of newer Omicron BA.4 and BA.5 subvariants (*8*). In contrast to the first wave of Omicron BA.1 variant infections, rates of reinfections remain considerably lower than primary infections, likely because protection improved after BA.1 and BA.2 infections and vaccination.

During March 3, 2020–September 30, 2022, SIREN recorded 18,319 participant infection episodes, of which 5,261 (28.7%) had valid sequence and infection data available, comprising 4,085 primary infections and 1,1176 reinfections. Our sequence yield was comparable to other studies (*8*,*9*), but we continue to expand data linkage and sample flows to improve data completeness.

SIREN sequencing identified several SARS-CoV-2 variants (Figure 2). Before Omicron subvariants emerged, 1,969 sequences with linked infection episode data were available: 521 unclassified/wild-type, 323 Alpha variant, 1,042 Delta variant, and 83

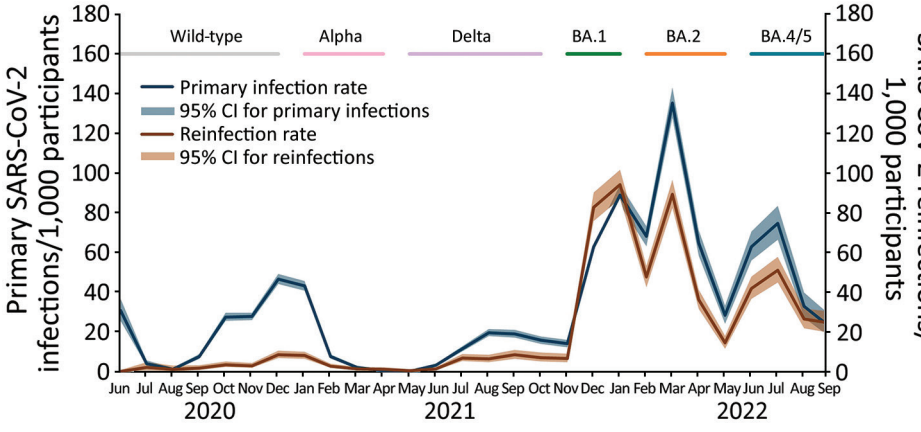

Figure 1. Rate of SARS-CoV-2 infections and reinfections detected through SIREN early warning system, United Kingdom, June 2020–September 2022. The SIREN study tested healthcare workers every 2 weeks via PCR and sequenced PCR-positive samples. We considered primary infection as infections among participants without prior infection and reinfections as infections among persons with prior infection. SIREN, SARS-CoV-2 Immunity and Reinfection.

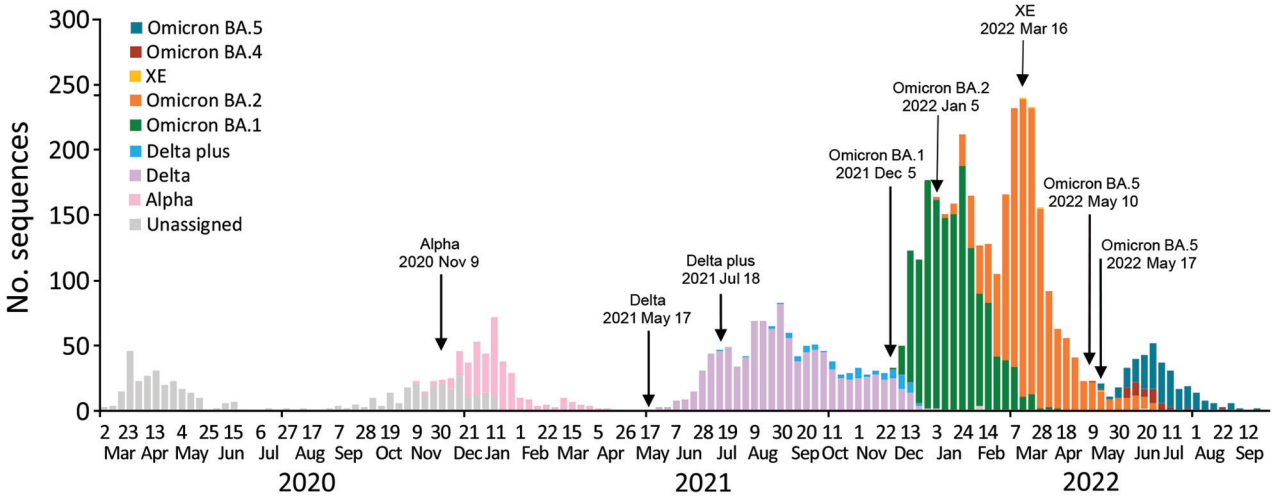

Figure 2. Number of sequenced samples by variant per week in SIREN early warning system, United Kingdom, March 2020–June 2022. The SIREN study tested healthcare workers every 2 weeks via PCR and sequenced PCR-positive samples. We have plotted all samples successfully sequenced and assigned a variant call or unclassified lineage. Dates of detection are noted for each variant. Of note, among >44,000 UK healthcare workers from 135 secondary care health organizations, we detected 521 cases of unclassified variants, 323 cases of Alpha, 1,042 cases of Delta, 83 cases of Delta plus, 1,487 cases of Omicron BA.1, 1,514 cases of Omicron BA.2, 4 cases of XE, 51 cases of Omicron BA.4, and 236 cases of Omicron BA.5. SIREN, SARS-CoV-2 Immunity and Reinfection.

Delta plus subvariant. Among these sequences, 8.3% (164/1,969) were reinfections and 91.7% (1,805/1,969) were primary infections.

The Omicron BA.1 subvariant was detected in SIREN on December 5, 2021, and 1,487 cases were detected by September 30, 2022; of those, 31.0% were reinfections. Omicron BA.2 was detected during January 5–September 30, 2022, and caused 1,514 cases, 27.3% of which were reinfections. Since March 2022, other Omicron subvariants have been identified within SIREN. The XE BA.1/BA.2 recombinant was detected from 4 primary infections on March 16, 2022. The BA.4 subvariant (25 primary infections and 26 reinfections) was detected on May 10, 2022, and the BA.5 subvariant (126 primary infections and 110 reinfections) was detected on May 17, 2022. Except for 4 XE cases, initial detection dates for Omicron subvariants within SIREN were an average of 16 days later than the Office for National Statistics (ONS) (*10*) and 27 days later than national surveillance (*8*). ONS detected BA.1 on November 29, 2021, national surveillance detected it November 3, 2021; ONS detected BA.2 on January 3, 2022, national surveillance detected it December 19, 2021; ONS detected BA.4 on April 4, 2022, national surveillance detected it April 12, 2022; and ONS detected BA.5 April 18, 2022, national surveillance detected it April 17, 2022 (*8*,*10*). We consider SIREN dates comparable with national surveillance data, which also contains sequence data from travelers and focused variant detection exercises.

Conclusions

Established early in the COVID-19 pandemic, SIREN has monitored infection trends and emerging variants for >2 years, directly informing the United Kingdom's national response (*2*–*4*), and contributing to Variant Technical Group briefings and government reports (*8*,*11*). After 4 successive variant waves with similar reinfection profiles, SIREN data showed that Omicron BA.1 and BA.2 subvariants emerged and caused a rapid rise in primary infection and reinfection rates among SIREN participants, regardless of vaccination status. Each subsequent Omicron subvariant was detected within a similar timeframe to national data (*8*), authenticating SIREN's use as a robust and representative surveillance tool.

The SIREN study population represents a highly exposed group who also have contact with vulnerable patients. In the absence of universal symptomatic PCR testing, SIREN provides a sustainable, focused, objective-driven sentinel surveillance platform and access to key epidemiologic variables, such as symptom severity. Although our cohort of predominantly healthy, working age, highly vaccinated adults are not representative of the general population, our study complements other national surveillance programs that target community and older populations (*10*,*12*). SIREN continues to improve its surveillance across a sentinel healthcare worker network in 135 national health organizations and support timely detection of infection

trends and emerging variants, keeping pace with other surveillance tools.

After a sixth wave of UK infections, concerns have grown around winter healthcare pressures combined with high rates of influenza observed in the Southern Hemisphere (*13*). Ongoing effective COVID-19 surveillance integrated with influenza and other respiratory pathogen surveillance is essential and achievable through SIREN's sentinel nature (*7*,*14*). SIREN will continue testing through March 31, 2023, and will continue to be a key asset in the UK surveillance strategy (*7*,*14*). The findings from SIREN can inform other countries' transitions from comprehensive surveillance to sentinel surveillance of key populations, such as healthcare workers.

The following additional members of the SIREN Study Group contributed data: Omoyeni Adebiyi, Nick Andrews, Tim Brooks, Davina Calbraith, Andre Charlett, Joanna Conneely, Paul Conneely, Silvia D'Arcangelo, Nabila Fowles-Gutierrez, Jacqueline Hewson, Kate Howell, Ferdinando Insalata, Robert Kyffin, Ezra Linley, Claire Neill, Anne-Marie O'Connell, Ashley Otter, Mary Ramsay, Cathy Rowe, Ayoub Saei, Noshin Sajedi, Amanda Semper, Jean Timeyin, Simon Tonge, Caio Tranquillini, Angela Dunne, Josie Evans, Nicole Sergenson, Jennifer Bishop, Jennifer Weir, Sally Stewart, Lynne Haahr, Laura Dobbie, Andrew Telfer, David Goldberg, Desy Nuryunarsih, Melanie Dembinsky, Desmond Areghan, Alexander Olaoye, Guy Stevens, Susannah Froude, Linda Tyson, Yvette Ellis, B. Larru, S. Mcwilliam, Anna Roynon, Sean Cutler, Stephen Winchester, Samuel Rowley, Stacey Pepper, Georgina Butt, Simantee Guha, Philippa Bakker, Clodagh Loughrey, A. Watt, Julia Roberts, Caroline Mulvaney Jones, Manny Bagary, Siobhan Keogh, Rebecca Chapman, Lucy Booth, Alison Grant, Rebecca Temple-Purcell, Joanne Howard, Emma Ward, Chinari Subudhi, Scott Latham, Lisa Barbour, Helena Sovriarova, N. Wong, R. Penn, A. Rajgopal, G. Boyd, Gosala Gopalakrishnan, Connor McAlpine, Amanda Whileman, Edward Harris, Joanna Ledger, Richard Laugharne, C. Jones, T. Barnes, Anna Rokakis, Banerjee SubhroOsuji, Carla Pothecary, John Geen, Nihil Chitalia, Tracy Edmunds, Sarah Creer, Joanna Wright, G. Harrison, S. Akhtar, Nicola Walker, Clare McAdam, V. Maxwell, K. Agwuh, Jennifer Graves, James Colton, Stephanie Willshaw, P. Ridley, A. O'Kelly, Janet Sinclair, Anna Cowley, Neringa Vilimiene, Helen Johnstone, Jane Democratis, Manjula Meda, David Boss, Simon Brake, Amanda Selassie, Rekha Plackal, Val Irvine, Catherine Sinclair, Badrinathan Chandrasekaran, Suzannah Pegler, Judith Radmore, Claire Thomas, Shivani Khan, Shekoo Mackay, Nicholas Easom, Philippa Burns, Zohra Omar, Tracy Lewis, Kenisha Lewis, Graham Pickard, Alison Brown, Sarah Hinch, Christian Hacon, Ben Burton, Jonnie Aeron-Thomas, Ray Chaudhuri, Kathryn Hollinshead, Robert Shorten, Mathew Anuj, Clair Favager, Kyra Holliday, Joanne Edgar, Sarah Baillon, J. Russell, A. Shah, Ananta Dave, Kelly Moran, Fran Westwell, Anu Chawla, David Adeboyeku, Ekaterina Watson, M. Williams, C. Pegg, A. Horsley, S. Ahmad, Diego Maseda, Murray Luckas, Yvonne Lester, Lauren Sach, John Ashcroft, Ismaelette Del Rosario, Chloe Reeks, Roxanne Crosby-Nwaobi, Lauren Finlayson, Joy Dawson, Devesh Dhasmana, Susan Fowler, Anne Todd, Euan Cameron, Harriet Carroll, Alison Thornton, Michael Murphy, Antonia Ho, Alexandra Cochrane, Lita Kovina, Karen Black, Manish Patel, Corrienne McCulloch, Kate Templeton, Joan Frieslick, Martin Malcolm, Louise Coke, Ngozi Elumogo, John Elliott, Beverly Wilkinson, Pratap Harbham, Mariyam Mirfenderesky, Stephanie Diaz, Janki Bhayani, T. Lewis, M Howard, Frances Johnston, Elinor Hanna, Peter Cowling, Jonathan Hatton, Imogen Gould, Sarah Brand, Charlotte Humphrey, Judith Dube, Kate Burrows, Johanna Mouland, Chris Norman, Jayne Goodwin, G. Pottinger, J. Giles, Holly Coles, Maya Joseph, D. Browne, H. Chenoweth, Stephanie Prince, Cressida Auckland, Tabitha Mahungu, Alison Rodger, Simon Warren, Esther Hanison, Helen Baxendale, Sumita Pai, Sarah Stone, Charles Piercy, Sarah Meisner, Debbie Delgado, Lehentha Mattocks, Vicky King, James Pethick, Ashok Dadrah, C. Kerrison, S. Gormley, Simon Tazzyman, Thushan de Silva, Shrikant Ambalkar, Lynne Allsop, Mandy Carnahan, Mandy Beekes, Johanne Tomlinson, Cathy Price, Kate James, Justin Pepperell, Tom Trinick, Yuri Protaschik, Raji Orath Prabakaran, Viji George, Fiona Thompson, Angel Boulos, Alice Neave, Ellene Thompson, Kerryanne Brown, Katherine Gray, Angela Houston, Tim Planche, Diane Wycherley, Rowan Pritchard Jones, Barzo Faris, B. Stewart, K. Nimako, Rebeccah Thomas, Claire Stafford, Nagesh Kalakonda, Sheena Khanduri, Helen Ashby, Natasha Mahabir, B. Payne, J. Harwood, Nikki White, Kathryn Court, Ruth Longfellow, Mihye Lee, Lauren Hughes, Marie Green, Pauline Mercer, Mathew Halkes, , Alun Roebuck, E. Wilson-Davies, Aaran Sinclair, Rajeka Lazarus, L. Berry, N. Aldridge, T. Reynolds, F. Game, Martin Wiselka, Christopher Holmes, Cristina Dragu, Therese Kelly, Joanne Gray, Christopher Duff, Penny Harris, Hannah Jory, James Powell, Charlotte Young, Aiden Plant, Lisa Richardson, Lisa Ditchfield, Zaman Qazzafi, R. Tilley, A. Moody, Maurice O'Kane, Tracy Donaghy, K. Shipman, R. Sierra, Zehra'a Al-Khafaji, Philippa Kemsley, Y. Huang, D. Harvey, L. Robinson, Sarah Board, Andrew Broadley, Claire Brookes, and Mags Szewczyk; and the Solent Research Team and the United Lincolnshire Hospitals NHS Trust Research Team.

Acknowledgments

We thank all the participants for their ongoing contributions and commitment to this study; all the research and laboratory teams for their hard work and support at all 135 sites and for making the study possible; colleagues at the UK Health Security Agency, Colindale, for processing all the self-swab PCRs and performing the sequencing; and those throughout the United Kingdom who have contributed to collation and analysis of the sequencing data.

This work was supported by the UK Health Security Agency; the UK Department of Health and Social Care with contributions from the governments in Northern Ireland, Wales, and Scotland; the National Institute for Health Research; and grants from the Medical Research Council (grant nos. NIHR200927 and MR/W02067X/1).

About the Author

Ms. Foulkes is the principal scientist for the SIREN Study at the UK Health Security Agency, London, England, UK. Her primary research interests are COVID-19 surveillance and field epidemiology. Dr. Monk is a SIREN clinical research fellow at the UK Health Security Agency, London. His primary research interests are emerging infectious disease dynamics, surveillance, and prevention.

References

1. Wallace S, Hall V, Charlett A, Kirwan PD, Cole M, Gillson N, et al. Impact of prior SARS-CoV-2 infection and COVID-19 vaccination on the subsequent incidence of COVID-19: a multicentre prospective cohort study among UK healthcare workers—the SIREN (Sarscov2 Immunity & REinfection EvaluatioN) study protocol. BMJ Open. 2022;12:e054336. https://doi.org/10.1136/bmjopen-2021-054336
2. Hall VJ, Foulkes S, Charlett A, Atti A, Monk EJM, Simmons R, et al.; SIREN Study Group. SARS-CoV-2 infection rates of antibody-positive compared with antibody-negative health-care workers in England: a large, multicentre, prospective cohort study (SIREN). Lancet. 2021;397:1459–69. https://doi.org/10.1016/S0140-6736(21)00675-9
3. Hall VJ, Foulkes S, Saei A, Andrews N, Oguti B, Charlett A, et al.; SIREN Study Group. COVID-19 vaccine coverage in health-care workers in England and effectiveness of BNT162b2 mRNA vaccine against infection (SIREN): a prospective, multicentre, cohort study. Lancet. 2021;397:1725–35. https://doi.org/10.1016/S0140-6736(21)00790-X
4. Hall V, Foulkes S, Insalata F, Kirwan P, Saei A, Atti A, et al.; SIREN Study Group. Protection against SARS-CoV-2 after Covid-19 vaccination and previous infection. N Engl J Med. 2022;386:1207–20. https://doi.org/10.1056/NEJMoa2118691
5. Atti A, Ferrari M, Castillo-Olivares J, Monk EJM, Gopal R, Patel M, et al. Serological profile of first SARS-CoV-2 reinfection cases detected within the SIREN study. J Infect. 2022;84:248–88. https://doi.org/10.1016/j.jinf.2021.09.019
6. Cabinet Office. COVID-19 response: living with COVID-19. 2022 May 06 [cited 2022 Jul 14]. https://www.gov.uk/government/publications/covid-19-response-living-with-covid-19
7. Suk JE, Pharris A, Beauté J, Colzani E, Needham H, Kinsman J, et al. Public health considerations for transitioning beyond the acute phase of the COVID-19 pandemic in the EU/EEA. Euro Surveill. 2022;27:2200155. https://doi.org/10.2807/1560-7917.ES.2022.27.17.2200155
8. UK Health Security Agency. SARS-CoV-2 variants of concern and variants under investigation in England; technical briefing 42; 20 May 2022 [cited 2022 Jul 14]. https://assets.publishing.service.gov.uk/government/uploads/system/uploads/attachment_data/file/1103534/Technical-Briefing-42-20May2022.pdf
9. European Centre for Disease Prevention and Control. Country overview report [cited 2022 Jul 22]. https://www.ecdc.europa.eu/en/covid-19/country-overviews
10. Office for National Statistics. Coronavirus (COVID-19) infection survey: technical data [cited 2022 Jul 22]. https://www.ons.gov.uk/peoplepopulationandcommunity/healthandsocialcare/conditionsanddiseases/datasets/covid19infectionsurveytechnicaldata
11. UK Health Security Agency. SIREN study. 2022 Jun 21 [cited 2022 Jul 14]. https://www.gov.uk/guidance/siren-study
12. Krutikov M, Palmer T, Donaldson A, Lorencatto F, Forbes G, Copas A, et al. Study protocol: understanding SARS-Cov-2 infection, immunity and its duration in care home residents and staff in England (VIVALDI). Wellcome Open Res. 2021;5:232. https://doi.org/10.12688/wellcomeopenres.16193.2
13. Australian Government Department of Health. Australian influenza surveillance report no. 6; 2022 Jun 19 [cited 2022 Jul 14]. https://www1.health.gov.au/internet/main/publishing.nsf/Content/828055131E7175CCCA25886B001C60FC/$File/flu-06-2022.pdf
14. European Centre for Disease Prevention and Control. COVID-19 surveillance guidance. 2021 Oct 1 [cited 2022 Jul 14]. https://www.ecdc.europa.eu/sites/default/files/documents/COVID-19-surveillance-guidance.pdf

Corresponding author: Michelle Cole, UK Health Security Agency, 61 Colindale Ave, London NW9 5HT, UK; email: michelle.cole@ukhsa.gov.uk

Efficient Inactivation of Monkeypox Virus by World Health Organization–Recommended Hand Rub Formulations and Alcohols

Toni L. Meister, Ronny Tao, Yannick Brüggemann, Daniel Todt, Joerg Steinmann, Joerg Timm, Ingo Drexler, Eike Steinmann

Increasing nonzoonotic human monkeypox virus (MPXV) infections urge reevaluation of inactivation strategies. We demonstrate efficient inactivation of MPXV by 2 World Health Organization–recommended alcohol-based hand rub solutions. When compared with other (re)emerging enveloped viruses, MPXV displayed the greatest stability. Our results support rigorous adherence to use of alcohol-based disinfectants.

The global spread of human monkeypox virus (MPXV) has activated the highest alert level of the World Health Organization (WHO), which declared the virus a public health emergency of international concern (*1*). MPXV is spreading among persons who have not traveled to disease-endemic areas (*2*). The associated novel clinical and epidemiologic patterns necessitate comprehensive investigations, including (re)evaluation of hygiene measures for preventing MPXV transmission. Given the remarkable stability of other pox viruses compared with other enveloped viruses, it is particularly useful to confirm which disinfectants and biocidal agents can inactivate MPXV (*3*). Moreover, in addition to direct contact with infected body fluids or lesions or respiratory secretions, MPXV can be transmitted indirectly through contaminated surfaces (fomites) (*4*). Hygienic hand antisepsis is one of the most useful measures in preventing healthcare- and outbreak-associated viral infections.

In 2009, the WHO proposed Guidelines on Hand Hygiene in Health Care, a document to implement use of 2 alcohol-based hand rubs (formulation I and II) for surgical and hygiene hand disinfection in healthcare settings and to reduce transmission of pathogens (*5*). However, inactivation efficacies of these products against MPVX have not been determined. We evaluated the WHO-recommended alcohol-based formulations against MPXV and performed a comparative inactivation analysis with other (re)emerging enveloped and reference viruses, including Zika virus, influenza A(H1N1) virus, Ebola virus, severe acute respiratory syndrome coronaviruses 1 and 2, and Middle East respiratory syndrome coronavirus.

The Study

We cultured Vero 76 cells in Dulbecco modified Eagle medium supplemented with 10% (vol/vol) fetal calf serum, 1% (vol/vol) nonessential amino acids, 100 IU/mL penicillin, 100 μg/mL streptomycin, and 2 mmol/L l-glutamine. For preparation of MPXV, we seeded cells at a concentration of 0.33×10^6 cells/mL in a 75-cm^2 flask in a total volume of 12 mL. The next day, the medium was changed and cells were inoculated with MPXV at a multiplicity of infection of 0.01 and incubated at 37°C until a visible cytopathic effect occurred. Infected cells were harvested by scraping, subjected to 3 freeze/thaw cycles, extensively vortexed and, together with the infectious supernatant purified from cell debris by subsequent centrifugation for 5 min at 1,500 rpm. The virus suspensions were aliquoted, titrated according to standard methods, and stored at −80°C until further use. Virus isolate MPXV-DUS_001 was originally obtained

Author affiliations: Ruhr University Bochum, Bochum, Germany (T.L. Meister, Y. Brüggemann, D. Todt, E. Steinmann); Heinrich-Heine-University, Düsseldorf, Germany (R. Tao, J. Timm, I. Drexler); European Virus Bioinformatics Center, Jena, Germany (D. Todt); Paracelsus Medical University, Nuremberg, Germany (J. Steinmann); University Hospital of Essen, Essen, Germany (J. Steinmann)

DOI: https://doi.org/10.3201/eid2901.221429

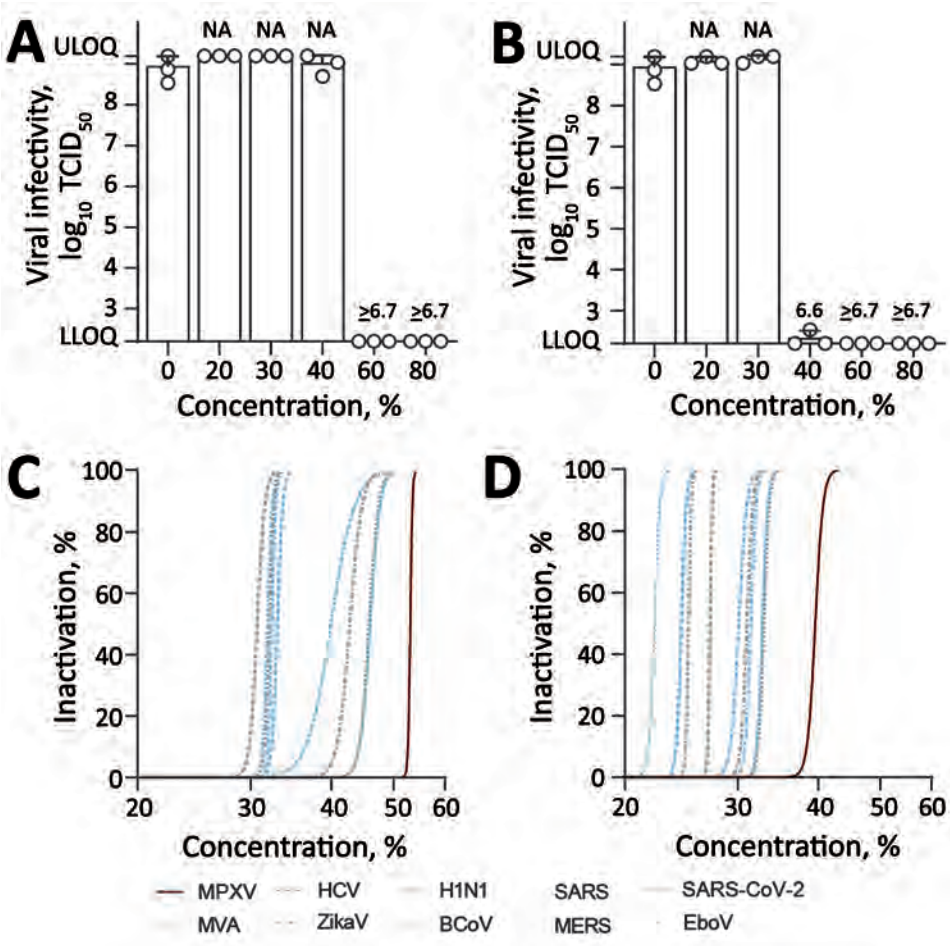

Figure 1. Virucidal activity of World Health Organization (WHO)–recommended hand rub formulations I and II for inactivating MPXV. A, B) Viral infectivity for WHO formulation I (A) and formulation II (B). Means of 3 independent experiments with SDs (error bars) and reduction factors (numbers above the bar) are shown. C, D) Regression analyses of inactivation of MPXV and (re)emerging enveloped or reference viruses, including ZIKV, EBOV, SARS-CoV, SARS-CoV-2, MERS-CoV, influenza A(H1N1) virus, BCoV, HCV, and MVA for WHO formulation I (C) and WHO formulation II (D). Dilutions of the WHO formulations ranging from 0% to 80% with an exposure time of 30 s. Viral titers are displayed as $TCID_{50}$/mL. BCoV, bovine coronavirus; EBOV, Ebola virus; HCV, hepatitis C virus; MERS-CoV, Middle East respiratory syndrome coronavirus; LLOQ, lower limit of quantification (1.58×10^2 $TCID_{50}$/mL); MPXV, monkeypox virus; MVA, modified vaccinia Ankara; NA, not applicable; SARS-CoV2, severe acute respiratory syndrome coronavirus 2; $TCID_{50}$, 50% tissue culture infectious dose; ULOQ, upper limit of quantification (1.58×10^9 $TCID_{50}$/mL); ZIKV, Zika virus.

from a patient in Düsseldorf, Germany, who has been infected early during the outbreak 2022, and the isolate was passaged twice on Vero 76 cells before experimental use.

We confirmed the presence of MPXV by a 2-step, quantitative, real-time reverse transcription PCR (qRT-PCR). The first step determines the presence of orthopoxvirus-specific DNA by using panorthopoxvirus□specific qRT-PCR, and the second step detects and differentiates MPXV clade I (former Congo Basin) and II (former West African) by using an MPXV-specific qRT-PCR. Isolate MPXV-DUS_001 was classified as MPXV clade II.

We assessed virucidal activity of WHO formulation I and II, as well as ethanol and 2-propanol, based on European guideline EN14476 as described (*6*). In brief, we mixed 8 parts of disinfectant with 1 part of interfering substance (bovine serum albumin, final concentration 0.3 g/L) and 1 part MPXV, then vortexed the suspension and incubated for 30 s at room temperature. We then performed an endpoint dilution assay on Vero 76 cells. After 7 days, we evaluated cytopathic effects microscopically and calculated the 50% tissue culture infectious dose per milliliter (Appendix, https://wwwnc.cdc.gov/EID/article/29/1/22-1429-App1.pdf). We tested all 4 disinfectants for final concentrations of 20%, 30%, 40%, 60%. and 80%.

We examined the virucidal activity of the WHO formulations I and II against MPXV by using a quantitative suspension test. MPXV was highly susceptible to both formulations (Figure 1). The WHO formulation I, based on 80% ethanol (vol/vol), efficiently inactivated the virus with reduction factors (RFs) ≥6.7 at concentrations of 60% and 80% (vol/vol) (Figure 1, panel A). Likewise, the WHO formulation II, based on 75% isopropanol (vol/vol), inactivated the virus with RFs ≥6.7 at concentrations of 60% and 80% (vol/vol) (Figure 1, panel B). A dilution of 40% (vol/vol) was still effective for the WHO formulation II with a RF of 6.6, whereas we observed no reduction in viral titer for WHO formulation I at a similar concentration. Subsequent regression analysis of both WHO formulations enabled a quantitative comparison of

MPXV inactivation with different other (re)emerging enveloped or reference viruses (Figure 2, panels C, D). Among all viruses, including its reference virus modified vaccinia Ankara, MPXV showed the highest stability against both tested WHO formulations.

Next, we examined the susceptibility of MPXV against the individual components (ethanol and 2-propanol) of both WHO formulations, which are also the main ingredients of numerous commercially available hand disinfections. Both ethanol (Figure 2, panel A) and 2-propanol (Figure 2, panel B) reduced viral titers to background levels with RFs ≥6.7 at concentrations ≥60% and ≥40% (vol/vol), respectively. A minimal concentration of 40% ethanol (vol/vol) nearly inactivated the virus completely (RF 6.6). For 2-propanol, a virucidal activity was observed at a minimal concentration of 30% (vol/vol) with a RF of 5.3.

Overall, both WHO formulations efficiently inactivated MPXV, but the 2-propanol–based WHO formulation II showed a slightly greater virucidal activity than the ethanol-based WHO formulation I. Nonetheless, MPXV showed the greatest stability to both formulations compared with other (re)emerging enveloped or reference viruses.

Conclusions

Poxvirus virions are known for their long-term environmental persistence (*3*,*7*). For example, infectious MPXV was recently reported to persist in a household environment for ≥15 days (*8*). Moreover, because of tight binding with fibrin matrixes of scab/crust material, virions shed from infectious lesion material are even more resistant to desiccation than other enveloped viruses (e.g., influenza virus, rubella virus) (*8*–*10*). Considering the high stability of other poxvirus virions, it is probable that MPXV will share this characteristic, requiring a comprehensive reevaluation of current hygiene measures.

Poxvirus virions are known for their long-term environmental persistence (*3*,*7*). For example, infectious MPXV was recently reported to persist in a household environment for ≥15 days (*8*). Moreover, because of tight binding with fibrin matrixes of scab/crust material, virions shed from infectious lesion material are even more resistant to desiccation than other enveloped viruses (e.g., influenza virus, rubella virus) (*8*–*10*). Considering the high stability of other poxvirus virions, it is probable that MPXV will share this characteristic, requiring a comprehensive reevaluation of current hygiene measures. The WHO recommends 2 inexpensive alcohol-based hand rub formulations to reduce the transmission of pathogens (*5*). We found that MPXV was efficiently inactivated by both formulations, supporting their use in healthcare systems and during MPXV outbreaks.

In addition, ethanol and 2-propanol inactivated the virus in during a 30-s exposure at a concentration of >30% (vol/vol). A comparative inactivation analyses with different (re)emerging enveloped or reference viruses showed that MPXV had the highest stability against both WHO formulations compared with other enveloped viruses. The susceptibility of the different viruses to the WHO formulations probably depends on virus-specific surface properties of their lipophilic envelope. Nonetheless, our results confirm modified vaccinia Ankara as a suitable model surrogate for MPXV to evaluate chemical disinfectants and antiseptics (*11*). WHO formulation II and 2-propanol were slightly more efficient in inactivating MPXV compared with WHO formulation I and ethanol. This difference can probably be explained by the additional carbon of 2-propanol, resulting in an enhanced lipophilicity against the viral membranes compared with ethanol (*12*). Our findings underscore the need and timely application of alcohol-based disinfectants as an effective measure for minimizing viral transmission and maximizing viral inactivation during the ongoing MPVX outbreak.

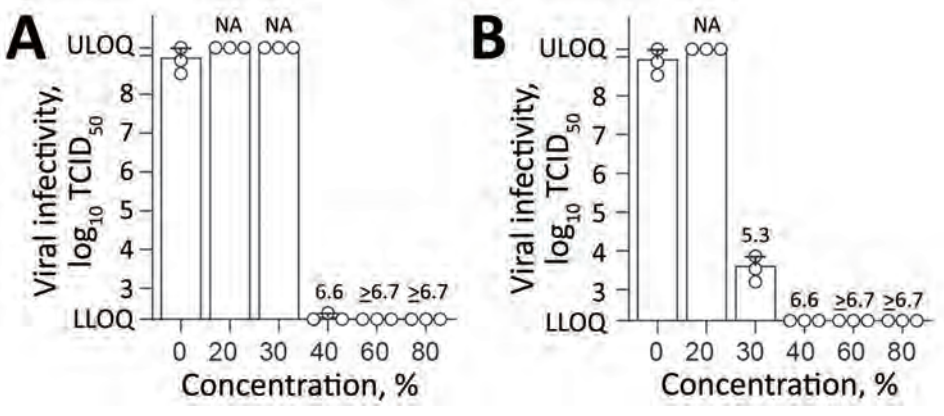

Figure 2. Effect of commercially available alcohols in inactivating monkeypox virus. A) Results for ethanol. B) Results for 2-propanol. Means of 3 independent experiments with SDs (error bars) are shown. Reduction factors are included above the bars. Biocide concentrations ranged from 0% to 80% with an exposure time of 30 s. Viral titers are displayed as $TCID_{50}$/mL values. LLOQ, lower limit of quantification (1.58×10^2 $TCID_{50}$/mL); NA, not applicable; $TCID_{50}$, 50% tissue culture infectious dose; ULOQ, upper limit of quantification (1.58×10^9 $TCID_{50}$/mL).

Acknowledgments

We thank the members of the Department for Molecular and Medical Virology, Ruhr University Bochum, Bochum, Germany for helpful suggestions and discussions.

This study was supported by the VIRus ALlianz (VIRAL) of North Rhine-Westphalia, Ministry of Culture and Science of the State of North Rhine-Westphalia (grant 323-8.03-151826). D.T. is supported by the German Federal Ministry of Education and Research (project VirBio, grant 01KI2106).

About the Author

Dr. Meister is a postdoctoral research scientist in the Department for Molecular and Medical Virology, Ruhr University Bochum, Bochum, Germany. Her primary research interests are coronavirus, hepatitis E virus, and MPVX.

References

1. World Health Organization. WHO Director-General declares the ongoing monkeypox outbreak a public health emergency of international concern [cited 2022 Nov 9]. https://www.who.int/europe/news/item/23-07-2022-who-director-general-declares-the-ongoing-monkeypox-outbreak-a-public-health-event-of-international-concern
2. World Health Organization. Multi-country monkeypox outbreak in non-endemic countries: update [2022 Nov 9]. https://www.who.int/emergencies/disease-outbreak-news/item/2022-DON388
3. Wißmann JE, Kirchhoff L, Brüggemann Y, Todt D, Steinmann J, Steinmann E. Persistence of pathogens on inanimate surfaces: a narrative review. Microorganisms. 2021;9:343. https://doi.org/10.3390/microorganisms9020343
4. Brown K, Leggat PA. Human monkeypox: current state of knowledge and implications for the future. Trop Med Infect Dis. 2016;1:E8. https://doi.org/10.3390/tropicalmed1010008
5. World Health Organization. WHO guidelines on hand hygiene in health care: first global patient safety challenge clean care is safer care. Geneva: The Organization; 2009.
6. Kratzel A, Todt D, V'kovski P, Steiner S, Gultom M, Thao TT, et al. Inactivation of severe acute respiratory syndrome coronavirus 2 by WHO-recommended hand rub formulations and alcohols. Emerg Infect Dis. 2020;26:1592–5. https://doi.org/10.3201/eid2607.200915
7. Kampf G. Efficacy of heat against the vaccinia virus, variola virus and monkeypox virus. J Hosp Infect. 2022;127:131–2. https://doi.org/10.1016/j.jhin.2022.06.008
8. Morgan CN, Whitehill F, Doty JB, Schulte J, Matheny A, Stringer J, et al. Environmental persistence of monkeypox virus on surfaces in household of person with travel-associated infection, Dallas, Texas, USA, 2021. Emerg Infect Dis. 2022;28:1982–9. https://doi.org/10.3201/eid2810.221047
9. Nolen LD, Osadebe L, Katomba J, Likofata J, Mukadi D, Monroe B, et al. Introduction of monkeypox into a community and household: risk factors and zoonotic reservoirs in the Democratic Republic of the Congo. Am J Trop Med Hyg. 2015;93:410–5. https://doi.org/10.4269/ajtmh.15-0168
10. Hutson CL, Carroll DS, Gallardo-Romero N, Weiss S, Clemmons C, Hughes CM, et al. Monkeypox disease transmission in an experimental setting: prairie dog animal model. PLoS One. 2011;6:e28295. https://doi.org/10.1371/journal.pone.0028295
11. Rabenau HF, Rapp I, Steinmann J. Can vaccinia virus be replaced by MVA virus for testing virucidal activity of chemical disinfectants? BMC Infect Dis. 2010;10:185. https://doi.org/10.1186/1471-2334-10-185
12. Schürmann W, Eggers HJ. Antiviral activity of an alcoholic hand disinfectant. Comparison of the in vitro suspension test with in vivo experiments on hands, and on individual fingertips. Antiviral Res. 1983;3:25–41. https://doi.org/10.1016/0166-3542(83)90012-8

Address for correspondence: Eike Steinmann, Ruhr-University Bochum, Universitaetsstr. 150, 44801 Bochum, Germany; email: eike.steinmann@rub.de

Detection of Monkeypox Virus DNA in Airport Wastewater, Rome, Italy

Giuseppina La Rosa, Pamela Mancini, Carolina Veneri, Giusy Bonanno Ferraro, Luca Lucentini, Marcello Iaconelli, Elisabetta Suffredini

Environmental surveillance can be a complementary tool for detecting pathogens circulating in communities. We detected monkeypox virus DNA in wastewater from Italy's largest airport by using real-time PCR assays targeting the G2R region and *F3L* and *N3R* genes and sequencing. Wastewater surveillance can be quickly adapted to investigate emerging threats.

Monkeypox virus (MPXV), a member of the family *Poxviridae*, causes monkeypox, a viral zoonosis detected in north Africa in the 1970s (*1*). MPXV can be transmitted between humans through contact with lesions, body fluids, respiratory droplets, and contaminated materials (*1*).

In May 2022, an epidemic of monkeypox in nonendemic regions outside Africa began receiving worldwide attention. On July 23, 2022, the World Health Organization declared monkeypox a public health emergency of international concern (*2*), and 24,973 monkeypox cases had been recognized in 45 countries throughout Europe by October 12, 2022 (*3*).

Rapid identification of outbreaks and clusters is critical for infection control. Sewage surveillance has been recognized as a powerful tool for assessing the circulation of pathogens. After the European Union issued Recommendation 2021/472 (http://data.europa.eu/eli/reco/2021/472/oj), wastewater surveillance was successfully used to track SARS-CoV-2 and its variants across EU countries (*4*). Studies have demonstrated MPXV DNA sheds from saliva, feces, urine, semen, and skin lesions (*5*–*7*), suggesting that the viral genome could occur in wastewater. Various research groups involved in SARS-CoV-2 environmental surveillance extended their efforts to investigate MPXV DNA in wastewater. Studies from the Netherlands and western California, USA, have documented successful detection of MPXV DNA in sewage (*8*; M.K. Wolfe et al., unpub. data, https://doi.org/10.1101/2022.07.25.22278043). We investigated whether we could detect MPXV in wastewater in Italy.

Author affiliation: Istituto Superiore di Sanità, Rome, Italy

DOI: https://doi.org/10.3201/eid2901.221311

The Study

We targeted the wastewater treatment plant (WTP) of Italy's largest airport, Fiumicino Airport, in Rome, which had ≈3,000,000 passengers/month during May–July 2022 (https://fiumicinoairport.com/statistics). This WTP has a global capacity of 4,000 m^3 per day. We collected 24-hour composite wastewater samples twice a week during May 30–August 3, 2022, for a total of 20 samples.

Before viral concentration, we pretreated samples in a water bath at 56°C for 30 min to inactivate the virus and protect laboratory technicians, as per a previous study (*9*). We used a polyethylene glycol/sodium chloride precipitation protocol originally developed for SARS-CoV-2 environmental surveillance (*10*,*11*) but modified the protocol by increasing the initial wastewater volume to 90 mL (2 tubes of 45 mL) and eluting all the extracted nucleic acids in 50 μL of elution buffer supplied with the kit. We used NucliSens miniMAG (bioMérieux, https://www.biomerieux.com) semi-automatic extraction platform to extract nucleic acids. We used OneStep PCR Inhibitor Removal Kit (Zymo Research, https://www.zymoresearch.com) to purify DNA.

We used 3 different real-time PCR assays: 2 published in 2004 that target the *N3R* and *F3L* genes (*12*), and 1 developed in 2010 by the US Centers for Disease Control and Prevention, G2R_G generic real-time PCR assay (*13*), which targets the G2R region of the tumor necrosis factor receptor gene. After comparing primers and probes with sequences of the current outbreak, we noted mismatches in primers, probes, or both. Therefore, we designed and tested novel primers and probes that had 100% nucleotide identity with current outbreak sequences, then compared these with the original primers and probes (Table 1). We used MPXV (Slovenia ex Gran

Canaria) DNA (European Virus Archive Global [EVAg]; https://www.european-virus-archive.com) as a control for testing primers and probes (Appendix, https://wwwnc.cdc.gov/EID/article/29/1/22-1311-App1.pdf). We further optimized the assays by evaluating different real-time PCR reagents and primer/probe concentrations (Appendix). We prepared reaction mixes in 25 µL by using TaqPath BactoPure Microbial Detection Master Mix (Thermo Fisher Scientific, https://www.thermofisher.com), 800 mmol of each primer, 500 nmol of the probe, and 5 µL of sample. Amplification conditions included an initial activation step at 95°C for 2 min and 50 cycles of 10 s at 95°C and 30 s at 60°C. We included 10-fold dilutions of the standardized EVAg MPXV DNA (range 740–0.74 copies/µL) in the runs as positive controls and for the rough estimation of viral loads. For each assay, we assessed the limit of detection at 50% (LOD_{50}) on a pure target (i.e., EVAg MPXV DNA) and on MPXV DNA diluted in nucleic acids previously extracted from wastewater samples collected in Europe before monkeypox emerged.

We designed nested PCR assays targeting the same regions as the real-time PCR assays to confirm results by amplicon sequencing using Primer3Plus software

Table 1. Primers and probes used to detect monkeypox virus DNA in airport wastewater, Rome, Italy*

PCR ID	Target	Primer name	Primer ID	Sequence, 5′ → 3′	Position†	Annealing temp. (°C)	Amplicon size	Ref.
1002	G2R	MPVX G F	2368	GGAAAATGTAAAGACAACGAATACAG	194459–84	60	90 bp	(*12*)
		MPVX G R	2369	GCTATCACATAATCTGGAAGCGTA	194525–48			
		MPVX G P	2370	FAM-AAGCCGTAATCTATG TTGTCTATCGTGTCC-BHQ1	194485–514			
1005	G2R	MPVX G F mod	2377	GGAAA**G**TGTAAAGACAACGAATACAG	194459–84	60	90 bp	(*12*)
		MPVX G R mod	2378	GCTATCACATAATCTG**A**AAGCGTA	194525–48			This study
		MPVX G P	2370	FAM-AAGCCGTAATCTATG TTGTCTATCGTGTCC-BHQ1	194485–514			
1003	*F3L*	F3L-F290	2371	CTCATTGATTTTTCGCGGGATA	46313–34	60	107 bp	(*11*)
		F3L-R396	2372	GACGATACTCCTCCTCGTTGGT	46398–419			
		F3Lp333S-MGB	2373	FAM-CATCAGAATCTGTAGGCCGT-MGBNFQ	46398–419			
1008	*F3L*	F3L-F290	2371	CTCATTGATTTTTCGCGGGATA	46313–34	60	107 bp	(*11*)
		F3L-R396 mod	2384	**A**ACGATACTCCTCCTCGTTGGT	46398–419			This study
		F3Lp333S-MGB	2373	FAM-CATCAGAATCTGTAGGCCGT-MGBNFQ	46398–419			
1004	*N3R*	N3R-F319	2374	AACAACCGTCCTACAATTAAACAACA	190641–66	60	139 bp	(*11*)
		N3R-R457	2375	CGCTATCGAACCATTTTTGTAGTCT	190755–79			
		N3Rp352S-MGB	2376	FAM-TATAACGGCGAAGAATATACT-MGBNFQ	190674–94			
1016	*N3R*	N3R-F319	2374	AACAACCGTCCTACAATTAAACAACA	190641–66	60	139 bp	(*11*)
		N3R-R457	2375	CGCTATCGAACCATTTTTGTAGTCT	190755–79			This study
		N3Rp352S-MGB mod	2381	FAM-TATAACGGCGA**C**GAATATACT-MGBNFQ	190674–94			
1006	G2R	G2R-1st cycle F	2379	ATAGCACCACATGCACCATC	194435–54	63	156 bp	This study
		G2R-1st cycle R	2380	AAAGGTATCCGAACCACACG	194590–71			
1005	G2R	MPVX G F mod	2377	GGAAAGTGTAAAGACAACGAATACAG	194459–84	61	90 bp	This study
		MPVX G R mod	2378	GCTATCACATAATCTGAAAGCGTA	194525–48			
1009	*F3L*	F3L-1st cycle F	2385	CAGGGTTAACACCTTTCCAA	46242–61	61	212 bp	This study
		F3L-1st cycle R	2386	TGATCTTCAACGTAGTGCTATGG	46453–31			
1008	*F3L*	F3L-F290	2371	CTCATTGATTTTTCGCGGGATA	46313–34	62	107 bp	(*11*)
		F3L-R396 mod	2384	AACGATACTCCTCCTCGTTGGT	46398–419			This study
1007	*N3R*	N3R-1st cycle F	2382	TCTATCTCGTTCATGGTCGGTAAT	190503–26	64	455 bp	This study
		N3R-1st cycle R	2383	CGCACTGTCTTATTCGCCATT	190957–37			
1004	*N3R*	N3R-F319	2374	AACAACCGTCCTACAATTAAACAACA	190641–66	64	139 bp	(*11*)
		N3R-R457	2375	CGCTATCGAACCATTTTTGTAGTCT	190755–79			

*Bold underlined text in bases represents modifications to the original primers and probes. ID, identification; F, forward; mod, modified; MPXV, monkeypox virus; R, reverse; ref., reference.
†Position based on monkeypox virus reference isolate MPXV_USA_2022_MA001, complete genome, GenBank accession no. ON563414.

Table 2. Wastewater sample results detecting monkeypox virus DNA in airport wastewater, Rome, Italy*

Sample ID	Collection date	Real-time RT-PCR (Cq values)			Nested RT-PCR		
		G2R	F3L	N3R	G2R	F3L	N3R
4419	2022 May 30	–	–	–	–	–	–
4420	2022 Jun 1	–	–	–	–	–	–
4421	2022 Jun 6	–	–	–	–	–	–
4422	2022 Jun 8	–	–	–	–	–	–
4444	2022 Jun 13	–	–	–	–	–	–
4445	2022 Jun 15	+ (40.18)	+ (39.59)		**+**	–	–
4453	2022 Jun 20	–	–	–	–	–	–
4454	2022 Jun 22	–	–	–	–	–	–
4460	2022 Jun 27	–	–	–	–	–	–
4461	2022 Jun 29	–	–	–	–	–	–
4474	2022 Jul 4	–	–	–	–	–	–
4475	2022 Jul 6	–	–	–	–	–	–
4476	2022 Jul 11	–	–	–	–	–	–
4477	2022 Jul 13	–	–	–	–	–	–
4478	2022 Jul 18	+ (38.37)	–	–	+	+	–
4479	2022 Jul 20	–	–	–	+	**+**	–
4480	2022 Jul 25	–	–	–	–	–	–
4481	2022 Jul 27	–	–	–	–	–	–
4482	2022 Aug 3	–	–	–	–	–	–
4483	2022 Aug 1	–	–	–	–	–	–

*Bold positive font (**+**) indicates sequence failure due to insufficient DNA target; amplification band of the expected length was confirmed by duplicate experiments. ID, identification; RT-PCR, reverse transcription PCR; –, negative; +, positive.

(https://www.primer3plus.com) (Table 1). We performed reactions by using 1 µL of 10 µmol primer and 2 µL of sample, and Platinum SuperFi II Green PCR Master Mix (Thermo Fisher Scientific) in a final volume of 25 µL. PCR amplicons on both strands were sequenced by Bio-Fab Research (https://www.biofabresearch.com).

All real-time PCR assays successfully amplified the EVAg MPXV DNA. Compared with the original assay, the modified G2R_G assay showed a decrease in the average quantification cycle (Cq) values of 1.34 cycles (21.93 vs. 23.28), demonstrating a better performance. Therefore, we performed subsequent optimization activities and screening of wastewater samples by using the F3L and N3R assays as originally designed but modified the G2R_G assay for our study.

On pure MPXV DNA, the real-time F3L assay had an LOD_{50} of 0.21 copies/µL, the N3L assay had an LOD_{50} of 0.31 copies/µL, and G2R_G had an LOD_{50} of 0.21 copies/µL. For nucleic acids extracted from sewage samples spiked with MPXV, F3L had an LOD_{50} of 0.43 copies/µL and 2.16 copies/reaction, N3L had an LOD50 of 0.33 copies/µL and 1.65 copies/reaction, and G2R_G had an LOD_{50} of 0.31 copies/µL and 1.55 copies/reaction (Appendix).

Cq values ranged from 38.37–40.18 for 2 wastewater samples that tested positive by real-time PCR (Table 2), indicating relatively low DNA concentrations in the tested samples. Consensus sequences found 100% similarity by BLAST analysis between study sequences and MPXV strains available in GenBank (accession no. OX248696), thus confirming the presence of MPXV DNA.

Conclusions

A crucial aim of infectious disease surveillance is early detection of cases, outbreaks, and clusters, which is essential for disease control. We explored possible methods for monitoring MPXV through wastewater surveillance, a well-established complementary epidemiologic tool used successfully for viral infectious diseases, including SARS-CoV-2 and polio.

Monkeypox prevalence in the general population was low at the time of sample collection, only 20 cases had been detected in Italy as of May 30, 2022. Thus, to maximize the probability of positive samples among those collected, we tested wastewater samples from a large transportation hub, through which millions of persons travel to and from numerous countries. Because harmonized methods for detecting MPXV in wastewater are not yet available, we tested 3 different real-time PCR assays previously designed for clinical samples. We modified the assays by introducing changes in the primer and probe sequences to mitigate the effect of nucleotide mismatches. Among 20 samples, 3 tested positive for MPXV by real-time or nested PCR and sequencing.

In the next stage, we will test wastewater samples from WTPs enrolled in official SARS-CoV-2 environmental surveillance throughout Italy, to map the geographic distribution of MPXV in the country. Further research efforts should focus on elucidating how detection of viral DNA in sewage can be related to reported and confirmed cases. Factors affecting MPXV detection in wastewater also should be studied, including routes and duration of

virus shedding by infected persons, environmental persistence, and analytical sensitivity of the methods used (*14*).

In conclusion, we adapted SARS-CoV-2 wastewater surveillance for MPXV detection in a large airport WTP. Our methods can be applied to wastewater-based epidemiology for monkeypox outbreaks and provides basic tools, including analytic methods. Wastewater surveillance can be rapidly adapted to detect emerging threats, including monkeypox.

This article was preprinted at https://medrxiv.org/cgi/content/short/2022.08.18.22278932v1.

Acknowledgments

We gratefully acknowledge the support of Cavina Lorenzo and Eleuteri Silvia, Aeroporti di Roma (ADR) Fiumicino Airport for wastewater sample collection. We also thank Claudia Del Giudice, Lidia Orlandi and Serena Maccaroni for their technical assistance.

This research was partially supported by collaboration agreement EC G.A. no. 060701/2021/864481/SUB/ ENV. C2, Support to Member States for the creation of systems, local collection points and digital infrastructures for monitoring COVID 19 and its variants in wastewater, Italy.

This publication was supported by the European Virus Archive Global (EVA-GLOBAL) project, which provided the monkeypox DNA for testing real-time PCR assays.

About the Author

Dr. La Rosa is an environmental virologist at the Department of Environment and Health, National Institute of Health (Istituto Superiore di Sanità), Rome, Italy. Her primary research interest is viral pathogen surveillance through the monitoring of sewer systems.

References

1. World Health Organization. Monkeypox 19 May 2022 [cited 2022 Aug 16]. https://www.who.int/news-room/fact-sheets/detail/monkeypox
2. World Health Organization. WHO Director-General declares the ongoing monkeypox outbreak a Public Health Emergency of International Concern, 23 Jul 2022 [cited 2022 Aug 16]. https://www.who.int/europe/news/item/23-07-2022-who-director-general-declares-the-ongoing-monkeypox-outbreak-a-public-health-event-of-international-concern#:~:text=On%20July%2023%2C%20the%20WHO,in%20the%20WHO%20European%20Region
3. European Centre for Disease Control and Prevention - World Health Organization. Joint ECDC-WHO Regional Office for Europe monkeypox surveillance bulletin 12 Oct 2022 [cited 2022 Aug 16]. https://monkeypoxreport.ecdc.europa.eu
4. European Commission. Coronavirus response: monitoring of wastewater contributes to tracking coronavirus and variants across all EU countries 17 Mar 2022 [cited 2022 Aug 16]. https://joint-research-centre.ec.europa.eu/jrc-news/coronavirus-response-monitoring-wastewater-contributes-tracking-coronavirus-and-variants-across-all-2022-03-17_en
5. Peiró-Mestres A, Fuertes I, Camprubí-Ferrer D, Marcos MÁ, Vilella A, Navarro M, et al.; Hospital Clinic de Barcelona Monkeypox Study Group. Frequent detection of monkeypox virus DNA in saliva, semen, and other clinical samples from 12 patients, Barcelona, Spain, May to June 2022. Euro Surveill. 2022;27:2200503. https://doi.org/10.2807/1560-7917.ES.2022.27.28.2200503
6. Lapa D, Carletti F, Mazzotta V, Matusali G, Pinnetti C, Meschi S, et al. INMI Monkeypox Study Group. Monkeypox virus isolation from a semen sample collected in the early phase of infection in a patient with prolonged seminal viral shedding. Lancet Infect Dis. 2022;22:1267–9. https://doi.org/10.1016/S1473-3099(22)00513-8
7. Antinori A, Mazzotta V, Vita S, Carletti F, Tacconi D, Lapini LE, et al.; INMI Monkeypox Group. Epidemiological, clinical and virological characteristics of four cases of monkeypox support transmission through sexual contact, Italy, May 2022. Euro Surveill. 2022;27:2200421. https://doi.org/10.2807/1560-7917.ES.2022.27.22.2200421
8. de Jonge EF, Peterse CM, Koelewijn JM, van der Drift AR, van der Beek RFHJ, Nagelkerke E, et al. The detection of monkeypox virus DNA in wastewater samples in the Netherlands. Sci Total Environ. 2022 Aug 31 [Epub ahead of print]. https://doi.org/10.1016/j.scitotenv.2022.158265
9. La Rosa G, Iaconelli M, Mancini P, Bonanno Ferraro G, Veneri C, Bonadonna L, et al. First detection of SARS-CoV-2 in untreated wastewaters in Italy. Sci Total Environ. 2020;736:139652. https://doi.org/10.1016/j.scitotenv.2020.139652
10. Wu F, Zhang J, Xiao A, Gu X, Lee WL, Armas F, et al. SARS-CoV-2 titers in wastewater are higher than expected from clinically confirmed cases. mSystems. 2020;5:e00614-20. https://doi.org/10.1128/mSystems.00614-20
11. Cutrupi F, Cadonna M, Manara S, Postinghel M, La Rosa G, Suffredini E, et al. The wave of the SARS-CoV-2 Omicron variant resulted in a rapid spike and decline as highlighted by municipal wastewater surveillance. Environ Technol Innov. 2022;28:102667. https://doi.org/10.1016/j.eti.2022.102667
12. Kulesh DA, Loveless BM, Norwood D, Garrison J, Whitehouse CA, Hartmann C, et al. Monkeypox virus detection in rodents using real-time 3′-minor groove binder TaqMan assays on the Roche LightCycler. Lab Invest. 2004;84:1200–8. https://doi.org/10.1038/labinvest.3700143
13. Li Y, Zhao H, Wilkins K, Hughes C, Damon IK. Real-time PCR assays for the specific detection of monkeypox virus West African and Congo Basin strain DNA. J Virol Methods. 2010;169:223–7. https://doi.org/10.1016/j.jviromet.2010.07.012
14. Tiwari A, Adhikari S, Kaya D, Islam MA, Malla B, Sherchan SP, et al. Monkeypox outbreak: wastewater and environmental surveillance perspective. Sci Total Environ. 2022;856:159166. https://doi.org/10.1016/j.scitotenv.2022.159166

Address for correspondence: Giuseppina La Rosa, Department of Environment and Health, Istituto Superiore di Sanità, Viale Regina Elena 299, Rome 00161, Italy; email: giuseppina.larosa@iss.it

Successful Treatment of *Balamuthia mandrillaris* Granulomatous Amebic Encephalitis with Nitroxoline

Natasha Spottiswoode, Douglas Pet, Annie Kim, Katherine Gruenberg, Maulik Shah, Amrutha Ramachandran, Matthew T. Laurie, Maham Zia, Camille Fouassier, Christine L. Boutros, Rufei Lu, Yueyuan Zhang, Venice Servellita, Andrew Bollen, Charles Y. Chiu, Michael R. Wilson, Liza Valdivia,[1] Joseph L. DeRisi[1]

A patient in California, USA, with rare and usually fatal *Balamuthia mandrillaris* granulomatous amebic encephalitis survived after receiving treatment with a regimen that included the repurposed drug nitroxoline. Nitroxoline, which is a quinolone typically used to treat urinary tract infections, was identified in a screen for drugs with amebicidal activity against *Balamuthia.*

Balamuthia mandrillaris is an ameba that can cause skin lesions, endophthalmitis, or granulomatous amebic encephalitis (GAE) in previously healthy patients. Routes of infection include possible soil exposure (*1*) and transplanted organs from infected donors (*2*,*3*). The mortality rate is high. During 1974–2016, of 109 *Balamuthia* GAE cases in the United States, 10 patients survived; mortality rate was >90% (*4*).

The recommended medication regimen for *Balamuthia* GAE includes pentamidine, sulfadiazine, azithromycin/clarithromycin, fluconazole, flucytosine, and miltefosine (*5*). This regimen is based on survivor case series, and results have been inconsistent. Of those medications, only miltefosine, pentamidine, and azithromycin exhibit in vitro evidence of amebicidal or amebistatic activity (*6*,*7*). Furthermore, in vitro activity requires high concentrations of drug that are implausible in vivo (50% inhibitory concentration for azithromycin 244 μM and miltefosine 62 μM) (*6*). We report a patient with *B. mandrillaris* granulomatous amebic encephalitis who survived after receiving treatment with nitroxoline, a drug typically used to treat urinary tract infections, which was identified in a screen for drugs with amebicidal activity against *Balamuthia.*

Author affiliations: University of California, San Francisco, California, USA (N. Spottiswoode, D. Pet, A. Kim, K. Gruenberg, M. Shah, Amrutha Ramachandran, Matthew T. Laurie, Maham Zia, Camille Fouassier, Christine L. Boutros, Rufei Lu, Yueyuan Zhang, Venice Servellita, Andrew Bollen, Charles Y. Chiu, Michael R. Wilson, Liza Valdivia, Joseph L. DeRisi); Chan Zuckerberg Biohub, San Francisco (Joseph L. DeRisi)

DOI: https://doi.org/10.3201/eid2901.221531

The Case

The patient was a man in his 50s, with no remarkable medical history, who received care at a hospital in northern California, USA, after experiencing a generalized seizure. Magnetic resonance imaging (MRI) demonstrated a solitary left temporal lobe T2 hyperintensity with gadolinium rim enhancement and surrounding edema. After receiving treatment with dexamethasone and levetiracetam, he was transferred to the University of California San Francisco Medical Center (UCSF) (Figure 1).

Examination by neurology consultants indicated disorientation, inattention, moderate aphasia, and mild right hemiparesis. The aphasia and hemiparesis improved during hospitalization, suggesting that those signs were postictal. Cerebrospinal fluid (CSF) testing revealed increased nucleated cells up to 80/UL (60% lymphocytes, 17% neutrophils, 23% monocytes), protein concentration 38 mg/dL, and glucose concentration 100 mg/dL. A biopsy sample from the left temporal lobe lesion was preliminarily reported as well-formed granulomata with acute inflammation (Figure 2, panel A**)**.

Cultures from the brain biopsy sample did not grow bacteria, fungi, or mycobacteria. We performed metagenomic next-generation sequencing (mNGS) on a CSF sample (*8*,*9*) and sent brain biopsy samples for universal broad-range PCR amplicon sequencing (uPCR) for bacteria, fungi, *Mycobacterium tuberculosis*,

[1]These authors contributed equally to this article.

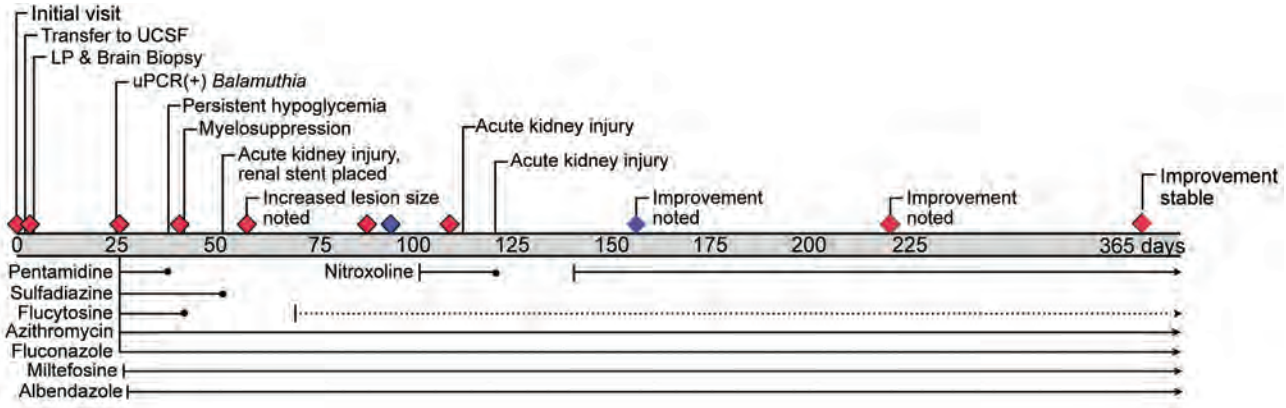

Figure 1. Timeline of events and medications for patient with granulomatous amebic encephalitis, California, USA. Grey bar shows days since initial evaluation; diamonds indicate interval magnetic resonance images; blue diamonds indicate magnetic resonance images taken before and after administration of nitroxoline. Medications at the bottom are other treatments administered. Solid lines refer to the dosages indicated in article text, and dotted lines indicate dose reduction. LP, lumbar puncture; UCSF, University of California, San Francisco Medical Center, San Francisco, California, USA; uPCR, universal broad-range PCR amplicon sequencing.

and nontuberculous mycobacteria. Rereview of neuropathology raised concern for amebic forms, prompting us to add uPCR of brain biopsy sample for ameba species (*10*). The patient was discharged.

On day 26 after the initial visit, Sanger sequencing of the uPCR amplicon was positive for *B. mandrillaris*. This diagnosis was confirmed by research-based mNGS of DNA extracted from the formalin-fixed, paraffin-embedded brain tissue under a remnant clinical sample biobanking protocol (UCSF IRB #10-01116; Appendix, https://wwwnc.cdc.gov/EID/article/28/1/22-1531-App1.pdf) (*11*). Results of all other studies, including mNGS of CSF, were negative.

On day 27, the patient was rehospitalized, again with disorientation and inattention. Repeat MRI showed disease progression with multiple new supratentorial and infratentorial lesions consistent with amebic abscesses. After consulting with the Centers for Disease Control and Prevention, we started administering sulfadiazine (1,500 mg orally 4×/d), fluconazole (1,000 mg [12 mg/kg] orally 1×/d), flucytosine (3,000 mg [37.5 mg/kg] 4×/d), pentamidine (330 mg [4 mg/kg] intravenously 1×/d), azithromycin (500 mg orally 1×/d), miltefosine (50 mg orally 3×/d), and albendazole (400 mg orally 1×/d) (Figure 1).

MRI on day 42 (15 days of the 7-drug regimen) showed moderately reduced lesion size, reduced edema, and no new lesions. However, severe medication toxicities developed. Hypoglycemia required discontinuation of pentamidine. Subsequent renal failure caused by sloughing of renal calyces required discontinuation of sulfadiazine and placement of bilateral nephrostomy tubes. The patient's kidney function improved but remained impaired (baseline estimated glomerular filtration rate 20). Decreased absolute neutrophil count necessitated stopping and then reducing flucytosine dose. The ongoing limited regimen included dose-reduced flucytosine, fluconazole, miltefosine, albendazole, and azithromycin. Brain MRI on day 59 (14 days on this limited regimen) showed interval increase in lesion size, with increased edema.

Given his worsening prognosis, the patient and his family agreed to trial treatment with nitroxoline, a quinolone antibiotic with in vitro amebicidal activity against *B. mandrillaris* (*6*). Nitroxoline was selected instead of compounds identified in other high-throughput screens (*12*) because it is available internationally to treat urinary tract infections and is well tolerated (*13*). Nitroxoline was authorized through an emergency use authorization (Food and Drug Administration Investigational New Drug no. 154939), and on day 103, we initiated treatment (250 mg orally 3×/d). All other medications were continued. The patient experienced a transient acute kidney injury; although the nephrology staff considered it unrelated to nitroxoline, we submitted a possible adverse event report.

On day 109, after 1 week of nitroxoline treatment, MRI showed decreased size of the cerebral abscesses and no new lesions compared with MRI before nitroxoline on day 96 (Figure 2, panel B). The patient was discharged, although neurologic examination continued to demonstrate mild disorientation and inattention. Recovery was complicated by a subsequent acute kidney injury because of malfunctioning ureteral stents, and nitroxoline administration was stopped

while creatinine clearance was <20 (days 122–143). Interval MRIs on days 156 and 220 (7 and 17 weeks after nitroxoline initiation) showed continued marked improvement in lesion size (Figure 2, panel B).

As of 15 months after initial evaluation, the patient continues to take nitroxoline, miltefosine, azithromycin, albendazole, fluconazole, and dose-reduced flucytosine. His infectious disease outpatient clinicians plan to sequentially discontinue medications after 1 year. He lives in the community, and his family assists with medication management and appointments.

Conclusions

Repurposed use of nitroxoline associated with survival from *B. mandrillaris* GAE demonstrates the potential of basic research to identify antiamebic agents that improve outcome of this rare and deadly disease. Given the limited options for treating *Balamuthia* GAE, several studies have used high-throughput screening tools to identify other amebicidal agents. Compounds from the Medicines for Malaria Ventures Pandemic Response Box underwent in vitro trials against *B. mandrillaris*, but the leading candidates have not been used in humans or are not commercially

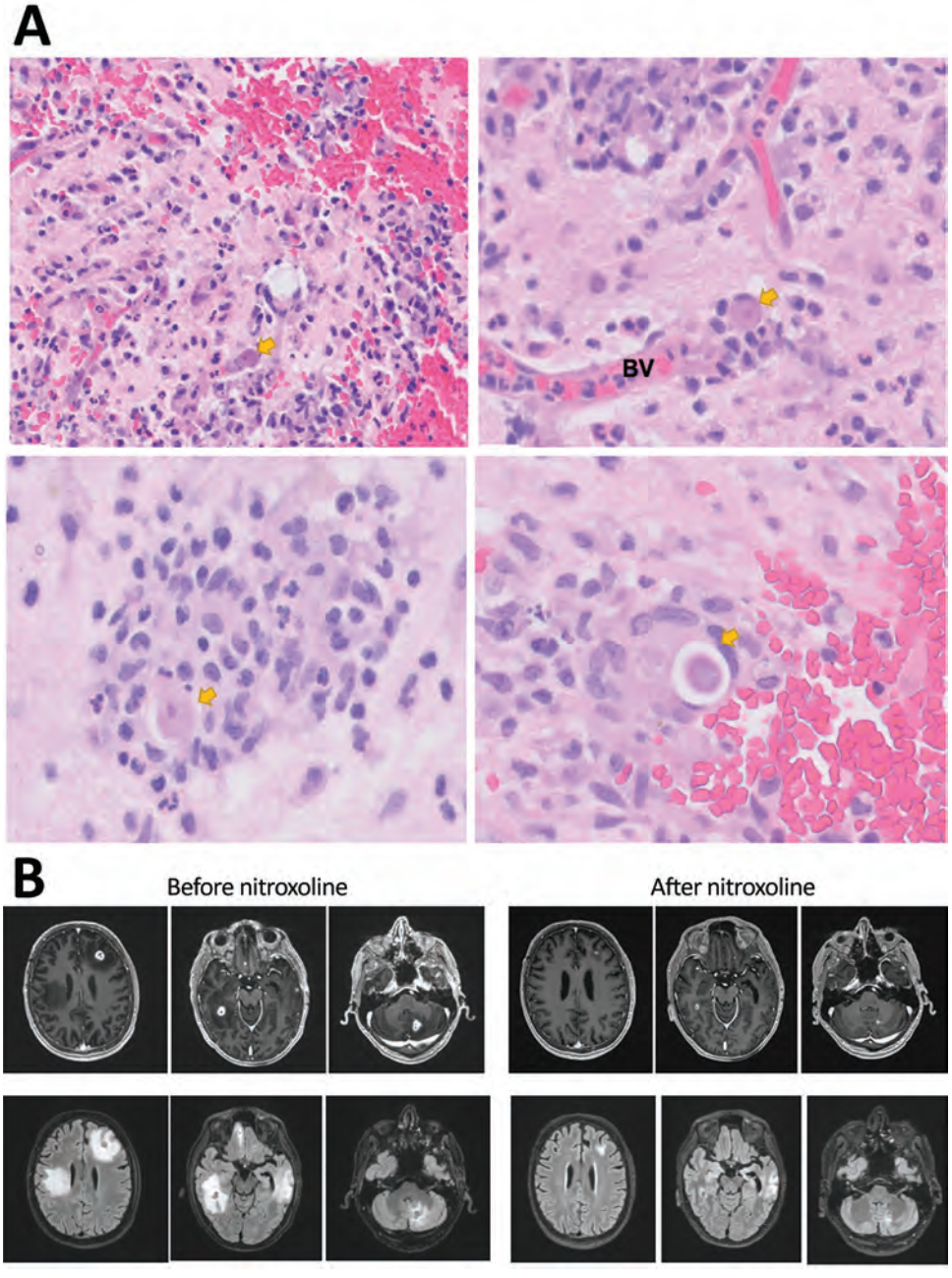

Figure 2. Diagnostic findings for patient with granulomatous amebic encephalitis, California, USA. A) Brain biopsy sample. Granulomas are noted in a perivascular pattern. Scattered structures (arrows) with large nuclei and abundant cytoplasma are concerning for amebic trophozoite forms. Occasional structures with a large nucleus present within a relatively rigid outline (lower right image) are suspicious for amebic cysts, the dormant, thick-walled life stage. B) Magnetic resonance images obtained before and after nitroxoline treatment. Upper row shows axial gadolinium-enhanced T1-weighted images; lower row shows axial fluid-attenuated inversion recovery images. Images in the left series were obtained on day 96 after initial visit, 1 week before nitroxoline initiation; images in the right series were obtained on day 156 after initial visit, 7 weeks after nitroxoline initiation. BV, blood vessel.

available (*12*). In the screening for the patient reported here, which identified nitroxoline as having amebicidal activity against *B. mandrillaris*, in vitro efficacy of nitroxoline against *B. mandrillaris* cysts and trophozoites was determined to be higher than that of currently recommended drugs and prevented tissue destruction in fibroblast and explant models of *B. mandrillaris* infection (*6*).

In vitro efficacy of nitroxoline is better than that of other antiamebic medications; it also is safe and well tolerated. In a review of its use in urinary tract infections, 9.8% of patients reported adverse events, primarily nausea (*13*). In contrast, current antiamebic treatments can cause severe toxicity, especially pentamidine and sulfadiazine. It is not known if nitroxoline penetrates the CNS, but our limited experience suggests that it may, especially in a patient with a compromised blood–brain barrier.

A barrier to treating *Balamuthia* GAE is diagnostic delay. Imaging characteristics are nonspecific, and more common pathologies are often misdiagnosed (e.g., neoplasm or pyogenic abscesses) (*4*). CSF findings are typically nonspecific, direct detection tests of CSF can be insensitive, and visualization of organisms in CSF is rare. Thus, diagnosis often requires brain biopsy, specialized pathology, or dedicated PCR testing.

Unbiased diagnostics, such as mNGS, offer the opportunity to streamline and accelerate diagnosis of rare pathogens such as *Balamuthia* (*8*). Multiple *Balamuthia* GAE cases have been diagnosed by CSF mNGS (*14*,*15*). In the case we report, results of CSF mNGS testing were negative, concordant with negative CSF uPCR and indicating that no abscesses had ruptured or were abutting the ventricles (*8*). However, results of uPCR and research-based mNGS of brain tissue were positive. Currently, clinical mNGS is not available for brain biopsy samples; clinical validation of this test may speed diagnoses of future cases. Despite the limitations of any case study, we suggest that accelerated diagnosis with unbiased techniques and early initiation of nitroxoline may offer promise to improve survival rates for patients with *Balamuthia* GAE.

Acknowledgments

We thank the patient and his family for participating in this study.

The Free-Living and Intestinal Ameba Laboratory, Division of Foodborne, Waterborne, and Environmental Diseases, National Center for Emerging and Zoonotic Infectious Diseases, Centers for Disease Control and Prevention, provided advice and guidance. Asieris Pharmaceuticals provided the nitroxoline pro bono. Heather Stone guided emergency authorization. David Sears, Dong Lee, Malcolm John, and Scott Grapentine were instrumental in preparing the Emergency Use Authorization and caring for the patient. Michael Reid and Erika Wallender provided advice. University of Washington Molecular Microbiology provided the full sequence of the universal PCR. Written informed consent was obtained from the patient for publication of this manuscript.

J.D.R. received funding from the Chan-Zuckerberg Biohub. M.R.W. received funding from the Westridge Foundation.

About the Author

Dr. Spottiswoode is a research fellow in the Division of HIV, Infectious Diseases, and Global Medicine at the University of California San Francisco. Her research interests include the use of novel diagnostic tools and the combination of pathogen metagenomics and host responses to understand disease pathophysiology and outcome.

References

1. Jackson BR, Kucerova Z, Roy SL, Aguirre G, Weiss J, Sriram R, et al. Serologic survey for exposure following fatal *Balamuthia mandrillaris* infection. Parasitol Res. 2014;113:1305–11. https://doi.org/10.1007/s00436-014-3769-0
2. Farnon EC, Kokko KE, Budge PJ, Mbaeyi C, Lutterloh EC, Qvarnstrom Y, et al.; Balamuthia Transplant Investigation Teams. Transmission of *Balamuthia mandrillaris* by organ transplantation. Clin Infect Dis. 2016;63:878–88. https://doi.org/10.1093/cid/ciw422
3. Gupte AA, Hocevar SN, Lea AS, Kulkarni RD, Schain DC, Casey MJ, et al. Transmission of *Balamuthia mandrillaris* through solid organ transplantation: utility of organ recipient serology to guide clinical management. Am J Transplant. 2014;14:1417–24. https://doi.org/10.1111/ajt.12726
4. Cope JR, Landa J, Nethercut H, Collier SA, Glaser C, Moser M, et al. The epidemiology and clinical features of *Balamuthia mandrillaris* disease in the United States, 1974-2016. Clin Infect Dis. 2019;68:1815–22. https://doi.org/10.1093/cid/ciy813
5. Centers for Disease Control and Prevention. Parasites—*Balamuthia mandrillis*—granulomatous amoebic encephalitis (GAE) [cited 2022 Jan 31]. https://www.cdc.gov/parasites/balamuthia/treatment.html
6. Laurie MT, White CV, Retallack H, Wu W, Moser MS, Sakanari JA, et al. Functional assessment of 2,177 U.S. and international drugs identifies the quinoline nitroxoline as a potent amoebicidal agent against the pathogen *Balamuthia mandrillaris*. MBio. 2018;9:e02051-18. https://doi.org/10.1128/mBio.02051-18
7. Schuster FL, Dunnebacke TH, Booton GC, Yagi S, Kohlmeier CK, Glaser C, et al. Environmental isolation of *Balamuthia mandrillaris* associated with a case of amebic encephalitis. J Clin Microbiol. 2003;41:3175–80. https://doi.org/10.1128/JCM.41.7.3175-3180.2003

8. Wilson MR, Sample HA, Zorn KC, Arevalo S, Yu G, Neuhaus J, et al. Clinical metagenomic sequencing for diagnosis of meningitis and encephalitis. N Engl J Med. 2019;380:2327–40. https://doi.org/10.1056/NEJMoa1803396
9. Miller S, Naccache SN, Samayoa E, Messacar K, Arevalo S, Federman S, et al. Laboratory validation of a clinical metagenomic sequencing assay for pathogen detection in cerebrospinal fluid. Genome Res. 2019;29:831–42. https://doi.org/10.1101/gr.238170.118
10. Rakeman JL, Bui U, Lafe K, Chen YC, Honeycutt RJ, Cookson BT. Multilocus DNA sequence comparisons rapidly identify pathogenic molds. J Clin Microbiol. 2005;43:3324–33. https://doi.org/10.1128/JCM.43.7.3324-3333.2005
11. Ramachandran PS, Ramesh A, Creswell FV, Wapniarski A, Narendra R, Quinn CM, et al. Integrating central nervous system metagenomics and host response for diagnosis of tuberculosis meningitis and its mimics. Nat Commun. 2022;13:1675. https://doi.org/10.1038/s41467-022-29353-x
12. Rice CA, Lares-Jiménez LF, Lares-Villa F, Kyle DE. *In vitro* screening of the open-source Medicines for Malaria Venture Malaria and pathogen boxes to discover novel compounds with activity against *Balamuthia mandrillaris*. Antimicrob Agents Chemother. 2020;64:e02233-19. https://doi.org/10.1128/AAC.02233-19
13. Naber KG, Niggemann H, Stein Gisela, Stein Guenter. Review of the literature and individual patients' data meta-analysis on efficacy and tolerance of nitroxoline in the treatment of uncomplicated urinary tract infections. BMC Infect Dis. 2014;14:628. https://doi.org/10.1186/s12879-014-0628-7
14. Haston JC, Rostad CA, Jerris RC, Milla SS, McCracken C, Pratt C, et al. Prospective cohort study of next-generation sequencing as a diagnostic modality for unexplained encephalitis in children. J Pediatric Infect Dis Soc. 2020;9:326–33. https://doi.org/10.1093/jpids/piz032
15. Wilson MR, Shanbhag NM, Reid MJ, Singhal NS, Gelfand JM, Sample HA, et al. Diagnosing *Balamuthia mandrillaris* encephalitis with metagenomic deep sequencing. Ann Neurol. 2015;78:722–30. https://doi.org/10.1002/ana.24499

Address for correspondence: Natasha Spottiswoode, Division of HIV, Infectious Disease, and Global Medicine, University of San Francisco, 513 Parnassus Ave, S380, San Francisco, CA 94143, USA: email: natasha.spottiswoode@ucsf.edu

etymologia revisited

Influenza

[in''floo-en'zə]

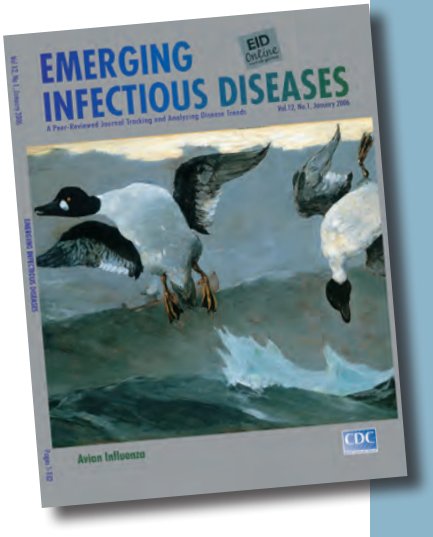

Originally published in January 2006

An acute viral infection of the respiratory tract. From Latin influentia,"to flow into"; in medieval times, intangible fluid given off by stars was believed to affect humans. The Italian influenza referred to any disease outbreak thought to be influenced by stars. In 1743, what Italians called an influenza di catarro ("epidemic of catarrh") spread across Europe, and the disease came to be known in English as simply "influenza."

Source:
Dorland's illustrated medical dictionary. 30th ed. Philadelphia: Saunders; 2003 and Quinion M. World wide words. 1998 Jan 3 [cited 2005 Dec 5]. Available from http://www.worldwidewords.org/topicalwords/tw-inf1.htm

Clinical Forms of Japanese Spotted Fever from Case-Series Study, Zigui County, Hubei Province, China, 2021

Zhongqiu Teng,[1] Ping Gong,[1] Wen Wang, Na Zhao, Xiaojing Jin, Xiangrong Sun, Haijian Zhou, Junlin Lu, Xuebing Lin, Bohai Wen, Biao Kan, Jianguo Xu, Tian Qin

We report a case-series study of 5 patients with Japanese spotted fever from the Three Gorges Area in China, including 1 fatal case. Seroprevalence of *Rickettsia japonica* was ≈12% among the local population. Our report highlights the emerging potential threat to human health of Japanese spotted fever in the area.

Japanese spotted fever (JSF), caused by the bacterium *Rickettsia japonica*, was first described in 1984 in Japan (*1*). It has been recognized in multiple countries in Asia, including Japan, South Korea, the Philippines, Thailand, and China (*1*–*5*), suggesting that it is endemic in Asia. In China, *R. japonica* has been detected in ticks from the central, southeast, and northeast regions (*6*–*8*). Since JSF cases were first found in Anhui Province in 2013 (*5*), a total of 39 have been reported in the Dabie Mountains on the borders of Henan, Anhui, and Hubei Provinces and in the Tianmu Mountains in Zhejiang Province on the eastern coast (Appendix Figure 1, https://wwwnc.cdc.gov/EID/article/29/1/22-0639-App1.pdf) (*9*–*11*).

The Study

Our study was approved by the ethics committees of the National Institute for Communicable Disease Control and Prevention (ICDC). During April–October 2021, five JSF cases were found in Zigui County, Hubei Province, in the Three Gorges area of China (Appendix Figure 1), including case 1, in which the patient died because of multiorgan failure. Among the 5 case-patients (3 female, 2 male), disease onset occurred during April–October (2 cases in spring, 3 in autumn); median age of case-patients was 53 years (range 47–70 years) (Table 1). All had histories of activity in fields, but none was aware of any tick bites. All initially manifested signs and symptoms of sudden fever (≥38.5°C), headache, chills, fatigue, chest tightness, shortness of breath, and dyspnea. All had rash and eschar (Appendix Figure 2), except for case-patient 1, who had no eschar. Case-patients 1, 3, and 5 experienced vomiting and case-patient 3 had abdominal pain. Medical laboratory tests (Table 2) showed that case-patients 1, 3, and 5 had thrombocytopenia and lymphopenia, case-patients 1 and 5 had neutrophilia, and case-patients 1 and 4 had mild anemia. All 5 patients had remarkably elevated levels of C-reactive protein and D-dimer, and except for case-patient 5, all had elevated liver-associated enzymes. Proteinuria was detected in case-patients 1, 2, 3, and 5. Case-patients 1, 3, and 5 had simultaneous edema and effusion and case-patient 5 showed multiple effusions (pelvic, pleural, pericardial, and ascites).

Most laboratory tests were flagged as abnormal for case-patient 1, who died. She received an initial antimicrobial treatment (Appendix) at the village clinic without a causative agent being identified and already had severe sepsis (sequential organ failure assessment score = 12) by the time she was admitted to the hospital on day 8 after symptom onset. Disseminated intravascular coagulation was diagnosed, and she died of multiple organ failure on day 9 despite

Author affiliations: State Key Laboratory of Infectious Disease Prevention and Control, Beijing, China (Z. Teng, W. Wang, N. Zhao, X. Jin, H. Zhou, B. Kan, J. Xu, T. Qin); National Institute for Communicable Disease Control and Prevention, Beijing (Z. Teng, W. Wang, N. Zhao, X. Jin, H. Zhou, B. Kan, J. Xu, T. Qin); Zigui People's Hospital, Yichang, China (P. Gong, J. Lu, X. Lin); Nanchang Municipal Center for Disease Control and Prevention, Nanchang, China (X. Sun); Beijing Institute of Microbiology and Epidemiology, Beijing (B. Wen)

DOI: https://doi.org/10.3201/eid2901.220639

[1]These authors contributed equally to this article.

Table 1. Epidemiologic and clinical characteristics of patients with *Rickettsia japonica* infection, Zigui County, Hubei Province, China

Characteristics	Case 1*	Case 2	Case 3	Case 4	Case 5
Sex	Female	Male	Male	Female	Female
Age, y	58	47	68	57	70
Month of admission	Apr	Jun	Sep	Sep	Oct
Occupation	Farmer	Village teacher	Farmer	Farmer	Farmer
Possible causative exposures	Picking tea, tea garden	Collecting bamboo, bamboo groves	Herding sheep, woodland	Farm work, fields	Farm work and chopping wood, fields and woodland
Previous illness	Healthy	Healthy	Hypertension	Healthy	Hypertension
Day of admission†	8	4	6	15	5
Signs and symptoms					
Highest temperature, °C	39.0	39.0	39.0	38.5	39.5
Fever type	Continued	Continued	Continued	Undetermined‡	Undetermined§
Headache	Present	Present	Present	Present	Present
Malaise	Present	Present	Present	Present	Present
Myalgia	Present	Present	Present	Present	Present
Chills	Present	Present	Present	Present	Present
Eschar	Absent	Present	Present	Present	Present
Rash (day)	Present (11)	Present (3)	Present (10)	Present (13)	Present (10)
Hypotension (day)	Present (9)	Absent	Absent	Absent	Absent
Dyspnea (day)	Present (9)	Present (6)	Present (10)	Present (15)	Present (5)
Vomiting (day)	Present (9)	Absent	Present (10)	Absent	Present (7)
Edema (day)	Face (9)	Absent	Lower extremities (10)	Absent	Lower extremities (10)
Clouding of consciousness	Present	Present	Present	Present	Present
Proteinuria	+++	+–	+	–	++
Anuria (day)	Present (9)	Absent	Absent	Absent	Absent
Abdominal pain	Absent	Absent	Present (11)	Absent	Absent
Pelvic effusion	Absent	Absent	Absent	Absent	Present (5)
Pleural effusion (day)	Present (9)	Absent	Present (10)	Absent	Present (5)
Pericardial effusion	Absent	Absent	Present (10)	Absent	Present (5)
Ascites effusion	Absent	Absent	Absent	Absent	Present (5)

*Fatal case.
†Day on which sign or symptom manifested in patient, when applicable. The day when the patients first experienced headache and fatigue was defined as Day 0.
‡Difficulty determining fever type because of drug intervention.
§Urine protein concentration: –, <0.1 g/L; +–, 0.1–0.2 g/L; +, 0.2–1.0 g/L; ++, 1.0–2.0 g/L; +++, 2.0–4.0 g/L.

continuous intensive therapy. The other 4 patients recovered without sequelae after receiving doxycycline or minocycline treatment (Appendix).

Using a PCR assay, we detected 6 rickettsial genes (*groEL*, *glt*A, *omp*A, *omp*B, *sca*4, and 17kDa gene) in a blood specimen from case-patient 1. In addition, we

Table 2. Laboratory findings of the patients with *Rickettsia japonica* infection, Zigui County, Hubei Province, China*

Laboratory findings*	Reference value	Case 1	Case 2	Case 3	Case 4	Case 5
Leukocyte, × 10^9 cells/L	4.0–10.0	9.09	3.50	7.78	8.45	9.15
Hemoglobin, g/L	110–150 (F), 120–160 (M)	109	130	127	105	115
Platelets, × 10^9/L	100–300	45	99	72	110	82
Lymphocytes, × 10^9 cells/L	0.8–3.5	0.52	0.72	0.91	2.29	0.64
Neutrophils, × 10^9 cells/L	1.8–6.3	8.11	2.55	5.80	5.80	7.90
CRP, mg/L	0.8–8.0	199.53	72.8	77.00	72.00	111.72
PCT, µg/L	<0.5	5.64	0.38	2.14	0.4	0.54
D-dimer, µg/mL	0–0.5	4.200	2.081	2.160	1.090	1.080
TBil, mg/L	3–13	38.0	12	12	9.3	11
DBil, mg/l	0–2.5	24.0	2.0	3.4	2.7	2.0
TBA, µmol/L	<10	43.1	3.9	8.6	4.8	4.9
TP, g/L	60–80	48.7	62.9	52.3	58.2	65
Albumin, g/L	35–55	23.8	36.2	30.6	35.6	35.9
A/G	1.5–2.5	1.0	1.4	1.4	1.6	1.2
ALT, U/L	0–35	21	69	177	167	16
AST, U/L	0–40	114	88	167	111	29
BUN, mmol/L	2.9–7.5	7.81	3.81	10.80	2.38	7.54
Creatinine, mg/L	40–100 (F), 50–110 (M),	93.2	84.9	74.1	58.2	83.9
Uric acid, µmol/L	150–357 (F), 200–416 (M)	378	301	259	182	210
LDH, U/L	100–300	587	412	403	433	368
Creatine kinase, U/L	18–198	257	186	51	48	125
α-HBDH, U/L	90–220	401	294	254	317	323
Sodium, mmol/L	135–145	137.7	141.9	132.9	131.4	136.5

*α-HBDH, α-hydroxybutyrate dehydrogenase; A/G, albumin/globulin ratio; ALT, alanine aminotransferase; AST, aspartate aminotransferase; BUN, blood urea nitrogen; CRP, C-reactive protein; DBil, direct bilirubin; LDH, lactate dehydrogenase; TBA, total bile acids; TBil, total bilirubin; TP, total protein.

amplified *groEL*, *glt*A, and 17kDa genes from case-patients 2, 3, and 5 but only *glt*A and 17kDa from case-patient 4. For all 5 patients, the genomic sequences of each amplified target gene were 100% identical to each other; phylogenetic analysis revealed that the causative agent was most closely related to *R. japonica* (Figure). We submitted the obtained sequences to GenBank (accession nos. OM966424–8 for *glt*A,

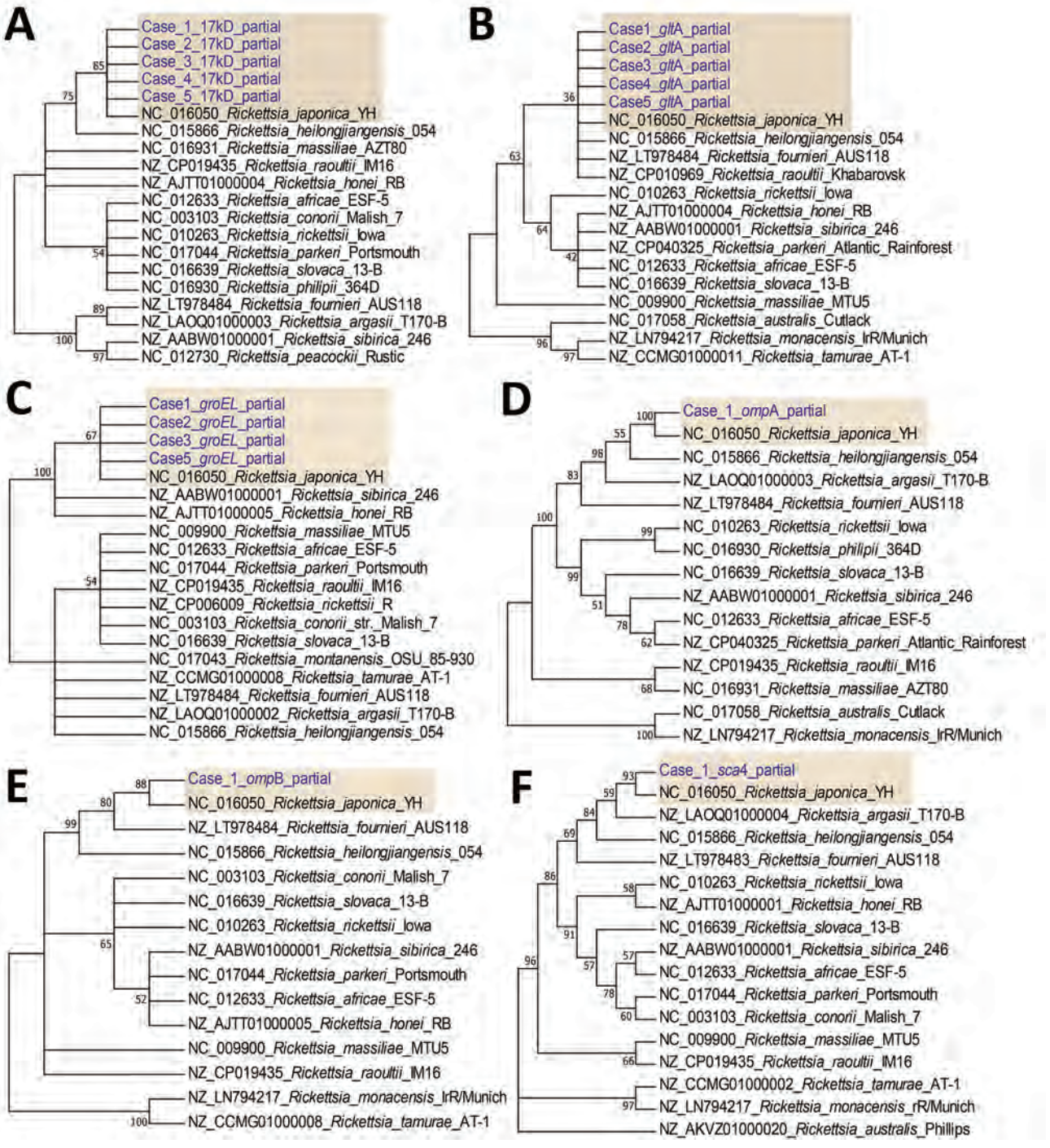

Figure. Bootstrap consensus phylogenetic tree constructed based on partial sequences of 17kDa (A), *glt*A (B), *groEL* (C), *omp*A (D), *omp*B (E), and *sca*4 (F) amplified from blood specimens from 5 spotted fever patients in Japan (yellow shading). We aligned sequences using MUSCLE within MEGA6 software (http://www.megasoftware.net). We analyzed phylogenetic relationships using the neighbor-joining method with 1,000 bootstrap replicates; boot values are shown next to the branches. Genbank accession numbers for the *Rickettsia* strains retrieved are indicated.

OM966422 for *omp*A, OM966423 for *omp*B, OM966412–6 for 17kDa, OM966417 for *sca*4, and OM966418–21 for *groEL*). We obtained 1 stable rickettsial isolate, designated *R. japonica* strain YC21, from the blood of case-patient 1 using Vero cell cultures (Appendix Figure 3) and obtained the whole genomic sequence from the isolate (GenBank BioProject PRJNA812951). Phylogenetic analysis based on core genes suggested that *R. japonica* strain YC21 was most closely related to *R. japonica* strain LA16/2015 (Appendix Figure 4); 30 virulence-associated genes of *R. japonica* strain YC21 (Appendix Table 2), predicted using the virulence factor database (http://www.mgc.ac.cn/VFs), were completely homologous to those of strain LA16/2015.

We used an immunofluorescence assay using *R. japonica* strain YC21 as coating antigen (a cutoff of 1:64 was determined by testing negative and positive samples) and *R. rickettsii* (Focus Diagnostics, http://focusdiagnostics.in) to test serum-specific antibodies from the 5 JSF patients and 100 healthy subjects recruited locally. Case-patients 2 and 3 were confirmed to have JSF on the basis of a ≥4-fold increase in *R. rickettsii*–specific and *R. japonica*–specific IgG titers between acute and convalescent phase serum (Appendix Table 3). At baseline, 12/100 (12%) of the healthy local donors tested positive (range, 1:128–1:1,024; geometric mean, 512) for *R. japonica*–specific IgG.

We measured cytokine and chemokine levels in the serum samples collected from the JSF patients (during acute phase) and 6 healthy donors (Appendix Table 4). The levels of interferon (IFN) γ, interleukin (IL) 6, IL-10, IL-1α, macrophage inflammatory protein 1β, IL-8, IFN gamma-induced protein 10, and monocyte chemoattractant protein 1 in the 4 surviving JSF patients were significantly higher than in the healthy donors ($p < 0.01$), consistent with previous reports, except for the exclusion of tumor necrosis factor α (*12*–*14*). In the case-patient who died, serum levels of IL-6, IL-10, and IFN-γ were 10-fold higher than those in the surviving case-patients and the levels of IL-4, INF-α, granulocyte-macrophage colony-stimulating factor, monocyte chemoattractant protein 1, macrophage inflammatory protein 1β, and IP-10 were 2-fold higher, suggesting that *R. japonica* infection might cause an unregulated hyperinflammatory state, potentially leading to cytokine release syndrome (*14*).

Conclusion

We identified 5 cases of JSF, including 1 in which the patient died, in Zigui County in the Three Gorges Area of China, where JSF has not previously been identified. Furthermore, our study revealed a high prevalence (12%) of *R. japonica* among residents, suggesting a new endemic area for JSF in China and indicating that JSF might be more widespread than previously thought. We should be alert to the potential risk for JSF, especially in areas where *R. japonica* is detected in vectors (Appendix Figure 1). The JSF cases were confirmed by PCR detection and serologic tests. A strain of *R. japonica* isolated from the blood of the patient who died was revealed to be most closely related to strains LA16/2015 and LA4/2015 detected in Zhejiang Province, suggesting that a virulent strain of *R. japonica* might have spread widely across China.

Delayed treatment is one of the worst prognostic factors for patients with JSF, and as a neglected infectious disease, it might not be considered during differential diagnosis. In our study, the patient who died manifested a faint rash, but without eschar, which resulted in delayed diagnosis and provision of correct antimicrobial treatment when she first visited the rural clinic. Profiling the patient's serum cytokine and chemokine levels indicated notably elevated IL-6, IL-10, and IFN-γ, characteristic of potential cytokine release syndrome. The primary findings on patient cytokines levels benefit understanding of immune response to *R. japonica* infection.

Our findings highlight the threat of JSF to public health in China. Healthcare workers, especially in rural areas where residents are at increased risk for tick exposure, should be aware of this potentially deadly infectious disease. Long-term surveillance and investigation of local hosts and vectors of *R. japonica* are necessary to improve the prevention and treatment of JSF.

Acknowledgments

We thank Jingdong Song for his assistance with acquiring scanning electron microscope images.

This work was supported by grants from the National Natural Science Foundation of China (grant no. 81671985), the Science Foundation for the State Key Laboratory for Infectious Disease Prevention and Control from China (grant no. 2019SKLID403, 2021SKLID507), and the Pathogen Monitoring Capability Improvement Project (grant no. 131031102000150003) from the National Health Commission of China.

About the Author

Dr. Teng is a research associate at the National Institute for Communicable Disease Control and Prevention, Chinese Center for Disease Control and Prevention. His research interests are detection and isolation of rickettsia and the epidemiology of rickettsioses.

References

1. Mahara F. Japanese spotted fever: report of 31 cases and review of the literature. Emerg Infect Dis. 1997;3:105–11. https://doi.org/10.3201/eid0302.970203
2. Camer GA, Alejandria M, Amor M, Satoh H, Muramatsu Y, Ueno H, et al. Detection of antibodies against spotted fever group Rickettsia (SFGR), typhus group Rickettsia (TGR), and *Coxiella burnetii* in human febrile patients in the Philippines. Jpn J Infect Dis. 2003;56:26–8.
3. Chung MH, Lee SH, Kim MJ, Lee JH, Kim ES, Lee JS, et al. Japanese spotted fever, South Korea. Emerg Infect Dis. 2006;12:1122–4. https://doi.org/10.3201/eid1207.051372
4. Gaywee J, Sunyakumthorn P, Rodkvamtook W, Ruang-areerate T, Mason CJ, Sirisopana N. Human infection with *Rickettsia* sp. related to *R. japonica*, Thailand. Emerg Infect Dis. 2007;13:657–9. https://doi.org/10.3201/eid1304.060585
5. Li J, Hu W, Wu T, Li HB, Hu W, Sun Y, et al. Japanese spotted fever in eastern China, 2013. Emerg Infect Dis. 2018;24:2107–9. https://doi.org/10.3201/eid2411.170264
6. Zhang L, Cui F, Wang L, Zhang L, Zhang J, Wang S, et al. Investigation of anaplasmosis in Yiyuan County, Shandong Province, China. Asian Pac J Trop Med. 2011;4:568–72. https://doi.org/10.1016/S1995-7645(11)60148-X
7. Yan P, Qiu Z, Zhang T, Li Y, Wang W, Li M, et al. Microbial diversity in the tick *Argas japonicus* (Acari: Argasidae) with a focus on *Rickettsia* pathogens. Med Vet Entomol. 2019;33:327–35. https://doi.org/10.1111/mve.12373
8. Lu M, Li F, Liao Y, Shen JJ, Xu JM, Chen YZ, et al. Epidemiology and diversity of Rickettsiales bacteria in humans and animals in Jiangsu and Jiangxi Provinces, China. Sci Rep. 2019;9:13176. https://doi.org/10.1038/s41598-019-49059-3
9. Lu Q, Yu J, Yu L, Zhang Y, Chen Y, Lin M, et al. *Rickettsia japonica* infections in humans, Zhejiang Province, China, 2015. Emerg Infect Dis. 2018;24:2077–9. https://doi.org/10.3201/eid2411.170044
10. Li W, Liu SN. *Rickettsia japonica* infections in Huanggang, China, in 2021. IDCases. 2021;26:e01309. https://doi.org/10.1016/j.idcr.2021.e01309
11. Li H, Zhang PH, Du J, Yang ZD, Cui N, Xing B, et al. *Rickettsia japonica* infections in humans, Xinyang, China, 2014–2017. Emerg Infect Dis. 2019;25:1719–22. https://doi.org/10.3201/eid2509.171421
12. Popivanova NI, Murdjeva MA, Baltadzhiev IG, Haydushka IA. Dynamics in serum cytokine responses during acute and convalescent stages of Mediterranean spotted fever. Folia Med (Plovdiv). 2011;53:36–43. https://doi.org/10.2478/v10153-010-0035-9
13. Kondo M, Matsushima Y, Mizutani K, Iida S, Habe K, Yamanaka K. Transition of serum cytokine concentration in *Rickettsia japonica* infection. Infect Dis Rep. 2020;12:127–31. https://doi.org/10.3390/idr12030023
14. Tai K, Iwasaki H, Ikegaya S, Takada N, Tamaki Y, Tabara K, et al. Significantly higher cytokine and chemokine levels in patients with Japanese spotted fever than in those with Tsutsugamushi disease. J Clin Microbiol. 2014;52:1938–46. https://doi.org/10.1128/JCM.03238-13

Address for correspondence: Tian Qin, State Key Laboratory of Infectious Diseases Prevention and Control, National Institute for Communicable Disease Control and Prevention, Chinese Center for Disease Control and Prevention, 155 Changbai Rd, Changping, Beijing 102206, China; email: qintian@icdc.cn

EID Podcast

Emerging Infectious Diseases Cover Art

Byron Breedlove, managing editor of the journal, elaborates on aesthetic considerations and historical factors, as well as the complexities of obtaining artwork for Emerging Infectious Diseases.

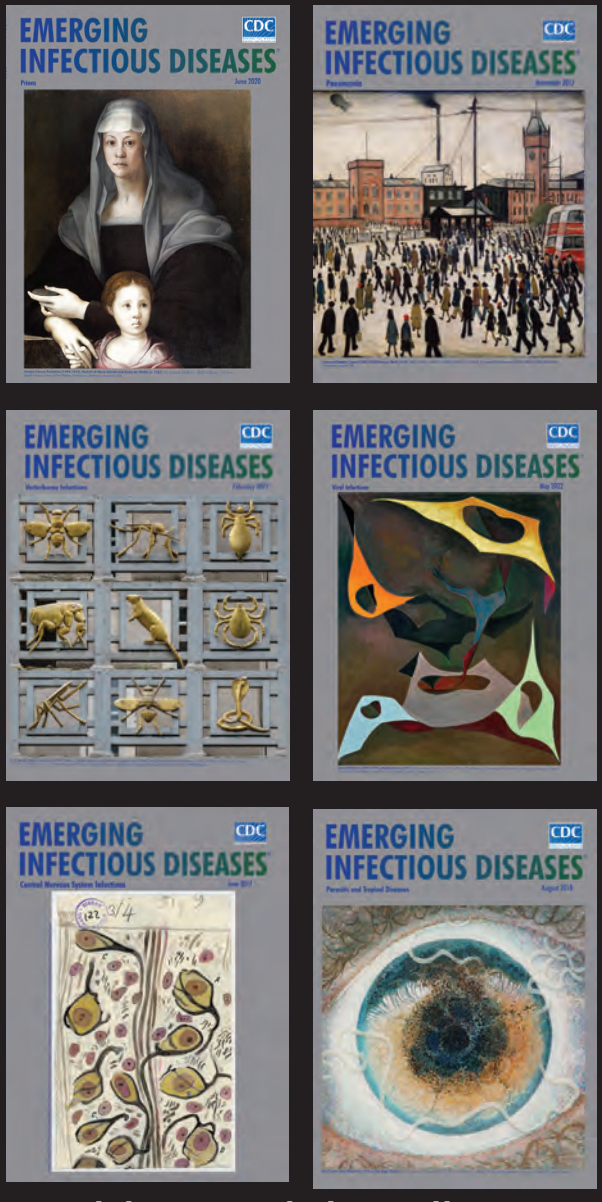

Visit our website to listen:

https://www2c.cdc.gov/podcasts/player.asp?f=8646224

EMERGING INFECTIOUS DISEASES

COVID-19 Symptoms by Variant Period in the North Carolina COVID-19 Community Research Partnership, North Carolina, USA

Michael E. DeWitt, Ashley H. Tjaden, David Herrington, John Schieffelin, Michael Gibbs, William S. Weintraub, John W. Sanders,[1] Sharon L. Edelstein,[1] on behalf of the COVID-19 Community Research Partnership

In North Carolina, USA, the SARS-CoV-2 Omicron variant was associated with changing symptomology in daily surveys, including increasing rates of self-reported cough and sore throat and decreased rates of loss of taste and smell. Compared with the pre-Delta period, Delta and Omicron (pre-BA.4/BA.5) variant periods were associated with shorter symptom duration.

The evolution of SARS-CoV-2 during the COVID-19 pandemic has raised interest in evolving disease manifestation and associated severity since early reports of its emergence in December 2019 (*1*). As SARS-CoV-2 variants have evolved, studies have focused on the differences in hospitalizations and deaths (*2*,*3*). Although case reports have described changes in symptoms, they are limited in scope and duration of follow-up (*4*–*8*). Moreover, because these retrospective case investigations are often event based, separating novel symptoms from preinfection symptoms is subject to recency bias (*9*), and does not establish a true distribution of these symptoms, unlike prospective syndromic surveillance. The purpose of this study was to describe the evolution of COVID-19 symptoms and their duration during each variant wave in the North Carolina COVID-19 Community Research Partnership (NC-CCRP), a multisite longitudinal symptom and serosurveillance study in North Carolina, USA, that included results from an electronic daily symptom survey regardless of infection status.

Author affiliations: Wake Forest University School of Medicine, Winston-Salem, North Carolina, USA (M.E. DeWitt, D. Herrington, J.W. Sanders); The George Washington University Milken Institute of Public Health, Rockville, Maryland, USA (A.H. Tjaden, S.L. Edelstein); Tulane School of Medicine, New Orleans, Louisiana, USA (J.S. Schieffelin); Atrium Health, Charlotte, North Carolina, USA (M.A. Gibbs); MedStar Health, Columbia, Maryland, USA (W.S. Weintraub); Georgetown University, Washington, DC, USA (W.S. Weintraub)

DOI: https://doi.org/10.3201/eid2901.221111

The Study

The NC-CCRP is one of the largest and longest running syndromic surveillance surveys of a convenience cohort in the United States. In the study, a total of 37,820 adult participants completed daily health and symptom logs during April 2020–April 2022 and captured 5,480 self-reported COVID-19 infections (*10*). Adults ≥18 years of age were recruited from the patient populations served by healthcare systems at 6 North Carolina sites via direct email outreach. Participants received a brief daily electronic survey by text or email to answer questions about COVID-19 exposures, symptoms, test results, receipt of vaccination, and risk behaviors. We obtained demographic information and healthcare worker occupation at baseline. Participants provided informed consent electronically. We defined variant periods as pre-Delta, Delta, and Omicron (pre-BA.4/BA.5) based on variant predominance in North Carolina (Figure 1). We defined symptomatic COVID-19 as the presence of ≥1 new symptom 2 weeks before or after the date of a self-reported positive viral test. A new symptom occurred if the symptom was not present in the 7 days before the report date. We defined reinfection as a positive test result >90 days after a previous positive test.

[1]These senior authors contributed equally to this article.

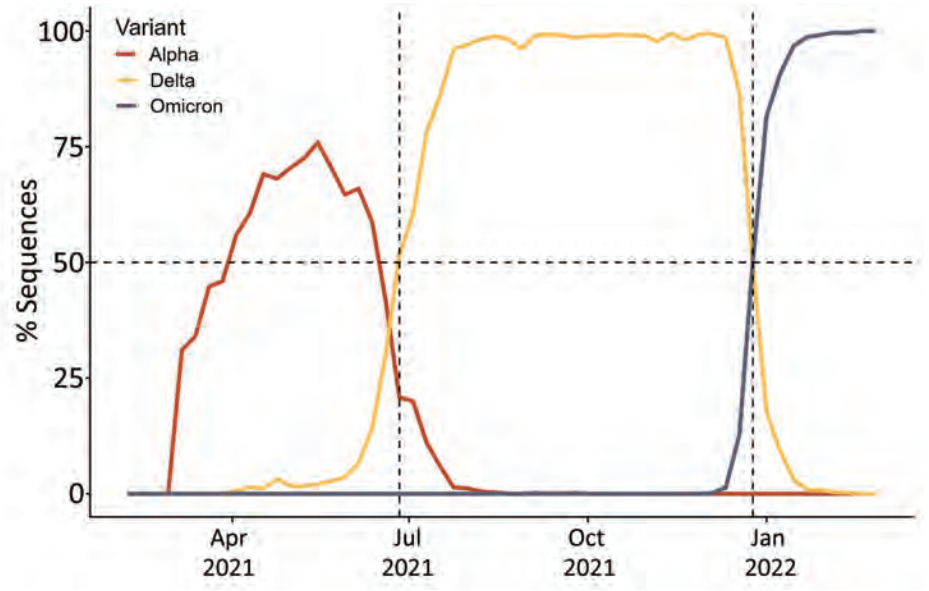

Figure 1. Overview of COVID-19 waves by variant in North Carolina, USA. We defined pre-Delta as an infection before June 26, 2021. Delta was the predominant variant during June 26–December 25, 2021, after which Omicron became dominant. Data were provided by North Carolina Department of Health and Human Services.

We estimated the duration of symptoms using a linear model fit to those persons who had a symptomatic episode during their infection where the predominant variant during infection was the independent variable. We included adjustments for participant sex, vaccination and booster status at infection, prior

Table 1. Overview of demographics and key characteristics of study population in the North Carolina COVID-19 Community Research Partnership study on COVID-19 reinfection, North Carolina, USA*

Characteristic	Pre-Delta, n = 37,711	Delta, n = 24,664	Omicron, n = 19,189
Median age, y (IQR)	49 (37–62)	53 (41–64)	55 (43–65)
Sex			
F	26,001 (69)	17,156 (70)	13,233 (69)
M	11,710 (31)	7,508 (30)	5,956 (31)
Race			
Asian	727 (1.9)	404 (1.6)	296 (1.5)
Black or African American	2,122 (5.6)	1,205 (4.9)	870 (4.5)
White	32,946 (87)	21,985 (89)	17,218 (90)
Other	1,916 (5.1)	1,070 (4.3)	805 (4.2)
Ethnicity			
Other	3,245 (8.6)	1,748 (7.1)	1,266 (6.6)
Hispanic or Latino	942 (2.5)	562 (2.3)	442 (2.3)
Mixed ethnicity	500 (1.3)	317 (1.3)	239 (1.2)
Not Hispanic/Latino	33,024 (88)	22,037 (89)	17,242 (90)
Healthcare worker	10,488 (28)	6,914 (28)	5,077 (26)
Site			
Atrium	8,362 (22)	6,112 (25)	4,983 (26)
Campbell	744 (2.0)	450 (1.8)	259 (1.3)
New Hanover	716 (1.9)	540 (2.2)	0 (0)
Vidant	1,367 (3.6)	692 (2.8)	0 (0)
Wake Forest	23,475 (62)	14,628 (59)	12,122 (63)
Wake Med	3,047 (8.1)	2,242 (9.1)	1,825 (9.5)
Median no. days reporting during wave (IQR)	169 (62–326)	129 (56–167)	47 (22–57)
Vaccination status			
Fully vaccinated by beginning of wave†	1,149 (3.0)	21,772 (88)	18,092 (94)
Fully vaccinated by end of wave†	24,264 (64)	22,597 (92)	18,112 (94)
Boosted by beginning of wave‡	0	122 (0.5)	14,595 (76)
Boosted by end of wave‡	6 (<0.1)	15,623 (63)	15,348 (80)
COVID-19 positive test§	1,908 (5.1)	1,472 (6.0)	2,090 (11)
Reinfection¶	8 (0.4)	43 (2.9)	132 (6.3)
Vaccine breakthrough infection	47 (2.5)	1,233 (84)	1,936 (93)
Booster breakthrough infection	0	360 (24)	1,444 (69)

*Values are no. (%) except as indicated. IQR, interquartile range.
†≥14 days after receipt of first dose if first dose is Johnson & Johnson/Janssen (https://www.jnj.com); ≥14 days after date of receipt of second dose if first dose is Pfizer-BioNTech (https://www.pfizer.com), Moderna (https://www.modernatx.com), other, or missing.
‡Self-reported receipt of a second dose ≥60 days following an initial Janssen vaccination or reported a third dose ≥60 days after the receipt of 2 doses of Pfizer/Moderna/other/missing.
§Self-reported.
¶Self-reported positive test (COVID-19 infection (sample by nasal swab, saliva or spit) ≥90 days after a prior positive test.

infection status, and participant age as potential confounding factors. We generated estimated marginal means to understand the pairwise comparisons between different variant waves. We analyzed symptom frequency and duration for the proportion of participants reporting each symptom and the duration of symptoms occurring ≥1 time during the episode. We used Fisher exact test or χ^2 test to determine symptom frequency between the variant waves and performed Kruskal-Wallis rank sum tests to identify differences in symptom duration. We used false-discovery rate corrections to adjust for multiple comparisons in which $\alpha = 0.05$. We conducted all analysis in R version 4.1.3 (The R Project for Statistical Computing, https://www.r-project.org).

Self-reported reinfections increased from 0.4% during pre-Delta and 2.9% during Delta to 6.3% during Omicron (Table 1). During the pre-Delta period, most infections were among persons not yet fully vaccinated (97.5%). During the Delta and Omicron periods, nearly all participants were fully vaccinated at the time of infection, 84% Delta and 93% Omicron

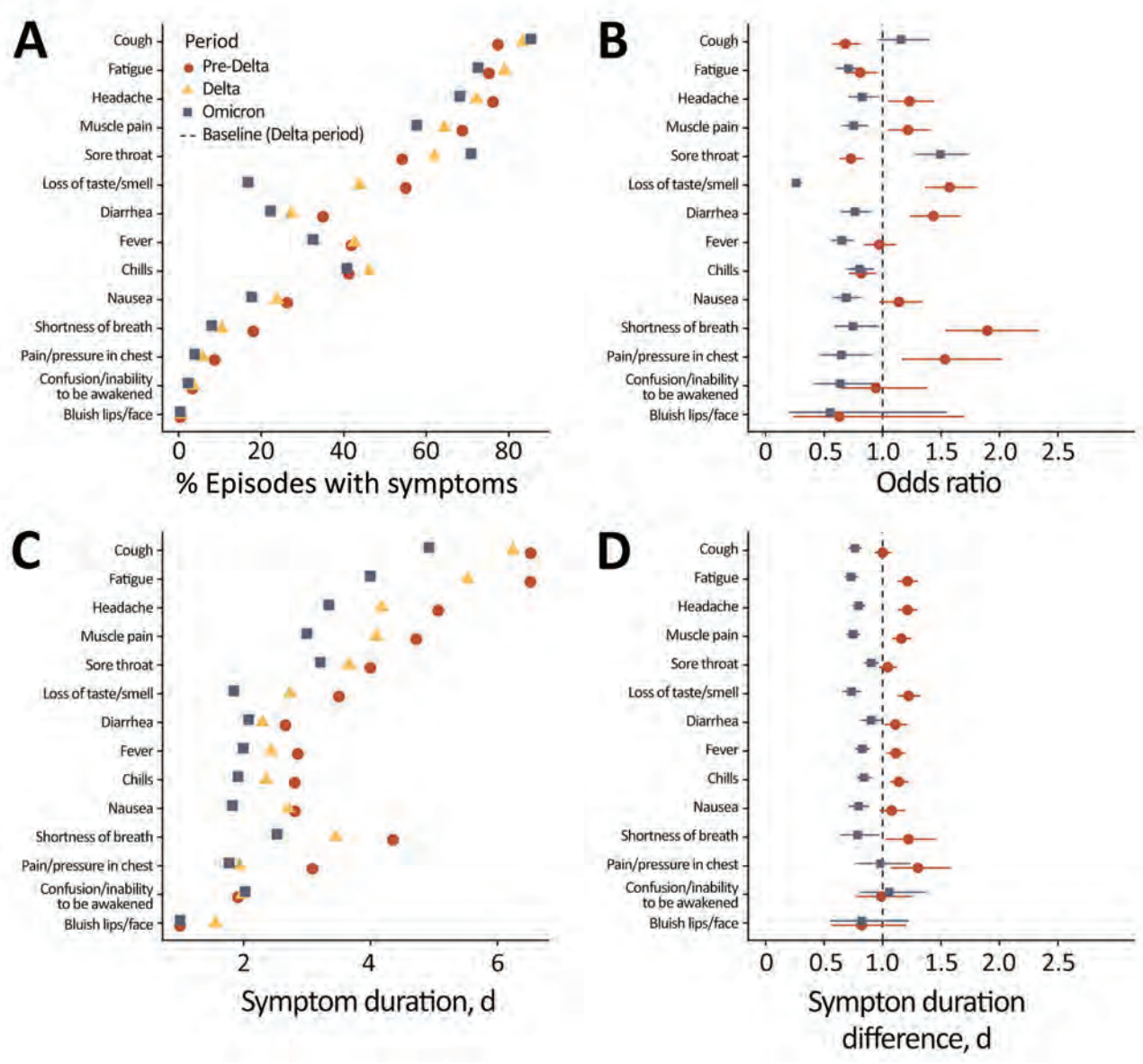

Figure 2. Reported COVID-19 symptoms by variant in the North Carolina COVID-19 Community Research Partnership, North Carolina, USA. A) Proportion of symptomatic persons reporting symptoms; we defined a symptomatic episode as the presence of any new symptoms in the 14-day window, where new means not occurring in the 7 days preceding the first observation of the symptom within the window. B) Odds ratio of reporting a symptom by variant wave using Delta as the baseline. C) Average length of participant-reported symptom duration in a symptomatic infection. D) Difference in symptom duration from Delta-period infections. Error bars represent 95% CIs.

Table 2. Symptom duration among participants reporting symptoms by variant wave in study of COVID-19 infection, North Carolina, USA*

Variant period	Beta (95% CI)†	p value	Marginal mean duration, d (95% CI)‡
Pre-Delta	NA	NA	9.7 (9.0–10.4)
Delta	−1.3 (−2.0 to −0.57)	<0.001	8.4 (7.8–9.1)
Omicron	−3.8 (−4.6 to −3.1)	<0.001	5.9 (5.3–6.4)

*Data are adjusted for age, vaccination status, boosting, reinfection, and sex. NA, not applicable.
†Differences from reference wave (pre-Delta) in the linear model.
‡Marginal mean represents the estimated mean duration of a symptomatic period across all levels of age, vaccination status, boosting, reinfection, and sex.

(Table 1), which corresponded to the higher rates of vaccination in the cohort during these periods. Survey participation rate declined from 37,711 participants during the pre-Delta period to 19,189 participants during the Omicron period; the median age increased from 49 to 55 years of age (Table 1).

Cough was the most frequent self-reported symptom in all waves; it increased from 77% pre-Delta to 85% during Omicron (p = 0.001) (Figure 2, panel A). Sore throat was more common during Omicron (71%), compared with 62% during Delta and 54% during pre-Delta (p<0.001). The largest change in proportion reporting a symptom was loss of taste or smell, which decreased from 55% during pre-Delta to 17% during Omicron (p<0.001). Compared with the pre-Delta period, the Delta (−1.26, 95% CI −1.95 to −0.57) and Omicron periods (−3.82, 95% CI −4.55 to −3.09) were associated with shorter symptom duration (Table 2; Figure 1, panel D). We conducted a sensitivity analysis to examine the effects of different comorbidities; we found that those with autoimmune, pulmonary, and renal diseases and obesity had longer symptom durations when adjusting for variant wave, age, vaccination, prior infection, and sex (Appendix Table 1, https://wwwnc.cdc.gov/EID/article/29/1/22-1111-App1.pdf). We observed no statistically significant interactions between variant period and comorbidity. A sensitivity analysis stratified by those who were and were not fully vaccinated before symptom onset found no appreciable difference in symptomology or length of symptoms than in the whole cohort combined (Appendix Tables 3–4). When we stratified results by variant, vaccination during Delta was associated with lower odds of reporting all individual symptoms except fatigue and sore throat (Appendix Figure 1).

Conclusions

Our results identify notable shifts in clinical manifestation and symptomology during the different phases of the COVID-19 pandemic. These findings support accumulating evidence of increasing occurrences of breakthrough infections in vaccinated and boosted participants and growing rates of reinfection commensurate with the rise in prevalence of the Omicron variant in the United States (*2*,*5*,*11*–*13*).

In this longitudinal survey of self-reported symptoms we found that variant waves were associated with differing symptom prevalence and duration. Overall, these findings largely confirm observations that symptomatic Omicron infections resolve faster with less severe symptomology, often resembling an upper respiratory infection without loss of taste and smell; and are less likely to result in hospitalization (*13*,*14*). Our estimates of marginal mean symptom duration and are consistent with Menni et al.; we found average duration of 8.4 (95% CI 7.8–9.1) days for Delta and 5.9 (95% CI 5.3–6.4) days for Omicron infections. Menni et al. found average symptom durations of 8.89 (95% CI 8.61–9.17) days for Delta and 6.87 (95% CI 6.58–7.16) days for Omicron infections in matched analysis of a prospective longitudinal syndromic study in the United Kingdom (*13*). Studies have shown that Omicron spike is associated with higher ACE2 binding affinity and less efficient S1/S2 cleavage than Delta, resulting in lower rates of syncytia formation (*15*). These changes in cellular tropism may explain the observed shift in symptom presentation and decreased symptom duration during Omicron.

A limitation of this study is that survey participant age declined during the study, whereas median age increased. Those who responded in later periods may have been more likely to report symptoms, and thus our estimates may overstate the duration and intensity of symptoms during the Omicron period. Respondents self-selected for participation, and some participants may be more likely to report symptoms than others, which is a limitation in self-reported symptom surveys. The survey also did not explicitly capture the use of at-home antigen tests, which expanded during the Omicron period.

Despite the lack of individual-level genomic sequencing, we detected significant differences in symptom manifestation and duration; our findings indicate that continued longitudinal syndromic surveillance could be an important component in measuring disease presentation, outcomes, and prevalence.

As COVID-19 becomes endemic and the immune landscape changes through vaccination and infection, understanding symptomology and clinical presentation will be needed to distinguish SARS-CoV-2 from other viral infections and provide insight into evolving pathology.

Acknowledgments

We thank the study participants for their commitment and dedication.

A complete list of study sites, investigators, and staff can be found in the Appendix. The COVID-19 Community Research Partnership is listed in https://www.clinicaltrials.gov (NCT04342884).

Programmatic, laboratory, and technical support was provided by Vysnova Partners, Inc., Oracle, Scanwell Health, and Neoteryx. The US Department of Health and Human Services provided funding for this work through the CARES Act (contract no. NC DHHS GTS #49927).

About the Author

Mr. DeWitt is a research data scientist and biostatistician in Infectious Diseases in the Department of Internal Medicine at Wake Forest University School of Medicine in Winston-Salem, North Carolina. His primary research interests are in the dynamics, detection, and surveillance of infectious diseases.

References

1. Huang C, Wang Y, Li X, Ren L, Zhao J, Hu Y, et al. Clinical features of patients infected with 2019 novel coronavirus in Wuhan, China. Lancet. 2020;395:497–506. https://doi.org/10.1016/S0140-6736(20)30183-5
2. Lewnard JA, Hong VX, Patel MM, Kahn R, Lipsitch M, Tartof SY. Clinical outcomes associated with SARS-CoV-2 Omicron (B.1.1.529) variant and BA.1/BA.1.1 or BA.2 subvariant infection in Southern California. Nat Med. 2022;28:1933–43. https://doi.org/10.1038/s41591-022-01887-z
3. Twohig KA, Nyberg T, Zaidi A, Thelwall S, Sinnathamby MA, Aliabadi S, et al.; COVID-19 Genomics UK (COG-UK) consortium. Hospital admission and emergency care attendance risk for SARS-CoV-2 delta (B.1.617.2) compared with alpha (B.1.1.7) variants of concern: a cohort study. Lancet Infect Dis. 2022;22:35–42. https://doi.org/10.1016/S1473-3099(21)00475-8
4. Ulyte A, Radtke T, Abela IA, Haile SR, Berger C, Huber M, et al. Clustering and longitudinal change in SARS-CoV-2 seroprevalence in school children in the canton of Zurich, Switzerland: prospective cohort study of 55 schools. BMJ. 2021;372:n616. https://doi.org/10.1136/bmj.n616
5. Brandal LT, MacDonald E, Veneti L, Ravlo T, Lange H, Naseer U, et al. Outbreak caused by the SARS-CoV-2 Omicron variant in Norway, November to December 2021. Euro Surveill. 2021;26:2101147. https://doi.org/10.2807/1560-7917.ES.2021.26.50.2101147
6. Espenhain L, Funk T, Overvad M, Edslev SM, Fonager J, Ingham AC, et al. Epidemiological characterisation of the first 785 SARS-CoV-2 Omicron variant cases in Denmark, December 2021. Euro Surveill. 2021;26:26. https://doi.org/10.2807/1560-7917.ES.2021.26.50.2101146
7. Lorthe E, Bellon M, Berthelot J, Michielin G, L'Huillier AG, Posfay-Barbe KM, et al.; SEROCoV-Schools Study Group. A SARS-CoV-2 omicron (B.1.1.529) variant outbreak in a primary school in Geneva, Switzerland. Lancet Infect Dis. 2022;22:767–8. https://doi.org/10.1016/S1473-3099(22)00267-5
8. CDC COVID-19 Response Team. SARS-CoV-2 B.1.1.529 (Omicron) variant—United States, December 1–8, 2021. MMWR Morb Mortal Wkly Rep. 2021;70:1731–4. https://doi.org/10.15585/mmwr.mm7050e1
9. Van den Bergh O, Walentynowicz M. Accuracy and bias in retrospective symptom reporting. Curr Opin Psychiatry.2016; 29:302–8. https://doi.org/10.1097/YCO.0000000000000267
10. Sanders JW; The COVID-19 Community Research Partnership. The COVID-19 Community Research Partneship; a multistate surveillance platform for characterizing the epidemiology of the SARS-CoV-2 pandemic. Biol Methods Protoc. 2022 Nov 28 [Epub ahead of print]. https://doi.org/10.1093/biomethods/bpac033
11. Tartof SY, Slezak JM, Fischer H, Hong V, Ackerson BK, Ranasinghe ON, et al. Effectiveness of mRNA BNT162b2 COVID-19 vaccine up to 6 months in a large integrated health system in the USA: a retrospective cohort study. Lancet. 2021;398:1407–16. https://doi.org/10.1016/S0140-6736(21)02183-8
12. Gray G, Collie S, Goga A, Garrett N, Champion J, Seocharan I, et al. Effectiveness of Ad26.COV2.S and BNT162b2 vaccines against Omicron variant in South Africa. N Engl J Med. 2022;386:2243–5. https://doi.org/10.1056/NEJMc2202061
13. Menni C, Valdes AM, Polidori L, Antonelli M, Penamakuri S, Nogal A, et al. Symptom prevalence, duration, and risk of hospital admission in individuals infected with SARS-CoV-2 during periods of omicron and delta variant dominance: a prospective observational study from the ZOE COVID Study. Lancet. 2022;399:1618–24. https://doi.org/10.1016/S0140-6736(22)00327-0
14. Vihta KD, Pouwels KB, Peto TEA, Pritchard E, House T, Studley R, et al. Omicron-associated changes in severe acute respiratory syndrome coronavirus 2 (SARS-CoV-2) symptoms in the United Kingdom. Clin Infect Dis. 2022 Aug 3 [Epub ahead of print]. https://doi.org/10.1093/cid/ciac613
15. Meng B, Abdullahi A, Ferreira IATM, Goonawardane N, Saito A, Kimura I, et al.; CITIID-NIHR BioResource COVID-19 Collaboration; Genotype to Phenotype Japan (G2P-Japan) Consortium; Ecuador-COVID19 Consortium. Altered TMPRSS2 usage by SARS-CoV-2 Omicron impacts infectivity and fusogenicity. Nature. 2022;603:706–14. https://doi.org/10.1038/s41586-022-04474-x

Address for correspondence: Michael DeWitt, Section on Infectious Diseases, Wake Forest University School of Medicine, Medical Center Blvd, Winston-Salem, NC 27157, USA; email: medewitt@wakehealth.edu

DAVID J. SENCER CDC MUSEUM

History·Legacy·Innovation

Dr. David J. Sencer, Mrs. Mountin and Jim Collins celebrate CDC's 25th anniversary, 1961.

CDC at 75

January 9, 2023–July 28, 2023

TEMPORARY EXHIBITIONS GALLERY

Opening January 9, *CDC at 75* is a commemorative exhibition that tells unique stories about the work of this fabled agency and provides a glimpse into the breadth and depth of CDC's history and vast accomplishments. It features rarely seen objects, documents, and media taken from the CDC Museum's rich collections and archives.

Hours

Monday–Wednesday: 9 a.m.–5 p.m.
Thursday: 9 a.m.–7 p.m.
Friday: 9 a.m.–5 p.m.
Closed weekends and federal holidays

Location

1600 Clifton Road, NE
Atlanta, GA
30329-4021
Phone (404) 639-0830

Admission and parking free • Vehicle inspection required
Government-issued photo ID required for adults over the age of 18
Passport required for non-U.S. citizens

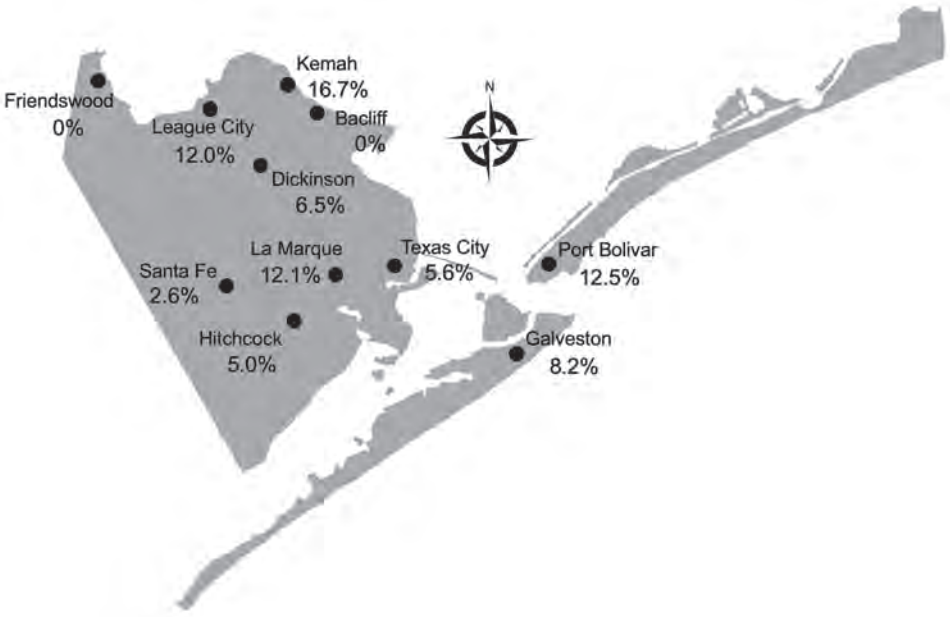

Figure. *Rickettsia typhi* seroprevalence in communities of Galveston County, Texas, USA, 2021. We tested 528 serum samples from persons across Galveston County by using indirect immunofluorescence assay and Western blot tests. Percentage seropositivity for each area is shown.

of Texas Medical Branch institutional review board (protocol no. 20-0259).

We tested 528 serum samples from persons across Galveston County (Table). Most (376/528, 71.2%) specimens were from female patients with a median age of 51 years. IFA reactivity was demonstrated in 46 (8.7%) persons, among whom 41 (7.8%) had confirmed seroreactivity (i.e., reactive by both IFA and Western blot). The geometric mean reciprocal titer was 521, which is much higher than the value of 197 we noted in 2013 ($p<0.04$). Seropositive specimens were found in all communities except Friendswood and Bacliff (Figure). Compared with the 1.6% (8/500) seroprevalence in the city of Galveston in 2013, which we obtained with the same methodology used in this study, we noted a higher seroprevalence in both the city of Galveston (8.2%, 12/146; $p<0.001$) and throughout Galveston County (7.8%, 41/528; $p<0.001$) in 2021.

The increased seroprevalence of *R. typhi* reactive antibodies supports the hypothesis that the increase in TGR cases reported in Galveston County is because of pathogen reemergence in this region, rather than enhanced clinical recognition alone. Considering the kinetics of *R. typhi* antibody (*8*), the higher geometric mean titer supports more recent seroconversion in the 2021 sample cohort, further supporting our hypothesis. Regional changes in the zoonotic transmission cycle could be contributing to this increase. Such changes might include a shift from the classic rat–rat flea urban transmission cycle to one involving opossums and cat fleas. In addition, another study demonstrated high *R. typhi* seropositivity (66.7%) in opossums and a high proportion of *R. typhi*–infected fleas (7%) collected from these animals in Galveston (*9*). More studies are needed to understand the ecology of TGR and risk to public health. Clinicians and public health officials should be aware of the increase of *R. typhi* seropositivity in the Galveston area and recognize the signs and symptoms of murine typhus.

Acknowledgments

We thank the staff of the University of Texas Medical Branch Clinical Laboratory for providing material for completion of this study.

About the Author

Dr. Blanton is an infectious disease physician and associate professor of medicine at the University of Texas Medical Branch, Galveston, Texas, USA. His research interests focus on the study of rickettsial diseases.

References

1. Civen R, Ngo V. Murine typhus: an unrecognized suburban vectorborne disease. Clin Infect Dis. 2008;46:913–8. https://doi.org/10.1086/527443
2. Azad AF, Radulovic S, Higgins JA, Noden BH, Troyer JM. Flea-borne rickettsioses: ecologic considerations. Emerg Infect Dis. 1997;3:319–27. https://doi.org/10.3201/eid0303.970308
3. Pratt HD. The changing picture of murine typhus in the United States. Ann N Y Acad Sci. 1958;70:516–27. https://doi.org/10.1111/j.1749-6632.1958.tb35408.x
4. Blanton LS, Vohra RF, Bouyer DH, Walker DH. Reemergence of murine typhus in Galveston, Texas, USA, 2013. Emerg Infect Dis. 2015;21:484–6. https://doi.org/10.3201/eid2103.140716

5. Ruiz K, Valcin R, Keiser P, Blanton LS. Rise in murine typhus in Galveston County, Texas, USA, 2018. Emerg Infect Dis. 2020;26:1044–6. https://doi.org/10.3201/eid2605.191505
6. Murray KO, Evert N, Mayes B, Fonken E, Erickson T, Garcia MN, et al. Typhus group rickettsiosis, Texas, USA, 2003–2013. Emerg Infect Dis. 2017;23:645–8. https://doi.org/10.3201/eid2304.160958
7. Vishwanath S. Antigenic relationships among the rickettsiae of the spotted fever and typhus groups. FEMS Microbiol Lett. 1991;81:341–4. https://doi.org/10.1111/j.1574-6968.1991.tb04783.x
8. Phakhounthong K, Mukaka M, Dittrich S, Tanganuchitcharnchai A, Day NPJ, White LJ, et al. The temporal dynamics of humoral immunity to *Rickettsia typhi* infection in murine typhus patients. Clin Microbiol Infect. 2020;26:781.e9-781.e16. https://doi.org/10.1016/j.cmi.2019.10.022
9. Blanton LS, Idowu BM, Tatsch TN, Henderson JM, Bouyer DH, Walker DH. Opossums and cat fleas: new insights in the ecology of murine typhus in Galveston, Texas. Am J Trop Med Hyg. 2016;95:457–61. https://doi.org/10.4269/ajtmh.16-0197

Address for correspondence: Lucas S. Blanton, University of Texas Medical Branch, 301 University Blvd, Galveston, TX 77555-0435, USA; email: lsblanto@utmb.edu

Short-Finned Pilot Whale Strandings Associated with Pilot Whale Morbillivirus, Brazil

Samira Costa-Silva, Carlos Sacristán, Rodrigo M. Soares, Vitor L. Carvalho, Pedro V. Castilho, Marta J. Cremer, Ana Carolina Ewbank, Arícia Duarte-Benvenuto, Thalita Faita, Pedro E. Navas-Suárez, Jenyffer V. Vieira, Letícia G. Pereira, Carolina F. Alves, Gabriela C. Souza, Giulia G. Lemos, Natália Silvestre-Perez, José L. Catão-Dias, Lara B. Keid

Author affiliations: Universidade de São Paulo, São Paulo, Brazil (S. Costa-Silva, C. Sacristán, R.M. Soares, A.C. Ewbank, A. Duarte-Benvenuto, T. Faita, P.E. Navas-Suárez, N. Sivestre-Perez, J. Catão-Dias); Centro de Investigación en Sanidad Animal (CISA-INIA), CSIC, Madrid, Spain (C. Sacristán); Associação de Pesquisa e Preservação de Ecossistemas Aquáticos, Caucáia, Brazil (V.L. Carvalho, L.G. Pereira); Universidade do Estado de Santa Catarina, Laguna, Brazil (P.V. Castilho, C.F. Alves, G.C. Souza); Universidade da Região de Joinville, Sao Francisco do Sul, Brazil (M.J. Cremer, J.V. Vieira, G.G. Lemos); Universidade de São Paulo, Pirassununga, Brazil (L.B. Keid)

DOI: https://doi.org/10.3201/eid2901.221549

Cetacean morbillivirus (CeMV) causes illness and death in cetaceans worldwide; the CeMV strains circulating in the Southern Hemisphere are poorly known. We detected a pilot whale CeMV strain in 3 short-finned pilot whales (*Globicephala macrorhynchus*) stranded in Brazil during July–October 2020. Our results confirm this virus circulates in this species.

Cetacean morbillivirus (CeMV; family Paramyxoviridae, genus *Morbillivirus*) is an important cause of illness and death in cetaceans (*1*). The genus *Morbillivirus* comprises 2 lineages: CeMV-1, which includes dolphin morbillivirus (DMV), porpoise morbillivirus (PMV), pilot whale morbillivirus (PWMV), and beaked whale morbillivirus (BWMV) strains; and CeMV-2, comprising the strain detected in Indo-Pacific bottlenose dolphins (*Tursiops aduncus*) in western Australia, the Fraser's dolphin morbillivirus (FDMV), and Guiana dolphin morbillivirus (GDMV) strains (*1*,*2*). GDMV has been the only strain reported in cetaceans in Brazil (*3*). Four cases of PWMV have been recorded in pilot whales of the Northern Hemisphere, on the Atlantic coast of the United States and in the Canary Islands, Spain (*4*,*5*).

During July–October 2020, four short-finned pilot whales (*Globicephala macrorhynchus*) stranded in Brazil: 2 in Ceará state (cases 1 and 2) and 2 in Santa Catarina state (cases 3 and 4). All the animals stranded alive and died within 24 hours (Appendix Figure 1, https://wwwnc.cdc.gov/EID/article/29/1/22-1549-App1.pdf). We performed standard necropsies and collected tissue samples, which we fixed in 10% buffered formalin for histopathology or froze at –20°C or –80°C for molecular analysis.

We performed RNA extractions of all available tissues with TRIzol-LS (Life Technologies Corporation, https://www.thermofisher.com). We performed a morbillivirus 2-step reverse transcription nested PCR to amplify the phosphoprotein gene (*6*). After DNA extraction with the QIAGEN Blood & Tissue Kit (QIAGEN, https://www.qiagen.com), we performed herpesvirus detection in lung (n = 2) and liver (n = 4) samples by nested pan-PCRs to amplify DNA polymerase and glycoprotein B genes (*7*); when those were positive, we tested the remaining

available tissues using the same protocols. We calculated percentage of identity among the obtained sequences and the closest ones from GenBank/EMBL/DDBJ based on p-distance. We used MEGA7 (https://www.megasoftware.net) to construct the phylogram (Figure).

Three animals, cases 1, 3 and 4, were morbillivirus-positive, amplified in central nervous system, lung, and pulmonary lymph node samples (Table, https://wwwnc.cdc.gov/EID/article/29/1/22-1549-T1.htm); sequences were submitted to GenBank (case 1, accession no. OP375347; case 3, OP375348; case 4, OP375349). Sequences from case 1 and 3 were identical and had a single nucleotide missense mutation (99.7% nt identity, 99.2% aa identity) when compared to the sequence from case 4. The sequences from cases 1 and 3 presented the highest nucleotide (99%) and amino acid identities (96.9%) with a PWMV sequence identified in 2 pilot whales in the Canary Islands, Spain (GenBank accession nos. KT006289 [animal 1], KT006290, and KT006291 [animal 2]). The sequence from case 4 had the highest nucleotide (99.2%) and amino acid similarities (97.7%) to the same PWMV sequences. Our sequences clustered with other PWMV sequences (Figure). In addition, we detected an alphaherpesvirus by the DNA polymerase protocol in a lung sample from case 3 (GenBank accession no. OP341880). The remaining tissue samples of case 3 (cerebellum, kidney, mesenteric lymph node, spleen, and liver) were

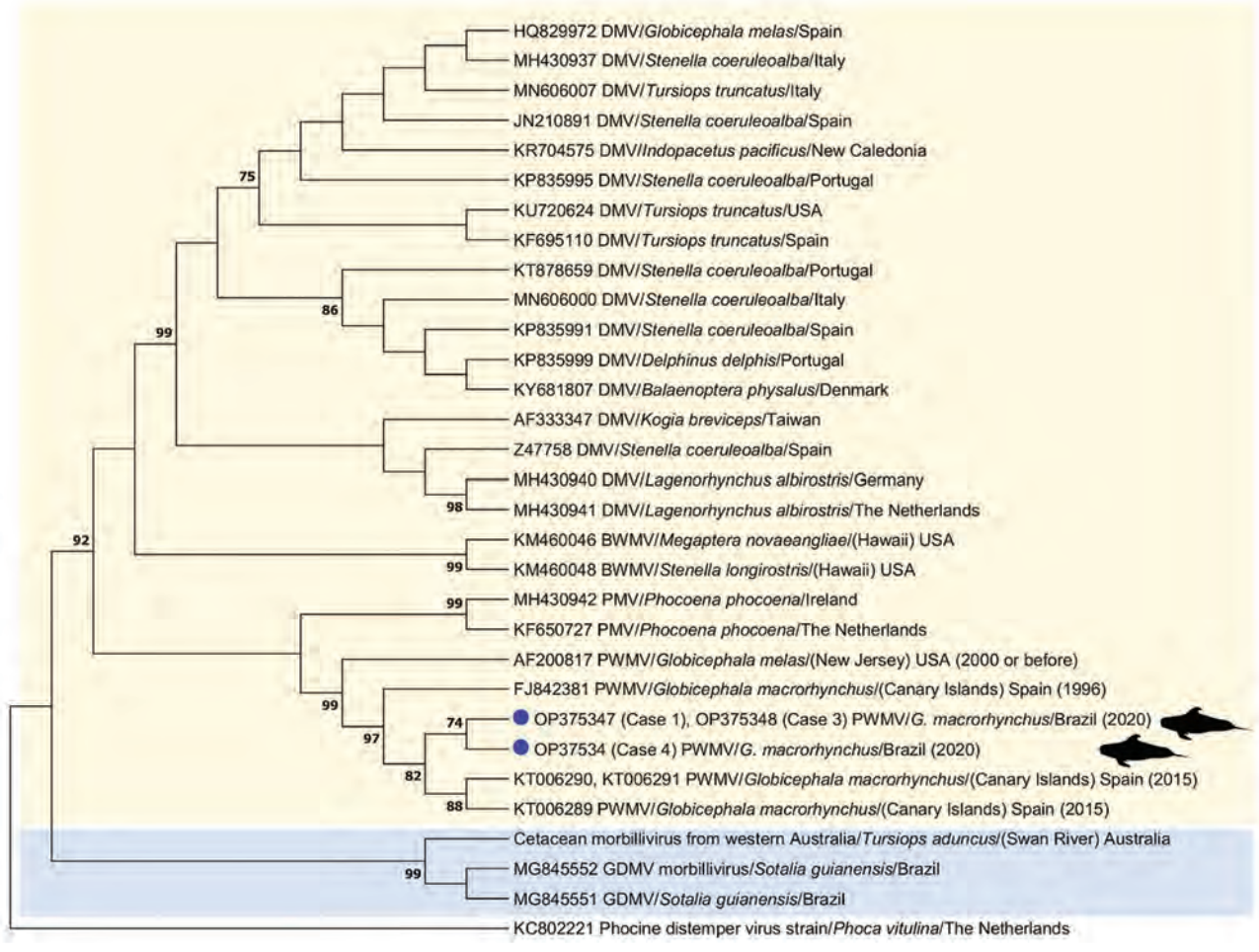

Figure. Maximum-likelihood phylogenetic tree based on Hasegawa-Khisino-Yano model with inversions gamma distribution and invariant sites of the phosphoprotein gene nucleotide sequences of cetacean morbillivirus PWMV obtained in Brazil (this study, blue circles), PWMV sequences previously described, and other morbillivirus strains described in cetaceans available from the GenBank/DDBJ/EMBL databases. Phocine distemper virus was selected as outgroup. The sequence identifier shows GenBank accession number, virus type, and location. Yellow shading indicates strains comprised in *Cetacean morbillivirus* lineage 1; blue shading indicates strains in lineage 2. Numbers at nodes indicate the bootstrap value; 1,000 bootstrap replications were selected, and bootstrap values <70 were omitted. BWMV, beaked whale morbillivirus; DMV, dolphin morbillivirus; GDMV, Guiana dolphin morbillivirus; PMV, porpoise morbillivirus; PWMV, pilot whale morbillivirus.

herpesvirus-negative by PCR. The obtained herpesvirus has the highest similarity (99.5% nt identity, 100% aa identity) to an alphaherpesvirus obtained in a striped dolphin (*Stenella coeruleoalba*) from Spain (GenBank accession no. GQ888671).

The general health of the CeMV-positive animals was poor, and all were undernourished. We compared the main pathologic findings in these animals to all other cases of PWMV strain reported in the literature (Table).

Pilot whales are susceptible to DMV and PWMV; DMV cause atypical pilot whale deaths in the Mediterranean Sea (*6*). By contrast, 4 cases of PWMV infections have been recorded; 1 in New Jersey, USA, and 3 in the Canary Islands, Spain (*4*–*6*,*9*,*10*). All of them had multiorgan infections (*4*,*5*). Case 1 likely had a subacute or systemic CeMV infection characterized by meningomyelitis with gliosis and lymphocytic bronchointerstitial pneumonia. Further studies are necessary to elucidate if cases 3 and 4 manifested an infection similar to the brain-only DMV form or a systemic infection with heterogenic dissemination. The poor nutritional condition observed in all PWMV-positive animals could be the result of decreased foraging capacity caused by encephalitis (*1*). Case 3 had alphaherpesvirus and CeMV co-infection, a comorbidity previously reported in cetaceans, including pilot whales (*5*,*10*); in this case, however, there were no associated herpesviral lesions. All PWMV-positive cetaceans we described were juveniles, which could be associated with maternal passive immunity loss.

The occurrence of pilot whale strandings in 2020 on the coast of Brazil could be considered atypical. Of interest, although case 1 was stranded >3,300 km away from case 3 along the coastline, it had the same PWMV sequence type, which suggests circulation of that type along the coast of Brazil. Further studies are necessary to understand the effects and epidemiology of morbillivirus in cetaceans in the South Atlantic Ocean. However, the high similarity between our sequences and the PWMV detected in the Northern Hemisphere confirms that this strain also circulates in South America pilot whales and might be enzootic in *Globicephala* sp. whales in the Atlantic Ocean.

Acknowledgments

We thank Aquasis, Universidade do Estado de Santa Catarina (UDESC), and Universidade da Região de Joinville (UNIVILLE) for logistic and technical support. We thank the Santos Basin Beach Monitoring Project (Projeto de Monitoramento de Praias da Bacia de Santos, PMP-BS) and Potiguar Basin Beach Monitoring Project (Projeto de Monitoramento de Praias da Bacia Potiguar, PMP-BP), conducted by Petrobrás, licensed by the Brazilian Institute of the Environment and Renewable Natural Resources of the Brazilian Ministry of Environment under ABIO no. 640/2015.

The Coordination for the Improvement of Higher Education Personnel (CAPES), National Council for Technological and Scientific Development (CNPq), and São Paulo Research Foundation (FAPESP) provided financial support. S.C.S. and A.C.E. received PhD fellowships by FAPESP (process nos. 2020/12434-9 and 2016/20956-0). L.B.K. received financial support from FAPESP (no. 2020/12434-9). J.L.C.-D., L.B.K. and M.J.C. are recipients of research productivity fellowships from CNPq (nos. 304999-18, 315619/2021-0, and 313577/2020-0, respectively),C.S. is a recipient of a Juan de la Cierva incorporación fellowship (no. IJC2020-046019-I) and received a postdoctoral grant by FAPESP (no. 2018/25069-7).

About the Author

Dr. Costa-Silva, a veterinarian specialist in marine mammals, completed this project as part of her PhD project in the Department of Preventive Veterinary Medicine and Animal Health, School of Veterinary Medicine and Animal Science, University of São Paulo.

References

1. Van Bressem MF, Duignan PJ, Banyard A, Barbieri M, Colegrove KM, De Guise S, et al. Cetacean morbillivirus: current knowledge and future directions. Viruses. 2014;6:5145–81. https://doi.org/10.3390/v6125145
2. West KL, Silva-Krott I, Landrau-Giovannetti N, Rotstein D, Saliki J, Raverty S, et al. Novel cetacean morbillivirus in a rare Fraser's dolphin (*Lagenodelphis hosei*) stranding from Maui, Hawai'i. Sci Rep. 2021;11:15986. https://doi.org/10.1038/s41598-021-94460-6
3. Groch KR, Groch KR, Kolesnikovas CKM, de Castilho PV, Moreira LMP, Barros CRMB, et al. Cetacean morbillivirus in southern right whales, Brazil. Transbound Emerg Dis. 2019;66:606–10. https://doi.org/10.1111/tbed.13048
4. Bellière EN, Esperón F, Fernández A, Arbelo M, Muñoz MJ, Sánchez-Vizcaíno JM. Phylogenetic analysis of a new cetacean morbillivirus from a short-finned pilot whale stranded in the Canary Islands. Res Vet Sci. 2011;90:324–8. https://doi.org/10.1016/j.rvsc.2010.05.038
5. Sierra E, Fernández A, Suárez-Santana C, Xuriach A, Zucca D, Bernaldo de Quirós Y, et al. Morbillivirus and pilot whale deaths, Canary Islands, Spain, 2015. Emerg Infect Dis. 2016;22:740–2. https://doi.org/10.3201/eid2204.150954
6. Fernández A, Esperón F, Herraéz P, de Los Monteros AE, Clavel C, Bernabé A, et al. Morbillivirus and pilot whale deaths, Mediterranean Sea. Emerg Infect Dis. 2008;14:792–4. https://doi.org/10.3201/eid1405.070948
7. Sacristán C, Esperón F, Ewbank AC, Costa-Silva S, Marigo J, Matushima ER, et al. Identification of novel gammaherpesviruses in a South American fur seal (*Arctocephalus australis*) with ulcerative skin lesions. J Wildl Dis. 2018;54:592–6. https://doi.org/10.7589/2017-09-224

8. Taubenberger JK, Tsai MM, Atkin TJ, Fanning TG, Krafft AE, Moeller RB, et al. Molecular genetic evidence of a novel morbillivirus in a long-finned pilot whale (*Globicephalus melas*). Emerg Infect Dis. 2000;6:42–5. https://doi.org/10.3201/eid0601.000107
9. Duignan PJ, House C, Geraci JR, Early G, Copland HG, Walsh MT, et al. Morbillivirus infection in two species of pilot whale (*Globicephala* sp.) from the western Atlantic. Mar Mamm Sci. 1995;11:150–62. https://doi.org/10.1111/j.1748-7692.1995.tb00514.x
10. Di Guardo G, Mazzariol S. Cetacean morbillivirus-associated pathology: knowns and unknowns. Front Microbiol. 2016;7:112. https://doi.org/10.3389/fmicb.2016.00112

Address for correspondence: Samira Costa-Silva, Av. Duque de Caxias Norte, 225, Bairro, Jardim Elite (campus da USP), Pirassununga, São Paulo, 13635-900, Brazil; email: costasilva.samira@gmail.com

Catheter-Related Bloodstream Infection Caused by *Mycolicibacterium iranicum*, California, USA

Elizabeth L. Ranson, Rebecca K. Tsevat, Benjamin von Bredow, Edwin Kamau, Shangxin Yang, Kavitha K. Prabaker

Author affiliations: University of California, Los Angeles, California, USA

DOI: https://doi.org/10.3201/eid2901.220851

We describe a case of catheter-related bacteremia caused by *Mycolicibacterium iranicum* in the United States. The case highlights the value of using next-generation sequencing to identify infrequent and emerging pathogens and the challenges associated with choosing appropriate treatments because of limited knowledge of drug resistance mechanisms in those emerging pathogens.

Mycolicibacterium iranicum is a rapidly growing mycobacterium (RGM) and emerging cause of respiratory, wound, blood, and central nervous system infections (*1*,*2*). Phylogenetic analyses have shown that *M. iranicum* is more closely related to environmental mycobacterial species than pathogenic species (*3*), and most outbreaks have been associated with exposure to contaminated water (*4*,*5*).

Reports of nontuberculous mycobacteria infections have been increasing worldwide (*6*,*7*), predominantly in immunocompromised patients with hematologic or oncologic medical conditions (*6*). The rise in RGM detection is likely because of increased prevalence of immunocompromising conditions and improved access to molecular diagnostics (*7*). Molecular techniques, especially sequencing multiple conserved genes, such as *rrs* (16S rRNA), *rpoB*, and *groEL* (*hsp65*) (*4*), have led to a dramatic increase in mycobacterial species identified during the past 30 years. We describe a case of *M. iranicum* bacteremia associated with a long-term percutaneous catheter in an immunocompromised patient.

A woman, 76 years of age, with a history of polymyositis and hypertrophic obstructive cardiomyopathy was admitted to an academic hospital in Los Angeles, California, USA, because of substernal chest pain and dyspnea that began 1 day before. Her medications included prednisone (15 mg/d) and intravenous immunoglobulin (20 g administered every 10 days through a port-a-cath that had been in place for several years). The patient had taken mycophenolate mofetil until a month before hospital admission. During each intravenous immunoglobulin infusion over the past 2 years, she had experienced fevers, which were attributed to an infusion reaction. The most recent infusion was 4 days before admission.

The patient reported fatigue and generalized weakness for several days and an unintentional 25-pound weight loss over the past year. On hospital day 2, she was febrile with a temperature of 101°F (Appendix Figure, https://wwwnc.cdc.gov/EID/article/29/1/22-0851-App1.pdf). Results of a preliminary work-up were unrevealing; however, after 4 days of incubation, multiple aerobic blood cultures (in BACTEC FX aerobic and F lytic media; Becton Dickinson, https://www.bd.com) taken from her port grew beaded, gram-positive rods with yellow mycobacteria-like colonies (Appendix Figure). Matrix-assisted laser desorption/ionization time-of-flight (MALDI-TOF) mass spectrometry failed to identify the isolate. We performed a laboratory-developed, next-generation sequencing-based test that identified the organism as *Mycolicibacterium iranicum*, which we further verified using k-mer–based phylogenic analysis (Figure) (*8*). Using a previously described method for detection of macrolide resistance in *Mycobacteroides abscessus* (*9*), we did not detect a functional *erm* gene.

When blood cultures demonstrated *Mycobacterium* sp., we changed therapy and administered

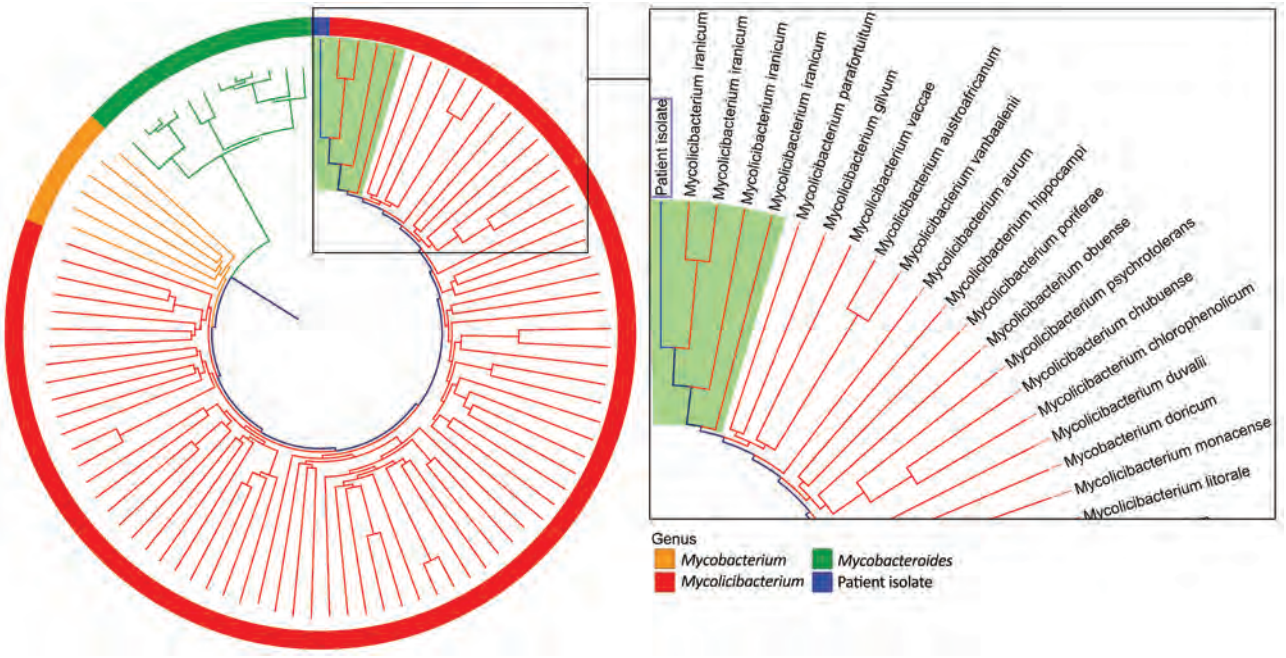

Figure. Phylogenetic tree of an isolate from a 76-year old woman in California, USA (blue box), compared with a selection of relevant members of the family Mycobacteriaceae in a case study of catheter-related bloodstream infection caused by *Mycolicibacterium iranicum.* Relatedness was determined by k-mer analysis. Reference genomes were from 4 *Mycolicibacterium iranicum* isolates, 74 other *Mycolicibacterium* spp., 12 *Mycobacteroides abscessus* isolates, and 6 clinically relevant slow-growing *Mycobacterium* spp. Light green background indicates *M. iranicum* isolates. The clinical isolate in this case study was clustered most closely with all 4 *M. iranicum* genomes. Tree is not scale and is designed to show clustering.

imipenem, amikacin, and azithromycin. We avoided fluoroquinolones because of the patient's history of seizures on ciprofloxacin. The patient's port was extracted. After 13 days, we changed her treatment regimen to doxycycline, azithromycin, and trimethoprim/sulfamethoxazole. Because of intolerable gastrointestinal symptoms, doxycycline treatment was discontinued. The patient was discharged, and azithromycin and trimethoprim/sulfamethoxazole treatments were continued with the presumption that her isolate was macrolide-susceptible because it lacked the *erm* gene. We determined the drug MIC by broth microdilution following Clinical and Laboratory Standards Institute guidelines, and the organism was susceptible to all drugs tested except clarithromycin, to which the organism was resistant with a MIC of 8.0 mg/L. After 4 weeks of therapy, when the MIC results were available, we discontinued azithromycin, added doxycycline, and continued trimethoprim/sulfamethoxazole treatment. The patient again did not tolerate doxycycline. After 6 weeks of targeted therapy, the patient's fevers resolved, blood cultures were negative, and therapy was ended.

Catheter-related bloodstream infections (CRBSIs) are the most common type of healthcare-associated RGM infection (*6*). Primary risk factors for RGM CRBSIs are immunosuppression, extended catheter placement, and previous antimicrobial therapy; our patient had all 3 risk factors (*4*–*6*). RGM form dense biofilms, which appear to be integral both to their survival in hostile environments and pathogenesis of CRBSIs (*5*,*7*). Successful treatment of nontuberculous mycobacterial CRBSIs usually necessitates catheter removal (*4*,*5*,*10*).

Except for 1 report of bacteremia resistant to clarithromycin, ethambutol, rifabutin, and trimethoprim/sulfamethoxazole, previously reported isolates of *M. iranicum* have been susceptible to all tested drugs (*1*,*2*). Macrolide resistance in RGM is best understood for *M. abscessus* in which specific *rrl* gene mutations mediate constitutive resistance, whereas an intact *erm*(41) gene confers inducible resistance (*9*). We used azithromycin when no *erm*(41)-like gene was detected in the patient's isolate, but susceptibility testing later revealed macrolide resistance. Macrolide resistance without *erm*(41) or other *erm*-like genes suggests that inducible macrolide resistance may be mediated by a different mechanism. Comparative genomic analysis suggests that *M. iranicum* could acquire multiple drug resistance genes by horizontal transfer (*3*). Molecular resistance mechanisms for *M. iranicum* are not well characterized, and

our case highlights the challenges of genotypic resistance prediction in uncommon RGM species.

In summary, we report a case of *M. iranicum* CRB-SI that was treated successfully with catheter removal and 2 weeks of amikacin and imipenem followed by 4 weeks of de facto monotherapy with trimethoprim/sulfamethoxazole. This case illustrates the value of using next generation sequencing to identify novel pathogens and the challenges of choosing appropriate treatment because of limited knowledge of drug-resistance mechanisms.

About the Author

Dr. Ranson is an infectious diseases fellow at the University of California, Los Angeles, CA. Her primary research interests focus on care delivery for people living with HIV and injection drug users.

References

1. Grandjean Lapierre S, Toro A, Drancourt M. *Mycobacterium iranicum* bacteremia and hemophagocytic lymphohistiocytosis: a case report. BMC Res Notes. 2017;10:372. https://doi.org/10.1186/s13104-017-2684-8
2. Shojaei H, Daley C, Gitti Z, Hashemi A, Heidarieh P, Moore ERB, et al. *Mycobacterium iranicum* sp. nov., a rapidly growing scotochromogenic species isolated from clinical specimens on three different continents. Int J Syst Evol Microbiol. 2013;63:1383–9. PubMed https://doi.org/10.1099/ijs.0.043562-0
3. Tan JL, Ngeow YF, Wee WY, Wong GJ, Ng HF, Choo SW. Comparative genomic analysis of *Mycobacterium iranicum* UM_TJL against representative mycobacterial species suggests its environmental origin. Sci Rep. 2014;4:7169. https://doi.org/10.1038/srep07169
4. Griffith DE, Aksamit T, Brown-Elliott BA, Catanzaro A, Daley C, Gordin F, et al.; ATS Mycobacterial Diseases Subcommittee; American Thoracic Society; Infectious Disease Society of America. An official ATS/IDSA statement: diagnosis, treatment, and prevention of nontuberculous mycobacterial diseases. Am J Respir Crit Care Med. 2007;175:367–416. https://doi.org/10.1164/rccm.200604-571ST
5. Rodriguez-Coste MA, Chirca I, Steed LL, Salgado CD. Epidemiology of rapidly growing *Mycobacteria* bloodstream infections. Am J Med Sci. 2016;351:253–8. https://doi.org/10.1016/j.amjms.2015.12.012
6. El Helou G, Viola GM, Hachem R, Han XY, Raad II. Rapidly growing mycobacterial bloodstream infections. Lancet Infect Dis. 2013;13:166–74. https://doi.org/10.1016/S1473-3099(12)70316-X
7. Martín-de-Hijas NZ, García-Almeida D, Ayala G, Fernández-Roblas R, Gadea I, Celdrán A, et al. Biofilm development by clinical strains of non-pigmented rapidly growing mycobacteria. Clin Microbiol Infect. 2009;15:931–6. https://doi.org/10.1111/j.1469-0691.2009.02882.x
8. Price TK, Realegeno S, Mirasol R, Tsan A, Chandrasekaran S, Garner OB, et al. Validation, implementation, and clinical utility of whole genome sequence-based bacterial identification in the clinical microbiology laboratory. J Mol Diagn. 2021;23:1468–77. https://doi.org/10.1016/j.jmoldx.2021.07.020
9. Realegeno S, Mirasol R, Garner OB, Yang S. Clinical whole genome sequencing for clarithromycin and amikacin resistance prediction and subspecies identification of *Mycobacterium abscessus*. J Mol Diagn. 2021;23:1460–7. https://doi.org/10.1016/j.jmoldx.2021.07.023
10. El Helou G, Hachem R, Viola GM, El Zakhem A, Chaftari AM, Jiang Y, et al. Management of rapidly growing mycobacterial bacteremia in cancer patients. Clin Infect Dis. 2013;56:843–6. https://doi.org/10.1093/cid/cis1032

Address for correspondence: Elizabeth L. Ranson, UCLA Division of Infectious Diseases, David Geffen School of Medicine at UCLA, 10833 Le Conte Ave, 52-215CHS, Los Angeles, CA, 90095, USA; email: eranson@mednet.ucla.edu

Monkeypox Virus Infection in 18-Year-Old Woman after Sexual Intercourse, France, September 2022

Alexandre Vallée, Audrey Chatelain, Marie Carbonnel, Catherine Racowsky, Erwan Fourn, David Zucman, Jean-Marc Ayoubi

Author affiliations: Foch Hospital, Suresnes, France (A. Vallée, A. Chatelain, M. Carbonnel, C. Racowsky, E. Fourn, D. Zucman, J.-M. Ayoubi); University of Versailles, Versailles, France (A. Chatelain, M. Carbonnel, J.-M. Ayoubi)

DOI: https://doi.org/10.3201/eid2901.221643

A monkeypox virus outbreak has spread worldwide since April 2022. We report a young woman in France positive for monkeypox virus transmitted through oral and vaginal sex. Ulceronecrotic lesions developed intravaginally and around her vulva. Health professionals should become familiar with all aspects of infection from this virus, including possible vertical transmission.

A monkeypox virus (MPXV) outbreak has spread worldwide since April 2022. Although the risk to the general public was previously considered low, the World Health Organization is now responding to this outbreak as a high priority to avoid further spread (*1*). The community of men who have sex with men appears to be particularly exposed (*2*), although

rare cases among women have been described. We report a sexually transmitted case of MPXV with typical genital lesions in a young woman in France. The study was approved by the Institutional Review Board of Foch Hospital (IRB no. IRB00012437 [approval no. 22-10-02]), Suresnes, France. Written consent for publication was obtained from the patient for clinical information and photographs. Deidentified data were securely transferred and stored.

On September 7, 2022, an 18-year-old woman sought care at the outpatient clinic of Foch Hospital for symptoms such as fever, myalgia, and multiple eruptions on her vulva that began 7 days earlier (Figure). She reported a headache began on September 2, 2022, followed by feverish episodes on September 2 that stopped on September 7. The first eruptions appeared on September 2 on the gluteal area and then spread. Rashes on her hands and wrists appeared on September 7. At examination, the patient showed no odynophagia, coughing, or sputum. A gynecological examination showed ulceronecrotic lesions around the vulva and intravaginally. The cutaneous lesions were infracentimetric pustules located on the torso, fingers, and palms of the hands and above the intergluteal groove. We observed bilateral laterocervical and inguinal lymphadenopathies, but no axillary lymphadenopathy or anal lesions were evident.

Tests for chlamydia and gonococcus on pharyngeal and self-collected anal swabs were negative, and no previous sexually transmitted infections were

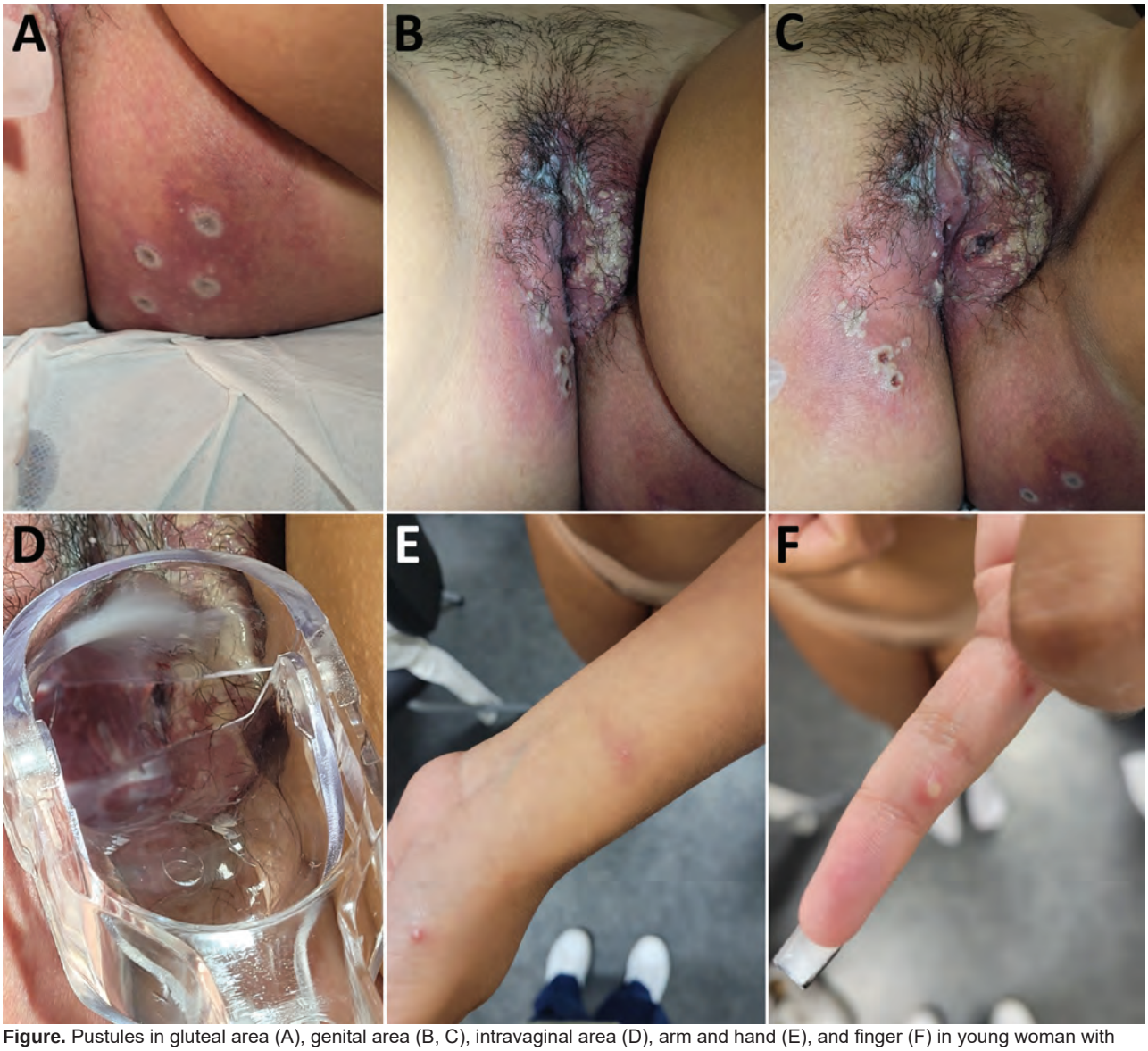

Figure. Pustules in gluteal area (A), genital area (B, C), intravaginal area (D), arm and hand (E), and finger (F) in young woman with monkeypox virus infection after sexual intercourse, France, September 2022.

reported for the patient or her boyfriend. Tests for HIV, syphilis, herpes, toxoplasmosis, rubella, and hepatitis (A, B, and C) were all negative for both persons. A real-time reverse transcription PCR, designed at the French National Reference Center of Orthopoxvirus, was performed on a pharyngeal swab sample from the patient on September 7 and tested positive for MPXV on September 8.

The patient had been in a relationship for 9 months with her boyfriend and had only had vaginal and oral intercourse with him; the most recent intercourse was 8 days before her first symptoms. On August 25, 2022, after a vacation in the southwest of France, her boyfriend began experiencing fever, pimples on his penis, and swollen inguinal glands. His rashes disappeared on September 1. We have no additional information for him. The main transmission hypothesis for MPXV in this case is oral and vaginal sex with the patient's boyfriend. She was not hospitalized but placed in confinement in her home. On October 12, the patient was seen at Foch Hospital for follow up, at which time the rashes were beginning to disappear (Appendix, https://wwwnc.cdc.gov/EID/article/29/1/22-1643-App1.pdf).

Most current MPXV outbreaks in Europe have involved young men who have sex with men who attend festivals and other public events (*3*). Conversely, data regarding MPXV cases in women are sparse; only a few cases have been reported in the literature (*4*). To date, only a small proportion of infections have been reported in women; only 1.2% of total cases in Europe have been reported in women (*5*). Our patient had a regular sexual partner who had MPXV symptoms, thus reinforcing that sexual transmission might play a predominant role in the outbreak (*2*).

Pharyngitis and rectal symptoms are being increasingly described as occurring after traditional skin lesions in MPXV infections (*6*), although these symptoms were not evident in our patient. The most reported clinical symptoms are painful perianal and genital lesions, together with fever, lymphadenopathy, headache, and malaise. Classic cases of MPXV included a febrile prodrome followed by generalized rash, although the ongoing outbreak has been characterized mainly by painless anogenital lesions, often without a prodrome. However, because of observed variability in clinical manifestations, the spread of the current MPXV outbreak might be underestimated.

To date, only 10 cases in pregnancy have been reported worldwide, predominantly in Brazil and the United States (*7*). Those cases were mainly reported by local media, and none were severe. However, studies in pregnant women remain limited. A transplacental transmission to the fetus might be responsible for congenital MPXV, although no cases of fetal malformations or death have been reported. Nevertheless, cases of vertical transmission with clinical signs of MPXV infection, such as cutaneous maculopapular lesions on the head, trunk, and extremities and hydrops, have been reported (*8*). A neonate born from an infected mother in the United States received prophylactic vaccinia immunoglobin and did not develop MPXV disease. Of note, the ACAM2000 vaccine (Sanofi, https://www.sanofi.com) is contraindicated during pregnancy because it is a vaccinia virus (live virus); other vaccines, such as third-generation vaccines (LC16m8 or JYNNEOS [Bavarian Nordic, https://www.bavarian-nordic.com]), are preferred in pregnant women (*9*). It is imperative that health professionals become familiar with all aspects of this disease affecting women (*10*).

About the Author

Dr. Vallée is head of the department of Epidemiology, Data, and Biostatistics at Foch Hospital, Suresnes, France. His primary research interests are epidemiology and clinical research.

References

1. Thornhill JP, Barkati S, Walmsley S, Rockstroh J, Antinori A, Harrison LB, et al.; SHARE-net Clinical Group. Monkeypox virus infection in humans across 16 countries—April–June 2022. N Engl J Med. 2022;387:679–91. https://doi.org/10.1056/NEJMoa2207323
2. Vallée A, Farfour E, Zucman D. Monkeypox virus: a novel sexually transmitted disease? A case report from France. Travel Med Infect Dis. 2022;49:102394. https://doi.org/10.1016/j.tmaid.2022.102394
3. Antinori A, Mazzotta V, Vita S, Carletti F, Tacconi D, Lapini LE, et al.; INMI Monkeypox Group. Epidemiological, clinical and virological characteristics of four cases of monkeypox support transmission through sexual contact, Italy, May 2022. Euro Surveill. 2022;27. https://doi.org/10.2807/1560-7917.ES.2022.27.22.2200421
4. Adler H, Gould S, Hine P, Snell LB, Wong W, Houlihan CF, et al.; NHS England High Consequence Infectious Diseases (Airborne) Network. Clinical features and management of human monkeypox: a retrospective observational study in the UK [Erratum in: Lancet Infect Dis. 2022;22:e177]. Lancet Infect Dis. 2022;22:1153–62. https://doi.org/10.1016/S1473-3099(22)00228-6
5. Vaughan AM, Cenciarelli O, Colombe S, Alves de Sousa L, Fischer N, Gossner CM, et al. A large multi-country outbreak of monkeypox across 41 countries in the WHO European Region, 7 March to 23 August 2022. Euro Surveill. 2022;27. https://doi.org/10.2807/1560-7917.ES.2022.27.36.2200620
6. Basgoz N, Brown CM, Smole SC, Madoff LC, Biddinger PD, Baugh JJ, et al. Case 24-2022: a 31-year-old man with perianal and penile ulcers, rectal pain, and rash. N Engl J Med. 2022;387:547–56. https://doi.org/10.1056/NEJMcpc2201244
7. Khalil A, Samara A, O'Brien P, Coutinho CM, Duarte G, Quintana SM, et al. Monkeypox in pregnancy: update on current outbreak. Lancet Infect Dis. 2022;22:1534–5.

8. D'Antonio F, Pagani G, Buca D, Khalil A. Monkeypox infection in pregnancy: a systematic review and metaanalysis. Am J Obstet Gynecol MFM. 2022;5:100747. https://doi.org/10.1016/j.ajogmf.2022.100747
9. Poland GA, Kennedy RB, Tosh PK. Prevention of monkeypox with vaccines: a rapid review. Lancet Infect Dis. 2022 Sep 15 [Epub ahead of print].
10. Kozlov M. Monkeypox outbreaks: 4 key questions researchers have. Nature. 2022;606:238–9. https://doi.org/10.1038/d41586-022-01493-6

Address for correspondence: Alexandre Vallée, Department of Epidemiology-Data-Biostatistics, Delegation of Clinical Research and Innovation (DRCI), Foch Hospital, 92150, Suresnes, France; email: al.vallee@hopital-foch.com

Monkeypox Virus Infection in 22-Year-Old Woman after Sexual Intercourse, New York, USA

Nawras Zayat, Shirley Huang, Jude Wafai, Melissa Philadelphia

Author affiliations: State University of New York Downstate Health Sciences University, Brooklyn, New York, USA (N. Zayat, S. Huang); St. George's University School of Medicine, West Indies, Grenada (J. Wafai); Kings County Hospital Center, Brooklyn (M. Philadelphia)

DOI: https://doi.org/10.3201/eid2901.221662

We report a case of a 22-year-old woman in New York, USA, who had painful vulvar and intravaginal lesions after sexual intercourse and tested positive for monkeypox virus. Literature documenting the clinical manifestations of monkeypox in female genitalia remains insufficient.

We report monkeypox virus infection in a 22-year-old woman with no remarkable medical history who sought care at the Kings County Hospital Center (Brooklyn, NY, USA) emergency department with numerous painful vulvar and intravaginal lesions. The patient reported a sexual encounter with 1 male partner 2.5 weeks before. She reported that they had vaginal sex and noted that her partner had a few dark bumps on his penis that resembled ingrown hairs. It was unknown if this partner had any sexually transmitted infections.

Two weeks after the encounter, the patient experienced onset of myalgias, fatigue, and fever. Two days after the onset of fever, she first noticed 3 mildly painful flesh-colored bumps, which progressed the following day and became white in color and more numerous. The lesions prompted the patient to go to the emergency department at an outside hospital. At arrival, the patient was febrile to 100.7° F. She underwent screening for sexually transmitted infections, including testing for monkeypox. She was discharged home with prescriptions of lidocaine, bacitracin, and ibuprofen as needed for pain while laboratory results were pending.

On day 3 after the lesions first appeared, they became larger and more painful, to the point of causing substantial distress when the woman sat, and had spread toward her perianal region. On day 4 after the lesions' appearance, the woman could no longer tolerate the pain and went to the emergency department at Kings County Hospital Center. At arrival, her temperature was 98.4° F, heart rate was 63 beats/min, respiratory rate was 18 breaths/min, and blood pressure was 118/72 mm Hg. Gynecologic examination revealed numerous singular, raised lesions that were umbilicated, ulcerated, vesicular, papular, and pustular, in different stages (Figure). The right labia majora was erythematous without any induration or fluctuance. We observed no lymphadenopathy on examination to the inguinal regions bilaterally. The vagina and cervix appeared normal otherwise. The uterus was small and mobile, and we noted no adnexal masses or tenderness. We observed no cutaneous lesions elsewhere in the body. Results of heart, lung, abdominal, and neurologic examinations were unremarkable.

The patient was tested for gonorrhea, chlamydia, HIV, herpes simplex virus, syphilis, and monkeypox. The patient also underwent a vulvar biopsy because the gynecology team was unfamiliar with the type of genital lesions she was experiencing. While waiting for the test results, the patient was informed by her male partner that he had tested positive for monkeypox virus earlier that day. The patient was admitted to the hospital and began a 14-day course of tecovirimat (600 mg every 12 h) with accompanying isolation precautions for 21 days as per the recommendations of the physicians within Kings County Hospital's Infectious Disease department. All results of laboratory tests were negative except for a positive PCR result for monkeypox virus. The

Figure. Numerous ulcerations with raised white borders extending from the labia minora into the vaginal walls in young woman with monkeypox virus infection, New York, USA

patient continued inpatient treatment with tecovirimat and was discharged on hospital day 3 without experiencing any other complications. Approximately 10 days after the onset of lesions, the patient reported in a follow-up telehealth visit that the lesions were decreasing in size and scabbing over and that the pain had greatly subsided.

Perineal, vaginal, and cervical lesions in women have rarely been described in the literature in the setting of a monkeypox infection. Furthermore, most cases documented from the 2022 monkeypox outbreak have primarily studied male genital lesions, with little to no mention of the clinical manifestations of monkeypox virus in female genitalia. In a literature search, we found a single case report documenting genital monkeypox lesions in a woman (*1*). In that case report, the patient experienced itchy, but painless, genital lesions extending down her labia majora that developed a week and a half after sexual intercourse with a new male partner (*1*). This patient also had a 2-day history of fever and myalgias (*1*). This patient's lesions and symptoms were similar to those of our patient's.

More research must be performed on the clinical manifestations of monkeypox, which would clarify the disease progression and help clinicians identify and diagnose this infection and properly treat patients. Monkeypox should be considered in the differential diagnosis of patients with genital lesions, especially in persons who are sexually active. Furthermore, there has been little study of how monkeypox virus manifests in women, especially during pregnancy, even though >400 cases have been reported in women in the United States in 2022 alone (*2*). Further consideration could elucidate the long term sequalae of monkeypox and its implications for health conditions such as pelvic inflammatory disorder, infertility, and cancer, which can occur with other sexually transmitted infections (*3*).

N.Z., S.H. and J.W. conceived and designed the work and acquired, analyzed, and interpreted the data. M.P. approved the final version of the manuscript.

About the Author

Dr. Zayat began his residency in obstetrics and gynecology at State University of New York Downstate in New York, NY, in July 2019. He is currently in his last year of residency and plans on pursuing a maternal fetal medicine fellowship. His primary research interests include women's health, HIV in pregnancy, and prevention of infectious diseases.

References

1. Portela-Dias J, Sereno S, Falcão-Reis I, Rasteiro C. Monkeypox infection with localized genital lesions in women. Am J Obstet Gynecol. 2022 Aug 27 [Epub ahead of print]. https://doi.org/10.1016/j.ajog.2022.08.046
2. Centers for Disease Control and Prevention. Monkeypox [cited 21 Sep 2022]. https://www.cdc.gov/poxvirus/monkeypox/index.html
3. Deal C, Cates W, Peeling R, Wald A. Long-term clinical sequelae of sexually transmitted infections in women [conference summary]. Emerg Infect Dis. 2004;10:e2. https://doi.org/10.3201/eid1011.040622_02

Address for correspondence: Nawras Zayat, SUNY Downstate Health Sciences University, 450 Clarkson Ave, Brooklyn, NY, 11203, USA; email: nawras.zayat@downstate.edu

SARS-CoV-2 Omicron BA.5 Infections in Vaccinated Persons, Rural Uganda

Joseph Mugisha, Bernard Mpairwe, Robert Newton, Matthew Cotten, My V.T. Phan

Author affiliations: Medical Research Council/Uganda Virus Research Institute and London School of Hygiene & Tropical Medicine, Uganda Research Unit, Entebbe, Uganda (J. Mugisha, B. Mpairwe, R. Newton, M. Cotten, M.V.T. Phan); University of York, York, United Kingdom (R. Newton); Medical Research Council–University of Glasgow Center for Virus Research, Glasgow, Scotland, United Kingdom (M. Cotten)

DOI: http://doi.org/10.3201/eid2901.220981

We describe a cluster of COVID-19 breakthrough infections after vaccination in Kyamulibwa, Kalungu District, Uganda. All but 1 infection were from SARS-CoV-2 Omicron strain BA.5.2.1. We identified 6 distinct genotypes by genome sequencing. Infections were mild, suggesting vaccination is not protective against infection but may limit disease severity.

The SARS-CoV-2 Omicron variant BA.5 was initially reported in South Africa in late February 2022 (*1*). The BA.5 variant, and especially the subvariant BA.5.2.1, has now spread to at least 104 countries globally; 197,425 genomes had been reported in GISAID (http://www.gisaid.org) as of September 16, 2022. The BA.5 spike protein shares substitutions with earlier Omicron variants but includes some of the Delta variant immune evasion changes. The BA.4/BA.5 viruses are reported to escape earlier Omicron immune responses, and vaccination does not fully block infection but may limit severity of disease (*2*–*5*). Infection of vaccinated persons (breakthrough infections) with SARS-CoV-2 strains is known, and such infections were reported recently among a highly vaccinated community within the US Embassy in Uganda (*6*). The frequency and outcomes of BA.5 vaccine breakthrough infections, both in Uganda and globally, are yet to be determined.

The Medical Research Council Unit in Uganda maintains a rural population cohort in Kyamulibwa, Kalungu District, southwestern Uganda (*7*). Unit staff were vaccinated as soon as vaccines were available in the country (March 2021), and most received at least 2 doses of COVID-19 vaccine by June 2021, with ongoing efforts for booster vaccination rolling out in the country. Staff members who had any symptoms indicating respiratory infections, including COVID-19, were routinely tested using Abbott's Panbio COVID-19 antigen rapid tests (Abbott, https://www.abbott.com). If cases of COVID-19 were detected, all staff were tested to detect asymptomatic cases. During such routine testing of staff members, a cluster of SARS-CoV-2 infections among vaccinated staff was detected. Test positivity during this period of infection was 18.5% (12 positive from 65 staff members tested), which was in the range of previous infection waves (January 3–10, 2022: 11.7%; June 6–14, 2021: 32.5%; November 30−December 1, 2020: 19.3%). Most infected staff members had mild symptoms, and all cases were quickly resolved (Appendix Table, https://wwwnc.cdc.gov/EID/article/29/1/22-0981-App1.pdf).

We performed sequencing by methods previously described (*8*). Nine cases yielded full genome SARS-CoV-2 sequences that we lineage-typed using Nextclade (*9*) and Pangolin (*10*) software; 8 of the 9 genomes were from the BA.5 lineage and 1 was BA.2.31, all variants within the Omicron variant-of-concern lineage. Although all 9 genomes belonged to the Omicron lineage, we detected 6 distinct subvariants (Figure). Genomes from cases 1, 2, 7, and 10 (all BA.5.2.1) were identical, suggesting a common infection source for these 4 cases. However, genomes for cases 4, 6, 11, and 12 genomes (also BA.5.2.1) were distinct from cases 1, 2, 7, and 10 and from each other, differing by 2–5 nt changes. The case 5 genome (BA.2.31) represents a 6th virus source for the cluster of breakthrough infections.

The detection of 5 distinct BA.5.2.1 sublineages found in Kalungu District in a short time period indicates multiple BA.5 sublineages were already circulating in other parts of Uganda and demonstrates the speed of movement of SARS-CoV-2. Uganda reported an increase in COVID-19 cases during this period, and both BA.5.2.1 and BA.2.31 virus strains potentially contributed to this increase in infections. Of note, 9 of the 12 COVID-19–positive staff members in this report routinely traveled on shared unit vehicles to and from Masaka or Kampala, which might account for the virus spread. In addition, the unit travel records show shared vehicle usage, suggesting a likely but not confirmed source of infection for cases 2, 7, and 10. The 3 infected staff members whose testing results did not yield sufficient PCR products for sequencing were asymptomatic, suggesting low viral loads (Appendix Table).

Many countries have reported increasing COVID-19 cases with BA.4 or BA.5 and derivatives as a major identified lineage. The global trend toward relaxed travel and quarantine restrictions and the mild

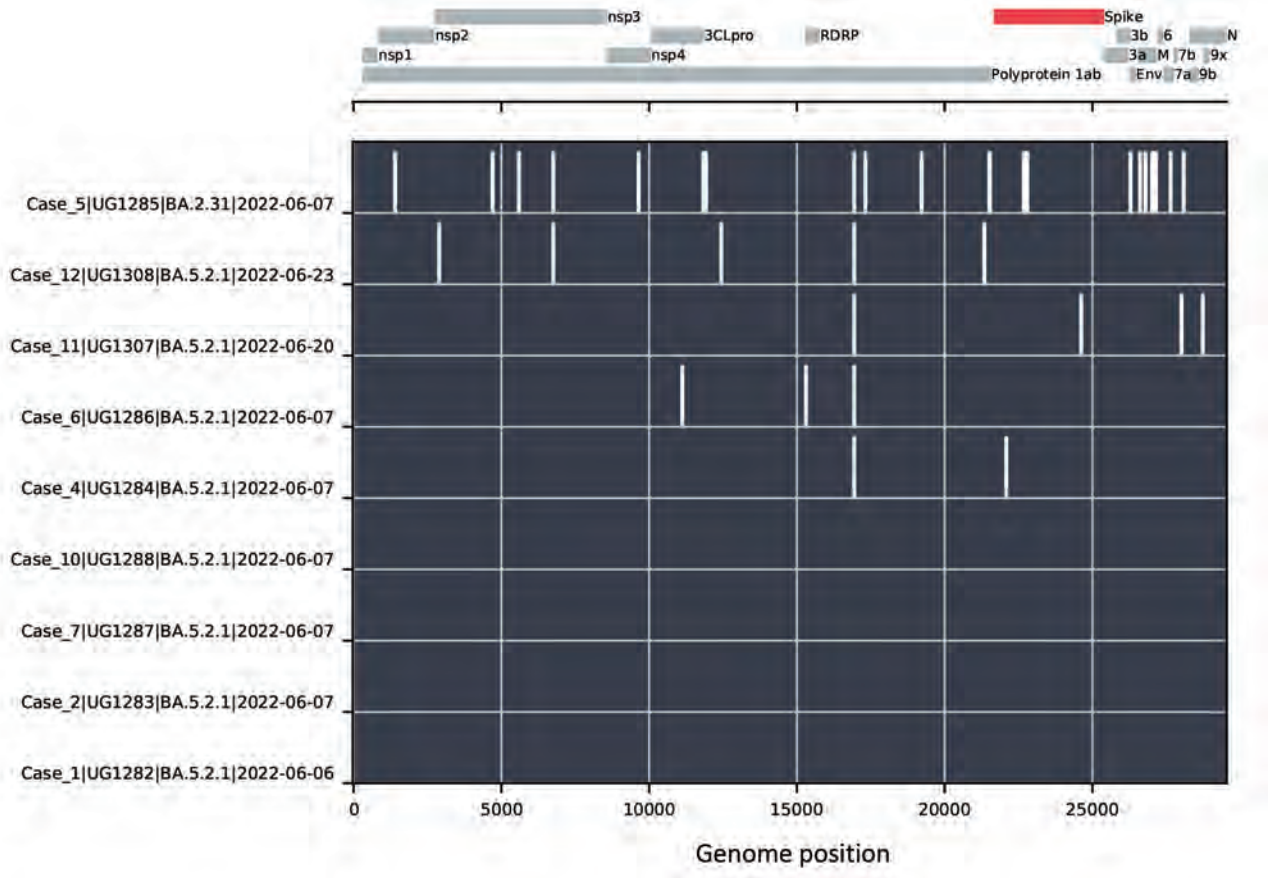

Figure. Nucleotide changes between SARS-CoV-2 genomes from a cluster of COVID-19–positive persons in Kyamulibwa, Kalungu District, rural Uganda. The lower portion of the chart shows nucleotide differences from the case 1 genome, plotted as white bars. The absence of bars in the BA.5.2.1 genomes from cases 1, 2, 7, and 10 indicates identical sequences. Case 5 was determined to be lineage BA.2.31, and cases 4, 6, 11, and 12 genomes demonstrated virus variants of lineage BA.5.2.1 distinct from the genomes from cases 1, 2, 7, and 10. A schematic of the SARS-CoV-2 genome is shown in the top portion of the chart, with protein coding regions marked.

infections in vaccinated and previously infected individuals might help enable global movement of these variants. This probably is evidenced by the timing of BA.5 appearance in rural Uganda within weeks of the variant being initially reported in other parts of the world (South Africa in late February 2022, Germany in mid-March 2022, the United States in late March 2022, Portugal in early April 2022, and Uganda in early June 2022).

In conclusion, the detection of 6 distinct sublineages of SARS-CoV-2 (5 of BA.5.2.1 and 1 of BA.2.31) in Kyamulibwa, Kalungu District, Uganda, within a short period indicates substantial diversity of and rapid movement of these viruses into and within Uganda. Combined with recent increases in reported SARS-CoV-2 infections throughout the country, our findings emphasize the need for vigilance, surveillance, and continued testing in this rural community and throughout the country. The mild nature of symptoms in these 12 cases, and in many vaccinated persons, reinforces the importance of community vaccination efforts.

Acknowledgments

We thank the staff and technicians working at the Kyamulibwa, Kalungu District field station that help make this work possible.

This work was supported by the UK Medical Research Council (MRC/UK Research and Innovation) and the UK Department for International Development under the MRC/DFID Concordat agreement (grant agreement no. MC_PC_20010) and Wellcome Trust, UK FCDO—Wellcome Epidemic Preparedness—Coronavirus (grant agreement no. 220977/Z/20/Z). The COVID-19 surveillance project in Kalungu District was supported with additional funding from the UK MRC (grant agreement no. MC_PC_20011).

This study was approved by the Uganda Virus Research Institute-Research and Ethics Committee (UVRI-REC Federalwide Assurance [FWA] FWA No. 00001354, study reference GC/127/20/04/771). Sequences described here are available from GISAID under accession numbers EPI_ISL_13332769–75, 15005215 and 15005216.

About the Author

Dr Mugisha is a medical scientist working at the Uganda Research Unit of the Medical Research Council/Uganda Virus Research Institute and London School of Hygiene & Tropical Medicine. During COVID-19, he has led surveillance activity in the unit's General Population Cohort in southwestern Uganda. His research interests are primarily on the health and social issues affecting older people in low- and middle-income countries.

References

1. Tegally H, Moir M, Everatt J, Giovanetti M, Scheepers C, Wilkinson E, et al. Emergence of SARS-CoV-2 Omicron lineages BA.4 and BA.5 in South Africa. Nat Med. 2022; 28(9):1785-1790. https://doi.org:10.1038/s41591-022-01911-2. PMID: 35760080
2. Kimura I, Yamasoba D, Tamura T, Nao N, Oda Y, Mitoma S, et al. Virological characteristics of the SARS-CoV-2 Omicron BA.2 subvariants, including BA.4 and BA.5. Cell, 2022;185(21):3992-4007.e16. ISSN 0092-8674 https://doi.org/10.1016/j.cell.2022.09.018.
3. Khan K, Karim F, Ganga Y, Bernstein M, Jule Z, Reedoy K, et al. Omicron BA.4/BA.5 escape neutralizing immunity elicited by BA.1 infection. Nat Commun. 2022;13(1):4686. https://doi.org:10.1038/s41467-022-32396-9. Erratum in: Nat Commun. 2022 Oct 13;13(1):6057. PMID: 35948557
4. Wang Q, Guo Y, Iketani S, Li Z, Mohri H, Wang M, et al. Antibody evasion by SARS-CoV-2 Omicron subvariants BA.2.12.1, BA.4 and BA.5. Nature. 2022;608:603-608. https://doi.org/10.1038/s41586-022-05053-w
5. Tuekprakhon A, Nutalai R, Dijokaite-Guraliuc A, Zhou D, Ginn HM, Selvaraj M, et al.; OPTIC Consortium; ISARIC4C Consortium. Antibody escape of SARS-CoV-2 Omicron BA.4 and BA.5 from vaccine and BA.1 serum. Cell. 2022;185:2422–2433.e13.
6. Harris JR, Owusu D, O'Laughlin K, Cohen AL, Ben Hamida A, Patel JC, et al. SARS-CoV-2 breakthrough infections among US Embassy staff members, Uganda, May–June 2021 [cited 2022 Jun 12]. Emerg Infect Dis. 2022;28:1279–80. https://doi.org/10.3201/eid2806.220427
7. Asiki G, Murphy G, Nakiyingi-Miiro J, Seeley J, Nsubuga RN, Karabarinde A, et al.; GPC team. The general population cohort in rural south-western Uganda: a platform for communicable and non-communicable disease studies [cited 2020 Mar 3]. Int J Epidemiol. 2013;42:129–41. https://doi.org/10.1093/ije/dys234
8. Cotten M, Bugembe DL, Kaleebu P, Phan MVT. Alternate primers for whole-genome SARS-CoV-2 sequencing. Virus Evol. 2021 Feb 4 [cited 2021 Mar 7]. https://academic.oup.com/ve/advance-article/doi/10.1093/ve/veab006/6128533
9. Aksamentov I, Roemer C, Hodcroft E, Neher R. Nextclade: clade assignment, mutation calling and quality control for viral genomes [cited 2022 Jun 13]. J Open Source Softw. 2021;6:3773. https://doi.org/10.21105/joss.03773
10. O'Toole Á, Scher E, Underwood A, Jackson B, Hill V, McCrone JT, et al. Assignment of epidemiological lineages in an emerging pandemic using the pangolin tool. Virus Evol. 2021;7:veab064. https://doi.org/10.1093/ve/veab064

Address for correspondence: Matthew Cotten, MRC/UVRI & LSHTM Uganda Research Unit, PO Box 49, Plot 51-59, Nakiwogo Road, Entebbe, Uganda; email: Matthew.Cotten@lshtm.ac.uk

Rapid SARS-CoV-2 Seroprevalence Survey in Central and Western Divisions of Fiji, 2021

Stephanie J. Curtis,[1] Abdul W. Shah,[1] Ana Ratu, Donald J. Wilson, Philip C. Hill, Phil Hulcome, Cathy Gaylard, Daniel Faktaufon, Talica Cabemaiwai, Isireli Rabukawaqa, Tevita Qoriniasi, Akesh Narayan, Susana Nakalevu, Pablo Romakin, Jemesa Tudravu, James Fong,[2] Nick Walsh[2]

Author affiliations: National Critical Care and Trauma Response Centre, Darwin, Northern Territory, Australia (S.J. Curtis, C. Gaylard, N. Walsh); Ministry of Health and Medical Services, Suva, Fiji (A.W. Shah, D. Faktaufon, T. Cabemaiwai, I. Rabukawaqa, T. Qoriniasi, A. Narayan, S. Nakalevu, P. Romakin, J. Tudravu, J. Fong); Fiji National University, Suva (A. Ratu, D.J. Wilson, P.C. Hill); University of Otago, Dunedin, New Zealand (P.C. Hill); Fiji Program Support Facility, Suva (P. Hulcome)

DOI: https://doi.org/10.3201/eid2901.221514

During November–December 2021, we performed a SARS-CoV-2 seroprevalence survey in Central and Western Divisions of Fiji. A total of 539 participants 8–70 years of age were 95.5% (95% CI 93.4%–97.1%) seropositive, indicating high community levels of immunity. Seroprevalence studies can inform public health responses to emerging SARS-CoV-2 variants.

In Fiji, the SARS-CoV-2 Delta variant wave occurred in a largely unvaccinated and nonimmune population during April–November 2021 (*1*). A risk-based COVID-19 vaccine rollout strategy commenced in March 2021, and, by late November 2021, a total of 90.6% of persons ≥18 years of age had received 2 vaccine doses and 97.3% had received 1 dose (*1*). Because of the high vaccination coverage, the government of Fiji had planned to reopen international borders by early December 2021.

Serosurveillance is a fundamental component of public health response to disease. Estimating disease epidemiology, including population immunity, by using serosurveillance can inform government policy. In November 2021, no serosurveillance data were available from any Pacific Island country or territory, and data from this region remain sparse (*2*). To inform public health decisions on the safe opening

[1]These first authors contributed equally to this article.

[2]These senior authors contributed equally to this article.

of international borders, we performed a rapid operational estimate of SARS-CoV-2 seroprevalence in Central and Western Divisions of Fiji.

We conducted a single cross-sectional serosurvey during November 24–December 1, 2021. The study population comprised persons deemed at higher risk for SARS-CoV-2 infection who were 8–70 years of age and located in Central and Western Divisions of Fiji. Persons at higher risk of infection included those who worked in healthcare, tourism, hospitality, retail, transportation, and education industries and primary or secondary school students. We used convenience sampling through nonrandom selection of study participants. The government of Fiji identified recruitment sites for persons at high risk for COVID-19 and directly invited those sites to identify potential study participants. We aimed to recruit 550 participants, including at least 50 unvaccinated persons, who were a nationally representative sample of sex and age within the community (*3*).

Field teams were trained in data collection protocols that aligned with the World Health Organization UNITY protocol (*4*). We approached potential participants at recruitment sites and administered a brief questionnaire (Appendix, https://wwwnc.cdc.gov/EID/article/29/1/22-1514-App1.pdf) and collected blood samples after informed consent was obtained. We tested serum samples for IgG against the receptor-binding domain of SARS-CoV-2 by using the SARS-CoV-2 Ab ELISA (Beijing Wantai Biologic, https://www.ystwt.cn), which has 96.7% sensitivity and 97.5% specificity across Alpha and Beta variants.

We merged questionnaire and laboratory data, summarized covariates, and estimated seroprevalence with 95% CIs. We performed analyses using R version 4.0.2 (The R Project for Statistical Computing, https://www.r-project.org). The Fiji National Human Research Ethics Committee reviewed all study materials and provided a letter of approval; however, formal ethics approval was not required.

We recruited 539 participants who were 30 ±14 years of age (mean ±SD); 47.3% (255/539) were male and 52.7% (284/539) female (Table). Most participants had received 2 doses of a COVID-19 vaccine (443/539, 82.2%), including 94.9% (463/488) of participants who were eligible for vaccination during the survey period. Overall seroprevalence was 95.5% (95% CI 93.4%–97.1%). Of those who had not received

Table. Participant characteristics from a rapid SARS-CoV-2 seroprevalence survey in Central and Western Divisions of Fiji, November–December 2021

Characteristics	No. (%)*	No. seropositive†	Seroprevalence, % (95% CI)
Total	539	515	95.5 (93.4–97.1)
Sex			
M	255 (47.3)	246	96.5 (93.2–98.3)
F	284 (52.7)	269	94.7 (91.3–97.0)
Age, years			
8–11	51 (9.5)	36	70.6 (56.0–82.1)
12–17	73 (13.5)	66	90.4 (80.7–95.7)
18–29	132 (24.5)	132	100 (96.5–100)
30–39	143 (26.5)	141	98.6 (94.5–99.8)
40–49	96 (17.8)	96	100 (95.2–100)
≥50	44 (8.2)	44	100 (90.0–100)
Ethnicity			
I-Taukei	269 (49.9)	259	96.3 (93.1–98.1)
Fijian of Indian descent	249 (46.2)	236	94.8 (91.0–97.1)
Fijian of other descent	21 (3.9)	20	95.2 (74.1–99.8)
Occupation industry			
Healthcare worker	158 (29.3)	157	99.4 (96.0–99.9)
Student	142 (26.3)	120	84.5 (77.3–89.8)
Transportation	94 (17.4)	94	100 (95.1–100)
Hotel	69 (12.8)	69	100 (93.4–100)
Education	40 (7.4)	39	97.5 (85.7–99.9)
Hospitality	36 (6.7)	36	100 (88.0–100)
COVID-19 vaccine status			
None	76 (14.1)	58	76.3 (64.9–85.0)
1 dose	20 (3.7)	16	80.0 (55.7–93.4)
2 doses	443 (82.2)	441	99.5 (98.2–99.9)
Self-reported previous COVID-19			
No	410 (76.1)	387	94.4 (91.6–96.3)
Yes	117 (21.7)	117	100 (96.0–100)
Unknown	12 (2.2)	11	91.7 (59.7–99.6)

*Percentage of total.
†Number seropositive for SARS-CoV-2.

a COVID-19 vaccine, 75% (58/76) were seropositive, including 70% (36/51) of children 8–11 years of age who were not eligible for vaccination during the survey period, indicating serum antibodies resulted from acquired infections.

We demonstrated a high level of immunity in participants ≥18 years of age in Central and Western Divisions of Fiji during late November and early December 2021. The results provided reassurance that international borders could open to fully vaccinated international travelers, without the necessity of previous hotel quarantine requirements, and relative safety of persons at higher risk for infection could be maintained. Our results highlighted a gap in pediatric vaccine coverage that included children 12–17 years of age who were eligible for vaccination during this investigation and were subsequently prioritized for vaccination by the government of Fiji.

The first limitation of our study is that direct extrapolation of the results to the general public is problematic because we conducted convenience sampling of the study population; however, the Central and Western Divisions account for about two thirds of the population of Fiji and were chosen because of resource availability. Second, our IgG measurements did not differentiate between immunity acquired by vaccination or infection or provide evidence of protection or population risk, particularly for severe COVID-19 (*5*). Hybrid immunity in our study population was likely high because of the recent national Delta variant outbreak and COVID-19 vaccination program (*6*). Third, our investigation occurred before the Omicron variant wave, which resulted in ≈12,000 notified COVID-19 cases during December 2021–February 2022 (*2*). However, the lower Omicron case notifications compared with the previous Delta wave of ≈52,000 cases support the likelihood that high population-level immunity attenuated illness from the highly transmissible Omicron variant when international borders reopened (*7*). Overall, further nationwide seroprevalence studies can inform the public health response as new COVID-19 variants emerge and demonstrate how population immunity might wane in the absence of continued COVID-19 vaccination efforts (*8*–*10*).

Acknowledgments

We thank the Fiji Ministry of Health and Human Services, including the dedicated fieldwork team, Australia's Fiji Program Support Facility, and the Australian High Commission team in Fiji, Department of Foreign Affairs and Trade, for their contributions to this study, and Kerryn Osborne for her help planning this initiative.

The seroprevalence survey was funded by the Australian Department of Foreign Affairs and Trade through the National Critical Care and Trauma Response Centre.

About the Author

Ms. Curtis is an epidemiologist at the National Critical Care and Trauma Response Centre. Her primary interests are epidemiology of infectious diseases, disease outbreak management, and public health emergency response.

References

1. Fiji Ministry of Health and Medical Services. COVID-19 update—29-10-2021 [cited 2021 Nov 19]. https://www.health.gov.fj/29-10-2021
2. Bergeri I, Whelan MG, Ware H, Subissi L, Nardone A, Lewis HC, et al. Global SARS-CoV-2 seroprevalence from January 2020 to April 2022: a systematic review and meta-analysis of standardized population-based studies. PLoS Med. 2022;19:e1004107. PubMed https://doi.org/10.1371/journal.pmed.1004107
3. Fiji Bureau of Statistics. 2017 Population and housing census—release 1 [cited 2021 Nov 19]. https://www.statsfiji.gov.fj/index.php/census-2017/census-2017-release-1
4. World Health Organization. Population-based age-stratified seroepidemiological investigation protocol for coronavirus 2019 (COVID-19) infection. 26 May 2020 [cited 2021 Nov 19]. https://www.who.int/publications/i/item/WHO-2019-nCoV-Seroepidemiology-2020.2
5. Feng S, Phillips DJ, White T, Sayal H, Aley PK, Bibi S, et al.; Oxford COVID Vaccine Trial Group. Correlates of protection against symptomatic and asymptomatic SARS-CoV-2 infection. Nat Med. 2021;27:2032–40. https://doi.org/10.1038/s41591-021-01540-1
6. Chen X, Chen Z, Azman AS, Deng X, Sun R, Zhao Z, et al. Serological evidence of human infection with SARS-CoV-2: a systematic review and meta-analysis. Lancet Glob Health. 2021;9:e598–609. https://doi.org/10.1016/S2214-109X(21)00026-7
7. Ito K, Piantham C, Nishiura H. Relative instantaneous reproduction number of Omicron SARS-CoV-2 variant with respect to the Delta variant in Denmark. J Med Virol. 2022;94:2265–8. https://doi.org/10.1002/jmv.27560
8. Ferdinands JM, Rao S, Dixon BE, Mitchell PK, DeSilva MB, Irving SA, et al. Waning 2-dose and 3-dose effectiveness of mRNA vaccines against COVID-19–associated emergency department and urgent care encounters and hospitalizations among adults during periods of Delta and Omicron variant predominance—VISION Network, 10 states, August 2021–January 2022. MMWR Morb Mortal Wkly Rep. 2022;71:255–63. https://doi.org/10.15585/mmwr.mm7107e2
9. Abu-Raddad LJ, Chemaitelly H, Bertollini R; National Study Group for COVID-19 Vaccination. Effectiveness of mRNA-1273 and BNT162b2 vaccines in Qatar. N Engl J Med. 2022;386:799–800. https://doi.org/10.1056/NEJMc2117933
10. Tseng HF, Ackerson BK, Luo Y, Sy LS, Talarico CA, Tian Y, et al. Effectiveness of mRNA-1273 against SARS-CoV-2 Omicron and Delta variants. Nat Med. 2022;28:1063–71. https://doi.org/10.1038/s41591-022-01753-y

Address for correspondence: Stephanie J. Curtis, Royal Darwin Hospital, Rocklands Drive, Tiwi, Northern Territory, 0810, Australia; email: stephanie.curtis@nt.gov.au

Up Close with Ticks

Byron Breedlove

Worldwide, only mosquitoes spread more vectorborne diseases than ticks; however, in temperate areas of North America, Europe, and Asia, ticks cause most vectorborne diseases. Ticks are vectors for multiple viruses, bacteria, and parasites that cause can cause an array of infectious diseases. Researcher Daniel Sonenshine notes, "Ticks transmit a greater variety of pathogenic microorganisms than any other hematophagous arthropod."

Ticks were spreading pathogens for millions of years before humans evolved. Biologist George Poinar, Jr., has found evidence of *Borrelia,* a type of spirochete-like bacteria that causes Lyme disease, in fossilized ticks preserved in 5−20-million-year-old amber. Much older fossilized ticks have been found in 99-million-year-old amber. However, that ticks are vectors for infectious diseases that affect humans was not confirmed until the early 20th Century.

Recently, these tiny arthropods gained additional notoriety by purportedly being the first living animals to be filmed under a scanning electron microscope. Science journalist James Gorman offers this colorful account: "Chain saws, hockey masks and the undead are all classic symbols of horror. But for a true shiver of dread, take a look at a tick. When seen with an electron microscope, a tick's mouth has what look like twin saws (chelicerae) flanking an appendage (a hypostome) that appears to be the kind of long, barbed sword that a villain in a video game might favor."

Images and videos from such research reveal new insights into how ticks penetrate and remain attached to hosts and transmit pathogens. They also confirm that some hand drawn illustrations of ticks from the late 19th century were remarkably detailed and accurate. This month's cover image, *Illustration of ticks (Ixodida)*, by George Marx, is an excellent example.

Born and educated in Germany, Marx enrolled in the gymnasium at Darmstadt in the Hesse district when he was 14 years old. His obituary notes that while he was a student there, Marx "proved himself so proficient in botany, and at the same time so able an artist, that to him was assigned the task of making the illustrations for the Flora of Gross-Gerua," the district seat in that part of Germany.

After earning his degree in pharmacy in 1860, Marx left Germany for the United States, where he served in the American Civil War, receiving an honorable discharge after experiencing a serious wound and illness. In 1865, Marx moved to Philadelphia, where he began

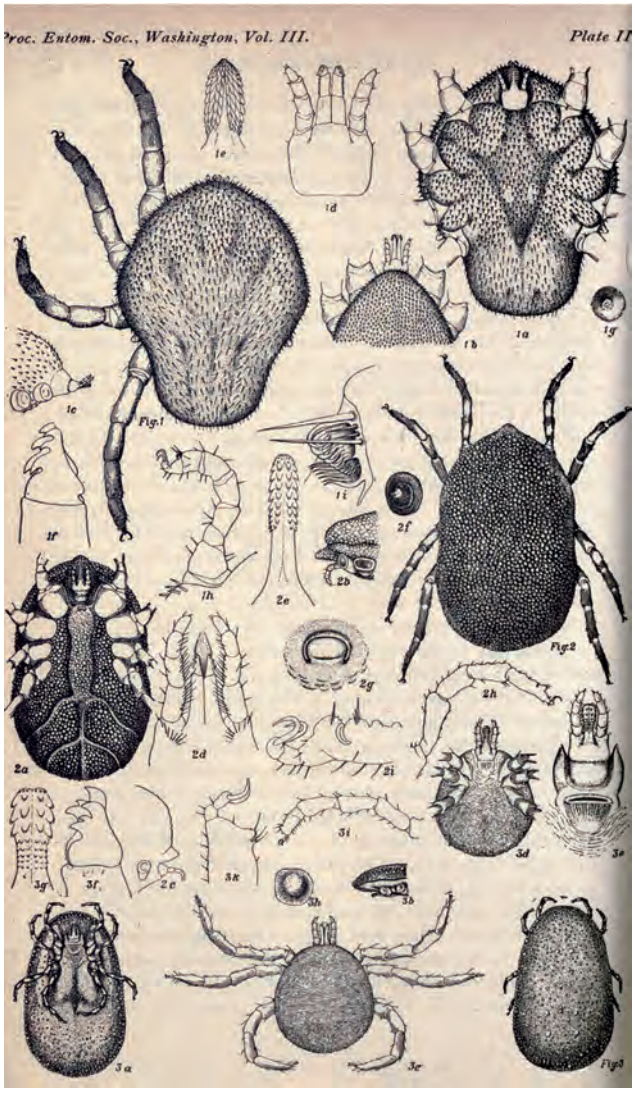

George Marx (1838−1895), *Illustration of ticks* (*Ixodida*), 1892. Plate II from Proceedings of the Entomological Society of Washington. Ink on paper. Public domain image from Biodiversity Heritage Library. Holding institution: Smithsonian Libraries, Washington, DC, USA.

Author affiliation: Centers for Disease Control and Prevention, Atlanta, Georgia, USA

DOI: https://doi.org/10.3201/eid2901.AC2901

collecting Arachnida. In 1878, Marx relocated to Washington, DC, after accepting a positon as a natural history illustrator in the Division of Entomology, US Department of Agriculture. Cited for his meticulous artwork, in 1889, Marx was selected to be chief of the department's newly established Division of Illustrations, where he worked and devoted much of his time to studying ticks until just before his death in early 1895. A charter member of the Entomological Society of Washinton, DC, Marx served as its fourth president. His obituary notes "... the various plates and figures which adorn his contributions to science are by far the best illustrations of Arachnids that have ever been produced in America."

His meticuolusly rendered *Illustration of ticks (Ixodida),* illustrates the appendages, forms, and features of 3 specimens accompanyed by his up-close depictions of the capitulum, maxillae, mandibles, stigma, and Haller's olfactory organ. One can imagine Marx peering through his microscopes and magnifying glasses, methodically rendering and notating his observations with pen and ink, then later refining his sketches for the finished composite.

In 1896, the year after Marx's death, Rocky Mountain spotted fever was identified in the Snake River Valley of Idaho, and in 1899, it was first described in a paper by E.E. Maxey. For a decade, its cause eluded researchers until a team led by Dr. Howard T. Ricketts discovered ticks' role in transmitting Rocky Mountain spotted fever to humans. Eisen and Paddock note that after the bacterium now known as *Rickettsia rickettsii* was discovered, "18 additional tickborne human pathogens have been recognized; remarkably, more than 40% of these agents have been described since 1980."

Tickborne viral diseases include Bourbon virus disease, Colorado tick fever, Crimean-Congo hemorrhagic fever, Heartland virus disease, Kyasanur Forest disease, and Powassan encephalitis. Among the tickborne bacterial diseases are anaplasmosis, bartonellosis, ehrlichiosis, Lyme disease, Rocky Mountain spotted fever, and tickborne relapsing fever. Microscopic parasites transmitted by ticks cause the disease babesiosis. The long list of diseases that ticks transmit to humans, none of which were known when Marx created his illustration, and their global incidence continue to increase.

Bibliography

1. Centers for Disease Control and Prevention. Diseases transmitted by ticks [cited 2022 Dec 1]. https://www.cdc.gov/ticks/diseases/index.html
2. Eisen RJ, Kugeler KJ, Eisen L, Beard CB, Paddock CD. Tick-borne zoonoses in the United States: persistent and emerging threats to human health. ILAR J. 2017;58:319–35. https://doi.org/10.1093/ilar/ilx005
3. Eisen RJ, Paddock CD. Tick and tickborne pathogen surveillance as a public health tool in the United States. J Med Entomol. 2021;58:1490–502. https://doi.org/10.1093/jme/tjaa087
4. Entomological Society of Washington. Obituary and bibliography of Dr. George Marx. Proc Entomol Soc Wash. 1894;3:195–201 [cited 2022 Dec 1]. https://www.biodiversitylibrary.org/page/2360491
5. Ishigaki Y, Nakamura Y, Oikawa Y, Yano Y, Kuwabata S, Nakagawa H, et al. Observation of live ticks (*Haemaphysalis flava*) by scanning electron microscopy under high vacuum pressure. PLoS One. 2012;7:e32676. https://doi.org/10.1371/journal.pone.0032676
6. Mallis A. American Entomologists. New Brunswick (NJ). Rutgers University Press, 1971. p. 408–10.
7. Maxey EE. Some observations on the so-called spotted fever of Idaho. Medical Sentinel. 1899;7:433–8.
8. Peñalver E, Arillo A, Delclòs X, Peris D, Grimaldi DA, Anderson SR, et al. Parasitised feathered dinosaurs as revealed by Cretaceous amber assemblages. Nat Commun. 2017;8:1924. https://doi.org/10.1038/s41467-017-01550-z
9. Poinar G Jr. Fossilized mammalian erythrocytes associated with a tick reveal ancient piroplasms. J Med Entomol. 2017;54:895–900. https://doi.org/10.1093/jme/tjw247
10. Richter D, Matuschka FR, Spielman A, Mahadevan L. How ticks get under your skin: insertion mechanics of the feeding apparatus of *Ixodes ricinus* ticks. Proc Biol Sci. 2013;280:20131758 . https://doi.org/10.1098/rspb.2013.1758
11. Rochlin I, Toledo A. Emerging tick-borne pathogens of public health importance: a mini-review. J Med Microbiol. 2020;69:781–91. https://doi.org/10.1099/jmm.0.001206
12. Rosenberg R, Lindsey NP, Fischer M, Gregory CJ, Hinckley AF, Mead PS, et al. Vital signs: trends in reported vectorborne disease cases—United States and Territories, 2004–2016. MMWR Morb Mortal Wkly Rep. 2018;67:496–501. https://doi.org/10.15585/mmwr.mm6717e1
13. Sonenshine DE. Range expansion of tick disease vectors in North America: implications for spread of tick-borne disease. Int J Environ Res Public Health. 2018;15:478. https://doi.org/10.3390/ijerph15030478

Address for correspondence: Byron Breedlove, EID Journal, Centers for Disease Control and Prevention, 1600 Clifton Rd NE, Mailstop H16-2, Atlanta, GA 30329-4027, USA; email: wbb1@cdc.gov

EMERGING INFECTIOUS DISEASES®

Upcoming Issue • High-Consequence Pathogens

Streptococcus dysgalactiae Blood Stream Infections, Norway, 1999–2021

Changing Disease Course of Pediatric Crimean-Congo Hemorrhagic Fever in Children

Sentinel Surveillance System Implementation and Evaluation for SARS-CoV-2 Genomic Data, Washington, 2020–2021

Incidence and Transmission Dynamics of *Bordetella pertussis* Infection in Rural and Urban Communities, South Africa, 2016–2018

Influence of Regional Terrain on Lassa Fever Virus Exposure, Republic of Guinea

Relationship between Telework Experience and Presenteeism during COVID-19 Pandemic, United States, March–November 2020

Age-Stratified Model to Assess Health Outcomes of COVID-19 Vaccination Strategies, Ghana

Circovirus Hepatitis Infection in Heart-Lung Transplant Patient

Novel Prion Strain as Cause of Chronic Wasting Disease in a Moose, Finland

Increased Multidrug-Resistant *Salmonella enterica* I Serotype 4,[5],12:i:- Infections Associated with Pork, United States, 2009–2018

Longitudinal Prepost Analysis of Electronic Health Information to Identify Possible COVID-19 Sequelae

Estimated Cases Averted by COVID-19 Electronic Exposure Notification, Pennsylvania, USA, November 8, 2020–January 2, 2021

(Mis)perception and Use of Unsterile Water in Home Medical Devices, PN View 360+ Survey, United States, August 2021

Characterization of *Candida auris* Discovered through Community Wastewater Surveillance during Healthcare Outbreak, Nevada, USA, 2022

Nipah Virus Exposure in Domestic and Peridomestic Animals Living in Human Outbreak Sites, Bangladesh

Successful Drug-Mediated Host Clearance of *Batrachochytrium salamandrivorans*

Powassan Virus Lineage I in Field-Collected *Dermacentor variabilis* Ticks, New York, USA

Next Generation Sequencing for Identifying Unknown Pathogens in Sentinel Immunocompromised Hosts

Occupational Monkeypox Virus Transmission to Healthcare Worker, California, USA, 2022

Familial Mpox Virus Infection Involving 2 Young Children

Detection of *Dirofilaria immitis* in a Dog Imported to Chile

Serologic Evidence of *Orientia* Infection among Rural Population, Cauca Department, Colombia

Metagenomic Sequencing of Monkeypox Virus, Northern Mexico

Epidemiology of SARS-CoV-2 Omicron BA.5 Infections, Macau, China, June–July 2022

Infant Botulism, Israel, 2007–2021

Complete list of articles in the February issue at https://wwwnc.cdc.gov/eid/#issue-296

Earning CME Credit

To obtain credit, you should first read the journal article. After reading the article, you should be able to answer the following, related, multiple-choice questions. To complete the questions (with a minimum 75% passing score) and earn continuing medical education (CME) credit, please go to http://www.medscape.org/journal/eid. Credit cannot be obtained for tests completed on paper, although you may use the worksheet below to keep a record of your answers.

You must be a registered user on http://www.medscape.org. If you are not registered on http://www.medscape.org, please click on the "Register" link on the right hand side of the website.

Only one answer is correct for each question. Once you successfully answer all post-test questions, you will be able to view and/or print your certificate. For questions regarding this activity, contact the accredited provider, CME@medscape.net. For technical assistance, contact CME@medscape.net. American Medical Association's Physician's Recognition Award (AMA PRA) credits are accepted in the US as evidence of participation in CME activities. For further information on this award, please go to https://www.ama-assn.org. The AMA has determined that physicians not licensed in the US who participate in this CME activity are eligible for AMA PRA Category 1 Credits™. Through agreements that the AMA has made with agencies in some countries, AMA PRA credit may be acceptable as evidence of participation in CME activities. If you are not licensed in the US, please complete the questions online, print the AMA PRA CME credit certificate, and present it to your national medical association for review.

Article Title

Comprehensive Review of Emergence and Virology of Tickborne Bourbon Virus in the United States

CME Questions

1. Which one of the following statements about the Bourbon virus is most accurate?

A. It is a DNA virus
B. It is a member of the *Thogotovirus* genus
C. It is a member of the orthopoxvirus family
D. It uses multiple glycoproteins for attachment and fusion

2. All US cases of infection with the Bourbon virus have occurred in which states?

A. Kansas, Oklahoma, and Missouri
B. Maine, New Hampshire, and Vermont
C. Virginia, West Virginia, and North Carolina
D. Colorado, Wyoming, and New Mexico

3. Which one of the following statements regarding the transmission of the Bourbon virus is most accurate?

A. The virus is only prevalent during the adult stage of Lone Star ticks
B. Lone Star ticks harbor the Bourbon virus exclusively
C. The most common animals that are seropositive for Bourbon virus are raccoons and white-tailed deer
D. Birds are an important amplifier of the Bourbon virus infection for humans

4. Which one of the following statements regarding the clinical presentation of the Bourbon virus infection is most accurate?

A. The latency period between tick bite and the onset of symptoms is about 2 weeks
B. Rash is uncommon
C. Leukocytosis is the most common finding on laboratory evaluation
D. Treatment for the Bourbon virus infection currently consists of supportive care

Earning CME Credit

To obtain credit, you should first read the journal article. After reading the article, you should be able to answer the following, related, multiple-choice questions. To complete the questions (with a minimum 75% passing score) and earn continuing medical education (CME) credit, please go to http://www.medscape.org/journal/eid. Credit cannot be obtained for tests completed on paper, although you may use the worksheet below to keep a record of your answers.

You must be a registered user on http://www.medscape.org. If you are not registered on http://www.medscape.org, please click on the "Register" link on the right hand side of the website.

Only one answer is correct for each question. Once you successfully answer all post-test questions, you will be able to view and/or print your certificate. For questions regarding this activity, contact the accredited provider, CME@medscape.net. For technical assistance, contact CME@medscape.net. American Medical Association's Physician's Recognition Award (AMA PRA) credits are accepted in the US as evidence of participation in CME activities. For further information on this award, please go to https://www.ama-assn.org. The AMA has determined that physicians not licensed in the US who participate in this CME activity are eligible for AMA PRA Category 1 Credits™. Through agreements that the AMA has made with agencies in some countries, AMA PRA credit may be acceptable as evidence of participation in CME activities. If you are not licensed in the US, please complete the questions online, print the AMA PRA CME credit certificate, and present it to your national medical association for review.

Article Title

Multicenter Case–Control Study of COVID-19–Associated Mucormycosis Outbreak, India

CME Questions

1. You are advising an inpatient COVID-19 treatment unit about prevention and management of COVID-19–associated mucormycosis (CAM). On the basis of the nationwide case-control study across 25 hospitals in India from January to June 2021 by Muthu and colleagues, which one of the following statements about risk factors for CAM, including potential associations of COVID-19 treatment practices with the occurrence of CAM, is correct?

A. Cumulative glucocorticoid dose was significantly associated with CAM
B. Zinc supplementation was associated with protection against CAM
C. Elevated C-reactive protein (CRP) and rural residence were not significantly associated with CAM
D. Diabetes mellitus and diabetic ketoacidosis (DKA) during COVID-19 were significantly associated with 2- to 3-fold increased risk for CAM

2. According to the nationwide case-control study across 25 hospitals in India from January to June 2021 by Muthu and colleagues, which one of the following statements about clinical outcomes of CAM and factors associated with mortality in CAM at 12 weeks is correct?

A. Mortality from CAM at 12 weeks was 12.2%
B. Pulmonary was the most common site for CAM
C. The most common organism causing mucormycosis was *Rhizomucor* spp.
D. Surgical resection and primary antifungal combination therapy were independently associated with better survival at 12 weeks

3. On the basis of the nationwide case-control study across 25 hospitals in India from January to June 2021 by Muthu and colleagues, which one of the following statements about clinical implications of risk factors for and clinical outcomes of CAM, including potential associations of COVID-19 treatment practices with the occurrence of CAM and factors associated with mortality in CAM at 12 weeks, is correct?

A. Hypoxemic COVID-19 patients should receive maximal glucocorticoid doses for 2 weeks
B. The findings support judicious use of COVID-19 therapies and optimal glycemic control to prevent CAM
C. The association between zinc supplementation and CAM was implausible and not supported by other evidence
D. The CAM outbreak during the COVID-19 pandemic was most likely related to factors other than COVID-19 or its treatment

DAVID J. SENCER CDC MUSEUM

History·Legacy·Innovation

Dr. David J. Sencer, Mrs. Mountin and Jim Collins celebrate CDC's 25th anniversary, 1961.

CDC at 75

January 9, 2023–July 28, 2023

TEMPORARY EXHIBITIONS GALLERY

Opening January 9, *CDC at 75* is a commemorative exhibition that tells unique stories about the work of this fabled agency and provides a glimpse into the breadth and depth of CDC's history and vast accomplishments. It features rarely seen objects, documents, and media taken from the CDC Museum's rich collections and archives.

Hours

Monday–Wednesday: 9 a.m.–5 p.m.
Thursday: 9 a.m.–7 p.m.
Friday: 9 a.m.–5 p.m.
Closed weekends and federal holidays

Location

1600 Clifton Road, NE
Atlanta, GA
30329-4021
Phone (404) 639-0830

Admission and parking free • Vehicle inspection required
Government-issued photo ID required for adults over the age of 18
Passport required for non-U.S. citizens